SHOUT
SHARE
IT

MBL

February 2004
Volume 206 • Number 1

THE BIOLOGICAL BULLETIN

Published by the Marine Biological Laboratory
www.biolbull.org

THE BIOLOGICAL BULLETIN
ONLINE

The Marine Biological Laboratory is pleased to announce that the full text of *The Biological Bulletin* is available online at

http://www.biolbull.org

The Biological Bulletin publishes outstanding experimental research on the full range of biological topics and organisms, from the fields of Neurobiology, Behavior, Physiology, Ecology, Evolution, Development and Reproduction, Cell Biology, Biomechanics, Symbiosis, and Systematics.

Published since 1897 by the Marine Biological Laboratory (MBL) in Woods Hole, Massachusetts, *The Biological Bulletin* is one of America's oldest peer-reviewed scientific journals.

The journal is aimed at a general readership, and especially invites articles about those novel phenomena and contexts characteristic of intersecting fields.

The Biological Bulletin Online contains the full content of each issue of the journal, including all figures and tables, beginning with the February 2001 issue (Volume 200, Number 1). The full text is searchable by keyword, and the cited references include hyperlinks to Medline. PDF files are available beginning in February 1990 (Volume 178, Number 1), some abstracts are available beginning with the October 1976 issue (Volume 151, Number 2), and some Tables of Contents are online beginning with the October 1965 issue (Volume 129, Number 2).

Each issue will be placed online approximately on the date it is mailed to subscribers; therefore the online site will be available prior to receipt of your paper copy. Online readers may want to sign up for the eTOC (electronic Table of Contents) service, which will deliver each new issue's table of contents *via* e-mail. The web site also provides access to information about the journal (such as Instructions to Authors, the Editorial Board, and subscription information), as well as access to the Marine Biological Laboratory's web site and other *Biological Bulletin* electronic publications.

The free trial period for access to *The Biological Bulletin* online has ended. Individuals and institutions who are subscribers to the journal in print or are members of the Marine Biological Laboratory Corporation may now activate their online subscriptions. All other access (*e.g.*, to Abstracts, eTOCs, searching, Instructions to Authors) remains freely available. Online access is included in the print subscription price.

For more information about subscribing or activating your online subscription, visit <www.biolbull.org/subscriptions>.

---

http://www.biolbull.org

NO SUCH THING AS GOOD VIBRATIONS.

BX51WI
ELECTROPHYSIOLOGY RESEARCH MICROSCOPE.

No other electrophysiology microscope eliminates vibrations like the Olympus BX51WI. The results are superb fluorescence and DIC capabilities under the challenging conditions of thick brain slice observation.

Olympus offers the most remarkable line of water immersion objectives. With the XLUMPFL 20× objective (NA 0.95 and WD 2.0mm) and a magnification changer, you'll never have to move the objective and disturb your experiment to switch between low and high magnifications.

Highly efficient wide-field fluorescence is at hand with the low-power XLFLUOR 4x/NA 0.28 or 2x/NA 0.14 objectives. Those objectives make GFP imaging of large fields easy and effective.

Olympus also offers an extensive line of dipping objectives that feature long working distances and large approach angles of over 40° for manipulator access.

The BX51WI provides excellent working conditions for in vivo brain slice IR-DIC application with an optical system tailored for high-contrast, high-resolution imaging.

THE OLYMPUS BX51WI. ROCKET SCIENCE™.

olympusamerica.com/microscopes 800-455-8236

OLYMPUS

© 2003 OLYMPUS AMERICA INC.

Cover

Most echinoderms are dioecious, but the sexes are usually indistinguishable on the basis of external structure. A very few species of brittle stars are, however, strikingly dimorphic, with a dwarf male clinging to a much larger female, usually mouth-to-mouth. Although this romantic posture suggests a role in reproduction, spawning has not previously been observed in these species. However, in this issue of *The Biological Bulletin* (p. 25) Hideyuki Tominaga and his colleagues describe the reproduction and development—from spawning to metamorphosis—of a dimorphic brittle star, *Ophiodaphne formata*. And they report further that these brittle stars, both couples and singles, have adopted a close living arrangement with sand dollars.

The upper portion of the cover shows an enlarged image of two brittle stars, coupled, and with their oral surfaces appressed. Her central disk is about 5 mm in diameter, his only 1 mm; and his arms are interdigitated with hers. At a much lower magnification (bottom left panel), we see this couple reclining on a host sand dollar, close to one of its five lunules. The female's aboral surface is fixed to the spiny oral surface of the sand dollar, and two of her arms are hooked over the edge of the lunule. A specimen of the host sand dollar from this study (*Astriclypeus manni*; diameter, about 14 cm) is shown in the lower right corner of the cover. But *O. formata* is not host-specific; two other species of sand dollars have been reported to accommodate this brittle star. Notice also that the figured specimen of *A. manni* bears two unpaired female brittle stars on its oral surface—near the lunules at 10 and 12 o'clock; thus, all *O. formata* are found on sand dollars, but only about half of the brittle stars are paired.

The sand dollars live in relatively shallow waters, partially buried in the sandy bottom. Thus, they provide the brittle stars with a ready, stable site of attachment on a shifting substrate; and the lunule protects against abrasion by the sand, which is the source of food for both organisms. At spawning, the gametes of brittle stars are released from bursal slits on the oral surface of the disk. The mouth-to-mouth posture brings those openings of the coupled male and female close together, maximizing the efficiency of fertilization. This is critical, because the population of brittle stars is sparse (only one of ten sand dollars is inhabited), and because these small animals produce a limited number of eggs. These relatively small eggs develop indirectly; but the time in development to metamorphosis is rapid, which minimizes transport of the brittle star larvae away from the habitat of the host sand dollars. Thus, Tominaga and colleagues suggest that the sexual dimorphism, the coupling behavior, and the characteristics of development all seem to be adaptations enabling a sparse population of brittle stars to survive on the sandy bottom of shallow seas.

The photographs on the cover were taken by Hideyuki Tominaga (Toyama University), and the cover was designed by Beth Liles (Marine Biological Laboratory, Woods Hole, Massachusetts).

THE
BIOLOGICAL BULLETIN
FEBRUARY 2004

Editor	MICHAEL J. GREENBERG	The Whitney Laboratory, University of Florida
Associate Editors	LOUIS E. BURNETT	Grice Marine Laboratory, College of Charleston
	R. ANDREW CAMERON	California Institute of Technology
	CHARLES D. DERBY	Georgia State University
	MICHAEL LABARBERA	University of Chicago
Section Editor	SHINYA INOUÉ, *Imaging and Microscopy*	Marine Biological Laboratory
Online Editors	JAMES A. BLAKE, *Keys to Marine Invertebrates of the Woods Hole Region*	ENSR Marine & Coastal Center, Woods Hole
	WILLIAM D. COHEN, *Marine Models Electronic Record and Compendia*	Hunter College, City University of New York
Editorial Board	PETER B. ARMSTRONG	University of California, Davis
	JOAN CERDÁ	Center of Aquaculture-IRTA, Spain
	ERNEST S. CHANG	Bodega Marine Lab., University of California, Davis
	THOMAS H. DIETZ	Louisiana State University
	RICHARD B. EMLET	Oregon Institute of Marine Biology, Univ. of Oregon
	DAVID EPEL	Hopkins Marine Station, Stanford University
	KENNETH M. HALANYCH	Auburn University, Alabama
	GREGORY HINKLE	Dana Farber Cancer Institute, Boston
	NANCY KNOWLTON	Scripps Inst. Oceanography & Smithsonian Tropical Res. Inst.
	MAKOTO KOBAYASHI	Hiroshima University of Economics, Japan
	ESTHER M. LEISE	University of North Carolina Greensboro
	DONAL T. MANAHAN	University of Southern California
	MARGARET MCFALL-NGAI	Kewalo Marine Laboratory, University of Hawaii
	MARK W. MILLER	Institute of Neurobiology, University of Puerto Rico
	TATSUO MOTOKAWA	Tokyo Institute of Technology, Japan
	YOSHITAKA NAGAHAMA	National Institute for Basic Biology, Japan
	SHERRY D. PAINTER	Marine Biomed. Inst., Univ. of Texas Medical Branch
	J. HERBERT WAITE	University of California, Santa Barbara
	PHIL YUND	University of New England, Biddeford, ME
	RICHARD K. ZIMMER	University of California, Los Angeles
Editorial Office	PAMELA CLAPP HINKLE	Managing Editor
	VICTORIA R. GIBSON	Staff Editor
	CAROL SCHACHINGER	Editorial Associate
	WENDY CHILD	Subscription & Advertising Administrator

Published by
MARINE BIOLOGICAL LABORATORY
WOODS HOLE, MASSACHUSETTS

http://www.biolbull.org

Marine Biological Laboratory,
Woods Hole Oceanographic Institution
Library

FEB 2 3 2004

Woods Hole, MA 02543

CONTENTS

VOLUME 206, NO. 1: FEBRUARY 2004

RESEARCH NOTE

Buresch, Kendra C., Jean G. Boal, Gregg T. Nagle, Jamie Knowles, Robert Nobuhara, Kate Sweeney, and Roger T. Hanlon
Experimental evidence that ovary and oviducal gland extracts influence male agonistic behavior in squids. 1

PHYSIOLOGY AND BIOMECHANICS

Motokawa, Tatsuo, Osamu Shintani, and Rüdiger Birenheide
Contraction and stiffness changes in collagenous arm ligaments of the stalked crinoid *Metacrinus rotundus* (Echinodermata) 4

NEUROBIOLOGY AND BEHAVIOR

Biggers, William J., and Hans Laufer
Identification of juvenile hormone-active alkylphenols in the lobster *Homarus americanus* and in marine sediments. 13

DEVELOPMENT AND REPRODUCTION

Tominaga, Hideyuki, Shogo Nakamura, and Miéko Komatsu
Reproduction and development of the conspicuously dimorphic brittle star *Ophiodaphne formata* (Ophiuroidea) 25

Temkin, M. H., and S. B. Bortolami
Waveform dynamics of spermatozeugmata during the transfer from paternal to maternal individuals of *Membranipora membranacea* 35

ECOLOGY AND EVOLUTION

Wang, Yongping, Zhe Xu, and Ximing Guo
Differences in the rDNA-bearing chromosome divide the Asian-Pacific and Atlantic species of *Crassostrea* (Bivalvia, Mollusca) 46

Maruyama, Yoshihiko K.
Occurrence in the field of a long-term, year-round, stable population of placozoans 55

THE BIOLOGICAL BULLETIN

THE BIOLOGICAL BULLETIN is published six times a year by the Marine Biological Laboratory, 7 MBL Street, Woods Hole, Massachusetts 02543.

Subscriptions and similar matter should be addressed to Subscription Administrator, THE BIOLOGICAL BULLETIN, Marine Biological Laboratory, 7 MBL Street, Woods Hole, Massachusetts 02543. Subscription includes both print and online journals. Subscription per year (six issues, two volumes): $325 for libraries; $120 for individuals. Subscription per volume (three issues): $165 for libraries; $70 for individuals. Back and single issues (subject to availability): $75 for libraries; $25 for individuals.

Communications relative to manuscripts should be sent to Michael J. Greenberg, Editor-in-Chief, or Pamela Clapp Hinkle, Managing Editor, at the Marine Biological Laboratory, 7 MBL Street, Woods Hole, Massachusetts 02543. Telephone: (508) 289-7149. FAX: 508-289-7922. E-mail: pclapp@mbl.edu.

http://www.biolbull.org

THE BIOLOGICAL BULLETIN is indexed in bibliographic services including *Index Medicus* and MEDLINE, *Chemical Abstracts, Current Contents, Elsevier BIOBASE/Current Awareness in Biological Sciences,* and *Geo Abstracts.*

Printed on acid free paper,
effective with Volume 180, Issue 1, 1991.

POSTMASTER: Send address changes to THE BIOLOGICAL BULLETIN, Marine Biological Laboratory,
7 MBL Street, Woods Hole, MA 02543.

Copyright © 2004, by the Marine Biological Laboratory

Periodicals postage paid at Woods Hole, MA, and additional mailing offices.
ISSN 0006-3185

INSTRUCTIONS TO AUTHORS

The Biological Bulletin accepts outstanding original research reports of general interest to biologists throughout the world. Papers are usually of intermediate length (10–40 manuscript pages). A limited number of solicited review papers may be accepted after formal review. A paper will usually appear within four months after its acceptance.

Very short, especially topical papers (less than 9 manuscript pages including tables, figures, and bibliography) will be published in a separate section entitled "Research Notes." A Research Note in *The Biological Bulletin* follows the format of similar notes in *Nature.* It should open with a summary paragraph of 150 to 200 words comprising the introduction and the conclusions. The rest of the text should continue on without subheadings, and there should be no more than 30 references. References should be referred to in the text by number, and listed in the Literature Cited section in the order that they appear in the text. Unlike references in *Nature,* references in the Research Notes section should conform in punctuation and arrangement to the style of recent issues of *The Biological Bulletin.* Materials and Methods should be incorporated into appropriate figure legends. See the article by Lee (October 2003, Vol. **205:** 99–101) for sample style. A Research Note will usually appear within two months after its acceptance.

The Editorial Board requests that regular manuscripts conform to the requirements set below; those manuscripts that do not conform will be returned to authors for correction before review.

1. ***Manuscripts.*** Manuscripts, including figures, should be submitted in quadruplicate, with the originals clearly marked. (Xerox copies of photographs are not acceptable for review purposes.) Please include an electronic copy of the text of the manuscript. Label the disk with the name of the first author and the name and version of the wordprocessing software used to create the file. If the file was not created in some version of Microsoft Word, save the text in rich text format (rtf). The submission letter accompanying the manuscript should include a telephone number, a FAX number, and (if possible) an E-mail address for the corresponding author. The original manuscript must be typed in no smaller than 12 pitch or 10 point, using double spacing (*including* figure legends, footnotes, bibliography, etc.) on one side of 16- or 20-lb. bond paper, 8 by 11 inches. Please, no right justification. Manuscripts should be proofread carefully and errors corrected legibly in black ink. Pages should be numbered consecutively. Margins on all sides should be at least 1 inch (2.5 cm). Manuscripts should conform to the *Council of Biology Editors Style Manual,* 5th Edition (Council of Biology Editors, 1983) and to American spelling. Unusual abbreviations should be kept to a minimum and should be spelled out on first reference as well as defined in a footnote on the title page. Manuscripts should be divided into the following components: Title page, Abstract (of no more than 200 words), Introduction, Materials and Methods, Results, Discussion, Acknowledgments, Literature Cited, Tables, and Figure Legends. In addition, authors should supply a list of words and phrases under which the article should be indexed.

2. ***Title page.*** The title page consists of a condensed title or running head of no more than 35 letters and spaces, the manuscript title, authors' names and appropriate addresses, and footnotes listing present addresses, acknowledgments or contribution numbers, and explanation of unusual abbreviations.

3. ***Figures.*** The dimensions of the printed page, 7 by 9 inches, should be kept in mind in preparing figures for publication. We recommend that figures be about 1 times the linear dimensions of the final printing desired, and that the ratio of the largest to the smallest letter or number and of the thickest to the thinnest line not exceed 1:1.5. Explanatory matter generally should be included in legends, although axes should always be identified on the illustration itself. Figures should be prepared for reproduction as either line cuts or halftones. Figures to be reproduced as line cuts should be unmounted glossy photographic reproductions or drawn in black ink on white paper, good-quality tracing cloth or plastic, or blue-lined coordinate paper. Those to be reproduced as halftones should be mounted on board, with both designating numbers or letters and scale bars affixed directly to the figures. All figures should be numbered in consecutive order, with no distinction between text and plate figures and cited, in order, in the text. The author's name and an arrow indicating orientation should appear on the reverse side of all figures.

Digital art: The Biological Bulletin will accept figures submitted in electronic form; however, digital art must conform to the following guidelines. Authors who create digital images are wholly responsible for the quality of their material, including color and halftone accuracy.

Format. Acceptable graphic formats are TIFF and EPS. Color submissions must be in EPS format, saved in CMKY mode.

Software. Preferred software is Adobe Illustrator or Adobe Photoshop for the Mac and Adobe Photoshop for Windows. Specific instructions for artwork created with various software programs are available on the Web at the Digital Art Information Site maintained by Cadmus Professional Communications at http://cpc.cadmus.com/da/

Resolution. The minimum requirements for resolution are 1200 DPI for line art and 300 for halftones.

Size. All digital artwork must be submitted at its actual printed size so that no scaling is necessary.

Multipanel figures. Figures consisting of individual parts (*e.g.*, panels A, B, C) must be assembled into final format and submitted as one file.

Hard copy. Files must be accompanied by hard copy for use in case the electronic version is unusable.

Disk identification. Disks must be clearly labeled with the following information: author name and manuscript number; format (PC or Macintosh); name and version of software used.

Color: The Biological Bulletin will publish color figures and plates, but must bill authors for the actual additional cost of printing in color. The process is expensive, so authors with more than one color image should—consistent with editorial concerns, especially citation of figures in order—combine them into a single plate to reduce the expense. On request, when supplied with a copy of a color illustration, the editorial staff will provide a pre-publication estimate of the printing cost.

4. ***Tables, footnotes, figure legends, etc.*** Authors should follow the style in a recent issue of *The Biological Bulletin* in preparing table headings, figure legends, and the like. Because of the high cost of setting tabular material in type, authors are asked to limit such material as much as possible. Tables, with their headings and footnotes, should be typed on separate sheets, numbered with consecutive Arabic numerals, and placed after the Literature Cited. Figure legends should contain enough information to make the figure intelligible separate from the text. Legends should be typed double spaced, with consecutive Arabic numbers, on a separate sheet at the end of the paper. Footnotes should be limited to authors' current addresses, acknowledgments or contribution numbers, and explanation of unusual abbreviations. All such footnotes should appear on the title page. Footnotes are not normally permitted in the body of the text.

5. ***Literature cited.*** In the text, literature should be cited by the Harvard system, with papers by more than two authors cited as Jones *et al.*, 1980. Personal communications and material in preparation or in press should be cited in the text only, with author's initials and institutions, unless the material has been formally accepted and a volume number can be supplied. The list of references following the text should be headed Literature Cited, and must be typed double spaced on separate pages, conforming in punctuation and arrangement to the style of recent issues of *The Biological Bulletin.* Citations should include complete titles and inclusive pagination. Journal abbreviations should normally follow those of the U. S. A. Standards Institute (USASI), as adopted by Biological Abstracts and Chemical Abstracts, with the minor differences set out below. The most generally useful list of biological journal titles is that published each year by Biological Abstracts (biosis List of Serials; the most recent issue). Foreign authors, and others who are accustomed to using The World List of Scientific Periodicals, may find a booklet published by the Biological Council of the U.K. (obtainable from the Institute of Biology, 41 Queen's Gate, London, S.W.7, England, U.K.) useful, since it sets out the World List abbreviations for most biological journals with notes of the USASI abbreviations where these differ. Chemical Abstracts publishes quarterly supplements of additional abbreviations. The following points of reference style for The Biological Bulletin differ from USASI (or modified World List) usage:

A. Journal abbreviations, and book titles, all underlined (for *italics*)

B. All components of abbreviations with initial capitals (not as European usage in World List *e.g., J. Cell. Comp. Physiol.* NOT *J. cell. comp. Physiol.*)

C. *All* abbreviated components must be followed by a period, whole word components *must not* (*i.e., J. Cancer Res.*)

D. Space between all components (*e.g., J. Cell. Comp. Physiol.*, not *J.Cell.Comp.Physiol.*)

E. Unusual words in journal titles should be spelled out in full, rather than employing new abbreviations invented by the author. For example, use *Rit Vísindafjélags Islendinga* without abbreviation.

F. All single word journal titles in full (*e.g., Veliger, Ecology, Brain*).

G. The order of abbreviated components should be the same as the word order of the complete title (*i.e., Proc.* and *Trans.* placed where they appear, not transposed as in some BIOLOGICAL ABSTRACTS listings).

H. A few well-known international journals in their preferred forms rather than WORLD LIST or USASI usage (*e.g., Nature, Science, Evolution* NOT *Nature, Lond., Science, N.Y.; Evolution, Lancaster, Pa.*)

6. ***Sequences.*** By the time a paper is sent to the press, all nucleotide or amino acid sequences and associated alignments should have been deposited in a generally accessible database (*e.g.*, GenBank, EMBL, SwissProt), and the sequence accession number should be provided.

7. ***Reprints, page proofs, and charges.*** Authors may purchase reprints in lots of 100. Forms for placing reprint orders are sent with page proofs. Reprints normally will be delivered about 2 to 3 months after the issue date. Authors will receive page proofs of articles shortly before publication. They will be charged the current cost of printers' time for corrections to these (other than corrections of printers' or editors' errors). Other than these charges for authors' alterations, *The Biological Bulletin* does not have page charges.

Reference: *Biol. Bull.* **206:** 1–3. (February 2004)
© 2004 Marine Biological Laboratory

Experimental Evidence That Ovary and Oviducal Gland Extracts Influence Male Agonistic Behavior in Squids

KENDRA C. BURESCH[1], JEAN G. BOAL[2], GREGG T. NAGLE[3], JAMIE KNOWLES[1], ROBERT NOBUHARA[1], KATE SWEENEY[1], AND ROGER T. HANLON[1,*]

[1] *Marine Resources Center, Marine Biological Laboratory, Woods Hole, Massachusetts 02543-1015;* [2] *Department of Biology, Millersville University of Pennsylvania, Millersville, Pennsylvania 17551-0302; and* [3] *Marine Biomedical Institute and Department of Anatomy and Neurosciences, University of Texas Medical Branch, Galveston, Texas 77555-1069*

Recent investigations of sensory and behavioral cues that initiate sexual selection processes in the squid Loligo pealeii *have determined that egg capsules deposited on the substrate provide a strong visual and chemotactile stimulus to males, even in the absence of females (1, 2, 3). The visual stimulus of egg capsules attracts males to the eggs, and when the males touch the eggs, they encounter a chemical stimulus that leads to highly aggressive fighting behavior. We have recently demonstrated that egg capsule extracts implanted in artificial egg capsules elicit this aggressive behavior (4). In this communication, we present evidence that the salient chemical factor originates in the ovary and perhaps the oviducal gland of the female reproductive tract.*

Cephalopods are highly visual animals, yet recent research has shown that chemical communication plays an important role in regulating some behaviors (5). It has long been known (6) that *Loligo pealeii* is attracted visually to egg capsules (each translucent egg capsule is about 4 cm long and contains 100–300 eggs) and that females frequently lay egg capsules adjacent to existing egg capsules (7, 8). A fortuitous field observation indicated that males are visually attracted by egg capsules, but that touching the eggs was essential to evoke the intra-male competition for mates (1). Thus it appears that both visual and chemical communication play a role in triggering a change from shoaling behavior to mating behavior when *L. pealeii* migrates inshore to spawn in spring. Our ultimate goal is to identify and characterize the compound (or compounds) that elicits this highly aggressive behavior in male squids.

Behavioral responses to natural eggs were compared with responses to artificial egg capsules coated with extracts (4) from one of four female reproductive organs or glands: ovary, oviducal gland, nidamental gland, or accessory nidamental gland. With the exception of ovary (see below), the equivalent of one-fifth of each gland was used to coat the artificial egg capsules. Six behaviors were selected to assess the level of aggression because they were conspicuous, easy to score, and reliable between observers. The general sequence of increased aggression in loliginid squids (9, 10), as shown by five of these behaviors, can be depicted as follows:

Raised arm → Fin-beating → Chase
→ Forward Lunge Grab (FLG) → Grapple

The sixth behavior, Splayed arms, is associated with defense of eggs or females and was also recorded. The frequency of any one of these six discrete behaviors was relatively low; consequently, the variable Total Aggression was computed as the sum of all occurrences of any of the six behaviors.

All experiments were conducted between May and August 2002. Squids were caught in Vineyard Sound (Falmouth, MA) using trawls or jigs. Reproductive organs were collected from 16 females. Each whole organ (except ovary, which was subsampled due to its large size) was individually extracted, centrifuged, and purified using separate C18 Sep-Pak cartridges (Waters Corp., Milford, MA) as de-

---

Received 8 August 2003; accepted 25 November 2003.

* To whom correspondence should be addressed. E-mail: rhanlon@mbl.edu

Table 1

Mean number of behaviors recorded during the 10-min trial period for each egg stimulus

Egg stimulus	n^{*}_{pr}	Egg touch	Raised arm	Fin-beating	# Chases	FLG**	Grapple	Splayed arms	Total aggr.†
Natural	7	2.71	3.29	1.00	12.29	9.86	1.29	3.86	31.57
Ovary	10	3.30	2.20	0.70	5.70	0.60	0.60	3.40	13.20
Oviducal	11	5.18	0.27	0.55	7.64	2.91	0.18	1.27	12.82
Nidamental accessory	10	1.90	0.30	0.10	1.30	0.70	0.00	0.80	3.20
Nidamental	10	3.00	0.30	0.10	1.30	0.50	0.20	1.10	3.50

* n_{pr} is the number of squid pairs tested.

** FLG is the behavior Forward-Lunge-Grab.

† Total Aggression is the sum of all instances of Raised arm, Fin-beating, Chase, FLG, Grapple, and Splayed arms.

scribed previously (4); C18 Sep-Paks bind small molecules, peptides, and small proteins.

Behavioral trials were conducted in round tanks with aerated, flow-through natural seawater. Trials were conducted according to the following protocol. A pair of squids was placed in the trial tank and allowed 30 min to reach baseline behavior (*i.e.*, agonistic interactions resulted in one squid becoming dominant and occupying the center of the tank, and both squids being calm and showing normal coloration). In the pre-test, a bundle of 16–20 natural egg capsules was added to the tank. Data collection began when one of the squids touched the egg capsules. Previous experiments demonstrated that uncoated artificial eggs elicited significantly fewer egg touches than either coated artificial eggs or natural eggs (Friedman two-way ANOVA by ranks; $F_r = 7.43$, $n = 14$; $P < 0.05$). Not all squids were attracted to natural eggs; pairs in which neither squid touched the eggs were removed from the experiment. Instances of five of the six discrete behaviors (Raised arm, Fin-beating, Forward-Lunge-Grab (FLG), Grapple, Splayed arms) were recorded continuously for 10 min. Chase was frequent and continuous; consequently it was recorded at 15-s intervals. Squids that did not respond aggressively (*i.e.*, touched eggs but stayed at baseline behavior—resting or calm swimming) during the pre-test were excluded from further experiments. After a minimum of 1 h to regain baseline behavior, experimental trials commenced. The mean time to return to baseline behavior after being exposed to an egg stimulus was determined previously to be 7.9 min (range 1–40 min; $n = 11$). The egg stimulus (natural egg capsules or artificial egg capsules) was added to the tank and behaviors were scored as before.

We expected to examine the differences in responses of squids (experimental trial response minus pre-test response) to control for variation in responses between squids; however, the variances in the calculated differences were higher than the variances of responses for either pre-test trials or experimental trials (*e.g.*, the variances for total aggression with real eggs were pre-test, 398; experimental trials, 369; differences, 692; $n = 7$). Consequently, only data from experimental trials were analyzed further. A Kruskal-Wallis analysis of variance by ranks (data were unitless and not normally distributed) was performed to determine which female reproductive organ elicited an agonistic response comparable to natural eggs. Multiple comparisons of treatments with the control were then performed. Note that statistical significance indicates that a treatment was not as effective as real eggs.

A total of 54 Raised arms, 22 Fin-beatings, 253 Chases, 119 FLGs, 19 Grapples, and 94 Splayed arms were recorded throughout the experiment ($n = 48$ pairs; means are listed in Table 1). Aggressive behavior ("Total Aggression" in Table 1) differed significantly between egg stimuli ($\chi^2 = 15.5$, df = 4, $P < 0.01$). Squids responded with the most aggression in response to natural eggs and with the least aggression in response to extracts from nidamental and accessory nidamental glands. Comparisons (11) of treatments *versus* the control (*i.e.*, natural eggs) revealed that aggressive responses to extracts from nidamental and accessory nidamental glands were significantly lower than responses to natural eggs. If we assume that more egg touches provide a greater stimulus for aggression, then it is reasonable to consider the aggression observed per egg touch. In this case, aggressive behavior again differed significantly between egg stimuli ($\chi^2 = 12.72$, df = 4, $P < 0.05$); however, comparisons (11) of treatments *versus* the control (*i.e.*, natural eggs) show that only extracts from ovaries elicited aggression statistically indistinguishable from that of real eggs (Fig. 1).

These results indicate that a chemical factor that induces agonistic interactions is produced in the ovary, and perhaps also in the oviducal gland, but not in the nidamental or accessory nidamental glands. The reversible binding of the chemical to C18 Sep-Pak cartridges suggests strongly that it is a soluble factor. Eggs are produced in the ovary and are transported into the oviducal gland, which is a specialized segment of the oviduct that is involved with secretion (12). The oviducal gland produces the inner jelly of the egg mass

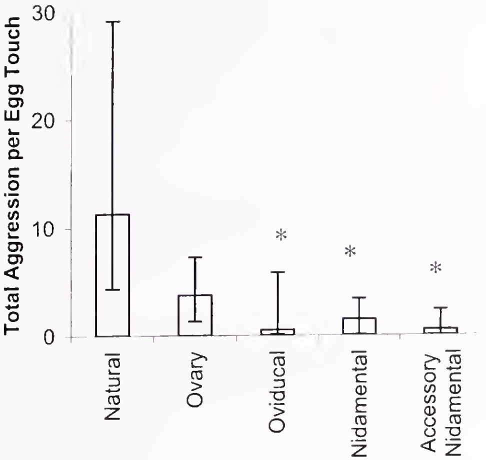

Figure 1. The median numbers of aggressive behaviors per egg touch (error bars indicate first and third quartiles) of squids after contact with natural eggs or contact with extracts from female reproductive glands (n = 48 pairs). An asterisk indicates that responses were significantly different from responses to natural eggs ($\chi^2 = 12.72$, df = 4, $P < 0.05$).

of *L. pealeii* (6). In contrast, the nidamental gland produces the outer coating of the egg capsule (12), and the accessory nidamental gland is responsible for coating the eggs with bacteria that may deter pathogens or reduce predation (13). There may be several chemical factors responsible for inducing agonistic behavior—for example, chemicals in the eggs themselves and perhaps in the inner jelly of the egg capsule secreted by the oviducal gland. If the chemical is indeed produced in the ovary, as suggested by these results, there must be some mechanism (*e.g.*, diffusion) by which the compound reaches the outer jelly coats of the egg capsule so that male squids can detect the compound when they touch the eggs.

Pheromones are key mediators of reproductive behaviors, and an understanding of their roles is essential to understanding the ecology and evolution of populations and species (14). Aquatic pheromones are particularly difficult to characterize because they are rapidly degraded (15); consequently, few invertebrate pheromones have been characterized in aquatic animals. However, a family of structurally related peptide pheromonal attractants ("attractins") has recently been characterized in five species of the opisthobranch *Aplysia* (16, 17), and the three-dimensional NMR solution structure of *A. californica* attractin has been determined (18). These peptide pheromones are secreted by the albumen gland, a large exocrine gland that packages the eggs into a cordon. Our results with squids suggest that the ovary and oviducal gland should be tested further, and that chemical factors in those organs should be chemically and behaviorally characterized. Clearly, more research is required to understand the mechanisms and functions of multiple sensory cues that play a critical role in initiating the sexual selection processes in *Loligo pealeii*.

Literature Cited

1. **Hanlon, R. T. 1996.** Evolutionary games that squids play: fighting, courting, sneaking, and mating behaviors used for sexual selection in *Loligo pealei*. *Biol. Bull.* **191:** 309–310.
2. **King, A. J., S. A. Adamo, and R. T. Hanlon. 1999.** Contact with squid egg capsules increases agonistic behavior in male squid (*Loligo pealei*). *Biol. Bull.* **197:** 256.
3. **King, A. J., S. A. Adamo, and R. T. Hanlon. 2003.** Agonistic behavior between male squid: squid egg mops provide sensory cues for swift conflict escalation. *Anim. Behav.* **66:** 49–58.
4. **Buresch, K. C., J. G. Boal, J. Knowles, J. Debose, A. Nichols, A. Erwin, S. D. Painter, G. T. Nagle, and R. T. Hanlon. 2003.** Contact chemosensory cues in egg bundles elicit male-male agonistic conflicts in the squid *Loligo pealeii* (Mollusca: Cephalopoda). *J. Chem. Ecol.* **29:** 529–542.
5. **Hanlon, R. T., and N. Shashar. 2002.** Aspects of the sensory ecology of cephalopods. Pp. 266–282 in *Sensory Processing in the Aquatic Environment*, S. P. Collin and N. J. Marshall, eds. Springer Verlag, New York. 446 pp.
6. **Drew, G. A. 1911.** Sexual activities of the squid, *Loligo pealii* (Les.). I. Copulation, egg-laying and fertilization. *J. Morphol.* **22:** 327–359.
7. **Arnold, J. M. 1962.** Mating behavior and social structure in *Loligo pealii*. *Biol. Bull.* **123:** 53–57.
8. **Griswold, C. A., and J. Prezioso. 1981.** *In situ* observations on reproductive behavior of the long-finned squid, *Loligo pealei*. *Fish. Bull.* **78:** 945–947.
9. **Hanlon, R. T., M. R. Maxwell, N. Shashar, E. R. Loew, and K.-L. Boyle. 1999.** An ethogram of body patterning behavior in the biomedically and commercially valuable squid *Loligo pealei* off Cape Cod, Massachusetts. *Biol. Bull.* **197:** 49–62.
10. **DiMarco, F. P., and R. T. Hanlon. 1997.** Agonistic behavior in the squid *Loligo plei* (Loliginidae, Teuthoidea): fighting tactics and the effects of size and resource value. *Ethology* **103:** 89–108.
11. **Siegel, S., and N. J. Castellan, Jr. 1988.** *Nonparametric Statistics for the Behavioral Sciences*. McGraw-Hill, New York. 399 pp.
12. **Lum-Kong, A. 1992.** A histological study of the accessory reproductive organs of female *Loligo forbesi* (Cephalopoda: Loliginidae). *J. Zool. (Lond.)* **226:** 469–490.
13. **Barbieri, E., K. Barry, A. Child, and N. Wainwright. 1997.** Antimicrobial activity in the microbial community of the accessory nidamental gland and egg cases of *Loligo pealei* (Cephalopoda: Loliginidae). *Biol. Bull.* **193:** 275–276.
14. **Zimmer, R. K., and C. A. Butman. 2000.** Chemical signaling processes in the marine environment. *Biol. Bull.* **198:** 168–187.
15. **Shimizu, Y. 1985.** Bioactive marine natural products with emphasis on handling of water-soluble compounds. *J. Nat. Prod.* **48:** 223–235.
16. **Painter, S. D., B. Clough, R. W. Garden, J. V. Sweedler, and G. T. Nagle. 1998.** Characterization of *Aplysia* attractin, the first water-borne peptide pheromone in invertebrates. *Biol. Bull.* **194:** 120–131.
17. **Painter, S. D., D.-B. G. Akalal, B. Clough, A. J. Susswein, M. Levy, and G. T. Nagle. 2000.** Characterization of four new members of the attractin family of peptide pheromones in *Aplysia*. *Soc. Neurosci. Abstr.* **26:** 1166.
18. **Garimella, R., Y. Xu, C. H. Schein, K. Rajarathnam, G. T. Nagle, S. D. Painter, and W. Braun. 2003.** NMR solution structure of attractin, a water-borne protein pheromone from the mollusk *Aplysia californica*. *Biochemistry* **42:** 9970–9979.

Reference: *Biol. Bull.* **206:** 4–12. (February 2004)
© 2004 Marine Biological Laboratory

Contraction and Stiffness Changes in Collagenous Arm Ligaments of the Stalked Crinoid *Metacrinus rotundus* (Echinodermata)

TATSUO MOTOKAWA*, OSAMU SHINTANI, AND RÜDIGER BIRENHEIDE

Department of Biological Sciences, Graduate School of Bioscience and Biotechnology,
Tokyo Institute of Technology, Meguro, Tokyo, 152-8551 Japan

Abstract. Shortening and stiffness were measured simultaneously in the aboral ligament of arms of sea lilies. Arm pieces were used from which oral tissues (including muscles) were removed, leaving only collagenous ligaments connecting arm ossicles. Chemical stimulation by means of artificial seawater with an elevated concentration of potassium caused both a bending movement and stiffness changes (either softening or stiffening). The movement lasted for 1.5–10 min, and bent posture was maintained. The observation that contraction was not necessarily associated with softening provided evidence against the hypothesis that the shortening of the aboral ligaments was driven by the elastic components that had been charged by the oral muscles and released their strain energy at the softening of the aboral ligaments. The speed of ligamental shortening was slower by at least one order of magnitude than that of muscles. Acetylcholine (10^{-5}–10^{-3} *M*) caused both contraction and softening. We conclude that the aboral ligament shows two mechanical activities based on different mechanisms: one is active contraction and the other is connective tissue catch in which passive mechanical properties show mutability. We suggest that there is neural coordination between the two mechanisms.

Introduction

Echinoderms are unique in possessing mechanically active collagenous connective tissues. The best-known example is catch connective tissue (mutable connective tissue), which changes its passive mechanical properties under nervous control (Motokawa, 1984; Wilkie, 1996). Catch connective tissues are found in various anatomical locations in all the classes of echinoderms, and they have been regarded as one of the major features that characterize the phylum Echinodermata (Motokawa, 1988). The catch connective tissue stiffens or softens. Such changes in passive mechanical properties become apparent only when an external force is applied and the reaction of the tissue to this force is measured.

Another kind of mechanically active connective tissue was recently found in echinoderms (Birenheide and Motokawa, 1996, 1998; Birenheide *et al.*, 2000). The collagenous ligaments in the arms and cirri of crinoids contract in response to chemical stimuli such as cholinergic agents and seawater with an elevated concentration of potassium. Although the mechanism of contraction has yet to be elucidated, it is evident that muscles are not directly involved in the contraction because no muscle cells were found in these ligaments (Birenheide and Motokawa, 1994; Birenheide *et al.*, 2000).

There remains the possibility that muscles are indirectly involved in the contraction of connective tissues. The aboral ligaments of crinoid arms are disposed in an antagonistic position to the muscles in arm articulations (Fig. 1a). Crinoid arms consist of a row of ossicles connected by ligaments and muscles (Fig. 1b). The face of each ossicle bears a fulcrum that corresponds to the fulcrum of the adjacent ossicle. Muscles are found only on the oral (upper) side of the fulcrum, whereas collagenous ligaments are found both orally and aborally. When muscles on the oral side of the fulcrum contract, the arm bends in the oral direction. The arm also shows aboral bending. Because the aboral ligaments are the only mechanically strong element on the aboral side of the fulcrum, they are no doubt responsible for

---

Received 19 June 2003; accepted 27 October 2003.

* To whom correspondence should be addressed. E-mail: tmotokaw@bio.titech.ac.jp

aboral bending. The conventional explanation has invoked elastic recoil (Birenheide and Motokawa, 1994). According to this view, elastic energy is stored in the aboral ligaments by passive stretch when oral bending is produced by the muscles. This strain energy is then released when the muscles relax, and the aboral ligaments shorten to cause aboral bending of the arm. This explanation regards the aboral ligament as being an antagonizing spring to the oral muscle.

The aboral ligaments are not, however, a simple spring. Arm preparations from which all the oral muscles have been removed keep a rather straight posture and show aboral bending upon chemical stimulation (Birenheide and Motokawa, 1996). Some locking mechanism for keeping the straight posture—and thus the charged state of the spring—would seem to be necessary, otherwise the aboral ligaments would spring back at the moment when the antagonizing muscles are removed. A possibility is that the ligament stores strain energy as an expanded spring by stiffening the tissue and releases it by softening, which results in shortening of the ligament. The "spring-with-a-lock" hypothesis for the contraction of crinoid arm ligaments seems to be a reasonable one because the arm ligaments contain fibrillin-like, and thus possibly elastic, microfibrils (Birenheide and Motokawa, 1994) and show mutability of stiffness (Birenheide and Motokawa, 1998). The hypothesis is also parsimonious because otherwise some unknown actively contractile machinery would have to be postulated.

The present study was designed to test the spring-with-a-lock hypothesis. We measured shortening and stiffness of the aboral ligaments simultaneously. The hypothesis predicts that softening should precede shortening. The results we obtained were contrary to the prediction and thus support our previous suggestion that the ligaments actively contract without the help of muscles (Birenheide and Motokawa, 1998; Birenheide *et al.*, 2000).

Materials and Methods

Specimens of the stalked crinoid *Metacrinus rotundus* Carpenter, 1882, were dredged from depths of 100–150 m in Suruga Bay off Numazu, Japan. Collected specimens were transported to our laboratory in Tokyo, where they were held in a tank containing recirculating seawater. The tank was kept dark and the water temperature was maintained at 14 °C. Nineteen individuals were used for experiments. They were used within 2 months after capture.

The arm of *Metacrinus rotundus* consists of a series of ossicles that are connected by ligaments and muscles. The skeletal joint of the ossicles is a transverse ridge that acts as a fulcrum. The muscles are found only on the oral side of the fulcrum, while ligaments are found on both sides (Fig. 1a). The aboral ligament was used in the present study. The aboral ligament consists of two parts, the main ligament and the much smaller ligament housed in a fossa. The results reported here refer to the combined properties of the two ligaments. An arm piece (length *ca.* 6 mm) containing five to seven ossicles was dissected from a sea lily. The oral side, containing coelomic canals, muscles, and most of the oral ligaments, was removed using a razor blade (Fig. 1b). The remaining oral tissue between ossicles was cut up to the fulcrum. The adjacent ossicles were thus connected by a mechanically strong aboral ligament and by a mechanically weak epidermis overlying the ligament, and also by a mechanically weak brachial nerve housed in a hole in the center of the ossicle.

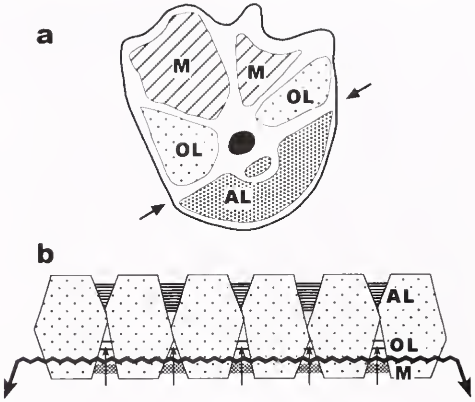

Figure 1. The articulation surface of an ossicle of *Metacrinus rotundus* (a), and the side view of an excised arm piece (b). Oral direction is to the top in a and to the bottom in b. (a) A transverse ridge (arrows) that acts as a fulcrum is arranged at an angle of about 60° to the oral-aboral plane. The ridges on the distal and the proximal side of each ossicle are arranged at angles of 60° and −60°, respectively. The central hole houses a brachial nerve. On the oral joint surface, two muscle bundles (M) and two bundles of oral ligaments (OL) insert into the ossicle. On the aboral joint surface, aboral ligaments (densely hatched area), which consists of a main aboral ligament (AL) and a small fossa ligament, insert into the ossicle. No muscles are found on the aboral side of the fulcrum. (b) An arm piece with six ossicles that are connected with each other by ligaments and muscles. The oral side, including muscle bundles, was removed from the arm piece with a razor blade, and the remaining oral tissues between the ossicles (arrows) were cut up to the fulcrum.

The experimental setup is shown in Figure 2. The proximal end of the arm piece was firmly fixed to a holder by both cyanoacrylate glue and mechanical clamping. The double fixing ensured that there would be no slippage between the sample and the holder when the sample was subjected to a push. The arm piece was held horizontally with the aboral side upward. A small L-shaped stainless steel plate weighing 140 mg was glued to the free end of the arm, and seawater was introduced to a trough. The position of the plate, and thus that of the arm tip, was recorded by an eddy current sensor (E2CA-AN4E, Omron, Japan) located in the floor of the trough. In this setup, any active contraction of the aboral ligaments results in an upward bending of the arm piece against the force of gravity; large softening of the ligaments would cause the arm piece to bend downward under gravity.

We constructed a device that allowed us to measure the stiffness of the ligament without restraining the free movement of the sample (Fig. 2). The device consisted of a force gauge (KSP-2-120-E-4, Kyowa, Japan) to which a probe of 1 mm diameter was attached. The gauge was fixed to a linear motion actuator (c-sx-30, THK, Japan) controlled by a microcomputer. The actuator produced vertical motion that allowed positioning of the probe in increments of 10 μm. The movements were controlled *via* a computer program written in BASIC. The program took data provided from the movement sensor and positioned the probe so that it was always 2 mm above the stainless steel plate attached to the arm piece. Any movement of the arm was followed by an immediate corresponding movement of the probe so that the distance between the probe tip and the specimen remained constant. At intervals determined by the experimenter, the probe was lowered until it touched the stainless steel plate. From this point the probe was lowered further for 0.2 mm, which caused downward displacement of the arm tip by the same amount. The force resulting from this downward displacement was recorded. The probe was then retracted to its position above the specimen. The speed of the probe was 4.2 mm/s, which was 100 times faster than the fastest arm-tip movement observed. The probe touched the arm for less than 91 ms. The bending stiffness was calculated as the peak force divided by the maximum excursion of the arm tip during the push, expressed as the percentage of the control value. The device thus enabled us to record stiffness changes and arm movement simultaneously.

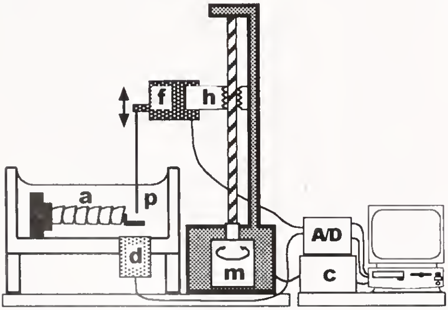

Figure 2. Schematic drawing of the experimental setup. An arm piece (a), whose size is drawn exaggerated, is held horizontally and aboral side up in a trough. A force gauge (f), to which a probe (p) is attached, is mounted on the moving head (h) of a linear motion acutator driven by a stepping motor (m). The vertical position of the moving head and thus that of the probe tip is precisely controlled. The position of the L-shaped metal plate glued to the distal end of the arm piece is monitored by a displacement sensor (d). Both force and displacement signals are fed to a computer through an analog-to-digital converter board (A/D). Feedback signals from the computer are given to the motor *via* a motor controller (c).

The sample was left in a trough for 10 min, and two successive downward pushes, separated by an interval of about 100 s, were applied to check that the stiffness and the baseline position of the arm tip were maintained. The stiffness at the second push was taken as the control value S_0. The stiffness change ΔS, expressed as a percentage, was calculated as follows: $\Delta S = 100 \times (S_1 - S_0)/S_0$, where S_1 is the stiffness after stimulation. A stiffness decrease was thus shown as a negative value. Chemicals for stimulation were introduced within 1 min after the second push. The speed of elevation of the arm tip was designated as the bending speed. The peak bending speed was the maximum speed of the upward bending of the arm tip. The average bending speed in artificial seawater with an elevated potassium concentration was calculated as follows. The peak height of the bending of the arm tip from the baseline was taken as 100%. The average bending speed was defined as 80% of the maximum excursion divided by the time needed to bend from 10% to 90% of the peak height. The reaction time for contraction was the time that elapsed from the application of chemical to the beginning of bending.

Artificial seawater (ASW) in the trough was constantly circulated *via* a pump through a water bath to keep the temperature at 14 °C. The composition of ASW was as follows (in mmol/l): NaCl, 433.7; KCl, 10.0; $CaCl_2$, 10.1; $MgCl_2$, 52.5; $NaHCO_3$, 2.5. The pH of all the solutions was adjusted to 8.2. ASW whose potassium concentration was raised to 100 m*M* (KASW) was prepared by reducing the sodium concentration so as to keep osmolarity constant. Acetylcholine solution (ACh) was prepared by diluting acetylcholine chloride (Nacalai Tesque, Japan) to the desired concentration in ASW. To rinse out the trough, both KASW and ACh were exchanged with ASW using the circulation pump.

Results

Control experiments

We performed control experiments to ensure that our experimental setup did not influence the movement or stiffness of the arm. When an arm piece glued to the stainless steel plate was left in seawater, the plate was kept in the same position for at least 30 min in most cases. After the 10-min resting period, a little drift of the position was observed in some samples; such samples were not used for experiments. Repeated stiffness measurements without chemical stimulation were performed. A typical result is given in Figure 3a, in which the upper trace is for the position of the arm tip, and the lower trace is for the force. The vertical bars in the upper trace show the downward deflection of the arm pushed by a probe. The upward

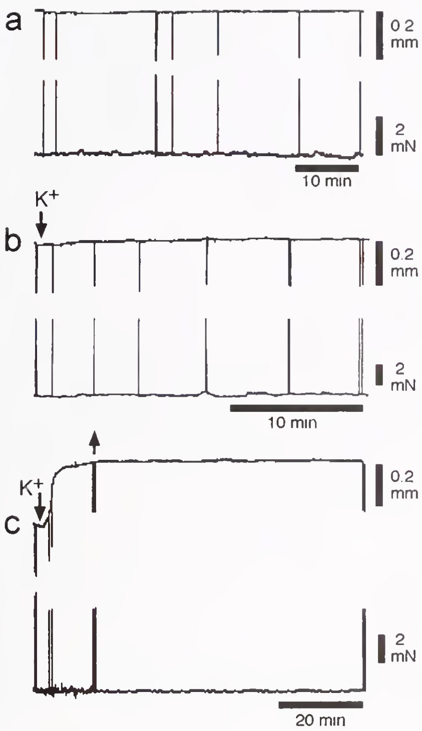

Figure 3. Control experiments. Upper traces show displacement, and lower traces show force. The vertical bars in the upper trace denote the passive downward movement of the arm when pushed, and the corresponding vertical bars in the lower trace denote the passive force exerted by the ligament in response to the push. (a) An example demonstrating that repeated pushes did not cause contraction or changes in stiffness. (b and c) Responses to chemical stimulation with artificial seawater with an elevated concentration of potassium (KASW) of a previously frozen arm piece (b) and a fresh arm piece (c). The arm pieces in b and c were cut from the same arm. The frozen sample did not respond, while the fresh one responded with contraction and stiffness decrease. In this and the following figures, a down-pointing arrow shows the introduction of a chemical, and an up-pointing arrow indicates a wash with artificial seawater.

deflections, corresponding to the downward bars, are the reaction forces to the pushes. The upper trace remained horizontal, which shows that the position of the arm tip remained the same after repeated pushes. The similar height of the upward vertical deflections shows that the stiffness remained almost the same after repeated pushes. When the first push was taken as the control, the stiffness change measured at the second push, applied 100 s after the first, was 0.63% ± 4.16% (average ± SD, $n = 18$). The range was −8% to +8%. The average was not statistically different from 0%, which implied no changes in stiffness (one-sample t-test, $P > 0.05$). After being pushed, the arm tip in most samples sprang back to almost the same position it held before the push. In some samples, however, small plastic deformations remained. Thus the averaged position after a push was a little lower than that before the push. It was −10.2 ± 24.9 μm (average ± SD, $n = 18$) when the initial position was taken as 0 and downward shift was expressed as negative, although the average value was not statistically different from 0 (one-sample t-test, $P > 0.05$). The range was −70 to +25 μm. The quick downward bending and release of the arm piece necessary for stiffness measurement thus did not provoke any active contractions or any subsequent stiffness changes. Based on the results above, the response to chemical stimulation was classified as "no contraction" when the upward excursion of the arm tip was less than +25 μm and as "no change in stiffness" when it was less than ±8%.

For each arm that was dissected, two pieces were removed: one piece was used soon after dissection, and the other was frozen at −20 °C overnight. The frozen sample was thawed and tested. The once-frozen, and thus no longer alive, samples did not respond to KASW. The stiffness and the position of the arm tip remained constant after repeated pushes (Fig. 3b). The fresh, unfrozen samples responded to KASW (Fig. 3c).

Responses to high-potassium seawater

Stimulation with KASW provoked two responses simultaneously. One was stiffness change, and the other was aboral bending due to the shortening of the ligament against the force of gravity. The combination of contraction and the direction of changes in stiffness was variable. The most frequent response was one in which both aboral bending and softening were observed (Fig. 3c and Fig. 4). In Figure 5, the relation between the maximal excursion of the contraction and the maximal stiffness change in a response was plotted for 20 samples stimulated by KASW. Most dots were found in the upper left quadrant, which corresponds to contraction with softening. Contraction was observed in 16 samples, 12 of which also showed softening. Although this seems to support the "spring-with-a-lock" hypothesis, there were marked exceptions. In three cases, contraction was associated not with softening but with stiffening (upper right quadrant in Fig. 5). In the case shown in Figure 6a and in the other two cases, the stiffness increased during contraction and remained so after the wash with seawater. The stiffness never fell below its value before stimulation, although some fluctuations were observed. Figure 6b shows an exceptional response. KASW caused contraction that started 1 min after stimulation. The stiffness measured at that time showed a small increase of 4%, which was classified as no change in stiffness according to our criterion. The contraction appeared to have almost reached a plateau

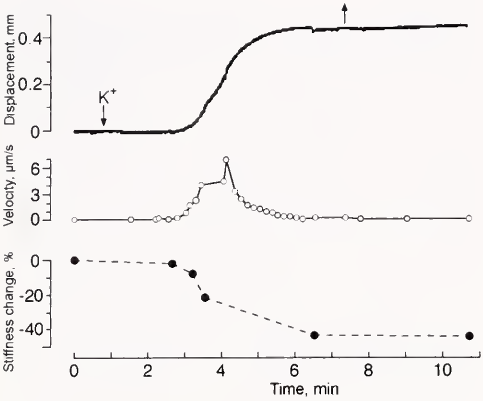

Figure 4. Typical response to artificial seawater with an elevated concentration of potassium (KASW). The upper trace is upward displacement of the arm tip, the middle trace is speed of upward bending of the arm tip, and the lower trace is softening. Both contraction and stiffness decrease were observed.

when KASW was washed out. The wash was followed by a further contraction accompanied by marked stiffening. This response is a clear demonstration that contraction was not associated with tissue softening. The contraction at wash was, however, not observed in other samples. Four arm pieces did not show contraction but did show stiffness changes. Figure 6c is such an example in which the stiffness almost doubled. Figure 6d is an example of tissue softening without contraction. In this example, the arm piece showed, instead of upward contraction, a little downward movement about 1 min after KASW stimulation. This arm piece did not fully spring back after a push by the probe but showed a persistent plastic deformation. Both the downward movement and the plastic deformation were probably produced by flow of the softened tissue due to gravity and to pushes with the probe. All the results above strongly suggested that the contraction and stiffness changes were separate responses, both independently activated by KASW. All the possible combinations—contraction with softening, contraction with stiffening, contraction with no stiffness changes, stiffening with no contraction, and softening with no contraction—were observed.

The most frequent response to KSW was contraction associated with softening, which was observed in 60% of the samples. Close inspection of the time courses of the contractile response and the softening response in these samples also supported the conclusion that these were independent of one another. In Figure 7, the maximum contraction height was taken as 100% and the maximum softening was taken as −100% in a response to KASW. In general, the extent of the softening increased as contraction proceeded. The two were, however, not tightly coupled. In the sample marked by crosses in Figure 7, the first plot showed an evident contraction with a small stiffness increase of 6.7%, though this value was regarded as no stiffness change according to our criterion. This example of contraction preceding softening was contrary to the expectation of the spring-with-a-lock hypothesis. In most responses, softening continued after the contraction had ceased.

The contraction by KASW became evident in about 30 s after the application of stimuli. The average reaction time for contraction was 31.5 ± 7.8 s (±SD, $n = 13$). The contraction curve was S-shaped. The upward bending movement continued for 1.5–10 min, and the raised arm position was maintained after movement stopped. The arm remained raised even after the wash with seawater for more than 1 h (Fig. 3c). The distance the arm tip moved was 40–1140 μm. The average was 384 ± 70 μm (mean ± SD, $n = 16$), which corresponded to an average of about 60 μm of elevation per joint. The bending speed reached a peak value in the middle of contraction (Fig. 4). The peak bending speed was quite variable, at 0.35–43.52 μm/s (6.47 ± 10.18 μm/s, mean ± SD, $n = 17$). The average bending speed ranged from 0.12 to 5.26 μm/s; the mean was 1.35 ± 1.28 μm/s (±SD, $n = 16$), which was about 0.2 μm/s elevation per joint.

Softening of the ligament was observed in 70% of the samples. In a typical example (Fig. 4), stiffness was halved during contraction and remained so after the movement ceased. The stiffness decrease was −35.8% ± 17.8%

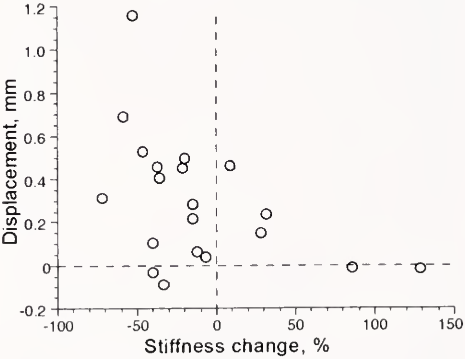

Figure 5. Relation between the maximum stiffness change and the maximum upward displacement of the arm tip in a response to artificial seawater with an elevated concentration of potassium (KASW). The former was plotted on the x-axis and the latter on the y-axis. Positive values of stiffness change denote stiffening, and negative values denote softening; positive values of displacement denote contraction, and negative values denote downward movement due to gravity.

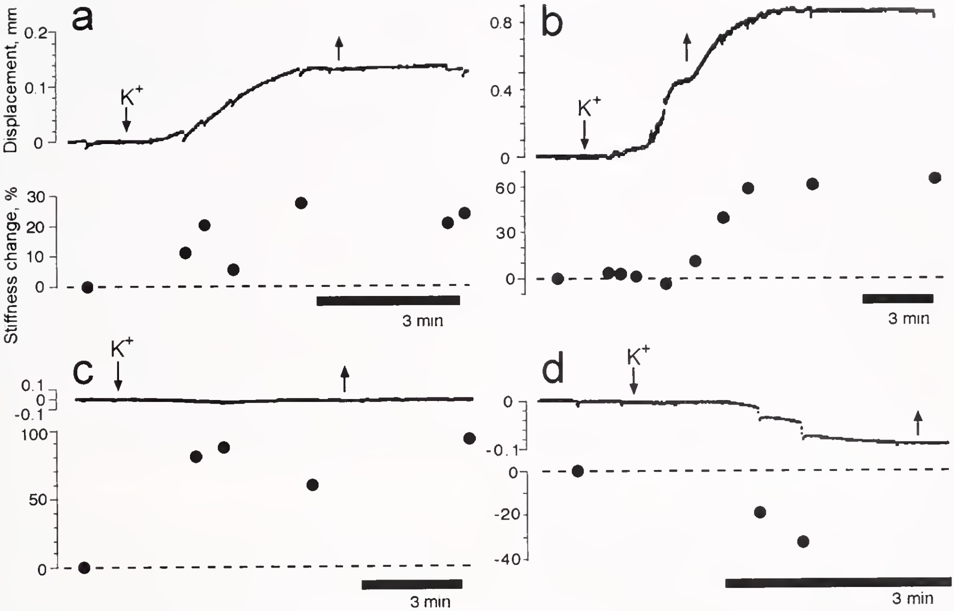

Figure 6. Responses to artificial seawater with an elevated concentration of potassium (KASW). The upper trace shows upward displacement of the arm tip, and the lower trace shows stiffness changes. Various combinations of contractile response and stiffness changes were observed. (a) Contraction associated with stiffening; (b) contraction without stiffness change in KASW, and contraction with stiffening when KASW was washed out; (c) no contraction, but marked stiffening; (d) no contraction, but softening.

(mean ± SD, $n = 14$). The stiffness remained decreased long after the KASW was washed out (Fig. 3c).

Responses to acetylcholine

We treated arm pieces with 10^{-5}–10^{-3} M solutions of acetylcholine in seawater. ACh 10^{-4} M and 10^{-3} M had similar effects, and 10^{-5} M provoked weaker responses. The typical response was contraction associated with softening (Fig. 8a, b). As in KASW, however, various combinations of contraction and stiffness changes were observed. Among 34 samples tested with 10^{-3} M ACh, 23 showed contraction with softening, 7 showed contraction without stiffness changes, and 4 showed softening without contraction. In 10^{-4} M ACh, 3 samples out of 8 showed contraction and softening, 2 showed contraction without stiffness changes, 2 showed no contraction but softening, and 1 neither contracted nor changed stiffness. Here again, contraction was not necessarily associated with tissue softening. It should be noted that the stiffness change was always softening; no stiffening was observed in ACh.

Contraction initiated by 10^{-3} M ACh became evident in

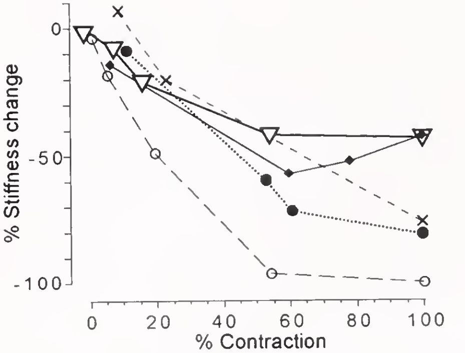

Figure 7. The relative degree of softening plotted against the relative degree of contraction in the samples that showed both softening and contraction to artificial seawater with an elevated concentration of potassium (KASW). Twelve samples showed both softening and contraction, but five examples are given here; the rest show curves similar to one of the curves shown in this figure. The final amount of contraction was taken as 100%, and the final amount of softening was taken as −100%. The time course of softening did not parallel that of contraction.

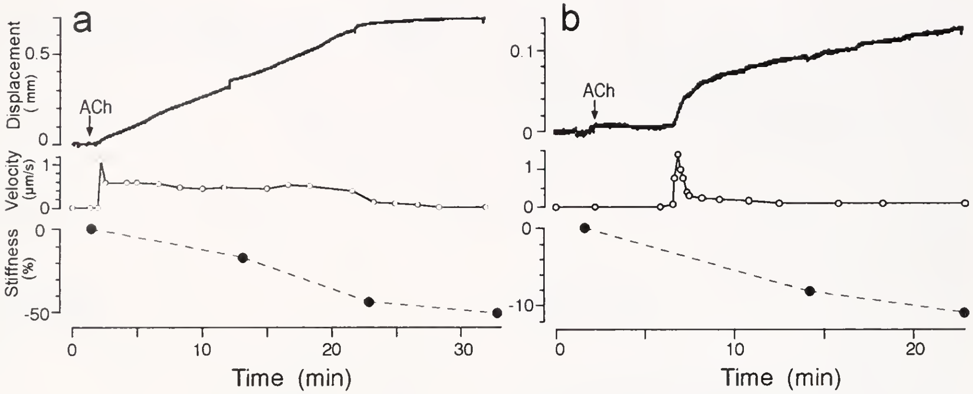

Figure 8. Typical responses to acetylcholine at concentrations of 10^{-3} *M* (a) and 10^{-4} *M* (b). The upper trace shows upward displacement of the arm tip, the middle trace shows speed of upward bending of the arm tip, and the lower trace shows softening. Both contraction and decrease in stiffness were observed.

about 30 s after the application of stimuli. The reaction time for contraction was 28.4 ± 3.4 s (average ± SD, $n = 7$). The bending speed peaked at the beginning, and then the contraction continued with ever-decreasing speed (Fig. 8b). The upward movement continued for more than 15 min. The arm remained raised even after ACh was washed out. After the peak in bending speed, contraction with a steady bending speed was observed for 10–20 min in some cases (see Fig. 8a). The peak bending speed in 10^{-3} *M* ACh was 0.72 µm/s on average (SD = 0.42, $n = 7$, range 0.16–1.23), and the distance moved in 15 min was 259 ± 228 µm (mean ± SD, $n = 8$). The peak bending speed was one order of magnitude less than in KASW (statistically significant difference by *t*-test, $P < 0.01$). Although contraction in ACh was slower than in KASW, it lasted longer, so the distance moved in 15 min reached a value similar to that found in KASW. The peak bending speed occurred at the beginning of contraction in ACh, but in the middle of contraction in KASW. The reaction time to the two chemicals was similar.

Softening of the ligament was observed in 79.4% of the samples treated with 10^{-3} *M* ACh and in 62.5% of the samples treated with 10^{-4} *M* ACh. The stiffness decrease due to 10^{-3} *M* ACh was −28.6% ± 11.7% (mean ± SD, $n = 6$).

Discussion

The simultaneous measurement of isotonic contraction and tissue stiffness revealed that the arm of a stalked crinoid from which arm muscles had been removed simultaneously shortened and changed in stiffness in response to chemical stimulation. Ligaments are undoubtedly responsible for these two mechanical activities, because other soft tissues connecting ossicles, such as nerves and covering thin epidermis, are mechanically quite weak. The mechanical responses are active ones in which living cells are involved, because arm preparations that had been frozen and rethawed never responded. The effectiveness of ACh in evoking these responses suggests the involvement of neural elements. Seawater with an elevated potassium concentration (KASW) possibly exerted its effects through cellular depolarization of neural elements and of some effector cells that are involved in the mechanical responses.

Evidence against the "spring-with-a-lock" hypothesis

The most frequent response was shortening of the arm in association with tissue softening. This result may well be taken as evidence for the "spring-with-a-lock" hypothesis in which the source of contraction is attributed to an extended spring that, after being stretched by the antagonizing muscles, then releases the strain energy stored in the stiffened tissue so that tissue softening causes shortening of the ligaments. This hypothesis predicts that softening must precede shortening. We obtained, however, examples contradicting this prediction. Some arm pieces showed shortening without stiffness changes, and some showed shortening associated with tissue stiffening. The latter was quite contrary to expectations based upon the hypothesis. Even among the examples of shortening with softening, inspection of the time course of the response revealed that shortening sometimes became evident before stiffness decreased. These results clearly showed that contraction did not necessarily require a foregoing softening, thus providing definitive evidence against the spring-with-a-lock hypothesis.

The time course of the shortening speed also suggested that the contraction was not simple elastic recoil. Although the maximum speed occurred in the middle of a contraction in KASW but at the start of contraction in ACh, no changes in stiffness corresponded to this difference. The ACh caused an initial fast contraction followed by a long slow contraction. The speed of the slow contraction was sometimes rather constant, although stiffness changes were observed during this period. This also suggested the independence of contraction and stiffness changes.

The spring-with-a-lock hypothesis was premised on the tight coupling between shortening and decrease in stiffness. Our observations, however, showed that shortening and changes in stiffness are separable. All the possible combinations of the two responses were encountered. The variety of responses, especially the shortening without stiffness changes and the stiffness changes without shortening, provides good evidence that contraction and stiffness changes are separable. The variety of responses also suggests that these two depend on different mechanisms.

Contraction and stiffness changes involve separate mechanisms

The present results are best explained by the presence of some active contractile machinery inside the ligaments. Stiffness control and active shortening may well depend on the same mechanism, as in most animals in which muscles are responsible for posture control, which involves both movement and stiffness changes. Active shortening implies force production, which would increase the resistance to stretch, causing an increase in stiffness during contraction. In the present study, however, most of the responses were contraction with a decrease in stiffness. Therefore, it is unlikely that contraction and stiffness changes share a common mechanism in these arm ligaments.

In a study of the stress-relaxation behavior of the cirral ligament of *Metacrinus rotundus,* we found that the collagenous ligament showed both stiffness changes and contraction (Birenheide *et al.*, 2000). The two responses were separable, although both were under cholinergic control. In the present study, we suggest that the same two responses are also under cholinergic control in arm ligaments.

Our present report provides the first measurement of stiffness changes in the arm ligaments of stalked crinoids. Such changes have already been reported in stalkless crinoids (Birenheide and Motokawa, 1998). The ability to change their passive mechanical properties seems to be a common character of the collagenous ligaments at the articulations of crinoids, since stiffness changes have also been reported in the ligaments of cirri (Wilkie, 1983; Birenheide *et al.*, 2000) and of stalks (Wilkie *et al.*, 1993, 1994). Stiffness changes serve to maintain body posture. They very likely share a common mechanism—connective tissue catch—which is found widely throughout the phylum Echinodermata (Motokawa, 1984; Wilkie, 1996). Although the mutability of the mechanical properties of collagenous connective tissues has been established and the importance of these properties in the supportive function is well appreciated (Motokawa, 1988), the molecular mechanism underlying connective tissue catch is incompletely understood. It seems, however, to involve the cellular secretion of proteins that directly affect the mechanical properties of the extracellular matrix (Tipper *et al.*, 2003).

We have reported shortening and force development in arm joints from which the muscles have been removed in the stalked crinoid *Metacrinus rotundus* and also in the stalkless crinoid *Oxycomanthus japonica* (Birenheide and Motokawa, 1996, 1998). The present study showed that such contractions derive from active contraction of collagenous ligaments. Non-muscular contractions in crinoids are not restricted to the arm joints. In spite of a thorough ultrastructural investigation, we found no muscle cells in the cirral joints, and yet we observed bending movements of these joints of *M. rotundus* in response to cholinergic agonists (Birenheide *et al.*, 2000). The spring-with-a-lock hypothesis is not applicable to cirri if antagonizing muscle bundles are supposed to be the force-producing engine. The coelomic canal has been proposed as a possible source of force production in crinoid arms and cirri (Holland and Grimmer, 1981; Candia Carnevali and Saita, 1985). This idea is not applicable to the present arm preparation from which the coelomic canal has been removed. Because of their mechanical weakness, other soft tissues connecting ossicles, such as the epidermis and brachial nerves, are unlikely to generate contractile forces. Therefore, we conclude that, both in arms and in cirri, the ligaments are responsible for the contraction and probably possess a common mechanism for active force production.

The present study shows that contraction is often associated with softening. Although we employed atypical examples of this as evidence against the tight coupling between contraction and tissue softening, the observation that the most frequent response was contraction associated with softening suggests that there is some coordination between contraction and stiffness changes. The association of contraction with softening is reasonable because softening probably facilitates shortening; otherwise, kinks would be produced. The stiffness of the aboral ligaments is probably also coordinated with contraction of the oral muscles. This may be one reason that the observed responses were variable. The variety of the responses suggests the presence of sophisticated control. A cholinergic system seems to be involved in the coordination between the contraction and the stiffness changes of ligaments.

The largest bending speed observed was 43.5 μm/s. A rough calculation from this value suggests that the maximum shortening speed of the ligament itself is 0.05 l_0/s, where l_0 is the length of the aboral ligament when the arm is straight. This is slower by one order of magnitude than reported for echinoderm muscles (Tsuchiya, 1985). The multi-joint structure of the arms, however, compensates for the slowness, because the speed of arm tip movement possibly increases in proportion to the number of joints.

The present study establishes that the collagenous ligaments of stalked crinoids show active contraction under nervous control. Among the animal kingdom, only crinoids have been documented to have such connective tissue contractions. The force-producing mechanism has yet to be elucidated.

Acknowledgments

This research was supported by a grant-in-aid for scientific research on priority area (A) "Molecular synchronization for design of new materials system" of the Ministry of Education, Science, Sports, and Culture of Japan.

Literature Cited

Birenheide, R., and T. Motokawa. 1994. Morphological basis and mechanics of arm movement in the stalked crinoid *Metacrinus rotundus* (Echinodermata, Crinoidea). *Mar. Biol.* **121:** 273–283.

Birenheide, R., and T. Motokawa. 1996. Contractile connective tissue in crinoids. *Biol. Bull.* **191:** 1–4.

Birenheide, R., and T. Motokawa. 1998. Crinoid ligaments: catch and contractility. Pp. 139–144 in *Echinoderm: San Francisco*, R. Mooi and M. Telford, eds. A. A. Balkema, Rotterdam.

Birenheide, R., K. Yokoyama, and T. Motokawa. 2000. Cirri of the stalked crinoid *Metacrinus rotundus:* neural elements and the effect of cholinergic agonists on mechanical properties. *Proc. R. Soc. Lond. B* **267:** 7–16.

Candia Carnevali, M. D., and A. Saita. 1985. Muscle system organization in echinoderms: II. Microscopic anatomy and functional significance of the muscle-ligament-skeleton system in the arm of comatulids (*Antedon mediterranea*). *J. Morphol.* **185:** 59–74.

Holland, N. D., and J. Grimmer. 1981. Fine structure of the cirri and a possible mechanism for their motility in stalkless crinoids (Echinodermata). *Cell Tissue Res.* **214:** 207–217.

Motokawa, T. 1984. Connective tissue catch in echinoderms. *Biol. Rev.* **59:** 255–270.

Motokawa, T. 1988. Catch connective tissue: a key character for echinoderms' success. Pp. 39–54 in *Echinoderm Biology*, R. D. Burke, P. V. Mladenov, P. Lambert, and R. L. Parsley, eds. A. A. Balkema, Rotterdam.

Tipper, J. P., G. Lyons-Levy, M. A. L. Atkinson, and A. Trotter. 2003. Purification, characterization and cloning of tensilin, the collagen-fibril binding and tissue-stiffening factor from *Cucumaria frondosa* dermis. *Matrix Biol.* **21:** 625–635.

Tsuchiya, T. 1985. The maximum shortening velocity of holothurian muscle and effects of tonicity change on it. *Comp. Biochem. Physiol. A* **81:** 397–401.

Wilkie, I. C. 1983. Nervously mediated change in the mechanical properties of the cirral ligaments of a crinoid. *Mar. Behav. Physiol.* **9:** 229–248.

Wilkie, I. C. 1996. Mutable collagenous tissue: extracellular matrix as mechano-effector. Pp. 61–102 in *Echinoderm Studies*, Vol. 5, M. Jangoux and J. M. Lawrence, eds. A. A. Balkema, Rotterdam.

Wilkie, I. C., R. H. Emson, and C. M. Young. 1993. Smart collagen in sea lilies. *Nature* **366:** 519–520.

Wilkie, I. C., R. H. Emson, and C. M. Young. 1994. Variable tensility of the ligaments in the stalk of a sea-liliy. *Comp. Biochem. Physiol. A* **109:** 633–641.

Reference: *Biol. Bull.* **206:** 13–24. (February 2004)
© 2004 Marine Biological Laboratory

Identification of Juvenile Hormone-Active Alkylphenols in the Lobster *Homarus americanus* and in Marine Sediments

WILLIAM J. BIGGERS[1] AND HANS LAUFER[2,*]

[1] *Department of Biology, Wilkes University, Wilkes-Barre, Pennsylvania 18766; and* [2] *Department of Molecular and Cell Biology, University of Connecticut, Storrs, Connecticut 06269, and the Marine Biological Laboratory, Woods Hole, Massachusetts 02543*

Abstract. We have identified, by gas chromatography/mass spectrometry, four alkylphenols that are present in the hemolymph and tissues of the American lobster *Homarus americanus* and in marine sediments. These alkylphenols are used industrially in antioxidant formulations for plastic and rubber polymer manufacturing, and are similar in structure to a known endocrine disruptor, bisphenol A. The compound 2-*t*-butyl-4-(dimethylbenzyl)phenol was present at concentrations of 0.02 to 1.15 μg/ml in hemolymph and 8.95 to 21.58 μg/g in sediments. A second compound, 2,4-bis-(dimethylbenzyl)phenol, was present at concentrations between 0.07 and 19.78 μg/ml in hemolymph and 138.94 to 224.89 μg/g in sediment, while a third compound, 2,6-bis-(*t*-butyl)-4-(dimethylbenzyl)phenol, was found at concentrations between 0.01 and 13.00 μg/ml in hemolymph, 2.55 and 6.11 μg/g in hepatopancreas, and 47.85 and 74.66 μg/g in sediment. A fourth compound, 2,4-bis-(dimethylbenzyl)-6-*t*-butylphenol, was found at concentrations of 0.20 to 70.71 μg/ml in hemolymph, 23.56 to 26.89 μg/g in hepatopancreas, and 90.68 to 125.58 μg/g in sediment. These compounds, along with bisphenol A, 4-dimethylbenzylphenol, and nonylphenol, display high juvenile hormone activity in bioassays. Alkylphenols at high concentrations are toxic to crustaceans and may contribute significantly to lobster mortality; at lower concentrations, they are likely to have endocrine-disrupting effects.

Introduction

The lobster population in western Long Island Sound has been decimated in recent years, and a variety of factors have been implicated, including elevated temperatures, anoxia, paramoeba infestation, and exposure to pesticides and other chemicals entering the marine environment (Long Island Sound Lobster Health Symposium, 2003). Since crustacean reproduction, development, and metamorphosis are known to be partly regulated by a juvenile hormone, methyl farnesoate (MF) (reviewed by Laufer and Biggers, 2001), we have joined these investigations, asking whether lobsters and marine sediments contain exogenous chemicals with juvenile-hormone activity (JH activity) that may affect the health of these crustaceans and act as endocrine disruptors.

MF is a sesquiterpenoid hormone that is similar in structure to insect juvenile hormones and is secreted by the mandibular organ. Previous investigations in our laboratory indicated that extracts of marine organisms and sediments display JH activity in insect cuticle bioassays (Biggers and Laufer, 1992; Biggers, 1994). Here we report the identification of four alkylphenols that are similar in structure to the endocrine disruptor bisphenol A and are present in sediment samples. We found these alkylphenols to possess high JH activity, and one of them was initially developed as a mosquito insecticide. We also report finding these four alkylphenols in lobster hemolymph and two alkylphenols in hepatopancreas tissue. These results suggest that these chemicals, like bisphenol A and other alkylphenols, may have widespread distribution in the marine environment where, at low concentrations, they may be acting as endocrine disruptors in the lobster, and at higher concentrations,

Received 2 July 2003; accepted 17 November 2003.

[*] To whom correspondence should be addressed. E-mail: laufer@uconn.edu

they may contribute to the high mortalities of lobsters in Long Island Sound and elsewhere.

Materials and Methods

Animals

Mature male and female lobsters, ranging in weight between 300 and 450 g (shorts) were collected from Long Island Sound and from Vineyard Sound, Massachusetts. Long Island Sound animals were kept in recirculating tanks at Storrs, Connecticut, and animals from Vineyard Sound were maintained in running seawater at the Marine Biological Laboratory, Woods Hole, Massachusetts. The animals were fed squid *ad libitum.* Immediately upon arrival, the animals were bled with 5-cc plastic syringes and 23-gauge needles.

Chemicals

The following chemicals were purchased from Sigma-Aldrich: 4-cumylphenol [also known as 4-dimethylbenzylphenol]; 2,4-bis-(dimethylbenzyl)phenol; bisphenol A [also known as 2,2-bis(4-hydroxyphenyl)propane]; nonylphenol-(mixed isomers); the juvenile hormones JH III and JH I; lutein; cholesterol; arachidonic acid; stearic acid; and farnesol. Pyriproxyfen was kindly provided by Dr. William Bowers (University of Arizona), and 2-*t*-butyl-4-(dimethylbenzyl)phenol, 2,6-bis-(*t*-butyl)-4-(dimethylbenzyl)phenol, 2,4-bis-(dimethylbenzyl)-6-*t*-butylphenol, and *trans-trans* methyl farnesoate were synthesized in the laboratory. Acetonitrile, acetone, and hexane used for extractions and in HPLC analysis were purchased from Fisher Chemical and were of HPLC grade.

Extraction of marine sediments

Samples were taken from the top 6–12 in. of marine sediment in the intertidal zones of Vineyard Sound, Massachusetts, and Great Bay, New Jersey. The sediments were filtered through a 1-mm wire sieve to remove large debris, then kept frozen at −20 °C. A 25-g portion (wet weight) of each sediment sample was extracted with 50 ml of acetone, and the yellowish acetone extract was filtered through Whatman #1 filter paper to remove particulates. Five milliliters of the acetone filtrate was evaporated to dryness under nitrogen in glass vials and resuspended in 200 μl of hexane. The resuspended extract (200 μl) was applied to the top of a PrepSep silica solid-phase extraction column (Fisher Scientific) that had been pre-equilibrated with 10 ml of hexane. The columns were eluted sequentially with solvents of increasing polarity: 3 ml hexane; 3 ml hexane/20% ethyl ether; and finally, 3 ml 100% ethyl ether. The 100% ethyl ether eluate, which was yellow and showed high JH activity, was stored at −20 °C. For GC/MS analysis, 1 ml of the ethyl ether eluate was evaporated to dryness under nitrogen, then resuspended in 200 μl of hexane in small amber vials that were stored at −20 °C before analysis. By this method, using chemical standards, extraction and recovery efficiencies for the four phenols were 95% for 2-*t*-butyl-4-(dimethylbenzyl)phenol and 2,6-bis-(*t*-butyl)-4-(dimethylbenzyl)phenol, 47% for 2,4-bis-(dimethylbenzyl)-phenol, and 50% for 2,4-bis-(dimethylbenzyl)-6-*t*-butylphenol.

Extraction of hemolymph and hepatopancreas

For each hemolymph sample, 2 ml was added into Pyrex culture tubes (prebaked at 250 °C before use) containing 2 ml of cold 4% NaCl and 2 ml of acetonitrile, and then kept frozen at −20 °C. Samples were extracted with 2 ml of hexane by vortexing for 5 min. The tubes were centrifuged at 600 × *g* for 30 min, and 1.5 ml of the hexane phase was pipetted off and evaporated with a stream of nitrogen to 150 μl in amber glass vials. Before analysis by GC/MS, the hexane extracts were stored at −20 °C.

Hepatopancreas from two lobsters was rinsed in 4% NaCl and weighed; 2 g of the tissue was homogenized in 4 ml of cold acetonitrile and extracted with 4 ml of 4% NaCl and 2 ml of hexane. The hexane phases were then processed as described for the hemolymph samples before analysis by GC/MS. By this method, using standards, extraction and recovery efficiencies for the four phenols were 90% for 2-*t*-butyl-4-(dimethylbenzyl)phenol and 2,6-bis-(*t*-butyl)-4-(dimethylbenzyl)phenol, and 45% for 2,4-bis-(dimethylbenzyl)phenol and 2,4-bis-(dimethylbenzyl)-6-*t*-butylphenol.

Gas chromatography/mass spectrometry analysis

The lobster extracts and marine sediments were analyzed by gas chromatography/mass spectrometry using a Hewlett-Packard HP 5890 GC/5970 MSD GC/MS equipped with a 12.5-m, 0.20-mm-diameter column of cross-linked dimethylsilicone with film thickness of 0.33 μm. The operating conditions for GC were an initial temperature of 35 °C for 2 min, followed by a 15 °C/min ramp to 270 °C, then a 10-min hold at 270 °C, for a total run time of 27.67 min. Operating conditions for MS analysis were set to detect ion masses of 50 to 500 MW, by electron impact ionization using the scan mode. Individual compounds were identified by comparing their mass spectra with published library spectra. Identification of the four phenolic compounds and diisooctylphthalate was confirmed by comparison of mass spectra and retention times with those of chemical standards that were either purchased, as were 2,4-bis-(dimethylbenzyl)phenol and diisooctylphthalate, or synthesized in the laboratory, as was 2-*t*-butyl-4-(dimethylbenzyl)phenol, 2,6-bis-(*t*-butyl)-4-(dimethylbenzyl)phenol, and 2,4-bis-(dimethylbenzyl)-6-*t*-butylphenol described below. The phenols were quantified by integration of peaks and comparison of peak areas with known amounts of authentic standards.

Chemical synthesis

The compounds 2-*t*-butyl-4-(dimethylbenzyl)phenol and 2,6-bis-(*t*-butyl)-4-(dimethylbenzyl)phenol were prepared by a Friedel-Crafts alkylation reaction. For synthesis, 15 g of 4-cumylphenol was dissolved in 75 ml of *t*-butylchloride in a 125-ml Ehrlenmeyer flask containing a stir bar. The reaction was started by addition of 100 mg of $FeCl_3$-$5H_20$ as catalyst with constant stirring at room temperature. The reaction was carried out in a fume hood to vent the evolved HCl gas. After 24 h, the reaction was stopped by transferring the reaction mixture to a 500-ml Ehrlenmeyer flask and adding 200 ml of distilled water. The phenols were extracted with 100 ml of hexane, and isolated and purified to 99% purity (determined by GC/MS) from the reaction mixture by normal-phase HPLC using a silica column (Varian microsorb, 250 mm, 100 A°) and hexane/6% acetone as running solvent.

The monophenol 2,4-bis-(dimethylbenzyl)-6-*t*-butylphenol was prepared using a Friedel-Crafts alkylation reaction, in the same way as were the other phenols, except that 15 g of 2,4-bis-(dimethylbenzyl)phenol was used as the starting material for synthesis, and the phenol product was purified by normal-phase HPLC using a running solvent of hexane/1% ethyl ether.

Bioassay for juvenile hormone activity

The phenolic compounds were assessed for JH activity using a rapid and sensitive assay based on their effects on the settlement and metamorphosis of larvae of the polychaete *Capitella* (Biggers and Laufer, 1996). The results of this bioassay are comparable to those of the *Galleria* JH bioassay: in both bioassays the test chemicals showed similar patterns of variation in JH activity. In this bioassay, no false positives or false negatives have been found for the compounds tested. Test chemicals were dissolved in 100% ethanol to give stock solutions of 0.1, 1, 10, and 100 μM, and aliquots of up to 100 μl of the stock solutions were added to 60-mm glass petri dishes each containing 10 ml of artificial seawater (Utikem, Co.), salinity 30 ppt, and 10 swimming 2-day-old metatrochophore larvae. Controls received up to 100 μl of ethanol. Dishes were swirled to disperse the test chemicals. Each concentration was tested in triplicate for every bioassay, and two bioassays were run (total dishes = 6, total number of larvae = 60) for each concentration tested. Settlement and metamorphosis of larvae was monitored using a stereobinocular microscope. After 1 h, the number of larvae that had settled and metamorphosed was recorded. Data are reported as EC_{50} values for each chemical, at the final concentration that induces 50% of the larvae to settle and metamorphose in 1 h.

Results

Alkylphenols in lobster hemolymph and hepatopancreas

The analysis of the hexane extracts of 14 samples of lobster hemolymph by GC/MS indicated the presence of four alkylphenols: 2-*t*-butyl-4-(dimethylbenzyl)phenol (molecular weight 268); 2,6-bis-(*t*-butyl)-4-(dimethylbenzyl)-phenol (molecular weight 324, CAS no. 34624-81-2), also named 2,6-*di-tert*-butyl-4-cumylphenol; 2,4-bis-(dimethylbenzyl)phenol (molecular weight 330, CAS no. 2772-45-4), also named 2,4-dicumylphenol; and 2,4-bis-(dimethylbenzyl)-6-*t*-butylphenol (molecular weight 386). The mass spectra for these chemicals matched those of the published library (Wiley) mass spectral database with a quality fit of more than 90%. Further confirming the identity of these compounds, the retention times of purchased or chemically synthesized standards also gave the same retention times and mass spectra as those of the compounds identified in the hemolymph (Figs. 1, 2, 3).

The levels of these four alkylphenols varied between lobsters. The compound 2-*t*-butyl-4-(dimethylbenzyl)phenol was found in 13 of the 14 lobsters analyzed, at concentrations ranging from 0.02 to 1.15 μg/ml of hemolymph, giving an average of 0.46 ± 0.11 μg/ml (mean ± standard error of the mean). The compound 2,6-bis-(*t*-butyl)-4-(dimethylbenzyl)phenol was present in the hemolymph of 11 of the 14 lobsters, at concentrations ranging from 0.01 to 13.00 μg/ml of hemolymph, with an average of 1.89 ± 1.14 μg/ml. The compound 2,4-bis-(dimethylbenzyl)phenol was detected in the hemolymph of all 14 lobsters analyzed, at concentrations ranging from 0.07 to 19.78 μg/ml of hemolymph, giving an average of 4.03 ± 1.52 μg/ml. The compound 2,4-bis-(dimethylbenzyl)-6-*t*-butylphenol was found in the hemolymph of 11 of the 14 lobsters, at concentrations ranging from 0.20 to 70.71 μg/ml of hemolymph, giving an average of 10.98 ± 6.414 μg/ml.

The relative amounts of these four phenols varied greatly between the two localities from which the lobsters were taken (Table 1). Lobsters from Long Island Sound showed much higher average concentrations of 2,6-bis-(*t*-butyl)-4-(dimethylbenzyl)phenol, 2,4-bis-(dimethylbenzyl)phenol, and 2,4-bis-(dimethylbenzyl)-6-*t*-butylphenol than those from Vineyard Sound, whereas lobsters from Vineyard Sound had much higher average concentrations of 2-*t*-butyl-4-(dimethylbenzyl)phenol. Interestingly, the phthalate ester diisooctylphthalate was also identified in lobster hemolymph, but only in the seven lobsters analyzed from Vineyard Sound, with concentrations ranging from 0.04 to 0.39 μg/ml of hemolymph.

Two of the phenols were also found in extracts made from the hepatopancreas of two additional lobsters. The concentrations of 2,6-bis-(*t*-butyl)-4-(dimethylbenzyl)phenol in the two hepatopancreas samples were found to be 2.55 and 6.11 μg/g of tissue, and concentrations of 2,4-bis-

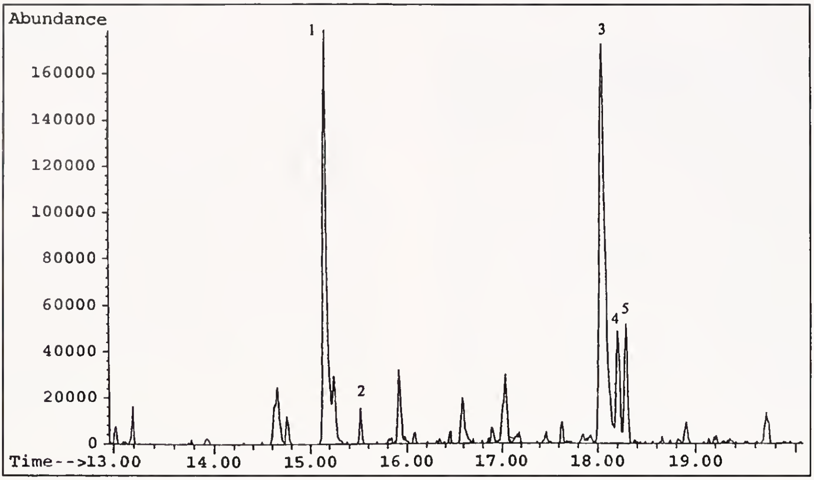

Figure 1. Gas chromatogram of a lobster hemolymph sample from Martha's Vineyard showing relative retention times of 2-*t*-butyl-4-(dimethylbenzyl)phenol, MW 268 (peak 1); 2,6-bis-(*t*-butyl)-4-(dimethylbenzyl)-phenol, MW 324 (peak 2); 2,4-bis-(dimethylbenzyl)phenol, MW 330 (peak 3); 2,4-bis(dimethylbenzyl)-6-*t*-butylphenol, MW 386 (peak 4); and diisooctylphthalate, MW 390 (peak 5).

(dimethylbenzyl)-6-*t*-butylphenol were 23.56 and 26.89 μg/g.

Alkylphenols in marine sediments

Analysis by GC/MS of ethyl ether fractions from silica columns, derived from a Vineyard Sound sediment sample and a Great Bay sediment sample, both of which showed high JH activity in the *Capitella* bioassays (data not shown), indicated the presence of the same four alkylphenols found in the lobster: 2-*t*-butyl-4-(dimethylbenzyl)phenol; 2,6-bis-(*t*-butyl)-4-(dimethylbenzyl)phenol, 2,4-bis-(dimethylbenzyl)phenol, and 2,4-bis-(dimethylbenzyl)-6-*t*-butylphenol (molecular weight 386).

The concentrations determined for these alkylphenols differed between the two sediment samples analyzed (Table 2). Concentrations of all four phenols were higher in the sediment sample from Great Bay, New Jersey (range from 21.58 to 251.01 μg/g of sediment) than in the sediment sample from Vineyard Sound, Massachusetts (range between 8.95 and 181.20 μg/g of sediment). Of considerable interest is the finding that both samples showed the same relative profiles, with 2,4-bis-(dimethylbenzyl)-6-*t*-butylphenol being found in the highest concentration of the four phenols, at 181.20 to 251.01 μg/g of sediment; followed by 2,4-bis-(dimethylbenzyl)phenol at concentrations ranging from 138.94 to 224.89 μg/g of sediment; followed by 2,6-bis-(*t*-butyl)-4-(dimethylbenzyl)phenol ranging in concentration from 49.47 to 77.89 μg/g; and with 2-*t*-butyl-4-(dimethylbenzyl)phenol being the lowest at 8.95 to 21.58 μg/g.

JH activity of alkylphenols

One of the phenols identified, 2,6-bis-(*t*-butyl)-4-(dimethylbenzyl)phenol, was previously developed as a juvenile-hormone mimic and mosquito insecticide (MON-0585) by the Monsanto Chemical Corporation (Sacher, 1971; Jakob and Schoof, 1972), so it was of great interest to examine these phenols for juvenile-hormone activity. Results of the *Capitella* bioassay showed that the MON-0585 compound had very high JH activity (EC_{50} at 0.5 μM) compared with MF, JH I, JH III, and the JH analog pyriproxyfen, which was also developed as an insecticide (Table 3). The other three alkylphenols identified also exhibited very high JH activity. Since these compounds share a high structural homology with the known xenoestrogens bisphenol A and 4-cumylphenol (Fig. 4), these latter chemicals were also tested for JH activity. Bisphenol A showed very high JH activity (EC_{50} of 0.05 μM), whereas 4-cumylphenol showed high activity (EC_{50} of 3 μM). Mixed isomers of nonylphenol, a well-known alkylphenol, also showed high JH activity (EC_{50} of 1 μM) (Table 3).

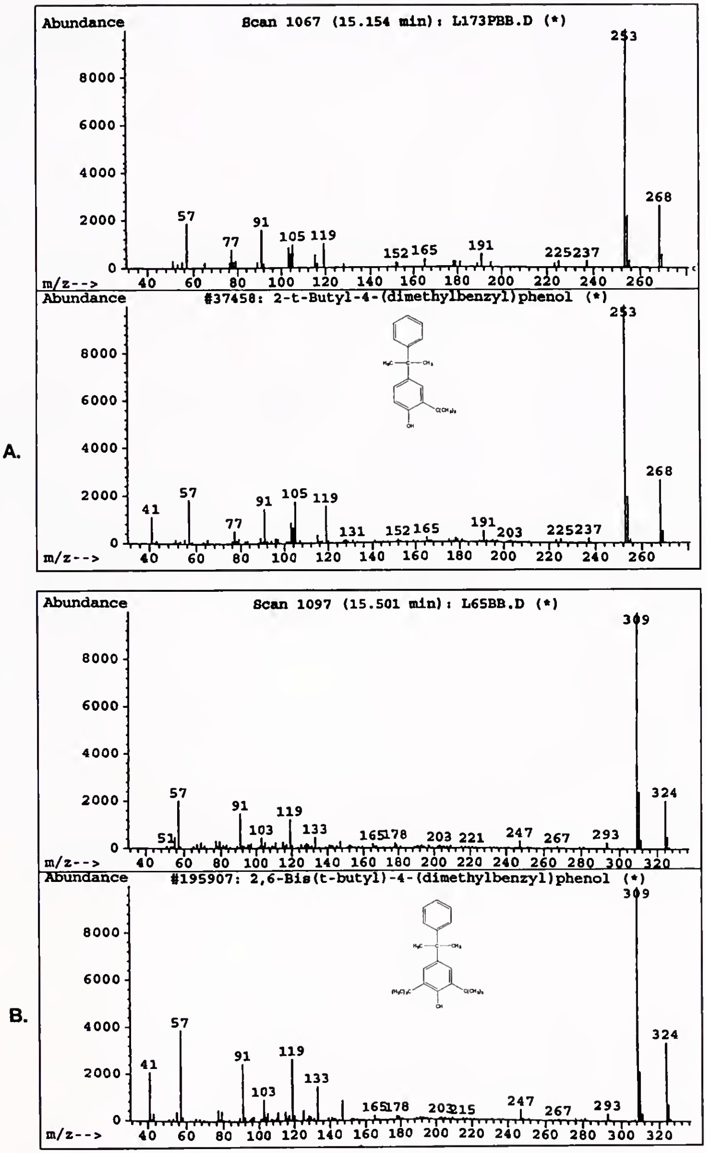

Figure 2. (A) 2-*t*-Butyl-4-(dimethylbenzyl)phenol. Mass spectra from lobster hemolymph (upper) and from reference library database, along with structure (lower) of 2-*t*-butyl-4-(dimethylbenzyl)phenol (molecular weight 286). (B) 2,6-Bis-(*t*-butyl)-4-(dimethylbenzyl)phenol. Mass spectra from lobster hemolymph (upper) and from reference library database, along with structure (lower) of 2,6-bis-(*t*-butyl)-4-(dimethylbenzyl)phenol (molecular weight 324).

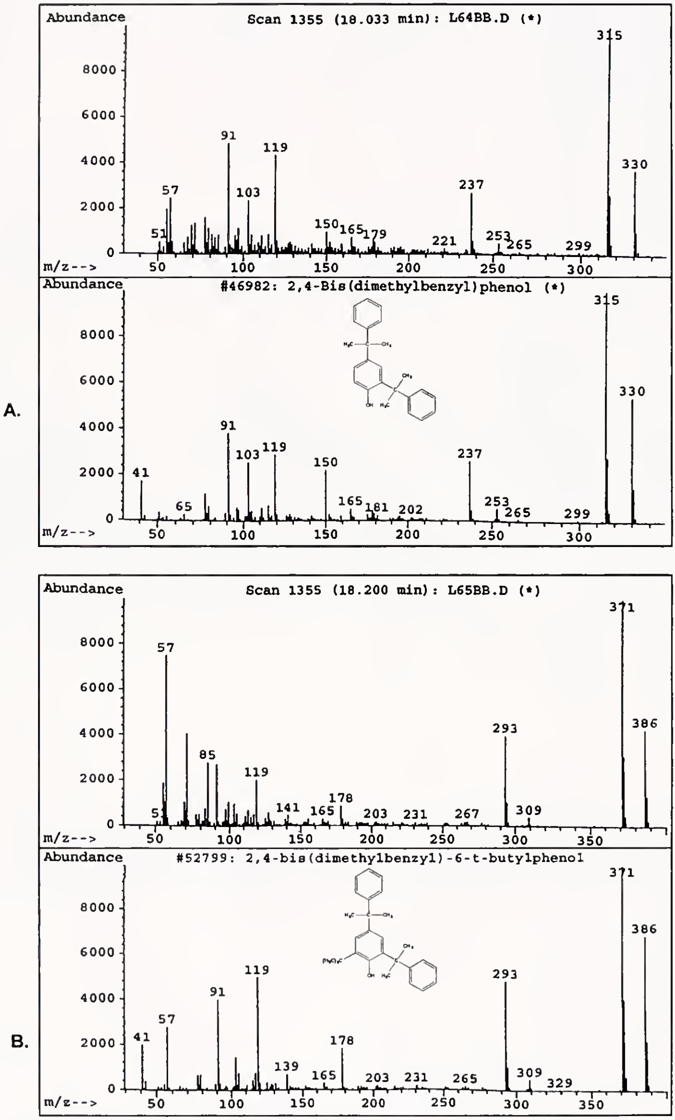

Figure 3. (A) 2,4-Bis-(dimethylbenzyl)phenol. Mass spectra from lobster hemolymph (upper) and from reference library database, along with structure (lower) of 2,4-bis-(dimethylbenzyl)phenol (molecular weight 330). (B) 2,4-Bis-(dimethylbenzyl)-6-*t*-butylphenol. Mass spectra from lobster hemolymph (upper) and from reference library database, along with structure (lower) of 2,4-bis-(dimethylbenzyl)-6-*t*-butylphenol (molecular weight 386).

Table 1

Relative concentrations of alkylphenols in hemolymph from lobsters collected from Long Island Sound (LIS) and Vineyard Sound (VS)

	Average hemolymph concentration (μg/ml) ± SEM		
Alkylphenol	LIS	VS	Combined (LIS + VS)
2-*t*-butyl-4-(dimethylbenzyl)phenol	0.10 ± 0.06	0.83 ± 0.07	0.46 ± 0.11
2,6-bis-(*t*-butyl)-4-(dimethylbenzyl)phenol	3.76 ± 2.11	0.03 ± 0.01	1.89 ± 1.14
2,4-bis-(dimethylbenzyl)phenol	5.17 ± 3.05	2.90 ± 0.55	4.03 ± 1.52
2,4-bis-(dimethylbenzyl)-6-*t*-butylphenol	21.50 ± 11.89	0.45 ± 0.09	10.98 ± 6.41

SEM: standard error of the mean.
$n = 7$ for each mean for LIS and VS; $n = 14$ for combined animals.

Discussion

Our analyses by GC/MS indicate the presence of alkylphenols in 14 samples of lobster hemolymph, 2 samples of hepatopancreas tissue, and two samples of marine sediment. Alkylphenols are used primarily in the production of alkylphenol ethoxylates (APEs), which are found in industrial and household detergents, surfactants, paints, and wetting agents, and which have applications in wood pulping, textile manufacture, plastics manufacture, and petroleum recovery, among other uses (Naylor *et al.*, 1992). Besides their use to produce APEs, alkylphenols are also used in the production of phenolic resins, as antioxidant stabilizers for plastics and polymers, and as curing agents (Ying *et al.*, 2002).

An estimated 500 million pounds of alkylphenols are used annually (Zintek *et al.*, 2003), and an estimated 500,000 tons of APEs are produced annually (Naylor *et al.*, 1992; Ying *et al.*, 2002). Environmental contamination by these chemicals and their breakdown products in rivers, oceans, and sediments is well known and widespread (Hale *et al.*, 2000). Of the 500,000 tons of APEs produced, about 60 percent are estimated to end up in the aquatic environment, as these chemicals and their breakdown products (which are alkylphenols) are released from wastewater outfalls or directly into the environment (Renner, 1997; Ying *et al.*, 2002). Alkylphenols have been detected in the water, in sediments, and in fish tissues (Lye *et al.*, 1999; van Heemst *et al.*, 1999); in sediments, levels have been reported to be as high as 70 μg/g in the United States (Ying *et al.*, 2002).

The alkylphenols identified in this report are similar in structure to bisphenol A (BPA), a well-known endocrine disruptor (Fig. 4). BPA is utilized primarily in the production of polycarbonate plastics. It is also a major antioxidant component of the epoxy resins used to line food cans and pipes, and is used in dental sealants (Staples *et al.*, 1998). Over 200,000 tons of BPA are produced annually by Japan

Table 2

Relative concentrations of alkylphenols in marine sediments from Vineyard Sound, Massachusetts (VS) and Great Bay, New Jersey (GB)

	Concentration (μg/gm sediment)	
Alkylphenol	VS	GB
2-*t*-butyl-4-(dimethylbenzyl)phenol	8.95	21.58
2,6-bis-(*t*-butyl)-4-(dimethylbenzyl)phenol	49.47	77.89
2,4-bis-(dimethylbenzyl)phenol	138.94	224.89
2,4-bis-(dimethylbenzyl)-6-*t*-butylphenol	181.20	251.05

Data shown is for one sediment sample from VS and one from GB.

Table 3

Juvenile hormone activity of alkylphenols compared with activity of known juvenile hormones, using a Capitella *settlement and metamorphosis bioassay*

Chemical tested	EC$_{50}$ (μM)
Juvenile hormones	
JH I	25
JH III	3
trans, trans-methyl farnesoate (crustacean juvenile hormone)	1
pyriproxyfen (JH-mimic)	8
Alkylphenols	
2-*t*-butyl-4-(dimethylbenzyl)phenol	1
2,4-bis-(dimethylbenzyl)phenol	2
2,6-bis-(*t*-butyl)-4-(dimethylbenzyl)phenol (JH-mimic MON-0585)	0.5
2,4-bis-(dimethylbenzyl)-6-*t*-butylphenol	1
4-cumylphenol	3
bisphenol A	0.05
nonylphenol (mixed isomers)	1
Other chemicals tested	
farnesol	40
arachidonic acid	70
stearic acid	410
cholesterol	NA
lutein	NA

NA: not active at highest concentration tested (1000 μM).

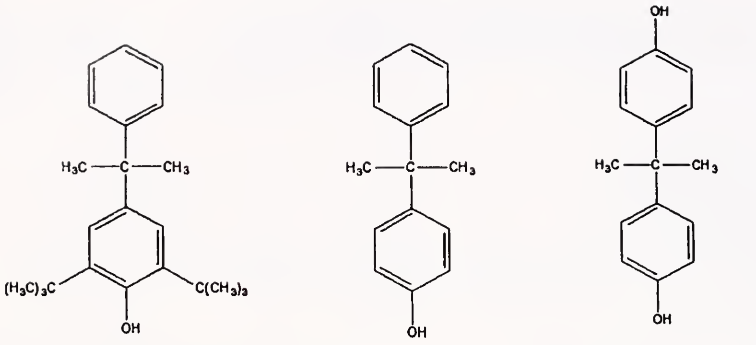

A. 2,6-bis-(t-butyl)-4-(dimethylbenzyl) phenol (MON-0585)

B. 4-cumylphenol

C. Bisphenol A

Figure 4. Comparison of chemical structures of 2,6-bis-(*t*-butyl)-4-(dimethylbenzyl)phenol, 4-dimethylbenzylphenol, and bisphenol A. (A) Chemical structure of the juvenile hormone mimic and mosquito insecticide MON-0585 (same as 2,6-bis-(*t*-butyl)-4-(dimethylbenzyl)phenol). (B) Chemical structure of 4-cumylphenol. (C) Chemical structure of the known endocrine disruptor bisphenol A.

alone (Kamiura *et al.*, 1997), and environmental contamination by this chemical has in recent years been of major public concern. The endocrine-disrupting effects of BPA have been demonstrated to alter the reproductive physiology and development of mammals (Stoker *et al.*, 1999; Takao *et al.*, 1999), fish, and invertebrates—including molting of the insect *Chironomus riparius* (Watts *et al.*, 2001; Segner *et al.*, 2003). BPA can leach from food cans and plastic bottles into foods and beverages and from there into the human digestive system; it subsequently travels through sewage treatment plants and eventually into river systems and oceans (Staples *et al.*, 1998; Fromme *et al.*, 2002). Furthermore, the plastic-particle waste that is prevalent in the oceans can also directly leach BPA into the environment (Sajiki and Yonekubo, 2003). BPA contamination in sediments is widespread; for example, levels have been reported as 0.05 μg/g dry weight in Ulsan Bay, Korea (Khim *et al.*, 2001), in Onsan Bay, Korea; as 0.20 μg/g dry weight (Koh *et al.*, 2002); and as 0.19 μg/g in Germany (Fromme *et al.*, 2002).

The four alkylphenols we have identified in lobsters and marine sediments are used together in antioxidant blend formulations for manufacturing rubber and plastic polymers. A patent by Russell *et al.* (2002) states that these phenols are found in the Wingstay C and Polystay C antioxidant formulations used in tire manufacturing by the Goodyear Tire and Rubber Co. Similarly, a patent by Messina *et al.* (1982) states that these phenols are added as stabilizers for organic polymers including rubbers and plastics. Other antioxidant applications include their use in pesticide formulations and in therapeutics (Smith, 2002). These phenolic antioxidants therefore appear to be widely employed in a fashion similar to BPA.

2,4-bis-(dimethylbenzyl)phenol

One alkylphenol we found in lobster hemolymph and marine sediments, 2,4-bis-(dimethylbenzyl)phenol, is sold under the tradename 2,4-dicumylphenol, or 2,4-DCP. This reagent is used in antioxidant mixtures (Messina *et al.*, 1982; Russell *et al.*, 2002) as previously mentioned, and appears to also have a use in surfactant formulations. This chemical is also released into the environment upon hydrolysis of the antioxidant plasticizer bis-(2,4-dicumylphenyl)pentaerythritol diphosphite. The use of this plasticizer in food containers is regulated by the food industry (Scientific Committee on Food, 2001). The 2,4-DCP compound is close in structure to that of 4-cumylphenol, another industrial alkylphenol (Fig. 4). Hale *et al.* (2000) reported levels of 4-cumylphenol as high as 70 μg/g of sediment in sediments near wastewater outfalls in the United States. To our knowledge, pollution by 2,4-bis-(dimethylbenzyl)phenol in sediments or aquatic life has not been reported. However, we found this phenol in sediments from Vineyard Sound at a concentration of 138.94 μg/g (wet weight) and at higher concentrations in Great Bay, New Jersey, at 224.89 μg/g, which is close to the concentration reported for 4-cumylphenol by Hale *et al.* (2000).

2,6-bis-(t-butyl)-4-(dimethylbenzyl)phenol

Concentrations of 2,6-bis-(*t*-butyl)-4-(dimethylbenzyl)-phenol were higher in lobsters taken from Long Island Sound than in those from Vineyard Sound, and this phenol was also found in sediment samples from the two locations. As previously mentioned, Monsanto developed this compound as a juvenile hormone mimic, named MON-0585, for application as a mosquito insecticide (Sacher, 1971; Jakob and Schoof, 1972); however, it was supposedly never brought to commercial use (Schaefer *et al.*, 1974). Like other alkylphenols and BPA, this one has also gained industrial use as an antioxidant in polymer manufacture (Hanauye *et al.*, 1976; Messina *et al.*, 1982; Russell *et al.*, 2002). Environmental contamination by this chemical has presumably not been documented before; however, it has been found in propolis, which is produced by bees and derived from the resins of tree bark and leaves (Hegazi and El Hady, 2002).

2-t-butyl-4-(dimethylbenzyl)phenol and 2,4-bis-(dimethylbenzyl)-6-t-butylphenol

The compounds 2-*t*-butyl-4-(dimethylbenzyl)phenol and 2,4-bis-(dimethylbenzyl)-6-*t*-butylphenol were both found in lobster hemolymph and marine sediments, and are used industrially in antioxidant blends for the manufacturing of rubber and other polymers (Messina *et al.*, 1982; Russell *et al.*, 2002). Interestingly, these phenols, along with 2,4-bis-(dimethylbenzyl)phenol, were found to be cyclooxgenase inhibitors that occur naturally in peat (Russell *et al.*, 2002). Under the tradename isobutylenated methylstyrenated phenol, the 2,4-bis-(dimethylbenzyl)-6-*t*-butylphenol compound is listed as having a high production volume (more than a million pounds produced per year) by the U.S. Environmental Protection Agency in its High Production Volume Challenge Program, which encourages manufacturers to investigate the toxicity of these chemicals (U.S. EPA, 2002). This compound has also been reported in sediments contaminated with coal tar sediments (Zeng and Hong, 2002). The 2-*t*-butyl-4-(dimethylbenzyl)phenol compound, however, has not been reported as a contaminant until now.

Probable sources of the alklphenols and likelihood of the presence of other phenols

Given that these identified alkylphenols are used in industrial antioxidant formulations similar to those of BPA, and that alkylphenol and BPA contamination is well known and widespread, it is likely that the source of these identified phenols is alkylphenol contamination originating from wastewater outfalls or released directly into the environment; these are the sources that have been identified for other alkylphenols and BPA (Ying *et al.*, 2002). Surface runoff from heavily traveled roadways containing tire residue may be a contributing source of these chemicals. It is to be noted, however, that three of these compounds were also found naturally in peat bog material (Russell *et al.*, 2002), indicating that they may be residues derived from breakdown of plant material. More research is needed to determine the sources of these chemicals. It should also be emphasized that the nonpolar extraction method employed, using hexane, may not be suitable for the extraction of some of the more polar phenols, such as BPA and 4-dimethylbenzylphenol, which may therefore also be present.

In support of the view that environmental contamination is a source for alkylphenols, the plasticizer diisooctylphthalate was also found in fairly high concentrations in the hemolymph of 7 of the 14 lobsters examined, indicating these lobsters indeed had exposure to plasticizers. Control experiments done in our laboratory showed that the phenols and diisooctylphthalate found were not derived from laboratory contamination by soap, glassware, pipettes, or syringes, and were not from the GC columns since control extractions did not produce these chemicals. It therefore appears that these alkylphenols, like other alkylphenols and BPA, result from environmental contamination. The relative levels of these phenols in the lobsters and sediments differed at different locations, and this presumably reflects different amounts and different formulations of alkylphenols used in different geographic areas. Alkylphenols may also have originated from nonlocal sources and been carried by currents.

Effects of alkylphenols on crustaceans

What effect these compounds have on lobsters is currently being investigated in our laboratory. Given that these phenols are similar in structure to BPA and show high JH activity in bioassays, it is likely that they have serious toxic and endocrine-disrupting effects. The high toxicity of alkyphenols to aquatic life has recently been documented by the U.S. Environmental Protection Agency, as has the fact that these chemicals persist in the environment, including sediments (U.S. EPA, 2003). Indeed, toxicity studies with 2,6-bis-(*t*-butyl)-4-(dimethylbenzyl)phenol (MON-0585) have shown that this compound does affect nontarget crustaceans (reviewed by Williams and Duke, 1979). In experiments by Costlow (1977), megalopa larvae of the blue crab *Callinectes sapidus* were all killed in water containing 10 ppm MON-0585, and 60% were killed in 1 ppm MON-0585. Sublethal behavioral effects of MON-0585 on the swimming speed and phototaxis of larvae of the crab *Rhithropanopeus harrisii* have also been reported (Forward and Costlow, 1976) and attributed to the effects of JH mimics on increased respiration (Slama and Kryspin, 1979). Thus lobster larval development and metamorphosis are likely to be affected by this compound at critical concentrations. The other three phenols found probably also have effects on lobster, since they also exhibit high JH activity and are structurally related to MON-0585 and BPA. For example, 4-nonylphenol is acutely toxic to lobsters, with an LC_{50} in seawater reported as 0.2 ppm (0.2 μg/ml) (Cox, 1996), and has been found to affect the development of other crustaceans, including barnacles, in which it inhibits settlement and induces synthesis of vitellin-like proteins (Billinghurst *et al.*, 1998, 2000). In our quantitative determinations, we found levels of 2,6-bis-(*t*-butyl)-4-(dimethylbenzyl)phenol (MON-0585) in the hemolymph of lobsters as high as 13 ppm, which Costlow (1977) found to be a lethal external concentration for crab larvae. The evidence thus indicates that these phenols may be contributing significantly to the lobster deaths seen in Long Island Sound, particularly under stressful environmental conditions such as high temperatures and hypoxia. Since JH mimics such as MON-0585 can increase respiration in insects (Slama and Kryspin, 1979) and possibly crustaceans (Forward and Costlow, 1976), these phenols may make the lobsters more susceptible to stress at low levels of oxygen. Furthermore, MON-0585 has been found to inhibit cuticle arylation and hardening in mosquitoes (Zomer and Lipke, 1981; Semensi and Sugumaran, 1986). We speculate that this compound may also interfere with cuticle formation and hardening in lobsters, making them more susceptible to chitinolytic microorganisms and shell disease. This disease has become increasingly prevalent in lobsters in recent years (Castro and Angell, 2000).

Because MON-0585 was developed as a juvenile hormone mimic, it is not surprising that other structurally related alkylphenols also possess JH activity: all four alkylphenols exhibited such activity in the *Capitella* bioassay when tested at concentrations found in the hemolymph (Tables 2, 3), raising the possibility that these alkylphenols may have JH-like effects on the lobster. Because reproduction, development, and metamorphosis in crustaceans are partly regulated by methyl farnesoate, a compound with juvenile hormone activity, the alkylphenols we investigated may function as endocrine disruptors in the lobster at low concentrations. Exogenous application of JH analogs can perturb normal metamorphosis and molting (reviewed by Laufer and Biggers, 2001). Like JH and its analogs, the JH-active alkylphenols may act through membrane-bound, intracellular, and nuclear receptors to bring about changes in morphogenesis and stimulation of vitellogenesis through vitellogenin gene induction and increased vitellogenin uptake (Engelmann, 1983; Sehnal, 1983; Wyatt, 1991; Davey and Gordon, 1996; Jones and Sharp, 1997). As evidence for this mechanism of action, both 4-nonylphenol and BPA have been found to induce vitellogenesis in vertebrates (Jones *et al.*, 2000).

To our knowledge, our results are the first to demonstrate that xenoestrogens such as BPA and nonylphenol have JH activity, indicating a possible relationship between estrogenicity and juvenile hormone activity, and the further possibility that estrogens and juvenile hormones share similar mechanisms of action.

Possible bioaccumulation and health effects of the identified alkylphenols

The presence of phenolic compounds in marine sediments suggests that lobsters may acquire them through the food chain as found for other polyaromatic hydrocarbons (Pruell *et al.*, 2000). Interestingly, in the report by Hale *et al.* (2000), levels of 4-cumylphenol in sediments was found to be much higher than those of 4-nonylphenol (70,000 μg/kg compared with 11,000 μg/kg), even though 80% of the alkylphenols used in formulations are nonylphenol ethoxylates (Ying *et al.*, 2002). This suggests that polyaromatic alkylphenols are more recalcitrant to biodegradation, as would be expected. It is therefore likely that, due to their polyaromatic structure, the alkylphenols we identified in the sediments are also more resistant to degradation and may accumulate in sediments and benthic invertebrates. These alkylphenols were also found in lobster hepatopancreas, and may be bioaccumulated there, as other polyaromatic hydrocarbons are known to be (McLeese and Metcalfe, 1979; James *et al.*, 1995). Bioaccumulation in seafoods has been documented for 4-nonylphenol (Ekelund *et al.*, 1990; Ferrara *et al.*, 2001). This raises concern for human health. Since 1995, the European community has placed a voluntary ban on the use of alkylphenol ethoxylates (APEs) due to the toxicity and endocrine-disruptor activity of the breakdown products (including 4-nonylphenol and 4-cumylphenol); use of these products has not been banned in the United States (Renner, 1997). This has sparked considerable debate among researchers and regulators. The potentially endocrine-disrupting effects of BPA have raised particular health concerns, especially since these are viewed as being potentially carcinogenic to humans (reviewed by Cox, 1996, and Lathers, 2002). Since the compounds identified are similar in structure to BPA, the presence of these compounds in lobsters may also warrant health concerns.

Acknowledgments

We acknowledge the help of Dr. Mike Syslo of the Massachusetts Division of Marine Fisheries lobster hatchery on Martha's Vineyard and Mrs. Penny Howell of the Connecticut Department of Environmental Protection for kindly supplying lobsters for this study. We also acknowledge Dr. Judith Grassle, Rutgers University, for kindly supplying marine sediment samples and *Capitella* stocks, and Dr. William Bowers, University of Arizona, for kindly supplying pyriproxyfen. In addition, we are grateful to Professor James M. Bobbitt, Professor James D. Stuart, and Mr. Christopher P. Capulong, of the Department of Chemistry, University of Connecticut, for helpful discussions on chemical synthesis and analysis. We also acknowledge the help and expertise of Mr. Marvin Thompson, manager of the mass spectrometry laboratory and the Department of Chemistry, University of Connecticut, for use of the GC/MS facilities. We gratefully acknowledge the Sea Grant College Program, NOAA, and the Connecticut Department of Environmental Protection for providing financial support for this research.

Literature Cited

Biggers, W. J. 1994. Effects of juvenile hormone-active compounds on larval settlement and metamorphosis of the polychaete annelid *Capitella* Sp. 1. Ph.D. dissertation, University of Connecticut.

Biggers, W. J., and H. Laufer. 1992. Chemical induction of settlement and metamorphosis of *Capitella capitata* sp. I. (Polychaetea) larvae by juvenile hormone-active compounds. *Invertebr. Reprod. Dev.* **22:** 39–46.

Biggers, W. J., and H. Laufer. 1996. Detection of juvenile hormone-active compounds by larvae of the marine annelid *Capitella* sp. I. *Arch. Insect Biochem. Physiol.* **32:** 475–484.

Billinghurst, Z., A. S. Clare, T. Fileman, J. McEvoy, J. Readman, and M. H. Depledge. 1998. Inhibition of barnacle settlement by the environmental oestrogen 4-nonylphenol and the natural oestrogen 17β-oestradiol. *Mar. Pollut. Bull.* **36:** 833–839.

Billinghurst, Z., A. S. Clare, K. Matsumura, and M. H. Depledge. 2000. Induction of cypris major protein in barnacle larvae by exposure to 4-n-nonylphenol and 17β-oestradiol. *Aquat. Toxicol.* **47:** 203–212.

Castro, K. M., and T. E. Angell. 2000. Prevalence and progression of shell disease in American lobster, *Homarus americanus*, from Rhode Island waters and the offshore canyons. *J. Shellfish Res.* **19:** 691–700.

Costlow, J. D. 1977. The effect of juvenile hormone mimics on development of the mud crab *Rhithropanopeus harrisii* (Gould). Pp. 439–457 in *Physiological Responses of Marine Biota to Pollutants*, F. J. Vernberg, A. Calabrese, F. P. Thurberg, and W. B. Vernberg, eds. Academic Press, New York.

Cox, C. 1996. Nonylphenol and related chemicals. *J. Pest. Reform* [Online] **16:** 15–20. Available: http://www.pesticide.org/nonyl.pdf [2003, 29 September].

Davey, K. G., and D. R. B. Gordon. 1996. Fenoxycarb and thyroid hormones have JH-like effects on follicle cells of *Locusta migratoria* in vitro. *Arch. Insect Biochem. Physiol.* 613–622.

Ekelund, R., A. Bergman, A. Granmo, and M. Berggren. 1990. Bioaccumulation of 4-nonylphenol in marine animals: a re-evaluation. *Environ. Pollut.* **64:** 107–120.

Engelmann, F. 1983. Vitellogenesis controlled by juvenile hormone. Pp. 259–270 in *Invertebrate Endocrinology, Vol. 1, Endocrinology of Insects*, R. G. H. Downer and H. Laufer, eds. A. R. Liss, New York.

Ferrara, F., F. Fabietti, M. Delise, A. P. Bocca, and E. Funari. 2001. Alkylphenolic compounds in edible molluscs of the Adriatic Sea (Italy). *Environ. Sci. Technol.* **35:** 3109–3112.

Forward, R. B., Jr., and J. D. Costlow, Jr. 1976. Crustacean larval behavior as an indicator of sublethal effects of an insect juvenile hormone mimic. Pp. 279–289 in *Estuarine Processes, Vol. 1, Uses, Stresses and Adaptation to the Estuary*, M. Wiley, ed. Academic Press, New York.

Fromme, H., T. Kuechler, T. Otto, K. Pilz, J. Mueller, and A. Wenzel. 2002. Occurrence of phthalates and bisphenol A and F in the environment. *Water Res.* **36:** 1429–1438.

Hale, R. C., C. L. Smith, P. DeFur, E. Harvey, E. Bush, M. J. LaGuardia, and G. G. Vadas. 2000. Nonylphenols in sediments and effluents associated with diverse wastewater outfalls. *Environ. Toxicol. Chem.* **19:** 946–952.

Hanauye, K., T. Takase, M. Iwasa, and M. Ito. 1976. Method for producing 2,6-di-tert.-butyl-4-cumyl phenol. *United States Patent* No. 3,933,928. [Online] Available: www.uspto.gov [2003, September 29].

Hegazi, A. G., and F. K. A. El Hady. 2002. Egyptian propolis: 3. Antioxidant, antimicrobial activities and chemical composition of propolis from reclaimed lands. *Z. Naturforsch. Sect. C* **57:** 395–402.

Jakub, W. L., and H. F. Schoof. 1972. Mosquito larvicide studies with MON 585, a juvenile hormone mimic. *Mosq. News* **32:** 6–10.

James, M. O., A. H. Altman, C. L. J. Li, and J. D. Schell. 1995. Biotransformation, hepatopancreas DNA binding and pharmacokinetics of benzo(a)pyrene after oral and parenteral administration to the American lobster, *Homarus americanus*. *Chem-Biol. Interact.* **95:** 141–160.

Jones, G., and P. A. Sharp. 1997. Ultraspiracle: an invertebrate nuclear receptor for juvenile hormones. *Proc. Natl. Acad. Sci. USA* **94:** 13499–13503.

Jones, P. D., W. M. DeCoen, L. Tremblay, and J. P. Giesy. 2000. Vitellogenin as a biomarker for environmental estrogens. *Water Sci. Technol.* **42:** 1–14.

Kamiura, T., Y. Tajima, and T. Nakahara. 1997. Determination of bisphenol A in air. *J. Environ. Chem.* **7:** 275–279.

Khim, J. S., K. T. Lee, K. Kannan, D. L. Villeneuve, J. P. Giesy, and C. H. Koh. 2001. Trace organic contaminants in sediment and water from Ulsan Bay and its vicinity, Korea. *Arch. Environ. Contam. Toxicol.* **40:** 141–150.

Koh, C. H., J. S. Khim, D. L. Villeneuve, K. Kannan, and J. P. Giesy. 2002. Analysis of trace organic contaminants in sediment, pore water, and water samples from Onsan Bay, Korea: instrumental analysis and *in vitro* gene expression assay. *Environ. Toxicol. Chem.* **21:** 1796–1803.

Lathers, C. M. 2002. Endocrine disruptors: a new scientific role for clinical pharmacologists? Impact on human health, wildlife, and the environment. *J. Clin. Pharmacol.* **42:** 7–23.

Laufer, H., and W. J. Biggers. 2001. Unifying concepts learned from methyl farnesoate for invertebrate reproduction and post-embryonic development. *Am. Zool.* **41:** 442–457.

Long Island Sound Lobster Health Symposium. 2003. *Symposium of the Long Island Sound Lobster Research Initiative and Connecticut Department of Environmental Protection*, CT-SG-03-03, N. C. Balcom, ed. Connecticut Sea Grant College Program, NOAA.

Lye, C. M., C. L. J. Frid, M. E. Gill, D. W. Cooper, and D. M. Jones. 1999. Estrogenic alkylphenols in fish tissues, sediments, and waters from the U.K. Tyne and Tees estuaries. *Environ. Sci. Technol.* **33:** 1009–1014.

McLeese, D. W., and C. D. Metcalfe. 1979. Toxicity of creosote to larval and adult lobsters *Homarus americanus* and *Crangon septemspinosa* and its accumulation in lobster hepatopancreas. *Bull. Environ. Contam. Toxicol.* **22:** 796–799.

Messina, G., L. Lorenzoni, and A. Fadda. 1982. Phenolic antioxidant compositions for organic polymers. *United States Patent* No. 4,439,570. [Online] Available: www.uspto.gov [2003, September 29].

Naylor, C. G., J. P. Mieure, W. J. Adams, J. A. Weeks, F. J. Castaldi, L. D. Ogle, and R. R. Romano. 1992. Alkylphenol ethoxylates in the environment. *J. Am. Oil Chem. Soc.* **69:** 695–703.

Pruell, R. J., B. K. Taplin, D. G. McGovern, R. McKinney, and S. B. Norton. 2000. Organic contaminant distributions in sediments, polychaetes (*Nereis virens*) and American lobster (*Homarus americanus*) from a laboratory food chain experiment. *Mar. Environ. Res.* **49:** 19–36.

Renner, R. 1997. European bans on surfactant trigger transatlantic debate. *Environ. Sci. Technol.* **31:** 316A–320A. [Online] July 1997. Available: http://pubs.acs.org/hotartcl/est/97/jul/euro.html [2003, September 29].

Russell, B. A., J. D. Miller, J. R. Cashman, and S. A. Weerawarna.

2002. Naturally occurring compounds and their derivatives as cyclooxygenase 2 and/or 5-lipoxygenase inhibitors. *United States Patent* No. 6,365,634. [Online] Available: www.uspto.gov [2003, September 29].

Sacher, R. 1971. A mosquito larvicide with favorable environmental properties. *Mosq. News* **31:** 513–516.

Sajiki, J., and J. Yonekubo. 2003. Leaching of bisphenol A (BPA) to seawater from polycarbonate plastic and its degradation by reactive oxygen species. *Chemosphere* **51:** 55–62.

Schaefer, C. H., T. Miura, F. S. Mulligan, III, and R. M. Takahashi. 1974. Insect development inhibitors: biological activity of RE17656, RE17937, and RE18286 against mosquitoes (Diptera:Culicidae). *Proc. Pap. Ann. Conf. Calif. Mosq. Control Assoc.* **42:** 147–151.

Scientific Committee on Food. 2001. Opinion of the Scientific Committee on Food on the 12th additional list of monomers and additives for food contact materials. Report CS/PM/GEN/M84. European Commission, Health and Consumer Protection Directorate-General, Brussels. [Online] Available: http://europa.eu.int/comm/food/fs/sc/scf/out84_en.pdf [2003, October 20].

Segner, H., K. Caroll, M. Fenske, C. R. Janssen, G. Maack, D. Pascoe, C. Schafers, G. F. Vandenbergh, M. Watts, and A. Wenzel. 2003. Identification of endocrine disrupting effects in aquatic vertebrates and invertebrates: report from the European IDEA project. *Ecotoxicol. Environ. Saf.* **54:** 302–314.

Sehnal, F. 1983. Juvenile hormone analogues. Pp. 657–672 in *Invertebrate Endocrinology, Vol. 1, Endocrinology of Insects,* R. G. H. Downer and H. Laufer, eds. A. R. Liss, New York.

Semensi, V., and M. Sugumaran. 1986. Effect of MON-0585 on sclerotization of *Aedes aegypti* cuticle. *Pestic. Biochem. Physiol.* **26:** 220–230.

Slama, K., and S. I. Kryspin. 1979. Hypermetabolic response induced by juvenile hormone analogs in an insect. *Z. Naturforsch. Biosci.* **34:** 599–607.

Smith, J. B. 2002. Zinc containing compositions for anti-viral use. *United States Patent* No. 6,475,526. [Online] Available: www.uspto.gov [2003, September 29].

Staples, C. A., P. B. Dom, G. M. Klecka, S. T. O'Block, and L. R. Harris. 1998. A review of the environmental fate, effects, and exposures of bisphenol A. *Chemosphere* **36:** 2149–2173.

Stoker, T. E., C. L. Robinette, B. H. Britt, S. C. Laws, and R. L. Cooper. 1999. Prepubertal exposure to compounds that increase prolactin secretion in the male rat: effects on the adult prostate. *Biol. Reprod.* **61:** 1636–1643.

Takan, T., W. Nanamiya, I. Nagano, K. Asaba, K. Kawabata, and K. Hashimoto. 1999. Exposure with the environmental estrogen bisphenol A disrupts the male reproductive tract in young mice. *Life Sciences* **65:** 2351–2357.

U.S. EPA (U.S. Environmental Protection Agency). 2002. High Production Volume (HPV) Challenge Program. Robust summaries and test plans: hindered phenols. EPA comments, American Chemistry Council. [Online] Available: http://www.epa.gov/chemrtk/hndrdphn/c13382tc.htm [2003, September 29].

U.S. EPA (U.S. Environmental Protection Agency). 2003. Design for the Environment. Key characteristics of laundry detergent ingredients. [Online] Available: http://www.epa.gov/dfe/pubs/laundry/techfact/keychar.htm [2003, September 29].

van Heemst, J. D. H., P. F. van Bergen, B. A. Stankiewicz, and J. W. de Leeuw. 1999. Multiple sources of alkylphenols produced upon pyrolysis of DOM, POM and recent sediments. *J. Anal. Appl. Pyrolysis* **52:** 239–256.

Watts, M. W., D. Pascoe, and K. Carroll. 2001. Chronic exposure to 17-alpha-ethinylestradiol and bisphenol A-effects on development and reproduction in the freshwater invertebrate *Chironomus riparius* (Diptera: Chironomidae). *Aquat. Toxicol.* **55:** 113–124.

Williams, A. B., and T. W. Duke. 1979. Crabs (Arthropoda: Crustacea: Decapoda: Brachyura). Pp. 171–233 in *Pollution Ecology of Estuarine Invertebrates,* C. W. Hart and L. H. Samuel, eds. Academic Press, New York.

Wyatt, G. R. 1991. Gene regulation in insect reproduction. *Invertebr. Reprod. Dev.* **20:** 1–35.

Ying, G.-G., B. Williams, and R. Kookana. 2002. Environmental fate of alkylphenols and alkylphenol ethoxylates—a review. *Environ. Int.* **28:** 215–226.

Zeng, Y., and P. K. A. Hong. 2002. Slurry-phase ozonation for remediation of sediments contaminated by polycyclic aromatic hydrocarbons. *J. Air Waste Manag. Assoc.* **52:** 58–68.

Zintek, L., D. Wesolowski, B. Paruchuri, P. Howe, A. Alwan, G. Azevedo, D. Hopkins, and J. Dorkin. 2003. Methods for determination of selected alkylphenols and bisphenol A in sediments and water. EPA Conference on Analysis of Pollutants in the Environment, 26th annual conference, Chicago, IL. U.S. Environmental Protection Agency, Office of Water, Office of Science and Technology, Engineering and Analysis Division, Washington, DC.

Zomer, E., and H. Lipke. 1981. Tyrosine metabolism in *Aedes aegypti* II. Arrest of sclerotization by MON 0585 and diflubenzuron. *Pestic. Biochem. Physiol.* **16:** 28–37.

Reference: *Biol. Bull.* **206:** 25–34. (February 2004)
© 2004 Marine Biological Laboratory

Reproduction and Development of the Conspicuously Dimorphic Brittle Star *Ophiodaphne formata* (Ophiuroidea)

HIDEYUKI TOMINAGA[1,*], SHOGO NAKAMURA[2], AND MIÉKO KOMATSU[1]

[1] *Department of Biology, Faculty of Science and* [2] *Department of Environmental Biology and Chemistry, Faculty of Science, Toyama University, Toyama, 930-8555, Japan*

Abstract. *Ophiodaphne formata* is a conspicuously dimorphic ophiuroid; the disk diameters are approximately 1 mm for males and 5 mm for females. The dwarf male clings to the larger female, with the oral surfaces and bursae of the paired ophiuroids closely appressed. Moreover, the female of each pair adheres aborally to the oral surface of a host sand dollar, *Astriclypeus manni.* Spawning and external fertilization occur in August, at Tsuruga Bay, Sea of Japan. Development of the dimorphic brittle star *O. formata* is described for the first time, from spawning through metamorphosis, with special attention to the formation of the skeletal system and the external morphology of early juveniles. Fertilized eggs are about 90 μm in diameter, pale pink, and negatively buoyant. The embryos undergo equal, total, and radial cleavage, and the larval skeleton first forms as a pair of tetraradiate spicules. Larval development proceeds to an 8-armed planktotrophic ophiopluteus, with skeletal elements that consist of a body rod and two recurrent rods. Three weeks after fertilization, all the pluteal arms, except for the postero-lateral arms, are absorbed, and the metamorphosing larvae sink to the bottom. Metamorphosis is completed 21.5 days after fertilization, and the resulting juvenile is pentagonal and approximately 270 μm in diameter. The smallest specimen (480 μm in disk diameter) collected by field sampling exhibited male features on the skeletal plates of the jaw and disk. Sexual dimorphism, the peculiar pairing behavior, and the close relationship with the host sand dollar may have evolved as distinct reproductive characteristics in this ophiuroid with its typical ophiopluteus larvae.

Introduction

The biology of reproduction has been reported in various echinoderms, and they are mostly dioecious (Hyman, 1955; Delavault, 1966; Lawrence, 1987). Sexual dimorphism is not common, but some species show external morphological differences in size, genital papillae, genital pores, and arm spines (Hyman, 1955; Delavault, 1966; Tyler and Tyler, 1966; Lawrence, 1987; O'Loughlin, 2001; Stöhr, 2001). In a few ophiuroids—*Ophiosphaera insignis, Amphiura scripta,* and *Astrochlamys bruneus*—the difference in size between males and females is very large (Brock, 1888; Koehler, 1904; Mortensen, 1933, 1936). In *O. insignis* and *A. scripta,* a dwarf male pairs with a much larger female, clinched mouth to mouth; and in *A. bruneus,* a smaller male attaches to the dorsal surface of a larger female. However, no spawning has been observed in these ophiuroids. Therefore, the pairing of a male and a female in these dimorphic species has not been demonstrated as a distinct reproductive behavior. Ophiuroid reproduction and development has been reviewed by Hyman (1955), Strathmann and Rumrill (1987), Hendler (1995), and Byrne and Selvakumaraswamy (2002), but neither the larva nor the metamorphosis of a dimorphic species has been described.

We have been studying an unusual sexually dimorphic ophiuroid, *Ophiodaphne formata,* which has two novel characteristics. First, the dwarf male and the larger female are coupled mouth to mouth, and we have observed this pairing throughout the year, even in the nonbreeding season. Second, these paired ophiuroids are only found firmly attached to the oral surface of a host sand dollar, *Astriclypeus manni.* The ophiuroid *O. formata* ranges from the Arabian coast to Indonesia (Koehler, 1905; Guille, 1981) and was recorded from off Minabe, Wakayama Prefecture (Honshu),

Received 13 January 2003; accepted 23 September 2003.

* To whom correspondence should be addressed. E-mail: hidetom@bb.cocone.jp

Japan, by Irimura (1981), who identified it, at first, as *Ophiodaphne materna.* He also reported that a large specimen and a smaller one—supposedly female and male, respectively—were found on the oral side of a sand dollar, *Clypeaster reticulatus,* clinched together mouth to mouth. However, the sex of the larger and smaller specimens was not verified in this very brief report. Later, Irimura and his coauthors (2001) classified specimens of this ophiuroid, which were collected at depths of 25.5–40 m, as *O. formata.*

In view of the unusual natural history of *O. formata,* the present study was initiated to confirm that pairing in this species is a reproductive behavior. Pairs of *O. formata* comprising a dwarf male and a much larger female were removed together from the oral side of the host sand dollar, *A. manni,* and kept in glass beakers. We observed spawning; then external fertilization occurred; and the fertilized eggs developed into 8-armed ophioplutei, which metamorphosed into juveniles. Thus, the developmental mode of the sexually dimorphic *O. formata* has now been defined.

Materials and Methods

In the summers of 1999 to 2001, adult sand dollars (*Astriclypeus manni*) were collected from depths of 5 m by scuba diving on the sandy bottom of Tsuruga Bay, Fukui Prefecture (central Japan, 35° 44′ N, 136° 03′ E). The sand dollars were examined for samples of paired and unpaired, young and adult *Ophiodaphne formata.* The ophiuroids (n = 245) were found on only about 1 out of 10 sand dollars, and 46% of them were paired (n = 112). When pairs were found, they were carefully removed from the sand dollars with fine forceps and placed into glass beakers containing filtered seawater. In 2002, about 20 individuals of *O. formata* were collected every 2 months for histological study of gonadal development.

A few days after the collection in August 2000, spawning occurred naturally, with no artificial stimuli, and the fertilized eggs were removed from the glass vessels and reared in 5-l glass beakers; density was maintained at one larva per 10 ml of filtered seawater. The water temperature was about 26 °C, approximately that at the collection site. Larval cultures were agitated with a plastic propeller rotating at 60 rpm. Seawater used for culture was obtained from the open sea and was filtered many times and renewed every 3 days. A small quantity (3 ml/l) of larval food in the form of a mixture of unicellular algae—*Dunaliella tertiolecta, Isochrysis galbana,* and *Chaetoceros gracilis*—was added to the culture when the seawater was changed.

The development of embryos and larvae, including skeletal formation, was observed by both light microscopy and polarized light microscopy. Measurements of living embryos and larvae were made with an ocular micrometer. For scanning electron microscopy, metamorphosing larvae and juveniles were fixed for 1 h in 2% OsO_4 in a 50 m*M* Na-cacodylate buffer (pH 7.4); the osmolarity of the fixative was adjusted by adding sucrose (final concentration 0.6 *M*), according to Komatsu *et al.* (1990). The fixed materials were dehydrated in an ethanol series, dried with a critical-point dryer (Hitachi, HCP-2), coated with gold-palladium (Hitachi, E101 Ion Sputter), and examined with a Hitachi S-2000 scanning electron microscope.

Histological observations of the reproductive organs were made to confirm their sex and maturity. Fresh specimens were measured, dissected, and fixed in Allen-Bouin's solution, followed by decalcification with 5% trichloroacetic acid for one week at 4 °C. These prepared gonadal tissues were serially sectioned at 4 μm by a routine paraffin method and stained with Delafield's hematoxylin and eosin.

Results

Pairing, symbiosis, and sexual dimorphism

Adult individuals of *Ophiodaphne formata* are diecious, and the disk diameter of mature specimens is about 1 mm in males and 5 mm in females. The oral surface of the dwarf male is pressed against the oral surface of the larger female, and the arms of the male cling to the female at the interradius position (Fig. 1A). Mature specimens, paired and unpaired, were situated next to a lunule on the oral side of the burrowing sand dollar *Astriclypeus manni,* which is considered to be their host (Fig. 1B, C). The female reaches upward to hook the terminal half of two arms over the edge of the lunule. She firmly fixes her aboral surface to the oral surface of the sand dollar by attaching her aboral skeletal elements to the oral spines of the host. Two of the tips of the male's arms are just visible protruding from under the female's disk (Fig. 1D). Most ophiuroids, whether paired or unpaired, were located at the lunule of the sand dollar as an attachment site, from which a radial food track leads away food particles to the sand dollar's mouth. However, some single young females and males were not located at the lunule, but on the oral plate of the sand dollar, closer to its mouth and anus.

In addition to the size dimorphism, external morphological differences between males and females are evident in such skeletal characteristics as the shape of the jaw, the number and size of disk scales, the number of arm spines, the presence or absence of parallel grooves on the radial shields and disk scales of the aboral disk, and tentacle scales on the oral side of the arm. The jaws of both males and females, present at each interradius, consist of one tooth, one oral shield, two adoral shields, two oral plates with infradental papillae, and two buccal scales. The jaw ossicles of females are stouter than those of males, and the oral plates and teeth are more apparent in the female (Fig. 2A, B). The aboral side of the smaller disk of the male is covered with scales that are less reduced in size and number than those of the female (Fig. 2C). The lateral arm plates of

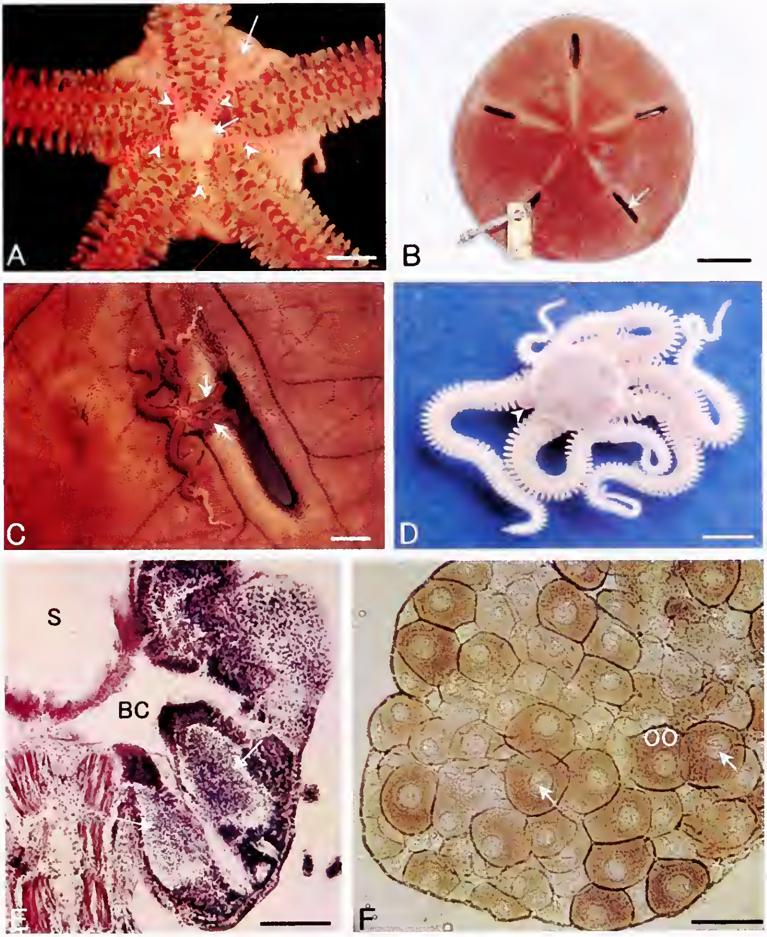

Figure 1. Male and female of *Ophiodaphne formata* and their host, *Astriclypeus manni*. (A) Magnified view of the female paired with a much smaller male of *O. formata*, both detached from the host shown in C. Note the dwarf male (short arrow), with his oral surface against that of the larger female (long arrow), and his arms (arrowheads) alternating with hers. Views of the female and male are oral and aboral, respectively. (B) Aboral view of a sand dollar, *A. manni*. Arrow indicates a lunule. (C) Female specimen of *O. formata* carrying a dwarf male close to the lunule on the oral side of *A. manni*. Note her position, with two arms (arrows) hooked over the edge of the lunule. (D) Aboral view of the female. The body of the male is hidden by the female, but the tips of two of his arms (arrowheads) are visible. (E) Horizontal section of a male specimen of *O. formata* with mature sperm (arrows) in a pair of testes situated at the interradius. The space above the testes is a body cavity (BC) near the stomach (S). (F) Compressed ovary filled with ova (OO) with germinal vesicle (arrows). Scale bars: 3 cm (B), 3 mm (C, D), 1 mm (A), and 100 μm (E, F).

males have 4 spines, whereas those of females have 8. Females possess grooves on their radial shields and disk scales of the disk (Fig. 2D, E) and tentacle scales on the oral side of the arm, while males do not (Fig. 2F, G).

In contrast to the sexual dimorphism in adults, recently metamorphosed juveniles, whose disks are about 400 μm in diameter, do not vary morphologically among individuals. However, the smallest specimen collected on a sand dollar

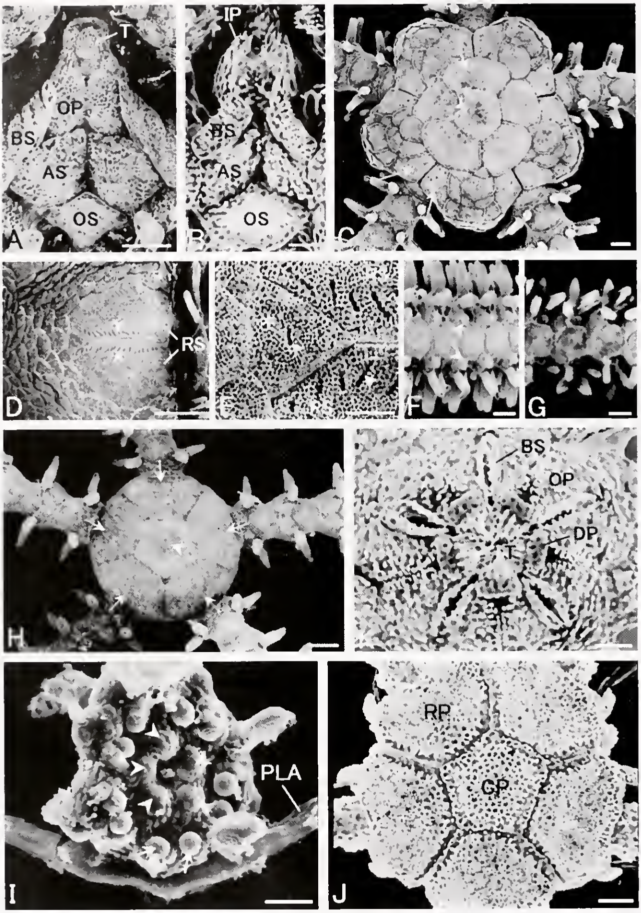

Figure 2. Skeletal structures of *Ophiodaphne formata*. A–K are scanning electron micrographs. (A) Adult female jaw in an interradius; oral view. Components: an oral shield (OS), two adoral shields (AS), two oral plates (OP), and a tooth (T). BS, buccal scale. (B) Adult male jaw in an interradius; oral view. Components of the jaw are the same as in female, but compare structures. IP, infradental papilla; other abbreviations as in (A). (C) Aboral skeletal system of an adult male detached from the host. Note that the disk is covered with scales: a central plate (arrowhead), five radial plates (short arrows), five pairs of radial shields (long arrows), and others. (D) Aboral view of grooves (arrowheads) on the radial shields (RS) of a female. (E) Grooves on the radial shields (RS) and the disk scale (asterisk) of a female at high magnification. (F) Oral view of tentacle scales (arrowheads) on the arm of a female. (G) Oral view of the arm of a male. Note absence of tentacle scales. (H) Aboral skeletal system of a young male brittle star detached from the host. Note the central plate (arrowhead) and five radial plates (arrows) on his disk. (I) Oral view of metamorphosing ophiopluteus with juvenile mouth formation and postero-lateral arm (PLA). Oral tube feet (arrowheads) are visible around the mouth, and tube feet (arrows) are more distal. (J) Central plate (CP) and five radial plates (RP) of a newly metamorphosed juvenile. Aboral view. (K) Oral view of jaws consisting of oral plates (OP), dental plates (DP), and tooth (T). BS indicates buccal scale. Same stage as in J. Scale bars: 500 μm (D, F), 200 μm (G), 100 μm (A, C, E, H), and 30 μm (B, I–K).

from the field (disk diameter 480 μm) exhibited male characteristics in the ossicle of the jaw and skeletal elements of the disk (Fig. 2H). The disk diameter of the smallest female specimen collected from the field was already 1.0 mm. These observations suggest that size differences corresponding to sexual dimorphism first appear in individuals with disk diameters of about 500 μm (males) and 1 mm (females).

Gonadal development and spawning

Sex in *O. formata* is distinguished by the color of the gonads upon dissection; the testes are creamy white, and the ovaries are pale pink. The gonads of both males and females were largest in specimens collected in August. Sections of gonad show that the testes are occupied, in early August, with numerous mature sperm (Fig. 1E), while the ovaries contain numerous oocytes, many of them fully grown and with a germinal vesicle (Fig. 1F). Later in August, after spawning, the ovaries are still large, but they contain no fully grown oocytes, and the center of the organ is occupied by a wide cavity, indicating degeneration. In October and December, the ovaries are smaller than in August. Though ovaries examined from January to May remain small, they are filled with developing oogonia and a few oocytes. Spawning in the laboratory begins when a paired female raises her disk from the bottom of the glass vessel to assume a shedding posture. The eggs and sperm are shed into each bursa, and are released outside through the genital slits at the base of the arms. The release is immediately followed by external fertilization.

We did not attempt to observe spawning in the field. However, our histological study of gonadal development—and our observation that eggs fertilized in August (but not in June, July or October) completed metamorphosis and developed into juveniles—all suggest that, in Tsuruga Bay, the breeding season for *O. formata* occurs during August.

Development

Early development. Fertilized eggs are spherical, about 90 μm in diameter, pale pink, and negatively buoyant (Fig. 3A). They have a transparent, nonsticky fertilization envelope, and a translucent, thick (10 μm) hyaline layer. A chronology of development, from fertilized egg to juvenile, is presented in Table 1. The cleavage is total, equal, and radial. At about 26 °C, the first division occurs at 2 h after fertilization, and as divisions continue (Fig. 3B), the embryos develop into blastulae (Fig. 3C). These blastulae are not wrinkled, unlike those of two other ophiuroids (*Ophiothrix oerstedi* and *Ophionereis schayeri*) and members of other echinoderm classes (Mladenov, 1979; Henry *et al.*, 1991; Chia *et al.*, 1993; Selvakumaraswamy and Byrne, 2000; Komatsu *et al.*, 2000). Nine hours after fertilization, the blastula hatches from the fertilization envelope (Fig. 3D), and primary mesenchyme cells in the vegetal pole wall are set free into the blastocoel (Fig. 3E). At this stage, blastulae in culture swim actively just beneath the water's surface. They become oval (180 μm long and 120 μm wide); and 12 h after fertilization, gastrulation occurs by invagination at the vegetal pole. During gastrulation, the embryo flattens dorso-ventrally (Fig. 3F).

Ophiopluteus stage. Twenty hours after fertilization, in the gastrula stage, the larval spicules begin to take a tetraradiate form (Fig. 3G, H). Then a pair of right and left coelomic pouches is formed on both sides of the tip of the archenteron. Figure 3I shows an early 2-armed ophiopluteus, 35 h after fertilization, taking the shape of a helmet as the postero-lateral arms appear. The antero-lateral arm buds are evident 60 h after fertilization (Fig. 3J). In this early 4-armed ophiopluteus, the archenteron has differentiated into a functional digestive tract: esophagus and stomach (Fig. 3J).

From the 2-armed to the 4-armed stage, two pair of recurrent rods arise successively, running parallel to the body rods (Fig. 3K). These recurrent rods extend to the center of the larval basket-like structure from paired points of divergence, and the body rods also arise from these points (DP in Fig. 3K). Thus, these recurrent rods, together with the body rods and transverse rods, constitute a bilateral, threefold skeletal structure. Immediately after the postero-lateral, antero-lateral, and body rods form, the post-oral rods also appear, and the postero-lateral rods extend horizontally and support the postero-lateral arms.

Four and a half days after fertilization, the post-oral arms are formed, and the ophioplutei develop to the 6-armed stage (Fig. 4A). Six and a half days after fertilization, they become 8-armed ophioplutei, bearing a 4th pair of arms, the postero-dorsal arms (Fig. 4C). At this stage, both the right and left coelomic pouches, the latter of which is further developed than the former, are divided into anterior and posterior sections on each side (Fig. 3L).

The body, the postero-lateral, the antero-lateral, the post-oral, and the postero-dorsal rods are not fenestrated and have no thorns. The length of the postero-lateral arm in the largest 8-armed ophiopluteus larvae is about 700 μm, and the postero-lateral rod is a spiral structure in the middle of this arm (Fig. 4C). These larval arm rods serve as flotation devices, and are absorbed as metamorphosis proceeds. Late 8-armed ophioplutei have neither ciliary epaulets nor vibratile lobes. The left posterior coelomic pouch is divided into a hydrocoel and somatocoel, and the former expands forward, gradually, along the stomach and esophagus, producing a 5-lobed hydrocoel (Fig. 3M, N and 4B). A hydrocoel lobe forms, passes through the left posterior coelomic pouch, and migrates around the esophagus of the 8-armed ophiopluteus larva just before the beginning of metamorphosis. After migrating and surrounding the esophagus for about a day, the 5-lobed hydrocoel develops into the water

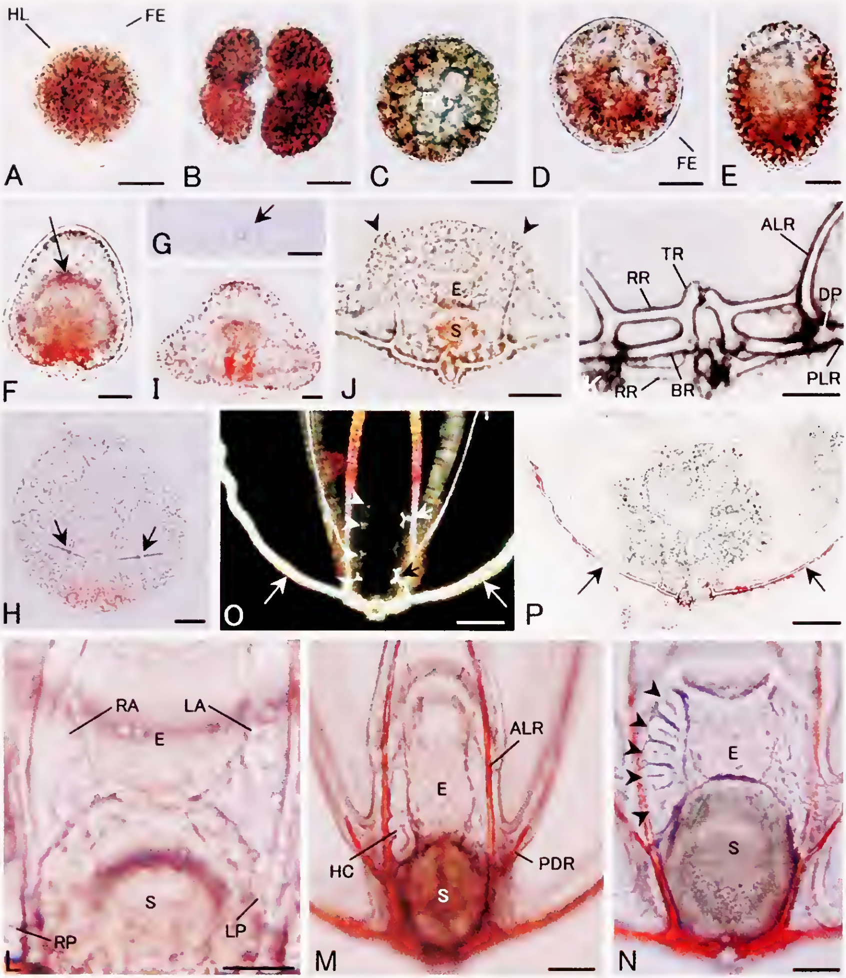

Figure 3. Early development of *Ophiodaphne formata.* (A–N and P are light micrographs; O is a polarized light micrograph.) (A) Fertilized egg surrounded by the fertilization envelope (FE) and hyaline layer (HL). (B) Four-cell stage, 2.5 h after fertilization. (C) Blastula with blastocoel (BC), 6.2 h after fertilization. (D) Hatching blastula, 9 h after fertilization. Note fertilization envelope (FE). (E) Swimming blastula. (F) Gastrula, 21 h after fertilization. Arrow indicates the archenteron. (G) Tetraradiate spicule (arrow) in gastrula at high magnification. (H) A pair of tetraradiate spicules (arrows) in a compressed gastrula; later stage than that shown in G. (I) Early 2-armed ophiopluteus, 1.5 d after fertilization. (J) Early 4-armed ophiopluteus with the antero-lateral arm buds (arrowheads), esophagus (E), and stomach (S), 2.5 d after fertilization. (K) Magnified view of skeletal structure of late 4-armed ophiopluteus. Two pairs of recurrent rods (RR) run parallel to the body rod (BR), and perpendicular to the transverse rods (TR), from the diverging points (DP). The postero-lateral rod (PLR) and antero-lateral rod (ALR) also arise from the diverging points. (L) Magnified view of esophagus (E) and stomach (S) in an 8-armed ophiopluteus. The right and left, anterior (RA, LA) and posterior (RP, LP) coelomic pouches are indicated. Oral view. (M) Late 8-armed ophiopluteus with hydrocoel (HC) along the stomach (S) and esophagus (E). Orange structures are antero-lateral rod (ALR) and postero-dorsal rod (PDR). Aboral view. (N) 8-armed ophiopluteus, more advanced than that shown in (M), with five-lobed hydrocoel (arrowheads) beside

Table 1

Chronology of development of Ophiodaphne formata *(26 °C)*

Time after fertilization	Stage
2 h	2-cell stage
2.5 h	4-cell stage
3 h	8-cell stage
3.5 h	16-cell stage
5 h	Morula
6.2 h	Blastula with blastocoel
9 h	Hatching
21 h	Gastrula, 140 μm long and 120 μm wide
1.5 d	2-armed ophiopluteus
2.5 d	4-armed ophiopluteus
4.5 d	6-armed ophiopluteus
6.5 d	8-armed ophiopluteus with posterior coelom
13.5 d	Hydrocoel formation
15.5 d	Left hydrocoel 5-lobed
18.5 d	Rudiments of adult skeleton appear as spicules
20.5 d	Metamorphic climax begins, larval arm degenerates rapidly
21.5 d	Completion of metamorphosis with absorption of larval arms

vascular system. The 6-armed and 8-armed ophioplutei have a mass of pigment cells including pigment granules, brownish and deep reddish, at the tips of the postero-lateral arms.

Metamorphosis. Eighteen and a half days after fertilization, the adult plates begin to form as fine spicules (Fig. 3O). These spicules correspond to the rudiments of the five terminal plates and large radial plates with a dorso-central plate. At this stage, the stomach and intestine are greenish. In the 8-armed ophiopluteus, 20 days after fertilization, the tip of the postero-lateral arms begin to swell, and the antero-lateral arms cross (Fig. 4C). Absorption of the post-oral and postero-dorsal arms begins 21 days after fertilization (Fig. 4D). Absorption of the left antero-lateral arm occurs and is followed by a decrease in the size of the right antero-lateral arm. Toward the end of metamorphosis, the left antero-lateral arm becomes much shorter than the right (Fig. 4E). The disk consists of small spicules that develop as a skeletal network (Fig. 3P). The spicules that will differentiate to become terminal and radial plates will migrate and will be situated at the tip of the arm and the margin of the disk. The metamorphosing larva is furnished by the rudimentary ophiuroid with a mouth, paired oral tube feet and tube feet; and it frequently creeps along the bottom (Fig. 2I).

Twenty-one and a half days after fertilization, metamorphosis is complete, and the left postero-lateral arm is absorbed, followed by the right (Table 1, Fig. 4F). Immediately after metamorphosis, the juveniles are pentagonal with short arms and spines (Fig. 4G). These paired short spines between the arms disappear as the juveniles grow (Fig. 1D, 2C). Newly metamorphosed juveniles are about 270 μm in disk diameter. They bear a terminal tentacle in the tip of each arm. On their aboral side, a central plate is situated in the center of the disk, surrounded by five radial plates (Fig. 2J). On the oral side, rudiments of five jaws begin to form (Fig. 2K). At this stage, the external morphology of skeletal elements does not vary among specimens.

After a period of 45 days (post-fertilization), the juveniles grow to approximately 400 μm in disk diameter, and are brown. They have five arms, each 130 μm long, consisting of one segment and a terminal plate (Fig. 4H). Although more than 200 juveniles survived in the laboratory for about 2 months after fertilization, they did not differentiate further and eventually died. One specimen collected from the natural habitat on 14 January 2002 was 480 μm in disk diameter (Fig. 2H). It possessed about 11 segments in each of its arms, which were approximately 1.6 mm long. We estimate that this field specimen was about 5 months old.

Discussion

We have described here, for the first time, the development—from spawning and fertilization through metamorphosis—of the sexually dimorphic ophiuroid *Ophiodaphne formata.* The pattern of development in *O. formata* is influenced by four characteristics. The egg is small, which is consistent with the observed indirect development through a planktotrophic ophiopluteus. However, the formation of tetraradiate larval spicules and the absence of a secondary vitellaria larva are features that tend to reduce the time to metamorphosis. Finally, the ciliated postero-lateral arms are retained, which may provide the juvenile brittle star with mobility for a brief presettlement exploration of the substrate. This suite of developmental characteristics is in accord with the novel natural history of *O. formata,* in which a dwarf male and a female are coupled and attached to the oral surface of the sand dollar *Astriclypeus manni,* mostly adjacent to the lunule.

Methods of inducing spawning in ophiuroids—except for a sudden change in water temperature reported for *Amphipholis kochii* by Yamashita (1985)—are not as precise or

esophagus (E) and upper part of stomach (S), 15.5 d after fertilization. Aboral view. (O) Skeletal system of late 8-armed ophiopluteus (polarized light micrograph). Postero-lateral rods (long arrows); rudimental radial plates (short arrows); terminal plates (arrowheads). Aboral view. (P) A pair of postero-lateral rods (arrows) of a metamorphosing ophiopluteus, compressed. Note the skeletal network for the resulting juvenile. Oral view. Scale bars: 100 μm (N, O, P), 50 μm (J, L), and 30 μm (A–I, K, M).

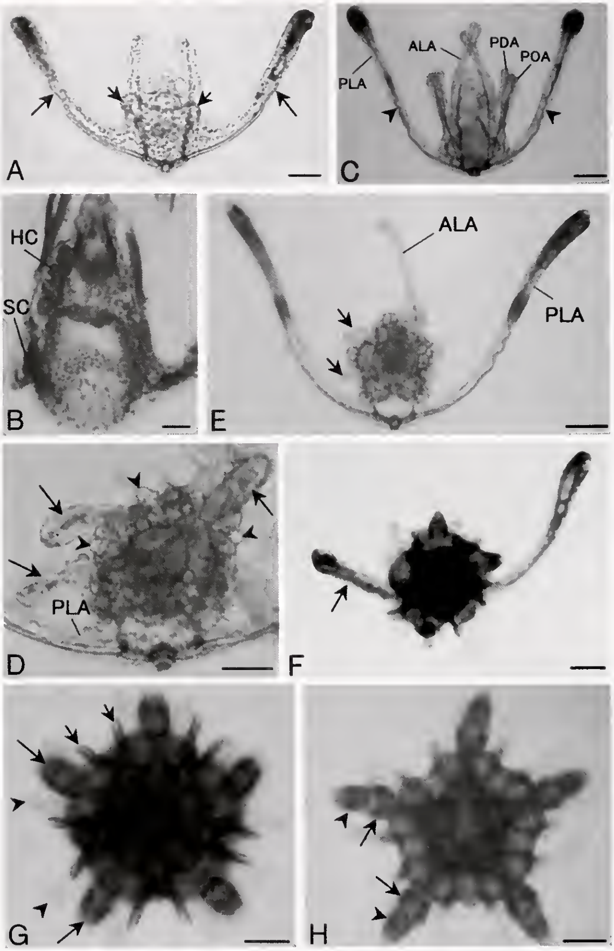

Figure 4. Development of *Ophiodaphne formata.* (A) Early 6-armed ophiopluteus, 4.5 d after fertilization. Long arrows indicate the postero-lateral arms, and short arrows, the post-oral arms. Oral view. (B) Histological longitudinal section (4 μm) of an 8-armed ophiopluteus showing the hydrocoel (HC) and somatocoel (SC). Same stage as shown in Figure 3N. Aboral view. (C) Metamorphosing ophiopluteus; oral view. Note the swollen tip of the postero-lateral arms (PLA), the crossed antero-lateral arms (ALA), and the spiral construction of the postero-lateral rods (arrowheads). (D–F) Successive stages of resorption of the larval arms. (D) Magnified aboral view of the ophiuroid rudiment, showing tube feet (arrowheads). The rudiment is within the metamorphosing ophiopluteus, which has a pair of postero-lateral arms (PLA) and reduced post-oral and postero-dorsal arms (arrows). (E) Metamorphosing ophiopluteus with a right antero-lateral arm (ALA) and other reduced larval arms (arrows) hanging on postero-lateral arms (PLA). Aboral view of the rudiment. (F) Metamorphosing ophiopluteus with a shorter left postero-lateral arm (arrow) than right, 20.5 d after fertilization. Aboral view. (G) Juvenile just after metamorphosis with terminal plates (long arrows), spines (short arrows), and tube feet (arrowheads), 21.5 d after fertilization. Aboral view. (H) Juvenile with arm segments (arrows). Arrowheads indicate terminal plates. Aboral view. Scale bars: 100 μm (C, E, F, H), and 50 μm (A, B, D, G).

reliable as those known for echinoids or asteroids (Strathmann and Rumrill, 1987). Fortunately, however, *O. formata* spawns spontaneously in the laboratory, so the entire process of development, from fertilized eggs to juveniles, has been observed in this study. The entire process has been observed in several other species: *Ophiothrix fragilis, Ophiocoma nigra, Ophiopholis aculeata, Ophiocoma pumila,* and *A. kochii* (MacBride, 1907; Narasimhamurti, 1933; Olsen, 1942; Mladenov, 1985; Yamashita, 1985), but none of these is a sexually dimorphic species. This study, therefore, is the first demonstration of a sexually dimorphic ophiuroid, developing through a typical ophiopluteus stage, and then into an 8-armed planktotrophic larva.

The mature ova of *O. formata* are 90 μm in diameter, similar in size to those of *O. fragilis, O. nigra,* and *A. kochii* (MacBride, 1907; Narasimhamurti, 1933; Yamashita, 1985). Mladenov (1979) summarized the quantitative characteristics of developmental patterns in ophiuroids and noted that species with small eggs (70–200 μm in diameter) undergo planktotrophic development and require 12–40 days to reach metamorphic competence. In the present study, *O. formata* completed metamorphosis within 21.5 days at 26 °C and thus fits the categorization of Mladenov (1979), as do *O. fragilis, O. nigra,* and *A. kochii.* Of these species, *O. fragilis* and *O. nigra* occur in relatively deep waters, whereas *A. kochii* is found under stones in the intertidal zone, along the Pacific coast of northern Japan, and *O. formata* inhabits the sandy bottom, 5 m deep, at Tsuruga Bay. A rapid metamorphosis should be advantageous to the shallow-water brittle stars, *O. formata* and *A. kochii,* for it would prevent dispersal to less advantageous deep habitats. In the case of the reproductive pairs of *O. formata,* which always live on a host sand dollar on the shallow sandy bottom, the requirement for rapid metamorphosis may be especially important.

Hyman (1955) generalized that an early ophiopluteus is furnished with a three-rayed skeletal rod, and Olsen (1942) and Strathmann and Rumrill (1987) reported this condition in *Amphipholis squamata* and *O. aculeata,* respectively. However, the present study reveals that the initial shape of the larval spicules in *O. formata* is tetraradiate, as in *Amphiura chiajei, Amphioplus abditus, A. kochii,* and *O. schayeri* (Fenaux, 1963; Hendler, 1978; Yamashita, 1985; Selvakumaraswamy and Byrne, 2000). Therefore, the rudiments of the skeletal rods in the ophiopluteus can form in two ways: triradiate or tetraradiate. The accelerated formation of tetraradiate spicules in the gastrula stage may reduce the time to metamorphosis and thus contribute to the rapid embryonic development in *O. formata.*

At settlement, ophioplutei generally release their postero-lateral arms (Olsen, 1942; Byrne and Selvakumaraswamy, 2002). In *O. formata,* however, the four pairs of larval arms are not discarded, but rather absorbed—first the post-oral and postero-dorsal arms, and then the antero-lateral and postero-lateral arms. Thus, the report of Balser (1998), that the released arms of an ophiopluteus can regenerate all the structures typical of the primary ophiopluteus, and that asexual reproduction of larval arms may be highly adaptive for life in the open ocean, does not apply to *O. formata.*

Ophiuroids live in all seas, in all types of sediment, and at all depths—from the intertidal zone to the abyssal region. Among these species, only *O. formata* is found on sand dollars, such as *A. manni* (Tominaga, 2001, and present materials), *Clypeaster reticulatus* (Irimura, 1981), and *C. japonicus* (Tominaga, unpubl.); and these host organisms are always in shallow waters, partially buried in the sandy bottom. In this study, the ophiuroids were never found on the sandy bottom; rather, the much larger female, carrying a dwarf male in a mouth-to-mouth position, is herself attached, by her aboral side, to the oral surface of the host *A. manni.* The lunule of the host may serve the female ophiuroid as a convenient site for attachment, or the concave shape of the lunule may provide protection from abrasion by the sand. Although we might suggest that a radial food track of the sand dollar, located close to the edge of the lunule (Fig. 1C), provides nutriment for the paired ophiuroids, this seems unlikely, because paired and unpaired females on the oral side of the sand dollar always turn their mouths to the sandy bottom to feed, not to a radial food track. Probably the association between the male and female and their morphological specializations have evolved as an adaptation to ensure mating success on this mobile and infaunal host. Although the pairing in *O. formata* is observed throughout the year, including in the nonbreeding season, this pairing behavior is probably essential to their reproduction, because spawning occurs while pairing.

Males and females of *O. formata* have a bursa on the oral surface which provides an opening for the gonad. Consequently, the most efficient posture for the male is to interdigitate his arms with the larger female, mouth to mouth, while he sheds sperm from his bursal slits. The posture is important because the low density of *O. formata* is in contrast to that of the more common shallow-water ophiuroids (Fujita, 1992). Thus, fertilization efficiency would probably be low if males and females of *O. formata* spawned separately on the sand and did not pair on their host. Probably *O. formata* selects *A. manni* as a host that provides a breeding site and thus raises the level of fertilization success, as suggested by Hendler (1991).

Acknowledgments

The authors wish to express their cordial thanks to Mr. T. Hashimoto and Mrs. Y. Hashimoto for their assistance with field sampling. Thanks are also extended to Miss H. Yamanishi for her cooperation in the developmental observations. They are grateful to Dr. S. Irimura for the identifica-

tion of and to Dr. G. Hendler for information and suggestions on *Ophiodaphne formata*.

Literature Cited

Balser, E. J. 1998. Cloning by ophiuroid echinoderm larvae. *Biol. Bull.* **194:** 187–193.

Brock, J. 1888. Die Ophiuriden fauna des indischen Archipels. *Z. Wiss. Zool.* **47:** 525–527.

Byrne, M., and P. Selvakumaraswamy. 2002. Phylum Echinodermata: Ophiuroidea. Pp. 483–498 in *Atlas of Marine Invertebrate Larvae*, C. M. Young, ed. Academic Press, London.

Chia, F. S., C. Oguro, and M. Komatsu. 1993. Sea-star (Asteroid) development. *Oceanogr. Mar. Biol. Annu. Rev.* **31:** 223–257.

Delavault, R. 1966. Determinism of sex. Pp. 615–638 in *Physiology of Echinodermata*, R. A. Boolootian, ed. Wiley-Interscience, New York.

Fenaux, L. 1963. Note préliminaire sur le dévelopment larvaire de *Amphiura chiajei* (Forbes). *Vie Milieu* **14:** 91–96.

Fujita, T. 1992. Dense beds of ophiuroids from the Paleozoic to the recent: the significance of bathyal populations. *Otsuchi Mar. Research Center Report* **18:** 25–21.

Guille, A. 1981. Echinoderms: Ophiurides. Pp. 435–439 in *Resultats des Campagnes MUSORSTOM*, Vol. 1. Museum national d'histoire naturelle, Paris.

Hendler, G. 1978. Development of *Amphioplus abditus* (Verrill) (Echinodermata: Ophiuroidea). II. Description and discussion of ophiuroid skeletal ontogeny and homologies. *Biol. Bull.* **154:** 79–95.

Hendler, G. 1991. Echinodermata: Ophiuroidea. Pp. 356–511 in *Reproduction of Marine Invertebrates*, Vol. 6, A. C. Giese, J. S. Pearse, and V. B. Pearse, eds. The Boxwood Press, Pacific Grove, CA.

Hendler, G. 1995. Class Ophiuroidea. Pp. 89–195 in *Sea Stars, Sea Urchins and Allies*. G. Hendler, J. E. Miller, D. L. Pawson, and P. M. Kier, eds. Smithsonian Institute Press, Washington DC.

Henry, J. J., G. A. Wray, and R. A. Raff. 1991. Mechanism of an alternate type of echinoderm blastula formation: the wrinkled blastula of the sea urchin *Heliocidaris erythrogramma*. *Dev. Growth Differ.* **33:** 317–328.

Hyman, L. H. 1955. *Echinodermata: The Invertebrates*, Vol. 4. McGraw-Hill, New York. 763 pp.

Irimura, S. 1981. Ophiurans from Tanabe Bay and its vicinity, with the description of a new species of *Ophiocentrus*. *Publ. Seto Mar. Biol. Lab.* **26:** 15–49.

Irimura, S., T. Fujita, and R. Ueshima. 2001. Preliminary report on the ophiuroids (Echinodermata) on the shelf off Shimoda, south of Izu Peninsula, central Japan (in Japanese with English summary). *Mem. Natl. Sci. Mus. (Tokyo)* **37:** 311–315.

Koehler, R. 1904. Ophiures nouvelles ou peu connues. *Mem. Soc. Zool. Fr.* **17:** 70–71.

Koehler, R. 1905. Ophiures littorales. *Siboga Exped. Monogr.* **45(b):** 1–142.

Komatsu, M., Y. T. Kano, and C. Oguro. 1990. Development of a true ovoviviparous sea star, *Asterina pseudoexigua pacifica* Hayashi. *Biol. Bull.* **179:** 254–263.

Komatsu, M., M. Sewell, S. F. Carson, and Fu-Shiang Chia. 2000. Larval development and metamorphosis of the sea star *Luidea foliolata* (Echinodermata: Asteroidea). *Species Diversity* **5:** 155–162.

Lawrence, J. M. 1987. *A Functional Biology of Echinoderms*. Croom Helm, London, 340 pp.

MacBride, E. W. 1907. The development of *Ophiothrix fragilis*. *Q. J. Microsc. Sci.* **51:** 557–606.

Mladenov, P. V. 1979. Unusual lecithotrophic development of the Caribbean brittle star *Ophiothrix oerstedi*. *Mar. Biol.* **55:** 55–62.

Mladenov, P. V. 1985. Development and metamorphosis of the brittle star *Ophiocoma pumila*: evolutionary and ecological implications. *Biol. Bull.* **168:** 285–295.

Mortensen, T. 1933. Papers from Dr. Th. Mortensen's Pacific Expedition 1914–16. LXIII. Biological observations on ophiuroids, with descriptions of two new genera and four new species. *Vidensk. Medd. Dan. Naturhist. Foren.* **93:** 171–194.

Mortensen, T. 1936. Echinoidea and Ophiuroidea. *Discov. Rep.* **12:** 199–348.

Narasimhamurti, N. 1933. The development of *Ophiocoma nigra*. *Q. J. Microsc. Sci.* **76:** 63–88.

O'Loughlin, P. M. 2001. The occurrence and role of a digitate genital papilla in holothurian. Pp. 363–368 in *Echinoderms 2000*, M. Barker, ed. Swetz and Zeitlinger, Lisse, The Netherlands.

Olsen, H. 1942. Development of the brittle-star *Ophiopholis aculeata* (O. Fr. Müller) with a short report on the outer hyaline layer. *Bergens Mus. Årbok. Naturvid.* **6:** 1–107.

Selvakumaraswamy, P., and M. Byrne. 2000. Vestigial ophiopluteal structures in the lecithotrophic larvae of *Ophionereis schayeri* (Ophiuroidea). *Biol. Bull.* **198:** 379–386.

Stöhr, S. 2001. *Amphipholis linopneusti* n. sp., a sexually dimorphic amphiurid brittle star (Echinodermata: Ophiuroidea), epizoic on a spatangoid sea urchin. Pp. 317–322 in *Echinoderms 2000*, M. Barker, ed. Swets and Zeitlinger, Lisse, The Netherlands.

Strathmann, R. R., and S. S. Rumrill. 1987. Phylum Echinodermata, class Ophiuroidea. Pp. 556–573 in *Reproduction and Development of Marine Invertebrates of the Northern Pacific Coast*, M. F. Strathmann, ed. University of Washington Press, Seattle.

Tominaga, H. 2001. The early development of the brittle star, *Ophiodaphne formata* (Koehler). P. 327 in *Echinoderms 2000*, M Barker, ed. Swets and Zeitlinger, Lisse, The Netherlands.

Tyler, A., and B. S. Tyler. 1966. The gametes: some procedures and properties. P. 642 in *Physiology of Echinodermata*, R. A. Boolootian, ed. Interscience Publishers, New York.

Yamashita, M. 1985. Embryonic development of the brittle-star *Amphipholis kochii* in laboratory culture. *Biol. Bull.* **169:** 131–142.

Reference: *Biol. Bull.* **206:** 35–45. (February 2004)
© 2004 Marine Biological Laboratory

Waveform Dynamics of Spermatozeugmata During the Transfer From Paternal to Maternal Individuals of *Membranipora membranacea*

M. H. TEMKIN[1,*] AND S. B. BORTOLAMI[2]

[1] *Biology Department, St. Lawrence University, Canton, New York 13617; and* [2] *Ashton Graybiel Spatial Orientation Laboratory, Brandeis University, Waltham, Massachusetts 02254*

Abstract. Analysis of standard (60 frames/s) and high-speed (200 frames/s) video records revealed that unencapsulated sperm aggregates (spermatozeugmata) of the gymnolaemate bryozoan *Membranipora membranacea* spontaneously generate at least three types of waveforms: small amplitude, large amplitude, and reverse. All three waveforms significantly differed from one another in amplitude. Additionally, small- and large-amplitude waveforms propagated from the base to the tip of axonemes, whereas the reverse waveform propagated from the tip to the base of axonemes. Small-amplitude waveforms, which were generated most frequently by spermatozeugmata in the paternal perivisceral coelom and in the water column after spawning, produced almost no curvature of the axoneme. Large-amplitude waveforms were produced by spermatozeugmata in the water column and within lophophores. Reverse waveforms were produced while spermatozeugmata moved tail-end forward through the paternal tentacles during spawning and after spermatozeugmata had contacted the intertentacular organ (ITO), a tubular structure that spermatozeugmata pass through to enter the maternal coelom and that eggs pass through to enter the seawater. The production of reverse waveforms by spermatozeugmata after reaching the ITO may be evidence for a behavioral response of bryozoan sperm to conspecific maternal individuals.

Introduction

Fertilization success for many benthic marine invertebrates is dependent on the transfer of sperm or an aggregate of sperm from males to females through the water column (see Franzén, 1956, 1998; Ryland and Bishop, 1993). Sperm aggregates may be either encapsulated (spermatophores) or unencapsulated (spermatozeugmata). The transfer of sperm, spermatophores, or spermatozeugmata from male to female conspecific benthic marine invertebrates may be influenced by numerous physical and biological factors. For example, water flow, population density, spawning synchrony, sperm chemoattractants, gamete longevity, and sperm motility are all factors that have been reported to increase or decrease fertilization success by altering the probability that sperm will find maternal individuals (see Ryland and Bishop, 1993; Levitan, 1995).

In species that transfer sperm from males to females through the water column, fertilization success may ultimately depend on sperm motility and behavior once a conspecific female has been approached or contacted. For example, sperm become attached to external maternal structures where they wait for eggs to be spawned, as in some sabellid polychaetes (*e.g.*, Daly and Golding, 1977; Rouse, 1996) and some bivalves (*e.g.*, Ó Foighil, 1985, 1989). In other species, sperm enter maternal individuals to fuse with eggs internally, as in some hydroids (see Miller, 1983), the sea cucumber *Leptosynapta clarki* (Sewell and Chia, 1994), the colonial ascidian *Diplosoma listerianum* (Bishop and Ryland, 1991; Burighel and Martinucci, 1994a, b), phoronids (see Zimmer, 1991), and the gymnolaemate bryozoan *Membranipora membranacea* (Temkin, 1994). Yet few observations have been made on how sperm attach to or enter conspecific females, or on how sperm locate eggs prior to fertilization.

Among gymnolaemate bryozoans, one of the most detailed descriptions of sperm transfer has been reported for *Membranipora membranacea* (Temkin, 1994). Zooids of

---

Received 12 September 2003; accepted 3 November 2003.

* To whom correspondence should be addressed. E-mail: mtemkin@stlawu.edu

Abbreviation: ITO, intertentacular organ.

M. membranacea colonies typically are functionally simultaneous hermaphrodites, and sperm in spermatozeugmata are transferred from paternal to maternal zooids through the water column (Temkin, 1994). Like those of other gymnolaemate bryozoans, the spermatogonia of *M. membranacea* migrate into the perivisceral coelom from the peritoneum of the body wall, or funiculus (a network of strand-like elements of the circulatory system), and form syncytial masses of spermatocytes around cytoplasmic masses or cytophores (see Reed, 1991; Franzén, 1998). Cells of a cytophore disassociate at the end of spermiogenesis in most gymnolaemates, but in species such as *M. membranacea*, sperm remain together, adhering to one another to form a spermatozeugma.

Gymnolaemate spermatozeugmata are aggregates of 32 or 64 euspermatozoa in which the cells are arranged parallel to one another in a hexagonal array, with all the heads at one end of the aggregate and all of the tails at the other (Bonnevie, 1907; Franzén, 1956, 1998; Zimmer and Woollacott, 1974) (Fig. 1). Spermatozeugmata of gymnolaemate bryozoans are held together by viscomechanical forces that tightly adhere sperm to one another along the head region, the tail-end half of the midpiece region, and almost all of the tail region (see Franzén, 1956, 1998; Temkin, 1994). The two regions of a spermatozeugma where sperm do not adhere to each other are the head-end half of the midpiece and the tip of the tail (Fig. 1).

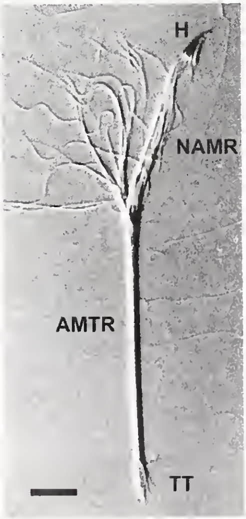

Figure 1. Differential interference contrast image of a partially disassociated spermatozeugma adhering to a glass slide. The head-end half of the spermatozeugma consists of the elongate head regions (H) that are adhering to one another and the nonadhering portions of the midpiece regions (NAMR). The tail-end half consists of the adhering portions of the midpiece and tail regions (AMTR) and the tips of the tails (TT). Sperm that have become partially disassociated from the aggregate generate a variety of waveforms. Scale bar = 12 μm.

Sperm of *M. membranacea* within spermatozeugmata generate waveforms, and movements of the midpiece regions may produce some of the motive forces required for both spawning and entry into maternal individuals (Temkin, 1994). Spermatozeugmata of *M. membranacea* are motile in the paternal coelom, like sperm of other gymnolaemate bryozoans (Marcus, 1938; Silén, 1966; Zimmer and Woollacott, 1974; Temkin, 1994). Prior to spawning, spermatozeugmata of *M. membranacea* become positioned in the perivisceral coelom between the body wall and the distomedial side of the pharynx, so that their tail ends are oriented toward the pore leading into the lophophoral coelom of the two distomedial tentacles (Temkin, 1994). Cilia located near the pore may help spermatozeugmata enter the lophophoral coelom of the distomedial tentacles (R. Zimmer, University of Southern California, pers. comm.). Spermatozeugmata move through the two distomedial tentacles, emerging tail-end first into the exhalant feeding currents of colonies. During their passage through the tentacle lumen, spermatozeugmata appeared to be pushed by waveforms produced in the midpiece region (Temkin, 1994).

In the laboratory, spermatozeugmata become quiescent after they are spawned, until they are drawn into the lophophores of conspecifics by colony feeding currents (Temkin, 1994). Spermatozeugmata retained within the lophophores of conspecifics often produce strong undulatory movements in the midpiece region (Temkin, 1994). While in the lophophore, spermatozeugmata may move headfirst into maternal individuals through the intertentacular organ (ITO). The ITO is a tubular secondary sex structure formed by the basal fusion of the two distomedial tentacles (see Silén, 1966; Reed, 1991). The ITO serves not only as the entry organ for spermatozeugmata, but also as the spawning organ for eggs (*e.g.*, Silén, 1966; Temkin, 1994). Temkin (1994) reported that spermatozeugmata that entered the distal pore of the ITO appeared to stop their undulatory movements and were drawn into the ITO. After entering maternal individuals, sperm of a spermatozeugma disassociate and migrate to the surface of the ovary, although the exact sequence of these two events is uncertain. In *M. membranacea*, sperm-egg fusion occurs during or shortly after ovulation and is monospermic (Temkin, 1994).

In this paper, we compare the waveforms generated by spermatozeugmata of *M. membranacea* within the paternal coeloms (perivisceral and lophophoral), in seawater after spawning, and within the lophophores of conspecifics. We describe three types of waveforms (small amplitude, large amplitude, and reverse) that are spontaneously generated by spermatozeugmata of *M. membranacea* during the transfer of aggregates from paternal to maternal zooids. In addition, we relate the functional significance of the waveforms to the structure of spermatozeugmata and to sperm transfer.

Materials and Methods

Colonies of *Membranipora membranacea* Linnaeus, 1767, were collected from waters near the Friday Harbor Laboratories (FHL), San Juan Island, Washington, and the Darling Marine Center (DMC), Walpole, Maine (for a phylogeographic analysis of these populations, see Schwaninger, 1999). The movements of spermatozeugmata within paternal coeloms, in seawater after spawning, and within the tentacle crown of maternal lophophores were videorecorded. Videorecordings were made using Panasonic cameras (60 frame/s) mounted on either Zeiss (FHL) or Olympus (DMC) research compound microscopes. Some *M. membranacea* colonies collected at the DMC were transported to Harvard University, where videorecordings were made using an NAC HSV-200 video camera (200 frames/s) mounted on a Zeiss Photo III compound microscope. To view spermatozeugmata within paternal coeloms and maternal lophophores, we examined "one-zooid-row" preparations that were placed on their sides in small petri dishes (Temkin, 1994). To make recordings of spermatozeugmata outside of the paternal coelom (seawater), individual spermatozeugma that had been recently spawned were removed from dishes containing one-zooid-row preparations and placed in depression slides containing 50 to 100 μl of 0.2-μm-filtered seawater (FSW) at room temperature.

Recorded sequences were viewed frame by frame to analyze the waveforms produced by spermatozeugmata during each trial. Waveforms produced by spermatozeugmata were distinguished based on waveform amplitude and direction of waveform propagation. The amplitudes of 10 waves for each of the three recognized waveforms were determined using the computer program Image Tool ver. 3.00 (University of Texas, http://ddsdx.uthscsa.edu/dig/itdesc.html), calibrated with an image of a stage micrometer, to measure digitized images of high-speed video frames. Systat 6 was used to calculate an analysis of variance (ANOVA), and Bonferroni adjusted pairwise comparisons were made to determine statistical differences among waveform amplitudes. The frequency of wave generation was measured in 25 reverse-waveform events for spermatozeugmata within the paternal coelom and calculated as the number of waves per second. In addition, waveform patterns generated by DMC spermatozeugmata in the paternal visceral coelom (n = 10) and in seawater after spawning (n = 10) were compared by determining the frequency and duration of reverse-waveform events. To be included in the comparison, spermatozeugmata had to have a video record of at least 20 s. Event frequencies were calculated as the number of waveform events per minute. Durations of reverse-waveform events during an individual trial were averaged. Two-sample t tests were calculated using Systat 6 to compare the frequencies and durations of reverse-waveform events between spermatozeugmata in the paternal coelom and water column.

Results

Waveform types

Spermatozeugmata of *Membranipora membranacea* from both the DMC and FHL generated three types of waveforms: small amplitude, large amplitude, and reverse. The amplitudes of these waveforms were greatest in the nonadhering portions of the midpiece regions of spermatozeugmata. The adhering portions of the midpiece and tail regions showed no apparent curvature during the generation of any of the three waveforms (Figs. 2, 3, and 4). An ANOVA and pairwise comparisons of means revealed that the amplitudes of the three waveforms significantly differed from one another (Table 1). Small-amplitude waveforms consisted of waves with amplitudes of 1.9 ± 1.6 μm (mean ± standard deviation, n = 10) that were generated from the base to the tip of axonemes (*i.e.*, head to tail). Sperm within a spermatozeugma typically produced small-amplitude waveforms asynchronously. Consequently, small-amplitude waveforms were difficult to observe unless sperm in an aggregate produced this type of waveform synchronously (Fig. 2). Small-amplitude waveforms produced almost no curvature in spermatozeugmata as waves moved along axonemes. Large-amplitude waveforms also propagated from the base to the tip of axonemes (Fig. 3), with amplitudes of 11.1 ± 3.0 μm (n = 10). During the generation of large-amplitude waveforms, spermatozeugmata undulated and rotated around their long axis. Reverse waveforms had amplitudes of 7.0 ± 2.4 μm (n = 10) and propagated from the tip to the base of axonemes (*i.e.*, tail to head) (Figs. 4 and 5); that is, reverse waveforms were propagated along the axoneme in a direction opposite to that of small- and large-amplitude waveforms. During reverse-waveform events in the paternal visceral coelom, waves were generated with a frequency of 11.0 ± 0.5 waves/s (n = 25). The generation of reverse waveforms was distinguished by the development of prominent bends near the junctions of (1) the heads and midpieces and (2) the nonadhering and adhering portions of midpieces (Figs. 4 and 5). The curvature in the anterior portions of a spermatozeugma during a reverse-waveform event causes the aggregate to bend over, giving a spermatozeugma the distinctive appearance of a question mark.

Location-specific waveform generation

Spermatozeugmata generated different patterns of waves depending on whether they were located in the paternal coeloms (visceral and lophophoral), water column, or ma-

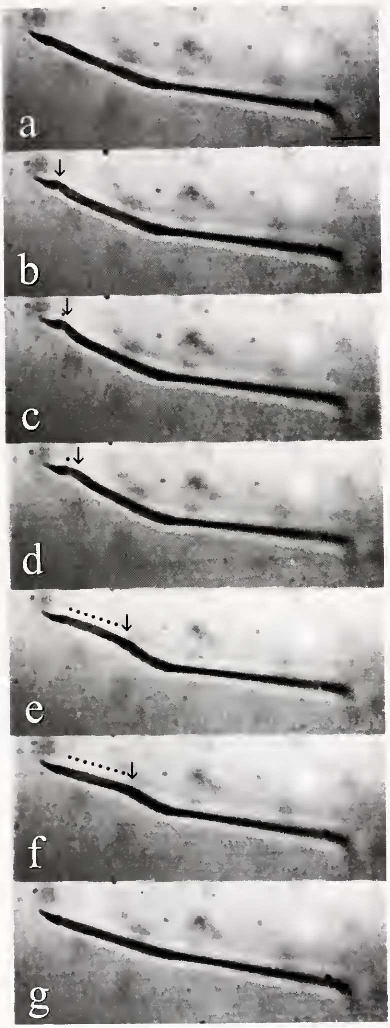

Figure 2. Synchronous production of a type I waveform by *Membranipora membranacea* spermatozeugma in seawater after spawning. (a) Asynchronous waveform production. (b–f) Propagation of wave (arrow) from the base to tip of axonemes. (g) Wave enters region of midpiece in which sperm are tightly adherent to each other and is no longer visible. Images are 10 ms apart. Dots indicate the propagation of the wave along the aggregate. The first dot in each series marks the position of the wave in (b). Scale bar = 30 μm.

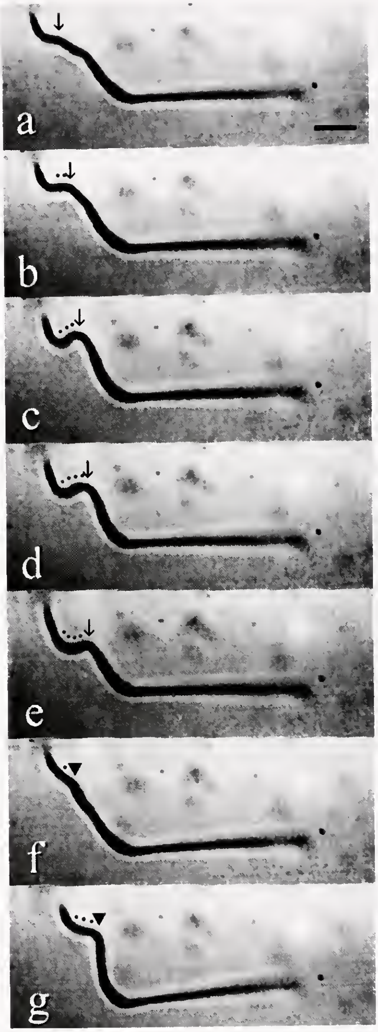

Figure 3. Generation of a type II waveform by *Membranipora membranacea* spermatozeugma in seawater after spawning. (a) A wave (arrow) forming just posterior to the heads. (b–e) The wave (arrow) propagating toward the tail end of the aggregate. (f, g) Generation of a second wave (arrowhead) after the first wave is no longer visible. Dots indicate the propagation of first wave along the aggregate. Images are 10 ms apart. Scale bar = 30 μm.

ternal lophophore. In the paternal visceral coelom and water column, spermatozeugmata generated predominantly the small-amplitude waveform, with periodic reverse-waveform events. Spermatozeugmata in the water column also sporadically generated a short series of large-amplitude waveforms. Two-sample *t* tests revealed significant differ-

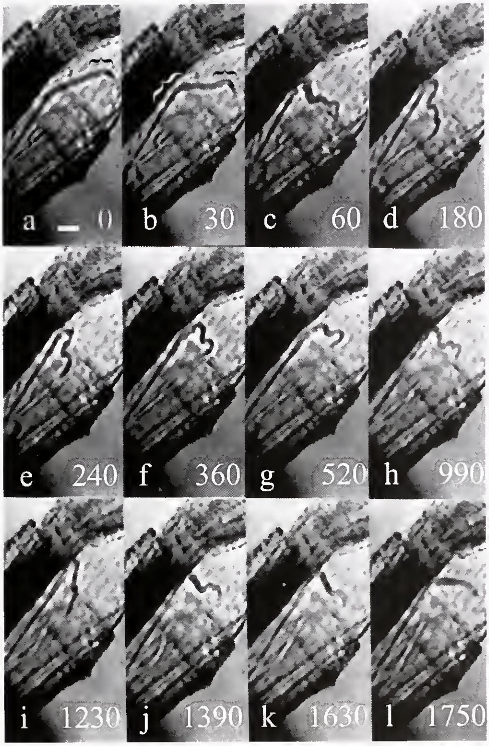

Figure 4. Variation in the conformation of a *Membranipora membranacea* spermatozeugma within paternal coelom during a 1750-ms reverse-waveform event. Values in lower right-hand corner of each image show elapsed time, from 0 to 1750 ms. (a, b) During the initiation of a reverse-waveform event, the spermatozeugma develops strong curvature near the junction of the heads and midpieces (black bracket) and near the junction of the nonadhering and adhering portions of the midpieces (white bracket). (c–j) Production of reverse waveforms bends the spermatozeugma into the shape of a cane or question mark. (k, l) Spermatozeugma returns to generating type I waveforms and a nearly linear conformation. Scale bar = 25 μm.

ences in the event frequencies (df = 18, $t = -3.04$, $P < 0.001$) and durations (df = 18, $t = -2.11$, $P < 0.05$) of reverse-waveform events between spermatozeugmata in the paternal visceral coelom and ones in the water column (Fig. 6). The reverse waveform was produced almost twice as often by spermatozeugmata in the paternal visceral coelom ($n = 10$, 9.4 ± 0.7 events/m) as by spermatozeugmata in the water column ($n = 10$, 5.6 ± 1.0 events/min). In addition, reverse-waveform events lasted about 1.5 times longer for spermatozeugmata in the paternal visceral coelom ($n = 10$, 0.94 ± 0.10 s) than for those in the water column ($n = 10$, 0.64 ± 0.11 s). During the production of reverse waveforms in the paternal perivisceral coelom and in seawater after spawning, spermatozeugmata were not observed to move in either a head-forward or a tail-forward direction.

Spermatozeugmata spent about 2.0 s in the lophophoral coelom during spawning. While traveling through the two distomedial tentacles into the external seawater, they generated reverse waveforms (Fig. 7). One sperm aggregate stopped producing the reverse waveform as it emerged from the tentacle and remained with its head end within the lophophoral coelom of the tentacle for about 10 s until reverse waveforms were generated again. With resumption of reverse-waveform production, the spermatozeugma pushed itself out of the tentacle.

Spawned spermatozeugmata were commonly swept into the lophophores of conspecifics by feeding currents. Most spermatozeugmata passed quickly through the lophophores without altering their waveform dynamics. However, when spermatozeugmata remained within the lophophores, they typically produced large-amplitude or reverse waveforms either continuously or periodically. Many of the spermatozeugmata generating large-amplitude waveforms escaped from the lophophores into the exhalant current of colonies. Spermatozeugmata generating large-amplitude waveforms were able either to swim directly out of the lophophores or to enter into the exhalant current stream of the lophophores. In one case, a spermatozeugma generating large-amplitude waveforms moved from the pharynx of a zooid, out through the mouth, and back into the lophophore. In other cases, spermatozeugmata within lophophores became positioned with their head ends at the distal pore of the ITO. Once their head ends contacted the distal surface of the ITOs, the

Table 1

Summary of statistical tests to determine differences among waveform amplitudes

Analysis of variance

Source	Sum-of-squares	df	Mean-square	F-ratio	P
Waveform type	399.29	2	199.64	34.60	0.000
Error	155.82	27	5.77		

Matrix of pairwise mean differences (below diagonal) and probabilities (above the diagonal)*

Waveform type	Small	Large	Reverse
Small		0.000	0.000
Large	8.9		0.003
Reverse	4.9	−4.0	

* Mean differences calculated using a mean squared error (MSE) model of 5.77 with 27 degrees of freedom; probabilities calculated using a Bonferroni adjustment.

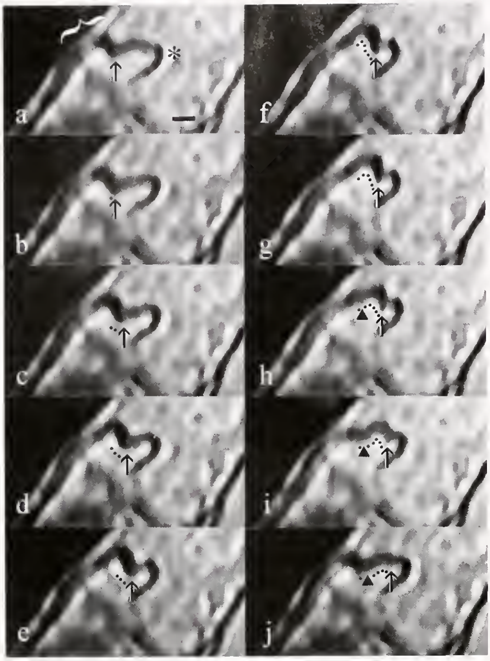

Figure 5. Propagation of reverse waveforms along the axonemes from the tips to the bases in a *Membranipora membranacea* spermatozeugma within the paternal coelom. Images are 10 ms apart. (a–j) The movement of a reverse waveform (arrow) from the midpoint of the nonadhering midpiece region toward the head end of the spermatozeugma. The white bracket and * in (a) indicate the curvature of the spermatozeugma occurring near the junction of the nonadhering and adhering portions of the midpieces and posterior to the heads, respectively. (h–j) A second wave (black arrowhead) becomes apparent and propagates toward the head end of the aggregate. The first dot of each tracking line indicates the original position of the first wave in (a). Scale bar = 20 μm.

spermatozeugmata altered their waveform dynamics to generate reverse waveforms within about 100 ms and attempted to enter the ITOs. The production of reverse waveforms bent the head ends of the spermatozeugmata toward the distal pore of the ITO (Fig. 8). Spermatozeugmata could not be observed after they entered ITOs because of cilia that line the lumen of the ITO. Consequently, we could not determine the waveforms produced by spermatozeugmata inside of ITOs.

To determine if the change from small-amplitude or large-amplitude waveform to reverse waveform after a spermatozeugma contacted an ITO was simply a touch response, the waveform dynamics of 25 spermatozeugmata were observed before and after they contacted a glass surface. In 18 cases, spermatozeugmata were producing a small-amplitude waveform when they contacted the substrate. Seventy-eight percent (14 of 18) of these spermatozeugmata continued to generate a small-amplitude waveform or a small-amplitude waveform with periodic reverse-waveform events. The remaining 22% (4 of 18) initially continued to produce a small-amplitude waveform, but later changed to reverse waveforms. Seven spermatozeugmata contacted the substrate during a reverse-waveform event, and all of them continued to generate reverse waveforms. Consequently, the change in waveform does not seem to be simply a touch response.

Discussion

Spermatozeugmata develop in a group of animals that is diverse in phylogeny and reproductive biology. For example, in addition to occurring in bryozoans, spermatozeugmata have been reported in marine and freshwater oligochaetes (see Ferraguti, 1983), gastropods (see Buckland-Nicks *et al.*, 1999, 2000), marine and freshwater bivalves (*e.g.*, Ó Foighil, 1985, 1989; Lynn, 1994; Jespersen *et al.*, 2001, 2002), insects (*e.g.*, Sahara and Kawamura, 2002), and fish (see Jamieson, 1991; Hayakawa *et al.*, 2002a). Marine and freshwater bivalves and some fish are similar to gymnolaemate bryozoans in that they spawn their spermatozeugmata into the water column. Gastropods, insects, and most fish transfer their spermatozeugmata directly from the male into the female reproductive tract using a form of copulation. Oligochaetes use a mechanism of pseudocopu-

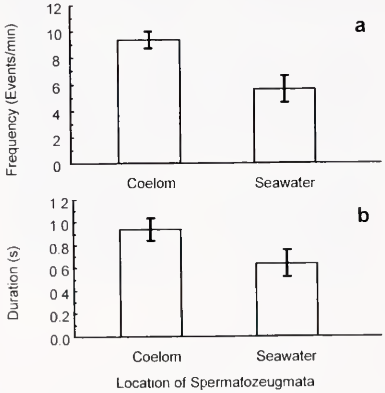

Figure 6. Event frequency (a) and duration (b) of reverse waveforms produced by *Membranipora membranacea* spermatozeugma within the paternal coelom ($n = 10$) and seawater ($n = 10$). Two sample t tests demonstrate that spermatozeugmata within the paternal coelom produce significantly more (df = 18, $t = -3.04$, $P < 0.001$) and longer (df = 18, $t = -2.11$, $P < 0.05$) reverse waveform events than spermatozeugmata in seawater.

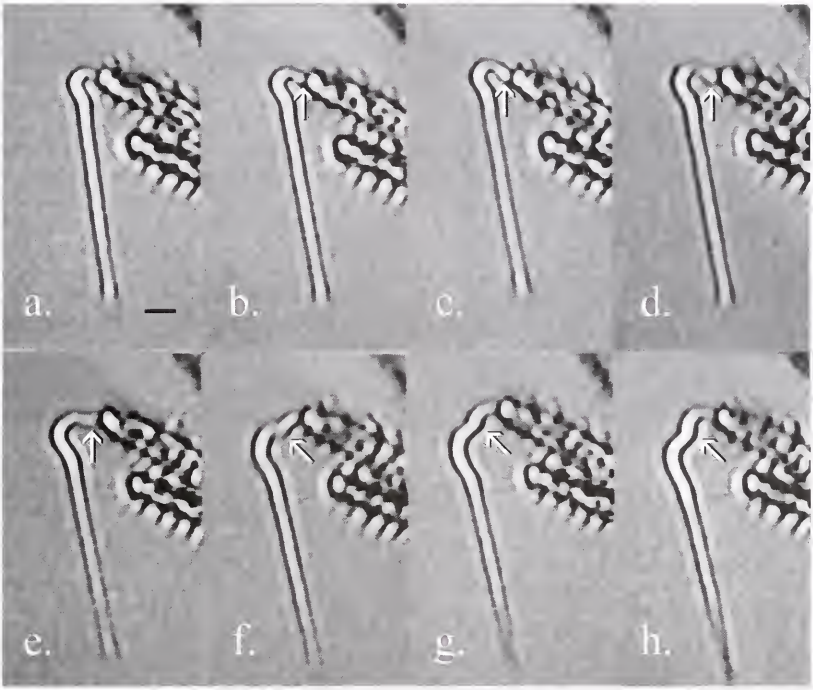

Figure 7. Spermatozeugma of *Membranipora membranacea* crawling out of a paternal tentacle tail-end forward by producing a reverse waveform. Images are 20 ms apart. Arrows indicate the position of the wave along the aggregate. Scale bar = 20 μm.

lation to deliver spermatozeugmata to the spermatheca of mating partners. The spermatozeugmata produced by many species of marine and freshwater oligochaetes, marine bivalves, gastropods, insects, and fish differ from the sperm aggregates of *Membranipora membranacea* in that they consist of dimorphic sperm (*e.g.*, Ferraguti *et al.*, 1989; Healy and Jamieson, 1993; Buckland-Nicks *et al.*, 2000; Jespersen *et al.*, 2001, 2002; Hayakawa *et al.*, 2002a; Sahara and Kawamura, 2002). One type of sperm, euspermatozoa, fertilizes eggs; the other type, paraspermatozoa, does not fuse with eggs, but instead is thought to enhance the fertilization success of euspermatozoa through a variety of mechanisms, including preventing sperm from other conspecific males from fertilizing eggs (see Buckland-Nicks *et al.*, 1999; Hayakawa *et al.*, 2002b; Sahara and Kawamura, 2002).

The production of spermatozeugmata by *M. membranacea* may increase fertilization success in three ways. First, "packaging" sperm together may reduce the loss of sperm during the transfer from paternal to maternal individuals (*e.g.*, Braidotti and Ferraguti, 1982; Ó Foighil, 1989; Lynn, 1994; Jespersen and Lutzen, 2001; Hayakawa *et al.*, 2002b). Among gymnolaemate bryozoans, *M. membranacea* has an uncommon reproductive biology (see Reed, 1991; Temkin and Zimmer, 2002). In most gymnolaemate bryozoans, the maternal zooids produce only one or a few eggs during each reproductive period; these are spawned to an external brood site, where they develop into lecithotrophic larvae, either coronate or pseudocyphonautes. In contrast, maternal zooids in species of *Membranipora* and *Electra*, as well as some species of *Alcyonidium*, *Farella*, and *Hypophorella*, produce many small, yolk-poor oocytes that are spawned into the water column, where they develop into planktotrophic cyphonautes. In *M. membranacea*, the synchronous development of groups of oocytes may result in the presence of as many as 25 ovulated primary oocytes in the perivisceral coelom at one time (Hageman, 1983). Consequently, the maternal zooids of *M. membranacea* likely need to acquire more sperm than most gymnolaemate bryozoans to fertilize their eggs. By transferring aggregates of sperm, the entry of one spermatozeugma into a maternal zooid delivers 64 sperm cells. In other gymnolaemate spe-

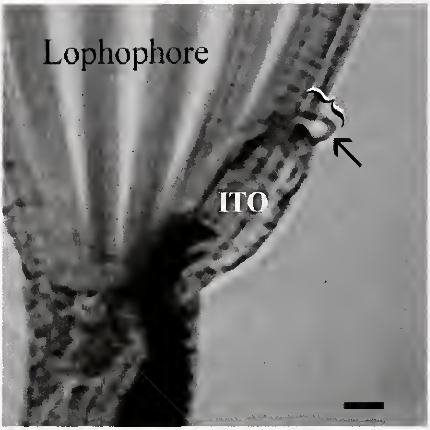

Figure 8. Spermatozeugma of *Membranipora membranacea* generating reverse waveforms after contacting the distal surface of an intertentacular organ (ITO) of a maternal individual. The anterior portion of the spermatozeugma (arrow) is projecting out of the lophophore between the two distomedial tentacles. The head end of the aggregate is in contact with the distal surface of the ITO. The anterior end of the spermatozeugma is strongly curved (bracket) due to the generation of reverse waveforms. As a result of the bend in the anterior portion of the aggregate, the spermatozeugma is able to enter the distal pore of the ITO. Scale bar = 50 μm.

cies that may face similar pressures to fertilize their eggs, spermatozeugmata occur in species of *Electra,* but have not yet been reported for species of *Alcyonidium, Farella,* and *Hypophorella.*

Second, the formation of spermatozeugmata has been suggested to increase fertilization success by increasing sperm longevity (Lynn, 1994). Currently, there are few data with which to assess the importance of spermatozeugmata on the longevity of bryozoan sperm after spawning. Manríquez *et al.* (2001) reported that the fertile half life of spawned *Celleporella hyalina* sperm at a concentration of 10 to 10^2 cells ml^{-1} was about 1.2 h. In another study, spermatozeugmata of *M. membranacea* were observed to remain motile for 36 h, although the ability of these sperm to fertilize eggs was not determined (Temkin, 1991).

Third, in some species, the formation of spermatozeugmata facilitates fertilization success by enhancing sperm motility. In organisms with dimorphic sperm, motile paraspermatozoa may transport euspermatozoa to sites of fertilization in oligochaetes and some gastropods (Ferraguti *et al.*, 1988; see Buckland-Nicks *et al.*, 2000). In contrast, the flagellar beat of euspermatozoa generates the motility associated with the spherical spermatozeugmata of the bivalve *Anodonta grandis* (Lynn, 1994). The movements of euspermatozoa contained within spermatozeugmata of *M. membranacea* are restricted because cells are bound together along most of their lengths by viscomechanical forces. The adherence of sperm to one another within a spermatozeugma of *M. membranacea* establishes a structural and functional division of the aggregate into head and tail halves. The head-end half consists of the head regions that are tightly adherent to each other and the nonadhering portions of the midpiece region. The head-end half is the region of a spermatozeugma in which waveforms achieve their greatest amplitude and where the aggregate undergoes conformational changes that create a strong curvature during the production of waveforms generated from the tip to the base of axonemes (*e.g.*, during reverse-waveform events). The tail-end half of a spermatozeugma forms a stiffened, rodlike region consisting of the adhering portions of the midpiece and tail regions. In fact, no discernible curvature was observed during the generation of any waveform in the tail-end half of spermatozeugmata during this study. Consequently, the forces that move spermatozeugmata of *M. membranacea* appear to be generated in the head-end half of the aggregates rather than along the entire length of the midpiece and tail regions.

Sperm in spermatozeugmata of *M. membranipora* may generate at least four types of waveforms. Here, we observed the spontaneous generation of three waveforms: small amplitude, large amplitude, and reverse. A fourth waveform type, in which the head-end halves of spermatozeugmata produce an effective stroke-recovery stroke movement similar to that of a cilium, can be induced by placing spermatozeugmata in seawater containing elevated levels of either Ca^{2+} or K^+ (Temkin, 2002). During small- and large-amplitude waveform events, waveforms are generated from the base to the tip of axonemes. In contrast, during reverse and cilium-like movements, waveforms are generated from the tip to the base of axonemes.

Modulating the direction of waveform propagation along the axoneme is a rare phenomenon among animal sperm (Afzelius, 1982; Baccetti *et al.*, 1989). The ability to naturally reverse the direction of waveform propagation has been reported for the sperm of the polyclad turbellarians *Notoplana atomata, Polyposthia similis,* and *Leptoplana tremellaris* (Hendelberg, 1965, 1983), the parasitic polychaete *Myzostomum cirriferum* (Afzelius, 1982, 1983), and the tephritid flies *Ceretitis capitata, Dacus oleae,* and *D. dorsalis* (Baccetti *et al.*, 1989). Among these organisms, modulating the direction of waveform propagation is not specific to any one organization of the axoneme or mode of sperm transfer. The sperm of *M. membranacea* have a 9 + 2 axoneme (Zimmer and Woollacott, 1974) and are transferred to maternal individuals through the water column aggregated into spermatozeugmata. The threadlike sperm of *N. atomata, P. similis,* and *L. tremellaris* contain two 9 + 1 axonemes and are copulated directly into the reproductive tract of females (Hendelberg, 1965, 1983). In *M. cirriferum,* sperm have a 9 + 0 axoneme and are packaged into spermatophores that are reciprocally transferred to the epidermis of hermaphroditic partners (Afzelius, 1983). The sperm of tephritid flies have a 9 + 9 + 2 axoneme and are directly copulated into the female reproductive tract as spermatodesmata, aggregates partially encapsulated around the head ends of the sperm (Baccetti *et al.*, 1989).

In *M. membranacea,* the motility of a spermatozeugma is dependent on the synchronous generation of waveforms by most sperm of the aggregate. At spawning, spermatozeugmata move through the paternal tentacles tail-end first, generating reverse waveforms that are translated along axonemes from tip to base. To explain how spermatozeugmata move through tentacles during spawning, we propose a crawling model. While in the tentacle lumen, spermatozeugmata generate reverse waveforms that push against the internal walls of the tentacles (Fig. 9). As reverse waveforms are generated from the tip to the base of the axoneme, spermatozeugmata move in a tail-forward direction. Since the generation of reverse waveforms did not seem to move spermatozeugmata in the paternal perivisceral coelom or in seawater, contact with a surface may be important for the effectiveness of reverse waveforms in moving spermatozeugmata. In contrast, generation of large-amplitude waveforms and cilium-like movements propels spermatozeugmata with the head-end forward without needing to push against a surface (Temkin, 2002). It seems likely that the generation of either large-amplitude waveforms or cilium-like movements pulls spermatozeugmata into ITOs. During this process, the adhering portions of the midpiece and tail appear rigid, which may have caused Temkin (1994) to report that the undulatory movements of spermatozeugmata stop after the head ends enter the ITO. The actual waveforms used by *M. membranacea* spermatozeugmata after entering ITOs remain to be determined, because the view of spermatozeugmata inside an ITO is obscured by the cilia that line the lumen of the organ.

The waveform patterns generated by sperm of *M. membranacea* in spermatozeugmata change after spawning into seawater. Temkin (1994) reported that spermatozeugmata seemed to become quiescent shortly after spawning. Unlike the quiescence of sea urchin (Gibbons, 1980), tunicate (Brokaw, 1984), and polychaete (Pacey *et al.*, 1994) sperm, in which the beat of the flagellum ceases, the apparent quiescence in *M. membranacea* spermatozeugmata is caused by the decrease in the frequency and duration of reverse waveforms after spermatozeugmata enter the water column. Evidence for a similar change in waveform dynamics for spermatozeugmata of *Electra pilosa* may be contained in a paper by Marcus (1926). Marcus (1926) reported that sperm of *E. pilosa* became immobile and died shortly after being transferred into seawater. Decreasing the frequency and duration of reverse-waveform events after spawning may allow spermatozeugmata to conserve energy and may increase the longevity of sperm in the water column. Ho and Suarez (2003) have shown that increases in wave amplitude in bull sperm require increases in ATP consumption. Since small-amplitude waveforms produce almost no curvature of the axoneme compared to large-amplitude and reverse waveforms, small-amplitude waveforms may require less energy to produce than the other waveforms. In *M. membranacea,* the actual consumption of ATP by spermatozeugmata inside and outside of the paternal visceral coelom remains to be determined.

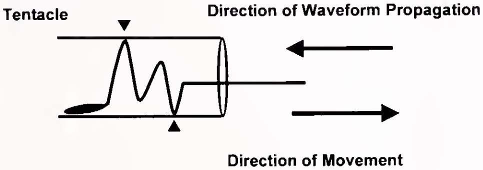

Figure 9. Model of spermatozeugma crawling tail-end forward through paternal tentacle during spawning. In the diagram, a spermatozeugma is moving from left to right. Reverse waveforms are being generated from the tip to the base of axonemes. Reverse waveforms push against the inner walls of the tentacle (arrowheads) and move the spermatozeugma tail-end forward.

In *M. membranacea,* spermatozeugmata also generate reverse waveforms after contacting an ITO. The ITO is oriented with its distal pore directed away from the funnel of the lophophore. Consequently, spermatozeugmata within lophophores cannot be oriented to enter maternal individuals unless they develop a bend. A spermatozeugma undergoing a reverse-waveform event develops a strong conformational change that curves the head end of an aggregate relative to its long axis. This conformation change bends the spermatozeugma toward the distal pore of the ITO. Once the head end of a sperm aggregate is inside an ITO, the spermatozeugma likely changes its waveform dynamics to generate a waveform that pulls it forward.

The generation of reverse waveforms by a spermatozeugma of *M. membranacea* after contacting an ITO may be a response to a substance either on the distal surface or emanating from the pores of the ITO that acts as a sperm chemoattractant. To date, no sperm chemoattractants have been identified for gymnolaemate bryozoans (see Reed, 1991). Nevertheless, the change in waveform dynamics at the ITO may be evidence for a behavioral response of gymnolaemate bryozoan sperm to contacting maternal tissue of conspecifics. Although external fertilization has been reported among gymnolaemate bryozoans (*e.g.*, Silén, 1966), all studies that have actually confirmed the presence of a sperm or male pronucleus in oocytes indicate that sperm-egg fusion occurs before or during ovulation (see Ryland and Bishop, 1993; Temkin, 1994, 1996).

Internal fertilization in gymnolaemate bryozoans probably involves the entry of spawned sperm into the maternal coelom, and is not the result of eggs and sperm being produced in the same perivisceral coelom by hermaphroditic zooids (see Ryland and Bishop, 1993; Temkin, 1994, 1996). Consequently, it is essential for spawned sperm to recognize the entryway into the maternal coelom, such as the ITO in *M. membranacea.* The presence of a sperm chemoattractant was also suggested by Silén (1966), based on his observations that sperm of *Electra posidoniae* attached to the abfrontal sides of tentacles began to produce "violent jerks" to move to the distal opening of the ITO at the time of egg spawning. ITOs have been reported to develop in species of seven gymnolaemate genera: *Membranipora, Electra, Alcyonidium, Conopeum, Farella, Victorella,* and *Bulbella.* Among these species, sperm entry through the ITO has been confirmed only for *M. membranacea* (Temkin, 1994). Silén (1966) reported that sperm entered the ITO of *Electra crustulena,* but he did not determine where sperm-egg fusion occurred. In species without ITOs, the supraneural pore, which represents the proximal pore of the ITO, has been hypothesized to serve as the entryway for sperm into the maternal coelom (see Silén, 1966). However, sperm entry through the supraneural pore has yet to be documented for any species.

Since spermatozeugmata are only known to occur in the gymnolaemate genera of *Membranipora* and *Electra,* the waveforms so far described for *M. membranacea* spermatozeugmata may not necessarily be produced by sperm of other gymnolaemate species. In fact, the waveforms produced by spermatozeugmata of *Electra* remain to be determined. However, some initial data on the waveforms generated by sperm of *Thalamoporella floridana* suggest that the waveforms observed for *M. membranacea* spermatozeugmata, including reverse waveforms, do occur in other gymnolaemate bryozoan sperm (Temkin, 2001). To understand the significance and evolution of spermatozeugmata and the waveform dynamics of gymnolaemate bryozoan sperm, further studies are required to determine how sperm locate, identify, and enter maternal individuals in gymnolaemate species that do not spawn spermatozeugmata or do not form ITOs.

Acknowledgments

We thank the following people for providing M. H. Temkin with laboratory space and facilities: Kevin Eckelbarger and Tim Miller at the Darling Marine Center in Maine, Mary Rice at the Smithsonian Marine Station at Fort Pierce, Dennis Willows and Richard Strathmann at the Friday Harbor Laboratories, and Robert Woollacott at Harvard University. Karel Liem generously allowed us to use his high-speed video equipment. We thank Brad Baldwin, Joe Erlichman, Marianne DiMarco-Temkin, Russel Zimmer, Michael LaBarbera, and an anonymous reviewer for reading and suggesting changes that improved the manuscript. This paper is dedicated to the memory of Dr. Larry R. McEdward.

Literature Cited

Afzelius, B. 1982. The flagellar apparatus of marine spermatozoa. Pp. 495–519 in *Prokaryotic and Eukaryotic Flagella,* W. Amos and J. Duckett, eds. Cambridge University Press, Cambridge.

Afzelius, B. A. 1983. The spermatozoon of *Myzostomum cirriferum* (Annelida, Myzostomida). *J. Ultrastruct. Res.* **83:** 58–68.

Baccetti, B. H., B. H. Gibbons, and I. R. Gibbons. 1989. Bidirectional swimming in spermatozoa of Tephritid flies. *J. Submicrosc. Cytol. Pathol.* **21:** 619–625.

Bishop, J. D. D., and J. S. Ryland. 1991. Storage of exogenous sperm by the compound ascidian *Diplosoma listerianum. Mar. Biol.* **108:** 111–118.

Bonnevie, K. 1907. Untersuchungen über Keimzellen. II. Physiologische Polyspermie bei Bryozoen. *Jenaische Zeitschreift für Naturwissenschaften* **42:** 567–598.

Braidotti, P., and M. Ferraguti. 1982. Two sperm types in the spermatozeugmata of *Tubifex tubifex* (Annelida, Oligochaeta). *J. Morphol.* **171:** 123–136.

Brokaw, C. J. 1984. Cyclic AMP-dependent activation of sea urchin and tunicate sperm motility. *Ann. N Y Acad. Sci.* **438:** 132–141.

Buckland-Nicks, J., I. Bryson, L. Hart, and V. Partridge. 1999. Sex and a snail's sperm: on the transport, storage, and fate of dimorphic sperm in Littorinidae. *Invertebr. Reprod. Dev.* **36:** 145–152.

Buckland-Nicks, J. A., J. M. Healy, B. G. M. Jamieson, and S. O'Leary. 2000. Paraspermatogenesis in *Littoraria (Palustorina) articulate,* with reference to other Littorinidae (Littorinoidea, Caenogastropoda). *Invertebr. Biol.* **119:** 254–264.

Burighel, P., and G. B. Martinucci. 1994a. Sexual reproduction in the compound ascidian *Diplosoma listerianum* (Tunicata). I. Metamorphosis, storage and phagocytosis of sperm in female duct. *Mar. Biol.* **118:** 489–498.

Burighel, P., and G. B. Martinucci. 1994b. Sexual reproduction in the compound ascidian *Diplosoma listerianum* (Tunicata). II. Sperm penetration through ovary wall and evidence of internal fertilization. *Mar. Biol.* **118:** 499–510.

Daly, J. M., and D. W. Golding. 1977. A description of the spermatheca of *Spirorbis spirorbis* (L.) (Polychaeta: Serpulidae) and evidence for a novel mode of sperm transmission. *J. Mar. Biol. Assoc. UK* **57:** 219–227.

Ferraguti, M. 1983. Annelida Clitellata. Pp. 343–376 in *Reproductive Biology of Invertebrates, Volume II, Spermatogenesis and Sperm Function,* G. K. Adiyodi and R. G. Adiyodi, eds. John Wiley, New York.

Ferraguti, M. G., G. Bernadini, G. Melone, and R. Dallai. 1988. Structure and function of the metachronal wave in *Tubifex tubifex* spermatozeugmata (Annelida, Oligochaeta). *J. Ultrastruct. Mol. Struct. Res.* **99:** 79–95.

Ferraguti, M., G. Grassi, and C. Erséus. 1989. Different models of tubificid spermatozeugmata. *Hydrobiologia* **180:** 73–82.

Franzén, Å. 1956. On spermiogenesis, morphology of the spermatozoan, and biology of fertilization among invertebrates. *Zool. Bidr. Upps.* **31:** 355–482.

Franzén, Å. 1998. Spermiogenesis, sperm structure and spermatozeugmata in the gymnolaematous bryozoan *Electra pilosa* (Bryozoa, Gymnolaemata). *Invertebr. Reprod. Dev.* **34:** 55–63.

Gibbons, B. H. 1980. Intermittent swimming in live sea urchin sperm. *J. Cell Biol.* **84:** 1–12.

Hageman, G. S. 1983. A fine structural analysis of ovarian morphology, oogenesis, and ovulation in the marine bryozoan *Membranipora serrilamella* (Cheilostomata, Anasca). Ph.D. dissertation, University of Southern California, Los Angeles, CA. 487 pp.

Hayakawa, Y., R. Akiyama, H. Munehara, and A. Komaru. 2002a. Dimorphic sperm influence semen distribution in a non-copulatory sculpin *Hemilepidotus gilberti. Environ. Biol. Fishes* **65:** 311–317.

Hayakawa, Y., H. Munehara, and A. Komaru. 2002b. Obstructive role of the dimorphic sperm in a non-copulatory marine sculpin, *Hemilepidotus gilberti,* to prevent other males' eusperm from fertilization. *Environ. Biol. Fishes* **64:** 419–427.

Healy, J. M., and B. G. M. Jamieson. 1993. Euspermatozoa, paraspermatozoa and spermatozeugmata of *Littoraria (Palustorina) articulata* (Prosobranchia: Caenogastropoda) with special reference to the pseudotrich. *Acta Zool.* **74:** 321–330.

Hendelberg, J. 1965. On different types of spermatozoa in Polycladida, Turbellaria. *Ark. Zool.* **18:** 267–304.

Hendelberg, J. 1983. Platyhelminthes—Turbellaria. Pp. 75–104 in *Reproductive Biology of Invertebrates, Volume II, Spermatogenesis and Sperm Function,* G. K. Adiyodi and R. G. Adiyodi, eds. John Wiley, New York.

Ho, H. C., and S. S. Suarez. 2003. Characterization of the intracellular calcium store at the base of the sperm flagellum that regulates hyperactivated motility. *Biol. Reprod.* **68:** 1590–1596.

Jamieson, B. G. M. 1991. *Fish Evolution and Systematics: Evidence from Spermatozoa.* Cambridge University Press, Cambridge. 319 pp.

Jespersen, Å., and J. Lützen. 2001. Ultrastructure of the seminal receptacle and the dimorphic sperm in the commensal bivalve *Mysella bidentata* (Veneroida; Galeommatoidea; Montacutidae). *Acta Zool.* **82:** 107–115.

Jespersen, Å., T. Kosuge, and J. Lützen. 2001. Sperm dimorphism and spermatozeugmata in the commensal bivalve *Pseudopythina macrophthalmensis* (Galeommatoidea, Kelliidae). *Zoomorphology* **120:** 177–189.

Jespersen, Å., J. Lützen, and B. Morton. 2002. Ultrastructure of dimorphic sperm and seminal receptacle in the hermaphrodites *Barrimysia siphonosomae* and *Pseudopythina ochetostomae* (Bivalvia, Galeommatoidea). *Zoomorphology* **121:** 159–172.

Levitan, D. R. 1995. The ecology of fertilization in free-spawning invertebrates. Pp. 123–156 in *Ecology of Marine Invertebrate Larvae,* L. R. McEdward, ed. CRC Press, New York.

Lynn, J. W. 1994. The ultrastructure of the sperm and motile spermatozeugmata released from the freshwater mussel *Anodonta grandis* (Mollusca, Bivalvia, Unionidae). *Can. J. Zool.* **72:** 1452–1461.

Manríquez, P. H., R. N. Hughes, and J. D. D. Bishop. 2001. Age-dependent loss of fertility in water-borne sperm of the bryozoan *Celleporella hyalina. Mar. Ecol. Prog. Ser.* **224:** 87–92.

Marcus, E. 1926. Beobachtungen und Versuche an lebenden Meeresbryozoen. *Zool. Jahrb. Abt. Syst.* **52:** 1–102.

Marcus, E. 1938. Bryozoarios marinhos brasilieros II. *Univ. Sao Paulo Fac. Filos. Cient. Let. Bol. Zool.* **2:** 1–196.

Miller, R. L. 1983. Cnidaria. Pp. 23–73 in *Reproductive Biology of Invertebrates, Volume II, Spermatogenesis and Sperm Function,* G. K. Adiyodi and R. G. Adiyodi, eds. John Wiley, New York.

Ó Foighil, D. 1985. Sperm transfer and storage in the brooding bivalve *Mysella tumida. Biol. Bull.* **169:** 602–614

Ó Foighil, D. 1989. Role of spermatozeugmata in the spawning ecology of the brood oyster *Ostrea edulis. Gamete Res.* **24:** 219–228.

Pacey, A. A., J. C. Cosson, and M. G. Bentley. 1994. Intermittent swimming in the spermatozoa of the lugworm *Arenicola marina* (L.) (Annelida: Polychaeta). *Cell Motil. Cytoskelet.* **29:** 186–194

Reed, C. G. 1991. Bryozoa. Pp. 85–245 in *Reproduction of Marine Invertebrates, Volume VI, Echinoderms and Lophophorates.* A. C. Giese, J. S. Pearse, and V. B. Pearse, eds. Boxwood Press, Pacific Grove, CA.

Rouse, G. W. 1996. Variability of sperm storage by females in the Sabellidae and Serpulidae (Polychaeta, Sabellida). *Zoomorphology* **116:** 179–193.

Ryland, J. S., and J. D. Bishop. 1993. Internal fertilization in hermaphroditic colonial invertebrates. *Oceanogr. Mar. Biol. Annu. Rev.* **31:** 445–477.

Sahara, K., and N. Kawamura. 2002. Double copulation of a female with sterile diploid and polyploid males recovers fertility in *Bombyx mori. Zygote* **10:** 23–29.

Schwaninger, H. R. 1999. Population structure of the widely dispersing marine bryozoan *Membranipora membranacea* (Cheilostomata): implications for population history, biogeography, and taxonomy. *Mar. Biol.* **135:** 411–423.

Sewell, M. A., and F.-S. Chia. 1994. Reproduction of the intraovarian brooding apodid *Leptosynapta clarki* (Echinodermata: Holothuroidea) in British Columbia. *Mar. Biol.* **121:** 285–300.

Silén, L. 1966. On the fertilization problem in the gymnolaematous Bryozoa. *Ophelia* **3:** 113–140.

Temkin, M. H. 1991. Fertilization in the gymnolaemate Bryozoa. Ph.D. dissertation, University of Southern California, Los Angeles, CA. 139 pp.

Temkin, M. H. 1994. Gamete spawning and fertilization in the gymnolaemate bryozoan *Membranipora membranacea. Biol. Bull.* **187:** 143–155.

Temkin, M. H. 1996. Comparative fertilization biology of gymnolaemate bryozoans. *Mar. Biol.* **127:** 329–339.

Temkin, M. H. 2001. A comparison of gymnolaemate bryozoan sperm waveform dynamics. *Am. Zool.* **41:** 1604.

Temkin, M. H. 2002. The effects of increased external Ca^{++} and K^{+} concentrations on the waveform dynamics of bryozoan spermatozeugmata. Pp. 315–320 in *Bryozoan Studies 2001,* P. N. Wyse Jackson, C. J. Buttler, and M. E. Spenser Jones, eds. Swets and Zeitlinger, Lisse, The Netherlands.

Temkin, M. H., and R. L. Zimmer. 2002. Phylum Bryozoa. Pp. 411–427 in *Atlas of Marine Invertebrate Larvae,* C. Young, ed. Academic Press, San Diego, CA.

Zimmer, R. L. 1991. Phoronida. Pp. 1–45 in *Reproduction of Marine Invertebrates, Volume VI, Echinoderms and Lophophorates.* A. C. Giese, J. S. Pearse, and V. B. Pearse, eds. Boxwood Press, Pacific Grove, CA.

Zimmer, R. L., and R. M. Woollacott. 1974. Morphology and biochemical modifications of the spermatozoan mitochondria of *Membranipora* (Bryozoa). *J. Cell Biol.* **63:** 385a.

Reference: *Biol. Bull.* **206:** 46–54. (February 2004)
© 2004 Marine Biological Laboratory

Differences in the rDNA-Bearing Chromosome Divide the Asian-Pacific and Atlantic Species of *Crassostrea* (Bivalvia, Mollusca)

YONGPING WANG[1,2], ZHE XU[1], AND XIMING GUO[1,*]

[1] *Haskin Shellfish Research Laboratory, Institute of Marine and Coastal Sciences, Rutgers University, 6959 Miller Avenue, Port Norris, New Jersey 08349; and* [2] *Experimental Marine Biology Laboratory, Institute of Oceanology, Chinese Academy of Sciences, 7 Nanhai Road, Qingdao, Shandong 266071, PRC*

Abstract. Karyotype and chromosomal location of the major ribosomal RNA genes (rDNA) were studied using fluorescence *in situ* hybridization (FISH) in five species of *Crassostrea:* three Asian-Pacific species (*C. gigas, C. plicatula,* and *C. ariakensis*) and two Atlantic species (*C. virginica* and *C. rhizophorae*). FISH probes were made by PCR amplification of the intergenic transcribed spacer between the 18S and 5.8S rRNA genes, and labeled with digoxigenin-11-dUTP. All five species had a haploid number of 10 chromosomes. The Atlantic species had 1–2 submetacentric chromosomes, while the three Pacific species had none. FISH with metaphase chromosomes detected a single telomeric locus for rDNA in all five species without any variation. In all three Pacific species, rDNA was located on the long arm of Chromosome 10 (10q)—the smallest chromosome. In the two Atlantic species, rDNA was located on the short arm of Chromosome 2 (2p)—the second longest chromosome. A review of other studies reveals the same distribution of NOR sites (putative rDNA loci) in three other species: on 10q in *C. sikamea* and *C. angulata* from the Pacific Ocean and on 2p in *C. gasar* from the western Atlantic. All data support the conclusion that differences in size and shape of the rDNA-bearing chromosome represent a major divide between Asian-Pacific and Atlantic species of *Crassostrea.* This finding suggests that chromosomal divergence can occur under seemingly conserved karyotypes and may play a role in reproductive isolation and speciation.

Introduction

Classification and phylogenetic analysis of oysters are problematic because oysters have few informative morphological characteristics. Shell coloration and morphology in oysters are highly variable and sensitive to environmental influence. Anatomy of soft tissue is difficult and provides only limited information. Phylogenetic analyses of oysters may have to rely on a multidiscipline approach using morphological, molecular, and cytogenetic characteristics. Molecular data have been used for phylogenetic analysis of oysters and have shown great promise (Banks *et al.*, 1993; Littlewood, 1994; Ó Foighil *et al.*, 1995, 1998; Ó Foighil and Taylor, 2000; Lapègue *et al.*, 2002). Cytogenetic analysis may provide additional characteristics for phylogenetic comparisons and insight about major genomic changes at chromosome levels. Chromosomal rearrangement and differentiation are important mechanisms for reproductive isolation and speciation in some taxa (White, 1978; King, 1993).

Most of the cytogenetic studies in oysters so far have focused on karyotyping, chromosome banding, and NOR (nucleolar organizer regions) staining in *Ostrea* species (Insua and Thiriot-Quiévreux, 1991; Li and Havenhand, 1997). Studies in *Crassostrea* are scarce and provide little interspecific comparison (Ladrón De Guevara *et al.*, 1996; Leitao *et al.*, 1999a, b). Although oysters have a low haploid number of 10 chromosomes (Nakamura, 1985), oyster chromosomes are small and similar in arm ratios, which makes

---

Received 17 June 2003; accepted 21 October 2003.

* To whom correspondence should be addressed. E-mail: xguo@hsrl.rutgers.edu

Abbreviations: CI, centromeric index; FISH, fluorescence *in situ* hybridization; NOR, nucleolar organizer region.

karyotypic analysis inherently difficult. Probably due to the small chromosome size and the lack of cell lines required for making elongated chromosomes, chromosome banding in oysters is difficult to obtain and reproduce. C- and G-banding patterns have been produced in three *Crassostrea* species (Rodriguez-Romero *et al.*, 1979; Leitão *et al.*, 1999a), but offered little help in the reliable identification of oyster chromosomes. Ag-NOR staining is also variable and often shows intraspecific variations in number and location, which poses problems for interspecific comparisons (Thiriot-Quiévreux and Insua, 1992; Ladrón De Guevara *et al.*, 1994).

Fluorescence *in situ* hybridization (FISH) is a relatively new technology and now widely used for chromosome identification, gene mapping, localization of gene expression, and studies on chromosome rearrangement in a variety of organisms (Swiger and Tucker, 1996; Nath and Johnson, 1999). By direct DNA base pair hybridization, FISH provides specific and reproducible localization of genes and DNA sequences on chromosomes. Repetitive DNA sequences and genes that are present in high copy numbers and tandem repeats are ideal for use as FISH probes because of their large target size. Unique sequences longer than 80 kb, such as P1 and BAC clones, can be readily mapped to chromosomes by FISH and used as chromosome-specific probes (Jiang *et al.*, 1995). Unique sequences shorter than 1 kb are generally difficult to assign by FISH, although not impossible (Schriml *et al.*, 1999). Chromosome paint probes have been developed to label specific chromosomes or chromosome regions in some organisms (Rabbitts *et al.*, 1995; Shi *et al.*, 1997). The unambiguous labeling and identification of chromosomes by FISH has made it possible to study chromosome rearrangements in cancer cells and at evolutionary scale.

FISH may provide a solution to the reliable identification of oyster chromosomes, which has not been possible through traditional karyotyping, and permit cross-species comparisons. The technique has recently been used to study oyster chromosomes and shows considerable advantages over traditional methods. Using FISH, a repetitive element has been mapped to centromeric regions of several chromosomes in the Pacific oyster *Crassostrea gigas* (Clabby *et al.*, 1996; Wang *et al.*, 2001), and the vertebrate telomere sequence (TAAGGG)n has been mapped to telomeres of three species of *Crassostrea* (Guo and Allen, 1997; Wang and Guo, 2001). Nine P1 clones have been assigned to specific chromosomes in *C. virginica* (Wang, 2001).

The major ribosomal RNA genes (rDNA), which correspond to NORs, have also been mapped by FISH in three species of *Crassostrea* (Zhang *et al.*, 1999; Xu *et al.*, 2001; Cross *et al.*, 2003). FISH analysis of rDNA provided validation for Ag-NOR staining and eliminated any uncertainty and intraspecific variations. Interestingly, Xu *et al.* (2001) found that the two species of *Crassostrea* studied, one Pacific and one Atlantic species, differ in the size and shape of the rDNA-bearing chromosome. In a species with an Asian-Pacific origin, *C. angulata,* the rDNA-bearing chromosome is the same size and shape as in the Pacific species, but differs from that in the Atlantic species (Cross *et al.*, 2003). To determine if the difference is shared by other species of *Crassostrea,* we used FISH to study the chromosomal location of rDNA in five *Crassostrea* species that are available to us, including the two species studied by Xu *et al.* (2001) but with different populations, two additional Asian-Pacific species (*C. plicatula* and *C. ariakensis*), and one additional Atlantic species (*C. rhizophorae*). Our results plus existing NOR data suggest that differences in the rDNA-bearing chromosome represent a major divide between Asian-Pacific and Atlantic species of *Crassostrea.*

Materials and Methods

Species studied

Five species of *Crassostrea* were included in this study: three Asian-Pacific species (*C. gigas* (Thunberg, 1793), *C. plicatula* (Gmelin, 1791), and *C. ariakensis* (Fujita, 1913)), and two Atlantic species (*C. virginica* (Gmelin, 1791) and *C. rhizophorae* (Guilding, 1828)). *C. gigas* was obtained from a hatchery in Penglai, Shandong, northern China. The *C. gigas* studied by Xu *et al.* (2001) was from a Rutgers stock originated from Washington State. The use of different stocks was intended to detect possible variation among populations. *C. plicatula* was collected from Qingdao, Shandong, northern China. *C. ariakensis* was collected from Yangjiang, Guangdong, southern China. *C. virginica* was from two sources: wild oysters from Delaware Bay and hybrids between Delaware Bay wild and a hatchery stock (NEH, the same stock used by Xu *et al.*, 2001) maintained at the Haskin Shellfish Research Laboratory (HSRL), Rutgers University, New Jersey. The hatchery stock, which originated from Long Island Sound, has been maintained at HSRL for over 10 generations (selected for disease-resistance). *C. rhizophorae* was the first-generation progeny of a Caribbean population produced and maintained at the Harbor Branch Oceanographic Institute, Ft. Pierce, Florida.

Chromosome preparation

For *C. plicatula* and *C. ariakensis,* chromosome metaphases were prepared from gill tissue. Oysters were incubated in 0.005% colchicine in seawater for 8–10 h. Gill tissues from five oysters of each species were dissected and treated with the hypotonic solution 0.075 *M* KCl for 30 min before being fixed in freshly prepared Carnoy's fixative (3:1 methanol/acetic acid, v:v). The fixative was changed twice, and fixed samples were stored at 4 °C. Metaphases of *C. gigas, C. virginica,* and *C. rhizophorae* were made from early embryos according to the protocol described by Xu *et* *al.* (2001). For embryo production, 3 females and 2 males of *C. gigas*, 4 females and 4 males of *C. virginica*, and 6 females and 3 males of *C. rhizophorae* were used.

Slides were prepared using an air-drying technique. Gill tissues were chopped into fine pieces and resuspended in freshly made fixative. Two or three drops of cell (from gills) or embryo suspension were loaded onto a clean slide and flooded with two drops of 1:1 methanol/acetic acid. Slides were air-dried and stored at −20 °C until FISH analysis.

Probe construction

Oyster genomic DNA was prepared from adductor muscle of *C. gigas* and *C. virginica* according to Doyle and Doyle (1987). Intergenic transcribed spacers between the 18S and 5.8S RNA genes (ITS1) were amplified, labeled by PCR incorporation of digoxigenin-11-dUTP, and used as FISH probes. Primers, 5′-GGTTTCTGTAGGTGAACCTGC and 5′-CTGCGTTCTTCATCGACCC, were designed using conserved sequences flanking the ITS1. ITS1 was used as the FISH probe so that the primer sequences were conserved and could allow universal amplification, while the internal sequences were variable and might permit species-specific detection. PCR amplification was conducted in 25 μl of a PCR mixture containing PCR buffer with 1.5 m*M* of $MgCl_2$, 0.4 mg/ml of BSA, 0.2 m*M* each of dATP, dCTP, and dGTP, 0.13 m*M* of dTTP, 0.07 m*M* of digoxigenin-11-dUTP, 0.5 U of Taq DNA polymerase, 1 μ*M* of each primer, and 1 μg of oyster genomic DNA. Digoxigenin-11-dUTP and other PCR reagents were purchased from Roche (Indianapolis, IN). PCR was performed in a DeltaCycler II system thermal cycler (ERICOMP Inc., San Diego, CA) with 30 cycles of 1 min of denaturing at 95 °C, 1 min of annealing at 50 °C, and 1 min of extension at 72 °C, and final extension at 72 °C for 5 min. PCR products were verified on 2% agarose gels. DIG-labeled PCR products were purified using G-50 columns (Roche) before being used as FISH probes.

Fluorescence in situ *hybridization*

Separate ITS1 probes were made for *C. gigas* and *C. virginica*, using their respective genomic DNA as templates. Both probes were tested for FISH in all five species. FISH was conducted according to protocols described by Xu *et al.* (2001). Before FISH, slides were stained with Leishman's stain for 3–5 min and screened for metaphases. Negative controls in which the FISH probe was replaced with distilled water were included to detect possible nonspecific hybridization. FISH signals were observed under a Nikon epi-fluorescence microscope equipped with a CCD camera and imaging system.

Chromosomes were measured for the calculation of relative length (RL) and centromeric index (CI), and classified according to criteria defined by Levan (1964). Ten metaphases were measured for each species. The CI of each chromosome represents the mean and standard deviation of the 10 metaphases. When the CI of a chromosome plus and minus the standard deviation overlapped two chromosome categories, the chromosome was designated with labels for two categories. Chromosomes were paired by length and arm ratio, and named 1 to 10 from the longest to the shortest.

Results

A diploid number, $2n = 20$, was found in all five oysters studied. Each karyotype consisted of 10 pairs of metacentric and sometimes submetacentric chromosomes. Karyotype analysis showed that all five species shared a similar karyotype (Table 1). The only noticeable difference between the three Pacific and two Atlantic species was that *C. virginica* and *C. rhizophorae* had 1–2 chromosomes that were clearly submetacentric, while the three Pacific species had no chromosomes that could be unquestionably defined as submetacentric. There were chromosomes in both Pacific and Atlantic species whose centromeric indexes overlapped ranges for metacentric (0.500–0.375) and submetacentric (0.374–0.250) chromosomes. These were classified as metacentric/submetacentric (m/sm in Table 1) chromosomes and not treated as submetacentric chromosomes. One chromosome in *C. virginica* and two chromosomes in *C. rhizophorae* were clearly submetacentric.

PCR amplification of ITS1 in *C. gigas* generated a single fragment of approximately 520 bp in length. Incorporation of digoxigenin-11-dUTP shifted the size of the PCR product to about 670 bp. The PCR product of the same primer pair in *C. virginica* was about 500 bp, slightly shorter than that from *C. gigas*. Both *C. gigas* (*Cg*) and *C. virginica* (*Cv*) probes were used for FISH analysis.

FISH with both *Cg* and *Cv* probes produced positive signals in all five species (Fig. 1). Two bright signals were detected in all metaphases analyzed in all five species without any variation (Table 2). The FISH signals were restricted to one locus (one pair of chromosomes) with no or little background signal elsewhere on the chromosomes. For interphase nuclei, the number of FISH signals varied between one and two. About 50%–68% of nuclei clearly had two FISH signals, while others had one or overlapping signals. In all five species studied, *Cg* and *Cv* probes produced identical results in the number and location of signals, but signal strength differed. In Pacific species, the signals produced by *Cg* probes were generally stronger than those produced by *Cv* probes; conversely, in Atlantic species, *Cv* probes usually produced stronger signals. Only FISH results with the *Cg* probe for Pacific species and the *Cv* probe for Atlantic species are presented in Figure 1. No FISH signal was observed in the negative controls.

Karyotype analysis of FISH signals showed that, in all

Table 1

Karyotype analysis of 10 metaphases in five Crassostrea *species*

Species chromosome	Relative length (mean ± SD)	Centromeric index (mean ± SD)	Classification[1]
C. gigas			
1	12.43 ± 0.25	0.41 ± 0.01	m
2	11.86 ± 0.55	0.46 ± 0.02	m
3	10.97 ± 0.40	0.45 ± 0.02	m
4	10.50 ± 0.16	0.43 ± 0.01	m
5	10.28 ± 0.42	0.38 ± 0.03	m/sm
6	9.88 ± 0.14	0.41 ± 0.01	m
7	9.43 ± 0.22	0.45 ± 0.02	m
8	9.29 ± 0.25	0.40 ± 0.03	m/sm
9	8.66 ± 0.22	0.41 ± 0.03	m
10	7.61 ± 0.53	0.42 ± 0.02	m
C. plicatula			
1	12.87 ± 0.37	0.46 ± 0.01	m
2	11.10 ± 0.27	0.41 ± 0.02	m
3	10.83 ± 0.31	0.46 ± 0.02	m
4	10.35 ± 0.29	0.41 ± 0.01	m
5	10.14 ± 0.49	0.45 ± 0.02	m
6	9.62 ± 0.05	0.45 ± 0.02	m
7	9.59 ± 0.24	0.39 ± 0.02	m/sm
8	9.09 ± 0.36	0.39 ± 0.02	m/sm
9	8.45 ± 0.38	0.39 ± 0.01	m
10	7.79 ± 0.28	0.40 ± 0.02	m
C. ariakensis			
1	12.03 ± 0.47	0.38 ± 0.02	m/sm
2	11.53 ± 0.39	0.46 ± 0.01	m
3	10.95 ± 0.59	0.40 ± 0.01	m
4	10.51 ± 0.37	0.41 ± 0.02	m
5	9.90 ± 0.81	0.45 ± 0.03	m
6	9.77 ± 0.35	0.46 ± 0.01	m
7	9.31 ± 0.44	0.42 ± 0.01	m
8	9.05 ± 0.22	0.40 ± 0.02	m
9	8.89 ± 0.32	0.44 ± 0.02	m
10	8.13 ± 0.56	0.39 ± 0.01	m
C. virginica			
1	12.51 ± 0.37	0.47 ± 0.01	m
2	11.64 ± 0.26	0.38 ± 0.01	m/sm
3	10.96 ± 0.29	0.41 ± 0.01	m
4	10.81 ± 0.23	0.47 ± 0.01	m
5	10.20 ± 0.31	0.40 ± 0.02	m
6	9.68 ± 0.30	0.47 ± 0.1	m
7	9.41 ± 0.25	0.40 ± 0.02	m
8	8.91 ± 0.22	0.41 ± 0.01	m
9	8.28 ± 0.21	0.35 ± 0.02	sm
10	7.61 ± 0.38	0.47 ± 0.01	m
C. rhizophorae			
1	12.23 ± 0.59	0.46 ± 0.02	m
2	12.22 ± 0.42	0.38 ± 0.01	m/sm
3	11.22 ± 0.39	0.40 ± 0.02	m
4	10.90 ± 0.16	0.46 ± 0.02	m
5	10.09 ± 0.49	0.32 ± 0.04	sm
6	9.96 ± 0.53	0.40 ± 0.01	m
7	9.45 ± 0.57	0.46 ± 0.01	m
8	8.70 ± 0.28	0.47 ± 0.02	m
9	7.83 ± 0.40	0.30 ± 0.03	sm
10	7.38 ± 0.65	0.46 ± 0.01	m

[1] m = metacentric chromosomes; sm = submetacentric chromosomes; m/sm = metacentric or submetacentric, centromeric indexes overlapping two categories.

three Pacific species (*C. gigas, C. plicatula,* and *C. ariakensis*), the FISH signals occurred on the long arms of Chromosome 10 (10q, Fig. 1, Table 2). The assignment was unambiguous because Chromosome 10 was clearly the smallest chromosome in all three species. In all three Pacific species, the signals were found at telomeric regions of the long arm. In the two Atlantic species (*C. virginica* and *C. rhizophorae*), however, FISH signals were found on the short arms of Chromosome 2 (2p, Fig. 1, Table 2). Chromosome 2 was the second longest chromosome in both species and was clearly distinguishable from Chromosome 1 and 3 by its centromeric index. Chromosome 2 in both Atlantic species had a centromeric index of 0.38 (m/sm), compared with 0.46–0.47 for Chromosome 1 and 0.40–0.41 for Chromosome 3 (Table 1). As in the Pacific species, FISH signals were restricted to telomere regions. Karyotypic alignments of the five *Crassostrea* species are presented in Figure 1F.

For both *C. gigas* and *C. virginica,* there was no intraspecific variation in the number and chromosomal location of the rDNA locus among oysters collected from different populations, as demonstrated by results from this study and Xu *et al.* (2001).

Discussion

Fluorescence in situ *hybridization validates nucleolar organizer regions, but not always*

This study provides unambiguous chromosomal assignment of rDNA in five species of *Crassostrea,* including different populations of two previously studied species, *C. gigas* and *C. virginica.* The number and location of the rDNA locus revealed by FISH are clear and without any variation. Despite the use of oysters from different populations, FISH results from this study agree with previous FISH analyses in both *C. gigas* and *C. virginica* (Zhang *et al.,* 1999; Xu *et al.,* 2001). FISH results presented here confirm that rDNA or the major rRNA genes are located at the NOR sites previously reported for *C. gigas* (Thiriot-Quiévreux and Insua, 1992). For *C. rhizophorae,* Lapègue *et al.* (2002) observed one NOR on the short arms of Chromosome 3, which corresponds to the rDNA loci we found on Chromosome 2. Chromosome 3 in Lapègue *et al.* (2002) appeared to be the second longest in the karyotype and had a centromeric index close to that of Chromosome 2 in our study.

For *C. virginica* and *C. ariakensis,* however, FISH results are in conflict with results from Ag-NOR staining. Leitão *et al.* (1999b) reported two NOR sites for *C. virginica* (Chromosomes 1 and 5) and *C. ariakensis* (Chromosomes 9 and 10) with considerable variation, while FISH in this study detected only one rDNA locus in the two species. Our FISH results are clear, consistent, and supported by early studies in *C. virginica* (Zhang *et al.,* 1999; Xu *et al.,* 2001). The

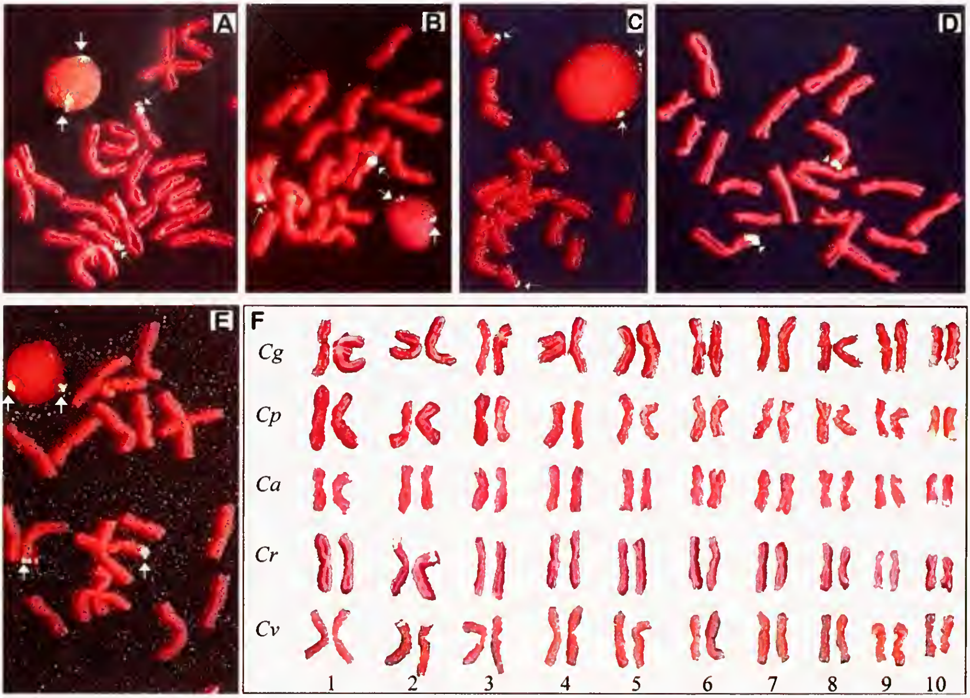

Figure 1. Fluorescence *in situ* hybridization (FISH) signals and chromosomal location of the major rRNA genes in five species of *Crassostrea*. (A) *C. gigas* rDNA probe on *C. gigas* chromosomes; (B) *C. gigas* probe on *C. plicatula;* (C) *C. gigas* probe on *C. ariakensis;* (D) *C. virginica* probe on *C. rhizophorae;* (E) *C. virginica* probe on *C. virginica;* (F) chromosome alignment of five species. Arrows show FISH signals.

discrepancy between the FISH and NOR data may be caused by either false-positive Ag-NOR staining or by a lack of correspondence between NORs and the major rRNA genes. Ag-NOR staining targets transcriptionally active NOR sites and is known to produce variable and inconsistent results in the number and sometimes the location of NORs within the same species (Insua and Thiriot-Quiévreux, 1993; Li and Havenhand, 1997). Also, Ag-NOR staining may not be able to separate major (18S-5.8S-28S) from minor (5S) rDNA and other actively transcribed genes. One of the two signals described by Leitão *et al.* (1999b) seems to correspond to the major rDNA locus in our study, but the nature of the other site is unknown. Based on preliminary FISH data (Wang and Guo, unpubl.), the extra NOR site in *C. virginica* is not the site of 5S rDNA. Clearly, Ag-NOR staining can accurately detect major rRNA genes sometimes—as shown by results from *C. gigas, C. rhizophorae,* and *C. angulata* (Thiriot-Quiévreux and Insua, 1992; Lapègue *et al.*, 2002; Cross *et al.*, 2003), but not always—as exemplified in *C. virginica* and *C. ariakensis.*

Table 2

Fluorescence in situ *hybridization with* C. gigas *and* C. virginica *rDNA probes on interphase nuclei and metaphase chromosomes in five species of* Crassostrea

Probe/species	% Nuclei with 2 signals (*n*)	% Metaphases with 2 signals (*n*)	Chromosomal location[1]
C. gigas probe			
C. gigas	60 (25)	100 (28)	10q
C. plicatula	60 (25)	100 (10)	10q
C. ariakensis	64 (14)	100 (10)	10q
C. virginica	66 (15)	100 (10)	2p
C. rhizophorae	67 (24)	100 (10)	2p
C. virginica probe			
C. gigas	50 (14)	100 (14)	10q
C. plicatula	55 (18)	100 (10)	10q
C. ariakensis	52 (15)	100 (13)	10q
C. virginica	65 (27)	100 (16)	2p
C. rhizophorae	68 (40)	100 (19)	2p

[1] All locations are telomeric.

Confirmation of NOR results by FISH is necessary. NOR sites, often two per genome, have been reported in several species of *Ostrea* (Insua and Thiriot-Quiévreux, 1991, 1993; Thiriot-Quiévreux and Insua, 1992; Li and Havenhand, 1997). It would be interesting to know if the NOR sites correspond to the major rRNA gene locus in the *Ostrea* species.

This study provides the first report on the karyotype of *C. plicatula*, whose taxonomic status is uncertain at this time. *C. plicatula* (formerly *Ostrea plicatula*) is commonly used to refer to a type of small oyster found in intertidal areas along most of China's coast (Wang *et al.*, 1993). Some believe that *C. plicatula* is the same species as *C. gigas* (Li and Qi, 1994; Yang *et al.*, 2000); others suggest that it is closely related to *C. ariakensis* (Yu *et al.*, 2003); and still others consider it an unresolved *Crassostrea* species and use the name of *Crassostrea* sp. instead (Xu, 1997). *C. plicatula* seems to be a different species from *Alectryonella plicatula* found in southern China (Li and Qi, 1994).

Differences between Pacific and Atlantic species

Results of this study clearly demonstrate that the major rDNA is located on the long arms of Chromosome 10 (the smallest) in all three Asian-Pacific species and on the short arms of Chromosome 2 (the second longest) in the two Atlantic species. A critical examination of NOR data indicates that the same pattern holds true in two other species: NORs (or the major rRNA genes, pending verification by FISH) are located on the long arms of Chromosome 10 in the Asian-Pacific species *C. sikamea* and on the short arms of Chromosome 2 in the eastern Atlantic (African) species *C. gasar* (Leitão *et al.*, 1999b; Lapègue *et al.*, 2002; Table 3). The Portuguese oyster *C. angulata* provides a unique and interesting case, adding support to the observed pattern. Both Ag-NOR staining and FISH have indicated that rDNA is located on the long arm of Chromosome 10, the same as in Pacific species (Leitão *et al.*, 1999b; Cross *et al.*, 2003). *C. angulata* is found along the northeastern coasts of the Atlantic and has been assumed to be native there. However, there are conflicting views on the taxonomic status and origin of this species. Some, on the basis of morphological and allozyme data, have suggested that *C. angulata* is the same species as the Pacific oyster *C. gigas* (Menzel, 1974; Buroker *et al.*, 1979). The prevailing view is that *C. angulata* is an Asian species that was introduced to Europe from Japan, although it is possible that *C. gigas* is an Atlantic species that was introduced to Japan from Portugal (Menzel, 1974). More recent analyses using mtDNA sequence data suggest that *C. angulata* is of Asian origin (likely from Taiwan), and that it is closely related, but not identical, to *C. gigas* from Japan (Boudry *et al.*, 1998; Ó Foighil *et al.* 1998). Whether *C. angulata* is the same species as *C. gigas* requires further study, but it is clear from molecular data that *C. angulata* is an Asian-Pacific species.

Another karyotypic difference between Asian-Pacific and Atlantic members of *Crassostrea* is the number of SM chromosomes. In this study, we observed one in *C. virginica*, two in *C. rhizophorae*, and none in the three Pacific species. Despite some variation, other studies also found more SM chromosomes in Atlantic than in Pacific species (Leitão *et al.*, 1999b; Lapègue *et al.*, 2002; Cross *et al.*, 2003). The karyotypic differences between all three Atlantic and five Pacific *Crassostrea* species studied so far are

Table 3

Summary of karyotypic differences in the rDNA-bearing chromosome and the number of submetacentric (SM) chromosomes between Asian-Pacific and Atlantic species of Crassostrea[1]

		Number of SM chromosomes				
Species	rDNA location	This study	Leitão *et al.* (1999b)	Lapègue *et al.* (2002)	Cross *et al.* (2003)	Average
Pacific species						
C. gigas	10q	0	0			0
C. ariakensis	10q	0	1			0.5
C. plicatula	10q	0				0
C. sikamea	10q[2]		0			0
C. angulata[3]	10q		1		0	0.5
Atlantic species						
C. virginica	2p	1	2			1.5
C. rhizophorae	2p	2		4		3.0
C. gasar	2p[2]		4	4		4.0

[1] Only chromosomes with a centromeric index + SD less than 0.375 were considered to be submetacentric for standardized comparisons.

[2] Based on Ag-NOR staining (Leitão *et al.*, 1999b; Lapègue *et al.*, 2002), pending verification by FISH.

[3] *C. angulata* is considered to be an Asian-Pacific species (Ó Foighil *et al.*, 1998; Boudry *et al.*, 1998).

summarized in Table 3. Differences in the rDNA-bearing chromosome and the number of SM chromosomes represent a major divide between Pacific and Atlantic members of the genus. Oysters are thought to have highly conserved karyotypes. All *Crassostrea* studied so far (about 13 species) have a haploid number of 10 chromosomes and similar karyotypes (Nakamura, 1985). The size and shape of the rDNA-bearing chromosome and the number of SM chromosomes are the first two clearly recognizable chromosomal divergences among species of *Crassostrea.*

There are likely other karyotypic differences between the Pacific and Atlantic species, and between this and other studies for the same species. We did not attempt to match individual chromosomes across species and studies. Chromosome identification in oysters is difficult because oyster chromosomes are similar in size and arm ratio. The accuracy of chromosome measurements varies considerably depending on the degree of chromosomal condensation, the quality of metaphases, and the staining methods used. Chromosome pairing, classification, and naming are prone to errors. In the absence of chromosome-specific FISH probes, chromosome alignment across species is not reliable in oysters and must be viewed with caution. However, difficulties in chromosome identification do not affect the conclusions of this study. The rDNA-bearing chromosomes in the Pacific and Atlantic species are strikingly and consistently different, and the difference in the number of SM chromosomes is independent of chromosome identity and supported by other studies.

The findings of this study suggest that chromosomal divergence among *Crassostrea* species is possible under a seemingly conserved karyotype. The divergence in karyotype is not surprising, and phylogenetic analysis using molecular data has shown that Pacific and Atlantic species of *Crassostrea* form two clades on phylogenetic trees (Littlewood, 1994; Ó Foighil *et al.*, 1998; Ó Foighil and Taylor, 2000; Lapègue *et al.*, 2002). Compared with molecular data, the rDNA-bearing chromosome provides a clear and simple divide between the two species groups, which may represent a single event of macroevolution at the chromosome level or accumulation of chromosome changes over time.

Divergence in karyotype can arise from chromosomal deletion, duplication, translocation, inversion, fission, fusion, and aneuploidy (White, 1978; King, 1993). In our case, the only recognizable difference so far is the size and shape of the rDNA-bearing chromosomes. It is not clear whether Chromosome 10 of the Pacific species is homologous to Chromosome 2 of the Atlantic species. If it is, the divergence may be caused by chromosomal duplications or deletions. If the two chromosomes have little homology other than in the rDNA regions, translocation would likely be responsible.

Chromosomal divergence and hybridization barrier

Major chromosomal divergence can cause reproductive isolation and speciation, by altering normal gene expression and regulation or causing problems for meiosis and fertility in hybrids (White, 1978; King, 1993; Noor *et al.*, 2001; Rieseberg, 2001). Biologically, there is a well-documented postzygotic hybridization barrier between Asian-Pacific and Atlantic species of *Crassostrea* (see review in Gaffney and Allen, 1993). Hybridization within the two geographic species groups produces viable offspring (Wang and Liu, 1959; Zhou *et al.*, 1982; Menzel, 1987; Allen and Gaffney, 1993). Hybridization between *C. virginica* and *C. gigas* or *C. ariakensis* results in high levels of fertilization and apparently normal larval development, but all hybrid larvae die within 2 weeks and before metamorphosis (Allen *et al.*, 1993). By demonstrating significant chromosomal divergence across the hybridization barrier, we raise the possibility that the chromosomal divergence may contribute to the formation of the barrier. Geographic isolation and genic mutations may have played important roles in the speciation of oysters. We present the chromosomal divergence hypothesis as a possible explanation for the postzygotic hybridization barrier between Atlantic and Asian-Pacific species of *Crassostrea,* while recognizing that the barrier may as well be genic. Additional data are needed to discriminate between the two hypotheses. There are about 15 extant members of *Crassostrea,* and most of them live in the Asian-Pacific region (Carriker and Gaffney, 1996). A survey of all species in the genus may reveal karyotypic variation within the geographic ranges. Species from the eastern Pacific and Indian Oceans would be most interesting. Similar studies in the oyster genera *Ostrea* and *Saccostrea* may provide insight into the phylogenetic relationships among the three major groups of Ostreidae.

Finally, this study provides the first chromosomal assignment by FISH of the major rRNA genes in *C. plicatula, C. ariakensis,* and *C. rhizophorae.* The unambiguous mapping of rDNA by FISH made it possible to identify major karyotypic differences between Asian-Pacific and Atlantic species of *Crassostrea.* Results of this study show that FISH is a powerful tool for cytogenetic analysis, especially in species where chromosome identification by traditional methods is challenging. Cytogenetic analysis in most marine invertebrates has been limited primarily due to difficulties of chromosome identification. The application of FISH techniques and development of chromosome-specific probes may enable chromosome identification and phylogenetic comparisons of molluscs and other marine invertebrates.

Acknowledgments

The authors thank Dr. John Scarpa for providing mangrove oysters and Prof. Fusui Zhang for helping with identifying *Crassostrea plicatula*. This study was conducted at Rutgers University and supported by grants from the National Sea Grant Marine Biotechnology Program (Grant B/T-9801), USDA NRI (Award No. 96-35205-3854), and the New Jersey Commission on Science and Technology (02-2042-007-11). Yongping Wang is partly supported by grants from China's Natural Science Foundation (No 39825121), the 863 program (Award 2001AA628150), and Chinese Academy of Sciences. This is Publication IMCS-2004-01 and NJSG-04-553.

Literature Cited

Allen, S. K., Jr., and P. M. Gaffney. 1993. Genetic confirmation of hybridization between *Crassostrea gigas* (Thunberg) and *Crassostrea rivularis* (Gould). *Aquaculture* **113:** 291–300.

Allen, S. K., Jr., P. M. Gaffney, J. Scarpa, and D. Bushek. 1993. Inviable hybrids of *Crassostrea virginica* (Gmelin) with *C. rivularis* (Gould) and *C. gigas* (Thunberg). *Aquaculture* **113:** 269–289.

Banks, M. A., D. Hedgecock, and C. Waters. 1993. Discrimination between closely related Pacific oyster species (*Crassostrea*) via mitochondrial DNA sequences coding for large subunit rRNA. *Mol. Mar. Biol. Biotechnol.* **2:** 129–136.

Boudry, P., S. Heurtebise, B. Collet, F. Cornette, and A. Gerard. 1998. Differentiation between populations of the Portuguese oyster, *Crassostrea angulata* (Lamark) and the Pacific oyster, *Crassostrea gigas* (Thunberg), revealed by mtDNA RFLP analysis. *J. Exp. Mar. Biol. Ecol.* **226:** 279–291.

Buroker, N. E., W. K. Hershberger, and K. K. Chew. 1979. Population genetics of the family Ostreidae. I. Intraspecific studies of *Crassostrea gigas* and *Saccostrea commercialis*. *Mar. Biol.* **54:** 157–169.

Carriker, M. R., and P. M. Gaffney. 1996. A catalogue of selected species of living oysters (*Ostreacea*) of the world. Pp. 1–15 in *The Eastern Oyster* Crassostrea virginica, V. S. Kennedy, R. I. E. Newell, and A. F. Eble, eds. Maryland Sea Grant College, College Park.

Clabby, C., U. Goswami, F. Flavin, N. P. Wilkins, J. A. Houghton, and R. Powell. 1996. Cloning, characterization and chromosomal location of a satellite DNA from the Pacific oyster, *Crassostrea gigas*. *Gene* **168:** 205–209.

Cross, I., L. Vega, and L. Rebordinos. 2003. Nucleolar organizing regions in *Crassostrea angulata:* chromosomal location and polymorphism. *Genetica* **119:** 65–74.

Doyle, J. J., and J. L. Doyle. 1987. A rapid DNA isolation procedure for small quantities of fresh leaf tissue. *Phytochem. Bull.* **19:** 11–15.

Gaffney, P. M., and S. K. Allen, Jr. 1993. Hybridization among *Crassostrea* species: a review. *Aquaculture* **116:** 1–13.

Guo, X., and S. K. Allen, Jr. 1997. Fluorescence *in situ* hybridization of the vertebrate telomere sequence to chromosome ends of the Pacific oyster, *Crassostrea gigas* Thunberg. *J. Shellfish Res.* **16:** 87–89.

Insua, A., and C. Thiriot-Quiévreux. 1991. The characterization of *Ostrea denselamellosa* (Mollusca, Bivalvia) chromosomes: karyotype, constitutive heterochromatin and nucleolus organizer regions. *Aquaculture* **97:** 317–325.

Insua, A., and C. Thiriot-Quiévreux. 1993. Karyotype and nucleolus organizer regions in *Ostrea puelchana* (Bivalvia: Ostreidae). *Veliger* **36:** 215–219.

Jiang, J., B. S. Gill, G. L. Wang, P. C. Ronald, and D. C. Ward. 1995. Metaphase and interphase fluorescence *in situ* hybridization mapping of the rice genome with bacterial artificial chromosomes. *Proc. Natl. Acad. Sci. USA* **92:** 4487–4491.

King, M. 1993. *Species Evolution: The Role of Chromosome Change.* Cambridge University Press, Cambridge.

Ladrón De Guevara, B., F. Winkler, and C. Palma. 1994. Karyotype description and the position of the nucleolar organizer region (NOR) in the Chilean oyster *Tiostrea chilensis* (Philippi) Chanley and Dinamani. Pp. 390–405 in *Genetics and Evolution of Aquatic Organisms*, A. R. Beaumont, ed. Chapman and Hall, London.

Ladrón De Guevara, B., F. Winkler, F. Rodriguez-Romero, and C. Palma-Rojas. 1996. Comparative karyology of four American oyster species. *Veliger* **39:** 260–266.

Lapègue, S., I. Boutet, A. Leitão, S. Heurtebise, P. Garcia, C. Thiriot-Quiévreux, and P. Boudry. 2002. Trans-Atlantic distribution of a mangrove oyster species revealed by 16S mtDNA and karyological analysis. *Biol. Bull.* **202:** 232–242.

Leitão, A., C. Thiriot-Quiévreux, P. Boudry, and I. Malheiro. 1999a. A 'G' chromosome banding study of three cupped oyster species: *Crassostrea gigas*, *Crassostrea angulata* and *Crassostrea virginica* (Mollusca: Bivalvia). *Genet. Sel. Evol.* **31:** 519–527.

Leitão, A., P. Boudry, J. Labat, and C. Thiriot-Quiévreux. 1999b. Comparative karyological study of cupped oyster species. *Malacologia* **41:** 175–186.

Levan, A., D. Fredga, and A. A. Sandberg. 1964. Nomenclature for centromeric position on chromosomes. *Hereditas* **52:** 201–220.

Li, X., and J. N. Havenhand. 1997. Karyotype, nucleolus organiser regions and constitutive heterochromatin in *Ostrea angasi* (Mollusca: Bivalvia): evidence of taxonomic relationships within the Ostreidae. *Mar. Biol.* **127:** 443–448.

Li, X., and Z. Qi. 1994. Studies on the comparative anatomy, systematic classification and evolution of Chinese oysters. *Studia Marina Sinica* **35:** 143–178. (In Chinese).

Littlewood, D. T. J. 1994. Molecular phylogenetics of cupped oysters based on partial 28S rRNA gene sequences. *Mol. Phylogenet. Evol.* **3:** 221–229.

Menzel, R. W. 1974. Portuguese and Japanese oysters are the same species. *J. Fish. Res. Board Can.* **31:** 453–456.

Menzel, W. 1987. Hybridization of oysters and clams. Pp. 47–59 in *Hybridization and Genetic Engineering in Aquaculture*, K. Tiews, ed. Heenemann, Berlin.

Nakamura, H. K. 1985. A review of molluscan cytogenetic information based on the CISMOCH-computerized index system for molluscan chromosomes. Bivalvia, Polyplacophora and Cephalopoda. *Venus Jpn. J. Malacol.* **44:** 193–226.

Nath, J., and K. L. Johnson. 1999. A review of fluorescence *in situ* hybridization (FISH): current status and future prospects. *Biotech. Histochem.* **75:** 54–78.

Noor, M. A. F., K. L. Grams, L. A. Bertucci, and J. Reiland. 2001. Chromosomal inversions and the reproductive isolation of species. *Proc. Natl. Acad. Sci. USA* **98:** 12,084–12,088.

Ó Foighil, D., and D. J. Taylor. 2000. Evolution of parental care and ovulation behavior in oysters. *Mol. Phylogenet. Evol.* **15:** 301–313.

Ó Foighil, D., P. M. Gaffney, and T. J. Hilbish. 1995. Differences in mitochondrial 16S ribosomal gene sequences allow discrimination among American (*Crassostrea virginica*) and Asian (*C. gigas*, *C. ariakensis*) oyster species. *J. Exp. Mar. Biol. Ecol.* **192:** 211–220.

Ó Foighil, D., P. M. Gaffney, A. E. Wilbur, and T. J. Hilbish. 1998. Mitochondrial cytochrome oxidase I gene sequences support an Asian origin for the Portuguese oyster *Crassostrea angulata*. *Mar. Biol.* **131:** 497–503.

Rabbitts, P., H. Impey, A. Heppell-Parton, C. Langford, C. Tease, N. Lowe, D. Bailey, M. Ferguson-Smith, and N. Carter. 1995. Chromosome specific paints from a high resolution flow karyotype of the mouse. *Nat. Genet.* **9:** 369–375.

Rieseberg, L. H. 2001. Chromosomal rearrangements and speciation. *Trends Ecol. Evol.* **16:** 351–358.

Rodriguez-Romero, F., A. Laguarda-Figueras, M. Uribe-Alcocer, and

M. L. Rojas-Lara. 1979. Distribution of "G" bands in the karyotype of *Crassostrea virginica. Venus Jpn. J. Malacol.* **38:** 180–184.

Schriml, L. M., H. M. Padilla-Nash, A. Coleman, P. Moen, W. G. Nash, J. Menninger, G. Jones, T. Ried, and M. Dean. 1999. Tyramide signal amplification (TSA)-FISH applied to mapping PCR labeled probes less than 1 kb in size. *Biotechniques* **27:** 608–613.

Shi, G., H. J. Weh, and D. K. Hossfeld. 1997. Reinterpretation of G-banded complex karyotypes by fluorescence *in situ* hybridization with chromosome-specific DNA painting probes and alpha-satellite centromere-specific DNA probes in malignant hematological disorders. *Am. J. Hematol.* **55:** 69–76.

Swiger, R. R., and J. D. Tucker. 1996. Fluorescence *in situ* hybridization: a brief review. *Environ. Mol. Mutagen.* **27:** 245–254.

Thiriot-Quiévreux, C., and A. Insua. 1992. Nucleolar organizer region variation in the chromosomes of three oyster species. *J. Exp. Mar. Biol. Ecol.* **157:** 33–40.

Wang, D., and H. Liu. 1959. Preliminary studies on artificial hybridization of oysters. *ACTA Zool. Sinica* **11:** 283–295. (In Chinese with French abstract).

Wang, R., Z. Wang, and J. Zhang. 1993. *Marine Molluscan Culture.* Qingdao Ocean University Press, Qingdao, China. (In Chinese).

Wang, Y. 2001. *Molecular Biological Characterization of Oyster Chromosomes.* Ph.D. dissertation, Institute of Oceanology, Chinese Academy of Sciences, Qingdao, China. (In Chinese).

Wang, Y., and X. Guo. 2001. Chromosomal mapping of the vertebrate telomeric sequence (TTAGGG)n in four bivalve molluscs by fluorescence *in situ* hybridization. *J. Shellfish Res.* **20:** 1187–1190.

Wang, Y., Z. Xu, and X. Guo. 2001. A centromeric satellite sequence in the Pacific oyster (*Crassostrea gigas* Thunberg) identified by fluorescence *in situ* hybridization. *Mar. Biotechnol.* **3:** 486–492.

White, M. J. D. 1978. *Modes of Speciation.* W. H. Freeman, San Francisco.

Xu, F. 1997. *Bivalve Mollusca of China.* Science Press, Beijing, China. (In Chinese).

Xu, Z., X. Guo, P. M. Gaffney, and J. C. Pierce. 2001. Chromosomal location of the major ribosomal RNA genes in *Crassostrea virginica* and *Crassostrea gigas. Veliger* **44:** 79–83.

Yang, R., Z. Yu, Z. Chen, X. Kong, and J. Dai. 2000. Allozyme variation within *Crassostrea plicatula* and *Crassostrea gigas* from Shandong coastal waters. *J. Fish. China* **24:** 130–133. (In Chinese with English abstract).

Yu, Z., X. Kong, L. Zhang, X. Guo, and J. Xiang. 2003. Taxonomic status of four *Crassostrea* oysters from China as inferred from mitochondrial DNA sequences. *J. Shellfish Res.* **22:** 31–38.

Zhang, Q. Y., G. Yu, R. K. Cooper, and T. R. Tiersch. 1999. Chromosomal location by fluorescence *in situ* hybridization of the 28S ribosomal RNA gene of the eastern oyster. *J. Shellfish Res.* **18:** 431–435.

Zhou, M., Y. Gao, and R. Wu. 1982. Preliminary studies on hybridization of *Crassostrea gigas* with *Ostrea rivularis* and *Ostrea plicatula. J. Fish. China* **6:** 235–241. (In Chinese with English abstract).

Reference: *Biol. Bull.* **206:** 55–60. (February 2004)
© 2004 Marine Biological Laboratory

Occurrence in the Field of a Long-Term, Year-Round, Stable Population of Placozoans

YOSHIHIKO K. MARUYAMA

Section of Marine Biological Science, Education and Research Center for Biological Resources,
Faculty of Life and Environmental Science, Shimane University, 194 Kamo, Saigo, Oki,
Shimane 685-0024, Japan

Abstract. Long-term field studies on placozoans (*Trichoplax adhaerens*), including both substrate sampling and slide sampling, were carried out at a subtidal site near Shirahama, Japan. Samples of natural substrate materials from the field, such as stones, shells, or fragments of coral, were particularly useful for obtaining placozoans. Results from the substrate sampling indicate that placozoans are present year-round at the study site. Large intermittent peaks in the number of animals collected at the study site occurred roughly once a year, between late summer and the beginning of winter. Placozoans were present every year from 1989 through 2000. A seawater aquarium was also studied and provided a considerable number of placozoans for more than 1 year.

Introduction

The placozoan *Trichoplax adhaerens* F. E. Schulze is a ciliated microscopic marine animal with a platelike morphology (Schulze, 1883; Grell, 1971, 1982; Miller, 1971a, b; Pearse *et al.*, 1987; Margulis and Schwartz, 1988; Grell and Ruthmann, 1991; Conn, 2000; Brusca and Brusca, 2003). The thin body consists only of an epithelium and an internal mesenchyme. The epithelium has two regions: an upper free, or dorsal, epithelium of cover cells and a lower attached, or ventral, epithelium of cylinder and gland cells (Grell and Benwitz, 1971; Pearse *et al.*, 1987; Grell and Ruthmann, 1991). Some differences between the central and marginal areas in the body have also been reported (Schwartz, 1984; Schuchert, 1993; Pearse *et al.*, 1994). When the densely ciliated ventral epithelium is in contact with the substrate, the animals display a gliding (or creeping) locomotion (Grell and Ruthmann, 1991). When the animal is fed, its shape changes periodically (Ueda *et al.*, 1999). For example, in addition to the gliding amoeboid platelike form, other forms (swarmers) (Thiemann and Ruthmann, 1991) have been described. Further, a swimming form has been reported (cited in Margulis and Schwartz, 1988; also see Levin and Bridges, 1995). *Trichoplax adhaerens* is considered to be the sole species in the phylum Placozoa (Grell, 1982; Grell and Ruthmann, 1991; Brusca and Brusca, 2003).

Placozoans have been found in seawater aquaria (Schulze, 1883; Miller, 1971a, b; Pearse *et al.*, 1987; Margulis and Schwartz, 1988; Grell and Ruthmann, 1991), as well as in various warm coastal areas (Grell and Benwitz, 1971; Sudzuki, 1977; Grell and López-Ochoterena, 1987; Pearse, 1989; Uehara *et al.*, 1989; Pearse *et al.*, 1994; V. B. Pearse, pers. comm.). Nevertheless, the biology of this microscopic animal under natural conditions is little known (Grell and Ruthmann, 1991).

In this study, which is based on long-term sampling of both glass slides and natural substrates, the occurrence of placozoans was examined at a subtidal site as well as in a seawater aquarium at the Seto Marine Biological Laboratory in Shirahama, Japan. Results of this study indicate that, in addition to their abundance in the seawater aquarium, placozoans are present at the study site year-round.

Materials and Methods

Sampling in the field

The study site was located at the east side of Tanjirikuzurenohana on the southern coast of Tanabe Bay, near the

Received 19 April 2000; accepted 17 November 2003.
E-mail: maruyama@life.shimane-u.ac.jp

Seto Marine Biological Laboratory of Kyoto University at Shirahama (Wakayama Prefecture, Japan). It was situated in the upper portion of the subtidal zone, about 1 m below the datum line in the tide table for Shirahama (tide tables issued by the Japan Meteorological Agency, Tokyo). Water temperatures were recorded (Fig. 1).

Slide sampling. Following Pearse (1989), specimens of placozoans were collected on glass slides (76 mm × 26 mm). Typically, seven clean slides were placed in a stainless steel slide rack (72 mm × 66 mm × 31 mm; ordinarily used in histology), and four sets of racks thus prepared were placed on the substrate at the study site. Later (19 to 68 days; 35 days on average), each of the racks was put separately into a plastic container filled with ambient seawater collected at the site and returned to the laboratory for observation. Sometimes, individual clean slides, not in racks, were placed at the site, and individual slides were also examined if the racks holding them disappeared unaccountably. On the day of retrieval, or the day after, new sets of slides were placed for the next observation.

Substrate sampling. Placozoans were also collected from samples of natural substrate materials ranging in size from pebble to cobble (according to the particle grade scale of Wentworth; *e.g.*, Lincoln *et al.*, 1998); for example, those of 4–8 cm in length are within this range. Stones, shells of molluscs (dead or alive), fragments of skeleton of hard corals (dead or alive), or mixtures thereof, were collected by hand at the study site and placed separately into containers of ambient seawater. These samples were brought to the laboratory for observation. The sampling was carried out at intervals of 12–68 days, 35 days on average.

Laboratory observations of placozoans from the field. In the slide sampling, each slide was quickly transferred into a plastic dish (90 mm in diameter) containing seawater from the field. Both surfaces of each slide were examined under a dissecting microscope. In the substrate sampling, each sample container was typically treated as follows. It was shaken for several seconds, and the resultant suspension was decanted into plastic dishes (90 mm in diameter). A few hours later, these dishes were observed under a dissecting microscope for placozoans, and within a few days (mostly, the day after), they were observed again. Placozoans could be seen; they were attached to and gliding along the bottom of the plastic dishes.

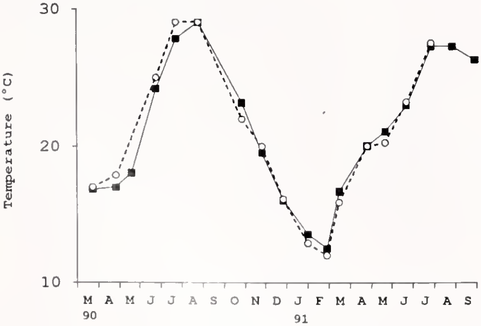

Figure 1. A profile of changes in water temperature at the study site and in the seawater aquarium. Abscissa, months from March 1990 through September 1991. Ordinate, temperature (°C) for the study site (squares, ■) and for the seawater aquarium (circles, ○).

When placozoans were found in these samples or on slides from the field (Fig. 2), they were transferred, with a mouth-controlled micropipette, to an observation chamber and further observed with a light microscope equipped with Nomarski optics. The thin platelike body form attached to the substrate on its ventral surface, its gliding ciliary movement, and the presence of shining spheres in the dorsal epithelium served to identify these animals as placozoans (Grell and Benwitz, 1971; Miller, 1971a; Grell and Ruthmann, 1991). Furthermore, the occurrence of birefringent granules in the subperipheral region (Miller, 1971a; Pearse *et al.*, 1994) usually served for identification.

Measurement of size in placozoans

Because the shape of placozoans continuously changes, determinations of size are only valid at the moment of measurement. Furthermore, only placozoans that were attached to either a glass or plastic substrate were measured. Under those circumstances, the lengths along the longest and shortest axes were measured with an ocular scale under a dissecting microscope, and the average of the two values was taken as the size of the individual.

Source of placozoans collected from stones

Samples of stones were collected at the study site and another subtidal site in Tanabe Bay (see a later section) and transported to the laboratory. Each sample consisted of a stone (4–8 cm in length) and an aliquot (typically, 30–70 ml) of the ambient seawater in a container. The stone in the container was transferred by hand into an aliquot (typically, 30–40 ml) of artificial seawater (ASW; Jamarin U, Jamarin Laboratory, Osaka) in a separate container; the ambient seawater (SW) was retained. Both containers—one with the ASW and the stone, and the other with the retained SW—were shaken similarly, and the fluids were then examined individually for placozoans, as described above; meanwhile the stone was discarded. The relative difference in the proportion of placozoans in the ASW and in the SW was calculated according to the expression $[(A - B)/(A + B)] \times 100$, where A is the number of placozoans in the ASW, and B is the number in the SW. The differences were

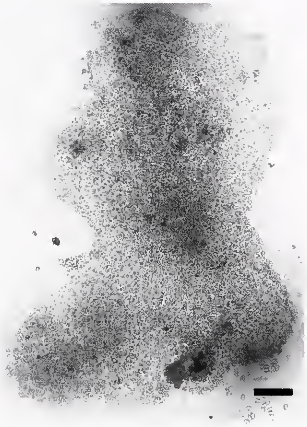

Figure 2. A placozoan on a slide from the study site. Bar, 100 μm.

statistically tested with a Student's t test, after arcsine transformation (Sokal and Rohlf, 1995) (Table 1).

Sampling at a seawater aquarium

Placozoans were also collected from the Kyoto University Aquarium at the Seto Marine Biological Laboratory. In a seawater aquarium in this facility, a square plastic basket was suspended; many hard corals were reared in the basket, and running seawater was continuously supplied from above. Water temperatures were recorded (Fig. 1).

Individual clean glass slides (76 mm × 26 mm), not in racks, were used here for sampling placozoans (slide sampling). About 10 slides were placed on the bottom of the basket with the corals. Later (19 to 44 days, 31 days on average), the slides were transferred to a container filled with seawater taken from the seawater supply system and were returned to the laboratory for observation under a dissecting microscope, as described above. When slides were removed, a new set of clean slides was placed for the next observation.

Results

Slide sampling at the subtidal study site

Slide samplings at the study site were carried out at intervals of 1 month on average for about 3 years, from November 1989 through December 1992. The samples yielded a total of 230 placozoans, which appeared in 13 of 33 (39%) samplings on 63 of 818 (7.7%) retrieved slides.

The number of placozoans changed with time, with large intermittent peaks in November 1990, September 1991, and August 1992 (arrows in Fig. 3). The percentage of slides with placozoans (placozoan-positive slides, or positive slides) was also higher in these months (Fig. 3). In addition, the number of racks containing slides with placozoans was also high in these months: 4 out of 4 in November 1990, 4 out of 4 in September 1991, and 3 out of 4 in August 1992.

The placozoans ranged in size from about 100 μm to 1200 μm (394 ± 179 μm, the mean ± SD of 227 individuals). All exhibited the platelike morphology (Fig. 2); but two placozoans obtained in November 1990 had a transparent balloonlike protrusion on the dorsal side, and two placozoans collected in September 1991 had a small protrusion.

Substrate sampling at the study site

Placozoans were found on all kinds of the substrate materials tested (stones, molluscan shells, corals), suggesting no specificity of placozoans for these particular substrates.

When samples of these materials were examined after collection at intervals of about 1 month (12–68 days, 35 days on average), for 2½ years, from July 1990 through December 1992, placozoans were found on all but two occasions (92%, 24 out of 26) (Fig. 4). Thus, placozoans were present virtually throughout the year at the study site.

A total of 199 placozoans were obtained from 39 out of the 114 (34%) samples. A large number of placozoans were obtained in November 1990 and August 1992 (Fig. 4). The percentage of positive samples varied with time, with peaks

Table 1

Source of placozoans collected from field samples of stones and ambient seawater

	Numbers of placozoans[a]		
Experiments	ASW + stone	SW	% Difference[b,c]
1	6	0	100
2	5	2	43
3	2	0	100
4	1	0	100
5	1	0	100

[a] The stone from each sample was transferred to artificial seawater (ASW), the stone and ASW were shaken, and the ASW was then examined for placozoans, as was the retained ambient seawater (SW) (see protocol in Materials and Methods). Only results from placozoan-positive samples are shown.

[b] % Difference, the relative value of the difference in number was calculated according to the equation $[(A - B)/(A + B)] \times 100$, where A and B represent the number of placozoans from ASW (+ stone) and SW, respectively.

[c] The % difference is significantly greater than 0% ($P < 0.05$); t test (see Materials and Methods).

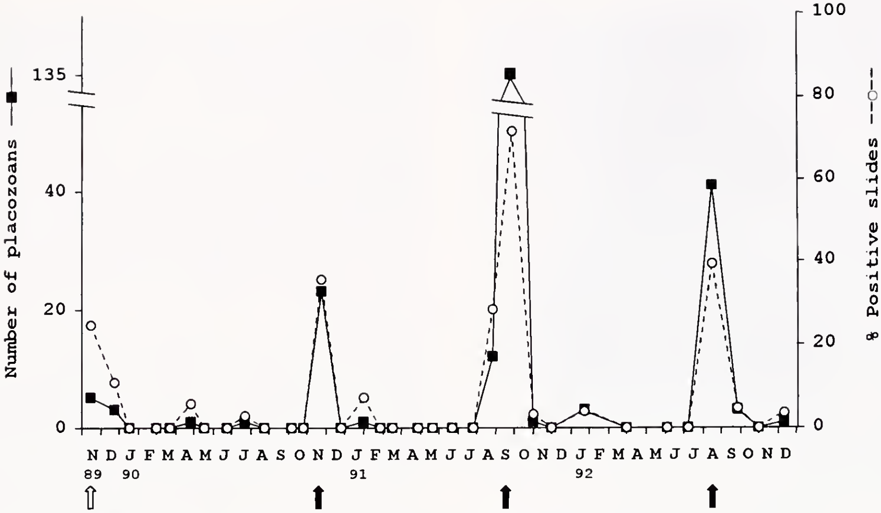

Figure 3. Slide sampling at the study site. Abscissa, months from November 1989 through December 1992. Ordinate (left), number of placozoans obtained from slides at each sampling (squares, ■); ordinate (right), percentage of placozoan-positive slides (circles, ○). Slides (10–34, 25 on average) that had been placed at the study site for about 1 month (19–68 days, 35 days on average) were used for the observations. Filled arrows indicate the timing of large intermittent peaks (November 1990, September 1991, and August 1992). The peak in November 1989 was also probably in this class (open arrow).

appearing in October 1990 to January 1991, September 1991, and August 1992 (see Fig. 4).

The placozoans obtained from substrate materials were, however, small. The animals collected from some samples ranged from 100 μm to 400 μm (132 ± 77 μm, mean ± SD of 52 individuals), and were frequently damaged at the periphery. Thus many of these placozoans had probably been fragmented during the sampling procedure. All, however, exhibited a platelike morphology.

Field sampling from 1993 through 2000

More recently, (August 1993–November 2000), samplings for placozoans, on either slides or natural substrates, were continued at the study site at a frequency of 1–3 times per year. Placozoans were present in every year. Moreover, placozoans were also present at other sites in this area of Shirahama, including a subtidal site and a tidal pool in Tanabe Bay as well as in Kanayama Bay.

Source of the placozoans collected from field samples of stones

Experiments were carried out to determine whether the placozoans obtained by substrate sampling were associated with the substrate or with the ambient seawater. Field samples of stones in containers of ambient seawater were used for this purpose ($n = 19$). The stone from each sample was individually transferred to artificial seawater (ASW + stone), the combination was shaken, and the ASW and the retained ambient seawater (SW) were examined for placozoans. Only two placozoans (mean size 94 μm) were found in the SW from 1 out of 19 samples, but 15 placozoans (85 ± 28 μm) were collected in the ASW from 5 out of 19 samples.

As shown in Table 1, in all these positive samples, placozoans were obtained from the ASW, and the placozoans were not equally distributed in the ASW and the SW (15 in the ASW and 2 in the SW; $P < 0.05$); and the proportion of placozoans in the ASW was enriched compared with that in the SW (Table 1). An association of some placozoans with the substrate (or other substrate material on it) rather than with the ambient seawater was suggested.

Sampling in the seawater aquarium

In earlier years, from November 1989 through August 1991, a seawater aquarium was also examined for placozoans. The slide sampling, carried out at intervals of 1 month

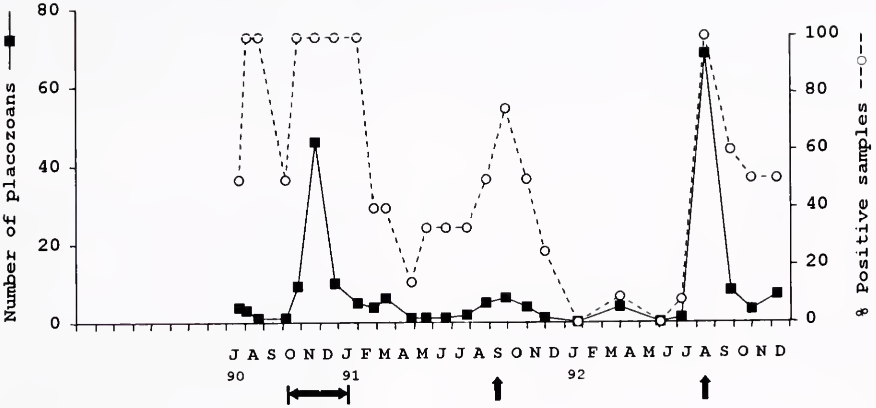

Figure 4. Substrate sampling at the study site. Abscissa, months from July 1990 through December 1992. Ordinate (left), number of placozoans obtained from samples of substrates at each sampling (squares, ■); ordinate (right), percentage of placozoan-positive samples (circles, ○). Samples of natural substrates were collected at intervals of about 1 month (12–68 days, 35 days on average). The number of samples was variable (1–13, 4 on average); 1–2 from July 1990 through January 1991, 3–7 from February 1991 through December 1991, 7–13 from January 1992 through July 1992, and 3–6 from August 1992 through December 1992. Arrows indicate peaks (October 1990 to January 1991, September 1991, and August 1992). The timing of the peaks is matched with that of the large intermittent peaks in Fig. 3.

on average for 1 ½ years, yielded a total of 1144 placozoans from the seawater aquarium (Fig. 5). The animals were obtained on most occasions (19 out of 22, or 86%) and inhabited 98 of 218 (45%) retrieved slides.

Both the number of placozoans at each sampling and the percentage of slides with placozoans (positive slides) varied with time (Fig. 5). Many placozoans were obtained in January, March, and April 1990, and August 1991. The percentage of positive slides was also high in these months.

All of the placozoans exhibited a platelike morphology. In one sampling, they ranged in size from about 100 μm to 300 μm (257 ± 59 μm, the mean ± SD of 8 individuals).

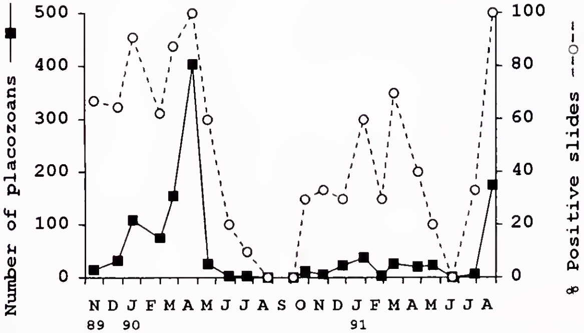

Figure 5. Slide sampling in the seawater aquarium. Abscissa, months from November 1989 through August 1991. Ordinate (left), number of placozoans obtained from slides at each sampling (squares, ■); ordinate (right), percentage of placozoan-positive slides (circles, ○). Slides (3–15, 10 on average) that had been placed in the seawater aquarium for about 1 month (19–44 days, 31 days on average) were observed. Note that the scale of the left ordinate is much larger than those in Figs. 3 and 4.

Discussion

This study, carried out from November 1989 to November 2000, at a study site in the subtidal waters in Shirahama, showed that placozoans were present year-round and in every year. Moreover, placozoans were also observed in July 1989 at and near To Island in Tanabe Bay (V. B. Pearse, pers. comm.). Further, a seawater aquarium used to hold transient stocks of local marine animals also yielded, over 1 year, a large number of placozoans. Thus, these animals have been observed for more than 11 years in the Shirahama area, and therefore, the population of placozoans can be considered to be stable.

Unexpectedly, the number of placozoans collected at the subtidal study site showed large, intermittent peaks that occurred roughly once a year, between late summer and the beginning of winter. Although the habitat of the seawater aquarium was quite different from that in the field, a peak also appeared in the aquarium samples. But this peak was shifted from that observed in the field samples. The significance of these fluctuations is unresolved.

Substrate sampling in this study was more direct and more productive for obtaining placozoans in the field than the slide sampling. But the number of organisms collected from substrate material is not certain, because some placozoans are apparently detached from this material during transport, before the sampling procedure in the laboratory (see Table 1). Another disadvantage of substrate sampling is that the fragile body may occasionally be damaged by excess shaking. Slide sampling seems to avoid this problem, providing placozoans without damage. The growth and reproductive patterns of placozoans on such slides with various other (mixed) organisms have been reported (Pearse, 1989). Slide sampling in this study also provided slides that could be used for rearing placozoans (data not shown). Therefore, a combination of both substrate and slide sampling seems to be the most effective way to study these microscopic animals from a local site.

Acknowledgments

This study was carried out at the Seto Marine Biological Laboratory during my stay there, and I thank the staff of the laboratory. I would like to express thanks to Dr. E. Harada for suggestions and encouragement during the study. I also thank Dr. V. B. Pearse for valuable comments and critical reading of the manuscript, and for kindly allowing me to refer to her data on placozoan sampling as a personal communication.

Literature Cited

Brusca, R. C., and G. J. Brusca. 2003. *Invertebrates*, 2nd ed. Sinauer Associates, Sunderland, MA. 936 pp.

Conn, D. B. 2000. *Atlas of Invertebrate Reproduction and Development*, 2nd ed. Wiley-Liss, New York. 300 pp.

Grell, K. G. 1971. *Trichoplax adhaerens* F. E. Schulze und die Entstehung der Metazoen. *Natwiss. Rundsch.* **24:** 160–161.

Grell, K. G. 1982. Placozoa. Page 639 in *Synopsis and Classification of Living Organisms*, Vol. 1. S. P. Parker, ed. McGraw-Hill, New York.

Grell, K. G., and G. Benwitz. 1971. Die Ultrastruktur von *Trichoplax adhaerens* F. E. Schulze. *Cytobiologie* **4:** 216–240.

Grell, K. G., and E. López-Ochoterena. 1987. A new record of *Trichoplax adhaerens* F. E. Schulze (Phylum Placozoa) in the Mexican Caribbean sea. *Anales del Instituto de Ciencias del Mar y Limnología, Universidad Nacional Autónoma de México* **14**(2): 255–256.

Grell, K. G., and A. Ruthmann. 1991. Placozoa. Pp. 13–27 in *Microscopic Anatomy of Invertebrates, Vol. 2, Placozoa, Porifera, Cnidaria, and Ctenophora*, F. W. Harrison and J. A. Westfall, eds. Wiley-Liss, New York.

Levin, L. A., and T. S. Bridges. 1995. Pattern and diversity in reproduction and development. Pp. 1–48 in *Ecology of Marine Invertebrate Larvae*. L. McEdward, ed. CRC Press, Boca Raton, FL.

Lincoln, R., G. Boxshall, and P. Clark. 1998. Appendix 14: Sediment particle size categories. Page 340 in *A Dictionary of Ecology, Evolution and Systematics*, 2nd ed. Cambridge University Press, Cambridge.

Margulis, L., and K. V. Schwartz. 1988. *Five Kingdoms: An Illustrated Guide to the Phyla of Life on Earth*, 2nd ed. W. H. Freeman, New York. 376 pp.

Miller, R. L. 1971a. Observations on *Trichoplax adhaerens* Schulze, 1883. *Am. Zool.* **11:** 698–699.

Miller, R. L. 1971b. *Trichoplax adhaerens* Schulze, 1883: return of an enigma. *Biol. Bull.* **141:** 374.

Pearse, V. B. 1989. Growth and behavior of *Trichoplax adhaerens:* first record of the phylum Placozoa in Hawaii. *Pac. Sci.* **43:** 117–121.

Pearse, V., J. Pearse, M. Buchsbaum, and R. Buchsbaum. 1987. *Living Invertebrates*. Blackwell Scientific Publications and The Boxwood Press, Pacific Grove, CA. 848 pp.

Pearse, V. B., T. Uehara, and R. L. Miller. 1994. Birefringent granules in placozoans (*Trichoplax adhaerens*). *Trans. Am. Microsc. Soc.* **113:** 385–389.

Schuchert, P. 1993. *Trichoplax adhaerens* (Phylum Placozoa) has cells that react with antibodies against the neuropeptide RFamide. *Acta Zool.* **74:** 115–117.

Schulze, F. E. 1883. *Trichoplax adhaerens*, nov. gen., nov. spec. *Zool. Anz.* **6:** 92–97.

Schwartz, V. 1984. The radial polar pattern of differentiation in *Trichoplax adhaerens* F. E. Schulze (Placozoa). *Z. Naturforsch. Sect. C* **39:** 818–832.

Sokal, R. R., and F. J. Rohlf. 1995. *Biometry: The Principles and Practice of Statistics in Biological Research*, 3d ed. W. H. Freeman, New York. 887 pp.

Sudzuki, M. 1977. Microscopical marine animals scarcely known from Japan. II. Occurrence of *Trichoplax* (Placozoa) in Shimoda. *Proc. Jpn. Soc. Syst. Zool.* **13:** 1–4.

Thiemann, M., and A. Ruthmann. 1991. Alternative modes of asexual reproduction in *Trichoplax adhaerens* (Placozoa). *Zoomorphology* **110:** 165–174.

Ueda, T., S. Koya, and Y. K. Maruyama. 1999. Dynamic patterns in the locomotion and feeding behaviors by the placozoan *Trichoplax adhaerens*. *Biosystems* **54:** 65–70.

Uehara, T., V. B. Pearse, and K. Yamazato. 1989. Birefringent particles observed in *Trichoplax adhaerens* (Placozoa), the simplest metazoan. *Zool. Sci.* **6:** 1209.

MARINE RESOURCES CENTER

MARINE BIOLOGICAL LABORATORY • WOODS HOLE, MA 02543 • (508)289-7700
WWW.MBL.EDU/SERVICES/MRC/INDEX.HTML

zebrafish facilities

Animal and Tissue Supply for Education & Research

- 150 aquatic species available for shipment via online catalog: <http://www.mbl.edu/animals/index.html>; phone: (508)289-7375; or e-mail: specimens@mbl.edu
- zebrafish colony containing limited mutant strains
- custom dissection and furnishing of specific organ and tissue samples

MRC Services Available

- basic water quality analysis
- veterinary services (clinical, histopathologic, microbial services, health certificates, etc.)
- aquatic systems design (mechanical, biological, engineering, etc.)
- educational tours and collecting trips aboard the R/V Gemma

Using the MRC for Your Research

- capability for advanced animal husbandry (temperature, light control, etc.)
- availability of year-round, developmental life stages
- adaptability of tank system design for live marine animal experimentation

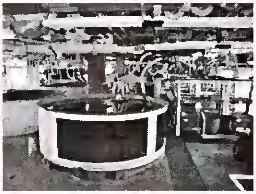

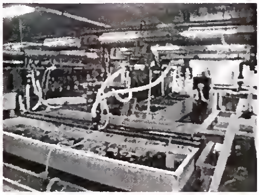

MBL
Marine Biological Laboratory • Woods Hole • MA

2004 Computational Neuroscience Courses

Contact: Carol Hamel
Admissions Coordinator
(508) 289-7401
admissions@mbl.edu

Applications are encouraged from women and members of underrepresented minorities.

The MBL is an Equal Opportunity/ Affirmative Action Employer.

Generous financial assistance is available!

www.mbl.edu/education

- **Methods in Computational Neuroscience**
  August 1 - August 29, 2004

Animals interact with a complex world, encountering a variety of challenges. This course introduces students to the computational and mathematical techniques that are used to address how the brain solves these problems at levels of neural organization ranging from single membrane channels to operations of the entire brain. Application Deadline: **March 5, 2004**

- **Neuroinformatics** ***August 14 - 29, 2004***

The ability to digitally acquire, store and analyze large volumes of multichannel data in the neurosciences, ranging from multiple spike trains to brain images, has given rise to a new and growing body of research. This two-week course is structured around the related issues, and will contain both pedagogical lectures on basic statistical techniques as well as focussed mini-workshops on specific neuroscience topics where applications of these techniques are critical Application Deadline: **March 16, 2004.**

MBL
Marine Biological Laboratory • Woods Hole • MA

2004 Microscopy Course

Optical Microscopy & Imaging in the Biomedical Sciences

October 5 - October 14, 2004

This course will enable the participant to obtain and interpret microscope images of high quality to perform quantitative optical measurements and to produce video and digital records for documentation and analysis.

Application Deadline: June 21, 2004

Contact: Carol Hamel, Admissions Coordinator, (508)289-7401, admissions@mbl.edu

Women and minorities encouraged to apply.
The MBL is an EEO/Affirmative Action Institution

www.mbl.edu/education

THE BIOLOGICAL BULLETIN

2004 Subscription Rates
Volumes 206-207

***Paid Subscriptions include both print and electronic subscriptions at:** www.biolbull.org

	Institutional*	**Individual***
One year subscription (6 issues - 2 volumes)	$325.00	$120.00
Single volume (3 issues)	$165.00	$70.00
Single Issues	$ 75.00	$25.00

*Surface delivery included in above prices.
For prompt delivery, we encourage subscribers outside the U.S. to request airmail service.

Airmail Delivery Charge

U.S. and Canada:	$ 45.00
Mexico:	$ 60.00
All other locations:	$100.00

Orders Must Be Prepaid in U.S. Dollars, Check Payable to The Marine Biological Laboratory

About *The Biological Bulletin*
ISSN: 0006-3185
Frequency: Bimonthly
Number of issues per year: 6
Months of Publication: February, April, June, August, October, December
Subscriptions entered for calendar year
Volume indexes contained in June and December issues
Annual report of the Marine Biological Laboratory contained in August issue
Most back issues available
Claims handled upon receipt
No agency discounts
Internet:
www.biolbull.org

Please address orders to:
Wendy Child
Subscriptions
The Biological Bulletin
Marine Biological Laboratory
7 MBL Street
Woods Hole, MA 02543-1015 U.S.A.
Fax: 508-289-7922 Tel: 508-289-7402 Email: wchild@mbl.edu

Published by the Marine Biological Laboratory
Woods Hole, Massachusetts, 02543 U.S.A.

THE BIOLOGICAL BULLETIN
(www.biolbull.org)
2004 SUBSCRIPTION FORM
(VOLUMES 206-207, 6 ISSUES)

(please print)

NAME: ______________________________

INSTITUTION: ______________________________

ADDRESS: ______________________________

CITY: ____________________ **STATE:** ____________________

POSTAL CODE: ______________ **COUNTRY:** ____________________

TELEPHONE: ______________ **FAX:** ____________________

E-MAIL ADDRESS ______________________________

All subscriptions run on the calendar year; price includes both print and online journals

☐ Please send me a 2004 subscription to *The Biological Bulletin* at the rate indicated below:

☐ Individual: $120.00 (6 ISSUES) ☐ Institutional : $325.00 (6 ISSUES)
☐ Individual: $70.00 (3 ISSUES) ☐ Institutional : $165.00 (3 ISSUES)

Check one: ☐ February April June or ☐ August October December

☐ Please send me the following back issue(s): ______________________

☐ Individual: at $25.00 (PER ISSUE) ☐ Institutional : at $75.00 (PER ISSUE)

Delivery Options

_____ Surface Delivery (Surface delivery is included in the subscription price.)
_____ Air delivery (Please add the correct amount to your payment.)

☐ U.S. and Canada: $46.00 ☐ Mexico: $60.00 ☐ All other locations: $100.00

Payment Options

_____ Enclosed is my check or U.S. money order for $ ______payable to The Marine Biological Laboratory

_____ Please charge my ☐ VISA, ☐ MasterCard ☐ Discover Card $________

_____ Please send me an invoice. (Note: Payment must be received before subscription commences.)

Account No.: ____________________ **Exp. Date:** ____________________

Signature: ____________________ **Date:** ____________________

Return this form with your check or credit information to:
Marine Biological Laboratory
Subscription Office ◆ The Biological Bulletin ◆ 7 MBL Street ◆ Woods Hole, MA 02543-1015

POSITION ANNOUNCEMENT

Editor-in-Chief
The Biological Bulletin

Start Date: January 2005
Term: Five years, renewable

The Editor-in-Chief is responsible for the overall editorial direction of the *Biological Bulletin*. The Editor-in-Chief appoints Associate Editors and members of the Editorial Board, decides which manuscripts are published, mediates editorial disputes, and sets policy for the journal.

The Editor-in-Chief is an independent contractor who reports to the Director and CEO of the Marine Biological Laboratory. Stipend for the position is $10,000 annually. The *Bulletin's* editorial offices are based in Woods Hole, but the Editor-in-Chief may work from his/her home institution. The Editor-in-Chief is expected to spend some part of the summer months in Woods Hole. Housing for up to one month will be provided in Woods Hole.

The successful candidate for this position will meet the following requirements:

- A broad understanding of biology, and a manifest interest in its diversity and comparative and integrative aspects
- A track-record of publishing in peer-reviewed journals
- Experience reviewing papers for scientific journals
- Proven skill as a substantive editor
- Ability to make tough decisions and willingness to work with other editors to reach a decision on difficult papers
- Demonstrated experience with the editorial process *(e.g.*, serving as an Editor or Associate Editor for a journal similar to the *Biological Bulletin*)
- The willingness and ability to commit the time required, approximately one day per week, to fulfill the duties outlined here for five years.

Job description:

The Editor-in-Chief devotes a minimum of six hours per week to the operation of the *Biological Bulletin*. The Editor's ongoing activities include 1) assigning submitted papers to the appropriate Associate Editor; 2) reading reviews and manuscripts to ensure fairness and technical accuracy; 3) writing editorial decision letters based on the reviews; 4) fielding telephone and e-mail queries on a daily basis from authors deciding whether to submit their work to the *Biological Bulletin*, authors who are unhappy about an editorial decision, and Associate Editors requesting guidance on such matters as the identity, availability, and number of reviewers, and editorial decisions and disputes; 5) communicating regularly (by telephone or e-mail) with the Managing Editor and other editorial staff members to plan future issues, to arrange the table of contents, to develop the issue cover, and to discuss organizational issues; 6) editing accepted manuscripts as necessary for substance, accuracy, and clarity; 7) selecting cover photos and writing associated legends; 8) informing editorial staff of noteworthy articles for the media; 9) as the deadline for each issue approaches, deciding which manuscripts will be published.

Nomination packets must include the following:

1. Letter of intent
2. Current CV
3. Vision Statement for the journal

Send nominations to:
Pamela Clapp Hinkle
Managing Editor, *Biological Bulletin*
Marine Biological Laboratory
7 MBL Street
Woods Hole, MA 02543
pclapp@mbl.edu

Marine Biological Laboratory • Woods Hole • Massachusetts

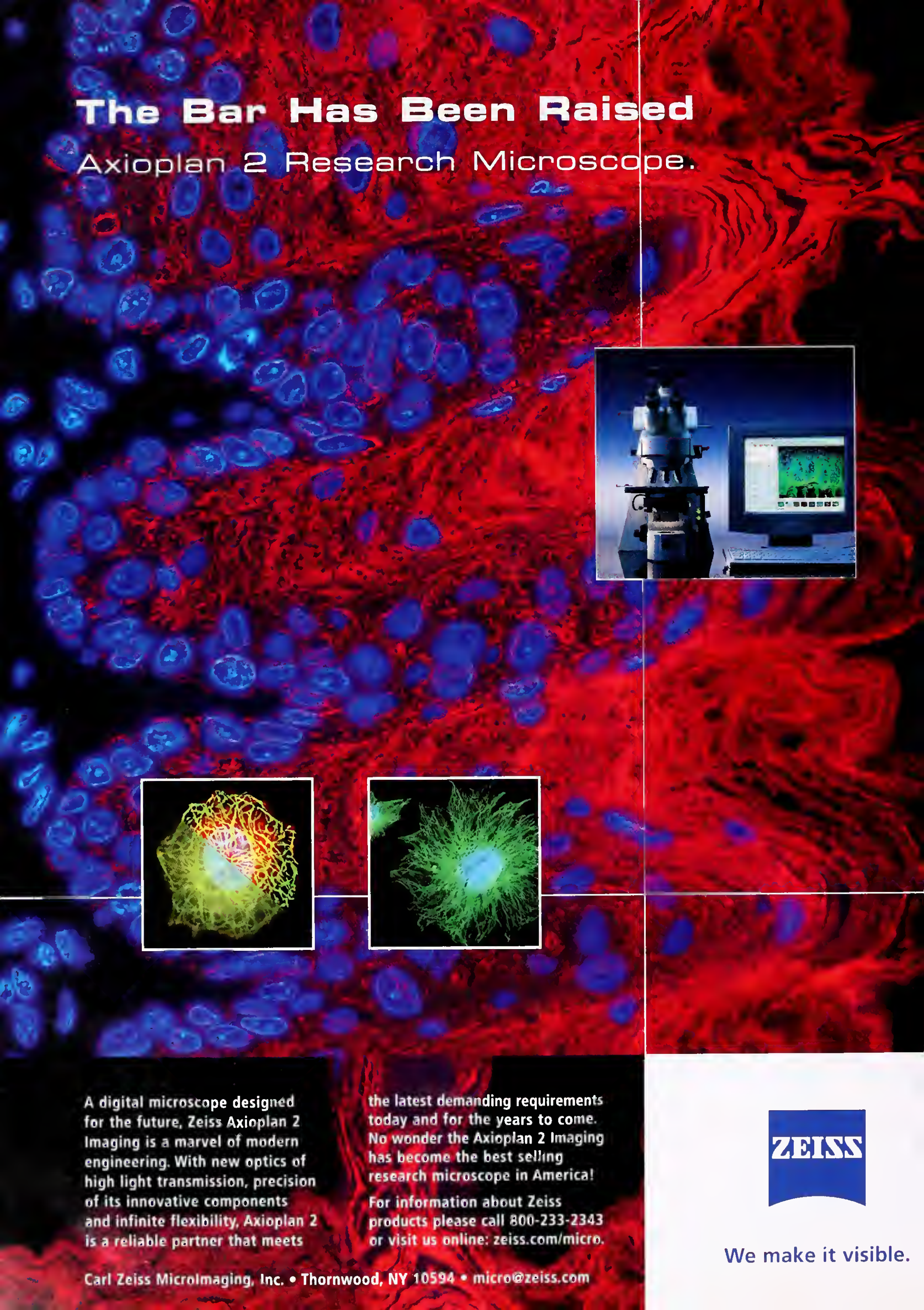

The Bar Has Been Raised

Axioplan 2 Research Microscope.

A digital microscope designed for the future, Zeiss Axioplan 2 Imaging is a marvel of modern engineering. With new optics of high light transmission, precision of its innovative components and infinite flexibility, Axioplan 2 is a reliable partner that meets the latest demanding requirements today and for the years to come. No wonder the Axioplan 2 Imaging has become the best selling research microscope in America!

For information about Zeiss products please call 800-233-2343 or visit us online: zeiss.com/micro.

Carl Zeiss MicroImaging, Inc. • Thornwood, NY 10594 • micro@zeiss.com

ZEISS

We make it visible.

April 2004

Volume 206 • Number 2

THE BIOLOGICAL BULLETIN

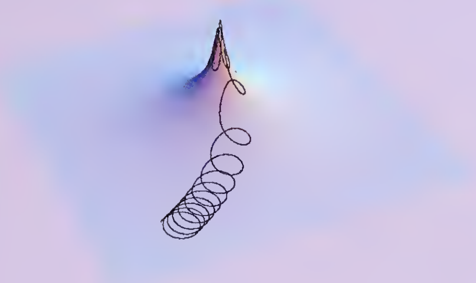

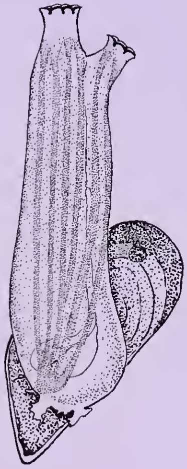

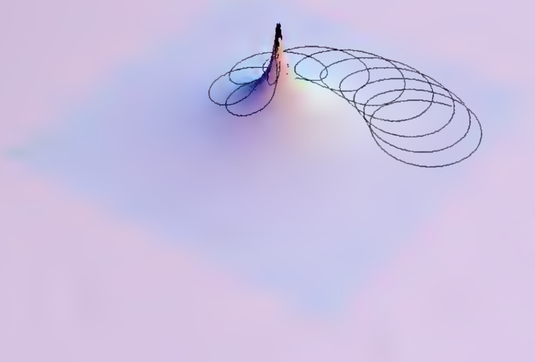

Published by the Marine Biological Laboratory

Woods Hole, Massachusetts

THE BIOLOGICAL BULLETIN
ONLINE

The Marine Biological Laboratory is pleased to announce that the full text of *The Biological Bulletin* is available online at

http://www.biolbull.org

The Biological Bulletin publishes outstanding experimental research on the full range of biological topics and organisms, from the fields of Neurobiology, Behavior, Physiology, Ecology, Evolution, Development and Reproduction, Cell Biology, Biomechanics, Symbiosis, and Systematics.

Published since 1897 by the Marine Biological Laboratory (MBL) in Woods Hole, Massachusetts, *The Biological Bulletin* is one of America's oldest peer-reviewed scientific journals.

The journal is aimed at a general readership, and especially invites articles about those novel phenomena and contexts characteristic of intersecting fields.

The Biological Bulletin Online contains the full content of each issue of the journal, including all figures and tables, beginning with the February 2001 issue (Volume 200, Number 1). The full text is searchable by keyword, and the cited references include hyperlinks to Medline. PDF files are available beginning in February 1990 (Volume 178, Number 1), some abstracts are available beginning with the October 1976 issue (Volume 151, Number 2), and some Tables of Contents are online beginning with the October 1965 issue (Volume 129, Number 2).

Each issue will be placed online approximately on the date it is mailed to subscribers; therefore the online site will be available prior to receipt of your paper copy. Online readers may want to sign up for the eTOC (electronic Table of Contents) service, which will deliver each new issue's table of contents *via* e-mail. The web site also provides access to information about the journal (such as Instructions to Authors, the Editorial Board, and subscription information), as well as access to the Marine Biological Laboratory's web site and other *Biological Bulletin* electronic publications.

The free trial period for access to *The Biological Bulletin* online has ended. Individuals and institutions who are subscribers to the journal in print or are members of the Marine Biological Laboratory Corporation may now activate their online subscriptions. All other access (*e.g.*, to Abstracts, eTOCs, searching, Instructions to Authors) remains freely available. Online access is included in the print subscription price.

For more information about subscribing or activating your online subscription, visit <www.biolbull.org/subscriptions>.

---

http://www.biolbull.org

WHEN IT COMES TO INPUT/OUTPUT FLEXIBILITY, NOTHING WILL GET YOU TO AN IMAGE FASTER.

SCIENCE
UTILITY
VEHICLE.

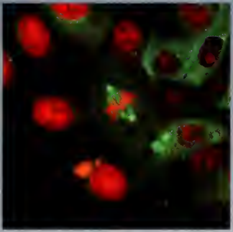

IX81
MOTORIZED
INVERTED
MICROSCOPE.

Olympus' most advanced motorized inverted microscope will position your research lab at the very vanguard of multi-wavelength advanced fluorescence, DIC and deconvolution techniques.

It's totally motorized from the built-in Z-Drive, 6-position nosepiece, 6-position condenser, 6-position fluorescence filter turret, and transmitted and UV shutters.

Nine access ports allow you to keep dedicated cameras and lasers in place and still have plenty of ports available for new devices.

The IX81 demonstrates Olympus' leadership in Total Internal Reflection Fluorescence Microscopy (TIRFM) with exceptional ease of operation and features such as the fully integrated TIRFM illuminator, a 1.45 NA TIRFM objective and the exclusive 1.65 NA objective.

The Olympus IX81 provides extraordinary system flexibility that will satisfy the most demanding research applications.

OLYMPUS
olympus

THE OLYMPUS IX81. ROCKET SCIENCE™.

olympusamerica.com/microscopes 800-455-8236

APR 29 2004

© 2003 OLYMPUS AMERICA INC

OLYMPUS®

Cover

The animals shown on the cover are *Ciona intestinalis*, an ascidian (here attached to a mussel), and *Muggiaea kochi*, a siphonophore. Fertilization in these marine organisms, as in many others, is external. But sperm survive only briefly in seawater, so they would be more effective if they could locate the eggs rapidly. More than 50 years ago, Jean Dan reported, in this journal, a specific attraction between the sperm and eggs of a hydromedusa (1). Since then, attractive substances that affect sperm motility and behavior have been widely detected in eggs and related structures and, in a few species, have been chemically identified.

The effect of a sperm-attracting factor, partially purified from the eggs of *Ciona intestinalis* (2), is illustrated in a video image on the cover (upper left). A pipette is filled with agar impregnated with attractant, and its tip (diameter, $\sim 30\ \mu\mathrm{m}$) is immersed in a drop of *Ciona* sperm suspension. In response to the gradient of factor, sperm swim in spiral paths with a constant radius and with a straight trajectory aimed toward the pipette tip—the source of attractant. Note that this characteristic behavior (chemotaxis) is unchanged as the sperm approaches the attractant and, therefore, as the local concentration of attractant increases. The chemotaxis of siphonophore sperm differs from that of *Ciona*: both the radius of the spiral and the direction of the trajectory change markedly as the sperm approaches the source of attractant. Thus, in their evolution, these two species have acquired different strategies for sperm chemotaxis.

As an approach to this phenomenon and, more generally, to the mechanisms underlying sperm chemotaxis, Makiko Ishikawa, Hidekazu Tsutsui, and their colleagues propose, in this issue of *The Biological Bulletin* (p. 95), two models of sperm chemotaxis—one for ascidians (*e.g.*, *Ciona intestinalis*), and one for siphonophores (*e.g.*, *Muggiaea kochi*). Both models are based on prior experimental evidence, and they share a common assumption: that the radius of the spiral path is inversely dependent upon the intracellular calcium ion concentration ($[\mathrm{Ca}^{2+}]_i$). Modeling the ascidian chemotaxis required one additional assumption: that the $[\mathrm{Ca}^{+2}]_i$, in turn, depend on the change in attractant concentration with time. The siphonophore model—in addition to the common assumption—requires also that $[\mathrm{Ca}^{+2}]_i$ depend on the local concentration of attractant, and that the enzymatic efflux of Ca^{+2} be substantially slower than its influx, raising the $[\mathrm{Ca}^{+2}]_i$.

On the cover, the two sets of calculated data are plotted on graphs representing (in the z axis) the profile of an attractant soon after it begins diffusing from a point source centered in a small area (4 mm^2). Note that this concentration gradient is small until very near the source of attractant, when it spikes. The ascidian model (top plot) is a spiral path that changes little until the sperm reaches the steep portion of the attraction gradient, very close to the source. In contrast, the siphonophore model is a wide spiral path that narrows markedly and curves tightly toward the source as the sperm approaches it (lower plot). Both models approximate experimental results.

This study suggests that only a small number of critical parameters are required to model sperm chemotaxis. Presumably these parameters reflect mechanisms underlying the behavior, and they may be amenable to experimentation, eventually explaining species differences and their adaptive significance.

The video image was provided by Makiko Ishikawa, and the plots of the ascidian and siphonophore model trajectories by Hidekazu Tsutsui (Misaki Marine Biological Station, Tokyo University). The drawing of *Ciona intestinalis* is from Millar, 1970 (3), and that of *Muggiaea kochi* is from Chun, 1882 (4). Stalwarts in the search for illustrations were George Mackie (University of Victoria, Canada), Claudia Mills (University of Washington), Phil Pugh (Southampton Oceanography Centre), Casey Dunn (Yale University and l'Observatoire Océanologique de Villefranche-sur-Mer), Gretchen Lambert (Seattle), Patricia Mather (Queensland Museum, Australia), and Nancy Stafford and Eleanor Uhlinger (MBL/WHOI Library, Woods Hole). The cover was designed by Beth Liles (Marine Biological Laboratory, Woods Hole).

1. **Dan, J. C. 1950.** *Biol. Bull.* **99:**412-415.
2. **Yoshida *et al.*, 1994.** *Dev. Growth Differ.* **36:**589-595.
3. **Millar, R. H. 1970.** *British Ascidians.* Academic Press, London.
4. **Chun, C. 1882.** *Sitzungsber. Preuss. Akad. Wiss.* **52:**1155-1172.

THE
BIOLOGICAL BULLETIN
APRIL 2004

Editor	MICHAEL J. GREENBERG	The Whitney Laboratory, University of Florida
Associate Editors	LOUIS E. BURNETT	Grice Marine Laboratory, College of Charleston
	R. ANDREW CAMERON	California Institute of Technology
	CHARLES D. DERBY	Georgia State University
	MICHAEL LABARBERA	University of Chicago
Section Editor	SHINYA INOUÉ, *Imaging and Microscopy*	Marine Biological Laboratory
Online Editors	JAMES A. BLAKE, *Keys to Marine Invertebrates of the Woods Hole Region*	ENSR Marine & Coastal Center, Woods Hole
	WILLIAM D. COHEN, *Marine Models Electronic Record and Compendia*	Hunter College, City University of New York
Editorial Board	PETER B. ARMSTRONG	University of California, Davis
	JOAN CERDÁ	Center of Aquaculture-IRTA, Spain
	ERNEST S. CHANG	Bodega Marine Lab., University of California, Davis
	THOMAS H. DIETZ	Louisiana State University
	RICHARD B. EMLET	Oregon Institute of Marine Biology, Univ. of Oregon
	DAVID EPEL	Hopkins Marine Station, Stanford University
	KENNETH M. HALANYCH	Auburn University, Alabama
	GREGORY HINKLE	Dana Farber Cancer Institute, Boston
	NANCY KNOWLTON	Scripps Inst. Oceanography & Smithsonian Tropical Res. Inst.
	MAKOTO KOBAYASHI	Hiroshima University of Economics, Japan
	ESTHER M. LEISE	University of North Carolina Greensboro
	DONAL T. MANAHAN	University of Southern California
	MARGARET MCFALL-NGAI	Kewalo Marine Laboratory, University of Hawaii
	MARK W. MILLER	Institute of Neurobiology, University of Puerto Rico
	TATSUO MOTOKAWA	Tokyo Institute of Technology, Japan
	YOSHITAKA NAGAHAMA	National Institute for Basic Biology, Japan
	SHERRY D. PAINTER	Marine Biomed. Inst., Univ. of Texas Medical Branch
	J. HERBERT WAITE	University of California, Santa Barbara
	PHIL YUND	University of New England, Biddeford, ME
	RICHARD K. ZIMMER	University of California, Los Angeles
Editorial Office	PAMELA CLAPP HINKLE	Managing Editor
	VICTORIA R. GIBSON	Staff Editor
	CAROL SCHACHINGER	Editorial Associate
	WENDY CHILD	Subscription & Advertising Administrator

Published by
MARINE BIOLOGICAL LABORATORY
WOODS HOLE, MASSACHUSETTS

http://www.biolbull.org

CONTENTS

Volume 206, No. 2: April 2004

RESEARCH NOTE

Edmunds, Peter J., and Ruth D. Gates
Size-dependent differences in the photophysiology of the reef coral *Porites astreoides* 61

NEUROBIOLOGY AND BEHAVIOR

Lindsay, Sara M., Timothy J. Riordan, Jr., and D. Forest
Identification and activity-dependent labeling of peripheral sensory structures on a spionid polychaete. 65

PHYSIOLOGY AND BIOMECHANICS

Harper, S. L., and C. L. Reiber
Physiological development of the embryonic and larval crayfish heart 78

Ehlinger, Gretchen S., and Richard A. Tankersley
Survival and development of horseshoe crab *(Limulus polyphemus)* embryos and larvae in hypersaline conditions. 87

CELL BIOLOGY

Ishikawa, Makiko, Hidekazu Tsutsui, Jacky Cosson, Yoshitaka Oka, and Masaaki Morisawa
Strategies for sperm chemotaxis in the siphonophores and ascidians: a numerical simulation study. 95

ECOLOGY AND EVOLUTION

Last, Kim S., and Peter J. W. Olive
Interaction between photoperiod and an endogenous seasonal factor in influencing the diel locomotor activity of the benthic polychaete *Nereis virens* Sars. 103

Greenwood, Paul G., Kyle Garry, April Hunter, and Miranda Jennings
Adaptable defense: a nudibranch mucus inhibits nematocyst discharge and changes with prey type . . . 113

THE BIOLOGICAL BULLETIN

THE BIOLOGICAL BULLETIN is published six times a year by the Marine Biological Laboratory, 7 MBL Street, Woods Hole, Massachusetts 02543.

Subscriptions and similar matter should be addressed to Subscription Administrator, THE BIOLOGICAL BULLETIN, Marine Biological Laboratory, 7 MBL Street, Woods Hole, Massachusetts 02543. Subscription includes both print and online journals. Subscription per year (six issues, two volumes): $325 for libraries; $120 for individuals. Subscription per volume (three issues): $165 for libraries; $70 for individuals. Back and single issues (subject to availability): $75 for libraries; $25 for individuals.

Communications relative to manuscripts should be sent to Michael J. Greenberg, Editor-in-Chief, or Pamela Clapp Hinkle, Managing Editor, at the Marine Biological Laboratory, 7 MBL Street, Woods Hole, Massachusetts 02543. Telephone: (508) 289-7149. FAX: 508-289-7922. E-mail: pclapp@mbl.edu.

http://www.biolbull.org

THE BIOLOGICAL BULLETIN is indexed in bibliographic services including *Index Medicus* and MEDLINE, *Chemical Abstracts, Current Contents, Elsevier BIOBASE/Current Awareness in Biological Sciences*, and *Geo Abstracts*.

Printed on acid free paper,
effective with Volume 180, Issue 1, 1991.

POSTMASTER: Send address changes to THE BIOLOGICAL BULLETIN, Marine Biological Laboratory,
7 MBL Street, Woods Hole, MA 02543.

Copyright © 2004, by the Marine Biological Laboratory

Periodicals postage paid at Woods Hole, MA, and additional mailing offices.
ISSN 0006-3185

INSTRUCTIONS TO AUTHORS

The Biological Bulletin accepts outstanding original research reports of general interest to biologists throughout the world. Papers are usually of intermediate length (10–40 manuscript pages). A limited number of solicited review papers may be accepted after formal review. A paper will usually appear within four months after its acceptance.

Very short, especially topical papers (less than 9 manuscript pages including tables, figures, and bibliography) will be published in a separate section entitled "Research Notes." A Research Note in *The Biological Bulletin* follows the format of similar notes in *Nature*. It should open with a summary paragraph of 150 to 200 words comprising the introduction and the conclusions. The rest of the text should continue on without subheadings, and there should be no more than 30 references. References should be referred to in the text by number, and listed in the Literature Cited section in the order that they appear in the text. Unlike references in *Nature*, references in the Research Notes section should conform in punctuation and arrangement to the style of recent issues of *The Biological Bulletin*. Materials and Methods should be incorporated into appropriate figure legends. See the article by Lee (October 2003, Vol. **205:** 99–101) for sample style. A Research Note will usually appear within two months after its acceptance.

The Editorial Board requests that regular manuscripts conform to the requirements set below; those manuscripts that do not conform will be returned to authors for correction before review.

1. ***Manuscripts.*** Manuscripts, including figures, should be submitted in quadruplicate, with the originals clearly marked. (Xerox copies of photographs are not acceptable for review purposes.) Please include an electronic copy of the text of the manuscript. Label the disk with the name of the first author and the name and version of the wordprocessing software used to create the file. If the file was not created in some version of Microsoft Word, save the text in rich text format (rtf). The submission letter accompanying the manuscript should include a telephone number, a FAX number, and (if possible) an E-mail address for the corresponding author. The original manuscript must be typed in no smaller than 12 pitch or 10 point, using double spacing (*including* figure legends, footnotes, bibliography, etc.) on one side of 16- or 20-lb. bond paper, 8 by 11 inches. Please, no right justification. Manuscripts should be proofread carefully and errors corrected legibly in black ink. Pages should be numbered consecutively. Margins on all sides should be at least 1 inch (2.5 cm). Manuscripts should conform to the *Council of Biology Editors Style Manual*, 5th Edition (Council of Biology Editors, 1983) and to American spelling. Unusual abbreviations should be kept to a minimum and should be spelled out on first reference as well as defined in a footnote on the title page. Manuscripts should be divided into the following components: Title page, Abstract (of no more than 200 words), Introduction, Materials and Methods, Results, Discussion, Acknowledgments, Literature Cited, Tables, and Figure Legends. In addition, authors should supply a list of words and phrases under which the article should be indexed.

2. ***Title page.*** The title page consists of a condensed title or running head of no more than 35 letters and spaces, the manuscript title, authors' names and appropriate addresses, and footnotes listing present addresses, acknowledgments or contribution numbers, and explanation of unusual abbreviations.

3. ***Figures.*** The dimensions of the printed page, 7 by 9 inches, should be kept in mind in preparing figures for publication. We recommend that figures be about 1 times the linear dimensions of the final printing desired, and that the ratio of the largest to the smallest letter or number and of the thickest to the thinnest line not exceed 1:1.5. Explanatory matter generally should be included in legends, although axes should always be identified on the illustration itself. Figures should be prepared for reproduction as either line cuts or halftones. Figures to be reproduced as line cuts should be unmounted glossy photographic reproductions or drawn in black ink on white paper, good-quality tracing cloth or plastic, or blue-lined coordinate paper. Those to be reproduced as halftones should be mounted on board, with both designating numbers or letters and scale bars affixed directly to the figures. All figures should be numbered in consecutive order, with no distinction between text and plate figures and cited, in order, in the text. The author's name and an arrow indicating orientation should appear on the reverse side of all figures.

Digital art: The Biological Bulletin will accept figures submitted in electronic form; however, digital art must conform to the following guidelines. Authors who create digital images are wholly responsible for the quality of their material, including color and halftone accuracy.

Format. Acceptable graphic formats are TIFF and EPS. Color submissions must be in EPS format, saved in CMKY mode.

Software. Preferred software is Adobe Illustrator or Adobe Photoshop for the Mac and Adobe Photoshop for Windows. Specific instructions for artwork created with various software programs are available on the Web at the Digital Art Information Site maintained by Cadmus Professional Communications at http://cpc.cadmus.com/da/

Resolution. The minimum requirements for resolution are 1200 DPI for line art and 300 for halftones.

Size. All digital artwork must be submitted at its actual printed size so that no scaling is necessary.

Multipanel figures. Figures consisting of individual parts (*e.g.*, panels A, B, C) must be assembled into final format and submitted as one file.

Hard copy. Files must be accompanied by hard copy for use in case the electronic version is unusable.

Disk identification. Disks must be clearly labeled with the following information: author name and manuscript number; format (PC or Macintosh); name and version of software used.

Color: The Biological Bulletin will publish color figures and plates, but must bill authors for the actual additional cost of printing in color. The process is expensive, so authors with more than one color image should—consistent with editorial concerns, especially citation of figures in order—combine them into a single plate to reduce the expense. On request, when supplied with a copy of a color illustration, the editorial staff will provide a pre-publication estimate of the printing cost.

4. ***Tables, footnotes, figure legends, etc.*** Authors should follow the style in a recent issue of *The Biological Bulletin* in preparing table headings, figure legends, and the like. Because of the high cost of setting tabular material in type, authors are asked to limit such material as much as possible. Tables, with their headings and footnotes, should be typed on separate sheets, numbered with consecutive Arabic numerals, and placed after the Literature Cited. Figure legends should contain enough information to make the figure intelligible separate from the text. Legends should be typed double spaced, with consecutive Arabic numbers, on a separate sheet at the end of the paper. Footnotes should be limited to authors' current addresses, acknowledgments or contribution numbers, and explanation of unusual abbreviations. All such footnotes should appear on the title page. Footnotes are not normally permitted in the body of the text.

5. ***Literature cited.*** In the text, literature should be cited by the Harvard system, with papers by more than two authors cited as Jones *et al.*, 1980. Personal communications and material in preparation or in press should be cited in the text only, with author's initials and institutions, unless the material has been formally accepted and a volume number can be supplied. The list of references following the text should be headed Literature Cited, and must be typed double spaced on separate pages, conforming in punctuation and arrangement to the style of recent issues of *The Biological Bulletin*. Citations should include complete titles and inclusive pagination. Journal abbreviations should normally follow those of the U. S. A. Standards Institute (USASI), as adopted by BIOLOGICAL ABSTRACTS and CHEMICAL ABSTRACTS, with the minor differences set out below. The most generally useful list of biological journal titles is that published each year by BIOLOGICAL ABSTRACTS (BIOSIS List of Serials; the most recent issue). Foreign authors, and others who are accustomed to using THE WORLD LIST OF SCIENTIFIC PERIODICALS, may find a booklet published by the Biological Council of the U.K. (obtainable from the Institute of Biology, 41 Queen's Gate, London, S.W.7, England, U.K.) useful, since it sets out the WORLD LIST abbreviations for most biological journals with notes of the USASI abbreviations where these differ. CHEMICAL ABSTRACTS publishes quarterly supplements of additional abbreviations. The following points of reference style for THE BIOLOGICAL BULLETIN differ from USASI (or modified WORLD LIST) usage:

A. Journal abbreviations, and book titles, all underlined (for *italics*)

B. All components of abbreviations with initial capitals (not as European usage in WORLD LIST *e.g., J. Cell. Comp. Physiol.* NOT *J. cell. comp. Physiol.*)

C. *All* abbreviated components must be followed by a period, whole word components *must not* (*i.e., J. Cancer Res.*)

D. Space between all components (*e.g., J. Cell. Comp. Physiol.*, not *J.Cell.Comp.Physiol.*)

E. Unusual words in journal titles should be spelled out in full, rather than employing new abbreviations invented by the author. For example, use *Rit Vísindafjélags Islendinga* without abbreviation.

F. All single word journal titles in full (*e.g., Veliger, Ecology, Brain*).

G. The order of abbreviated components should be the same as the word order of the complete title (*i.e., Proc.* and *Trans.* placed where they appear, not transposed as in some BIOLOGICAL ABSTRACTS listings).

H. A few well-known international journals in their preferred forms rather than WORLD LIST or USASI usage (*e.g., Nature, Science, Evolution* NOT *Nature, Lond., Science, N.Y.; Evolution, Lancaster, Pa.*)

6. ***Sequences.*** By the time a paper is sent to the press, all nucleotide or amino acid sequences and associated alignments should have been deposited in a generally accessible database (*e.g.*, GenBank, EMBL, SwissProt), and the sequence accession number should be provided.

7. ***Reprints, page proofs, and charges.*** Authors may purchase reprints in lots of 100. Forms for placing reprint orders are sent with page proofs. Reprints normally will be delivered about 2 to 3 months after the issue date. Authors will receive page proofs of articles shortly before publication. They will be charged the current cost of printers' time for corrections to these (other than corrections of printers' or editors' errors). Other than these charges for authors' alterations, *The Biological Bulletin* does not have page charges.

Reference: *Biol. Bull.* **206:** 61–64. (April 2004)
© 2004 Marine Biological Laboratory

Size-Dependent Differences in the Photophysiology of the Reef Coral *Porites astreoides*

PETER J. EDMUNDS[1,*] AND RUTH D. GATES[2]

[1] *Department of Biology, California State University, 18111 Nordhoff Street, Northridge, California 91330-8303; and* [2] *The Hawai'i Institute of Marine Biology, University of Hawaii Manoa, P.O. Box 1346, Kaneohe, Hawai'i 96744*

The recruitment and survival of juvenile corals is central to the maintenance of coral reef communities and the repopulation of denuded reef substrata. Although it is widely accepted that the mortality of scleractinians is inversely proportional to size, the biotic and abiotic factors that drive this trend remain unclear. Here we measure the mortality of corals on the reefs of St. John (U.S. Virgin Islands) to demonstrate that small corals are more likely to die than their larger counterparts, and we explore whether the photophysiological performance of juveniles in two size classes can provide some insight into why smaller corals are so vulnerable. To evaluate photophysiological performance, we examined chlorophyll fluorescence in two size classes (mean diameters 15 mm and 45 mm) of juvenile colonies of Porites astreoides *exposed for short periods to ambient and elevated temperatures. Our results show that the photophysiology of these size classes differs under ambient conditions, with dark-adapted quantum yield (F_v/F_m) being significantly higher in smaller compared to bigger juveniles. As expected, the photophysiology of both size classes is negatively impacted by thermal stress, and although size-related trends are evident in our data, the interaction between size and temperature is not statistically significant. Thus, while there is size dependency in the photophysiological performance of juvenile colonies of* P. astreoides, *the link between this aspect of scleractinian biology and the higher mortality of small juvenile corals in the face of high thermal stress remains unclear.*

As a context for this study, we draw on mortality data for different size classes of corals at five sites on the shallow reefs of St. John. Between 1996 and 2002, the annual mortality of all juvenile corals <20 mm in diameter was 2-fold higher than for corals of 21–40 mm in diameter (Fig. 1), and in genera such as *Porites*, the smallest juveniles experienced a 4.3-fold higher mortality rate than their larger counterparts (Fig. 1). Using these data as a rationale, we compared the photophysiology of two size classes of juvenile colonies of *Porites astreoides* in January 2003. Corals were collected from 6–8 m depth on the west fore reef at Discovery Bay, Jamaica, to represent two significantly different size classes ($t = 17.960$, df $= 26$, $P < 0.001$) with mean diameters of 15 ± 2 mm and 45 ± 6 mm, hereafter described as sizes I and II, respectively. These corals were exposed to ambient (≈27 °C) and elevated temperatures (31.6 °C) for 6 h in the light followed by 2 h in the dark, and the impact of these environmental conditions was evaluated by using pulse amplitude modulation (PAM) fluorometry to measure each coral's photophysiological performance at the end of the 8-h incubation (Fig. 2). The duration of these experiments reflects previously published studies that show an 8-h exposure to high temperature to be sufficient to elicit a photophysiological response in reef corals (1, 2). Throughout the incubations the corals were inspected for signs of stress, such as the production of mucus or the loss of color, but no such responses were observed.

The analysis of the photosynthetic performance of *P. astreoides* by means of PAM fluorometry revealed that the dark-adapted (maximal) quantum yield of photosystem (PS) II (calculated as F_v/F_m which is defined in Fig. 2), differed significantly between size classes and treatments, but that the interaction between size and treatment was not significant (Table 1, Fig. 2). At ambient temperatures, F_v/F_m was 3% to 6% higher in size I *versus* size II juvenile corals, and exposure to the elevated temperature reduced F_v/F_m by 10% in size I and 12% in size II juveniles. Because F_v/F_m

---

Received 10 October 2003; accepted 12 January 2004.

* To whom correspondence should be addressed. E-mail: peter.edmunds@csun.edu

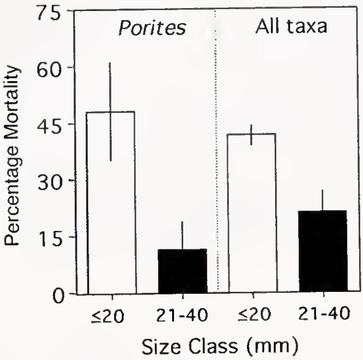

Figure 1. The mortality of juvenile corals at 5–6 m depth along the south coast of St. John, U.S. Virgin Islands. Juvenile corals at five sites were identified to genus, sized (diameter), and tagged. To determine mortality, each coral was relocated a year later and scored as dead or alive (12). Sample sizes and taxonomic composition of the corals varied each year, but most belonged to the genera *Porites*, *Agaricia*, *Siderastrea*, and *Favia*. Mortality was calculated for *Porites* spp. (including *P. astreoides*) and for juveniles pooled by taxon (11 genera), and was determined separately for corals ≤ 20 mm in diameter (small) and between 21 and 40 mm in diameter (big). Mean annual percentage mortality is displayed (±SE; n = 6 years), and differed significantly between small and big juveniles for both *Porites* (t = 2.306, df = 10, P = 0.044) and the pooled taxa (t = 3.076, df = 10, P = 0.012; statistical analyses were carried out with arcsine-transformed percentage mortality). *Porites* mortality was calculated using 58 corals between 1996 and 1997, 46 between 1997 and 1998, 28 between 1998 and 1999, 5 between 1999 and 2000, 17 between 2000 and 2001, and 37 between 2001 and 2002; the sample sizes for all juvenile corals were 395, 187, 105, 28, 57, and 92, respectively.

measures the efficiency of exciting electrons with light energy in PSII, a decline in F_v/F_m reflects a reduction in the efficiency of the photochemical pathways culminating in carbon fixation (3). Thus, our results show that for *P. astreoides*, the photochemical pathways of smaller juveniles are slightly more efficient than those in their larger counterparts, but that their photophysiology is equally impaired by short exposures to elevated temperatures, at least in corals collected and analyzed in the winter.

To explore these size-dependent differences in photophysiology in more detail, we examined nonphotosynthetic quenching in the same corals by qualitatively comparing rapid light curves. Nonphotosynthetic quenching (q_N) is a measure of excess light energy absorbed by the PSII antenna system and dissipated as heat through photoprotective mechanisms such as xanthophyll cycling (3, 4); q_N is calculated from the relationship $q_N = (F_m - F_{m'})/(F_m - F_o)$, where F_m and F_o are defined in Figure 2, and $F_{m'}$ is the maximal fluorescence in the light. We selected q_N because it is more sensitive to thermal stress than variable fluorescence [F_v (5)], and therefore is likely to display more subtle responses to high temperature than F_v/F_m. As expected, q_N appears sensitive to a number of factors; however, most relevant to the current discussion are the differences in response of q_N for sizes I and II juvenile corals under the

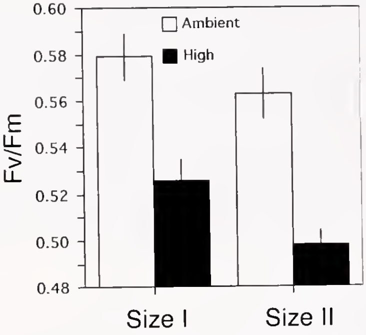

Figure 2. A comparison of the photophysiology of two size classes of juvenile colonies of *Porites astreoides*. Temperature treatments were established in 10-l tanks placed in an air-conditioned room where they received sunlight from an adjacent window [119 ± 5 μmol photons · s^{-1} · m^{-2} (mean ± SD, n = 2), recorded with a spherical Li-Cor sensor at noon]. The tanks were aerated and filled with fresh seawater daily, and maintained at 26.1 ± 0.4 °C (mean ± SE, n = 6, ambient treatment; on reef ≈ 27 °C) and 31.6 ± 0.3 °C (mean ± SE, n = 6, elevated treatment). A randomized block experimental design was used to test for the effects of size and temperature, where each block corresponded to one day of experiments with one coral of each size class allocated to each treatment. Incubations began at noon, and after 6 h the tanks were covered and the corals dark-adapted for at least 2 h prior to assessing their photophysiology. A pulse amplitude modulation fluorometer (PAM-210, Walz GmbH) was used to quantify chlorophyll fluorescence in the dark-adapted state and at each of 11 standard light levels. Fluorescence measurements were obtained by positioning the sensor just above the tissue on the upper surface of a coral colony sitting in seawater at the appropriate incubation temperature. Two sets of recordings were obtained from different positions on each coral, and the average was used as a statistical replicate. Minimal and maximal fluorescences for dark-adapted corals (F_o and F_m, respectively) were measured, and the results displayed as PSII quantum yield [$F_v/F_m = (F_m - F_o)/F_m$; mean ± SE shown ($n$ = 7)]. F_v/F_m differed significantly between size classes and treatments, but there was no statistical interaction between the two (Table 1).

Table 1

Results of a three-way randomized block ANOVA comparing dark-adapted quantum yield of PSII (F_v/F_m) *between size classes (fixed factor I) and treatments (fixed factor II), with the block being the day that the experiment was completed*

Source	SS	df	MS	F	P
Size class	0.0033	1	0.0033	5.5303	0.030
Treatment	0.0241	1	0.0241	40.6022	<0.001
Block	0.0031	6	0.0005	0.8657	0.538
Size class × Treatment	0.0002	1	0.0002	0.3210	0.578
Error	0.0107	18	0.0006		

same light and temperature conditions (Fig. 3). For example, when corals are exposed to elevated temperature at <120 μmol photons · s^{-1} · m^{-2}, q_N is more severely depressed in size I corals than in their larger counterparts (size II). Interestingly, at higher light intensities of ≥ 367 μmol photons · s^{-1} · m^{-2}, this trend is reversed and the size II juveniles incubated at the higher temperature exhibit a greater depression in q_N than do size I corals. Although qualitative, the nuances in our results provide some evidence that the photophysiology of two size classes of juveniles of *P. astreoides* respond differently to the combination of light and temperature used in our experiments. The most parsimonious conclusion is that the two size classes are functionally different in photophysiology (as described by F_v/F_m and q_N); it remains to be demonstrated whether these differences are reflected in their tolerance to thermal stress and in their inverse size-dependent mortality. Perhaps the smallest corals die faster than the bigger corals simply because they are so easily overwhelmed (and killed completely) by sources of mortality other than thermal stress, for example sedimentation or predation (6).

The size-dependent differences in dark-adapted yield (Fig. 2) under ambient conditions likely reflect the functional implications of other well-known aspects of coral biology. For example, conspecifics belonging to different size classes may harbor distinct "types" of symbiotic zooxanthellae (7), each with the physiological characteristics and functional limits most suited to the ontogenetic rigors facing corals of a particular size. Alternatively, the symbionts harbored by size I and size II juvenile corals might be identical, but the communication between the symbiotic partners might be tailored to meet the unique demands of their specific developmental stage, such as the rapid growth necessary for small juveniles to escape the risks of overgrowth and predation (8). Or perhaps allometric scaling of biological traits (9) mediates the differences in photophysiology. For example, size-dependent changes in coral tissue biomass and thickness (9) could create variable shading of zooxanthellae through behavioral responses (10), and rapid protein metabolism in fast-growing small corals could reduce the nitrogen limitation of the symbiotic algae, thereby enhancing the efficiency of photochemical conversion (11). Regardless of the mechanisms underlying our results, we believe that further investigation of size-dependent variation in juvenile corals is likely to be valuable in understanding the environmental thresholds and biology of these complex symbiotic organisms.

Acknowledgments

This research was facilitated by S. Genovese and the East/West Marine Biology Program of Northeastern University, and is dedicated to Mr. Brown, whose tireless spirit and hard work has done much to support our research in Jamaica for the last two decades. We thank R. C. Carpenter and J. Kübler for comments that improved earlier drafts of this paper. Funding was provided in part by the Sea Grant Program of the University of Puerto Rico (grant #R-101-2-02) and the Reef Assessment Program of the Virgin Islands National Park (both to PJE). This is contribution number 119 of the CSUN Marine Biology Program, 677 of the Discovery Bay Marine Laboratory and 1176 of the Hawai'i Institute of Marine Biology.

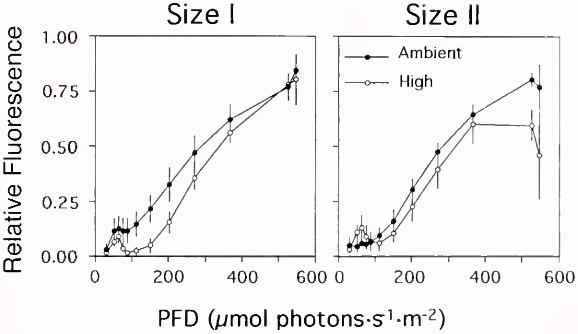

Figure 3. Quenching analyses for size I and size II juvenile corals exposed to ambient and elevated temperature treatments. Measurements were obtained using chlorophyll fluorescence after exposure to each of 11 irradiances for 1 min in the software-driven protocol supplied by the manufacturer (Run 9, Walz GmbH). Results are displayed for nonphotosynthetic quenching (q_N) (mean ± SE, $n = 7$ for each datum) and allow for a qualitative comparison of relative photosynthetic performance between size classes and treatments. One important limitation of this analysis is that photosynthetic equilibrium is probably not achieved within the 1-min irradiance exposures employed.

Literature Cited

1. **Jones, R. J., O. Hoegh-Guldberg, A. W. D. Larkum, and U. Shreiber. 1998.** Temperature-induced bleaching of corals begins with impairment of the CO_2 fixation mechanism in zooxanthellae. *Plant Cell Environment* **21:** 1219–1230.
2. **Warner, M. E., W. K. Fitt, and G. W. Schmidt. 1999.** Damage to photosystem II in symbiotic dinoflagellates: a determinant of coral bleaching. *Proc. Natl. Acad. Sci. USA* **96:** 8007–8012.
3. **Maxwell, K., and G. N. Johnson. 2000.** Chlorophyll fluorescence—a practical guide. *J. Exp. Botany* **51:** 659–668.
4. **Brown, B. E., I. Ambarsari, M. E. Warner, W. K. Fitt, R. P. Dunne, S. W. Gibbs, and D. G. Cummings. 1999.** Diurnal changes in photochemical efficiency and xanthophylls concentrations in shallow water reef corals: evidence of photoinhibition and photoprotection. *Coral Reefs* **18:** 99–105.
5. **Shreiber, U., U. Schliwa, and W. Bilger. 1986.** Continuous recording of photochemical and non-photochemical chlorophyll fluorescence quenching with a new type of modulation fluorometer. *Photosynthesis Research* **10:** 51–62.
6. **Hughes, T. P., and J. B. C. Jackson. 1985.** Population dynamics and life histories of foliaceous corals. *Ecol. Monogr.* **55:** 141–166.
7. **Coffroth, M. A., S. R. Santos, and T. L. Goulet. 2001.** Early ontogenetic expression of specificity in a cnidarian-algal symbiosis. *Mar. Ecol. Prog. Ser.* **222:** 85–96.
8. **Jackson, J. B. C. 1977.** Competition on marine hard substrata: the adaptive significance of solitary and colonial strategies. *Am. Nat.* **980:** 743–767.
9. **Vollmer, S. V., and P. J. Edmunds. 2000.** Allometric scaling in small colonies of the scleractinian coral *Siderastrea siderea* (Ellis and Solander). *Biol. Bull.* **199:** 21–28.
10. **Brown, B. E., C. A. Downs, R. P. Dunne, and S. W. Gibb. 2002.** Preliminary evidence for tissue retraction as a factor in photoprotection of corals incapable of xanthophyll cycling. *J. Exp. Mar. Biol. Ecol.* **277:** 129–144.
11. **Falkowski, P. G., Z. Dubinsky, L. Muscatine, and L. McCloskey. 1993.** Population control in symbiotic corals. *Bioscience* **43:** 606–611.
12. **Edmunds, P. J. 2000.** Patterns in the distribution of juvenile corals and coral reef community structure in St. John, US Virgin Islands. *Mar. Ecol. Prog. Ser.* **202:** 113–124.

Reference: *Biol. Bull.* **206:** 65–77. (April 2004)
© 2004 Marine Biological Laboratory

Identification and Activity-Dependent Labeling of Peripheral Sensory Structures on a Spionid Polychaete

SARA M. LINDSAY*, TIMOTHY J. RIORDAN, JR., AND D. FOREST

School of Marine Sciences, 5751 Murray Hall, University of Maine, Orono, Maine 04469

Abstract. In marine sedimentary habitats, chemoreception is thought to coordinate feeding in many deposit-feeding invertebrates such as polychaetes, snails, and clams. Relatively little is known, however, about the chemosensory structures and mechanism of signal transduction in deposit feeders. Using electron microscopy, confocal laser scanning microscopy (CLSM), and immunohistochemistry, we investigated the structure and function of putative chemosensory cells on the feeding appendages of a deposit-feeding polychaete species, *Dipolydora quadrilobata*. Tufts of putative sensory cilia were distributed over the prostomium and feeding palps and typically occurred next to pores. Examination of these regions with transmission electron microscopy revealed multiciliated cells with adjacent glandular cells beneath the pores. The sensory cells of prostomium and palps were similar, displaying an abundance of apical mitochondria and relatively short ciliary rootlets. Staining with antiserum against acetylated α-tubulin was examined by CLSM, and revealed axonal processes from putative sensory tufts on the palp surface to palp nerves, as well as many free nerve endings. Activity-dependent cell labeling experiments were used to test the sensitivity of putative sensory cells on the palps to an amino acid mixture that elicited feeding in previous behavioral experiments. In static exposures, the number of lateral and abfrontal cells labeled in response to the amino acid mixture was significantly greater than in the controls. Ultrastructural, positional, and now physiological evidence strongly suggests that spionid feeding palps are equipped with sensory cells, at least some of which function as chemoreceptors.

Introduction

In marine sedimentary habitats, deposit-feeding invertebrates such as polychaetes, bivalves, gastropods, crustaceans, holothurians, and hemichordates are abundant members of the macrofauna. These organisms ingest large volumes of sediment with typically low food value, often processing one or more body weights of sediment each day (reviewed in Lopez and Levinton, 1987). They also disturb the sediment as they burrow or build tubes. As bioturbators, deposit feeders have a profound influence on the biological, chemical, geological, and even physical properties of their habitat. Deposit feeders affect sediment transport and distribution (*e.g.*, Nittrouer and Sternberg, 1981; Suchanek, 1983; Shull, 2001), sediment geochemistry (Marinelli, 1992; Aller, 1994), sediment microbial communities (Findlay *et al.*, 1990; Grossman and Reichardt, 1991; Plante and Mayer, 1994), nutrient cycling (Widbom and Frithsen, 1995; Christensen *et al.*, 2000), and fate of pollutants (Mayer *et al.*, 1996; Weston *et al.*, 2000). Sediment disturbance by deposit feeders mediates competitive interactions (*e.g.*, Rhoads and Young, 1970; Woodin, 1976; Wilson, 1981; Brenchley, 1981), and influences animal distribution patterns and dispersal (Wilson, 1981; Gunther, 1992; Brey, 1991), as well as recruitment (Williams, 1980; Posey, 1986; Luckenbach, 1987; Hines *et al.*, 1989; Olafsson, 1989; Flach, 1992). In addition, deposit feeders can influence recruitment directly by ingesting larvae and juveniles (Wilson, 1980; Tamaki, 1985; Miliekovsky, 1974; Elmgren *et al.*, 1986; Albertsson and Leonardsson, 2001).

Rates of sediment mobilization by deposit feeders depend on food supply. In the last two decades, behavioral, physiological, and mathematical modeling approaches have been applied to the question of what makes some sediments better food than others (*e.g.*, review by Jumars, 1993). Largely absent from this body of research, however, are studies that investigate the cues that initiate ingestion and modulate feeding rates in deposit feeders. Jumars (1993)

Received 17 September 2002; accepted 4 February 2004.

* To whom correspondence should be addressed. E-mail: slindsay@maine.edu

suggested several stimuli that could operate to regulate ingestion rate: smell, taste, distension of the gut, and internal detection of the absorbed products in body fluids. The physiological and molecular mechanisms for detecting these stimuli remain poorly understood for most deposit feeders.

Chemoreception is implicated in the coordination of feeding by a variety of deposit feeders. For example, fresh fecal material depresses feeding rate in the snail *Hydrobia truncata* (Forbes and Lopez, 1986) and the spionid polychaete *Pseudopolydora kempi japonica* (Miller and Jumars, 1986). Phagostimulants are implicated as well. When given a choice, the common deposit-feeding polychaete *Streblospio benedicti* fed preferentially on organically enriched sediments rather than on unaltered sediments (Kihslinger and Woodin, 2000). Feeding rate in a deposit-feeding hemichordate was strongly correlated with sediment chlorophyll *a* concentrations (Karrh and Miller, 1994). Robertson *et al.* (1980) found that fiddler crabs, *Uca pugilator*, fed selectively in diatom-enriched patches of sediment and could resolve patches at the millimeter scale by probing with sensory setae on their legs. Fiddler crabs have also been the focus of several studies that explicitly tested the effects of chemical compounds on deposit feeders. A variety of amino acids, peptides, and sugars appear to stimulate feeding (Robertson *et al.*, 1981; Rittschof and Buswell, 1989; Weissburg and Zimmer-Faust, 1991; Weissburg, 1993). Similarly, Ferner and Jumars (1999) found that dissolved cues (amino acids and complex mixtures) influenced the feeding behavior of several spionid polychaetes. We recently extended this work to show that particle-bound amino acids and sugars influence feeding in the spionid polychaete *Dipolydora quadrilobata* (Riordan and Lindsay, 2002).

Although chemical mediation of deposit feeding seems likely, relatively little is known about the chemosensory structures and mechanism of signal transduction in deposit feeders. One exception is fiddler crabs. Weissburg and colleagues have identified gender-specific differences in fiddler crab feeding behavior in response to chemical cues, and these are linked to differences in the number and sensitivity of chemoreceptor neurons (Weissburg, 1993, 1999; Weissburg and Derby, 1995; Weissburg *et al.*, 1996). Recent work (Weissburg, 2001) suggests the adenylate-cyclase–cAMP second messenger cascade mediates inhibition of chemosensory neurons, and that gender-specific differences in this pathway contribute to the physiological and behavioral differences in fiddler crab chemosensitivity.

Among the polychaetes, nuchal organs are presumed to be involved in chemoreception based on histological, ultrastructural, and positional criteria (Storch and Schlötzer-Schrehardt, 1988; Purschke, 1997). Several authors have speculated that nuchal organs may be involved in food selection (Rullier, 1951; Rhode, 1990; Nozais *et al.*, 1997) or reproduction (Schlötzer-Schrehardt, 1987), although they may also be involved in osmoregulation (Fewou and Dhainaut-Courtois, 1995). Nuchal organs typically are paired epidermal structures found on the dorsal side of the prostomium or peristomium (*i.e.*, the anterior presegmental region). Some spionid polychaetes (not *Dipolydora quadrilobata*) also have metameric nuchal organs on their bodies (Jelsing, 2002). Cephalic nuchal organs are typically composed of ciliated supporting cells, bipolar primary sensory cells with cilia, unmodified epidermal cells, and retractor muscle cells in those species in which nuchal organs can be retracted (reviewed by Purschke, 1997).

Other presumed chemosensory structures have been described from polychaetes, including epidermal papillae of the deposit-feeding lugworm *Arenicola marina* (Jouin *et al.*, 1985), compound sensory organs on the prostomial cirri and palps of *Nereis diversicolor* (Dorsett and Hyde, 1969), and the parapodial cirri of nereidid polychaetes (Boilly-Marer, 1972). In *Platynereis dumerlii*, the receptors of the parapodial cirri function in perception of sexual pheromones (Boilly-Marer, 1968, 1974). Peripheral sensory structures have also been observed on the feeding palps, prostomia, and peristomia of several spionid polychaete species (Dauer, 1984, 1987, 1991, 1997; Worsaee, 2001). With the exception of the nereidid pheromone receptors, studies demonstrating functions of these putative polychaete chemoreceptors are largely absent. The goals of this study were to (1) describe the distribution and ultrastructure of peripheral sensory cells of the spionid polychaete *Dipolydora quadrilobata*, and (2) assign a functional role to these structures by using an immunohistochemical approach that labeled cells responding to chemical cues that elicited behavioral responses in *D. quadrilobata* (Riordan and Lindsay, 2002).

Materials and Methods

Collection and maintenance of animals

Individuals of *Dipolydora quadrilobata* (Jacobi 1883) were sieved (0.5 mm) out of cores collected from the mudflats of Lowe's Cove at the University of Maine's Darling Marine Laboratory (Walpole, ME, USA) on several days in September and October of 2000, and March, April, and May of 2001. Animals and natural sediments were transported to the University of Maine in Orono and maintained in aquaria inside an environmental chamber (14 °C:10 °C, 12 h light:dark cycle). Individual worms that measured 10–20 mm in length and showed no signs of gametogenesis, loss of segments, or other bodily damage were used in the experiments.

Electron microscopy

For scanning electron microscopy (SEM), intact worms were relaxed in chilled 37% magnesium chloride, fixed in

3% glutaraldehyde in 0.1 *M* phosphate buffer with 10% sucrose, post-fixed in 1% osmium tetroxide in 0.1 *M* phosphate buffer, and dehydrated in an ethanol series. Samples were then critical-point-dried with liquid CO_2, mounted on stubs, and coated with gold palladium in a Conductavac I (SpeeVac, Inc.) sputter coater. Samples were viewed with an AMRay AMR1000A scanning electron microscope operating at 5 kV. Negatives were scanned at 800 dpi with an HP Scanjet 7400C flatbed scanner equipped with an HP Scanjet XPA attachment, and the images were saved as TIFF files.

For transmission electron microscopy (TEM), worms were relaxed in chilled 37% magnesium chloride, fixed in 3% glutaraldehyde in phosphate buffer with 10% sucrose, post-fixed in 1% osmium tetroxide in 0.1 *M* phosphate buffer, dehydrated in an acetone series, and embedded in Spurr's resin. Ultrathin sections were collected onto slot grids, then stained with 0.5% lead citrate and 2% uranyl acetate. Samples were viewed with a Phillips CM10 transmission electron microscope operating at 80 kV. Negatives were scanned at 800 dpi with an HP Scanjet 7400C flatbed scanner equipped with a HP Scanjet XPA attachment, and the images were saved as TIFF files.

Confocal laser scanning microscopy

Worms were relaxed in a 37% $MgCl_2$ solution for 5 min, then fixed overnight at 4 °C in a solution of 4% formaldehyde in artificial seawater (ASW, 32‰, pH 7.4, Forty Fathoms Crystal Sea Marine Mix, Marine Enterprises International, Baltimore, MD). After three 10-min rinses in ASW, worms were soaked for 5 h in a blocking solution containing 0.5% Triton-X 100 and 0.5% bovine serum albumin (BSA). The primary antibody (1° Ab), monoclonal mouse anti-acetylated α-tubulin (Sigma, St. Louis; clone 6-11B-1), was diluted 1:100 with 0.5% Triton X-100 in ASW and applied overnight (about 18 h). Specimens were then rinsed in ASW and incubated for 5 h with FITC-conjugated goat anti-mouse secondary antibodies (Sigma; Fc specific IgG) diluted 1:100 in 0.5% Triton X-100/ASW. After a final series of ASW rinses, worms were mounted on glass slides in Fluoromount-G (Southern Biotechnology Associates, Birmingham, AL). Preparations were imaged with a Leica TCS SP2 confocal laser scanning microscope. Negative controls to test for the specificity of primary antibodies were prepared by treating specimens as described, but omitting the 1° Ab. Repeated incubations were performed, and at least 10 worms were used to test for reproducibility.

Activity-dependent cell labeling

We adapted the method used by Michel *et al.* (1999) to label activated olfactory neurons in zebrafish and spiny lobsters. This method exploits the ability of cationic guanidinium analogs to enter into stimulated neurons and metabolically active cells (Dwyer *et al.*, 1980; Picco and Menini, 1993). These analogs enter active neurons through nonspecific cation channels activated and opened by the binding of a ligand with its receptor protein. Sequestration of the analogs in these cells allows for the activity-dependent labeling of individual receptor neurons.

For example, the guanidinium analog, 1-amino-4-guanidobutane (= agmatine), has been shown to enter into receptor neurons through such open cation channels (Yoshikami, 1981). When coupled with known stimulatory cues in solution and perfused over olfactory organs, agmatine accumulates in activated odorant receptor neurons (Michel *et al.*, 1999; Steullet *et al.*, 2000). Cells stimulated by a cue accumulate agmatine and can be identified using an anti-agmatine IgG antibody followed by silver intensification labeling (Marc, 1995, 1999a, b). We presented agmatine plus a mixture of amino acids known to elicit behavioral responses to individual specimens of *Dipolydora quadrilobata* in both flow-through and static experiments.

Flow trials. Individual worms were immersed in artificial seawater (ASW, in m*M*: 423 NaCl, 9 KCl, 13 $CaCl_2$, 23 $MgCl_2$, 26 $MgSO_4$ (Cavanaugh, 1975) pH adjusted to 7.2) inside a small coverslip perfusion chamber (Warner Instruments, Model #RC 21B). Odorant stimuli were added to the ASW perfusion fluid in 5-s pulses every 60 s for 60 min. The ASW and the odorant stimuli solutions were held in 60-ml syringes connected to the perfusion chamber through rubber tubing and a manifold. Fluid flow from the syringes was by gravity feed, and flow rates (0.5 cm s^{-1}) were controlled by stopcock valves; fluid flow was turned on and off by electronically activated pinch valves (Warner Instruments, model VC-6). Stimuli included 20 m*M* agmatine sulfate (AGB) in ASW (control, n = 4 worms) and 20 m*M* AGB plus a mixture of amino acids (1 m*M* each of proline, alanine, threonine, valine, taurine, and glycine) in ASW (treatment, n = 5 worms). Following the 60-min stimulation period, ASW was perfused over the worms for 5 min to remove residual AGB. Worms were then immersed in fresh ASW and relaxed by placing them in a freezer (−20 °C) for 10 min prior to fixing. Whole worms were placed in fixative (1% paraformaldehyde, 2% glutaraldehyde in 0.2 *M* phosphate buffer with 10% sucrose (w/v), pH 7.2) from overnight to several days.

No flow (static) trials. Individual worms were immersed in 10 ml ASW inside a small petri dish, and 10 ml of either 40 m*M* AGB in ASW (control, n = 6 worms) or 40 m*M* AGB plus the mixture of amino acids in ASW (treatment, n = 6 worms) was slowly added by pipette. Worms were exposed to the treatments for 60 min, during which time they were relatively quiescent in the dishes, immersed in fresh ASW for 5 min to remove residual AGB, and relaxed by placing them in a freezer (−20 °C) for 10 min prior to fixing. Whole worms were placed in fixative (1% paraformaldehyde, 2% glutaraldehyde in 0.2 *M* phosphate buffer with 10% sucrose (w/v), pH 7.2) from overnight to several days.

Tissue processing, immunolabeling, and visualization

Fixed worms were rinsed in a phosphate buffer (PB: 1.76 g $NaH_2PO_4 \cdot H_2O$ + 7.67 g Na_2HPO_4 in 1 l of deionized water), dehydrated through a graded series of absolute ethanol and acetone, embedded in Epon 812 resin, cured, and sectioned using a microtome and glass knives. An average of 156 sections were processed for each individual. Semi-thick sections (2 μm) were placed in 7-mm wells of a Teflon-coated spot slide (Erie Scientific), deplasticized in a 1:5 v/v solution of mature sodium ethoxide in anhydrous ethanol, and subsequently washed in three changes of anhydrous ethanol. The slides were rinsed in deionized water, air-dried, and then incubated overnight in a 1:100 dilution of a polyclonal rabbit anti-AGB IgG antibody (Signature Immunologics and courtesy of R. Marc, University of Utah School of Medicine). The slides were then rinsed in PB, washed in 1% goat serum in PB plus 0.05% thimerosal (1% GSPBT) for 10 min, and incubated in a 1:50 dilution of a 1-nm gold conjugated anti-rabbit IgG antibody for 60 min. After a final PB wash and air-drying, labeled cells were visualized using silver intensification (Marc, 1999a, b). The silver nitrate solution for silver intensification was prepared by mixing three solutions: 5 ml of solution A (114 mg citric acid + 342 mg sodium citrate in 6 ml of deionized water), 1 ml of solution B (0.5 g hydroquinone in 15 ml of deionized water), and 1 ml of 1% aqueous silver nitrate. Following a dip in 5% acetic acid to stop the intensification reaction, the slides were washed in deionized water for 10 min, air-dried, and mounted in Permount (Fisher) for viewing on a light microscope.

Image digitization and analysis

Images of the sections were captured digitally using a Javelin JE12HMV video camera mounted on an Olympus BX60 light microscope. Video signals were passed to a frame grabber board (Scion LG 3) in a Dell Optiplex GX110 computer. The images were analyzed using the Scion ImagePC software, Beta ver. 4.02 (Scion Corporation, Frederick, MD). Cells labeled with agmatine were identified by quantifying the pixel intensity inside a cell of interest in the digitized images and comparing it to the pixel intensity of an unlabeled region adjacent to the cell (*e.g.* Michel *et al.*, 1999). The mean and standard deviation of the pixel intensity inside cells of interest was used to calculate a 95% confidence interval; cells were counted as labeled if the lower limit of this interval was higher than the upper limit of the unlabeled region. Two strategies were used to avoid double-counting of labeled cells. First, cells were counted only if the distal processes and apical cilia were present in the same plane as the labeled cell body; these processes typically were not coplanar in more than one adjacent section. Second, the locations of labeled cells in a single section were compared to labeled cells in adjacent sections to avoid counting the same cell twice.

Labeled cells were grouped by type according to their location within the sections (Fig. 1). Abfrontal cells were located behind a straight line drawn across the sections and tangent to the back of the food groove. Lateral cells were found between the food groove and the abfrontal cilia. Cells immediately adjacent to the frontal ciliated food groove were called laterofrontal cells. And cells located within the frontal ciliated food groove were called frontal cells. Because different numbers of sections were analyzed for each worm, we calculated the number of labeled cells per 100 μm palp length, based on the total number of sections analyzed per individual. The resulting data were compared among treatments using a nonparametric Kruskal-Wallis analysis of variance (SAS version 9, SAS Institute, Inc.). Data from flow experiments and static experiments were analyzed separately.

To estimate the total number of each cell type in any length of palp, serial sections made from the palps (middle portion) of four worms were stained with a toluidene blue stain. Toluidene blue stains acidic cell parts (*i.e.*, nucleus) and allows the different types of cells to be identified and counted. Individual cells were traced through the sections to avoid double-counting. On average, about 121 μm of palp tissue was sectioned for each of these worms, representing about 5% of the average length of the palps of *D. quadrilobata*.

Results

Distribution of peripheral sensory cells

Scanning electron microscopy revealed tufts of cilia (*i.e.*, cirri, *sensu* Worsaae, 2001) distributed on the palps and prostomium of *Dipolydora quadrilobata* (Fig. 2). Tufts of putative sensory cilia were found on all surfaces of the prostomium (Fig. 2B) and were typically adjacent to pores (Fig. 2B). The cilia of the prostomial tufts were nonmotile and relatively short; they numbered about 13–20 cilia per tuft (Fig. 2C). On the palps, we observed motile cilia arrayed in a row immediately adjacent to each side of the food groove (laterofrontal, Fig. 3A, B), and tufts of motile cilia arrayed in a second lateral row and on the abfrontal surface (Fig. 3A, B). Laterofrontal, lateral, and abfrontal cilia occurred with similar frequency along the length of the palp (Fig. 3C). The putative sensory tufts of cilia on the abfrontal surface seemed regularly dispersed; and, interestingly, we observed fewer adjacent pores than on the prostomium. The cilia of the abfrontal surfaces were longer than

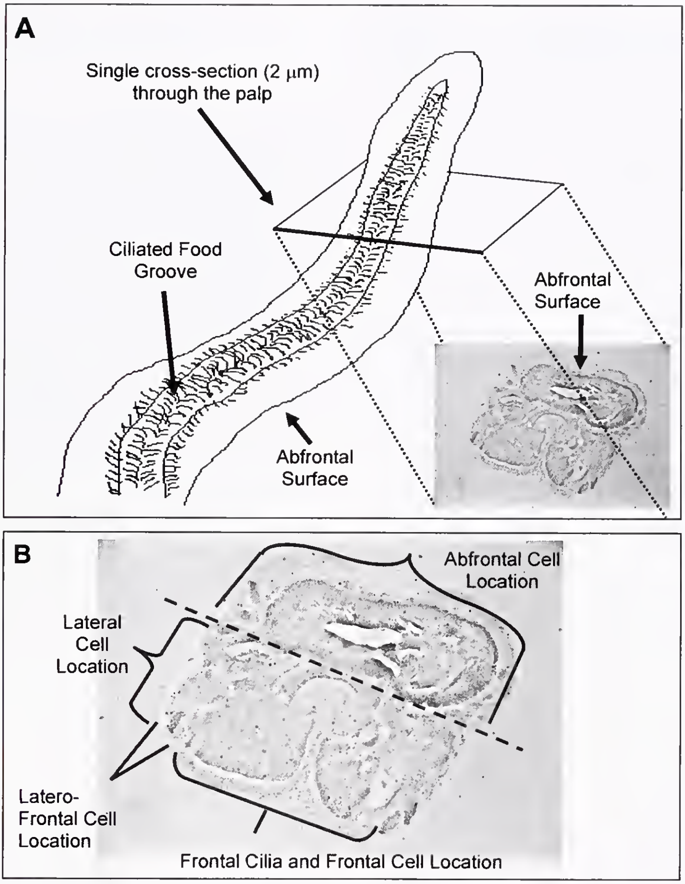
A
Single cross-section (2 μm) through the palp
Ciliated Food Groove
Abfrontal Surface
Abfrontal Surface
B
Abfrontal Cell Location
Lateral Cell Location
Latero-Frontal Cell Location
Frontal Cilia and Frontal Cell Location

Figure 1. (A) Gross palp morphology and section placement for cell labeling studies in *Dipolydora quadrilobata*. (B) Cell type location within sections. Cells along the food groove and within the frontal cilia were designated frontal cells. Cells immediately adjacent to the frontal cilia were designated laterofrontal cells. Cells behind a line drawn across the back end of the food groove were designated abfrontal cells. Cells in front of that line and lateral to the frontal surface were designated lateral cells.

those of the prostomium, and there were fewer cilia per tuft (7–14) (Fig. 3C, inset).

Sensory cell ultrastructure

Palp and prostomial sensory cells shared similar ultrastructural characteristics. All were multiciliated and contained many apical mitochondria (Figs. 4, 5). Laterofrontal cells on the palp were typically adjacent to glandular cells (Fig. 4) associated with pores on the surface. Gland cells contained either globules of very electron-dense material (Fig. 4C) or less dense material that appeared to be mucus (not shown). Abfrontal cells of the palp were restricted by the muscle layers below, and cell bodies often projected laterally (Fig. 5). Ciliary rootlets of both palp and prostomial cells, when observed, were short relative to the length of the cell body (Fig. 5A). All cilia were readily distinguishable from the microvillar cuticle (Figs. 4, 5) and displayed a characteristic 9 × 2 + 2 microtubular arrangement in cross-section.

Confocal laser scanning microscopy

The antibody for acetylated α-tubulin targets nerve axons and cilia axoneme microtubules. Cilia of the food groove,

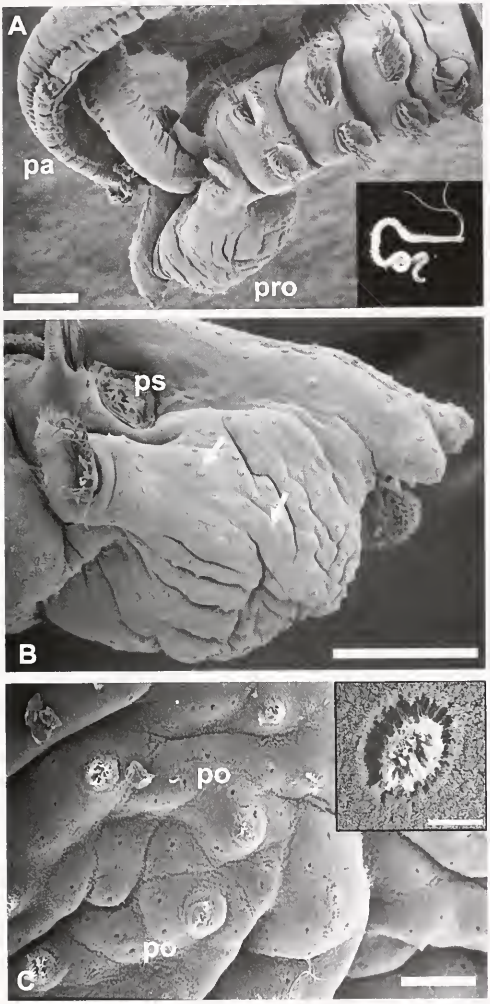

Figure 2. Peripheral sensory cells on the prostomium of *Dipolydora quadrilobata*. (A) Anterior profile, showing palps (pa) and prostomium (pro); scale = 100 μm. Inset shows entire worm. (B) Ciliated structures are distributed on the entire surface of the prostomium (arrows); palps were removed, leaving a scar (ps); scale = 100 μm. (C) Pores (po) are found adjacent to the sensory structures on the prostomium; scale = 10 μm. Inset shows the sensory cilia of the prostomium; inset scale = 2.5 μm.

lateral and abfrontal surfaces of palp, as well as the main palp nerve and several smaller palp nerves projecting to the central nervous system showed acetylated α-tubulin reactivity (Fig. 6A). Our initial observations clearly show axons that project from the cilia of putative lateral and abfrontal sensory tufts to the palp nerves (Fig. 6B). There are also many nerves with apparent free endings on the palp surface (*i.e.*, not associated with ciliated cells). A more detailed

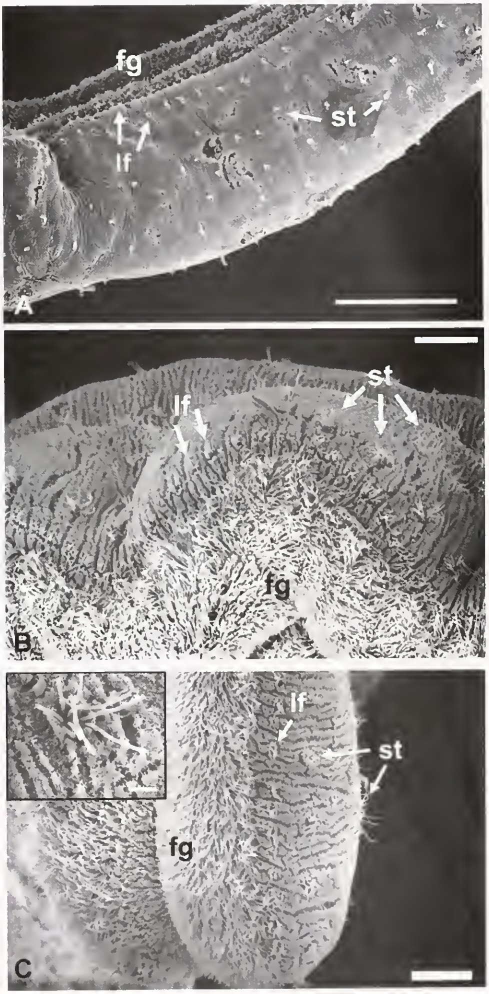

Figure 3. Peripheral sensory cells on the palp of *Dipolydora quadrilobata*. (A) Lateral view of the middle portion of a feeding palp, showing frontal food groove (fg), laterofrontal cilia (lf), and tufts of nonmotile sensory cilia (st) on the lateral and abfrontal surfaces of the palp; scale = 50 μm. (B) Middle portion of the feeding palp showing laterofrontal (lf) cilia adjacent to the frontal food groove (fg), as well as laterally distributed sensory tufts (st); scale = 10 μM. (C) Distal portion of feeding palp showing the food groove (fg), laterofrontal (lf) cilia, and sensory tufts (st); scale = 10 μm. Inset: palp sensory tufts appear to be similar to those on the prostomium; inset scale = 1 μm.

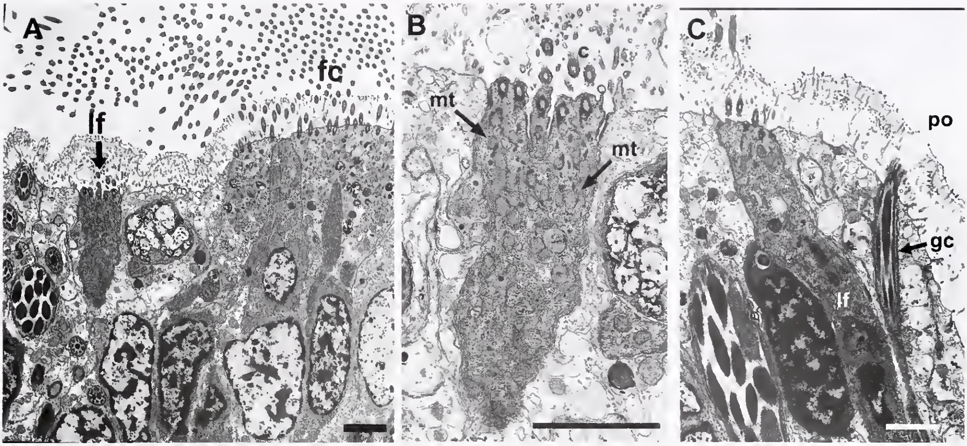

Figure 4. Ultrastructure of *Dipolydora quadrilobata* palp laterofrontal cells. (A) Semi-oblique section through palp food groove showing dense field of frontal cilia (fc) and adjacent laterofrontal cell (lf); scale = 2 μm. (B) Same laterofrontal cell showing numerous cilia (c) and many apical mitochondria (mt); scale = 2 μm; the basal portion of the cell projects out of the plane of section. (C) Another semi-oblique section of the palp reveals the laterofrontal cell and adjacent glandular cell (gc) with pore (po); scale = 2 μm.

examination of the innervation of these peripheral sensory cells, as well as their reactivity to anti-serotonin and anti-FMRFamide, is in progress.

Activity-dependent labeling

Four types of putative sensory cells were labeled by exposing the palps of *D. quadrilobata* to agmatine and the amino acid mixture: frontal, laterofrontal, lateral, and abfrontal cells (Fig. 7). These four cell types all have cellular processes extending through the epidermis to the surface of the palp (Fig. 7), many with visible cilia extending from the surface of the palp. Frontal and laterofrontal cells were generally found as groups of several cells close to one another at the periphery of the food groove, and often most of these cells were labeled. In contrast, labeled lateral and abfrontal cells were always found in isolation.

The occurrence of labeled cells in the flow-through perfusion experiment was quite variable (Fig. 8A). Pooling all cell types, there was no significant effect of amino acids (cue) on cell labeling (Kruskal-Wallis $\chi^2 = 0.74$, d.f. = 1, $P = 0.39$, $n = 27$). There was a non-significant trend toward greater labeling in the controls for laterofrontal and frontal cells (*e.g.,* Kruskal-Wallis test of the difference between the number of frontal cells labeled in the presence of amino acids compared to controls: $\chi^2 = 2.7655$, d.f. = 1, $P = 0.09$, $n = 9$). Relatively fewer cells were labeled in the static experiments (Fig. 8B, note axis scale). In contrast to the flow experiment, however, addition of amino acids significantly increased cell labeling with agmatine compared to controls in all cell types pooled (Kruskal-Wallis, $\chi^2 = 9.88$, d.f. = 1, $P = 0.002$, $n = 36$). We observed the greatest amount of labeling in lateral and abfrontal cells (Fig. 8B).

Based on counts from the serial sections stained with toluidine blue, frontal cells and laterofrontal cells occur at about the same frequency, averaging 27 frontal cells and 28 laterofrontal cells per 100 μm of palp. Lateral and abfrontal cells occur less frequently, at a combined average rate of 11 cells per 100 μm of palp. Given an average palp length of 2.55 mm for *D. quadrilobata,* and assuming no changes in distribution along the length of the palp, we can then expect approximately 688 frontal cells, 714 laterofrontal cells, and a total of 280 lateral and abfrontal cells to occur on a single palp. Based on the occurrence of labeling that we observed in static trials only, we conservatively estimate that 14% of the total number of lateral and abfrontal cells, 4% of the total number of laterofrontal cells, and 3% of the total number of frontal cells were labeled by agmatine in the presence of amino acids.

Discussion

The diversity of chemosensory organs among marine organisms is great, from crustacean aesthetasc sensilla to molluscan osphradium, rhinophores, and oral tentacles, to polychaete nuchal organs (Laverack, 1968; Emery, 1992). Despite this diversity, the transduction of externally detected signals to the brain follows a similar pathway, beginning with the activation of a chemoreceptor cell that leads to the central nervous system. The structural common denominator for all chemosensory cells is the presence of ciliary or microvillar extensions into the environment. The peripheral cells of the spionid palps and prostomium clearly meet this requirement (Figs. 2, 3).

Dauer (1984, 1987, 1991, 1997) and Worsaee (2001) observed nonmotile cilia on palps and prostomia of several spionid species, including *Dipolydora quadrilobata*, and classified them as sensory on the basis of scanning electron microscopy data and positional criteria. Our initial TEM observations (Figs. 4, 5) support these classifications, and suggest that these peripheral sensory cells have features similar to the caudal chemoreceptors that Jouin *et al.*, (1985) described in *Arenicola marina*—namely an abundance of apical mitochondria and short ciliary rootlets. Confocal laser scanning microscopy further reveals axonal processes to palp nerves from the lateral and abfrontal sensory tufts (Fig. 6), as well as many free nerve endings projecting to the lateral and abfrontal surfaces of the palps.

Assigning function to cells based solely on morphological criteria can be difficult, however. For example, it appears that no single morphological character defines chemoreceptor cilia: on the crustacean aesthetasc, olfactory cilia can have "significant" ciliary rootlets and motile cilia (Grünert and Ache, 1988). We used the activity-dependent labeling experiments to explore the possible function of the palp sensory cells. Although we designed the experiment to assay for cell activity in the presence or absence of chemical cues (amino acids), it is important to note that this method of labeling active sensory cells does not discriminate between types of receptors. It simply identifies cells that have accumulated agmatine, regardless of the stimulus source. Thus, the labeled cells may include a variety of sensory cell types. The initial stimulation of a mechanoreceptor (*i.e.*, stretching or bending of the cell membrane or a protruding cilium) in at least one invertebrate (the crayfish) opens a stretch-activated ion channel that appears to be permeable to divalent cations (Edwards *et al.*, 1981). Chemoreceptor transduction proceeds similarly, with the binding of a ligand to the receptor in the membrane causing the activation and opening of ion channels. In both cases, such cation-permeable channels should be permeable to agmatine, and therefore both mechanoreceptors and chemoreceptors could be labeled using this technique.

Spionid palps are probably equipped with mechanosen-

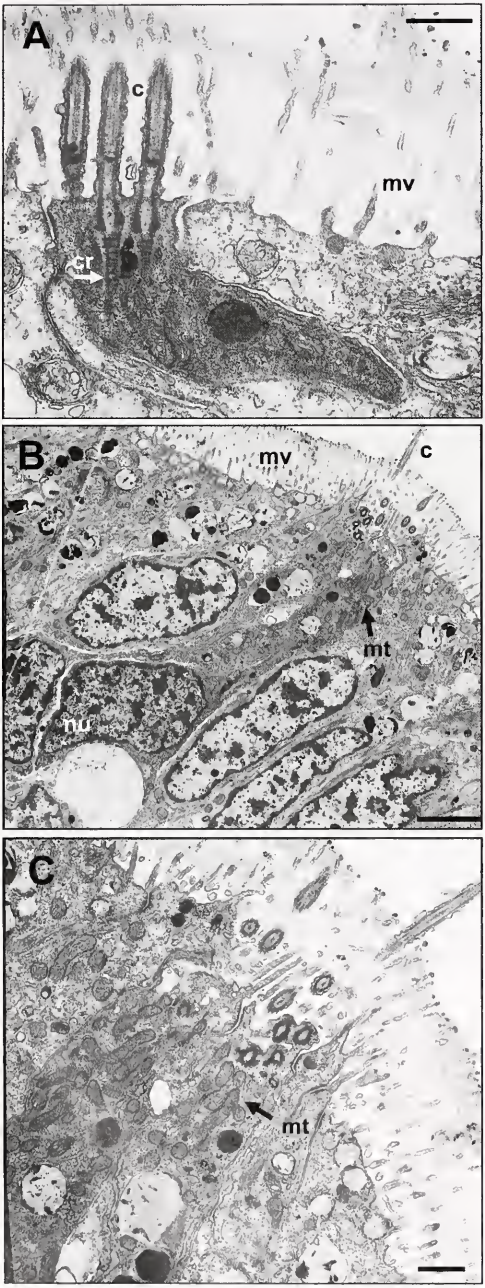

Figure 5. Ultrastructure of *Dipolydora quadrilobata* palp abfrontal cell and prostomial sensory cells. (A) Constrained by a muscle layer below, this abfrontal palp sensory cell projects laterally. Cilia (c) are readily distinguished from the microvilli (mv) of the cuticle; ciliary rootlets (cr) appear relatively short; scale = 0.5 μm. (B) Prostomial sensory cells have a similar structure, with cilia (c) projecting through the microvillar (mv) cuticle, numerous mitochondria (mt), and a bilobed nucleus (nu); scale = 2 μm. (C) Higher magnification of the same cell, showing apical mitochondria (mt); scale = 0.7 μm.

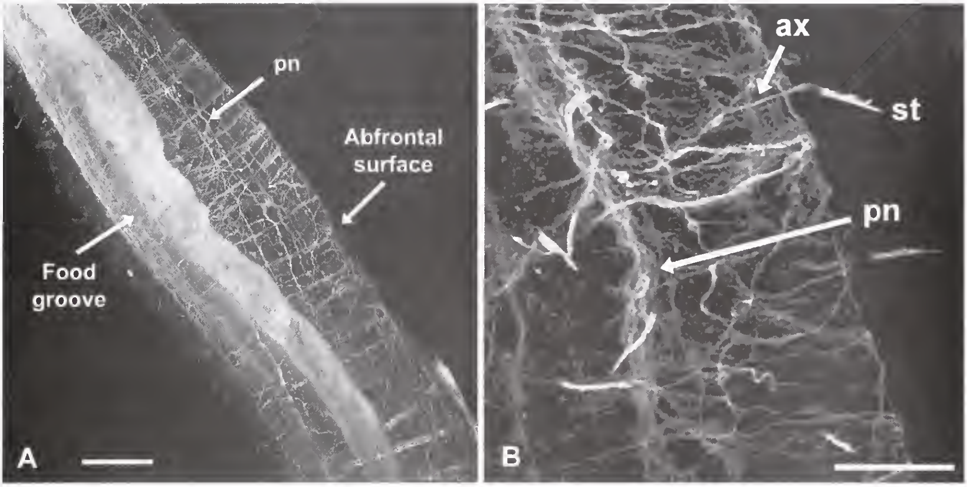

Figure 6. Fluorescence of anti-acetylated α-tubulin in *Dipolydora quadrilobata* palps examined with confocal laser scanning microscopy reveals (A) palp nerves (pn), and cilia of the frontal food groove (scale bar 40 μm) as well as (B) cilia of the abfrontal putative sensory tufts (st), their axons (ax), and their proximity to the palp nerves (pn); scale = 25 μm).

sory cells. Many spionids (including *D. quadrilobata;* T. Riordan, pers. obs.) switch from deposit feeding to suspension feeding in the presence of higher flow rates (Taghon *et al.*, 1980; Dauer *et al.*, 1981). This switch is probably mediated by mechanosensory detection of flow rates. In addition, when suspension feeding, spionids collect suspended particles that directly intercept the palps. Cilia lining the edge of the frontal food groove (*i.e.*, laterofrontal cilia) and inside the food groove (*i.e.*, frontal cilia) move such particles toward the mouth (Dauer, 1984, 1985, 1987), and may be mechanosensitive. For example, the laterofrontal cilia of one spionid, *Paraprionospio pinnata*, beat only when contacted by a suspended particle (Dauer, 1985), suggesting a mechanosensory influence on activity.

The experiments we conducted did not explicitly isolate mechanical stimulation as a factor affecting cell labeling; thus we cannot make any conclusions about a possible mechanosensory function for the palp sensory cells. However, the trend toward increased labeling of the laterofrontal and frontal cells in the flow-through controls (Fig. 8A) is intriguing, and the possibility that these cells function as mechanoreceptors should be further examined using electrophysiological approaches. It is also possible that the increased labeling in controls was due to the presence of agmatine, which itself is a potent chemical cue in zebrafish (Michel *et al.*, 1999). In the static trials, significantly more cells were labeled in the presence of amino acids and agmatine than in agmatine alone (Fig. 8B); increased labeling was especially pronounced in the lateral and abfrontal cells. There was virtually no labeling in the agmatine controls. These results suggest that the lateral and abfrontal cells are chemosensory, although it is possible that the cells were stimulated by a response triggered elsewhere on the body. We believe that body movement was an unlikely stimulus, however, because the worms were quiescent during the static trials.

If we accept that the lateral and abfrontal ciliated tufts are chemosensory, then the question arises whether the cells function as distance or contact chemoreceptors. When spionid polychaetes are deposit feeding, they typically probe the sediment surface with the distal portion of the palps (Dauer *et al.*, 1981; Lindsay, pers. obs.), using the abfrontal surface to contact the sediment surface. Previously, we showed that *D. quadrilobata* increased active feeding, including sediment probing, when presented with particle-bound amino acids and sugars (Riordan and Lindsay, 2002). Because a waterborne cue was minimal or nonexistent, we concluded that the palps mediated the response. In addition, Ferner and Jumars (1999) reported repeated "pore-water-sniffing" behavior by *Boccardia proboscidea* in which the palps were raised into the water column, sank passively onto the sediment, and then quickly returned to an upright position. Again, it was the abfrontal palp surface that contacted the sediment. Given such behaviors, we speculate that the abfrontal cells act as contact chemoreceptors. Yet spionids also use their palps to "monitor" the water column (Dauer *et al.*, 1981; Ferner and Jumars, 1999), and the lateral and

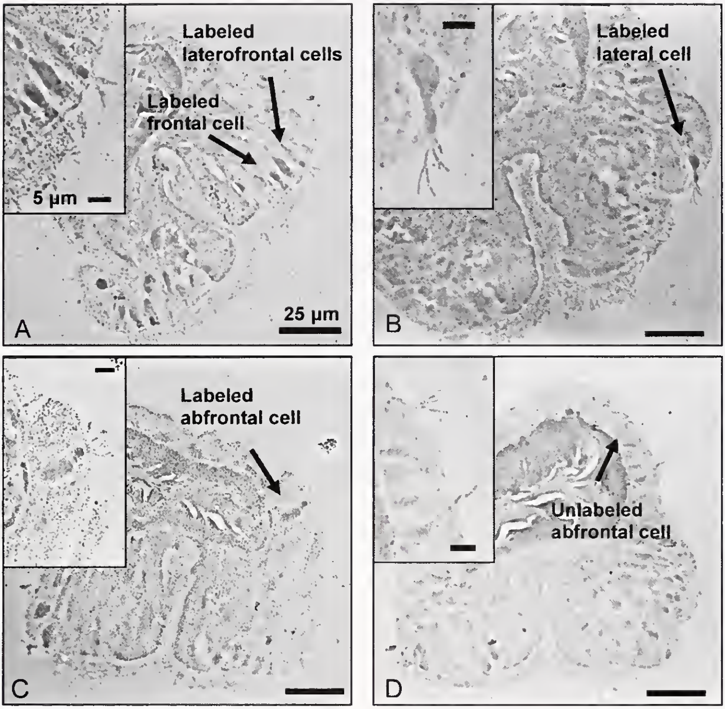

Figure 7. Labeling of *Dipolydora quadrilobata* palp cells by agmatine in the presence and absence of the amino acid mixture. (A) Semi-thin section from palp exposed to agmatine + amino acids showing labeled laterofrontal and frontal cells; scale = 25 μm. Inset shows the same cells at higher magnification; scale = 5 μm. (B) Semi-thin section from palp exposed to agmatine + amino acids showing labeled lateral cell; scale = 25 μm. Inset shows the same cell at higher magnification; scale = 5 μm. (C) Semi-thin section from palp exposed to agmatine + amino acids showing labeled abfrontal cell; scale = 25 μm. Inset shows the same cell at higher magnification; scale = 5 μm. (D) Semi-thin section from palp exposed to agmatine without amino acids (control), showing unlabeled abfrontal cell and its cilia projecting from the cuticle; scale = 25 μm. Inset shows the same cell at higher magnification; scale = 5 μm.

abfrontal sensory cells might also function as distance chemoreceptors.

Among invertebrates, preliminary studies suggest that gustatory ("taste," or contact chemosensitive) and olfactory ("smell," or distance chemosensitive) sensory neurons show a considerable amount of structural similarity (Dionne and Dubin, 1994). For example, two populations of sensory cells are distributed on the sensory tentacles of the nudibranch *Phestilla sibogae*. The intraepithelial sensory cells (contact or short-distance chemoreceptors) and subepithelial sensory cells (olfaction) have distinct spatial distributions, axonal organizations, and sensitivity to chemical cues, yet have very similar electrophysiological and pharmacological characteristics (Boudko *et al.*, 1997, 1999). Our experiments with *D. quadrilobata* demonstrate that the lateral and abfrontal sensory cells of the palps recognize both dissolved (*i.e.*, lacking contact, this paper) and adsorbed (*i.e.*, contact necessary, Riordan and Lindsay, 2002) cues. The initial ultrastructural information reveals no significant differences among the groups of palp sensory cells (laterofrontal, lateral, and abfrontal). Characterization of the innervation patterns and immunoreactivity to serotonin and FMRFamide is ongoing.

Conclusion

Previous research established that selection of particles of certain sizes by spionid palps can be influenced by mucus adhesion strength and particle "stickiness" (Jumars *et al.*, 1982; Taghon, 1982; Dauer, 1985). Qian and Chia (1997) have speculated about a possible sensory role the palps may play in selective feeding, and putative sensory structures

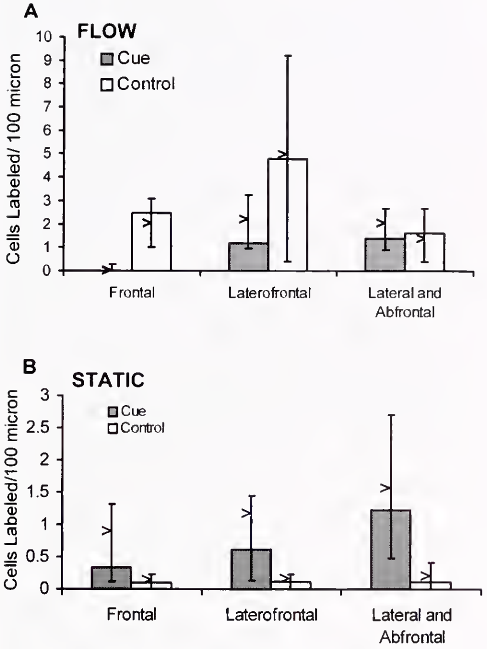

Figure 8. Number of cells per 100 μm of palp of *Dipolydora quadrilobata* that were labeled by agmatine in the presence (cue) and absence (control) of the amino acid mixture. (A) Results from the flow experiment using 20 m*M* agmatine. Numerous sections were collected from each of four control individuals and five treatment (cue) individuals; medians are presented, and error bars indicate the 75th and 25th percentile values. ">" indicates the value of the mean. (B) Results from the static experiment using 40 m*M* agmatine. Numerous sections were collected from each of six control individuals and six treatment (cue) individuals; medians are presented and error bars indicate the 75th and 25th percentile values. ">" indicates the value of the mean.

have been identified on the palps (Dauer, 1984, 1987, 1991, 1997; Worsaee, 2001), but direct evidence linking sensory cells to selective behavior was lacking. This study presents the first physiological evidence that the peripheral sensory receptors on spionid polychaete palps detect chemical stimuli that elicit a selective feeding response. The percentage of peripheral cells that were labeled in the presence of amino acids varied by cell type (3% to 14%), and was greatest for the cells located on the lateral and abfrontal surfaces of the palps. This rate of labeling is similar to that observed for olfactory neurons in spiny lobster aesthetascs (0.5% to 4.6%, Steullet *et al.*, 2000). For spionid polychaetes, ultrastructural, positional, and now physiological evidence strongly suggests that the feeding palps are equipped with lateral and abfrontal sensory cells that function as chemoreceptors. Electrophysiological experiments will be required to determine whether these cells and the laterofrontal cells might also function as mechanoreceptors.

Acknowledgments

We thank Kelly Edwards for his valuable technical assistance in the EM lab and Jennifer Jackson for her help collecting and sorting worms. Brad Calloway and Geoff Daniels of Leica Microsystems, Inc., assisted in obtaining the image shown in Figure 6A during the Analytical and Quantitative Light Microscopy course at the Marine Biological Laboratory, May 2003. Robert Marc, University of Utah School of Medicine, kindly provided anti-agmatine antibody. Comments from Charles Derby and two anonymous reviewers significantly improved the manuscript and we are grateful. TJR was supported in part by the Maine Sea Grant Program and the School of Marine Sciences at the University of Maine. This research was supported by NSF grants OCE-9973327 and OCE-0221229 to SML and by the Office of the Vice President for Research at the University of Maine.

Literature Cited

Albertsson, J., and K. Leonardsson. 2001. Deposit-feeding amphipods (*Monoporeia affinis*) reduce the recruitment of copepod nauplii from benthic resting eggs in the northern Baltic Sea. *Mar. Biol.* **138:** 793–801.

Aller, R. C. 1994. Bioturbation and remineralization of sedimentary organic matter: effects of redox oscillation. *Chem. Geol.* **114:** 331–345.

Boilly-Marer, Y. 1968. Sur le rôle chimiorecepteur des cirris parapodiaux hétéronéréidiens de *Platynereis dumerilii* Aud. et M. Edwards. *C. R. Acad. Sci. (Paris) Ser. D* **266:** 1538–1585.

Boilly-Marer, Y. 1972. Étude ultrastructurale des cirres parapodiaux de Néréidiens atoques (Annelides, Polychètes). *Z. Zellforsch.* **131:** 309–327.

Boilly-Marer, Y. 1974. Étude expérimentale du comportement nuptiale de *Platynereis dumerilii* (Annelida, Polychaeta): chémoréception, émission des produits genitaux. *Mar. Biol.* **24:** 167–179.

Boudko, D. Y., M. Switzer-Dunlap, and M. G. Hadfield. 1997. Morphology, electrophysiology and pharmacology of anterior sensory pathways in the nudibranch mollusc, *Phestilla sibogae*. *Soc. Neurosci. Abstr.* **23:** 1787.

Boudko, D. Y., M. Switzer-Dunlap, and M. G. Hadfield. 1999. Cellular and subcellular structure of anterior sensory pathways in *Phestilla sibogae* (Gastropoda, Nudibrachia). *J. Comp. Neurol.* **403:** 39–52.

Brenchley, G. A. 1981. Disturbance and community structure: an experimental study of bioturbation in marine soft-bottom environments. *J. Mar. Res.* **39:** 767–790.

Brey, T. 1991. The relative significance of biological and physical disturbance: an example from intertidal and subtidal sandy bottom communities. *Estuar. Coast. Shelf Sci.* **33:** 339–360.

Cavanaugh, G. M. 1975. *Formulae and Methods VI.* The Marine Biological Laboratory, Woods Hole, MA.

Christensen, B., A. Vedel, and E. Kristensen. 2000. Carbon and nitrogen fluxes in sediment inhabited by suspension-feeding (*Nereis diversicolor*) and non-suspension-feeding (*Nereis virens*) polychaetes. *Mar. Ecol. Prog. Ser.* **192:** 203–217.

Dauer, D. M. 1984. Functional morphology and feeding behavior of *Streblospio benedicti* (Polychaeta: Spionidae). Pp. 418–429 *in Proceedings of the First International Polychaete Conference, Sydney,*

P. A. Hutchings, ed. The Linnean Society of New South Wales, Sydney.

Dauer, D. M. 1985. Functional morphology and feeding behavior of *Paraprionospio pinnata* (Polychaeta: Spionidae). *Mar. Biol.* **85:** 143–151.

Dauer, D. M. 1987. Systematic significance of the morphology of spionid polychaete palps. *Bull. Biol. Soc. Wash.* **7:** 41–45.

Dauer, D. M. 1991. Functional morphology and feeding behavior of *Polydora commensalis* (Polychaeta: Spionidae). *Ophelia* Suppl. **5:** 607–614.

Dauer, D. M. 1997. Functional morphology and feeding behavior of *Marenzelleria viridis* (Polychaeta: Spionidae). *Bull. Mar. Sci.* **60:** 512–516.

Dauer, D. M., C. A. Maybury, and R. M. Ewing. 1981. Feeding behavior and general ecology of several spionid polychaetes from the Chesapeake Bay. *J. Exp. Mar. Biol. Ecol.* **54:** 21–38.

Dionne, V. E., and A. E. Dubin. 1994. Transduction diversity in olfaction. *J. Exp. Biol.* **194:** 1–21.

Dorsett, D. A., and R. Hyde. 1969. The fine structure of the compound sense organs on the cirri of *Nereis diversicolor. Z. Zellforsch.* **97:** 512–527.

Dwyer, T. M., D. J. Adams, and B. Hille. 1980. The permeability of the endplate channel to organic cations in frog muscle. *J. Gen. Physiol.* **75:** 469–492.

Edwards, C., D. Ottoson, B. Rydqvist, and C. Swerup. 1981. The permeability of the transducer membrane of the crayfish stretch receptor to calcium and other divalent cations. *Neuroscience* **6:** 1455–1460.

Elmgren, R., S. Ankar, B. Marteleur, and G. Ejdung. 1986. Adult interference with postlarvae in soft-sediments: the *Pontoporeia-Macoma* example. *Ecology* **67:** 827–836.

Emery, D. J. 1992. Fine structure of olfactory epithelia of gastropod molluscs. *Microsc. Res. Tech.* **22:** 307–324.

Ferner, M. C., and P. A. Jumars. 1999. Responses of deposit-feeding spionid polychaetes to dissolved chemical cues. *J. Exp. Mar. Biol. Ecol.* **236:** 89–106.

Fewou, J., and N. Dhainaut-Courtois. 1995. Research on polychaete annelid osmoregulatory peptide(s) by immunocytochemical and physiological approaches. Computer reconstruction of the brain and evidence for a role of angiotensin-like molecules in *Nereis (Hediste) diversicolor* OF Muller. *Biol. Cell.* **85:** 21–33.

Findlay, R. H., M. B. Trexler, and D. C. White. 1990. Response of a benthic microbial community to biotic disturbance. *Mar. Ecol. Prog. Ser.* **62:** 135–148.

Flach, E. C. 1992. Disturbance of benthic infauna by sediment-reworking activities of the lugworm *Arenicola marina. Neth. J. Sea Res.* **30:** 81–89.

Forbes, V. E., and G. R. Lopez. 1986. Changes in feeding and crawling rates of *Hydrobia truncata* (Prosobranchia: Hydrobiidae) in response to sedimentary chlorophyll-a and recently egested sediment. *Mar. Ecol. Prog. Ser.* **33:** 287–294.

Grossman, S., and W. Reichardt. 1991. Impact of *Arenicola marina* on bacteria in intertidal sediments. *Mar. Ecol. Prog. Ser.* **77:** 85–93.

Grünert, U., and B. W. Ache. 1988. Ultrastructure of the aesthetasc (olfactory) sensilla of the spiny lobster, *Panulirus argus. Cell Tissue Res.* **251:** 95–103.

Gunther, C.-P. 1992. Dispersal of intertidal invertebrates: a strategy to react to disturbances of different scales? *Neth. J. Sea Res.* **30:** 45–56.

Hines, A. H., M. H. Posey, and P. J. Haddon. 1989. Effects of adult suspension- and deposit-feeding bivalves on recruitment of estuarine infauna. *Veliger* **32:** 109–119.

Jelsing, J. 2002. Ultrastructural investigations on the cephalic and metameric nuchal organs of *Spio* cf. *filicornis* (Polychaeta, Spionidae). *Zoomorphology* **121:** 213–220.

Jouin, C., C. Tchernigovtzeff, M. F. Baucher, and A. Toulmond. 1985. Fine structure of probable mechano- and chemoreceptors in the caudal epidermis of the lugworm *Arenicola marina* (Annelida, Polychaeta). *Zoomorphology* **105:** 76–82.

Jumars, P. A. 1993. Gourmands of mud: diet selection in marine deposit feeders. Pp. 124–156 *in Diet Selection: An Interdisciplinary Approach to Foraging Behaviour*, R. N. Hughes, ed. Blackwell Scientific Publications, Oxford.

Jumars, P. A., R. F. L. Self, and A. R. M. Nowell. 1982. Mechanics of particle selection by tentaculate deposit feeders. *J. Exp. Mar. Biol. Ecol.* **64:** 47–70.

Karrh, R. R., and D. C. Miller. 1994. Functional response of a surface-deposit feeder, *Saccoglossus kowalevskii. Limnol. Oceanogr.* **39:** 1455–1464.

Kihslinger, R. L., and S. A. Woodin. 2000. Food patches and a surface deposit feeding spionid polychaete. *Mar. Ecol. Prog. Ser.* **201:** 233–239.

Laverack, M. S. 1968. On the receptors of marine invertebrates. *Oceanogr. Mar. Biol. Annu. Rev.* **6:** 249–324.

Lopez, G. R., and J. S. Levinton. 1987. Ecology of deposit-feeding animals in marine sediments. *Q. Rev. Biol.* **62:** 235–260.

Luckenbach, M. W. 1987. Effects of adult infauna on new recruits: implications for the role of biogenic refuges. *J. Exp. Mar. Biol. Ecol.* **105:** 197–206.

Marc, R. E. 1995. Visualization of glutamate-gated channel permeation: high resolution mapping of neuronal subpopulations. *Soc. Neurosci. Abstr.* **21:** 781–786.

Marc, R. E. 1999a. Kainate activation of horizontal, bipolar, amacrine, and ganglion cells in the rabbit retina. *J. Comp. Neurol.* **407:** 65–76.

Marc, R. E. 1999b. Mapping glutamatergic drive in the vertebrate retina with a channel-permeant organic cation. *J. Comp. Neurol.* **407:** 47–64.

Marinelli, R. L. 1992. Effects of polychaetes on silicate dynamics and fluxes in sediments: importance of species, animal activity and polychaete effects on benthic diatoms. *J. Mar. Res.* **50:** 745–779.

Mayer, L. M., Z. Chen, R. H. Findlay, R. H. Fang, S. Sampson, R. F. L. Self, P. A. Jumars, C. Quetel, and O. F. X. Donard. 1996. Bioavailability of sedimentary contaminants subject to deposit-feeder ingestion. *Environ. Sci. Technol.* **30:** 2641–2645.

Michel, W. C., P. Steullet, H. S. Cate, C. J. Burns, A. B. Zhainazarov, and C. D. Derby. 1999. High-resolution functional labeling of vertebrate and invertebrate olfactory receptor neurons using agmatine, a channel-permeant cation. *J. Neurosci. Meth.* **90:** 143–156.

Mileikovsky, S. A. 1974. On predation of pelagic larvae and early juveniles of marine bottom invertebrates by adult benthic invertebrates and their passing alive through their predators. *Mar. Biol.* **26:** 303–311.

Miller, D. C., and P. A. Jumars. 1986. Pellet accumulation, sediment supply, and crowding as determinants of surface deposit-feeding rate in *Pseudopolydora kempi japonica* Imajima and Hartman (Polychaeta: Spionidae). *J. Exp. Mar. Biol. Ecol.* **99:** 1–17.

Nittrouer, C. A., and R. W. Sternberg. 1981. The formation of sedimentary strata in an allochthonous shelf environment: the Washington continental shelf. *Mar. Geol.* **42:** 201–232.

Nozais, C., J. C. Duchene, and M. Bhaud. 1997. Control of position in the water column by the larvae of *Poecilochaetus serpens* (Polychaeta): the importance of mucus secretion. *J. Exp. Mar. Biol. Ecol.* **210:** 91–106.

Olafsson, E. B. 1989. Contrasting influences of suspension-feeding and deposit-feeding populations of *Macoma balthica* on infaunal recruitment. *Mar. Ecol. Prog. Ser.* **55:** 171–179.

Picco, C., and A. Menini. 1993. The permeability of the cGMP-activated channel to organic cations in retinal rods of the tiger salamander. *J. Physiol.* **460:** 741–758.

Plante, C. J., and L. M. Mayer. 1994. Distribution and efficiency of bacteriolysis in the gut of *Arenicola marina* and three additional deposit feeders. *Mar. Ecol. Prog. Ser.* **109:** 193–194.

Posey, M. H. 1986. Changes in a benthic community associated with dense beds of a burrowing deposit feeder, *Callianassa californiensis. Mar. Ecol. Prog. Ser.* **31:** 15–22.

Purschke, G. 1997. Ultrastructure of nuchal organs in polychaetes (Annelida)—new results and review. *Acta Zool.* **78:** 123–143.

Qian, P., and F. Chia. 1997. Structure of feeding palps and feeding behavior of the spionid polychaete *Polydora polybranchia. Bull. Mar. Sci.* **60:** 502–511.

Rhoads, D. C., and D. K. Young. 1970. The influence of deposit-feeding organisms on sediment stability and community trophic structure. *J. Mar. Res.* **28:** 150–174.

Rhode, B. 1990. Ultrastructure of nuchal organs in some marine polychaetes. *J. Morphol.* **206:** 95–107.

Riordan, T. J., Jr., and S. M. Lindsay. 2002. Feeding responses to particle-bound cues by a deposit-feeding spionid polychaete, *Dipolydora quadrilobata* (Jacobi 1883). *J. Exp. Mar. Biol. Ecol.* **277:** 79–95.

Rittschuf, D., and C. U. Buswell. 1989. Stimulation of feeding behavior in three species of fiddler crabs by hexose sugars. *Chem. Senses* **14:** 121–130.

Robertson, J. R., K. Bancroft, G. Vermeer, and K. Plaisier. 1980. Experimental studies on the foraging behavior of the sand fiddler crab *Uca pugilator* (Bosc 1802). *J. Exp. Mar. Biol. Ecol.* **44:** 67–83.

Robertson, J. R., J. A. Fudge, and G. K. Vermeer. 1981. Chemical and live feeding stimulants of the sand fiddler crab *Uca pugilator* (Bosc). *J. Exp. Mar. Biol. Ecol.* **53:** 47–64.

Rullier, F. 1951. Étude morphologique, histologique, et physiologique de l'organe nuchal chez annelids polychaetes sédentaires. *Ann. Inst. Océanogr. Monaco* **25:** 207–341.

Schlötzer-Schrehardt, U. 1987. Ultrastructural investigations of the nuchal organs of *Pygospio elegans* (Polychaeta). II. Adult nuchal and dorsal organs. *Zoomorphology* **107:** 169–179.

Shull, D. H. 2001. Transition-matrix model of bioturbation and radionuclide diagenesis. *Limnol. Oceanogr.* **46:** 905–916.

Steullet, P., H. S. Cate, W. C. Michel, and C. D. Derby. 2000. Functional units of a compound nose: aesthetasc sensilla house similar populations of olfactory receptor neurons on the crustacean antennule. *J. Comp. Neurol.* **418:** 270–280.

Storch, V., and U. Schlötzer-Schrehardt. 1988. Sensory structures. Pp. 121–133 in *The Ultrastructure of Polychaeta. Microfauna Marina*, Vol. 4. W. Westheide, and C. O. Hermans, eds. Gustav Fischer Verlag, New York.

Suchanek, T. H. 1983. Control of seagrass communities and sediment distribution by *Callianassa* (Crustacea, Thalassinidea) bioturbation. *J. Mar. Res.* **41:** 281–298.

Taghon, G. L. 1982. Optimal foraging by deposit-feeding invertebrates: roles of particle size and organic coating. *Oecologia* **52:** 295–304.

Taghon, G. L., A. R. M. Nowell, and P. A. Jumars. 1980. Induction of suspension feeding in spionid polychaetes by high particle fluxes. *Science* **210:** 562–564.

Tamaki, A. 1985. Inhibition of larval recruitment of *Armandia* sp. (Polychaeta: Opheliidae) by established adults of *Pseudopolydora paucibranchiata* (Okuda) (Polychaeta: Spionidae) on an intertidal sand flat. *J. Exp. Mar. Biol. Ecol.* **87:** 67–82.

Weissburg, M. J. 1993. Sex and the single forager: gender-specific energy maximizing strategies in the fiddler crab *Uca pugnax. Ecology* **74:** 279–291.

Weissburg, M. J. 1999. Sex-specific tuning and dose-response functions in male fiddler crabs, *Uca pugnax. J. Comp. Physiol. A.* **353:** 787–804.

Weissburg, M. J. 2001. Sex, sensitivity, and second messengers: differential effect of cyclic nucleotide mediated inhibition in the chemosensory system of fiddler crabs. *J. Comp. Physiol. A* **187:** 489–498.

Weissburg, M. J., and C. D. Derby. 1995. Regulation of sex-specific behavior in fiddler crabs: physiological properties of chemoreceptor neurons in claws and legs of males and females. *J. Comp. Physiol. A* **176:** 513–526.

Weissburg, M. J., and R. K. Zimmer-Faust. 1991. Ontogeny *versus* phylogeny in determining patterns of chemoreception: initial studies with fiddler crabs. *Biol. Bull.* **181:** 205–215.

Weissburg, M. J., J. Pearce, C. K. Govind, and C. D. Derby. 1996. Sexually dimorphic patterns of neural organization in the feeding appendages of fiddler crabs. *Cell Tissue Res.* **286:** 155–166.

Weston, D. P., D. L. Penry, and L. K. Gulmann. 2000. The role of ingestion as a route of contaminant bioaccumulation in a deposit-feeding polychaete. *Arch. Environ. Contam. Toxicol.* **38:** 446–454.

Widbom, B., and J. B. Frithsen. 1995. Structuring factors in a marine soft-bottom community during eutrophication—an experiment with radio-labeled phytodetritus. *Oecologia* **101:** 156–168.

Williams, J. G. 1980. The influence of adults on settlement of spat of the clam, *Tapes japonica. J. Mar. Res.* **38:** 729–741.

Wilson, W. H., Jr. 1980. A laboratory investigation of the effect of a terebellid polychaete on the survivorship of Nereid polychaete larvae. *J. Exp. Mar. Biol. Ecol.* **46:** 73–80.

Wilson, W. H., Jr. 1981. Sediment-mediated interactions in a densely populated infaunal assemblage: the effects of the polychaete *Abarenicola pacifica. J. Mar. Res.* **39:** 735–748.

Woodin, S. A. 1976. Adult-larval interactions in dense infaunal assemblages: patterns of abundance. *J. Mar. Res.* **34:** 25–41.

Worsaae, K. 2001. The systematic significance of palp morphology in the *Polydora* complex (Polychaeta: Spionidae). *Zool. Anz.* **240:** 47–59.

Yoshikami, D. 1981. Transmitter sensitivity of neurons assayed by autoradiography. *Science.* **212:** 929–930.

Reference: *Biol. Bull.* **206:** 78–86. (April 2004)
© 2004 Marine Biological Laboratory

Physiological Development of the Embryonic and Larval Crayfish Heart

S. L. HARPER[1] AND C. L. REIBER[2,*]

[1] *U.S. Environmental Protection Agency, Environmental Sciences Division/ORD, P.O. Box 93478, Las Vegas, Nevada 89193-3478; and* [2] *Department of Biology, 4505 Maryland Parkway, Box 454004, University of Nevada, Las Vegas, Nevada 89154-4004*

Abstract. The cardiovascular system is the first system to become functional in a developing animal and must perform key physiological functions even as it develops and grows. The ontogeny of cardiac physiology was studied throughout embryonic and larval developmental stages in the red swamp crayfish *Procambarus clarkii* using videomicroscopic dimensional analysis. The heart begins to contract by day 13 of development (at 25 °C, 20 kPa O_2). Cardiac output is primarily regulated by changes in heart rate because stroke volume remains relatively constant throughout embryogenesis. Prior to eclosion, heart rate and cardiac output decreased significantly. Previous data suggest that the decrease in cardiac parameters prior to hatching may be due to an oxygen limitation to the embryo. Throughout development, metabolizing mass and embryonic oxygen consumption increased, while egg surface area remained constant. The surface area of the egg membrane is a constraint on gas exchange; this limitation, in combination with the increasing oxygen demand of the embryo, results in an inadequate diffusive supply of oxygen to developing tissues. To determine if the decrease in cardiac function was the result of an internal hypoxia experienced during late embryonic development, early and late-stage embryos were exposed to hyperoxic water (Po_2 = 40 kPa O_2). Heart rate in late-stage embryos exposed to hyperoxic water increased significantly over control values, which suggests that the suppression in cardiac function observed in late-stage embryos is due to a limited oxygen supply.

Introduction

Crustaceans exhibit a diverse array of metabolic and physiological responses to aquatic hypoxia (Reiber, 1995). Typically, hypoxic exposure results in a decreased heart rate (bradycardia) in decapod crustaceans (McMahon and Burnett, 1990; Wilkens, 1993; McGaw *et al.*, 1994; Reiber, 1995; Reiber and McMahon, 1998). This hypoxia-induced bradycardia has been well documented in adult red swamp crayfish (*Procambarus clarkii*) (Reiber, 1995, 1997; Chapman and Reiber, 1998; Reiber and McMahon, 1998). However, an examination of heart rate alone does not provide a complete picture of cardiac performance. Cardiac output and stroke volume are broader measures of cardiac performance that can vary over wide ranges with little or no variation in heart rate (Orlando and Pinder, 1995). Furthermore, heart rate and stroke volume can vary independently of each other in decapods (McMahon and Burnett, 1990). Therefore, the cardiovascular response of decapods to a given perturbation can be understood only by evaluating heart rate, stroke volume, and cardiac output rather than just heart rate.

Cardiac performance in adult red swamp crayfish is altered when the animals are exposed to levels of oxygen below the critical level needed to maintain aerobic metabolism (P_{CRIT}) (approximately 5 kPa O_2 at 25 °C) (Reiber, 1995). Reiber (1995) found a decrease in heart rate and an increase in stroke volume in adult red swamp crayfish exposed to hypoxic conditions. The increase in stroke volume and maintenance of cardiac output is likely due to increased pericardial sinus pressure coupled with increased filling pressure, an increase in diastolic filling time, and an increased end diastolic volume (Reiber, 1995).

Information on cardiac function and hypoxic responses in embryonic and larval crustaceans is limited (Spicer, 1994;

Received 22 October 2001; accepted 3 February 2004.

* To whom correspondence should be addressed. E-mail: Reiber@ccmail.nevada.edu

Spicer and Morritt, 1996; Reiber, 1997). Cardiac functions in embryos and larvae can be quite different from those of adults because centers of metabolic activity shift during development (Reiber, 1997). Additionally, embryonic crayfish cannot escape hypoxic waters: the embryos are attached to the female's pleopods, and the brooding female typically remains sequestered within the burrow where the water can become oxygen-depleted due to both crayfish and microbial respiration (Payette and McGaw, 2003). To survive, the embryonic and larval crayfish must possess physiological mechanisms for dealing with hypoxia, and these may differ from adult responses. Fluid convection on either side of the egg membrane would allow for greater oxygen extraction from the environment by eliminating boundary layers and maintaining a diffusional gradient. The embryo itself does not move around within the egg to aid convective processes, so cardiac development is critical to embryonic viability because it provides the only source of internal convection to facilitate gas movement within the egg (Seymour and Bradford, 1995).

In late-stage crayfish embryos, E-Stage XVI, cardiac activity is not significantly responsive to hypoxic exposure, whereas in E-Stage XIV, the heart rate decreases significantly when water Po_2 is dropped to 5 kPa (an adult-like response) (Reiber, 1995; refer to table 1 for staging). Reiber (1995) attributed the lack of response in the late-stage embryos to the possibility that they are already internally hypoxic (experiencing levels of oxygen below their metabolic demands). This hypothesis was supported by the finding that the heart rates for animals at E-Stage XVI were the same as those for E-Stage XIV embryos during hypoxic exposure (2 kPa) (Reiber, 1995).

The current study evaluates cardiac physiology and metabolic function throughout early development of the red swamp crayfish. To determine whether embryos are experiencing an internal hypoxia just prior to hatching, oxygen consumption was measured along with metabolizing mass and exchange surface area throughout development. Subsequently, early and late-stage embryos were exposed to acutely hyperoxic conditions. It was expected that cardiac function in late stage embryos would be impaired due to an internal hypoxia caused by an increase in metabolizing mass and the limits in the surface area for gas exchange. Such physiological cardiovascular impairment would result in a decrease in cardiac parameters that would be alleviated by exposure to hyperoxic water.

Materials and Methods

Crayfish breeding

Adult male and female crayfish (*Procambarus clarkii* [Girard, 1852) were purchased from the Atchafalaya Biological Supply Co., Inc. Animals were maintained in the laboratory in 35-l aquaria (5–6 animals to an aquarium) filled with dechlorinated tap water (25 °C, pH = 7.0, conductivity = 150–300 μS) and fed twice a week (romaine lettuce and liver). Mature females were separated from other animals and placed into individual 2-l containers (25 °C and 10:14 dark/light cycle), where they were held for 3–4 days, after which a sexually mature male was placed in the container and the pair was observed for mating behavior. If mating did not ensue within 20 min, the male was replaced with another male and again observed for copulatory behavior. If copulation occurred, the animals were left together for 5 h and then separated to prevent cannibalism. After mating, females were placed into a nursery aquarium (25 °C) and observed daily until eggs were laid.

Experimental apparatus

Crayfish embryos or larvae were removed from females, staged according to Harper and Reiber (2001), and then attached to an applicator stick using cyanoacrylate gel glue. A minimal amount of gel glue was applied to the flattened end of the applicator stick and pressed against the egg or larva. Care was taken to minimize obstruction of the egg's respiratory surface area yet provide a firm holdfast for attachment. Animals were then placed into a flow-through experimental chamber (Harper and Reiber, 1999) where they were held for 30 min. Larval crayfish were not observed to struggle or show swimming behaviors during the experimental period. Water (25 °C, pH = 7.0, Po_2 = 20 kPa) was pumped (12 ml · min^{-1}) through the experimental chamber and then over a Clark-type polarographic oxygen electrode to determine Po_2. The Po_2 and temperature of the reservoir water were established and maintained using a gas mixing system (Cameron Instrument Company, GF-3/MP) and a circulating water bath (VWR Scientific, 1160). Changes in heart shape were monitored using a microscope (Leica MZ 12.5) equipped with a video camera (Mintron, 05-70D), super VHS video recording system (Panasonic, PV-4661), and Horita time code generator (VG-50).

Ontogeny of heart rate, stroke volume, and cardiac output

Seven crayfish from each of seven developmental stages were used: embryonic stages E-Stage XIII, E-Stage XIV, E-Stage XV, and E-Stage XVI, and larval stages L-Stage I, L-Stage II, and L-Stage III (see Reiber, 1995; and Reiber and Harper, 2001, for details on the correlation between days of development at 25 °C and developmental stage for these stages). Heart rate and stroke volume were obtained using frame-by-frame (60 Hz sampling speed) analysis of the videotape on an editing tape player (Panasonic, AG-DS550). Heart rate for each animal is presented as the mean number of beats per minute calculated from three 30-s intervals. To determine cardiac volumes (end diastolic volume and end systolic volume), embryonic and larval crayfish hearts were modeled as a prolate spheroid (cardiac volume = $4/3\pi ab^2$), where a and b are half of the measured long and short axes of the heart, respectively (Keller *et al.*, 1991, 1994; Taber *et al.*, 1992; Schwerte and Pelster, 2000; and Harper and Reiber, 2001). In early embryos (Stage XIII), the length of both the long and short axes of the heart were averaged over a minimum of 10 cardiac cycles to account for peristaltic-like contractions when the heartbeat is initiated. The geometric equation used to model the heart takes into account cardiac growth with development (*i.e.*, the increasing length and width of the heart as measured within each developmental stage). In later developmental stages (embryonic and larval) the heart remains a prolate spheroid; it changes only in its ratio of length to width. The equation for a prolate spheroid can be applied even if the changes are somewhat disproportional (*i.e.*, a longer thinner prolate spheroid models mathematically the same as a shorter thicker prolate spheroid). The basic geometry of the heart remains the same throughout development, with changes occurring primarily in the long and short axes. Stroke volume was calculated from the difference between end diastolic volume (EDV) and end systolic volume (ESV). Cardiac output was calculated as the product of stroke volume and heart rate. Heart rate, stroke volume, and cardiac output were determined for each developmental stage.

Oxygen consumption

Closed-system respirometry was used to determine embryonic oxygen consumption. Six animals were placed in a 50-ml syringe filled with aerated water and placed on an oscillating plate at 25 °C. A 5-ml water sample was injected into a chamber holding a Clark-type polarographic oxygen electrode after 30, 60, and 90 min. Three replicates were run for each of the following stages: E-Stage II, E-Stage XIII, E-Stage XV, E-Stage XVI, L-Stage I, and L-Stage III. Two syringes lacking animals were run to account for bacterial respiration, which was found to be negligible. Fluid volume and water $P\text{O}_2$ in the experimental chamber were decreased by a total of 15 ml and 6.6 kPa O_2 (minimum) over the 90-min course of the experiments. This change in volume was adjusted for when calculating oxygen consumption. Rates of oxygen consumption over the experimental period were consistent, indicating that the small reduction in oxygen availability did not adversely affect the animals. Mass-specific oxygen consumption is reported as microliters of O_2 per milligram (wet mass) per hour. Oxygen consumption rate was calculated according to the formula $V\text{O}_2 = (V_r \times \Delta P_{\text{WO2}} \times \beta_{\text{WO2}})/\Delta t \times W$; where $V\text{O}_2$ is oxygen consumption, V_r is the volume of water in the respirometer, ΔP_{WO2} is the change in water $P\text{O}_2$, β_{WO2} is the capacitance of oxygen in water, Δt is the duration in minutes, and W is the wet weight of the animal.

Lipid and metabolizing mass

Embryonic crayfish were collected from gravid females at E-Stage II, E-Stage XIII, E-Stage XV, and E-Stage XVI, and larval crayfish were collected at L-Stage I and L-Stage III. Egg diameter and larval length were measured (n = 7 per stage). Egg surface area was calculated using the formula for a sphere (surface area (mm^2) = $4\pi r^2$). Surface area was calculated only for embryos. Each embryo and larva was dried with a Kimwipe for 10 s prior to weighing and placed on a clean, preweighed coverslip. To determine the metabolically active mass (tissue) of the embryo or larva, the nonmetabolic (lipid) portion of the body was first removed by puncturing the wall of the animal and isolating the lipid onto the coverslip. The lipid-free animal was then weighed. The egg membrane and exoskeleton were not separated from the active metabolizing mass but were assumed to contribute little to mass error because they constitute only a small proportion of overall mass. Furthermore, errors in this estimate were likely similar among stages of development. Non-lipid mass was calculated as the difference in animal mass before and after removal of lipids.

Hyperoxic exposure

Animals at E-Stage XIV (n = 13) and E-Stage XVI (n = 13) were held individually under experimental chamber conditions for 30 min followed by heart rate measurements to determine control values. Control and experimental $P\text{O}_2$ values were established and maintained using a gas mixing system (Cameron Instrument Company, GF-3/MP). Embryos were exposed to normoxic (20 kPa O_2) and hyperoxic (40 kPa O_2) water for 30 min. Heart rate was determined as previously described for both control and experimental conditions at E-Stage XIV and E-Stage XVI.

Statistical analysis

Means and standard errors were calculated for each stage (n = 7) for data on egg surface area, lipid mass, metabolizing mass, and oxygen consumption rate. An analysis of variance was used to determine overall effects of development on the dependent variables (SigmaStat, ver. 2.03). A Bonferroni t-test was used for pairwise multiple comparisons where a significance of $P \leq 0.05$ was found. Lipid/metabolizing mass ratios failed normality tests, thus an analysis of variance based on ranks and a Tukey test were used. Baseline cardiac parameters were established by pooling values obtained for each stage (n = 7) and calculating a mean and standard error. The effects of developmental stage on cardiac parameters were assessed using a one-way analysis of variance (SigmaStat, ver. 2.03). Where developmental effects were shown to be significant ($P < 0.05$), group means were compared using the Newman-Keuls multiple range test. A Student's t-test was used to compare embryonic response to normoxic and hyperoxic exposure with significance at the level of $P = 0.05$. Embryos within a developmental stage ($n = 13$) were used for comparison.

Results

Ontogeny of heart rate, stroke volume, and cardiac output

Uncoordinated cardiac contractions began in embryonic crayfish by E-Stage XIII of development, with a mean heart rate of 160 ± 3 (SEM) beats · min^{-1} (bpm). At the onset of cardiac contractions heart rate was irregular, characterized by short bursts of activity (*e.g.*, 300 bpm), very long peristaltic-like contractions (*e.g.*, 48 bpm), and intermittent periods of cardiac arrest (maximum of 11 s). Therefore, heart rate was determined by averaging over the six 30-s time periods. Heart rate varied significantly with development ($P = 0.05$, $F = 7.29$). Mean heart rate remained unchanged (163 ± 2 bpm) through E-Stage XIV, after which it increased significantly ($P = 0.05$, $F = 3.64$) to 192 ± 6 bpm at E-Stage XV. At E-Stage XVI, heart rate decreased significantly ($P = 0.05$, $F = 3.01$) to 149 ± 3 bpm and remained at this rate until eclosion. Upon hatching, heart rate increased significantly ($P = 0.05$, $F = 5.11$) to 255 ± 9 bpm and remained at this level through all three larval stages (Fig. 1a).

Both stroke volume and cardiac output showed little variation throughout embryonic development (Fig. 1b, c). However, after hatching (L-Stage I), stroke volume increased significantly ($P = 0.05$, $F = 42.17$) from 3.8 ± 0.9 (SEM) nl/beat to 12.4 ± 1.8 nl/beat, and cardiac output increased significantly ($P = 0.05$, $F = 281.55$) from 178 ± 96 (SEM) nl · min^{-1} pre-hatching (E-Stage XVI) to 3130 ± 46 nl · min^{-1} at the first larval stage. Stroke volume decreased significantly ($P < 0.001$, $F = 21.64$) from the first larval stage (12.4 ± 1.8 nl · beat^{-1}) to the second larval stage (6.07 ± 1.9 nl · beat^{-1}), with no significant change occurring from the second to third larval stages. During larval development, cardiac output followed stroke volume, decreasing significantly ($P = 0.05$, $F = 77.17$) at L-Stage II and then remaining stable into L-Stage III (1660 ± 43 to 1747 ± 47 nl · min^{-1}).

The effects of cardiac differentiation and elongation on the ontogeny of cardiac physiology can be assessed using the data relating the length and width of the heart at end diastole to days of development (Fig. 2). The pattern of cardiac development reveals that the heart grows in length from 8.3 ± 0.3 (SEM) to 11.0 ± 0.4 μm (32.5% increase) as compared to width from 5.9 ± 0.2 (SEM) to 8.4 ± 0.3 μm (42.4% increase), through embryonic development. There is a greater absolute increase in the length as opposed to the width of the heart during development, which results in a dramatic increase in the length-to-width ratio after eclosion.

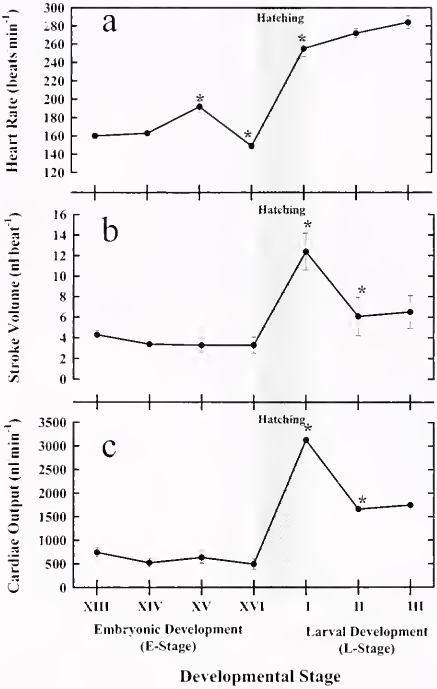

Figure 1. Ontogeny of (a) heart rate, (b) stroke volume, and (c) cardiac output in the red swamp crayfish *Procambarus clarkii*. * indicates significant difference from the previous stage at the level of $P = 0.05$. Shaded area indicates when hatching occurs. Values are shown as means ± standard error, $n \geq 7$ at each stage. Embryonic and larval stages correspond to the following days of development at 25 °C: E-Stage XIII = 12–14 days, E-Stage XIV = 14–17 days, E-Stage XV = 17–19 days, E-Stage XVI = 19–21 days, L-Stage I = 21–23 days, L-Stage II = 23–25 days, and L-Stage III = 25–27 days.

Oxygen consumption

Oxygen consumption increased significantly between E-Stage IV (4.03 ± 0.50 (SEM) μl $O_2 \cdot mg^{-1} \cdot h^{-1}$) and E-Stage XIII (71.33 ± 5.19 μl $O_2 \cdot mg^{-1} \cdot h^{-1}$) ($P = 0.05$, $t = 4.05$) and between E-Stage XIII and E-Stage XV (148.14 ± 13.61 μl $O_2 \cdot mg^{-1} \cdot h^{-1}$) ($P = 0.05$, $t = 5.21$) (Fig. 3). Just before hatching, E-Stage XVI, metabolic oxygen consumption did not increase significantly from the previous stage. Larval stages showed a significant increase in oxygen consumption (L-Stage I, $P < 0.001$, $t = 7.597$ and L-Stage III, $P < 0.001$, $t = 16.953$).

Lipid/metabolizing mass

Embryo diameter (used to calculate membrane area) did not change significantly through embryonic development.

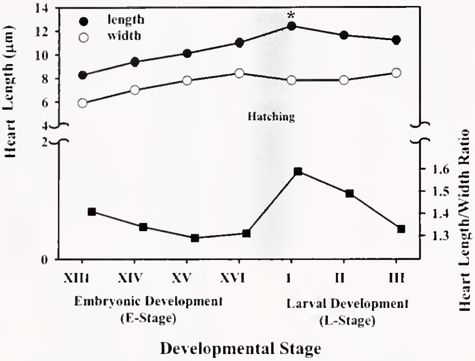

Figure 2. Length and width measurements of the heart with development. Solid circles represent length, open circles represent width, and solid squares represent length/width ratio. * indicates significant difference from the previous stage at the level of $P = 0.05$. Values are shown as means ± standard error, $n \geq 7$ at each stage. Error bars fall within symbols. See legend to Figure 1 for correspondence between stage and length of development.

After eclosion, larval length increased significantly from the first (2.61 ± 0.03 (SEM) mm) to the third larval instar (3.38 ± 0.02 mm) ($P = 0.001$, $t = 5.61$) (Fig. 4a). Calculated surface area of the egg membrane decreased significantly just prior to eclosion ($P = 0.05$, $t = 3.17$) (Fig. 4b). Animal mass also decreased significantly just prior to hatching (4.31 ± 0.07 (SEM) mg to 3.78 ± 0.10 mg) ($P < 0.001$, $t = 4.65$) but increased significantly by the first larval stage (3.78 ± 0.10 mg to 4.95 ± 0.03 mg) ($P < 0.001$, $t = 10.31$) (Fig. 4c).

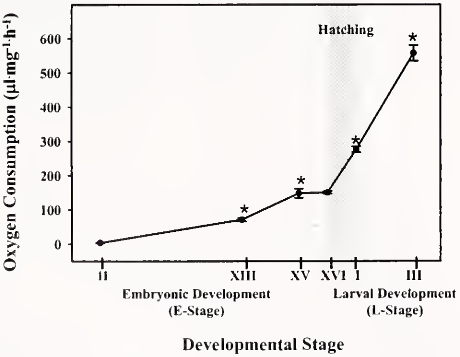

Figure 3. Oxygen consumption for embryonic and larval crayfish. * indicates significant difference from the previous stage at the level of $P = 0.05$. Shaded area indicates when hatching occurs. Values are shown as means ± standard error, $n \geq 3$ at each stage. Embryonic and larval stages correspond to the following days of development at 25 °C: E-Stage II = 2–4 days, E-Stage XIII = 12–14 days, E-Stage XV = 17–19 days, E-Stage XVI = 19–21 days, L-Stage I = 21–23 days, and L-Stage III = 25–27 days.

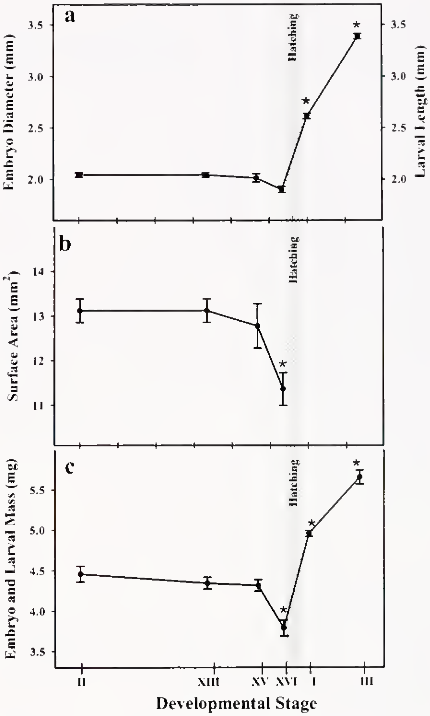

Figure 4. (a) Diameter of embryo or length of larval crayfish at various stages throughout development. (b) Surface area calculated from diameter measurements on embryonic crayfish. Surface area measurements not applicable to larvae. (c) Mass of developing crayfish. * indicates significant difference from the previous stage at the level of $P = 0.05$. Shaded area indicates when hatching occurs. Values are shown as means ± standard error, $n \geq 7$ at each stage. See Figure 3 for correspondence between stage and length of development.

Lipid content of the egg decreased significantly from E-Stage XIII (2.41 ± 0.06 (SEM) mg) to E-Stage XV (1.85 ± 0.20 mg) ($P = 0.05$, $t = 3.52$) and from L-Stage I (1.64 ± 0.06 mg) to L-Stage III (0.64 ± 0.02 mg) ($P < 0.001$, $t = 6.32$) (Fig. 5a). As lipid content decreased, metabolizing mass increased significantly between E-Stage XIII (1.93 ± 0.08 mg) and E-Stage XV (2.46 ± 0.17 mg) ($P = 0.05$, $t = 3.92$) (Fig. 5b). Metabolizing mass increased throughout embryonic development, although egg membrane surface area did not change significantly. The metabolizing mass of the first larval stage (3.31 ± 0.04 mg)

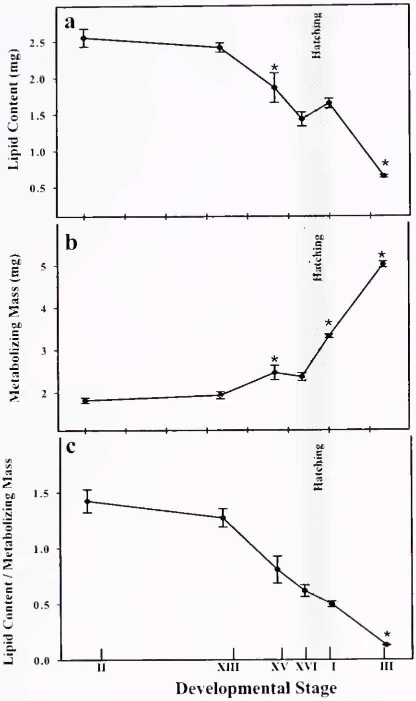

Figure 5. (a) Lipid content of developing crayfish. (b) Metabolizing mass of developing crayfish. (c) Ratio of lipid content to metabolizing mass in the developing crayfish. * indicates significant difference from the previous stage at the level of $P = 0.05$. Shaded area indicates when hatching occurs. Values are shown as means ± standard error, $n \geq 7$ at each stage. See Figure 3 for correspondence between stage and length of development.

($P < 0.001$, $t = 6.35$) increased significantly by the third larval stage (5.01 ± 0.07 mg) ($P < 0.001$, $t = 12.598$). The ratio of lipid to metabolizing mass declined significantly ($P = 0.001$, $q = 7.040$) over the embryonic and larval development period from 1.43 ± 0.10 (SEM) at E-Stage IV to 0.12 ± 0.01 at L-Stage III but did not change significantly from one stage to the next (Fig. 5c).

Hyperoxic exposure

E-Stage XIV and E-Stage XVI embryos were selected to represent animals thought to be under internally normoxic and hypoxic conditions, respectively. If embryonic cardiac function is depressed in late-stage embryos because they are oxygen-deficient, then an increase in the oxygen diffusion gradient should partially restore oxygen delivery and thus allow heart rate to increase. No significant change was observed in E-Stage XIV animals when exposed to hyperoxic water (Fig. 6). However, heart rate increased significantly in E-Stage XVI animals ($P < 0.001$, $F = 21.73$) (from 138 ± 6 to 159 ± 6 bpm) when exposed to hyperoxic water (40 kPa O_2).

Discussion

The mechanisms by which embryonic cardiac contractions are initiated in crayfish are not clearly understood. Cardiac contractions, which result in the movement of hemolymph within the embryo, appear to facilitate gas transport in developing crustaceans (Reiber, 1997). Burggren and Territo (1995) have suggested that these early cardiac contractions may serve an angiogenic function in lower vertebrates. Early in development, the fundamental driving forces that influence developing physiological systems are often similar, even among taxa from diverse animal groups. All organisms must balance immediate environmental needs against long-term physiological requirements. Crayfish, like other animals, rely on diffusion for both exchange and internal delivery of respiratory gases during early embryonic development (Burggren and Pinder, 1991; Reiber, 1997). Eventually, however, they attain a mass at which diffusion alone can no longer adequately meet gas exchange demands; at this point the active movement of fluids (hemolymph) as a result of cardiac pumping is initiated. The heart rate in most animals changes as development proceeds from embryo through immature or larval stages to adult, yet the patterns of change are not consistent among species in lower vertebrates (Burggren and Pinder, 1991; Farrell, 1991; Hou and Burggren, 1995; Icardo, 1996) or invertebrates (Cooke, 1988; Spicer and Morritt, 1996).

Spicer and Morritt (1996) have shown that the timing of

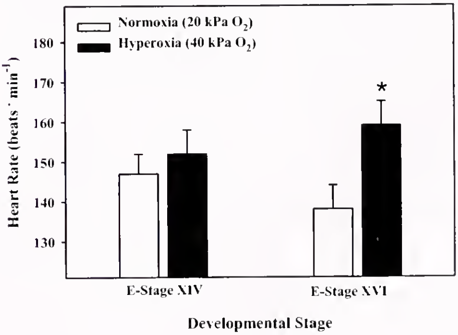

Figure 6. Heart rate of two stages of embryonic crayfish exposed to hyperoxic water (40 kPa). * indicates significant difference from control ($P = 0.05$). E-Stage XIV correlates to 14–17 days of development at 25 °C and E-Stage XVI to 19–21 days.

key developmental events, such as the initiation of cardiac contractions, is not consistent among aquatic crustaceans. However, some generalizations can be made about the ontogeny of cardiac physiology and function from the first appearance of cardiac contractions to maturity. Whether segmentation in an animal occurs pre- or post-hatch appears to be linked with the onset of beating of the heart because segmentation of the thoracic cavity precedes initiation of the heartbeat (Spicer, 1994; Spicer and Morritt, 1996). The relationship between body mass and heart rate does not conform to a single power curve model; rather it depends on the organogenesis of the heart itself. In the crayfish *Procambarus clarkii,* the heart grew proportionally in width and length throughout embryonic development; yet just after hatching, the length of the heart increased in slightly greater proportion than width, resulting in a large and rapid increase in the length-to-width ratio. As suggested by Spicer and Morritt (1996), this probably represents the switch from differentiation of cardiac tissue to the elongation phase of cardiac development. After hatching, larval mass increased significantly while heart rate remained fairly constant. This developmental pattern—a decrease in heart rate with increasing body size after cardiac development is complete and elongation has commenced—was described by Spicer and Morritt (1996) in the water flea *Daphnia magna,* the amphipod *Gammarus duebeni,* the lobster *Nephrops norvegicus,* and the brine shrimp *Artemia franciscana.*

Many adult crustaceans adjust stroke volume rather than heart rate to modulate cardiac output (Reviewed by McMahon and Burnett, 1990; McGaw *et al.,* 1994; Reiber, 1995; Reiber and McMahon, 1998). However, stroke volume does not appear to be as tightly regulated as heart rate during the embryonic development of crayfish. Embryonic crayfish apparently use heart rate as a primary mechanism to regulate cardiac output, as stroke volume remains constant throughout embryogenesis. We present three explanations for the lack of change in stroke volume during embryonic development. The first explanation is that the increased dimensions of the heart are offset by a reduction in contractility with development. The dimensions of the heart measured in diastole increased throughout embryonic development. Systolic measurements also increased throughout development, implying that the heart was contracting to a lesser degree. The reduced force of contraction ultimately decreases the ejection fraction of the ventricle and leads to an increased residual volume of the heart such that, although the heart is growing in size, the volume of blood pumped per beat remains the same. A second explanation for the maintenance of stroke volume with development is the thickening of the heart walls. Measurements for stroke volume were obtained using the outer diameter of the heart, which may not account for thickening of the myocardium with development. After hatching, elongation of the heart and a decrease in systolic volume contribute to the significant rise in stroke volume observed in the larval crayfish. It is the maintenance of stroke volume throughout embryogenesis that dictates that cardiac output is driven by heart rate alone early in development. A third possibility is that the maintenance of stroke volume may be due to increased afterload as a result of increased vascular pressure developed during angiogenesis, as is the case with zebrafish embryos (Pelster and Burggren, 1996).

Reiber (1997) postulated that cardiac parameters decline just prior to hatching because internal convective processes are insufficient to facilitate adequate gas exchange in the face of a limited gas exchange area. Throughout embryonic development in the red swamp crayfish, the metabolizing portion of the embryo increased in mass as it utilized the lipid-rich yolk as metabolic fuel. Embryonic crayfish appear to rely on oxidative phosphorylation throughout embryogenesis; however, they can switch to anaerobic metabolism when exposed to decreased oxygen concentrations (Chiba and Chichibu, 1993). Metabolic rates increased throughout development as metabolizing mass increased and as organogenesis and differentiation gave way to functional systems. We observed a significant increase in oxygen consumption at E-Stage XIII, when the heart starts beating. After eclosion, another significant increase is observed in each larval stage; these changes could be associated with increases in the animal's activity (DeSilva *et al.,* 1986). Increased metabolic rates have significant consequences for the oxygen supply system since the supply of oxygen must be matched with the metabolic demands of the embryo. We observed an increase in the oxygen consumption of the crayfish throughout embryonic and larval development, except at the point prior to hatching when the embryos are thought to be internally hypoxic and could be relying on anaerobic metabolic pathways.

Embryonic aerobic metabolism cannot be sustained under severe hypoxic conditions. Myocardial anaerobic capabilities are typically limited or nonexistent, which makes this tissue particularly sensitive to hypoxia; thus, if the embryo can no longer maintain aerobic metabolism, the heart should already be failing. Cardiac function declined during embryonic development in the crayfish, most likely due to an internal hypoxia resulting from the embryo's oxygen requirements exceeding the diffusive capacity of its outer egg membranes. Prior to hatching, an internal hypoxia could result in direct inhibition of cardiac metabolism and cardiac function, as is observed in larval frogs (Fritsche and Burggren, 1996). In the crayfish, eclosion removes the physical limitation to gas exchange (the egg membrane) and active respiratory mechanisms (gill ventilation) are initiated. Cardiac functions can then increase after hatching, as the animal becomes more active and organ systems mature.

To determine whether the diminution in cardiac function observed in late-stage embryos was due to an internal hypoxia, the diffusional gradient of oxygen was increased by exposing the embryo to hyperoxic water. The finding that this exposure increased the heart rate in late-stage crayfish embryos but not in early embryos suggests that oxygen limitation is at least one factor responsible for reducing the heart rate in late-stage embryos. However, the increase in heart rate observed in late-stage embryos exposed to hyperoxia could also be explained by changes in the oxygen conductance of the egg membrane. In amphibian eggs, the oxygen conductance of the egg membrane is related to the stage of the embryo and is not directly influenced by environmental factors (Seymour and Bradford, 1995). If the same is true for crayfish, the early stages might not respond to an increase in $P\mathrm{o}_2$ because the conductance of the membrane limits the oxygen diffusion across the membrane. However, this would not account for the reduction in heart rate observed in late-stage embryos. It is far more likely that these embryos are experiencing an internal hypoxia that decreases cardiac parameters and is alleviated by exposure to high ambient $P\mathrm{o}_2$. An alternative explanation for depressed cardiac function in late-stage embryos is a shift in the oxygen sensitivity of the embryos throughout development. It is possible that late-stage embryos are less sensitive to water $P\mathrm{o}_2$ than earlier stages. However, if this were the reason for the depression of cardiac function, then increasing water $P\mathrm{o}_2$ would not have had the observed effect on cardiac parameters in the late-stage embryos.

Other mechanisms that could underlie the observed patterns of cardiac function during development include (1) intrinsic changes in membrane permeability and in myocyte characteristics such as the ion channels, and (2) the development of, or changes in, extrinsic controls (Fritsche, 1997). The decreases observed in egg surface area and animal mass may contribute to the decreases observed in cardiac parameters just prior to hatching. Lastly, it should be noted that the shifts in heart rate and stroke volume could coincide with the pacemaker of the heart switching from a myogenic to a neurogenic mechanism of cardiac regulation (Yamagishi, 1990; Yamagishi and Hirose, 1992; Chapman and Reiber, 1998; Harper and Reiber, 2000). Previous data on the extrinsic regulatory mechanisms of the embryonic crayfish cardiovascular system have been difficult to interpret. Embryonic crayfish hearts appear to be initially myogenic and to become neurogenic later in development (Chapman and Reiber, 1998; Harper and Reiber, 2000). The timing of this event could correspond with the shifts in cardiac function observed during embryonic development in the crayfish.

Acknowledgments

This research was supported by NSF grant IBN-98874534 (C.L.R.) and the University of Nevada Las Vegas Graduate Student Association grant (S.L.H.).

Literature Cited

Burggren, W. W., and A. W. Pinder. 1991. Ontogeny of cardiovascular and respiratory physiology in lower vertebrates. *Annu. Rev. Physiol.* **53:** 107–135.

Burggren, W. W., and P. R. Territo. 1995. Early development of blood oxygen transport. Pp. 45–56 in *Hypoxia and Brain*, J. Jouston and J. Coates, eds., Queen City Printer, Burlington, VT.

Chiba, A., and S. Chichibu. 1993. Phosphorylation in crayfish (*Procambarus clarkii*) eggs during hatching. *Comp. Biochem. Physiol. B* **106:** 433–436.

Chapman, S. L., and C. L. Reiber. 1998. Ontogeny of cardiac regulation in the crayfish. *Am. Zool.* **37:** 42A.

Cooke, I. M. 1988. Studies on the crustacean cardiac ganglion. *Comp. Biochem. Physiol. C* **91:** 205–218.

DeSilva, C. D., S. Premawansa, and C. N. Keemiyahetty. 1986. Oxygen consumption in *Oreochromis miloticus* (L.) in relation to development, salinity, temperature, and time of day. *J. Fish Biol.* **29:** 267–277.

Farrell, A. P. 1991. From hagfish to tuna: a perspective on cardiac function in fish. *Physiol. Zool.* **64:** 1137–1164.

Fritsche, R. 1997. Ontogeny of cardiovascular control in amphibians. *Am. Zool.* **37:** 23–30.

Fritsche, R., and W. Burggren. 1996. Development of cardiovascular responses to hypoxia in larvae of the frog *Xenopus laevis*. *Am. J. Physiol.* **40:** R912–R917.

Harper, S. L., and C. L. Reiber. 1999. Influence of hypoxia on cardiac functions in the grass shrimp (*Palaemonetes pugio* Holthuis). *Comp. Biochem. Physiol. A* **124:** 569–573.

Harper, S. L., and C. L. Reiber. 2000. Developmental cardiac response to GABA in the red swamp crayfish *Procambarus clarkii* and the relevance to crayfish burrow ecology. *J. Ariz.-Nev. Acad. Sci.* **32:** 158–163.

Harper, S. L., and C. L. Reiber. 2001. Ontogeny of neurohormonal regulation of the cardiovascular system in the crayfish *Procambarus clarkii*. *J. Comp. Physiol. B.* **171:** 577–583.

Hou, P.-C. L., and W. W. Burggren. 1995. Blood pressure and heart rate during larval development in the anuran amphibian *Xenopus laevis*. *Am. J. Physiol.* **269:** R1120–R1125.

Icardo, J. M. 1996. Developmental biology of the early vertebrate heart. *J. Exp. Zool.* **275:** 144–161.

Keller, B. B., N. Hu, P. J. Serrino, and E. B. Clark. 1991. Ventricular pressure-area loop characteristics in the stage 16 to 24 chick embryo. *Circ. Res.* **68**(1): 226–230.

Keller, B. B., J. P. Tinney, and N. Hu. 1994. Embryonic ventricular diastolic and systolic pressure-volume relations. *Cardiol. Young* **4:** 19–27.

McGaw, I. J., C. N. Airriess, and B. R. McMahon. 1994. Patterns of haemolymph-flow variation in decapod crustaceans. *Mar. Biol.* **121:** 53–60.

McMahon, B. R., and L. E. Burnett. 1990. The crustacean open circulatory system: a re-examination. *Physiol. Zool.* **63:** 35–71.

Orlando, K., and A. W. Pinder. 1995. Larval cardiorespiratory ontogeny and allometry in *Xenopus laevis*. *Physiol. Zool.* **68:** 63–75.

Payette, A. L., and I. J. McGaw. 2003. Thermoregulatory behavior of the crayfish *Procambarus clarkii* in a burrow environment. *Comp. Biochem. Physiol. A.* **136:** 539–556.

Pelster, B., and W. W. Burggren. 1996. Disruption of hemoglobin oxygen transport does not impact oxygen-dependent physiological processes in developing embryos of zebra fish (*Danio rerio*). *Circ. Res.* **79:** 358–362.

Reiber, C. L. 1995. Physiological adaptations of crayfish to the hypoxic environment. *Am. Zool.* **35:** 1–11.

Reiber, C. L. 1997. Ontogeny of cardiac and ventilatory function in the crayfish *Procambarus clarkii*. *Am. Zool.* **37:** 82–91.

Reiber, C. L., and S. L. Harper. 2001. Perspectives on cardiac physiological ontogeny in crustaceans. (Zoologische Jahrbucher) (Zoology: Analysis of complex systems): Zoology of Complex Systems. **104**(1): 103–113.

Reiber, C. L., and B. R. McMahon. 1998. The effects of progressive hypoxia on the crustacean cardiovascular system: a comparison of the freshwater crayfish, (*Procambarus clarkii*), and the lobster (*Homarus americanus*). *J. Comp. Physiol. B* **168:** 168–176.

Schwerte, T., and B. Pelster. 2000. Digital motion analysis as a tool for analyzing the shape and performance of the circulatory system in transparent animals. *J. Exp. Biol.* **203:** 1659–1669.

Seymour, R. S., and D. F. Bradford. 1995. Respiration of amphibian eggs. *Physiol. Zool.* **68:** 1–25.

Spicer, J. I. 1994. Ontogeny of cardiac function in the brine shrimp *Artemia franciscana* Kellogg 1906 (Branchiopoda: Anostraca). *J. Exp. Zool.* **270:** 508–516.

Spicer, J. I., and D. Morritt. 1996. Ontogenic changes in cardiac function in crustaceans. *Comp. Biochem. Physiol. A* **114:** 81–89.

Taber, L. A., B. B. Keller, and E. B. Clark. 1992. Cardiac mechanism in the stage 16 chick embryo. *J. Biomech. Eng.* **114:** 427–434.

Wilkens, J. L. 1993. Re-evaluation of the stretch sensitivity hypothesis of crustacean hearts: Hypoxia, not lack of stretch, causes reduction in heart rate of isolated hearts. *J. Exp. Biol.* **176:** 223–232.

Yamagishi, H. 1990. Physiological change of the heart beat in juvenile stage of the isopod crustacean, *Ligia exotica. Zool. Sci.* **7:** 1037–1042.

Yamagishi, H., and E. Hirose. 1992. Nervous regulation of the myogenic heart in early juveniles of the isopod crustacean, *Ligia exotica. Comp. Physiol.* **11:** 141–148.

Reference: *Biol. Bull.* **206:** 87–94. (April 2004)
© 2004 Marine Biological Laboratory

Survival and Development of Horseshoe Crab (*Limulus polyphemus*) Embryos and Larvae in Hypersaline Conditions

GRETCHEN S. EHLINGER* AND RICHARD A. TANKERSLEY

Florida Institute of Technology, Department of Biological Sciences, 150 W. University Blvd., Melbourne, Florida 32901

Abstract. The horseshoe crab *Limulus polyphemus* spawns in the mid- to upper intertidal zone where females deposit eggs in nests below the sediment surface. Although adult crabs generally inhabit subtidal regions of estuaries with salinities from 5 to 34 ppt, developing embryos and larvae within nests are often exposed to more extreme conditions of salinity and temperature during summer spawning periods. To test whether these conditions have a negative impact on early development and survival, we determined development time, survival, and molt cycle duration for *L. polyphemus* embryos and larvae raised at 20 combinations of salinity (range: 30–60 ppt) and temperature (range: 25–40 °C). Additionally, the effect of hyperosmotic and hypoosmotic shock on the osmolarity of the perivitelline fluid of embryos was determined at salinities between 5 and 90 ppt. The embryos completed their development and molted at salinities below 60 ppt, yet failed to develop at temperatures of 35 °C or higher. Larval survival was high at salinities of 10–70 ppt but declined significantly at more extreme salinities (*i.e.*, 5, 80, and 90 ppt). Perivitelline fluid remained nearly isoosmotic over the range of salinities tested. Results indicate that temperature and salinity influence the rate of crab development, but only the extremes of these conditions have an effect on survival.

Introduction

Estuaries are physiologically challenging habitats for organisms because of the temporal and spatial variation in environmental conditions. Among environmental variables, salinity and temperature are two factors that especially influence the survival and growth of marine invertebrates (Kinne, 1970, 1971). Salinity influences many physiological functions and is therefore important in regulating the distribution of estuarine and marine organisms. Estuarine species are generally euryhaline and eurythermal and, therefore, more tolerant of widely ranging temperatures and salinities than marine species (Costlow *et al.*, 1966; Laughlin and French, 1989; Goncalves *et al.*, 1995). Because the range of conditions that an organism can survive may change throughout development (Kinne, 1970, 1971; Charmantier *et al.*, 1988), ontogenetic differences in temperature and salinity tolerance often enable larvae, juveniles, and adults to inhabit different habitats or regions of estuaries (Charmantier *et al.*, 1988).

The American horseshoe crab *Limulus polyphemus* (L.) occurs in estuaries along the east coast of North America, where the general salinity range is 5 to 34 ppt. Although its densities are highest in portions of the estuary with higher and variable salinities, the species also inhabits regions with lower salinities (Shuster, 1982). The adults and juveniles live in subtidal benthic habitats, but embryonic and early larval development occurs in intertidal areas. Females dig nests near the waterline in the mid- to upper intertidal zone and deposit up to 20,000 eggs per clutch 10–25 cm below the sediment surface (Shuster and Botton, 1985; Brockmann, 1990; Penn and Brockmann, 1994). Peak spawning occurs in the late spring to early summer (Cohen and Brockmann, 1983; Barlow *et al.*, 1986), generally near the time of high tide during new and full moons (Rudloe, 1980; Cohen and Brockmann, 1983; Barlow *et al.*, 1986). Eggs are laid in sandy areas that are regularly inundated in tidal systems and have variable frequencies and periods of inun-

---

Received 4 August 2003; accepted 13 January 2004.

* To whom correspondence should be addressed. Current address: Florida Fish and Wildlife Conservation Commission, Jacksonville Field Laboratory, 6134 Authority Ave, Jacksonville, FL 32221. E-mail: Gretchen.Ehlinger@fwc.state.fl.us

dation in nontidal areas (Rudloe, 1985; Penn and Brockmann, 1994). Because the nests are located on the beach, the embryos and larvae may be exposed to fluctuations in temperature and salinity that are greater than those experienced by adults in subtidal areas. During low tide, nests may be exposed to freshwater during rainfall and to rapid changes in temperature when the beach is heated by the sun. Thus, developing embryos might be expected to tolerate rapid and wide fluctuations in temperature and salinity. Alternatively, they may be protected from changes in external conditions by the perivitelline fluid, the fluid inside the inner egg membrane, which may buffer embryos from changes in external conditions, especially salinity.

Adult horseshoe crabs also inhabit lagoons and coastal embayments with a much broader salinity range (5–55 ppt) due to shallow conditions and relatively high rates of evaporation and freshwater input (Pritchard, 1967; Robertson, 1970; Shuster, 1982; Botton *et al.*, 1988; Ehlinger *et al.*, 2003). One such habitat is the Indian River Lagoon (IRL) located along the east coast of Florida, USA. The IRL consists of three shallow (1–3 m) sub-basins, the Indian River, Banana River, and Mosquito Lagoon, that extend about 250 km parallel to the Atlantic coast (Smith, 1987; De Freese, 1991). Although appreciable tidal changes occur in the immediate vicinity of the five inlets that link the IRL to the ocean, most of the system is virtually tideless (tidal amplitudes < 5 cm; Smith, 1993). Despite the presence of spawning adults, densities of *L. polyphemus* larvae in the IRL are low compared to levels in tidally dominated habitats such as Delaware Bay and the Gulf coast of Florida (Rudloe, 1979; Ehlinger *et al.*, 2003; M. L. Botton, Fordham University, pers. comm.). One possible cause of this low larval abundance is physiological stress. A recent study of the spawning and reproductive behavior of horseshoe crabs inhabiting the IRL indicates that water temperatures and salinities during the spawning season reach levels as high as 45 °C and 55 ppt, which may surpass the tolerance limits of the embryos or prevent larval development and hatching (Ehlinger, 2002).

In estuarine habitats of New England and the mid-Atlantic region, low salinities caused by snow melt and freshwater runoff are more common than high salinities. Therefore, most studies on the effect of salinity on embryonic development have focused on hypoosmotic stress and tolerance to low salinities. Previous studies indicate that the optimal salinity for the development of horseshoe crab embryos is between 20 and 30 ppt (Jegla and Costlow, 1982; Laughlin, 1983; Sugita, 1988). Temperature also affects the rate of embryonic development and the duration of posthatch intermolt stages, with the optimal temperature for development ranging from 25 °C to 30 °C (Jegla and Costlow, 1982). Laughlin (1983) concluded that the effect of salinity is secondary to that of temperature, since the duration of larval development was similar among salinity treatments but differed significantly among temperature treatments.

No published studies have examined the tolerance of *L. polyphemus* embryos to salinities higher than 40 ppt. The objectives of this study were to determine the effect of high temperatures and salinities on embryonic and larval development and to determine the salinity tolerance of *L. polyphemus* larvae. The effect of hyperosmotic shock on the osmotic concentration of the perivitelline fluid within the eggs was also examined. The results indicate that *L. polyphemus* embryos and larvae can tolerate a wide range of salinities (30–60 ppt), but they are more sensitive to high temperatures (≥35 °C).

Materials and Methods

Adult specimens of *Limulus polyphemus* were collected by hand during the spawning season (February–May 2002) from the Indian River Lagoon, Florida. Crabs were obtained from two sites: (1) Pineda Causeway, Banana River (28°12′33″N, 80°38′12″W) and (2) Peacock Pocket, Indian River (28°39′41″N, 80°43′45″W). The crabs were maintained in the laboratory in a recirculating fiberglass tank (2.7 m × 1.7 m × 1 m) containing natural seawater (temperature 20–23 °C; salinity 30 ppt). For all experiments, eggs were fertilized by artificial insemination, and the embryos were cultured in the laboratory according to standard procedures (Brown and Clapper, 1981; Sekiguchi, 1988). Sperm collected from males by manual stimulation of the genital operculum were diluted with filtered seawater to make a 10% (vol/vol) sperm solution. Eggs collected from females by direct extraction from the ovaries were washed several times with 5-μm filtered seawater, placed in petri dishes (diameter 8.5 cm; height 1.4 cm) containing 50 ml of filtered seawater, and fertilized with 1 ml of the sperm solution. The eggs were incubated with sperm for 1 h and then rinsed with filtered seawater to remove excess sperm. To determine whether fertilization was successful, a subset of the eggs was stained with a solution of 0.1% neutral red and observed under a dissecting microscope for signs of cleavage and gastrulation (Sekiguchi, 1988). The developmental stage of the embryos was determined using the classification scheme of Sekiguchi (1988).

Effect of high temperature and salinity on embryonic and larval development

To determine whether high temperature and salinity influence the rate and success of embryonic development and the duration of the larval stage following hatching, fertilized eggs were reared under one of 20 combinations of salinity and temperature (salinities: 30, 40, 50, 60 ppt; temperature: 25, 30, 33, 35, 40 °C). Thirty eggs were placed in individual wells (1.5 cm diameter × 1.5 cm depth) of a multiwell tissue culture dish containing 3 ml of filtered natural seawater at each temperature-salinity combination. For each combination, 10 dishes were placed in a thermostatically controlled incubator (Precision Scientific, Winchester, VA) to maintain a constant temperature. To avoid temperature and osmotic shock, all eggs were fertilized at 25 °C and 30 ppt, and the temperature and salinity were increased by 5 °C and 5 ppt each day until the target treatment combination was reached. Seawater was changed every other day, and dishes were checked daily for the presence of newly hatched larvae and juveniles. Eggs that showed no sign of development after 75 days were excluded from the analysis. The effects of temperature and salinity on the time to hatching and molting to the first juvenile instar were determined using a two-factor analysis of variance (ANOVA; SYSTAT 10.0, SPSS Inc.). If the overall analysis indicated significant treatment effects, comparisons among treatment levels were conducted using Tukey pairwise comparisons (SYSTAT 10.0).

Salinity tolerance of larvae

To determine the salinity tolerance of *L. polyphemus* larvae, embryos were reared at 30 °C and 30 ppt until they hatched to the trilobite larva stage. Within 24 h of hatching, 24 larvae were placed in individual wells (1.5 cm diameter × 1.5 cm depth) of a multiwell culture dish containing 3 ml of filtered seawater at salinities of 5, 10, 20, 30, 40, 50, 60, 70, 80, and 90 ppt. Larval survival was monitored daily for 30 days. Larvae were considered dead when they were inactive (no leg or book-gill movement) and unresponsive to mechanical stimulation. Time to death (in days) or time of molting to the first juvenile instar (in days) was recorded. Survivorship curves for larvae in each of the salinity treatments were constructed using the product-limit method (Kaplan-Meier method: Muenchow, 1986; Kleinbaum, 1996). Survival functions were compared among treatments using the Mantel log-rank test (χ^2 approximation, SYSTAT 10.0, SPSS Inc.). The same analysis was used to compare the duration of the larval stage, with time to molting as the dependent variable. Larvae that were alive but had not molted after 30 days of exposure were treated as right-censored observations in the analysis.

Osmotic concentration of the perivitelline fluid

To determine the effect of changes in external salinity on the osmotic concentration of the perivitelline fluid surrounding developing embryos, *L. polyphemus* eggs reared at 25 °C and 30 ppt were transferred, after the fourth embryonic molt, to one of 10 test salinities (5, 10, 20, 30, 40, 50, 60, 70, 80, and 90 ppt). The osmotic concentration of the perivitelline fluid of a subset of randomly selected eggs (n = 10) from each salinity treatment was determined at 0, 0.5, 1, 2, 4, and 6 h following exposure. Thus, a total of 60 eggs (10 eggs × 6 time exposures) were tested at each combination of salinity and temperature. Perivitelline fluid within the egg was collected by using the tip of a micropipette to carefully tear the egg's outer membrane and then to draw up 10 μl of perivitelline fluid. Osmolarity was determined with a vapor pressure osmometer (Vapro model 5520, Westcor Inc., Logan, Utah) calibrated with standards of 290 and 1000 mmol kg^{-1}. The effect of the salinity of the external medium on the osmolarity of the fluid over time was determined using a two-factor analysis of variance (salinity and time as factors; SYSTAT 10.0, SPSS Inc.). Comparisons between experimental treatments and the control (*i.e.*, 30 ppt) were conducted using *a priori* directed contrasts (SYSTAT 10.0).

Results

Effect of high temperature and salinity on embryonic and larval development

Both high temperatures and salinities significantly affected the success of embryonic development in *Limulus polyphemus.* At 35 °C, eggs developed to embryonic stage 20, where the embryo is enclosed by a clear membrane and the legs and gills are visible (Sekiguchi, 1988); but at all salinities, these embryos failed to hatch to trilobite larvae after 75 days. At 40 °C, eggs showed no signs of development after 75 days at all salinities. Development and hatching were normal at all other temperatures. Temperature and salinity also had a significant effect on time to hatching (Fig. 1, F = 52.02, df = 6, 202, $P < 0.001$). At all test salinities, embryonic development took longer at 25 °C than at 30 and 33 °C (Tukey pairwise comparisons, Fig. 1, Table 1). At 25 °C, time to hatching increased significantly as the salinity increased (Fig. 1, Table 1). Embryos maintained at 30 °C and 33 °C and 30 and 40 ppt had similar hatching

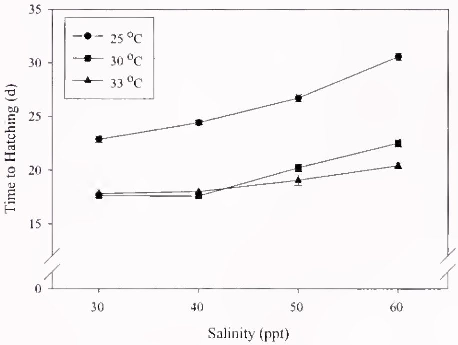

Figure 1. Mean (±SE) number of days from fertilization to hatching of *Limulus polyphemus* embryos at 25 °C, 30 °C, and 33 °C and at 30, 40, 50, and 60 ppt. No hatching occurred in any of the test salinities at 35 °C and 40 °C. n = 30 for each trial.

Table 1

Matrix of pairwise comparison probabilities (Tukey test) for days to hatching for Limulus polyphemus *embryos*

	T/S											
T/S	25/30	25/40	25/50	25/60	30/30	30/40	30/50	30/60	33/30	33/40	33/50	33/60
n =	27	29	30	26	26	27	25	28	27	29	27	25
25/30	1.00											
25/40	<0.01	1.00										
25/50	<0.01	<0.01	1.00									
25/60	<0.01	<0.01	<0.01	1.00								
30/30	<0.01	<0.01	<0.01	<0.01	1.00							
30/40	<0.01	<0.01	<0.01	<0.01	**0.97**	1.00						
30/50	<0.01	<0.01	<0.01	<0.01	<0.01	<0.01	1.00					
30/60	**0.03**	<0.01	<0.01	<0.01	<0.01	<0.01	0.01	1.00				
33/30	<0.01	<0.01	<0.01	<0.01	**0.86**	**1.00**	<0.01	<0.01	1.00			
33/40	<0.01	<0.01	<0.01	<0.01	**0.46**	**1.00**	<0.01	<0.01	**1.00**	1.00		
33/50	<0.01	<0.01	<0.01	<0.01	<0.01	<0.01	<0.01	<0.01	<0.01	<0.01	1.00	
33/60	<0.01	<0.01	<0.01	<0.01	<0.01	<0.01	0.01	<0.01	<0.01	<0.01	<0.01	1.00

T = temperature (°C); S = salinity (ppt); *n* = sample size. Bold type indicates pairwise comparisons that are not statistically significant.

rates (Table 1), but hatching was delayed significantly in more hypersaline conditions (50 and 60 ppt, Fig. 1). Optimal temperature and salinity conditions for development to stage 21 were 30–33 °C and 30–40 ppt.

The duration of the trilobite larva stage (time from hatching to molting to the first juvenile instar) decreased significantly with increasing temperature ($F = 3.79$, df = 6, 202, $P < 0.001$, Fig. 2), yet was similar for all salinity treatments ($F = 0.22$, df = 6, 202, $P = 0.64$). Larval stage duration was shortest at 30–33 °C and was significantly longer at 25 °C (Tukey test, Fig. 2, Table 2). Development times were similar for larvae maintained at 30 °C and 33 °C (Fig. 2, Table 2).

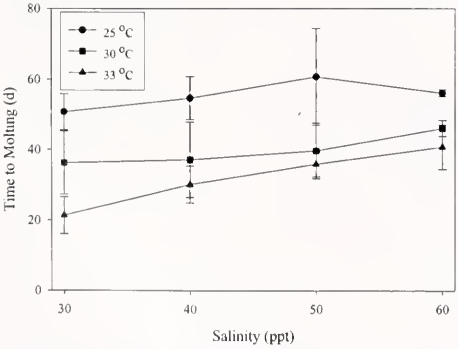

Figure 2. Mean (±SE) time to molting to the first juvenile stage (in days) of *Limulus polyphemus* at 25 °C, 30 °C, and 33 °C and 30, 40, 50, and 60 ppt. Sample sizes are provided in Table 2.

Salinity tolerance of larvae

All *L. polyphemus* trilobite larvae survived for 30 days at salinities ranging from 10 to 70 ppt; they died only in the extreme salinities of 5, 80, and 90 ppt (Fig. 3). Comparisons of the survival curves among salinity treatments indicated that survival was significantly reduced relative to control levels only when larvae were maintained at 90 ppt ($\chi^2 = 33.0$, df = 2, $P < 0.01$, Fig. 3). The time to 50% mortality (TM_{50}) was ≈16.0 days in 90 ppt. Salinity also had a significant effect on molting rate of larvae to the first juvenile instar ($\chi^2 = 12.1$, df = 4, $P < 0.01$, Fig. 4). Larval stage duration increased at salinities above and below 30 ppt (Fig. 4). Molting did not occur after 30 days at the most extreme salinities tested (≤10 ppt or ≥70 ppt).

Osmotic concentration of the perivitelline fluid

Salinity significantly affected the osmotic concentration of the perivitelline fluid of *L. polyphemus* eggs (Fig. 5, $F = 176.81$, df = 9, 45, $P < 0.01$). When developing embryos were placed in hypoosmotic solutions (5, 10, and 20 ppt), the osmolarity of the perivitelline fluid decreased significantly within 0.5 h of exposure (Fig. 5). After the first hour, fluid osmolarity leveled off and remained relatively constant for the remainder of the experiment (Fig. 5). At 30 ppt, the osmolarity of the perivitelline fluid did not change significantly throughout the exposure period ($F = 0.098$, df = 9, 45, $P = 0.925$, Fig. 5). When embryos were exposed to more hyperosmotic conditions (>30 ppt), the fluid osmolarity increased significantly within the first 0.5 hour and initially reached levels that were slightly above that of the bathing medium (Fig. 5). However, the osmolarity de-

Table 2

Matrix of pairwise comparison probabilities (Tukey test) for time to hatching to the first juvenile instar for Limulus polyphemus *larvae*

	T/S											
T/S	25/30	25/40	25/50	25/60	30/30	30/40	30/50	30/60	33/30	33/40	33/50	33/60
n =	26	27	26	23	24	25	22	25	24	27	24	24
25/30	1.00											
25/40	**1.00**	1.00										
25/50	**0.68**	**0.12**	1.00									
25/60	**0.98**	**0.38**	**1.00**	1.00								
30/30	**0.04**	**0.04**	<0.01	<0.01	1.00							
30/40	0.01	0.01	<0.01	0.01	**1.00**	1.00						
30/50	**0.02**	**0.02**	0.01	<0.01	**0.97**	**1.00**	1.00					
30/60	**0.03**	0.01	**0.04**	<0.01	**0.08**	**0.39**	**0.73**	1.00				
33/30	<0.01	<0.01	<0.01	<0.01	**0.06**	**0.09**	**0.39**	**0.05**	1.00			
33/40	<0.01	<0.01	<0.01	<0.01	**0.08**	**0.13**	**0.06**	**0.07**	**0.77**	1.00		
33/50	<0.01	<0.01	<0.01	<0.01	**0.49**	**0.10**	**0.10**	**0.09**	**0.08**	**0.86**	1.00	
33/60	<0.01	<0.01	<0.01	<0.01	**0.49**	**0.93**	**1.00**	**1.00**	**0.11**	**0.25**	**1.00**	1.00

T = temperature (°C); S = salinity (ppt); *n* = sample size. Bold type indicates pairwise comparisons that are not statistically significant.

creased after 1 h and remained at levels slightly above that of the bathing medium (Fig. 5). Similar changes in the osmotic concentration of the perivitelline fluid occurred when eggs were exposed to salinities above 40 ppt. Yet the magnitude of the change and its duration increased with increasing hyperosmotic shock (Fig. 5). After 6 h, the perivitelline fluid of all embryos was nearly isoosmotic with the bathing medium (Fig. 6).

Discussion

In estuaries, *Limulus polyphemus* is exposed to rapid fluctuations in salinity, particularly in intertidal areas where embryos and larvae undergo development. The results of the current study support earlier reports that *L. polyphemus* embryos and larvae are remarkably hardy and able to withstand the fluctuating and often harsh environmental conditions of intertidal areas (Jegla and Costlow, 1982; Palumbi and Johnson, 1982; Sugita, 1988; Botton *et al.,* 1988). Although both embryos and larvae completed development in hypersaline conditions, time to hatching and metamorphosis was delayed at salinities above 40 ppt (Fig. 1). Posthatching development was not affected by salinity (Fig. 2). Optimal salinities for development were between 30 and 40 ppt, which differs slightly from previous reports of optimal values between 20 and 30 ppt (Jegla and Costlow, 1982; Laughlin, 1983; Sugita, 1988). This difference may

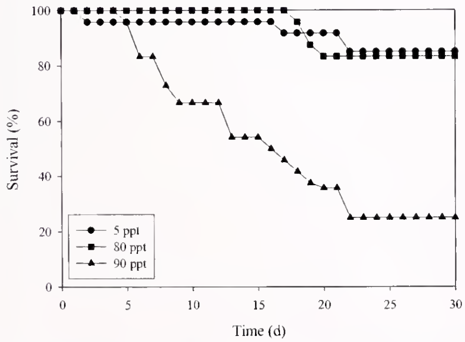

Figure 3. Kaplan-Meier survival curves for *Limulus polyphemus* larvae subjected to salinities ranging from 5 to 90 ppt for 30 days. All larvae survived in salinities from 10 to 70 ppt. *n* = 24 for each trial.

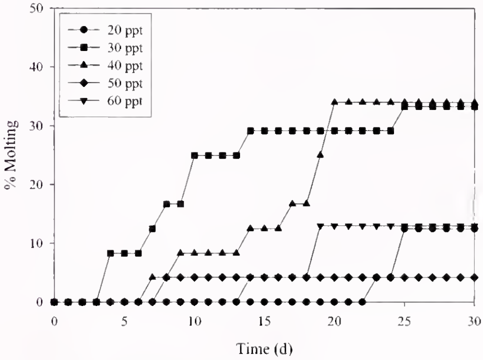

Figure 4. Kaplan-Meier curves for time until molting for *Limulus polyphemus* larvae subjected to salinities ranging from 5 to 90 ppt for 30 days. *n* = 24 for each trial.

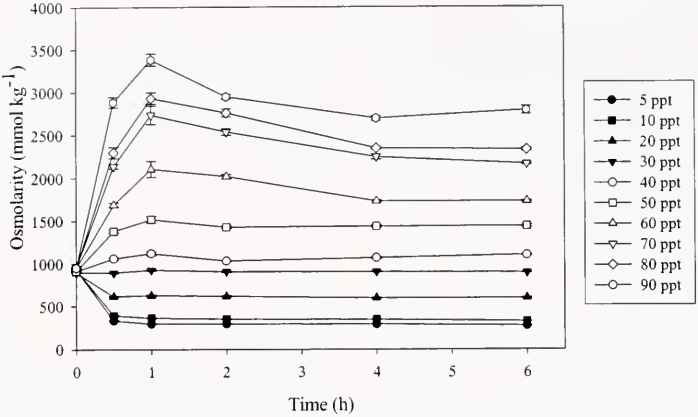

Figure 5. Mean (±SE) osmotic concentration of the perivitelline fluid at 0, 0.5, 1, 2, 4, and 6 h after exposure to salinities ranging from 5 to 90 ppt.

be the result of acclimation by the adults to the extreme salinity conditions found in the IRL compared to other estuaries because it is a nontidal, shallow lagoon.

The results of the current study indicate that eggs and embryos of *L. polyphemus* are more sensitive to high temperatures than to high salinities (Figs. 1 and 2). Optimal temperatures for development were 30–33 °C, yet temperatures 35 °C and above were lethal to embryos and adversely affected larval growth and development. This differs slightly from previous studies in which lower temperatures produced optimal development (25–30 °C: Jegla and Costlow, 1982; Laughlin, 1983; Sugita, 1988). Another difference is that hatching did not occur at temperatures above 33 °C in our study, whereas other researchers reported hatching at temperatures up to 35 °C (Jegla and Costlow, 1982; Laughlin, 1983).

Temperature tolerance in *L. polyphemus* varies with life-history stage: older stages are better able to withstand ex-

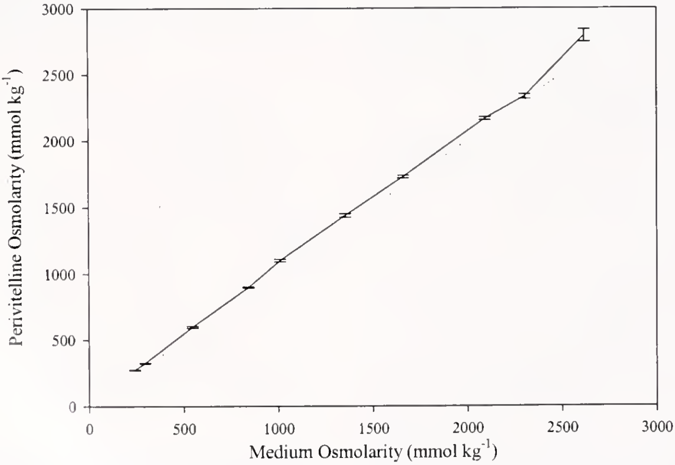

Figure 6. Variations in the perivitelline osmolarity of *Limulus polyphemus* eggs as a function of the bathing medium following 6 h of exposure. Values are means (±SE). The dashed line is the isoosmotic line.

treme temperatures (Fraenkel, 1960; Jegla and Costlow, 1982; Laughlin, 1983). In the current study, embryos could not tolerate temperatures above 33 °C (Fig. 1). Reynolds and Casterlin (1979) found that juveniles were tolerant of temperatures from 15 °C to 40 °C. The lethal temperature for 1-h exposure is 44 °C for adults, although they can survive more than 72 h at 40 °C (Fraenkel, 1960). Thus, adults are more tolerant than embryos to high temperatures since embryos failed to develop and hatch at temperatures of 35 °C.

Salinity tolerance also varies with life-history stage. Embryos developed, hatched, and molted to the first juvenile instar at 60 ppt (Figs. 1 and 2), and larvae survived at salinities from 10 to 70 ppt (Fig. 3). Juveniles (12th instar) are able to withstand salinities of 12 ppt for several days, but as salinity decreases, mortality increases, and survival time decreases (Reynolds and Casterlin, 1979). Adults can withstand direct transfer from 25 ppt to 13 ppt with no adverse effects, but transfer to 6 ppt causes swelling of the limb joints and gills (Robertson, 1970). Our results indicate that larvae are more tolerant of sudden hyposalinity shock than adults and juveniles. This may be due to ontogenetic differences that enable embryos and larvae to tolerate the rapid fluctuations in salinity that typically occur in intertidal nesting areas. These results are consistent with studies of other estuarine and marine arthropod species that found that tolerance to a wide range of salinities is greater in the larval stage than in the adult. For example, the larvae of the coastal crabs *Armases ricordi* and *A. roberti* are tolerant of a wider range of salinities than the adult stages and, as a consequence, have different habitats (Diesel and Schuh, 1998). The larvae of the Chinese mitten crab *Eriocheir sinensis* also has a much wider salinity tolerance than the juveniles and adults (Anger, 1991).

Temperature and salinity have been found to affect the physiology and growth of *L. polyphemus* (Jegla and Costlow, 1982). Temperatures and salinities are higher in the IRL than in the northern portion of the range for the species. Therefore, the IRL population of horseshoe crabs may be able to withstand higher temperatures and salinities as a result of acclimatization, leading to the slightly higher optimal ranges for development and growth found in this study. Temperature may also have an effect on size and growth, leading to geographic differences in size. Adults tend to be larger in temperate regions, with the smaller adults occurring in the warm tropical waters of Yucatan and the cold waters north of Cape Cod, Massachusetts (Shuster, 1979; Reynolds and Casterlin, 1979). Shuster (1979) also found significantly smaller adults that matured one or two molts earlier at locations with salinities below 18 ppt.

When exposed to hyperosmotic and hypoosmotic stress, the perivitelline fluid contained within the outer membrane of *L. polyphemus* embryos changed rapidly and became nearly isoosmotic to the surrounding medium (Figs. 5 and 6). Since the osmotic concentration of the perivitelline fluid changes with the surrounding medium, the perivitelline fluid does not buffer developing embryos from changes in external salinity. Partial regulation of perivitelline fluid osmolarity may be a common trait among members of the Xiphosura, since Sugita (1988) reported similar results for embryos of *Tachypleus tridentatus*, the Japanese horseshoe crab. Sekiguchi (1988) found that the osmotic concentration of the perivitelline fluid of *L. polyphemus* and *T. tridentatus* embryos bathed in high-salinity waters changed during the exposure period, attaining a slightly higher value than the surrounding medium. Sekiguchi (1988) also found that inorganic ions pass freely through the inner egg membrane. Thus, osmoactive substances secreted by the embryo, but which cannot pass through the inner egg membrane, are most likely responsible for the slightly higher osmolarity of the perivitelline fluid relative to the outer medium. Since the perivitelline fluid of the eggs conforms osmotically to the surrounding medium, one would expect the egg volume to change initially, and then return to its original level once the egg has reached the osmolarity of the surrounding medium. Ehlinger (2002) found that the volume of eggs exposed to salinities from 5 to 90 ppt changed over a 6-h exposure period: in general, volume decreased in hyperosmotic solutions and increased in hypoosmotic solutions. These results differ from those reported by Jegla and Costlow (1982), who found that egg volume did not change conspicuously when exposed to salinities of 10 and 40 ppt.

The wide salinity tolerance of embryos and larvae of *L. polyphemus* is an important adaptation to the extreme conditions in the intertidal nursery habitat. Such variability in tolerance may be an advantage in species that live in a highly variable, unpredictable environment (Anger, 1991). Embryos and larvae of *L. polyphemus* are exposed to and can tolerate a much wider range of salinities than juveniles and adults. This enables the embryos to survive and hatch in shallow lagoons and embayments with rapidly fluctuating salinities. Larvae are able to tolerate salinities from 20 to 70 ppt, which they experience in intertidal areas where they develop and molt to larger stages before they migrate farther offshore (Rudloe, 1979). This tolerance for extreme temperatures and salinities is particularly important in nontidal estuarine systems and lagoons, such as the IRL. Although embryos and larvae of *L. polyphemus* are able to withstand the high salinities experienced in the IRL, temperatures during summer spawning and development periods may exceed tolerance limits, thus leading to the lower abundance of embryos and larvae in the IRL.

Acknowledgments

Research supported by National Park Service Grant No. CA5180990049. We thank Canaveral National Seashore, Merritt Island National Wildlife Refuge, and NASA/

Kennedy Space Center for access to the collection sites. We thank Drs. M. Botton, M. Bush, E. Irlandi, and J. Lin for their comments on an early version of this manuscript. We are grateful to M. Mota, E. Reyier, and D. Scheidt for their assistance in collecting adult crabs, A. Brenner and K. Smolarek for their assistance in the lab, and Dr. J. Grimwade for use of laboratory equipment. We thank two anonymous reviewers for their critical review of this manuscript.

Literature Cited

Anger, K. 1991. Effects of temperature and salinity on the larval development of the Chinese mitten crab *Eriocheir sinensis* (Decapoda: Grapsidae). *Mar. Ecol. Prog. Ser.* **72:** 103–110.

Barlow, R. B., Jr., M. K. Powers, H. Howard, and L. Kass. 1986. Migration of *Limulus* for mating: relation to lunar phase, tide height, and sunlight. *Biol. Bull.* **171:** 310–329.

Botton, M. L., R. E. Loveland, and T. R. Jacobsen. 1988. Beach erosion and geochemical factors: influence on spawning success of horseshoe crabs (*Limulus polyphemus*) in Delaware Bay. *Mar. Biol.* **99:** 325–332.

Brockmann, H. J. 1990. Mating behavior of horseshoe crab, *Limulus polyphemus*. *Behavior* **114:** 206–220.

Brown, G. G., and D. L. Clapper. 1981. Procedures for maintaining adults, collecting gametes, and culturing embryos and juveniles of the horseshoe crab, *Limulus polyphemus* L. Pp. 268–290 in *Laboratory Animal Management: Marine Invertebrates*. Committee on Marine Invertebrates. National Academy Press, Washington, DC.

Charmantier, G., M. Charmantier-Daures, N. Bouaricha, P. Thuet, D. E. Aiken, and J.-P. Trilles. 1988. Ontogeny of osmoregulation and salinity tolerance in two decapod crustaceans: *Homarus americanus* and *Penaeus japonicus*. *Biol. Bull.* **175:** 102–110.

Cohen, J. A., and H. J. Brockmann. 1983. Breeding activity and mate selection in the horseshoe crab, *Limulus polyphemus*. *Bull. Mar. Sci.* **33:** 274–281.

Costlow, J. D., C. G. Bookhout, and R. J. Monroe. 1966. Studies on the larval development of the crab, *Rhithropanopeus harrisii* (Gould). I. The effect of salinity and temperature on larval development. *Physiol. Zool.* **39:** 81–100.

De Freese, D. E. 1991. Threats to biological diversity in marine and estuarine ecosystems of Florida. *Coast. Manage.* **19:** 73–101.

Diesel, R., and M. Schuh. 1998. Effects of salinity and starvation on larval development of the crabs *Armases ricordi* and *A. roberti* (Decapoda: Grapsidae) from Jamaica, with notes on the biology and ecology of adults. *J. Crustac. Biol.* **18:** 423–436.

Ehlinger, G. S. 2002. Spawning behavior and larval biology of the American horseshoe crab, *Limulus polyphemus*, in a microtidal coastal lagoon. Ph.D. dissertation, Florida Institute of Technology, Melbourne, FL. 133 pp.

Ehlinger, G. S., R. A. Tankersley, and M. B. Bush. 2003. Spatial and temporal patterns of spawning and larval hatching by the horseshoe crab, *Limulus polyphemus*, in a microtidal coastal lagoon. *Estuaries* **26:** 631–640.

Fraenkel, G. 1960. Lethal high temperature for three marine invertebrates: *Limulus polyphemus, Littorina littorea* and *Pagurus longicarpus*. *Oikos* **11:** 171–182.

Goncalves, F., R. Ribeiro, and A. M. V. M. Soares. 1995. Laboratory study of effects of temperature and salinity on survival and larval development of a population of *Rhithropanopeus harrisii* from the Mondego River estuary, Portugal. *Mar. Biol.* **121:** 639–645.

Jegla, T. C., and J. D. Costlow. 1982. Temperature and salinity effects on developmental and early posthatch stages of *Limulus*. Pp. 103–113 in *Physiology and Biology of Horseshoe Crabs: Studies on Normal and Environmentally Stressed Animals*, J. Bonaventura, C. Bonaventura, and S. Tesh, eds. Alan R. Liss, New York.

Kinne, O. 1970. Temperature. Pp. 321–514 in *Marine Ecology*, Vol. I, Part 1, O. Kinne, ed. Wiley-Interscience, New York.

Kinne, O. 1971. Salinity. Pp. 683–995 in *Marine Ecology*, Vol. 1, Part 2, O. Kinne, ed. Wiley-Interscience, New York.

Kleinbaum, D. G. 1996. *Survival Analysis: A Self-Learning Text*. Springer, New York.

Laughlin, R. 1983. The effects of temperature and salinity on larval growth of the horseshoe crab *Limulus polyphemus*. *Biol. Bull.* **164:** 93–103.

Laughlin, R. B., and W. French. 1989. Differences in responses to factorial combinations of temperature and salinity by zoeae from two geographically isolated populations of the mud crab *Rhithropanopeus harrisii*. *Mar. Biol.* **102:** 387–395.

Muenchow, G. 1986. Ecological use of failure time analysis. *Ecology* **67:** 246–250.

Palumbi, S. R., and B. A. Johnson. 1982. A note on the influence of life-history stage on metabolic adaptation: the responses of *Limulus* eggs and larvae to hypoxia. Pp. 115–124 in *Physiology and Biology of Horseshoe Crabs: Studies on Normal and Environmentally Stressed Animals*, J. Bonaventura, C. Bonaventura, and S. Tesh, eds. Alan R. Liss, New York.

Penn, D., and H. J. Brockmann. 1994. Nest-site selection in the horseshoe crab, *Limulus polyphemus*. *Biol. Bull.* **187:** 373–384.

Pritchard, D. W. 1967. What is an estuary: physical viewpoint. Pp. 1–157 in *Estuaries*, G. H. Lauff, ed. American Association for the Advancement of Science, Washington, DC.

Reynolds, W. W., and M. E. Casterlin. 1979. Thermoregulatory behavior and diel activity of *Limulus polyphemus*. Pp. 47–59 in *Biomedical Applications of the Horseshoe Crab (Limulidae)*, E. Cohen, ed. Alan R. Liss, New York.

Robertson, J. D. 1970. Osmotic and ionic regulation in the horseshoe crab *Limulus polyphemus* (Linneaus). *Biol. Bull.* **138:** 157–183.

Rudloe, A. 1979. Locomotor and light responses of larvae of the horseshoe crab, *Limulus polyphemus* (L.). *Biol. Bull.* **157:** 494–505.

Rudloe, A. E. 1980. The breeding behavior and patterns of movement of horseshoe crabs, *Limulus polyphemus*, in the vicinity of breeding beaches in Apalachee Bay, Florida. *Estuaries* **3:** 177–183.

Rudloe, A. E. 1985. Variation in the expression of lunar and tidal behavior rhythms in the horseshoe crab, *Limulus polyphemus*. *Bull. Mar. Sci.* **36:** 388–395.

Sekiguchi, K. 1988. *Biology of Horseshoe Crabs*. Science House, Tokyo.

Shuster, C. N. 1979. Distribution of the American horseshoe "crab," *Limulus polyphemus* (L.). Pp. 3–26 in *Biomedical Applications of the Horseshoe Crab (Limulidae)*, E. Cohen, ed. Alan R. Liss, New York.

Shuster, C. N. 1982. A pictorial review of the natural history and ecology of the horseshoe crab, *Limulus polyphemus*, with reference to other Limulidae. Pp. 1–52 in *Physiology and Biology of Horseshoe Crabs: Studies on Normal and Environmentally Stressed Animals*, J. Bonaventura, C. Bonaventura, and S. Tesh, eds. Alan R. Liss, New York.

Shuster, C. N., Jr., and M. L. Botton. 1985. A contribution to the population biology of horseshoe crabs, *Limulus polyphemus* in Delaware Bay. *Estuaries* **8:** 363–372.

Smith, N. P. 1987. An introduction to the tides of Florida's Indian River Lagoon. I. Water levels. *Fla. Sci.* **50:** 49–61.

Smith, N. P. 1993. Tidal and wind-driven transport between Indian River and Mosquito Lagoon, Florida. *Fla. Sci.* **56:** 235–246.

Sugita, H. 1988. Environmental adaptations of embryos. Pp. 195–224 in *Biology of Horseshoe Crabs*, K. Sekiguchi, ed. Science House, Tokyo.

Reference: *Biol. Bull.* **206:** 95–102. (April 2004)
© 2004 Marine Biological Laboratory

Strategies for Sperm Chemotaxis in the Siphonophores and Ascidians: A Numerical Simulation Study

MAKIKO ISHIKAWA[1,*], HIDEKAZU TSUTSUI[1,†], JACKY COSSON[2], YOSHITAKA OKA[1,‡],
AND MASAAKI MORISAWA[1]

[1] *Misaki Marine Biological Station, Graduate School of Science, The University of Tokyo, Japan; and*
[2] *Observatoire Oceanologique de Villefrance-sur-Mer, CNRS, France*

Abstract. Chemotactic swimming behaviors of spermatozoa toward an egg have been reported in various species. The strategies underlying these behaviors, however, are poorly understood. We focused on two types of chemotaxis, one in the siphonophores and the second in the ascidians, and then proposed two models based on experimental data. Both models assumed that the radius of the path curvature of a swimming spermatozoon depends on $[Ca^{2+}]_i$, the intracellular calcium concentration. The chemotaxis in the siphonophores could be simulated in a model that assumes that $[Ca^{2+}]_i$ depends on the local concentration of the attractant in the vicinity of the spermatozoon and that a substantial time period is required for the clearance of transient high $[Ca^{2+}]_i$. In the case of ascidians, trajectories similar to those in experiments could be adequately simulated by a variant of this model that assumes that $[Ca^{2+}]_i$ depends on the time derivative of the attractant concentration. The properties of these strategies and future problems are discussed in relation to these models.

Introduction

After the first discovery of the chemotactic behavior of spermatozoa toward an egg by Dan (1950), sperm chemotaxis has been reported in various animal species (Miller, 1977; Eisenbach, 1999), and chemoattractants that mediate such behaviors have been identified in a few cases (Ward *et al.*, 1985; Coll *et al.*, 1994; Olson *et al.*, 2001; Yoshida *et al.*, 2002). Furthermore, recent cell biological studies revealed some of the intracellular enzymatic signaling cascade evoked by the attractant stimulations (Yoshida *et al.*, 2003; Kaupp *et al.*, 2003). However, a major question that anyone who observed this phenomenon has to bear in mind remains poorly answered: How does such a tiny spermatozoon succeed in finding an attractant source?

What makes this question both more mysterious and more interesting is the fact that distinct swimming trajectories have been observed for spermatozoa of different species, which implies that different strategies for chemotaxis may underlie these behaviors. For example, the chemotactic behavior in the siphonophores has been described as follows (Cosson *et al.*, 1984): spermatozoa show trajectories of large diameter (700–1000 μm) while swimming far from the "cupule," which in these species is an extracellular structure of the egg and serves as an attractant source, and trajectories of smaller diameter (200 μm) in the vicinity of the cupule; the transition between the two modes is progressive. In the ascidians, on the other hand, spermatozoa exhibit characteristic "chemotactic turns" during chemotaxis, but the curvature of the trajectories has no noticeable dependence on the distance to the attractant source (Yoshida *et al.*, 1993, 2002; Ishikawa, 2000). The behavior of sea urchin spermatozoa seems to be a little more complicated but still exhibits unambiguous chemotaxis (Ward *et al.*, 1985). Thus, it appears that spermatozoa in different species often respond to the attractant differently, although the goal is the same in all cases—to find an egg and facilitate fertilization.

One approach to revealing the underlying strategies for sperm chemotaxis may be to build a model based on the experimental observations and then study how the model works. In the present paper, we propose two models, one

---

Received 8 July 2003; accepted 4 February 2004.

[*] Present address: Department of Geology, National Science Museum, Japan.

[†] Author to whom correspondence should be addressed. Present address: Laboratory for Cell Function Dynamics, Brain Science Institute, RIKEN, Hirosawa 2-1, Saitama 351-0198, Japan. E-mail: tsutsui@brain.riken.go.jp

[‡] Present address: Department of Biological Sciences, Graduate School of Science, The University of Tokyo, Japan.

applied to the siphonophores and the second to the ascidians. We focused on these two taxa because their swimming behaviors are simple but clearly distinct, and also because substantial experimental data are available in the literature (see Results for details). These experimental results were simplified, as summarized in Figure 1, and incorporated into the models, which required only a few simple and reasonable assumptions. We show that numerical calculations of sperm trajectory using the two models result in trajectories very similar to those observed experimentally.

Materials and Methods

General remarks on the models

It has been suggested that spermatozoa swim with three-dimensional beating waves whose characteristics confine them to a two-dimensional space when they are confronted with the interfaces between two media such as water/air or glass/water (Cosson *et al.*, 2003). For this reason as well as to simplify the observation of sperm trajectories under a microscope, our experiments have been restricted mainly to spermatozoa located at the glass/water interface of the laboratory chambers. Since experimental background is necessary to test the validity of a model, the models we used were also limited to two dimensions. At the interface, most spermatozoa of siphonophores and ascidians show circular movement, usually in one preferred direction. A reasonable explanation is that the movement in the three-dimensional free environment is helical and that some of the initially homogeneously suspended spermatozoa were going upward and tended to be confined to the air/water interface, while others were going downward, to the water/glass interface, as was shown for sea urchin spermatozoa (see Cosson *et al.*, 2003). Sperm confined to the glass surface still exhibit unambiguous chemotaxis as reported thus far, and this behavior is our topic in the present study.

In our model, a spermatozoon is treated as a mathematical point. This point circulates in the x-y plane in one direction (clockwise for the ascidian spermatozoa observed in the vicinity of the glass slide surface, and counterclockwise for the siphonophore spermatozoa), with a radius of curvature that changes depending on the attractant concentration and

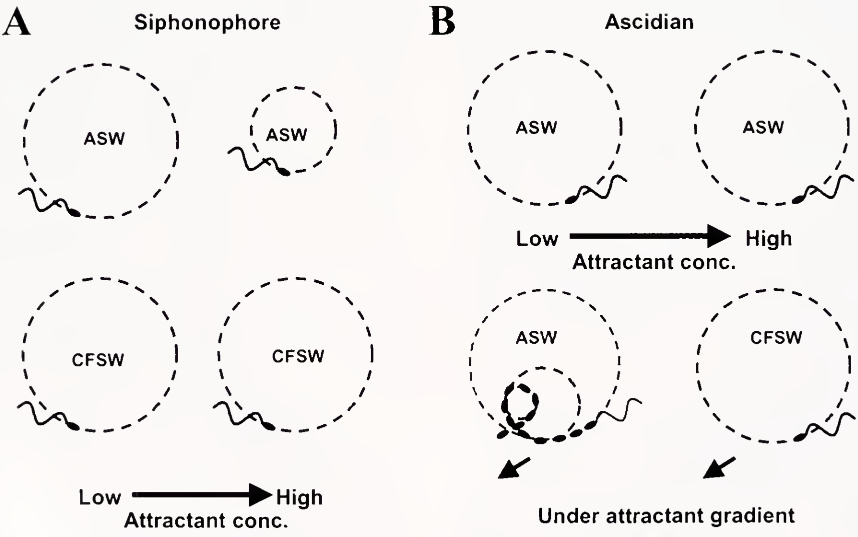

Figure 1. A summary, based on previous reports, of spermatozoa behavior in the presence of the attractant in two species of siphonophore (*Muggiaea kochi, Chelopheyes appendiculata*) and one species of ascidian (*Ciona intestinalis*). (A) In the siphonophores, the curvature is negatively dependent on the attractant concentration in artificial seawater (ASW, *top*), but the dependence is lost in Ca^{2+}-free seawater (CFSW, *bottom*). (B) In the ascidians, no such dependence is observed, even in ASW (*top*), but a rapid modulation of the curvature leading to a turning behavior occurs in the presence of the attractant gradient (*bottom left*). Arrows indicate direction of the attractant source. The curvature is larger when swimming toward the source and smaller when swimming in the opposite direction. A short delay in the response has been often observed in this correlation (Ishikawa, 2000; Yoshida *et al.*, 2002). In CFSW, no such modulation in the curvature is observed, even under the attractant gradient (*bottom left*).

on time. Let us define some parameters: t, time; $\mathbf{p}(t)$, position of sperm at t; $\mathbf{v}(t) = v\{\cos(\phi(t)), \sin(\phi(t))\}$, velocity vector of sperm; $r(t)$, curvature; and $c(\mathbf{p})$, attractant concentration sensed by the sperm at position $\mathbf{p}$ (Fig. 2A). Since no significant changes in the swimming velocity were found during the chemotactic behavior in these species (Cosson *et al.*, 1984; Ishikawa, 2000; Yoshida *et al.*, 2002), let us assume the amplitude of the velocity vector as constant ($=v$). Numerical integration of sperm movement was evaluated as follows with a time step (Δt) of 1.0 ms:

$$\mathbf{p}(t + \Delta t) = \mathbf{p}(t) + \Delta t\mathbf{v}(t) \qquad \text{(Eq. 1)}$$

$$\phi(t + \Delta t) = \phi(t) + \Delta tv/r(t) \qquad \text{(Eq. 2)}$$

Updating the angular component of velocity, but not the vector itself, as in the equation (2), moderates the accumulation of error during the integrations for a long time period. All the calculations and graphical outputs were done by using the Mathematica 3.0 program (Wolfram Research).

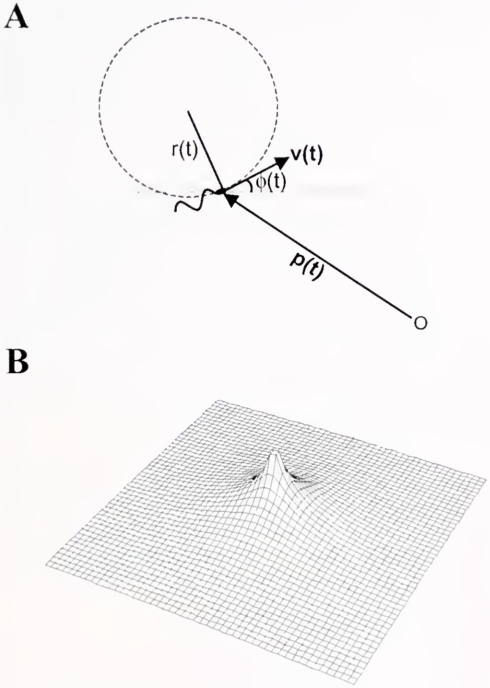

Figure 2. (A) A schematic drawing that shows the four parameters used in the calculation of sperm trajectory. O, the origin; p, position at t (vector); v, velocity (vector); ϕ, angular component of v (scalar); r, radius of curvature (scalar). (B) A computed snapshot of the chemoattractant gradient used in the present study. The attractant concentration profile in the square area of ±1 mm of the x-y plane is plotted in the z-axis. The peak (hilltop) corresponds to the chemoattractant source located at the origin ($x = y = 0$).

Attractant profile

For most observations of chemotaxis, the following experimental design was adopted: a glass pipette filled with chemoattractant or any fluid (within agar-gel in many cases) to be tested was placed in a drop of water containing dispersed sperm cells. This allows a spatial gradient of attractant concentration to be established rapidly: sperm located in the vicinity of an attractant source usually approach it within no more than tens of seconds. Since molecules such as an organic compound or a small protein normally have diffusion coefficients in water of $\sim 10^{-10}$ m^2/s or smaller, it is an acceptable approximation that the attractant profile does not change much during the approach of the spermatozoon. In our model, therefore, we simply used a computed snapshot of a solution of a diffusion equation as an attractant profile (Fig. 2B). Moreover, the drop is largely spread on the slide but is much thinner in the z-axis, so variation of attractant concentration along the z-axis should be small. Therefore, we consider the attractant gradient field with a two-dimensional diffusion equation with a coefficient of D:

$$\delta c/\delta t = D(\delta^2 c/\delta x^2 + \delta^2 c/\delta y^2) \qquad \text{(Eq. 3)}$$

In the polar coordinates of ρ, θ ($x = \rho\cos(\theta)$, $y = \rho\sin(\theta)$), equation (3) can be expressed as

$$\delta c/\delta t = D(\delta^2 c/\delta\rho^2 + 1/\rho\delta c/\delta\rho + 1/\rho^2\delta^2 c/\delta\theta^2) \qquad \text{(Eq. 4)}$$

Since we assume a situation of spatial symmetry, the last term of equation (4) can be regarded to be zero.

$$\delta c/\delta t = D(\delta^2 c/\delta\rho^2 + 1/\rho\delta c/\delta\rho) \qquad \text{(Eq. 5)}$$

As a boundary condition, we assumed that the concentration at the origin (*i.e.*, the tip of a pipette) is always kept at a high level ($c(0) = 1$). We set D as 2.0×10^{-10} m^2/s and used a numerical solution of equation (5) at $t = 60$ s as the profile for subsequent trajectory calculations (Fig. 2B). We also tried some other static attractant profile models (exponential, parabolic, solution of the diffusion equation at different times, etc.) and found that most definitions resulted in qualitatively similar responses to what we show next.

Results

The siphonophore model

Some properties of sperm-swimming in siphonophores are summarized in Figure 1A. This summary is based on observations of *Muggiaea kochi* and *Chelophyes appendiculata* (Cosson *et al.*, 1984). In artificial seawater (ASW), the spermatozoa show trajectories of larger diameter (700–

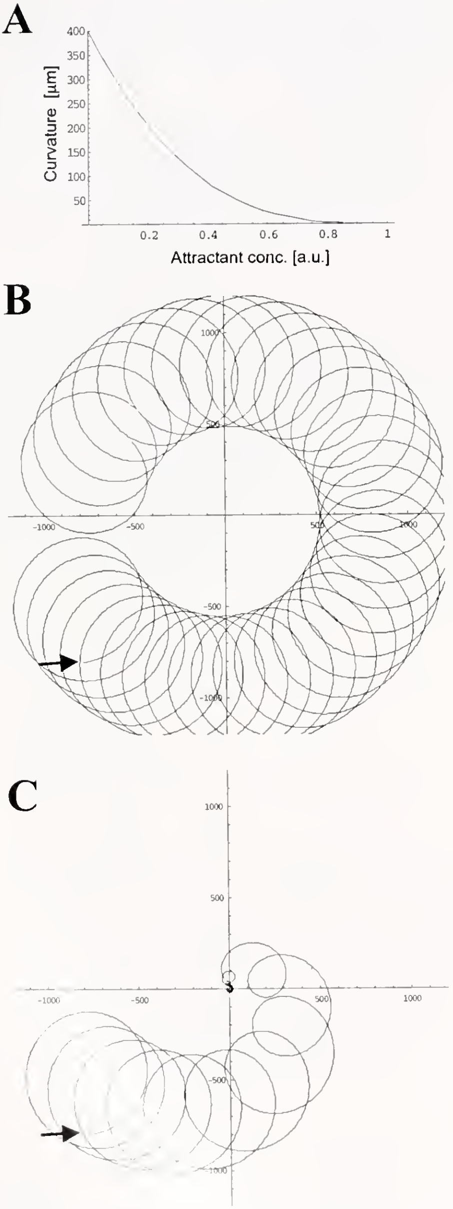

Figure 3. Simulations of the siphonophore model. (A) A cubic function as one of the examples of a function that negatively correlates attractant concentration to curvature of the trajectory. (B) A trajectory simulated with the function shown in (A). Time to lower $[\mathrm{Ca}^{2+}]_i$ is not considered. The sperm started at position $(x, y) = (-800\ \mu\mathrm{m}, -800\ \mu\mathrm{m})$ with an initial angle of 0.1 radian and a constant speed of 500 µm/s (arrow). The trajectory during the initial 40 s is shown. (C) A trajectory simulated under the same conditions as in (B), except that τ of 0.5 s is incorporated as a decay-time constant to lower $[\mathrm{Ca}^{2+}]_i$.

1000 µm) while they are far from the attractant source (~5 mm), and smaller trajectories (~200 µm) near the attractant source (~0.2 mm). However, this dependence on distance from the attractant was lost in the absence of external Ca^{2+}, which suggests that Ca^{2+} influx is involved in the modulation of the curvature of trajectories. We incorporated these findings into the assumptions set in the model as follows:

(a) Curvature decreases as intracellular Ca^{2+} concentration, ($[\mathrm{Ca}^{2+}]_i$), increases (*i.e.*, a negative correlation).

(b) $[\mathrm{Ca}^{2+}]_i$ positively correlates with $c(\boldsymbol{p})$, the attractant concentration which is sensed by the sperm.

Assumption (a) also agrees with the evidence that spermatozoa treated with a Ca^{2+} ionophore showed a curvature of ~200 µm, which increased up to ~800 µm at lower Ca^{2+} concentration. Since any quantitative relationship among these factors in real spermatozoa is not yet available, we set some trial functions and studied the behavior. We first tried a simple linear correlation between $[\mathrm{Ca}^{2+}]_i$ and $c(\boldsymbol{p})$, and a cubic function for $[\mathrm{Ca}^{2+}]_i$ and $r(t)$ (Fig. 3A):

$$[\mathrm{Ca}^{2+}]_i = c(\boldsymbol{p}) \quad (0 < c < 1; [\text{arbitral unit (a.u.)}]) \qquad (\text{Eq. } 6)$$

$$r(t) = 400(1 - [\mathrm{Ca}^{2+}]_i)^3\ [\mu\mathrm{m}] \quad (0 < [\mathrm{Ca}^{2+}] < 1; [\text{a.u.}]) \qquad (\text{Eq. } 7)$$

This now allows us to study how spermatozoa swim under these conditions. The results show that the trajectories generated by such conditions are far from chemotactic behavior. Spermatozoa do circle around the attractant source but never finally approach the egg (Fig. 3B). This result is not surprising because our present system is fully symmetric in terms of time and space components. When using functions other than those of equations (6 and 7), no chemotaxis is observed at all. However, a remarkable change occurs if we incorporate an additional condition:

(c) $[\mathrm{Ca}^{2+}]_i$ has different rates of increase and decrease (slow to decrease).

This condition is not unlikely, because pumping of the cytosolic Ca^{2+} out of the cell or into the intracellular store against the electrochemical gradient across the membrane is an enzymatic process, which is energy-consuming, whereas Ca^{2+} influx generally occurs rapidly. Therefore, we then incorporated this additional condition as follows:

$$\Delta[\mathrm{Ca}^{2+}]_i/\Delta t = -1/\tau([\mathrm{Ca}^{2+}]_i - c(\boldsymbol{p})) \quad \text{when} \quad [\mathrm{Ca}^{2+}]_i > c(\boldsymbol{p}) \qquad (\text{Eq. } 6')$$

where τ is the decay time constant. This condition was applied only when $[Ca^{2+}]_i > c(\boldsymbol{p})$; otherwise, equation (6) was applied as before. When trajectories were calculated with these new sets of conditions (6, 6′, 7), we found that the incorporation of a time component for the Ca^{2+} decay results in chemotactic trajectories (Fig. 3C) that are not unlike those obtained in the experimental observations. Likewise, chemotactic trajectories were reconstructed for a wide range of arbitrarily selected functions that relate '$c(\boldsymbol{p})$' to '$[Ca^{2+}]_i$' positively instead of by equation (6), and relate '$[Ca^{2+}]_i$' to '$r(t)$' negatively instead of by equation (7), even though some of them, of course, showed heavily distorted trajectories of approach toward the attractant source and unusually long or short times of approach.

The ascidian model

The behavior of ascidian sperm is quite different from that in the siphonophore sperm. The behavior illustrated in Figure 1B is based on observations of *Ciona intestinalis* by Ishikawa (2000) and Yoshida *et al.* (1993). In the presence of an attractant without a gradient, the curvature of the sperm trajectory is independent of the concentration of the attractant, and is close to that in the absence of the attractant (Fig. 1B). Under the gradient of attractant concentration, however, spermatozoa show rapid changes in their track diameters, so-called chemotactic turns. Since this turning behavior is lost in the calcium-free seawater (CFSW) or in the presence of Ca^{2+} channel inhibitors, it has been suggested that rapid changes of diameter are dependent on $[Ca^{2+}]_i$. Therefore, we again incorporated condition (a), as we did in the siphonophore model. Next, we need to infer the relationship between $[Ca^{2+}]_i$ and $c(\boldsymbol{p})$, the attractant concentration that the spermatozoan senses. Since modulation of diameter occurs only in the presence of an attractant gradient, we assumed that $[Ca^{2+}]_i$ depends on the temporal changes of $c(\boldsymbol{p})$ but not on the "absolute" concentration itself. Thus, we assume a second condition:

(d) $[Ca^{2+}]_i$ negatively correlates to the time derivative of the attractant concentration.

With conditions (a) and (d), it follows that $r(t)$ positively correlates to $\Delta c(\boldsymbol{p}(t))/\Delta t$, the time derivative of the attract-

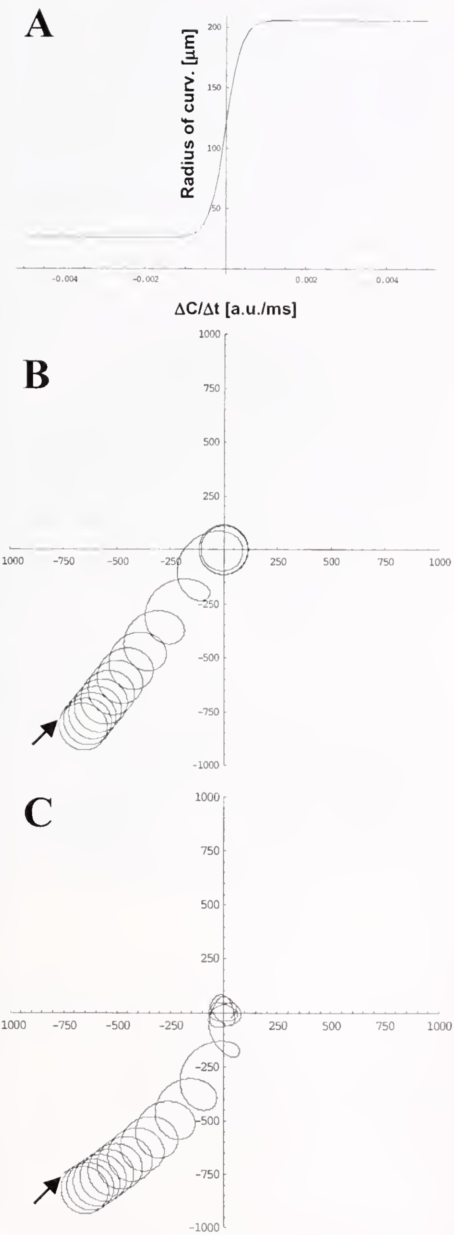

Figure 4. Simulations of the ascidian model. (A) A sigmoid function as one of the examples of a function that positively correlates time-derived attractant concentration to the curvature of the trajectory. (B) A trajectory simulated with the function shown in (A). The sperm started at position (x, y) = (−750 μm, −750 μm) with an initial angle of 0.8 radian and a constant speed of 250 μm/s (arrow). The trajectory during the initial 40 s is shown. (C) A trajectory simulated under the same conditions as in (B), except that a delay of 150 ms in the response of curvature to the time-derived attractant concentration is incorporated.

ant concentration. This assumption was incorporated in the ascidian model as follows:

$$r(t) = F(\Delta c(p(t))/\Delta t) \qquad \text{(Eq. 8)}$$

Where F is the function that positively correlates $\delta c/\delta t$ with $r(t)$. We studied sperm behavior with a sigmoid function for F (Fig. 4A) and found that this condition alone is sufficient to show chemotactic trajectories with successive turns when approaching the attractant source (Fig. 4B). We further incorporated a delay in the sperm response of $r(t)$ to $\Delta c(p(t))/\Delta t$ with a time range of tens of milliseconds, because such a delay has been found in the analysis of the trajectory of real sperm (Ishikawa, 2000; Yoshida *et al.*, 2002). This resulted in similar trajectories, but with a twist (Fig. 4C), which is often observed in real chemotaxis in the ascidian. Thus, we find that the delay of sperm response is not an absolute necessity for chemotactic behavior in the case of the ascidian model, but this parameter results in trajectories that are somewhat more realistic.

Discussion

In the present study, we proposed two comprehensive models for strategies of sperm chemotaxis in the siphonophores and the ascidians. With these models, chemotactic trajectories similar to those observed for real spermatozoa could be reconstructed. We found that there are at least two ways to identify the location of the "hilltop"—the source of the chemoattractant—without looking around for it. The siphonophore's way is to "walk" circularly, with large-diameter curvatures at low altitude and smaller ones at higher altitude. This alone is not enough for success; however, success can be achieved if any increase in curvature is followed by a time lag. In the ascidian's way, one needs to sense the steepness (gradient) but not the height (absolute concentration): the curvature is large when climbing steeply uphill, medium when the slope is gentle, and small when going downhill. The time-delay condition is not always necessary, but such a delay introduces twists into the trajectory.

Even though these models employ some conditions based on experimental results, these conditions may seem to be oversimplified. However, the goal of the present modeling study is not to simulate the natural behavior of the spermatozoa perfectly but to find out what elements are needed to reconstruct the phenomenon of interest. For this purpose, it is necessary to focus on a small number of important parameters.

Nonetheless, some lines of evidence in addition to those mentioned earlier, support our simplification of the conditions. First, it has been shown that asymmetrical bending waves are induced when a high concentration of Ca^{2+} is applied to the flagella of demembranated sea urchin sperm (Brokaw, 1979). This may support our condition (a). Next, it was recently suggested that a store-operated Ca^{2+} channel (SOC) regulates chemotaxis in the ascidian (Yoshida *et al.*, 2002). Involvement of such a SOC may account for the time delay in the curvature response to the temporal changes in the attractant concentration: this feature was often observed in the experiments and is introduced into the ascidian model (Fig. 4C), since activation of the SOC requires depletion of internal Ca^{2+} stores evoked by the releasing signals such as inositol 1,4,5-phosphate.

Quantitative comparison of the model outputs with experimental results is very important for validation of the models. Unfortunately, we are not ready to do such a study because the models currently have high degrees of freedom. The two functions, one that relates attractant stimulus with $[Ca^{2+}]_i$ and the other that relates $[Ca^{2+}]_i$ with curvature, cannot yet be quantitatively defined. Of course, one desirable experiment might be to experimentally define these functions and then to carry out a quantitative comparison. But this requires many very difficult technical break-

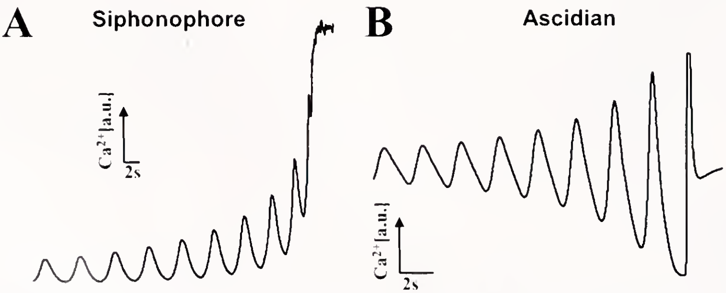

Figure 5. Changes in $[Ca^{2+}]_i$ during chemotaxis. (A) Plot of $[Ca^{2+}]_i$ as a function of time in the modeled chemotaxis for siphonophores (Fig. 3C). (B) Plot of $[Ca^{2+}]_i$ *versus* time in the modeled chemotaxis for the ascidian (Fig. 4B). It is assumed that $[Ca^{2+}]_i$ is proportional to the inverse of the radius of curvature.

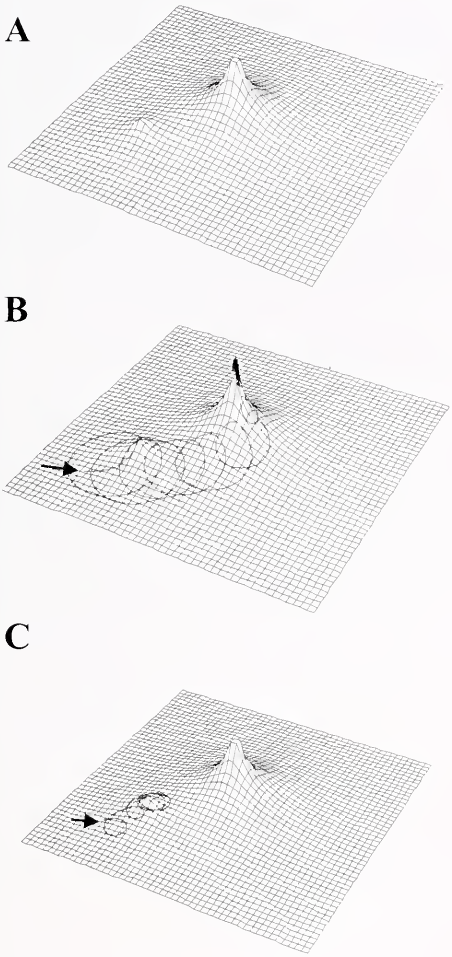

Figure 6. A difference in the sensitivity to a local attractant peak between the siphonophore and ascidian strategies. (A) A secondary source with one-fourth the attractant concentration of the main one is added at the position $(x, y) = (-500\ \mu\text{m}, -500\ \mu\text{m})$. (B) Sperm trajectory with the siphonophore model under the dual peak profile in (A). The trajectory is superimposed upon the attractant profile. Note that the spermatozoa found the main peak. The initial condition is same as that in Fig. 3B. (C) Sperm trajectory simulated with the ascidian model. Note that the spermatozoa now found the local peak instead of the main peak. The initial condition is the same as that in Fig. 4B. Arrows in (B) and (C) indicate the initial positions and directions.

throughs such as quantification of local attractant concentration, application of an attractant stimulus varying with time, and so on. Another indirect but more practical experiment would be to measure $[\text{Ca}^{2+}]_i$ during chemotaxis. Our models predict that there will be a temporal $[\text{Ca}^{2+}]_i$ pattern during chemotaxis specific to each model: $[\text{Ca}^{2+}]_i$ oscillates in both models, and the base level elevates in the siphonophores but not in the ascidians (Fig. 5). Even though measurement of $[\text{Ca}^{2+}]_i$ in swimming spermatozoa is still technically challenging, mainly due to the small volume of cytoplasm and fast movements of the sperm, we hope that recent innovations in Ca^{2+} indicators and image sensors will make it possible in the future.

What is the significance of the difference in the two strategies? Since temporal change of the attractant concentration is the critical parameter for the modulation of curvature in the ascidian model, we expect that the ascidian spermatozoon is more sensitive to local change of concentration than the siphonophore spermatozoon, in which the absolute concentration value is the most critical. Simulation under two attractant sources, one of high concentration and the other of low concentration, led to the expected results: the ascidian spermatozoa found the lower peak of attractant in the vicinity, and the siphonophore spermatozoa reached the higher peak (Fig. 6). Thus, an interesting future problem would be to test this prediction in biological experiments. One may also be interested in possible relationships between such characteristics of sperm strategy and the environment that the species are facing. However, such a question cannot be addressed currently. Most of our knowledge has been limited to sperm in two-dimensional laboratory conditions, even though the goal should be to reach a deep understanding of strategy in the three-dimensional natural environment. Since theoretical treatments suggests that drag forces near the interface have substantial effects on the flagellar motion of sperm (Katz, 1974), we should avoid applying knowledge gained in two dimensions thoughtlessly in building three-dimensional models. One needs to know how parameters that describe three-dimensional helical motions are affected by the attractant gradient. To accomplish this goal, we hope that techniques to measure sperm trajectories in the three-dimensional environment, as pioneered by Crenshaw *et al.* (2000), will soon be more accessible.

Acknowledgments

We thank Dr. M. Yoshida and Dr. K. Yoshimura of the University of Tokyo for helpful discussions, and the staff of MMBS for encouragement. The CNRS, JSPS, and MEXT are acknowledged for support of J. Cosson at the occasion of several stays in Japan. This work was supported by grants-in-aid from the Ministry of Education, Culture, Sports, Science and Technology of Japan to M.M.

Literature Cited

Brokaw, C. J. 1979. Calcium-induced asymmetrical beating of Triton-demembranated sea urchin sperm flagella. *J. Cell Biol.* **82:** 401–411.

Coll, J. C., B. F. Bowden, G. V. Meehan, G. M. König, A. R. Carroll, D. M. Tapiolas, P. M. Alino, A. Heaton, R. De Nys, P. A. Leone, M. Maida, T. L. Acetet, R. H. Willis, R. C. Babcock, B. L. Willis, Z. Florian, M. N. Clayton, and R. L. Miller. 1994. Chemical aspects of mass spawning in corals. I. Sperm-attractant molecules in the eggs of the scleractinian coral *Montipora digitata*. *Mar. Biol.* **118:** 177–182.

Cosson, M. P., D. Carré, and J. Cosson. 1984. Sperm chemotaxis in siphonophores. II. Calcium-dependent asymmetrical movement of spermatozoa induced by the attractant. *J. Cell Sci.* **68:** 163–181.

Cosson, J., P. Huitorel, and C. Gagnon. 2003. How spermatozoa come to be confined to surfaces. *Cell Motil. Cytoskelet.* **54:** 56–63.

Crenshaw, H. C., C. N. Ciampaglio, and M. McHenry. 2000. Analysis of the three-dimensional trajectories of organisms: estimates of velocity, curvature and torsion from positional information. *J. Exp. Biol.* **203:** 961–982.

Dan, J. C. 1950. Fertilization in the medusan *Spirocodon saltarix*. *Biol. Bull.* **99:** 412–415.

Eisenbach, M. 1999. Sperm chemotaxis. *Rev. Reprod.* **4:** 56–66.

Ishikawa, M. 2000. Strategy and regulation of sperm chemotactic behavior in the ascidian, *Ciona intestinalis*. M.S. thesis, University of Tokyo. (In Japanese).

Katz, D. F. 1974. On the propulsion of micro-organisms near solid boundaries. *J. Fluid Mech.* **64:** 33–49.

Kaupp, U. B., J. Solzin, E. Hildebrand, J. E. Brown, A. Helbig, V. Hagen, M. Beyermann, F. Pampaloni, and I. Weyand. 2003. The signal flow and motor response controlling chemotaxis of sea urchin sperm. *Nat. Cell Biol.* **5:** 109–117.

Miller, R. L. 1977. Distribution of sperm chemotaxis in the animal kingdom. Pp. 99–199 in *Advances in Invertebrate Reproduction*, Vol. 1. K. G. Adiyogi and R. G. Adiyogi, eds. Peralam Kenoth, Kerala, India.

Olson, J. H., X. Xiang, T. Ziegert, A. Kittelson, A. Rawls, A. L. Bieber, and D. E. Chandler. 2001. Allurin, a 21-kDa sperm chemoattractant from *Xenopus* egg jelly, is related to mammalian sperm-binding proteins. *Proc. Natl. Acad. Sci. USA* **98:** 11,205–11,210.

Ward, G. E., C. J. Brokaw, D. L. Garbers, and V. D. Vacquier. 1985. Chemotaxis of *Arbacia punctulata* spermatozoa to resact, a peptide from the egg jelly layer. *J. Cell Biol.* **101:** 2324–2329.

Yoshida, M., K. Inaba, and M. Morisawa. 1993. Sperm chemotaxis during the process of fertilization in the ascidians *Ciona savignyi* and *Ciona intestinalis*. *Dev. Biol.* **157:** 497–506.

Yoshida, M., M. Murata, K. Inaba, and M. Morisawa. 2002. A chemoattractant for ascidian spermatozoa is a sulfated steroid. *Proc. Natl. Acad. Sci. USA* **99:** 14,831–14,836.

Yoshida, M., M. Ishikawa, H. Izumi, R. De Santis, and M. Morisawa. 2003. Store-operated calcium channel regulates the chemotactic behavior of ascidian sperm. *Proc. Natl. Acad. Sci. USA* **100:** 149–154.

Reference: *Biol. Bull.* **206:** 103–112. (April 2004)
© 2004 Marine Biological Laboratory

Interaction Between Photoperiod and an Endogenous Seasonal Factor in Influencing the Diel Locomotor Activity of the Benthic Polychaete *Nereis virens* Sars

KIM S. LAST* AND PETER J. W. OLIVE

School of Marine Sciences and Technology, Ridley Building, University of Newcastle upon Tyne, NE1 7RU, United Kingdom

Abstract. The locomotor activity of *Nereis virens* Sars associated with food prospecting was investigated in response to photoperiod and season using an actograph. Experimental animals which had been reared under natural photoperiods were exposed to two constant photoperiodic treatments, LD 16:8 and LD 8:16, in both the autumn and winter and in the absence of tidal entrainment. Autocorrelation analysis of rhythmicity showed that during the autumn, animals under the LD 16:8 photoperiod displayed a strong nocturnal rhythm of activity, whereas animals under the LD 8:16 photoperiod showed only a weak nocturnal activity rhythm. This is believed to represent an autumn feeding cessation that is triggered when the animals pass through a critical photoperiod $LD_{crit} <12:>12$. Later in the winter, however, animals exposed to both photoperiodic treatments showed strong rhythms of foraging activity irrespective of the imposed photoperiod. It is suggested that the autumn cessation may maximize the fitness of *N. virens*, a spring-breeding semelparous organism, by reducing risk during gamete maturation, while spontaneous resurgence of activity after the winter solstice permits animals that are not physiologically competent to spawn to accrue further metabolic reserves. This response is believed to be initiated by a seasonal (possibly circannual) endogenous oscillator or interval timer.

Introduction

Nereis virens Sars, one of the largest marine annelids, has proven to be an interesting model for studies of semelparous life histories with mixed age at maturity (Olive *et al.*, 1997, 2000, 2001). While age at maturity varies between 1 and 7 or more years, any one worm can breed only once, whereupon spawning is followed by death. A key transition in this life history occurs during the autumn preceding eventual breeding when the final stages of gametogenesis are initiated, culminating in individuals becoming gravid and spawning during the following spring. The profound influence of the photoperiod on the behavior and physiology of *N. virens* has already been demonstrated. Transition through the critical photoperiod ($LD_{crit} <12:>12$) at the end of September (Last *et al.*, 1999) initiates sexual maturation and gamete development, which may culminate in sexual reproduction and death in any particular year (Olive *et al.*, 1997). When semiquantitative methods were used to determine the prospecting behavior of this polychaete, it was shown (Last and Olive, 1999) that the frequency at which animals emerged from their burrows in the autumn was much higher under a photoperiod of LD (light/dark) 16:8 than under LD 8:16. In a potentially long-lived but strictly semelparous organism such as *N. virens*, there is strong selection for the avoidance of risk during the final stages of sexual maturation when accumulated reserves are being converted to gametogenic tissues (Olive *et al.*, 2001). It is reasonable, therefore, to interpret the level of foraging activity as indicating the onset of a physiological state, responsive to relative daylength, during which sexual maturation occurs. Observations made during the late spring and summer, however (Last and Olive, 1999), showed that the differences in foraging activity between LD 16:8 and LD 8:16 were not as marked, but were still significantly different. It was therefore suggested that a covert temporal rhythm must underlie the overt activity of emergence in *N. virens*, and that the emergent patterns also involve expression of a

Received 23 September 2003; accepted 25 February 2004.

* To whom correspondence should be addressed. E-mail: k.s.last@ncl.ac.uk

response to a seasonal (or circannual) clock, since exposure to a constant LD 8:16 photoperiod does not induce the same physiological response at all times of the year.

Photoperiodism in marine animals is less intensively studied than in terrestrial organisms, but "photoperiod-like" phenomena have been documented in several marine species, including the echinoderm *Picaster ochraceus* (Pearse and Eernisse, 1982), the copepod *Labidocera aestiva* (Marcus, 1986), and the polychaetes *Neanthes limnicola* (Fong and Pearce, 1992a, b) and *Harmothoe imbicata* (Garwood and Olive, 1982). The difference between the environmental and the evolutionary history in marine organisms requires that these processes be investigated to understand environmental signal transduction in the control of life-history events and to determine whether these observations are likely to be the consequence of a common clock mechanism. Confirmation that they are such a consequence would have important implications for our understanding of the evolution of clock-based processes.

To test the suggestion that an endogenous long-term rhythm moderates responses to fixed photoperiodic inputs in *N. virens*, we used an actographic procedure (Last, 2003) to monitor its emergence (foraging) behavior and examined the spontaneous diel activity patterns of individual animals maintained under fixed LD cycles for several months.

Materials and Methods

Two experiments were conducted using the polychaete *Nereis virens*. Short-term assays of activity were carried out in the autumn and winter to assess the strength of diel "out-of-burrow" activity both within and between seasons under rectilinear photoperiods (that is, light and dark periods without simulated dawn and dusk). Concurrently, a long-term experiment was used to determine any spontaneous changes in activity under constant rectilinear photoperiods with time.

Two time periods were used for the short-term assay: six days in September in the autumn of 1998 (A98) and six days in February in the winter of 1999 (W99). Both A98 and W99 animals had been born from the same broodstock (16 March 1998), and as a consequence, the experimental animals for W99 were 5 months older than those used for A98. To prevent any size- or maturation-related bias in feeding rates, all animals chosen were of about the same weight, 2.5 ± 0.1 g, with all coelomic oocytes having a diameter ≤120 μm. All animals (n = 16) were collected from a commercial supplier (Seabait Ltd.) a week prior to the experiments, which took place under controlled conditions in the laboratory. Since birth, animals had been maintained outside under natural photoperiods, so the natural photoperiod at the time of collection was LD 13:11 for A98 and LD 11:13 for W99. After acclimatization, animals were introduced into the actographs (see below) and maintained under one of two photoperiods, LD 16:8 or LD 8:16, that approximated the photoperiodic extremes between midsummer and midwinter at a latitude of 55° north (where the animals were collected).

Data obtained from the actographic recording were analyzed for two factors: (1) variability in the diel activity of individuals both between photoperiodic treatments and seasons, and (2) overall changes in "strength" of rhythm. Variability in diel activity was visually represented using actograms, while the strength of rhythm was characterized with autocorrelation analysis (Dowse and Ringo, 1989; Palmer *et al.*, 1994; Dutilleul, 1995). This statistic provides a measure of the strength to the rhythm that is not affected by the overall level of activity: the less noisy the data between cycles and the higher the signal, the stronger the rhythm. Since the autocorrelation output is normally distributed around the lag time that most closely matches the period of that particular rhythm, robust parametric statistics can be applied.

The concurrent long-term experiment was carried out for 9 months under constant LD 16:8 and LD 8:16 photoperiods, using animals from the same broodstock that were born naturally at Seabait Ltd. on 16 March 1998 and reared continuously outside under natural photoperiods until the start of these investigations. As with experiments A98 and W99, the animals chosen had about the same weight (2.5 ± 0.1 g) and sexual maturity (oocyte diameter ≤120 μm). All stock animals (n = 100) for this experiment were maintained continuously under photoperiods of LD 16:8 or LD 8:16. Such continuous rectilinear photoperiods have previously been used to detect circannual rhythms (Randall *et al.*, 1998; Nisimura and Numata, 2001) without the possibly detrimental effects of inducing a free-running state by using continuous light or darkness. Each month between September 1998 and June 1999, four animals were selected at random from stock aquaria in the laboratory and placed into the artificial burrows of the actograph. Their activity was then recorded for 6 to 7 days under the two photoperiodic treatments, LD 16:8 and LD 8:16. At other times, the animals were maintained under the respective photoperiodic treatments LD 16:8 and LD 8:16 in stock aquaria. Hourly actograph data were summed into 48-h epochs and partitioned into mean monthly actograms. The mean data points were plotted against maximum overall activity that normalized the amplitude between treatments and made direct comparisons possible.

To prevent transient behavioral activity for both short (A98 and W99) and long-term assays, animals were always acclimatized for 7 days under their new photoregimes.

The actograph consisted of two aquaria housed in light-tight photoperiodically controlled chambers. Artificial burrows consisting of lengths of PVC tubing were inserted through the bottoms of these experimental aquaria and connected to infra-red optocouplers that were broken as soon as any animal emerged. Out-of-burrow activity for all animals was monitored using a data logger. A complete description of the actographic procedures has been published in Last (2003). The aquaria were supplied with recirculating seawater, salinity 34 to 36‰, that had been biologically trickle-filtered and sterilized with UV light; temperatures in the aquaria were maintained constant at ≈16 °C. Every 2 days during the middle of the photophase (the light portion of the cycle) the experimental animals were fed coarse trout pellets to and above the maximum that they would consume.

Results

Analysis of locomotor activity in N. virens: *Autumn (A98)*

Actograms. The mean hourly activity (beam breaks) of all animals over 7 days in the autumn when maintained under LD 16:8 and LD 8:16 photoperiods is shown in Figure 1. Note that these animals are from natural photoperiods of LD 13:11. The main onset of activity under both treatments occurred at 0000 (midnight) GMT immediately after the lights-off signal. All activity was much reduced during the photophase. Thus the type of activity under both treatments can be described as a nocturnal diel pattern of foraging behavior. Under LD 16:8 (Fig. 1a), activity was consistently high for each successive scotophase (the dark portion of the cycle) but with substantial within-treatment variability between individuals, as shown by the standard deviation bars. Under LD 8:16, however (Fig. 1b), the distinction between onset and cessation of activity was less marked except for days 1 and 2. All animals were similarly inactive except during the first scotophase, which showed raised activity levels comparable with those animals under LD 16:8. The mean number of emergence events for animals under LD 16:8 was significantly greater (Student's t test: $t = 3.23$, $P < 0.05$) for each consecutive 24-h period than for animals under LD 8:16.

Strength-of-rhythm analysis of activity data. Autocorrelation analysis showed that animals maintained under LD 8:16 in the autumn have a significantly weaker rhythm of activity than those under LD 16:8 (t test: $t = 2.54$, $P < 0.05$). This demonstrates that strength of rhythm in the autumn is dependent on the imposed photoperiodic treatment.

Analysis of locomotor activity of N. virens: *Winter (W99)*

Actograms. The mean hourly activity (beam breaks) of all animals over 6 days in the winter when maintained under LD 16:8 and LD 8:16 photoperiods is shown in Figure 2. Note that these animals are from natural photoperiods of LD 11:13. Under both photoperiods, activity was consistently high for each successive scotophase despite the relatively high within-treatment variability between individuals, as shown by the standard deviation bars. There was no significant difference (t test: $t = 2.09$, $P > 0.05$) in the number of emergence events for animals under LD 16:8 and animals under LD 8:16 for each consecutive 24-h period. This is in striking contrast to the results recorded 5 months earlier under the same photoperiodic treatments.

Strength-of-rhythm analysis of activity data. The strength of the activity rhythm of animals maintained under LD 16:8 was not significantly different (t test: $t = 0.65$, $P > 0.1$) from those maintained under LD 8:16. This demonstrates that strength of rhythm in the winter is independent of the imposed photoperiodic treatment.

Comparative analysis in strength of rhythm: Autumn and winter

Autocorrelation analysis of rhythm strength is not affected by overall amplitude of activity, and hence a comparative analysis of activity between treatments (LD 16:8 and LD 8:16) and between seasons (A98 and W99) was possible even though overall activity in A98 was higher than in W99. The strength of rhythm of animals maintained under LD 16:8 in the autumn was significantly (t test: $t = 2.54$, $P < 0.05$) stronger than that of animals under LD 8:16 at this time. No significant difference (t test: $t = 0.27$, $P > 0.1$) was observed in strength of rhythm in animals maintained under a photoperiod of LD 16:8 in the autumn compared to animals maintained under the same photoperiod in the winter. Similarly, no significant difference (t test: $t = 0.65$, $P > 0.1$) was observed in strength of rhythm in animals maintained under LD 16:8 or LD 8:16 photoperiods in the winter. Finally the strength of rhythm of animals maintained under the LD 8:16 photoperiod in the winter was significantly (t test: $t = 3.29$, $P < 0.01$) stronger than that of animals under the LD 8:16 photoperiod in the autumn. In the autumn, the most noticeable between-treatment variation was the much reduced overall activity and strength of rhythm under LD 8:16 compared to LD 16:8. In the winter, no such differences in strength were observed since the strength of rhythm was high in all animals irrespective of photoperiod.

Analysis of long-term locomotor activity of N. virens

The results from each experimental treatment (LD 16:8 and LD 8:16) were pooled to plot a three-dimensional (3D) topographical graph of activity (y-axis) over time (x-axis) and month (secondary x-axis) (Fig. 3a, b). Dashed rectangles beneath the x-axis represent the times of the imposed scotophase. The surface topography represents the mean hourly activity of four animals over the duration of 6 to 8 days every month for 9 months. (Note: these results do not include data from the short-term A98 and W99 experiments).

Figure 3a shows the pattern of locomotor activity under

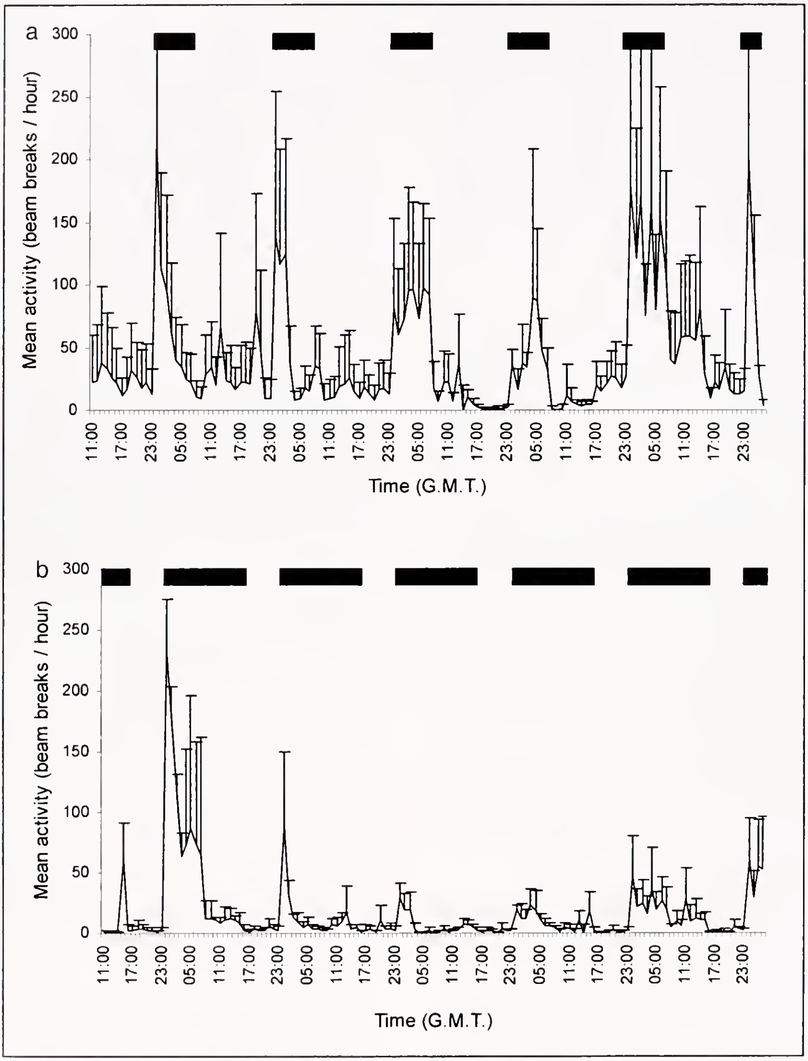

Figure 1. The mean beam breaks/hour (+SD) representative of foraging excursions under different photoperiods in the autumn (A98) for *Nereis virens*, where the black rectangles represent times of artificial scotophase. (a) LD 16:8, *n* = 4; (b) LD 8:16, *n* =4.

LD 16:8 over the duration of the experiment. Most of the activity was restricted to the scotophase, except transiently in September and March, when late photophase activity was also observed. Little difference was seen between mean activities over each successive 48-h period for the duration of 9 months. Activity was typically initiated around the time of the lights-off signal (steep topographical relief) and continued to be high throughout all scotophases.

Figure 3b shows the pattern of locomotor activity under LD 8:16. Between September and December there was no

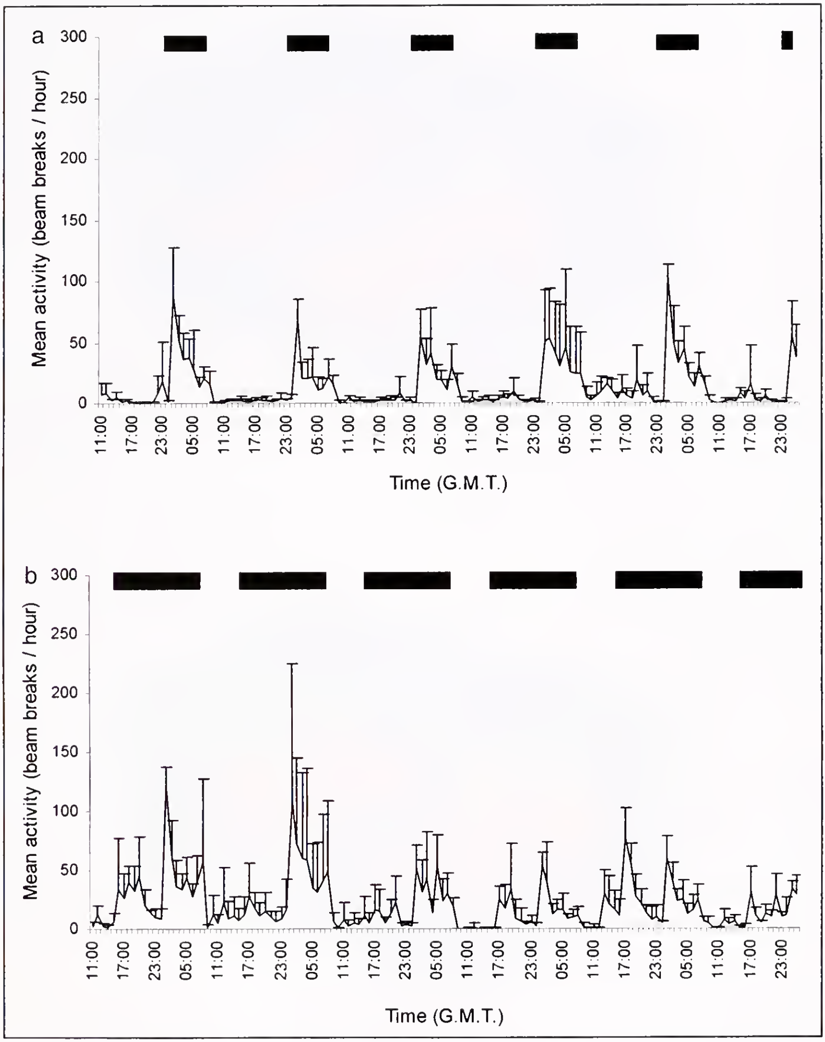

Figure 2. The mean beam breaks/hour (+SD) representative of foraging excursions under different photoperiods in the winter (W99) for *Nereis virens*, where the black rectangles represent times of artificial scotophase. (a) LD 16:8, n = 4; (b) LD 8:16, n = 4.

activity in either the photophase or the scotophase. Nocturnal activity increased dramatically after December, and then continued until termination of the experiment in June. This elevated activity occurred spontaneously and independently of any environmental signal. The major peak of activity was generally seen directly after lights-off, with raised activity during the rest of the scotophase. Activity during the photophase was low. A perturbation was observed in March, when activity dropped significantly for the duration of the month. This is represented by the trough running the length of the graph from left to right.

The results from the topographical data for LD 16:8 and

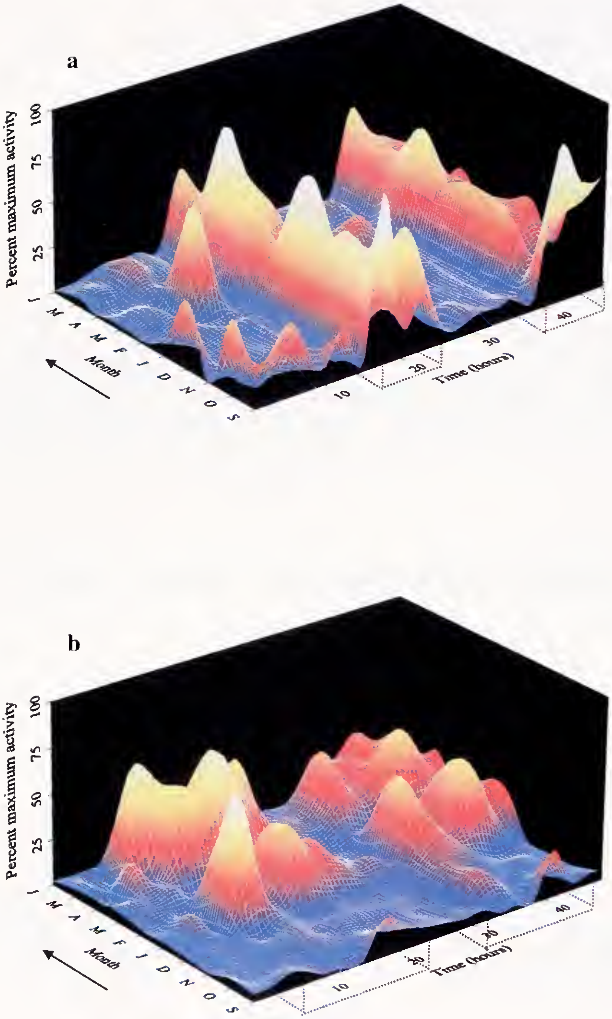

Figure 3. Three-dimensional plot showing the topography of mean monthly activity (September to June) in *Nereis virens* under different static photoperiods. Dashed rectangles beneath the *x*-axis represent times of the scotophase. Data points constituting surface topography number about 7000. (a) LD 16:8, *n* = 4: Nearly all activity is confined to the scotophase except for perturbations in September, October, and March. (b) LD 8:16, *n* = 4: Note the cessation of activity between September and the middle of December. At the beginning of January, a spontaneous resurgence of activity during the scotophase occurs, which is continuous for the rest of the experiment except for a decline in activity in March.

LD 8:16 are summarized schematically in relation to the natural photoperiod in Figure 4. At the start of the experiment in September, the natural photoperiod was LD 13:11. All animals placed under the LD 16:8 photoperiod (Fig. 4a) showed strong, nocturnal activity that continued until March, when the natural photoperiod was once again LD

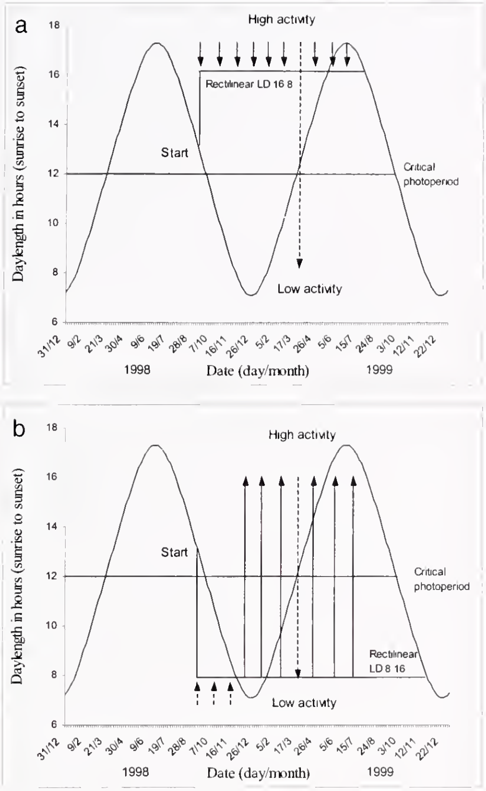

Figure 4. Schematic summaries of the results for the static rectilinear 9-month experiment under LD 16:8 (a) and LD 8:16 (b). Ambient day length (sunrise to sunset) is shown over time at latitude 55° N, giving the temporal position of the rectilinear photoperiodic treatments and type of activity in relation to the ambient photoperiods outside the laboratory. Solid arrows indicate where activity in *Nereis virens* is high; dotted arrows indicate where activity is low.

12:12. At this time, additional activity was noted during the later part of the photophase. After March, activity was once again restricted solely to the scotophase. Animals placed under the LD 8:16 photoperiod, however, displayed a quite different activity pattern (Fig. 4b). In these animals, all activity was relatively low for 3 months, during the time when natural photophases are diminishing in the natural habitat (LD <12:>12). By the middle of December, the time when the natural scotophase is at its longest at this latitude (17 h), a spontaneous recovery of activity during the scotophase was observed. This pattern of elevated nocturnal activity continued in the laboratory at a time when the nights in the natural environment were gradually shortening. At the spring equinox in March, when natural photoperiods were once again LD 12:12, overall activity dropped substantially. From April to June, however, activity was once again elevated.

Discussion

The results presented here demonstrate that the pattern of locomotor activity expressed by *Nereis virens* is influenced by both the photoperiod to which the animals are subjected and the time of year in which the behavioral assay is conducted. Photoperiod and time of year appear to interact and modulate overall activity patterns, giving rise to variability in the daily nocturnal activity patterns and in the overall strength of the rhythm associated with foraging activity.

Our results also show that the activity of this polychaete is predominantly nocturnal under all photoperiods, irrespective of season. The photophase suppressed activity in animals under both photoperiodic treatments, and we believe that spurious beam breaks during the photophase constitute primarily "within-burrow" rather than "out-of-burrow" activity (Last, 2003). We hypothesize that the conserved nature of this nocturnal response reflects a strong selective advantage as a predator-avoidance mechanism, since feeding excursions for *N. virens* are associated with predation risk from shorebirds and pleuronectenoid fish, which are all well-known diurnal, visual feeders (Thijssen *et al.*, 1974; Carter *et al.*, 1991; Wilson, 1991), and such risk is reduced under cover of darkness.

Activity in the autumn

Under the LD 16:8 photoperiod in the autumn, the actogram showed a high level of nocturnal activity (Fig. 1a), which is synonymous with a high feeding rate (Last, 2003). In contrast, those animals under LD 8:16 displayed relatively reduced overall activity (Fig. 1b) signifying a low feeding rate. These findings are similar to those of Last and Olive (1999) using semiquantitative, manual methods to assess the degree of foraging activity at a similar time of year.

Photoperiodism necessitates the presence of an underlying endogenous clock. The results of experiment A98 support the presence of such an oscillator in *N. virens*. During the first scotophase, animals under LD 8:16 ceased activity at between 1000 and 1100 GMT (Fig. 1b), 10–11 h after the onset of activity. This was surprising since the lights-on signal for these animals was at 1600 GMT, and inactivity was thus not expected for a further 7–8 h. The animals used in the A98 experiment would have been experiencing natural photoregimes of LD 12:12, suggesting that the observed time of activity cessation was due to the entrainment of past photoperiodic regimes. We hypothesize that the nocturnal activity cessation under LD 8:16 may reflect a *proactive* response to the anticipated time of sunrise, therefore providing indirect evidence for an endogenous timer. This response is surprising since these animals had been acclimatized to this photoperiod for a week.

Activity in subsequent scotophases rapidly became bimodal (Fig. 1b) with activity peaks in both early and late scotophases. Similar daily changes in activity under various photoperiods have been recorded for the locomotory activity patterns of the onion fly *Delia antiqua* (Watari and Arai, 1997). When this diurnal fly was subjected to photoperiods in which LD >8:<16, two peaks of activity were always observed. The first occurred in the early photophase and the second in the late photophase. Under short photoperiods (where LD <8:>16), the activity peaks fused as the "window" of diurnal activity became smaller. For this species, it was suggested that the main, late-photophase activity peak was due to a *predictive* circadian oscillator, whereas the early-photophase peak was solely due to a *reactive* lights-on response. For the experiment described here using *N. virens*, the response is interpreted as being an adjustment to the new photoperiodic cue, or Zeitgeber, where the observed inactivity at the expected dawn is evidence for transient behavior prior to attaining a steady state in the following scotophases.

Coupling between the environmental Zeitgeber and the endogenous oscillator occurs through entrainment (Aschoff, 1965). The results illustrate that the process of entrainment of an activity rhythm in the autumn experiment depends on the photoperiodic regime. Subjecting animals to a photoperiod of LD 8:16 considerably reduced the strength of the rhythm. We believe that this represents the initial stages of the autumn feeding cessation, which is triggered when the animals pass through a critical photoperiod $LD_{crit} <12:>12$ (Last *et al.*, 1999), a characteristic physiological response at this time of year. This photoperiodically mediated change in activity provides an interesting result. At a time when the nights were becoming longer and hence, for these nocturnal animals, the "potential" for nocturnal feeding was gradually increasing, all activity became much reduced. It has been demonstrated elsewhere (Last and Olive, 1999) that under a photoperiod of LD 8:16, rates of somatic growth, segmentation, and regeneration all become much reduced and energy is channeled into future reproductive growth through changes in vitellogenesis or vitellin incorporation into the developing oocytes (Rees and Olive, 1999). We regard this as the initiation of a switch from somatic to reproductive growth. The photoperiodic transition therefore appears to trigger a change in physiological state (McNamara and Houston, 1996) from one in which essentially somatic growth processes predominate to one in which acquired resources are redeployed to sexual development. It seems at first surprising that this change in physiological state is not restricted to animals that will breed in the following spring, but occurs in all individuals regardless of age or state of maturity. A fitness model based on the life history of *N. virens* suggests, however, that when either or both net foraging risk and net foraging gain vary seasonally, a substantial fitness benefit accrues when all members of a mixed-age population respond to environmental signals and reduce foraging at times of maximum risk or minimum benefit (Olive *et al.*, 2000, 2001).

Parallels can be drawn with the Salmonidae, in which temperature and daylength alone do not dictate physiological changes. Bimodality in wild fish will separate animals destined to smolt in the following spring from those that are not (Thorpe *et al.*, 1980; Skilbrei, 1991), a mechanism that has long been known to be photoperiodically induced (Villarreal *et al.*, 1988). In *S. salar*, the advancement of smoltification through photoperiodic manipulation has been shown (Duston and Saunders, 1995) to largely reduce the effects of bimodality and has provided evidence that, in the salmonids at least, a coupling between threshold length, photoperiod (and the circadian clock), and time of year (the seasonal/circannual clock) determines bimodal segregation of individuals and maturational development.

Activity in the winter

The seasonal modulation of activity in *N. virens* was further exemplified when the same experiments were repeated in the winter. Whereas in the autumn there had been a nearly complete cessation of foraging activity under LD 8:16 (Figs. 1b and 3b), by the winter the amplitude of activity under LD 8:16 (Fig. 2b) had dramatically increased and was high compared to activity in the autumn or under LD 16:8 (Fig. 2a). In addition, the results of autocorrelation analysis showed no significant between-treatment difference in mean strength of rhythm between winter LD 8:16 and LD 16:8. We postulate that, for animals that have not reached some critical state of sexual maturity, the optimum strategy must change as the optimum time for breeding approaches. In these animals, renewed foraging increases the probability that sufficient energy reserves will be accrued for reproduction one year later. Since out-of-burrow foraging by *N. virens* is inevitably associated with predation risk, increased nocturnal activity at this time will maximize exploitation of the feeding time and minimize the risk of predation from diurnal predators. Animals that have reached a critical state of maturity become susceptible to a feedback response from the maturing gametes (Porchet and Cardon, 1976; Golding and Yuwono, 1994). This seasonally mediated change in activity under LD 8:16 occurred independently of photoperiodic treatment, which is suggestive of an endogenous seasonal (and possibly circannual) rhythm of activity or the operation of some long-term interval timer.

Interestingly, the mean peak activity during the first two nights occurred around midnight (Fig. 2b), which cannot readily be explained at this stage. We hypothesize that, as in the A98 experiment (Fig. 1b), activity onset may have been due to a "memory" of past photoperiodic regimes. The 7-day acclimatization period imposed on these animals under their new photoregime may not have been long enough to prevent transient activity before a new steady state had been reached. The observed "snapshot" of activity under the autumn and winter photoperiodic treatments may be influenced by the photoperiodic history of the animals. In view of these results, a long-term assay under constant photoperiods was deemed the only suitable method for establishing true endogenous behavior without transient manifestations. Under those conditions, any spontaneous changes in activity would imply the effects of a purely endogenous, rather than exogenous, response to an innate underlying seasonal oscillator or interval timer.

Long-term activity patterns in N. virens

The results shown in Figure 3b demonstrate that a long-term regulator of activity does indeed exist in the polychaete *N. virens.* This endogenous modulation is revealed under a constant LD 8:16 photoperiod, 3 months after the transition through the critical photoperiod LD_{crit} <12:>12 previously described by Last *et al.* (1999). The resurgence of activity under this photoperiod was spontaneous and, irrespective of the experimental photoperiod, occurred around the time of the winter solstice. Subjecting animals to a photoperiod of LD 16:8 will result in the negative masking (Aschoff, 1960) of any long-term endogenous oscillators.

Proactive anticipation of the spring equinox has been suggested previously for other nereid polychaetes (Olive and Garwood, 1983; Fong and Pearse, 1992a, b), and the results presented here provide further evidence for the expression of an overt endogenous seasonal clock in the Nereidae. Perturbations in the activity patterns of *N. virens* were observed under both photoperiodic treatments in March. Under LD 16:8, a late photophase peak was observed prior to the scotophase (Figs. 3a and 4a), and under LD 8:16 a marked drop in activity was observed in both the photophase and the scotophase (Figs. 3b and 4b). These perturbations occurred when the animals would, under natural photoperiods, pass through the spring critical photoperiod (where LD_{crit} >12:<12). The significance of these perturbations is not yet clear, but may indicate a change in the sensitivity of the endogenous pacemaker to the external photoperiod around the time of the spring equinox.

Seasonally overt changes in physiological state and behavior of this long-lived polychaete do not occur solely as a direct response to changes in proximate factors such as temperature and, particularly, daylength. We believe that while seasonally changing daylengths will actively drive changes in physiological state through photoperiodism at certain times of the year, at other times, photoperiod acts as a Zeitgeber to entrain an endogenous seasonal rhythm. Such a mechanism has also been implicated in another marine invertebrate, *Pisaster ochraceus.* In this sea star, gametogenesis can be shifted by maintaining the animals on a seasonally changing photoperiod regime out-of-phase with ambient photoperiods (Pearse *et al.*, 1986). Like our results, this finding is suggestive of an endogenous annual calendar.

To infer that these results are evidence for a circannual rhythm in *N. virens* would be premature since the observed response could have also been caused by an interval timer measuring a time period of approximately 90 days. Work is in progress to examine the endogenous modulation of activity patterns over the duration of years instead of months. We provide here evidence of a long-term modulation of activity in *N. virens* under fixed photoperiods. This mechanism modulates the response of individuals to the natural photoperiod according to real time and may be an essential adaptive component of the photoperiodically adjusted seasonal cycle of growth and reproduction.

Acknowledgments

This work was supported by the award of a NERC Industrial Case Studentship to K.S.L. and the DEMA thematic award GST/02/2164, NERC/T/S/200/00273 to P.J.W.O. Current funding to P.J.W.O. is from the NERC Environmental Genomics Programme NERC/T/S/2001/0273. We wish to acknowledge the additional financial support of the Industrial Sponsors Seabait Ltd., Ashington Village, Northumberland, NE63 9NW, for the supply of the experimental material as well as for allowing us to use procedures subject to patent. Thanks finally to the constructive comments of the anonymous referees and C. D. Derby.

Literature Cited

Aschoff, J. 1960. Exogenous and endogenous components in circadian rhythms. *Cold Spring Harbor Symp.* **25:** 11–28.

Aschoff, J. 1965. Circadian rhythms in man. *Science* **148:** 1427–1432.

Carter, C. G., D. J. Grove, and D. M. Carter. 1991. Trophic resource partitioning between two coexisting flatfish species off the north coast of Anglesey, North Wales. *Neth. J. Sea Res.* **23:** 325–335.

Dowse, H. B., and J. M. Ringo. 1989. The search for hidden periodicities in biological time-series revisited. *J. Theor. Biol.* **139:** 487–515.

Duston, J., and R. L. Saunders. 1995. Advancing smolting to autumn in age 0+ Atlantic salmon by photoperiod, and long-term performance in sea water. *Aquaculture* **135:** 295–309.

Dutilleul, P. 1995. Rhythms and autocorrelation analysis. *Biol. Rhythm Res.* **26:** 173–193.

Fong, P. P., and J. S. Pearse. 1992a. Evidence for a programmed circannual life cycle modulated by increasing daylengths in *Neanthes limnicola* (Polychaeta: Nereidae) from central California. *Biol. Bull.* **182:** 289–297.

Fong, P. P., and J. S. Pearse. 1992b. Photoperiodic regulation of parturition in the self fertilising viviparous polychaete *Neanthes limnicola* from central California. *Mar. Biol.* **112:** 81–89.

Garwood, P. R., and P. J. W. Olive. 1982. The influence of photoperiod on oocyte growth and its role in the control of the reproductive cycle of the polychaete *Harmothoe imbricata* (L.). *Int. J. Invertebr. Reprod.* **5:** 161–165.

Golding, D. W., and E. Yuwono. 1994. Latent capacities for gametogenic cycling in the semelparous invertebrate *Nereis*. *Proc. Natl. Acad. Sci. USA* **91:** 11777–11781.

Last, K. S. 2003. An actograph and its use in the study of foraging behaviour in the benthic polychaete, *Nereis virens* Sars. *J. Exp. Mar. Biol. Ecol.* **287:** 237–248.

Last, K. S., and P. J. W. Olive. 1999. Photoperiodic control of growth and segment proliferation by *Nereis (Neanthes) virens* Sars in relation to real time and state of maturity. *Mar. Biol.* **134:** 191–199.

Last, K. S., P. J. W. Olive, and A. Edwards. 1999. An actographic study of diel activity in the semelparous polychaete *Nereis (Neanthes) virens* Sars in relation to the annual cycle of growth. *Invertebr. Reprod. Dev.* **35:** 141–145.

Marcus, N. H. 1986. Population dynamics of marine copepods: the importance of photoperiodism. *Am. Zool.* **26:** 469–477.

McNamara, J. M., and A. I. Houston. 1996. State-dependent life-histories. *Nature* **380:** 215–221.

Nisimura, T., and H. Numata. 2001. Endogenous timing mechanism controlling the circannual pupation rhythm of the varied carpet beetle *Anthrenus verbasci*. *J. Comp. Physiol. A* **187:** 433–440.

Olive, P. J. W., and P. R. Garwood. 1983. The importance of long term endogenous rhythms in the maintenance of reproductive cycles of marine invertebrates—a reappraisal. *Int. J. Invertebr. Reprod.* **6:** 339–347.

Olive, P. J. W., J. Fletcher, S. Rees, and G. Desrosiers. 1997. Interactions of environmental temperature with photoperiod in determining age at maturity in a semelparous polychaete *Nereis (Neanthes) virens* Sars. *J. Therm. Biol.* **22:** 489–497.

Olive, P. J. W., C. Lewis, and V. Beardall. 2000. Fitness components of seasonal reproduction: an analysis using *Nereis virens* as a life history model. *Oceanol. Acta* **23:** 377–389.

Olive, P. J. W., C. Lewis, V. Beardall, K. Last, and M. G. Bentley. 2001. Fitness consequences of seasonal reproduction: experiments on the polychaete *Nereis virens* Sars. Pp. 321–341 in *Environment and Animal Development*, D. Atkinson and M. Thorndyke, eds. Bios Scientific Publishers, Oxford.

Palmer, J. D., B. G. Williams, and H. B. Dowse. 1994. The statistical analysis of tidal rhythms: tests of the relative effectiveness of five methods using model simulations and actual data. *Mar. Behav. Physiol.* **24:** 165–182.

Pearse, J. S., and D. J. Eernisse. 1982. Photoperiodic regulation of gametogenesis and gonadal growth in the sea star *Pisaster ochraceus*. *Mar. Biol.* **67:** 121–125.

Pearse, J. S., D. J. Eernisse, V. B. Pearse, and K. A. Beauchamp. 1986. Photoperiodic regulation of gametogenesis in sea stars, with evidence for an annual calendar independent of fixed daylength. *Am. Zool.* **26:** 417–431.

Porchet, M., and C. Cardon. 1976. The inhibitory feed-back mechanism coming from oocyte and acting on brain endocrine activity in Nereidae. *Gen. Comp. Endocrinol.* **30:** 378–390.

Randall, C. F., N. R. Bromage, J. Duston, and J. Symes. 1998. Photoperiod induced phase shifts of the endogenous clock controlling reproduction in the rainbow trout: a circannual phase response curve. *J. Reprod. Fertil.* **112:** 399–405.

Rees, S. W., and P. J. W. Olive. 1999. Photoperiodic changes influence the incorporation of vitellin yolk protein by oocytes of the semelparous polychaete *Nereis (Neanthes) virens*. *Comp. Biochem. Physiol. A* **123:** 213–220.

Skilbrei, O. T. 1991. Importance of threshold length and photoperiod for the development of bimodal length frequency distribution in Atlantic salmon (*Salmo salar*). *Can. J. Fish. Aquat. Sci.* **48:** 2163–2172.

Thijssen, R., A. J. Lever, and J. Lever. 1974. Food composition and feeding periodicity of 0-group plaice (*Pleuronectes platessa*) in the tidal area of a sandy beach. *Neth. J. Sea Res.* **8:** 369–377.

Thorpe, J. E., C. Talbot, and C. A. Villarreal. 1980. Bimodality in growth and smolting in Atlantic salmon, *Salmo salar* L. *Aquaculture* **28:** 123–132.

Villarreal, C. A., J. E. Thorpe, and M. S. Miles. 1988. Influence of photoperiod on growth changes in juvenile Atlantic salmon, *Salmo salar* L. *J. Fish Biol.* **33:** 15–30.

Watari, Y., and T. Arai. 1997. Effects of photoperiod and aging on locomotor activity rhythms in the onion fly, *Delia antiqua*. *J. Insect Physiol.* **43:** 567–576.

Wilson, W. H. 1991. The importance of epibenthic predation and ice disturbance in a Bay of Fundy mudflat. *Ophelia* **5:** 507–514.

Reference: *Biol. Bull.* **206:** 113–120. (April 2004)
© 2004 Marine Biological Laboratory

Adaptable Defense: A Nudibranch Mucus Inhibits Nematocyst Discharge and Changes With Prey Type

PAUL G. GREENWOOD*, KYLE GARRY, APRIL HUNTER, AND MIRANDA JENNINGS

Colby College, Department of Biology, 5732 Mayflower Hill, Waterville, Maine 04901

Abstract. Nudibranchs that feed on cnidarians must defend themselves from the prey's nematocysts or risk their own injury or death. While a nudibranch's mucus has been thought to protect the animal from nematocyst discharge, an inhibition of discharge by nudibranch mucus has never been shown. The current study investigated whether mucus from the aeolid nudibranch *Aeolidia papillosa* would inhibit nematocyst discharge from four species of sea anemone prey. Sea anemone tentacles were contacted with mucus-coated gelatin probes, and nematocyst discharge was quantified and compared with control probes of gelatin only. Mucus from *A. papillosa* inhibited the discharge of nematocysts from sea anemone tentacles. This inhibition was specifically limited to the anemone species on which the nudibranch had been feeding. When the prey species was changed, the mucus changed within 2 weeks to inhibit the nematocyst discharge of the new prey species. The nudibranchs apparently produce the inhibitory mucus rather than simply becoming coated in anemone mucus during feeding. Because of the intimate association between most aeolid nudibranchs and their prey, an adaptable mucus protection could have a significant impact on the behavior, distribution, and life history of the nudibranchs.

Introduction

All predators must overcome their prey's defenses to feed. In the case of nudibranchs that feed on cnidarians, the predator must defend itself from the prey's nematocysts or risk its own injury or death (Harris, 1973; Conklin and Mariscal, 1977). Nematocysts from non-prey cnidarians can kill the nudibranch (Grosvenor, 1903); even the prey species can be dangerous if the individual is large enough (Harris, 1973, 1986; Conklin and Mariscal, 1977). Defenses that might protect aeolids from nematocysts include behaviors that limit contact of the nudibranch with the prey (Grosvenor, 1903), morphological adaptations such as ellipsoid vacuolate cells of the epithelium (Graham, 1938; Porter and Rivera, 1980; Martin and Walther, 2003) or a cuticle that lines the mouth region of the nudibranch (Edmunds, 1966), and copious mucous secretions (Graham, 1938; Russell, 1942; Edmunds, 1966).

It has been hypothesized for over a century that the nudibranch's mucus serves as a protective barrier against nematocysts (Boutan, 1898). Grosvenor (1903) suggested that there might be some acclimatization to nematocysts as part of the mucous defense, because copious mucus was not enough to protect nudibranchs from different cnidarian species. However, Salvini-Plawen (1972) hypothesized that "hyper-viscous" mucous secretions would inhibit nematocyst discharge generally and that it would be unnecessary to adapt the protective nature of mucus to specific prey. Conklin and Mariscal (1977) noted that the aeolid nudibranch *Spurilla neapolitana* was apparently stung by its prey anemones during the first few minutes of feeding but the nudibranchs' behavior indicated that nematocyst discharge then ceased. These authors hypothesized that aeolids might produce or acquire (from the prey) a substance that prevented nematocyst discharge. Recently Mauch and Elliott (1997) found that mucus from the aeolid nudibranch *Aeolidia papillosa* caused fewer nematocysts to discharge from its potential prey, the sea anemone *Anthopleura elegantissima*, than mucus from other gastropods did. Mauch and Elliott (1997) hypothesized that the nudibranchs might adapt their mucus as protection from their cnidarian prey, but the nudibranch mucus was tested on only one species of cnidarian.

While a few nudibranchs are highly specialized and feed exclusively on one prey species, most nudibranch species

Received 2 July 2002; accepted 21 January 2004.

* To whom correspondence should be addressed. E-mail: pggreenw@colby.edu

can feed on several different prey species (Thompson, 1976; Todd *et al.*, 2001). Monophagous species might have defensive mucus that works well against the nematocysts of a single prey species, but the more generalist feeders need an effective defense against a number of cnidarian species (with different nematocyst types). Such nudibranchs might require defensive mucus that changes properties depending upon which prey is being consumed.

The current study investigated whether mucus from the aeolid nudibranch *Aeolidia papillosa* inhibited nematocyst discharge from different sea anemone species, and whether the inhibitory nature of the mucus changed when the prey species was changed. Individuals of *A. papillosa* feed almost exclusively on sea anemones (Hall and Todd, 1986). In its New England subtidal habitat, *A. papillosa* is frequently found among populations of the sea anemone *Metridium senile,* but is also found associated with a variety of other sea anemone species (Harris, 1973; Reidy, 1996). Individuals of *A. papillosa* have been induced to change prey species in the laboratory (Hall *et al.,* 1982; Hall and Todd, 1984, 1986), but in the field a single prey species may dominate a large area. Concentrated prey distribution and low nudibranch mobility means that individual nudibranchs might spend most of their lives closely associated with just one prey species (Harris, 1973, 1987; Todd, 1983). Because of this intimate association between *A. papillosa* and its prey, protection from the prey's nematocysts has a significant impact on the behavior, distribution, and life history of the nudibranch.

We used mucus-coated gelatin probes in a highly reproducible method (Watson and Hudson, 1994) to investigate the effects of *A. papillosa* mucus on nematocyst discharge. When gelatin probes are touched to sea anemone tentacles, nematocysts that discharge into the gelatin remain attached to the probe and are easily counted (Watson and Hessinger, 1989; Watson *et al.*, 1999). In this study, mucus-coated gelatin probes were used to mimic the contact of a nudibranch to the sea anemones. We also probed sea anemones in the presence of N-acetylneuraminic acid (NANA). NANA, which mimics the complex molecules containing N-acetylated sugars commonly found on the sea anemones' normal prey (Thorington and Hessinger, 1988), has been found to increase the sensitivity of sea anemone nematocytes to mechanical stimulation (Thorington and Hessinger, 1988, 1990, 1998; Watson and Hessinger, 1994). With NANA, we can therefore determine whether nudibranch mucus actually inhibits nematocyst discharge or simply provides no stimulus for discharge.

Materials and Methods

Animal collection and maintenance

Individuals of the nudibranch *Aeolidia papillosa* and the sea anemone *Metridium senile* were collected from a floating commercial fishing dock in Portsmouth, New Hampshire. Individuals of *A. papillosa* and the sea anemones *Urticina felina* and *Aulactinia stella* were collected midway through the littoral zone on bedrock at west Quoddy Head in Lubec, Maine (courtesy of C. Sisson). Twelve individuals of *A. papillosa,* living among individuals of the sea anemone *Anthopleura elegantissima,* were collected from the low intertidal zone on the coast of California (supplied by Pacific Biomarine Supply, Venice, CA). Individuals of *A. elegantissima* were collected from the low intertidal zone of San Juan Island, Washington (courtesy of D. Duggins). All animals were kept in refrigerated aquaria with recirculating and refiltered seawater (11 °C, 31‰ salinity, pH 8.2) collected at the Darling Laboratory, University of Maine, Walpole, Maine. Anemones were kept in separate plastic or glass containers within the aquaria, and the nudibranchs were placed in separate acrylic plastic containers, segregated according to the sea anemone species on which they were feeding. Sea anemones were fed frozen brine shrimp every 2 days, and the nudibranchs were fed sea anemones *ad libidum.* The sea anemones that were used as prey all had pedal disk diameters less than 3 cm, and the nudibranchs ranged in length from 1 cm to 7 cm. Individuals of *M. senile* were held for no more than 2 months before being replaced with other animals; the other species of sea anemones were held for less than a month.

Control probes, mucus-coated probes, and general probing of sea anemone tentacles

We used gelatin probes to quantify nematocyst discharge from tentacles of sea anemones. Each probe was made by coating one end of a 6-cm length of monofilament fishing line (Stren, 6-lb-test or 17-lb-test) with 25% (weight/volume) gelatin in E-pure deionized water (modified slightly from Watson and Hudson, 1994). Occasionally, the gelatin did not adhere well to the probe, and such probes were discarded. The gelatin adhered better to the 17-lb-test line than to the 6-lb-test line, so the number of probes discarded was smaller when the heavier line was used, as it indeed was, in later experiments. Probes that were coated with only gelatin served as controls.

To prepare an experimental mucus-coated probe, a nudibranch was removed from the water and a gelatin probe was gently wiped across its dorsal surface (from anterior to posterior) four times. Three mucus-coated probes were made from each nudibranch. Anemones that had not been fed for between 24 and 36 hs were placed into separate glass dishes that contained a probing solution of either filtered seawater alone, or filtered seawater and NANA. Ten minutes after the anemones were placed into the probing solution, each dish was placed under an Olympus SC30 stereomicroscope, and probing began with the edge of the probe tip being lightly touched to one tentacle about 5 mm proximal to the tentacle tip. Three control probes and three experimental probes, all prepared from the same nudibranch, were used to probe each anemone. Used probes were fixed in 2.5% glutaraldehyde in filtered seawater for at least 30 s and then placed into 3 drops of deionized water on a microscope slide. Individual nematocysts that had discharged into the gelatin were counted, using an Olympus CK2 inverted phase contrast microscope equipped with a 40× objective lens. In early experiments with probes made from 6-lb-test monofilament line, we counted nematocyst capsules from at least three fields of view, and the mean was calculated for each probe. In later experiments, when we used probes made from 17-lb-test line, the nematocyst capsules from one central field of view were counted. Using these techniques, between 75% and 100% of the discharged nematocysts on each probe were counted, and both types of probes yielded highly reproducible results.

Does a nudibranch's mucus inhibit the nematocyst discharge from the tentacles of its prey species?

Probes were coated with mucus from 12 individuals of *Aeolidia papillosa* of mixed sizes that had been feeding on the sea anemone *Metridium senile* and with mucus from 6 individuals of *A. papillosa* of mixed sizes that had been feeding on the sea anemone *Urticina felina.* These mucus-coated probes were then used to probe feeding tentacles from the sea anemones *M. senile, U. felina,* and *Aulactinia stella.* In each experiment, one anemone was always tested with three control probes and then, immediately afterwards, with three experimental (mucus-coated) probes; the experimental probes were coated with mucus from an individual nudibranch. The mean number of discharged nematocysts in the three probes was used to calculate a grand mean of nematocyst discharge in response to mucus from each nudibranch. These grand means were tested for normality and equal variances and then analyzed using Student's t tests (or the Mann-Whitney U test when variances were unequal) to compare nematocyst discharge into mucus-coated probes with discharge into control probes for each species. To minimize the effects of captivity on nematocyst discharge, each species of anemone was tested within 2 weeks of its collection.

If the prey species is changed, will the effect of the nudibranch mucus on nematocyst discharge also change?

Seven specimens of *A. papillosa* were collected from several New England localities and were fed *U. felina* for 16 days in the laboratory. During that period, mucus-coated probes were used to test nematocyst discharge from the tentacles of *U. felina* and *M. senile.* The nudibranchs' prey was then switched from *U. felina* to *M. senile* and, over a 2-week interval, mucus-coated probes were used periodically to test nematocyst discharge from both sea anemone species. Because the baseline number of nematocysts differed between the two sea anemone species, these data were converted to relative values, where a relative value of 1.0 represents the average number of nematocysts discharged into control probes. Data collected from mucus-coated probes for each day were converted to an average relative discharge based on controls for that day from the same anemones. Results from tests on each sea anemone species were analyzed by ANOVA and with Scheffé's test for pairwise comparisons.

If a second prey species is offered, will the effect of the nudibranch mucus on nematocyst discharge change?

Four individuals of *A. papillosa* were fed the sea anemone *M. senile* for 21 days. Mucus-coated probes were used to test nematocyst discharge from feeding tentacles of *M. senile* and the sea anemone *Anthopleura elegantissima.* The nudibranchs were then offered both *M. senile* and *Anthopleura elegantissima. Anthopleura elegantissima* is not found on the coast of New England, so the experimental nudibranchs could not have encountered this prey species before. Fourteen days later, mucus-coated probes were used to test nematocyst discharge from the tentacles of both species of prey anemone. Data were converted to relative discharge values as described for the previous experiment and analyzed using Student's t tests.

Does the nudibranch produce its own inhibitory mucus or simply become covered in the prey's mucus?

Any inhibitory effect of the nudibranch's mucus coating could be a result of the nudibranch being coated in the mucus of the prey species during feeding. To test this possibility, we compared the inhibitory effectiveness of mucus removed from a particular region of a nudibranch with mucus removed from that same region 45 min after wiping that area clean. Probes were coated with mucus from eight individuals of *A. papillosa* of mixed sizes that had been feeding on the sea anemone *M. senile.* The probes were coated with mucus from the dorsal surface of the nudibranch immediately behind the heart. Each nudibranch was then transferred to fresh filtered seawater. Sterile cotton swabs were used to wipe the mucus from the dorsal surface of the nudibranch and from the surrounding cerata. Six additional swabs were used to wipe the nudibranch a total of seven times, and the nudibranch was again transferred to fresh filtered seawater. After the nudibranch was allowed to recover from this treatment for 45 min, additional probes were coated with mucus from its dorsal surface immediately behind the heart. The mucus-coated probes were then all used to probe feeding tentacles of *M. senile.* Three probes were coated with mucus from each nudibranch for each treatment (unswabbed and swabbed). Counting of all probes was done blind. The mean number of discharged nemato-

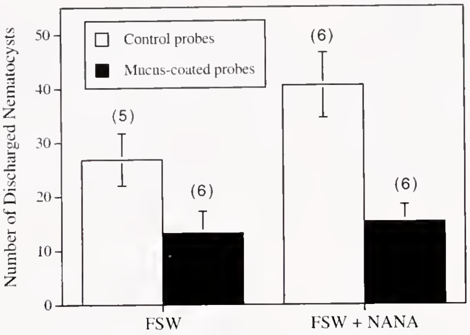

Figure 1. Number of nematocysts discharged into control probes or into probes coated with mucus from individuals of *Aeolidia papillosa* that had been feeding on *Metridium senile*. Mucus-coated probes were used to probe tentacles of the sea anemone *M. senile* in both filtered seawater (FSW) and FSW containing 10^{-7} *M* N-acetylneuraminic acid (FSW + NANA), and compared against control probes of gelatin only. The numbers in parentheses are the numbers of anemones used (control probes) or the numbers of nudibranchs used (mucus-coated probes) per test.

cysts into mucus-coated probes from unswabbed nudibranchs was compared to nematocyst discharge into mucus-coated probes from swabbed nudibranchs and into control probes. Analysis was done by ANOVA and with Scheffé's test for pairwise comparisons.

We also investigated whether the mucus of *M. senile* individuals inhibited discharge from other individuals of *M. senile* held in separate containers. Individual sea anemones were transferred to filtered seawater, allowed to recover for 10 min, transferred to fresh filtered seawater again, allowed to recover for 10 min, and finally transferred to a dry, clean glass dish. The sea anemone secreted mucus for 10 min and was removed from the dish. The mucus was removed from the dish and stored in sterile microcentrifuge tubes. Gelatin probes were placed into the mucus for 2 min and used to probe different individuals of *M. senile*. Three probes were coated with mucus from each of four anemones. The mean number of discharged nematocysts in the mucus-coated probes was compared to that number in control probes with no mucus. Data were analyzed using Student's *t* tests as described above.

Results

Does a nudibranch's mucus inhibit the nematocyst discharge from the tentacles of its prey species?

When tentacles of the sea anemone *Metridium senile* were probed with control probes in seawater, a baseline discharge response was observed (Fig. 1). The nematocysts that discharged into the gelatin were mostly basitrichous isorhizas along with some microbasic p-mastigophores. Gelatin probes coated with mucus from the nudibranch *Aeolidia papillosa* that had been feeding on *M. senile* elicited 51% fewer nematocysts to discharge from *M. senile* than control probes did (Student's *t* test, $t_9 = 5.1$, $P = 0.0006$) (Fig. 1). When probing was done in seawater containing 10^{-7} *M* NANA, the number of nematocysts that discharged into mucus-coated probes was almost 65% less than the number that discharged into control probes (Student's *t* test, $t_{10} = 9.1$, $P < 0.0001$) (Fig. 1), but the mean number of discharges into control probes was higher than when NANA was omitted (Student's *t* test, $t_9 = 4.1$, $P < 0.003$). For each anemone species, probing in 10^{-7} *M* NANA elicited a greater number of discharged nematocysts than probing in seawater alone (Fig. 2). Statistical results were as follows: for *M. senile*, Student's *t* test, $t_9 = 4.1$, $P < 0.003$; for *Aulactinia stella*, Student's *t* test, $t_2 = 4.5$, $P < 0.05$; for *Anthopleura elegantissima*, Student's *t* test, $t_4 = 5.0$, $P = 0.008$. Because it increased the response, 10^{-7} *M* NANA was used for all subsequent experiments.

When probes coated with mucus from *A. papillosa* that had been feeding on *M. senile* were used to probe the sea anemones *Urticina felina* and *Aulactinia stella*, there was a small but nonsignificant increase in nematocyst discharge over controls (for *U. felina*, Student's *t* test, $t_{10} = 0.394$, $P = 0.70$; for *Aulactinia stella*, Student's *t* test, $t_{26} = 0.76$, $P = 0.46$) (Fig. 3). As before, significantly fewer nematocysts discharged into mucus-coated probes from tentacles of *M. senile* than into control probes (Student's *t* test, $t_8 = 9.0$, $P < 0.0001$) (Fig. 3). Nematocysts from *U. felina* were mostly microbasic p-mastigophores and some basitrichous isorhizas. Nematocysts from *Aulactinia stella* were basitrichous isorhizas and microbasic p-mastigophores in about equal numbers. The mucus effectiveness was sim-

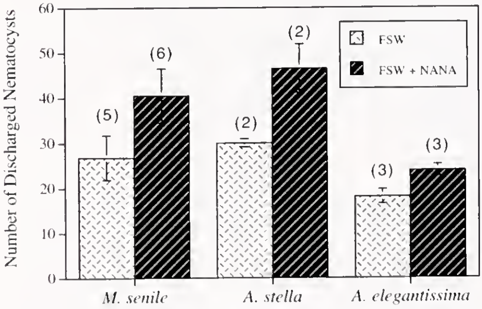

Figure 2. Number of nematocysts discharged into control probes. Tentacles of the sea anemones *Metridium senile*, *Aulactinia stella*, and *Anthopleura elegantissima* were probed in filtered seawater (FSW) and tentacles of other individuals of each species were probed in FSW containing 10^{-7} *M* N-acetylneuraminic acid (FSW + NANA). The numbers in parentheses are the numbers of anemones used per test.

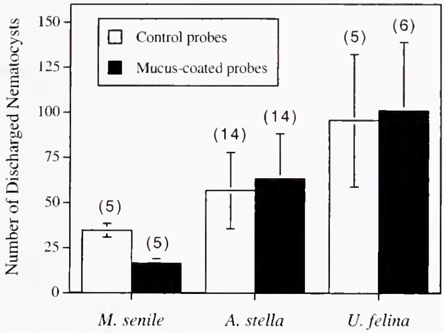

Figure 3. Number of nematocysts discharged into control probes or into probes coated with mucus from individuals of *Aeolidia papillosa* that had been feeding on *Metridium senile* (±SD). Mucus-coated probes were used to probe tentacles of the sea anemones *M. senile, Aulactinia stella,* and *Urticina felina* (in 10^{-7} *M* N-acetylneuraminic acid) and were compared against control probes of gelatin only. The numbers in parentheses are the numbers of anemones used (control probes) or the numbers of nudibranchs used (mucus-coated probes) per test.

ilar among individual nudibranchs regardless of their size (ANOVA, $F_{6,48} = 0.76$, $P = 0.61$).

When gelatin probes coated with mucus from individuals of *A. papillosa* that had been feeding upon *U. felina* were tested on the tentacles of *U. felina,* nematocyst discharge was 67% less than discharge into the control probes (Mann-Whitney *U* test, $U_{4,6} = 24$, $P = 0.01$) (Fig. 4). When probes coated with mucus from *A. papillosa* that had been feeding on *U. felina* were used to probe the sea anemones *M. senile* and *Aulactinia stella,* nematocyst discharge was no different than in controls (for *M. senile,* Student's *t* test, $t_6 = 1.10$, $P = 0.31$; for *Aulactinia stella,* Student's *t* test, $t_6 = 1.96$, $P = 0.098$) (Fig. 4).

If the prey species is changed, will the effect of the nudibranch mucus on nematocyst discharge also change?

Seven individuals of *A. papillosa* that had been collected from several different New England localities were fed *U. felina* for 16 days in the laboratory. As before, nematocyst discharge into mucus-coated probes was 50% less than nematocyst discharge into control probes for *U. felina,* but not for *M. senile* (Fig. 5). The nudibranchs' prey was then switched from *U. felina* to *M. senile,* and over a period of 2 weeks, the mucus from the nudibranchs was tested periodically against both sea anemone species. Over the course of the experiment, the number of nematocysts that discharged into mucus-coated probes increased when *M. senile* was probed (ANOVA, $F_{4,21} = 8.20$, $P = 0.0004$) and decreased when *U. felina* was probed (ANOVA, $F_{3,19} = 23.12$, $P < 0.0001$). Within 10 days after the prey switch, touching *M. senile* tentacles with mucus-coated probes elicited the discharge of 75% fewer nematocysts than control probes did (Scheffé's test, $P = 0.0067$) (Fig. 5). By the end of the experiment, touching *U. felina* tentacles with mucus-coated probes again resulted in a small but nonsignificant

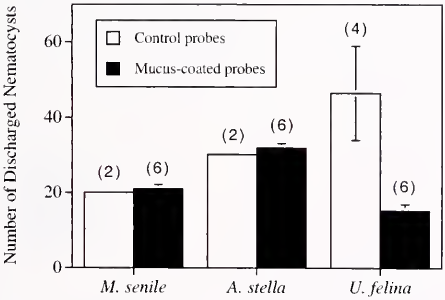

Figure 4. Number of nematocysts discharged into control probes or into probes coated with mucus from individuals of *Aeolidia papillosa* that had been feeding on *Urticina felina* (±SD). Mucus-coated probes were used to probe tentacles of the sea anemones *Metridium senile, Aulactinia stella,* and *U. felina* (in 10^{-7} *M* N-acetylneuraminic acid) and were compared against control probes of gelatin only. The numbers in parentheses are the numbers of anemones used (control probes) or the numbers of nudibranchs used (mucus-coated probes) per test.

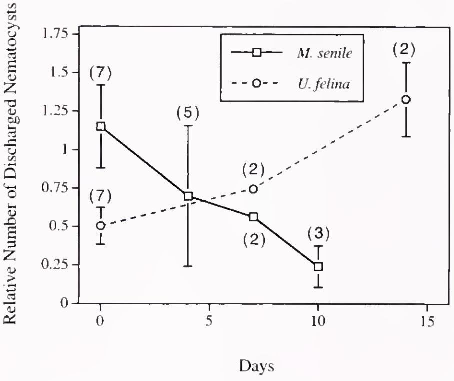

Figure 5. The effect of *Aeolidia papillosa* mucus on the relative number of discharged nematocysts following prey switch from the sea anemone *Urticina felina* to the sea anemone *Metridium senile* (±SD). Mucus-coated probes were used to probe tentacles of the sea anemones *U. felina* and *M. senile* (in 10^{-7} *M* N-acetylneuraminic acid), and were compared against controls for each species for a period of 2 weeks. A relative value of 1.0 corresponds to the number of nematocysts discharged into control probes on Day 0 for each sea anemone species. Data obtained from mucus-coated probes for each day were normalized against controls for that day and for each species of sea anemone. The numbers in parentheses are the numbers of nudibranchs used per test.

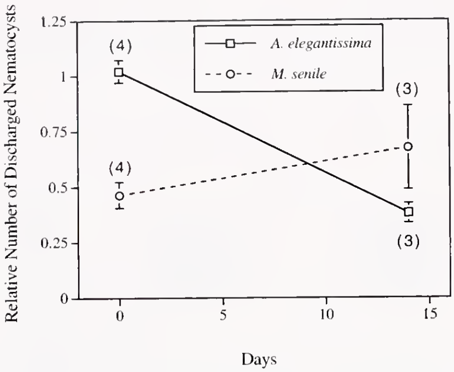

Figure 6. The effect of *Aeolidia papillosa* mucus on the relative number of discharged nematocysts following prey switch from the sea anemone *Metridium senile* only to *both M. senile* and the sea anemone *Anthopleura elegantissima*. Mucus-coated probes were used to probe tentacles of the sea anemones *M. senile* and *A. elegantissima* (in 10^{-7} *M* N-acetylneuraminic acid), and were compared against controls for each species after 2 weeks. A relative value of 1.0 corresponds to the number of nematocysts discharged into control probes on Day 0 for each sea anemone species. Data obtained from mucus-coated probes for each day were normalized against controls for that day and for each species of sea anemone. The numbers in parentheses are the numbers of nudibranchs used per test.

increase in nematocyst discharge over that into control probes (Scheffé's test, $P = 0.072$) (Fig. 5).

If a second prey species is offered, will the effect of the nudibranch mucus on nematocyst discharge change?

Four individuals of *A. papillosa* were fed *M. senile* for at least 21 days, and tentacles of both *M. senile* and *Anthopleura elegantissima* were tested with mucus-coated probes. *M. senile* nematocyst discharge was 56% lower into mucus-coated probes than into control probes (Student's *t* test, $t_6 = 9.6$, $P < 0.0001$); *Anthopleura elegantissima* nematocyst discharge into mucus-coated probes was not different from discharge into control probes (Student's *t* test, $t_6 = 0.545$, $P = 0.61$) (Fig. 6). Nematocysts from *Anthopleura elegantissima* were all basitrichous isorhizas. The nudibranchs were then offered both *M. senile* and *Anthopleura elegantissima*. After the nudibranchs had been feeding on both prey species for 14 days, testing with mucus-coated probes showed nematocyst discharges 34% lower than control probes for *M. senile* (Student's *t* test, $t_4 = 2.78$, $P = 0.05$) and 64% lower than control probes for *Anthopleura elegantissima* (Student's *t* test, $t_4 = 17.06$, $P < 0.0001$) (Fig. 6).

Does the nudibranch produce its own inhibitory mucus or simply become covered in the prey's mucus?

Mucus was wiped away from the dorsal surface of eight individuals of *A. papillosa* that had been feeding on the sea anemone *M. senile*. Forty-five min later, gelatin probes coated with new mucus from those same nudibranchs were used to probe tentacles of *M. senile*. Nematocyst discharge into those probes was no different from nematocyst discharge into probes coated with mucus from the same eight individuals of *A. papillosa* before wiping the mucus away (Scheffé's test, $P = 0.60$) (Fig. 7). Nematocyst discharge into both groups of mucus-coated probes was well under half the number that discharged into control probes (ANOVA, $F_{2,16} = 10.54$, $P = 0.001$) (Fig. 7).

When probes coated with *M. senile* mucus were used to probe tentacles of other individuals of *M. senile*, nematocysts discharged into the probes in numbers no different than into control probes (Student's *t* test, $t_6 = 1.14$, $P = 0.30$) (Fig. 8).

Discussion

The present study shows, for the first time, that the mucus from a nudibranch specifically inhibits the discharge of nematocysts from sea anemone tentacles. This inhibition of nematocyst discharge is limited to the anemone species on which the nudibranch has been feeding. Moreover, the nudibranch mucus changes to inhibit the nematocyst discharge of a different sea anemone species if the nudibranch

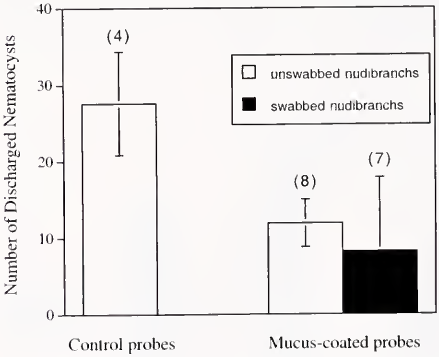

Figure 7. The number of nematocysts discharged into control probes or into probes coated with mucus from individuals of *Aeolidia papillosa* that had been feeding on *Metridium senile*. Probing of *M. senile* tentacles was done in 10^{-7} *M* N-acetylneuraminic acid. Mucus-coated probes were prepared both before the original mucous coating was removed from the nudibranch (unswabbed nudibranchs) and 45 min after mucus removal (swabbed nudibranchs). The numbers in parentheses are the numbers of anemones used (control probes) or the numbers of nudibranchs used (mucus-coated probes) per test.

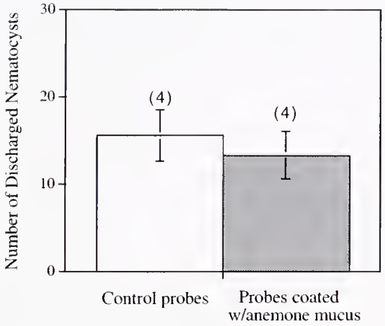

Figure 8. The number of nematocysts discharged into control probes or into probes coated with mucus from individuals of the sea anemone *Metridium senile*. Probing of *M. senile* tentacles was done in 10^{-7} *M* N-acetylneuraminic acid. The numbers in parentheses are the numbers of anemones used per test.

begins to feed on that new species. If nudibranchs are fed two different species of sea anemone, their mucus inhibits nematocyst discharge from both prey species. Nudibranchs produce their own inhibitory mucus and do not simply mimic sea anemones by becoming covered with anemone mucus during feeding.

Mucus from nudibranchs that had been fed the sea anemone *Metridium senile* greatly inhibited nematocyst discharge from *M. senile*, but not from *Urticina felina* or *Aulactinia stella* (Fig. 3). Likewise, mucus from nudibranchs that had been fed *U. felina* inhibited nematocyst discharge from *U. felina*, but not from *M. senile* or *Aulactinia stella* (Fig. 4). Within 10 days after the prey of *A. papillosa* was changed from *U. felina* to *M. senile*, the mucus of *A. papillosa* no longer inhibited nematocyst discharge from *U. felina*, but did inhibit nematocyst discharge from *M. senile* (Fig. 5). In another experiment, *A. papillosa* was fed both *M. senile* and *Anthopleura elegantissima*. After 2 weeks, the mucus of the nudibranch inhibited nematocyst discharge from both *M. senile* and *Anthopleura elegantissima* (Fig. 6). Overall, *A. papillosa* mucus reduced nematocyst discharge from all prey anemones by 60% below control levels (60.3% ± 4.1%).

Mucus from nudibranchs that had been freshly swabbed of their previous mucous coating inhibited nematocyst discharge from anemone prey (Fig. 7), indicating that the nudibranchs do not simply become covered with anemone mucus. Mucus from nudibranchs held in the same aquarium with sea anemones did not inhibit nematocyst discharge from that species. This suggests that the nudibranch mucus is altered only after feeding. Whether the mucus of *A. papillosa* is altered by the nudibranch itself or if compounds acquired from the prey are subsequently incorporated into the mucus is not yet known. Nudibranchs acquire numerous prey compounds and use them for their own defense from predators (Avila *et al.*, 1991; McClintock *et al.*, 1994), but some nudibranchs also synthesize their own chemical defenses (Cimino *et al.*, 1983; Faulkner, 1992). Because sea anemones do not sting themselves or clonemates, there might be compounds that prevent nematocyst discharge on or within the sea anemone (Pantin, 1942; Ertman and Davenport, 1981), but so far such compounds have not been identified in any cnidarians. In addition, we found in this study that mucus from individuals of one color morph of *M. senile* did not inhibit nematocyst discharge from another color morph of *M. senile* (Fig. 8), indicating that a prey species' mucus is not necessarily inhibitory to other members of that species. Therefore, the nudibranchs are not relying solely on compounds acquired from the prey's mucus. Aeolid nudibranchs secrete mucus and other secretions from gland cells found in various locations on their bodies (Edmunds, 1966). Histochemical evidence suggests that most species (including *A. papillosa*) have acidic mucopolysaccharides as at least part of the mucus (Edmunds, 1966; Porter and Rivera, 1983), but other components, which are not well characterized, may be secreted from gland cells and mix with the mucus on the surface of the nudibranch (Edmunds, 1966). The mucous secretion we used to coat the gelatin probes probably includes components from any or all of these gland cells.

Most of our studies were done in the presence of N-acetylneuraminic acid (NANA), which increased the baseline number of nematocysts that discharged into the gelatin probes (Fig. 2). Because the nudibranch mucus inhibited nematocyst discharge in the presence of NANA (Fig. 1), the mucus must either reduce the mechanical stimulation caused by the nudibranch while feeding or inhibit the signal pathway leading to nematocyst discharge. When nudibranch mucus was tested against non-prey sea anemones, nematocyst discharge actually increased by a modest, but consistent, number over controls (11.8% ± 4.5%). Therefore nudibranch mucus may actually promote nematocyst discharge in species that are not the current prey. *Aeolidia papillosa* shows a strong preference for its most recent prey species (Hall *et al.*, 1982). Because the mucus of *A. papillosa* inhibits nematocyst discharge from current prey species but not from other potential prey species, one might expect the current prey species to remain the preferred prey of the nudibranch.

Acknowledgments

We thank J. Elliott, C. Sisson, W. H. Wilson, and three anonymous reviewers for many helpful comments on the manuscript and for suggestions of additional experiments. This research was partially supported by the Merck Charitable Foundation and by NSF Grant STI-9602639.

Literature Cited

Avila, C., G. Cimino, A. Fontana, M. Gavagnin, J. Ortea, and E. Trivellone. 1991. Defensive strategy of two *Hypselodoris* nudibranchs from Italian and Spanish coasts. *J. Chem. Ecol.* **17:** 625–636.

Boutan, L. 1898. Moeurs de l'*Eolis papillosa* Linne. *Arch. Zool. Exp. Gen.* **6:** 37–42.

Cimino, G., S. De Rosa, S. De Stefano, G. Sodano, and G. Villani. 1983. Dorid nudibranch elaborates its own chemical defense. *Science* **219:** 1237–1238.

Conklin, E. J., and R. N. Mariscal. 1977. Feeding behavior, ceras structure, and nematocyst storage in the aeolid nudibranch, *Spurilla neapolitana* (Mollusca). *Bull. Mar. Sci.* **27:** 658–667.

Edmunds, M. 1966. Protective mechanisms in the Eolidacea (Mollusca: Nudibranchia). *J. Linn. Soc. Lond. Zool.* **46:** 27–71.

Ertman, S. C., and D. Davenport. 1981. Tentacular nematocyte discharge and "self-recognition" in *Anthopleura elegantissima* Brandt. *Biol. Bull.* **161:** 366–370.

Faulkner, D. J. 1992. Chemical defenses of marine molluscs. Pp. 119–163 in *Ecological Roles of Marine Natural Products,* V. J. Paul, ed. Constock Publishing, Ithaca, NY.

Graham, A. 1938. The structure and function of the alimentary canal of aeolid molluscs, with a discussion on their nematocysts. *Trans. R. Soc. Edinb.* **59:** 267–307.

Grosvenor, G. H. 1903. On the nematocysts of aeolids. *Proc. R. Soc. Lond.* **72:** 462–486.

Hall, S. J., and C. D. Todd. 1984. Prey-species selection by the anemone predator *Aeolidia papillosa* (L.): the influence of ingestive conditioning and previous dietary history, and a test for switching behaviour. *J. Exp. Mar. Biol. Ecol.* **82:** 11–33.

Hall, S. J., and C. D. Todd. 1986. Growth and reproduction in the aeolid nudibranch *Aeolidia papillosa* (L). *J. Molluscan Stud.* **52:** 193–205.

Hall, S. J., C. D. Todd, and A. D. Gordon. 1982. The influence of ingestive conditioning on the prey species selection in *Aeolidia papillosa* (Mollusca: Nudibranchia). *J. Anim. Ecol.* **51:** 907–921.

Harris, L. G. 1973. Nudibranch associations. Pp. 213–315 in *Current Topics in Comparative Pathobiology,* Vol. 2, T. C. Cheng, ed. Academic Press, New York.

Harris, L. G. 1986. Size-selective predation in a sea anemone, nudibranch, and fish food chain. *Veliger* **29:** 38–47.

Harris, L. G. 1987. Aeolid nudibranchs as predators and prey. *Am. Malacol. Bull.* **5:** 287–292.

Martin, R., and P. Walther. 2003. Protective mechanisms against the action of nematocysts in the epidermis of *Cratena peregrina* and *Flabellina affinis* (Gastropoda, Nudibranchia). *Zoomorphology* **122:** 25–35.

Mauch, S., and J. Elliott. 1997. Protection of the nudibranch *Aeolidia papillosa* from nematocyst discharge of the sea anemone *Anthopleura elegantissima. Veliger* **40:** 148–151.

McClintock, J. B., B. J. Baker, M. Slattery, J. N. Heine, P. J. Bryan, W. Yoshida, M. T. Davies-Coleman, and D. J. Faulkner. 1994. Chemical defense of the common Antarctic shallow water nudibranch *Tritoniella belli* Eliot (Mollusca: Tritonidae) and its prey, *Clavularia frankliniana* Rouel (Cnidaria: Octocorallia). *J. Chem. Ecol.* **20:** 3361–3372.

Pantin, C. F. A. 1942. The excitation of nematocysts. *J. Exp. Biol.* **19:** 294–310.

Porter, K. J., and E. R. Rivera. 1980. The Golgi apparatus in epidermal mucoid and ellipsoid-vacuolate cells of *Aeolidia papillosa* and *Coryphella rufibranchialis* (Nudibranchia). *Protoplasma* **102:** 217–233.

Porter, K. J., and E. R. Rivera. 1983. Light and electron microscopic cytochemistry of the epidermal mucoid cells of *Aeolidia papillosa* and *Coryphella rufibranchialis* (Mollusca, Nudibranchia). *Protoplasma* **114:** 14–22.

Reidy, S. E. 1996. A comparison of settlement, growth and mortality in the nudibranch *Aeolidia papillosa* when offered the anemones *Metridium senile* and *Urticina crassicornis. Am. Zool.* **36:** 106A.

Russell, H. D. 1942. Observations on the feeding of *Aeolidia papillosa* L., with notes on the hatching of the veligers of *Cuthona amoena* A. and H. *Nautilus* **55:** 80–82.

Salvini-Plawen, L. v. 1972. Cnidaria as food sources for marine invertebrates. *Cah. Biol. Mar.* **13:** 385–400.

Thompson, T. E. 1976. *Biology of Opisthobranch Molluscs,* Vol. I. Ray Society, London. 207 pp.

Thorington, G. U., and D. A. Hessinger. 1988. Control of cnida discharge: I. Evidence for two classes of chemoreceptor. *Biol. Bull.* **174:** 163–171.

Thorington, G. U., and D. A. Hessinger. 1990. Control of cnida discharge: III. Spirocysts are regulated by three classes of chemoreceptors. *Biol. Bull.* **178:** 74–83.

Thorington, G. U., and D. A. Hessinger. 1998. Efferent mechanisms of discharging cnidae: II. A nematocyst release response in the sea anemone tentacle. *Biol. Bull.* **195:** 145–155.

Todd, C. D. 1983. Reproductive and trophic ecology of nudibranch molluscs. Pp. 225–259 in *The Mollusca, Vol. 6, Ecology,* W. D. Russell-Hunter, ed. Academic Press, Orlando, FL.

Todd, C. D., W. J. Lambert, and J. Davies. 2001. Some perspectives on the biology and ecology of nudibranch molluscs: generalisations and variations on the theme that prove the rule. *Boll. Malacol.* **37:** 105–120.

Watson, G. M., and D. A. Hessinger. 1989. Cnidocyte mechanoreceptors are tuned to the movements of swimming prey by chemoreceptors. *Science* **243:** 1589–1591.

Watson, G. M., and D. A. Hessinger. 1994. Antagonistic frequency tuning of hair bundles by different chemoreceptors regulates nematocyst discharge. *J. Exp. Biol.* **187:** 57–73.

Watson, G. M., and R. R. Hudson. 1994. Frequency and amplitude tuning of nematocyst discharge by proline. *J. Exp. Zool.* **268:** 177–185.

Watson, G. M., S. Venable, R. R. Hudson, and J. J. Repass. 1999. ATP enhances repair of hair bundles in sea anemones. *Hear. Res.* **136:** 1–12.

THE BIOLOGICAL BULLETIN

2004 Subscription Rates
Volumes 206-207

***Paid Subscriptions include both print and electronic subscriptions at:** www.biolbull.org

	Institutional*	**Individual***
One year subscription (6 issues - 2 volumes)	$325.00	$120.00
Single volume (3 issues)	$165.00	$70.00
Single Issues	$ 75.00	$25.00

*Surface delivery included in above prices.
For prompt delivery, we encourage subscribers outside the U.S. to request airmail service.

Airmail Delivery Charge

U.S. and Canada:	$ 45.00
Mexico:	$ 60.00
All other locations:	$100.00

Orders Must Be Prepaid in U.S. Dollars, Check Payable to The Marine Biological Laboratory

About *The Biological Bulletin*
ISSN: 0006-3185
Frequency: Bimonthly
Number of issues per year: 6
Months of Publication: February, April, June, August, October, December
Subscriptions entered for calendar year
Volume indexes contained in June and December issues
Annual report of the Marine Biological Laboratory contained in August issue
Most back issues available
Claims handled upon receipt
No agency discounts
Internet:
www.biolbull.org

Please address orders to:
Wendy Child
Subscriptions
The Biological Bulletin
Marine Biological Laboratory
7 MBL Street
Woods Hole, MA 02543-1015 U.S.A.
Fax: 508-289-7922 Tel: 508-289-7402 Email: wchild@mbl.edu

Published by the Marine Biological Laboratory
Woods Hole, Massachusetts, 02543 U.S.A.

THE BIOLOGICAL BULLETIN
(www.biolbull.org)
2004 SUBSCRIPTION FORM
(VOLUMES 206-207, 6 ISSUES)

(please print)
NAME: ______________________________
INSTITUTION: ______________________________
ADDRESS: ______________________________
CITY: ________________ **STATE:** ________________
POSTAL CODE: ________________ **COUNTRY:** ________________
TELEPHONE: ________________ **FAX:** ________________
E-MAIL ADDRESS ______________________________

All subscriptions run on the calendar year; price includes both print and online journals

☐ Please send me a 2004 subscription to *The Biological Bulletin* at the rate indicated below:

☐ Individual: $120.00 (6 ISSUES) ☐ Institutional : $325.00 (6 ISSUES)
☐ Individual: $70.00 (3 ISSUES) ☐ Institutional : $165.00 (3 ISSUES)

Check one: ☐ February April June or ☐ August October December

☐ Please send me the following back issue(s): ________________

☐ Individual: at $25.00 (PER ISSUE) ☐ Institutional : at $75.00 (PER ISSUE)

Delivery Options

_____ Surface Delivery (Surface delivery is included in the subscription price.)
_____ Air delivery (Please add the correct amount to your payment.)

☐ U.S. and Canada: $46.00 ☐ Mexico: $60.00 ☐ All other locations: $100.00

Payment Options

_____ Enclosed is my check or U.S. money order for $ _____payable to The Marine Biological Laboratory

_____ Please charge my ☐ VISA, ☐ MasterCard ☐ Discover Card $________

_____ Please send me an invoice. (Note: Payment must be received before subscription commences.)

Account No.: ________________ **Exp. Date:** ________________

Signature:________________ **Date:** ________________

Return this form with your check or credit information to:
Marine Biological Laboratory
Subscription Office ◆ The Biological Bulletin ◆7 MBL Street ◆ Woods Hole, MA 02543-1015

MARINE RESOURCES CENTER

MARINE BIOLOGICAL LABORATORY • WOODS HOLE, MA 02543 • (508)289-7700
WWW.MBL.EDU/SERVICES/MRC/INDEX.HTML

zebrafish facilities

Animal and Tissue Supply for Education & Research

- 150 aquatic species available for shipment via online catalog: <http://www.mbl.edu/animals/index.html>; phone: (508)289-7375; or e-mail: specimens@mbl.edu
- zebrafish colony containing limited mutant strains
- custom dissection and furnishing of specific organ and tissue samples

MRC Services Available

- basic water quality analysis
- veterinary services (clinical, histopathologic, microbial services, health certificates, etc.)
- aquatic systems design (mechanical, biological, engineering, etc.)
- educational tours and collecting trips aboard the R/V Gemma

Using the MRC for Your Research

- capability for advanced animal husbandry (temperature, light control, etc.)
- availability of year-round, developmental life stages
- adaptability of tank system design for live marine animal experimentation

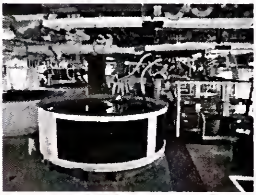

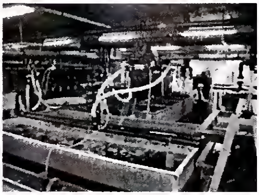

OGL-OCEAN GENOME LEGACY

■ *EXECUTIVE DIRECTOR*

A new not-for-profit foundation devoted to the preservation, distribution and evolutionary genomics of DNA from marine organisms is seeking an **EXECUTIVE DIRECTOR.**

The successful candidate will have a Ph.D. in cell or molecular biology, 4+ years' experience in molecular biology, and be highly motivated to work at the bench. Responsibilities will include the assembly of a small team of scientists for the long-term preservation of marine organism DNA, development of tissue culture techniques for marine invertebrate cells, construction of genome libraries, and evolutionary genomics of special marine transition groups.

The OGL laboratory will be temporarily located at New England Biolabs, Inc., Beverly, MA until a new facility is constructed in Ipswitch, MA.

Applicants should send a resume and three references to: ***Carol Ann Zapustas, New England Biolabs, Inc., 32 Tozer Road, Beverly, MA 01915.***

OCEAN GENOME LEGACY

An Equal Opportunity Employer.

MBL

Marine Biological Laboratory • Woods Hole • MA

Advances in Genome Technology and Bioinformatics

October 5 - November 3, 2004

A comprehensive, four-week course in genome science that will integrate bioinformatics with the latest laboratory techniques for genome sequencing, genome analysis, and high throughput gene expression.

Application Deadline: June 16, 2004

Contact: Carol Hamel, Admissions Coordinator, (508) 289-7401, admissions@mbl.edu; 7 MBL Street, Woods Hole, MA 02543
Applications are encouraged from women and members of underrepresented minorities. The MBL is an Equal Opportunity/Affirmative Action Employer.

www.mbl.edu/education

POSITION ANNOUNCEMENT

Editor-in-Chief
The Biological Bulletin

Start Date: January 2005
Term: Five years, renewable

The Editor-in-Chief is responsible for the overall editorial direction of the *Biological Bulletin*. The Editor-in-Chief appoints Associate Editors and members of the Editorial Board, decides which manuscripts are published, mediates editorial disputes, and sets policy for the journal.

The Editor-in-Chief is an independent contractor who reports to the Director and CEO of the Marine Biological Laboratory. Stipend for the position is $10,000 annually. The *Bulletin's* editorial offices are based in Woods Hole, but the Editor-in-Chief may work from his/her home institution. The Editor-in-Chief is expected to spend some part of the summer months in Woods Hole. Housing for up to one month will be provided in Woods Hole.

The successful candidate for this position will meet the following requirements:

- A broad understanding of biology, and a manifest interest in its diversity and comparative and integrative aspects
- A track-record of publishing in peer-reviewed journals
- Experience reviewing papers for scientific journals
- Proven skill as a substantive editor
- Ability to make tough decisions and willingness to work with other editors to reach a decision on difficult papers
- Demonstrated experience with the editorial process *(e.g.*, serving as an Editor or Associate Editor for a journal similar to the *Biological Bulletin*)
- The willingness and ability to commit the time required, approximately one day per week, to fulfill the duties outlined here for five years.

Job description:

The Editor-in-Chief devotes a minimum of six hours per week to the operation of the *Biological Bulletin*. The Editor's ongoing activities include 1) assigning submitted papers to the appropriate Associate Editor; 2) reading reviews and manuscripts to ensure fairness and technical accuracy; 3) writing editorial decision letters based on the reviews; 4) fielding telephone and e-mail queries on a daily basis from authors deciding whether to submit their work to the *Biological Bulletin*, authors who are unhappy about an editorial decision, and Associate Editors requesting guidance on such matters as the identity, availability, and number of reviewers, and editorial decisions and disputes; 5) communicating regularly (by telephone or e-mail) with the Managing Editor and other editorial staff members to plan future issues, to arrange the table of contents, to develop the issue cover, and to discuss organizational issues; 6) editing accepted manuscripts as necessary for substance, accuracy, and clarity; 7) selecting cover photos and writing associated legends; 8) informing editorial staff of noteworthy articles for the media; 9) as the deadline for each issue approaches, deciding which manuscripts will be published.

Nomination packets must include the following:

1. Letter of intent
2. Current CV
3. Vision Statement for the journal

Send nominations to:

Pamela Clapp Hinkle
Managing Editor, *Biological Bulletin*
Marine Biological Laboratory
7 MBL Street
Woods Hole, MA 02543
pclapp@mbl.edu

Marine Biological Laboratory • Woods Hole • Massachusetts

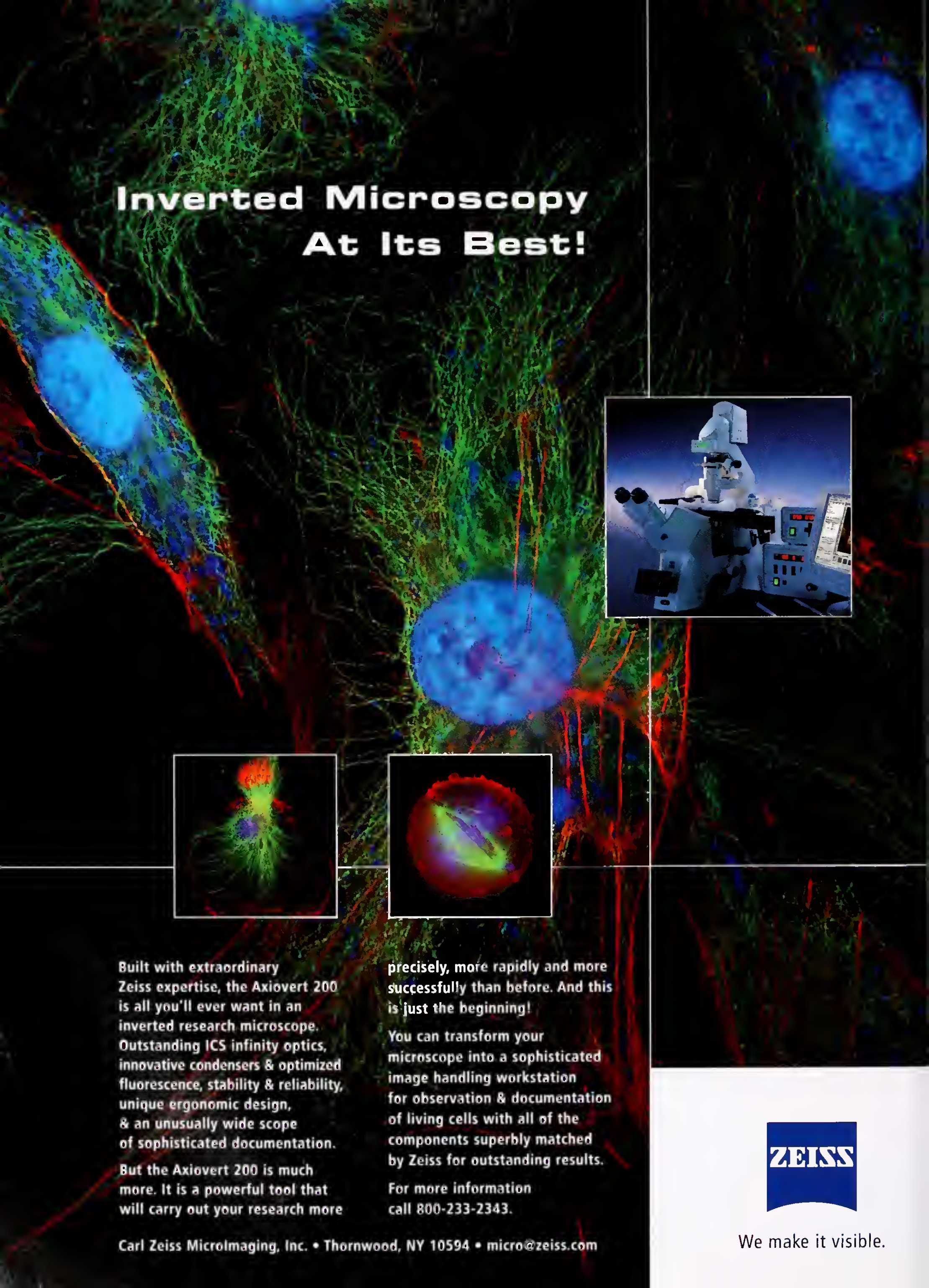

Built with extraordinary Zeiss expertise, the Axiovert 200 is all you'll ever want in an inverted research microscope. Outstanding ICS infinity optics, innovative condensers & optimized fluorescence, stability & reliability, unique ergonomic design, & an unusually wide scope of sophisticated documentation.

But the Axiovert 200 is much more. It is a powerful tool that will carry out your research more precisely, more rapidly and more successfully than before. And this is just the beginning!

You can transform your microscope into a sophisticated image handling workstation for observation & documentation of living cells with all of the components superbly matched by Zeiss for outstanding results.

For more information call 800-233-2343.

Carl Zeiss MicroImaging, Inc. • Thornwood, NY 10594 • micro@zeiss.com

June 2004

Volume 206 • Number 3

THE BIOLOGICAL BULLETIN

Published by the Marine Biological Laboratory
Woods Hole, Massachusetts

THE BIOLOGICAL BULLETIN
ONLINE

The Marine Biological Laboratory is pleased to announce that the full text of *The Biological Bulletin* is available online at

http://www.biolbull.org

The Biological Bulletin publishes outstanding experimental research on the full range of biological topics and organisms, from the fields of Neurobiology, Behavior, Physiology, Ecology, Evolution, Development and Reproduction, Cell Biology, Biomechanics, Symbiosis, and Systematics.

Published since 1897 by the Marine Biological Laboratory (MBL) in Woods Hole, Massachusetts, *The Biological Bulletin* is one of America's oldest peer-reviewed scientific journals.

The journal is aimed at a general readership, and especially invites articles about those novel phenomena and contexts characteristic of intersecting fields.

The Biological Bulletin Online contains the full content of each issue of the journal, including all figures and tables, beginning with the February 2001 issue (Volume 200, Number 1). The full text is searchable by keyword, and the cited references include hyperlinks to Medline. PDF files are available beginning in February 1990 (Volume 178, Number 1), some abstracts are available beginning with the October 1976 issue (Volume 151, Number 2), and some Tables of Contents are online beginning with the October 1965 issue (Volume 129, Number 2).

Each issue will be placed online approximately on the date it is mailed to subscribers; therefore the online site will be available prior to receipt of your paper copy. Online readers may want to sign up for the eTOC (electronic Table of Contents) service, which will deliver each new issue's table of contents *via* e-mail. The web site also provides access to information about the journal (such as Instructions to Authors, the Editorial Board, and subscription information), as well as access to the Marine Biological Laboratory's web site and other *Biological Bulletin* electronic publications.

The free trial period for access to *The Biological Bulletin* online has ended. Individuals and institutions who are subscribers to the journal in print or are members of the Marine Biological Laboratory Corporation may now activate their online subscriptions. All other access (*e.g.*, to Abstracts, eTOCs, searching, Instructions to Authors) remains freely available. Online access is included in the print subscription price.

For more information about subscribing or activating your online subscription, visit <www.biolbull.org/subscriptions>.

---

http://www.biolbull.org

THE BRAIN REPAIR SHOP

A TRON-generation kid with a computer-monitor tan liberated by confocal technology. A tennis jock from Sweden who traded her rocket for a FluoView™ 300 and a stethoscope. A criminalist from the LAPD now in hot pursuit of outlaw cells. Unique talents brought together by Principal Investigator Dan Peterson to chase down the Big Answer: How to harness endogenous brain stem cells that can repair, and send them to other places in the brain that *need* repair. "Our bread and butter is confocal microscopy," Peterson says. "We're like portrait photographers. We light, compose, direct, position – all to get the cell ready for its close-up."
And to improve the human condition at the end of the day.

OLYMPUS MICROSCOPES. ROCKET SCIENCE™.

Find out more about Olympus microscopes at www.olympusamerica.com/microscopes 800-455-8236

Christopher Vega, Ph D Research Associate
Anna Hallbergson M D Ph D Student
Daniel A Peterson, Ph D Lab Director
Christine Sanders - Research Assistant
Department of Neuroscience
Rosalind Franklin University
of Medicine and Science

OLYMPUS®
Your Vision, Our Future

CONTENTS

VOLUME 206, NO. 3: JUNE 2004

RESEARCH NOTE

Li, Natasha K., and Mark W. Denny
Limits to phenotypic plasticity: flow effects on barnacle feeding appendages 121

SEA MONSTERS

Pierce, Sidney K., Steven E. Massey, Nicholas E. Curtis, Gerald N. Smith, Jr., Carlos Olavarría, and Timothy K. Maugel
Microscopic, biochemical, and molecular characteristics of the Chilean Blob and a comparison with the remains of other sea monsters: nothing but whales. . . 125

ECOLOGY AND EVOLUTION

Díaz, Eliecer R., and Martin Thiel
Chemical and visual communication during mate searching in rock shrimp 134

Johnson, Sheri L., and Philip O. Yund
Remarkable longevity of dilute sperm in a free-spawning colonial ascidian 144

Phillippi, Aimee, Ellen Hamann, and Philip O. Yund
Fertilization in an egg-brooding colonial ascidian does not vary with population density. 152

Swanson, Rebecca L., Jane E. Williamson, Rocky De Nys, Naresh Kumar, Martin P. Bucknall, and Peter D. Steinberg
Induction of settlement of larvae of the sea urchin *Holopneustes purpurascens* by histamine from a host alga 161

Ferrell, David L.
Fitness consequences of allorecognition-mediated agonistic interactions in the colonial hydroid *Hydractinia [GM]* 173

INNATE IMMUNITY

Holman, Jeremy D., Karen G. Burnett, and Louis E. Burnett
Effects of hypercapnic hypoxia on the clearance of *Vibrio campbellii* in the Atlantic blue crab, *Callinectes sapidus* Rathbun. 188

* * *

Index for Volume 206 197

THE BIOLOGICAL BULLETIN

THE BIOLOGICAL BULLETIN is published six times a year by the Marine Biological Laboratory, 7 MBL Street, Woods Hole, Massachusetts 02543.

Subscriptions and similar matter should be addressed to Subscription Administrator, THE BIOLOGICAL BULLETIN, Marine Biological Laboratory, 7 MBL Street, Woods Hole, Massachusetts 02543. Subscription includes both print and online journals. Subscription per year (six issues, two volumes): $325 for libraries; $120 for individuals. Subscription per volume (three issues): $165 for libraries; $70 for individuals. Back and single issues (subject to availability): $75 for libraries; $25 for individuals.

Communications relative to manuscripts should be sent to Michael J. Greenberg, Editor-in-Chief, or Pamela Clapp Hinkle, Managing Editor, at the Marine Biological Laboratory, 7 MBL Street, Woods Hole, Massachusetts 02543. Telephone: (508) 289-7149. FAX: 508-289-7922. E-mail: pclapp@mbl.edu.

http://www.biolbull.org

THE BIOLOGICAL BULLETIN is indexed in bibliographic services including *Index Medicus* and MEDLINE, *Chemical Abstracts, Current Contents, Elsevier BIOBASE/Current Awareness in Biological Sciences*, and *Geo Abstracts*.

Printed on acid free paper,
effective with Volume 180, Issue 1, 1991.

POSTMASTER: Send address changes to THE BIOLOGICAL BULLETIN, Marine Biological Laboratory,
7 MBL Street, Woods Hole, MA 02543.

Copyright © 2004, by the Marine Biological Laboratory

Periodicals postage paid at Woods Hole, MA, and additional mailing offices.
ISSN 0006-3185

INSTRUCTIONS TO AUTHORS

The Biological Bulletin accepts outstanding original research reports of general interest to biologists throughout the world. Papers are usually of intermediate length (10–40 manuscript pages). A limited number of solicited review papers may be accepted after formal review. A paper will usually appear within four months after its acceptance.

Very short, especially topical papers (less than 9 manuscript pages including tables, figures, and bibliography) will be published in a separate section entitled "Research Notes." A Research Note in *The Biological Bulletin* follows the format of similar notes in *Nature*. It should open with a summary paragraph of 150 to 200 words comprising the introduction and the conclusions. The rest of the text should continue on without subheadings, and there should be no more than 30 references. References should be referred to in the text by number, and listed in the Literature Cited section in the order that they appear in the text. Unlike references in *Nature*, references in the Research Notes section should conform in punctuation and arrangement to the style of recent issues of *The Biological Bulletin*. Materials and Methods should be incorporated into appropriate figure legends. See the article by Lee (October 2003, Vol. **205:** 99–101) for sample style. A Research Note will usually appear within two months after its acceptance.

The Editorial Board requests that regular manuscripts conform to the requirements set below; those manuscripts that do not conform will be returned to authors for correction before review.

1. ***Manuscripts.*** Manuscripts, including figures, should be submitted in quadruplicate, with the originals clearly marked. (Xerox copies of photographs are not acceptable for review purposes.) Please include an electronic copy of the text of the manuscript. Label the disk with the name of the first author and the name and version of the wordprocessing software used to create the file. If the file was not created in some version of Microsoft Word, save the text in rich text format (rtf). The submission letter accompanying the manuscript should include a telephone number, a FAX number, and (if possible) an E-mail address for the corresponding author. The original manuscript must be typed in no smaller than 12 pitch or 10 point, using double spacing (*including* figure legends, footnotes, bibliography, etc.) on one side of 16- or 20-lb. bond paper, 8 by 11 inches. Please, no right justification. Manuscripts should be proofread carefully and errors corrected legibly in black ink. Pages should be numbered consecutively. Margins on all sides should be at least 1 inch (2.5 cm). Manuscripts should conform to the *Council of Biology Editors Style Manual*, 5th Edition (Council of Biology Editors, 1983) and to American spelling. Unusual abbreviations should be kept to a minimum and should be spelled out on first reference as well as defined in a footnote on the title page. Manuscripts should be divided into the following components: Title page, Abstract (of no more than 200 words), Introduction, Materials and Methods, Results, Discussion, Acknowledgments, Literature Cited, Tables, and Figure Legends. In addition, authors should supply a list of words and phrases under which the article should be indexed.

2. ***Title page.*** The title page consists of a condensed title or running head of no more than 35 letters and spaces, the manuscript title, authors' names and appropriate addresses, and footnotes listing present addresses, acknowledgments or contribution numbers, and explanation of unusual abbreviations.

3. ***Figures.*** The dimensions of the printed page, 7 by 9 inches, should be kept in mind in preparing figures for publication. We recommend that figures be about 1 times the linear dimensions of the final printing desired, and that the ratio of the largest to the smallest letter or number and of the thickest to the thinnest line not exceed 1:1.5. Explanatory matter generally should be included in legends, although axes should always be identified on the illustration itself. Figures should be prepared for reproduction as either line cuts or halftones. Figures to be reproduced as line cuts should be unmounted glossy photographic reproductions or drawn in black ink on white paper, good-quality tracing cloth or plastic, or blue-lined coordinate paper. Those to be reproduced as halftones should be mounted on board, with both designating numbers or letters and scale bars affixed directly to the figures. All figures should be numbered in consecutive order, with no distinction between text and plate figures and cited, in order, in the text. The author's name and an arrow indicating orientation should appear on the reverse side of all figures.

Digital art: The Biological Bulletin will accept figures submitted in electronic form; however, digital art must conform to the following guidelines. Authors who create digital images are wholly responsible for the quality of their material, including color and halftone accuracy.

Format. Acceptable graphic formats are TIFF and EPS. Color submissions must be in EPS format, saved in CMKY mode.

Software. Preferred software is Adobe Illustrator or Adobe Photoshop for the Mac and Adobe Photoshop for Windows. Specific instructions for artwork created with various software programs are available on the Web at the Digital Art Information Site maintained by Cadmus Professional Communications at http://cpc.cadmus.com/da/

Resolution. The minimum requirements for resolution are 1200 DPI for line art and 300 for halftones.

Size. All digital artwork must be submitted at its actual printed size so that no scaling is necessary.

Multipanel figures. Figures consisting of individual parts (*e.g.*, panels A, B, C) must be assembled into final format and submitted as one file.

Hard copy. Files must be accompanied by hard copy for use in case the electronic version is unusable.

Disk identification. Disks must be clearly labeled with the following information: author name and manuscript number; format (PC or Macintosh); name and version of software used.

Color: The Biological Bulletin will publish color figures and plates, but must bill authors for the actual additional cost of printing in color. The process is expensive, so authors with more than one color image should—consistent with editorial concerns, especially citation of figures in order—combine them into a single plate to reduce the expense. On request, when supplied with a copy of a color illustration, the editorial staff will provide a pre-publication estimate of the printing cost.

4. ***Tables, footnotes, figure legends, etc.*** Authors should follow the style in a recent issue of *The Biological Bulletin* in preparing table headings, figure legends, and the like. Because of the high cost of setting tabular material in type, authors are asked to limit such material as much as possible. Tables, with their headings and footnotes, should be typed on separate sheets, numbered with consecutive Arabic numerals, and placed after the Literature Cited. Figure legends should contain enough information to make the figure intelligible separate from the text. Legends should be typed double spaced, with consecutive Arabic numbers, on a separate sheet at the end of the paper. Footnotes should be limited to authors' current addresses, acknowledgments or contribution numbers, and explanation of unusual abbreviations. All such footnotes should appear on the title page. Footnotes are not normally permitted in the body of the text.

5. ***Literature cited.*** In the text, literature should be cited by the Harvard system, with papers by more than two authors cited as Jones *et al.*, 1980. Personal communications and material in preparation or in press should be cited in the text only, with author's initials and institutions, unless the material has been formally accepted and a volume number can be supplied. The list of references following the text should be headed Literature Cited, and must be typed double spaced on separate pages, conforming in punctuation and arrangement to the style of recent issues of *The Biological Bulletin*. Citations should include complete titles and inclusive pagination. Journal abbreviations should normally follow those of the U. S. A. Standards Institute (USASI), as adopted by BIOLOGICAL ABSTRACTS and CHEMICAL ABSTRACTS, with the minor differences set out below. The most generally useful list of biological journal titles is that published each year by BIOLOGICAL ABSTRACTS (BIOSIS List of Serials; the most recent issue). Foreign authors, and others who are accustomed to using THE WORLD LIST OF SCIENTIFIC PERIODICALS, may find a booklet published by the Biological Council of the U.K. (obtainable from the Institute of Biology, 41 Queen's Gate, London, S.W.7, England, U.K.) useful, since it sets out the WORLD LIST abbreviations for most biological journals with notes of the USASI abbreviations where these differ. CHEMICAL ABSTRACTS publishes quarterly supplements of additional abbreviations. The following points of reference style for THE BIOLOGICAL BULLETIN differ from USASI (or modified WORLD LIST) usage:

A. Journal abbreviations, and book titles, all underlined (for *italics*)

B. All components of abbreviations with initial capitals (not as European usage in WORLD LIST *e.g., J. Cell. Comp. Physiol.* NOT *J. cell. comp. Physiol.*)

C. *All* abbreviated components must be followed by a period, whole word components *must not* (*i.e., J. Cancer Res.*)

D. Space between all components (*e.g., J. Cell. Comp. Physiol.*, not *J.Cell.Comp.Physiol.*)

E. Unusual words in journal titles should be spelled out in full, rather than employing new abbreviations invented by the author. For example, use *Rit Vísindafjélags Islendinga* without abbreviation.

F. All single word journal titles in full (*e.g., Veliger, Ecology, Brain*).

G. The order of abbreviated components should be the same as the word order of the complete title (*i.e., Proc.* and *Trans.* placed where they appear, not transposed as in some BIOLOGICAL ABSTRACTS listings).

H. A few well-known international journals in their preferred forms rather than WORLD LIST or USASI usage (*e.g., Nature, Science, Evolution* NOT *Nature, Lond., Science, N.Y.; Evolution, Lancaster, Pa.*)

6. ***Sequences.*** By the time a paper is sent to the press, all nucleotide or amino acid sequences and associated alignments should have been deposited in a generally accessible database (*e.g.*, GenBank, EMBL, SwissProt), and the sequence accession number should be provided.

7. ***Reprints, page proofs, and charges.*** Authors may purchase reprints in lots of 100. Forms for placing reprint orders are sent with page proofs. Reprints normally will be delivered about 2 to 3 months after the issue date. Authors will receive page proofs of articles shortly before publication. They will be charged the current cost of printers' time for corrections to these (other than corrections of printers' or editors' errors). Other than these charges for authors' alterations, *The Biological Bulletin* does not have page charges.

CONTENTS
for Volume 206

No. 1: February 2004

RESEARCH NOTE

Buresch, Kendra C., Jean G. Boal, Gregg T. Nagle, Jamie Knowles, Robert Nobuhara, Kate Sweeney, and Roger T. Hanlon
Experimental evidence that ovary and oviducal gland extracts influence male agonistic behavior in squids 1

PHYSIOLOGY AND BIOMECHANICS

Motokawa, Tatsuo, Osamu Shintani, and Rüdiger Birenheide
Contraction and stiffness changes in collagenous arm ligaments of the stalked crinoid *Metacrinus rotundus* (Echinodermata) 4

NEUROBIOLOGY AND BEHAVIOR

Biggers, William J., and Hans Laufer
Identification of juvenile hormone-active alkylphenols in the lobster *Homarus americanus* and in marine sediments. 13

DEVELOPMENT AND REPRODUCTION

Tominaga, Hideyuki, Shogo Nakamura, and Miéko Komatsu
Reproduction and development of the conspicuously dimorphic brittle star *Ophiodaphne formata* (Ophiuroidea) 25

Temkin, M. H., and S. B. Bortolami
Waveform dynamics of spermatozeugmata during the transfer from paternal to maternal individuals of *Membranipora membranacea* 35

ECOLOGY AND EVOLUTION

Wang, Yongping, Zhe Xu, and Ximing Guo
Differences in the rDNA-bearing chromosome divide the Asian-Pacific and Atlantic species of *Crassostrea* (Bivalvia, Mollusca) 46

Maruyama, Yoshihiko K.
Occurrence in the field of a long-term, year-round, stable population of placozoans 55

No. 2: April 2004

RESEARCH NOTE

Edmunds, Peter J., and Ruth D. Gates
Size-dependent differences in the photophysiology of the reef coral *Porites astreoides* 61

NEUROBIOLOGY AND BEHAVIOR

Lindsay, Sara M., Timothy J. Riordan, Jr., and D. Forest
Identification and activity-dependent labeling of peripheral sensory structures on a spionid polychaete. 65

PHYSIOLOGY AND BIOMECHANICS

Harper, S. L., and C. L. Reiber
Physiological development of the embryonic and larval crayfish heart 78

Ehlinger, Gretchen S., and Richard A. Tankersley
Survival and development of horseshoe crab (*Limulus polyphemus*) embryos and larvae in hypersaline conditions. 87

CELL BIOLOGY

Ishikawa, Makiko, Hidekazu Tsutsui, Jacky Cosson, Yoshitaka Oka, and Masaaki Morisawa
Strategies for sperm chemotaxis in the siphonophores and ascidians: a numerical simulation study. 95

ECOLOGY AND EVOLUTION

Last, Kim S., and Peter J. W. Olive
Interaction between photoperiod and an endogenous seasonal factor in influencing the diel locomotor activity of the benthic polychaete *Nereis virens* Sars. 103

Greenwood, Paul G., Kyle Garry, April Hunter, and Miranda Jennings
Adaptable defense: a nudibranch mucus inhibits nematocyst discharge and changes with prey type . . . 113

No. 3: June 2004

RESEARCH NOTE

Li, Natasha K., and Mark W. Denny
Limits to phenotypic plasticity: flow effects on barnacle feeding appendages 121

SEA MONSTERS

Pierce, Sidney K., Steven E. Massey, Nicholas E. Curtis, Gerald N. Smith, Jr., Carlos Olavarría, and Timothy K. Maugel
Microscopic, biochemical, and molecular characteristics of the Chilean Blob and a comparison with the remains of other sea monsters: nothing but whales. . . 125

ECOLOGY AND EVOLUTION

Díaz, Eliecer R., and Martin Thiel
Chemical and visual communication during mate searching in rock shrimp 134
Johnson, Sheri L., and Philip O. Yund
Remarkable longevity of dilute sperm in a free-spawning colonial ascidian 144
Phillippi, Aimee, Ellen Hamann, and Philip O. Yund
Fertilization in an egg-brooding colonial ascidian does not vary with population density. 152
Swanson, Rebecca L., Jane E. Williamson, Rocky De Nys, Naresh Kumar, Martin P. Bucknall, and Peter D. Steinberg
Induction of settlement of larvae of the sea urchin *Holopneustes purpurascens* by histamine from a host alga 161
Ferrell, David L.
Fitness consequences of allorecognition-mediated agonistic interactions in the colonial hydroid *Hydractinia [GM]* 173

INNATE IMMUNITY

Holman, Jeremy D., Karen G. Burnett, and Louis E. Burnett
Effects of hypercapnic hypoxia on the clearance of *Vibrio campbellii* in the Atlantic blue crab, *Callinectes sapidus* Rathbun. 188

* * *

Index for Volume 206 197

Reference: *Biol. Bull.* **206:** 121–124. (June 2004)
© 2004 Marine Biological Laboratory

Limits to Phenotypic Plasticity: Flow Effects on Barnacle Feeding Appendages

NATASHA K. LI* AND MARK W. DENNY

Hopkins Marine Station, Stanford University, Pacific Grove, California 93950

Phenotypic plasticity, the capacity of a given genotype to produce differing morphologies in response to the environment, is widespread among marine organisms (1). For example, acorn barnacles feed by extending specialized appendages (the cirral legs) into flow, and the length of the cirri is plastic: the higher the velocity, the shorter the feeding legs (2, 3). However, this effect has been explored only for flows less than 4.6 m/s, slow compared to typical flows measured at sites on wave-exposed shores. What happens at faster speeds? Leg lengths of Balanus glandula *Darwin, 1854, an acorn barnacle, were measured at 15 sites in Monterey, California, across flows ranging from 0.5 to 14.0 m/s. Similar to previous findings, a plastic response in leg length was noted for the four sites with water velocities less than 3 m/s. However, no plastic response was present at the 11 sites exposed to faster velocities, despite a 4-fold variation in speed. We conclude that the velocity at which the plastic response occurs has an upper limit of 2–4 m/s, a velocity commonly exceeded within the typical habitat of this species.*

Acorn barnacles provide an excellent opportunity for examining plastic response because they are sessile (and therefore cannot move in response to the environment), molt their exoskeleton (providing periodic opportunity for morphological change), and occur across a wide range of flow conditions. Helmuth and Denny (4) measured maximal wave-induced water velocities at 222 sites along the rocky intertidal shore at Hopkins Marine Station (HMS) in Pacific Grove, California (36°36′N, 121°53′W), and the variation in velocity at each site was expressed as a function of offshore significant wave height (the average height of the highest one-third of waves). These measurements allowed us to select sites exposed to a range of wave-induced water velocities. Eleven sites, each 1.5 m above the mean lower low water (MLLW), were selected for collection of *B. glandula*. Because of the exposure of this shore, all HMS sites except one are subjected to water velocities greater than those encountered in previous studies on *B. glandula* (2, 3). Therefore, four additional sites were selected at the Monterey Wharf in Monterey, California (~2 km from HMS), where barnacles are subjected to a range of slower flows. At each site, 10 barnacles were collected, and the length of each cirrus was measured.

Offshore significant wave height was measured four times per day for 30 days prior to the barnacle collections, and the largest significant wave height occurring when the tidal height was greater than 1.5 m above MLLW was noted for each day. These data, in conjunction with the relationships measured by Helmuth and Denny (4), allowed us to estimate the daily maximal water velocities imposed at each collection site. Marchinko (3) found that transplanted specimens of *B. glandula* begin modifying their cirral length in response to their new environment somewhere between 7 and 18 days after first exposure. There was no evidence of alteration at day 7 and significant alteration by day 18, continuing through day 30. To incorporate this lag in response time, we used the water velocities recorded 10–30 days prior to sampling as an index of the flows to which the barnacles could have responded. Previous studies have examined only the relationship between cirrus length and average daily maximum velocity, although the barnacles could be responding to maximum velocity, average velocity, or some other aspect of flow. We employ both the average daily maximum (ADM) velocity and overall maximum (OM) velocity.

Received 5 February 2004; accepted 31 March 2004.

* To whom correspondence should be addressed. Present address: American Institute of Mathematics, 360 Portage Ave, Palo Alto, CA 94305. E-mail: nkli@stanfordalumni.org

Abbreviations: ADM, average daily maximum; ANCOVA, analysis of covariance; HMS, Hopkins Marine Station; MLLW, mean lower low water; OM, overall maximum.

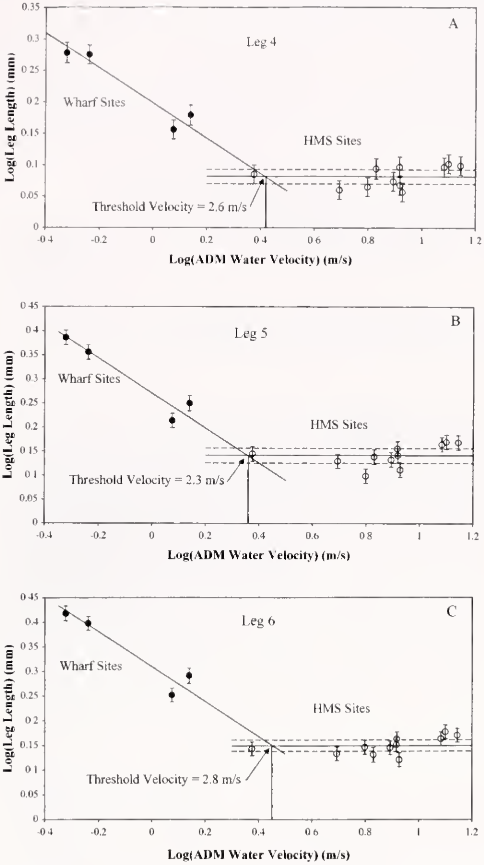

Figure 1. Average length of three feeding legs of *Balanus glandula* from 15 sites of differing wave exposure in Monterey Bay, California. Wave exposure was calculated as the average of daily maximum velocities encountered for 10–30 days prior to collection. Legs 4, 5, and 6 refer to the fourth, fifth, and posterior-most (sixth) pair of thoracic legs of these balanomorph barnacles. Leg lengths ($n = 10$ per site) were standardized to a common prosoma wet mass of 0.0079 g by ANCOVA. Reduced major axis regression lines are shown for the low-flow Wharf data. Lines representing the mean and 95% confidence intervals are shown for the HMS sites. (A) Average $\log_{10}$ length of leg 4. (B) Average $\log_{10}$ length of leg 5. (C) Average $\log_{10}$ length of leg 6. Reduced major axis regression statistics are given in Table 1. Error bars are standard errors of the log-transformed data, calculated by ANCOVA (Table 2).

Water velocities during high tide at the Monterey Wharf sites were measured using a Marsh-McBirney 511 electromagnetic flow meter. The probe was placed about 0.5 m seaward of the collection points, and the velocity was sampled every 30 s for 20 min at each site. The maximum velocity encountered was then used in conjunction with the co-occurring offshore wave height as a means of estimating maximal velocity. We assume that the velocity can be modeled using solitary wave theory (10), $U = k(gh)^{0.5}$ (where U is velocity, g is the acceleration of gravity, and h is offshore significant wave height), and the constant of proportionality, k, was calculated for each site. Velocities could then be calculated for days 10–30 prior to barnacle collection from average daily maximum offshore wave significant height measurements. Note that in the summer of 2002 (when barnacles were collected), wave heights in Monterey Bay were consistently small, and variation among days was minimal.

We collected 10 solitary, uncrowded specimens of *Balanus glandula* from rock surfaces within 6 cm of each dynamometer for 11 sites along HMS on 5 and 6 May 2002. At the Monterey Wharf, barnacles were collected from rocks at four sites with differing wave exposures on 20 July 2002. The staggered collection dates may have allowed seasonal variation in barnacle morphology, but we assume that any such variation is unlikely to account for the extreme differences in cirral lengths found between the sites. At each site, barnacles of various sizes were collected. All barnacles were dissected on the day of collection. The prosoma (the fleshy part of the body without the shell) was extracted, blotted with a paper towel, and weighed to the nearest 0.1 mg as a measure of wet body mass. The posterior three cirri (legs 4, 5, and 6) were then dissected from the left side of the prosoma. Both the exopodite and the endopodite of each leg were placed together on a microscope slide in a drop of saltwater. The slides were viewed and legs traced onto paper with the use of a camera lucida attached to the microscope. A calibration length measurement was taken using a stage micrometer. The traced length of each leg was then measured to the nearest micrometer by using a piece of cotton string placed against the tracing. The legs were measured from the base of the ramus to each tip, excluding the propodite segments.

Analysis of covariance was conducted using SYSTAT (Systat Software Inc., ver. 6.0 for Macintosh). All sites exhibited a common slope of mass *versus* leg length. Separate ANCOVA tests were done on each leg (4, 5, and 6). Least-square means of barnacle leg length for a standard body mass were computed by ANCOVA. A Tukey HSD test was performed to detect differences between velocities and least-square mean leg lengths. Reduced major axis regressions were calculated using the least squares standardized means (5). All regression and ANCOVA analyses were performed on $\log_{10}$-$\log_{10}$ transformed data, as per Arsenault *et al.* (3).

All cirral legs (legs 4, 5, and 6) were significantly longer at the protected Monterey Wharf sites than at the exposed HMS sites. For example, the average length of leg 6 at the two wharf sites with ADM velocities less than 0.6 m/s was 2.56 mm, nearly 1.8 times that at HMS (avg. length = 1.42 mm), where ADM velocities exceeded 2.4 m/s. On the basis of evidence from previous studies (2, 3), we assume that this difference is due to a plastic response to flow. In contrast, the differences among the HMS sites were not significant, despite a range of velocities from 2.4 to 14.0 m/s. Furthermore, among the Monterey Wharf sites, there was a significant difference between the sites with lower velocities (0.48 and 0.58 m/s ADM) and higher velocities (1.19 and 1.38 m/s ADM).

Among the HMS sites, there was no significant correlation between leg length and either measure of water velocity ($P > 0.05$). In contrast, at the Monterey Wharf sites, leg length and water velocity were significantly correlated, and we explored this correlation using reduced major axis regressions for the logarithm of leg lengths *versus* the logarithm of either ADM or OM velocity (Fig. 1 and Table 1). We employed reduced major axis regression because the variables involved have different scales and are subject to measurement errors that are not easily specified (5). (Note that leg measurements were standardized to a common prosomal wet weight; see Table 2.) Among the Monterey Wharf sites, leg length is significantly negatively correlated with flow velocity, with slopes varying from −0.28 to −0.36 depending on the cirrus. The relationship using ADM velocities is shown in Figure 1. The intersection of the Wharf regression and HMS mean (with 95% confidence interval) using ADM velocity occurred between 2.0 and 3.1 m/s (average of intersection with the mean: 2.6 m/s) depending on the cirrus (Fig. 1). The intersection using OM velocity (not shown) occurred between 3.0 and 4.6 m/s (average of intersection with mean: 3.6 m/s). Because of the small number of data points ($n = 4$), we could not calculate confidence bands for the reduced major axis regressions.

The morphology of the cirri of *B. glandula* is likely to affect their ability to act as effective filters. The longer the legs, the more area they can subtend and the farther they can extend into the water flow, and therefore the more water they can potentially filter. However, if the legs grow too long, hydrodynamic forces could cause them to buckle or bend, and thereby to lose their functionality. The ability to vary leg lengths appropriately in response to different water velocities would therefore appear to be advantageous. Indeed, barnacles seem capable of adjusting leg lengths within one or two molts of exposure to different wave velocities (3), and Arsenault *et al.* (2) suggest that this "tuning" results in a precise power relationship between leg length and water velocity. Our results suggest, however, that there is a threshold water velocity (~2.6 m/s using ADM velocity, ~3.6 m/s using OM velocity) above which barnacles cease responding plastically to flow. Above this velocity, the large drag forces experienced might not allow legs of any practical length to act as effective filters, and a plastic response would lose its advantage. Previous studies have reported that acorn barnacles adjust their feeding behavior across a range of low water velocities (0–0.15 m/s [6, 7]) and maintain their feeding activity at water velocities of at least 0.25 m/s (8, 9), but we know of no direct observations at greater velocities. Our results suggest that acorn barnacles on wave-exposed shores may be able to feed only during the relatively slow backwash as waves recede.

Table 1

Reduced major axis linear regression equations for the average log_{10}(leg length) (mm) of Balanus glandula *as a function of the average log_{10} of two measures of water velocity (m/s) under breaking waves*

	Regression statistics			
Trait	slope	intercept	r^2	P
A. Average daily maximum water velocity (ADM)				
leg 4	−0.279	0.198	0.9148	<0.001
leg 5	−0.362	0.271	0.9146	<0.001
leg 6	−0.354	0.310	0.901	<0.001
B. Overall maximum water velocity (OM)				
leg 4	−0.279	0.245	0.9148	<0.001
leg 5	−0.362	0.332	0.9146	<0.001
leg 6	−0.354	0.370	0.901	<0.001

Regressions for ADM and OM velocity have identical slopes because (for our method of estimating velocity at these sites) OM velocity is a constant multiple of ADM velocity. Data are shown only for the Monterey Wharf sites. No significant correlations were found among the sites at Hopkins Marine Station ($P > 0.05$). Sample size (n) for each leg is 4.

Table 2

Analysis of covariance results for measurements of Balanus glandula

Source of variation	df	Mean-square	F	P
Log(ramus length of fourth thoracic leg)				
Field site	14	0.052	22.876	<0.001
Covariate(log(prosoma wet mass))	1	0.392	172.237	<0.001
Residual	134	0.002		
Log(ramus length of fifth thoracic leg)				
Field site	14	0.069	31.817	<0.001
Covariate(log(prosoma wet mass))	1	0.359	166.552	<0.001
Residual	134	0.002		
Log(ramus length of sixth thoracic leg)				
Field site	14	0.082	40.281	<0.001
Covariate(log(prosoma wet mass))	1	0.369	180.598	<0.001
Residual	134	0.002		

Arsenault *et al.* (2) propose that the tight relationship between leg length and water velocity might allow barnacles to be used to measure local wave exposure. Our results suggest that barnacle leg length can, indeed, be a reliable indicator of wave exposure, but only for sites at which the ADM water velocity is less than about 3 m/s. Note also that the exponents of the power relationship found by Arsenault *et al.* (2) (−0.32 to −0.43) are slightly different from those found here (−0.28 to −0.36). This disparity could be an artifact of the small number of data points ($n = 6$, Arsenault *et al.* [2]; $n = 4$, this study), but also could possibly be accounted for by differences in mean barnacle size (0.0219 g, Arsenault *et al.* [2]; 0.0079 g, this study), method used to estimate water velocity, or substantial latitudinal difference in collection site. Therefore, local calibration might be necessary if barnacles are to be used as "exposure meters."

Studies to date have examined only the ultimate relationship between maximum velocities and cirral length. As with any correlation, further research is needed to elucidate the mechanisms that account for the relationship.

Acknowledgments

We thank J. Watanabe for his invaluable statistical help, even while traveling the globe.

Literature Cited

1. **Pigliucci, M. 2001.** *Phenotypic Plasticity: Beyond Nature and Nurture.* Johns Hopkins University Press, Baltimore, MD.
2. **Arsenault, D., K. B. Marchinko, and A. R. Palmer. 2001.** Precise tuning of barnacle leg length to coastal wave action. *Proc. R. Soc. Lond. B* **268:** 2149–2154.
3. **Marchinko, K. B. 2003.** Dramatic phenotypic plasticity in barnacle legs (*Balanus glandula* Darwin): magnitude, age dependence, and speed of response. *Evolution* **57:** 1281–1290.
4. **Helmuth, B., and M. W. Denny. 2003.** Predicting wave exposure in the rocky intertidal zone: Do bigger waves always lead to larger forces? *Limnol. Oceanogr.* **48:** 1338–1345.
5. **Sokal, R., and F. J. Rohlf. 2000.** *Biometry: the Principles and Practice of Statistics in Biological Research,* 3rd ed. W. H. Freeman, New York. Pp. 541–548.
6. **Trager, G. C., J.-S. Hwang, and J. R. Strickler. 1990.** Barnacle suspension feeding in variable flow. *Mar. Biol.* **105:** 117–127.
7. **Trager, G. C., D. Coughlin, A. Genin, Y. Achituv, and A. Gangopadhyay. 1992.** Foraging to the rhythm of ocean waves: porcelain crabs and barnacles synchronize feeding with flow oscillations. *J. Exp. Mar. Biol. Ecol.* **164:** 73–86.
8. **Eckman, J. E., and D. O. Duggins. 1993.** Effects of flow speed on growth of benthic suspension feeders. *Biol. Bull.* **185:** 28–41.
9. **Sanford, E., D. Bermudez, M. D. Bertness, and S. D. Gaines. 1994.** Flow, flood supply and acorn barnacle population dynamics. *Mar. Ecol. Prog. Ser.* **104:** 49–62.
10. **Gaylord, B. 1999.** Detailing agents of physical disturbance: wave-induced velocities and accelerations of a rocky shore. *J. Exp. Mar. Biol. Ecol.* **239:** 85–124.

Reference: *Biol. Bull.* **206:** 125–133. (June 2004)
© 2004 Marine Biological Laboratory

Microscopic, Biochemical, and Molecular Characteristics of the Chilean Blob and a Comparison With the Remains of Other Sea Monsters: Nothing but Whales

SIDNEY K. PIERCE[1,*], STEVEN E. MASSEY[1], NICHOLAS E. CURTIS[1],
GERALD N. SMITH, JR.[2], CARLOS OLAVARRÍA[3], AND TIMOTHY K. MAUGEL[4]

[1] *Department of Biology, University of South Florida, Tampa, Florida 33620;* [2] *Department of Medicine, Division of Rheumatology, Indiana University School of Medicine, Indianapolis, Indiana 46202;* [3] *Centro de Estudios del Cuaternario Fuego-Patagonia y Antártica Punta Arenas, Chile, and School of Biological Sciences, University of Auckland, Private Bag 92019, Auckland, New Zealand; and* [4] *Department of Biology, University of Maryland, College Park, Maryland 20742*

Abstract. We have employed electron microscopic, biochemical, and molecular techniques to clarify the species of origin of the "Chilean Blob," the remains of a large sea creature that beached on the Chilean coast in July 2003. Electron microscopy revealed that the remains are largely composed of an acellular, fibrous network reminiscent of the collagen fiber network in whale blubber. Amino acid analyses of an acid hydrolysate indicated that the fibers are composed of 31% glycine residues and also contain hydroxyproline and hydroxylysine, all diagnostic of collagen. Using primers designed to the mitochondrial gene *nad2*, an 800-bp product of the polymerase chain reaction (PCR) was amplified from DNA that had been purified from the carcass. The DNA sequence of the PCR product was 100% identical to *nad2* of sperm whale (*Physeter catadon*). These results unequivocally demonstrate that the Chilean Blob is the almost completely decomposed remains of the blubber layer of a sperm whale. This identification is the same as those we have obtained before from other relics such as the so-called giant octopus of St. Augustine (Florida), the Tasmanian West Coast Monster, two Bermuda Blobs, and the Nantucket Blob. It is clear now that all of these blobs of popular and cryptozoological interest are, in fact, the decomposed remains of large cetaceans.

Introduction

Sea monsters have been reported since ancient times. For instance, Homer described the sea monsters *Scylla* and *Charybdis*; the Bible spoke of *Leviathan*; and St. Brendan encountered the beast *Jasconius*. Later on, world-roving mariners such as Columbus, Magellan, and Cook described encounters with sea monsters. Many of these accounts have been variously attributed to early descriptions of cetaceans or other large aquatic mammals, to misidentification of natural phenomena, or simply to overactive imaginations. Because the deep sea is still difficult to explore, tales of large marine creatures, new to science, are rarely substantiated through direct field observations. However, a few monsters, like the Nordic tale of the *Kraken*—a large and ferocious squid-like animal—may have a basis in reality, as shown by the recovery last year of an intact colossal squid *Mesonychoteuthis hamiltoni* (http://news.nationalgeographic.com/news/2003/04/0423_030423_seamonsters.html), complete with hooklike tentacles and eyes the size of dinner plates.

For over a century the amorphous, decomposed remains of large animals have washed onto beaches around the world. Lacking a skeleton, or other identifiable morphology, a positive identification of the remains is problematic, especially by untrained observers. Wild claims, especially in the nonscientific literature, are regularly made that the blobs are the remains of sea monsters. For example, the Tasmanian West Coast Monster is still referred to as a monster,

---

Received 13 February 2004; accepted 5 April 2004.

[*] To whom correspondence should be addressed. E-mail: pierce@cas.usf.edu

although an Australian scientific team, led by W. Bryden, visited the carcass 2 years after it beached and identified it as a whale (Wall, 1981). Other relics such as the St. Augustine (Florida) Sea Monster and the Bermuda Blob are still described by some as the remains of a gigantic octopus (*Octopus giganteus*), even though A. E. Verrill—who named the St. Augustine specimen sight unseen—recanted his identification in favor of whale remains (Verrill, 1897a, b, c), and in spite of microscopic and biochemical analyses showing that they were nothing more than the collagenous matrix of whale blubber (Pierce *et al.*, 1995)

Last summer another blob washed ashore, this time on a beach in Chile (Fig. 1). The Chilean Blob rapidly generated a large amount of media interest around the world, and several immediate, and varied, identifications were made (including *O. giganteus*), almost all by novices with no more evidence than images of the carcass on the beach displayed on the Internet. Yet Chilean scientists, including G. P. Sanino of the Centre for Marine Mammals Research Leviathan in Santiago, had visited the grounding site and had identified the remains as that of a whale (pers. comm.).

To augment the gross anatomical observations of the carcass, we have obtained samples of the Chilean relic and have used a variety of techniques—including polymerase chain reaction (PCR) on recovered DNA—to establish its true identity. In addition, we have compared the results with those we have obtained from several other blobs, including some that have previously been reported (Pierce *et al.*, 1995).

Materials and Methods

Samples of carcasses

All of the carcasses were sampled by others and sent to us in a variety of states of preservation. The Chilean Blob (Fig. 1) was sampled from its location on Pinuno Beach, Los Muermos, Chile, within a few days after it was discovered on 26 July 2003, by Elsa Cabrera of the Chilean Centro de Conservación Cetacea. Some of the tissue was preserved in ethanol, and some was fresh frozen. The material was shipped to Tampa by overnight express, and the frozen tissue had thawed by the time it reached us. The St. Augustine carcass was originally sampled by Dewitt Webb, M.D., in 1896. Apparently it was initially preserved in formalin, which solution it was in when given to us by Professor Eugenie Clark in 1995 (Pierce *et al.*, 1995). Bermuda Blob 1, also provided by Professor Clark, washed onto Bermuda in 1995 and was also preserved in formalin when it was sampled (Pierce *et al.*, 1995). Bermuda Blob 2 beached in January 1997. Professor Wolfgang Sterrer of the Bermuda Biological Laboratory provided us with both formalin-fixed and fresh-frozen samples. The Tasmanian West Coast monster arrived on the beach in northwestern Tasmania in 1960, where it sat, mostly buried in sand, until it was sampled in

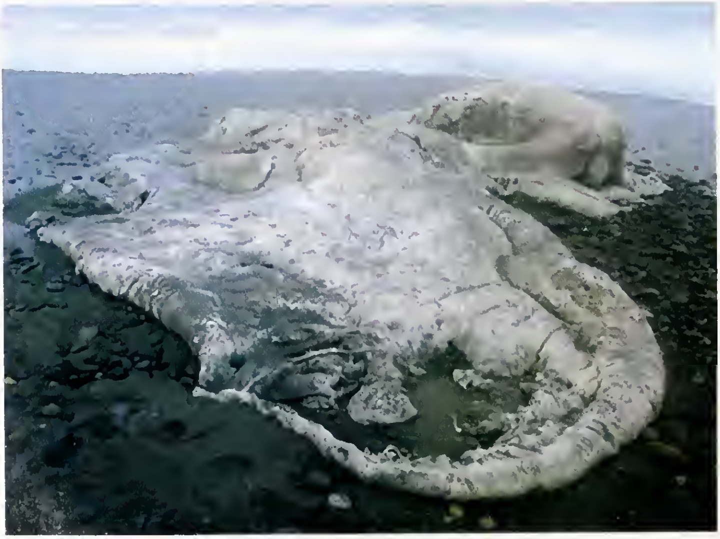

Figure 1. The Chilean carcass as it was found on Pinuno Beach. Photo by Elsa Cabrera (© E. Cabrera, 2003).

1962. After the existence of the monster was called to our attention by Leonard Wall—a member of the scientific party that sampled it—Curator A. P. Andrews of the Tasmanian Museum and Art Gallery in Hobart provided us with a sample in an unknown fixative which, by its odor, contained ethanol. Finally, the Nantucket Blob washed onto Nantucket Island, Massachusetts, sometime during November 1996. A sample was collected, frozen, and sent to us by personnel in the Nantucket Shellfish Warden's office.

Microscopy

The original conditions of preservation of the relics were unsatisfactory for electron microscopy. So, small pieces were cut off of each and soaked, at least overnight, in several changes of filtered (0.2 μm) artificial seawater. They were then placed into 2% glutaraldehyde and taken through the same fixation, embedding, and sectioning procedures that were described previously for the St. Augustine and Bermuda Blob 1 carcasses (Pierce *et al.*, 1995). The sections were viewed and photographed with a transmission electron microscope (Zeiss EM 10 or Phillips Morgagni).

Hydrolysis

Preliminary examination of the samples prepared for microscopy suggested strongly that all of the remains were almost exclusively composed of collagen fibers, as we had found before with the St. Augustine and Bermuda Blob 1 carcasses (Pierce *et al.*, 1995). To confirm the collagen identification, the amino acid compositions of hydrolysates of the carcass samples was determined as follows. Small pieces were cut off and soaked in seawater as above. Each piece was placed into 5N HCl and heated overnight at 100 °C. The hydrolysate was neutralized with concentrated NaOH, mixed 1:1 with ethanol, brought to a boil, and finally centrifuged at 20,000 × *g* for 20 min. The supernatant was lyophilized, and the residue was taken up in an appropriate volume of lithium citrate buffer. The amino acid composition of this solution was determined with a ninhydrin-based, HPLC analysis (Pierce *et al.*, 1995). Amino acid composition was calculated as residues/1000 amino acids.

Molecular analysis

The Chilean carcass was subjected to two independent molecular analyses. First, in Tampa (done by authors SEM and NEC), DNA was obtained from the frozen-thawed, unfixed tissue by phenol/chloroform extraction, followed by ethanol precipitation. The DNA was amplified in PCR using the temperature profile described previously (Carr *et al.*, 2002). The sequence of the universal primers corresponded to the vertebrate mitochondrial *nad2* gene—the same sequence used to identify *Physeter catadon* (= *macrocephalus*) (sperm whale) as the source of the Newfoundland Blob (Carr *et al.*, 2002). A single, 800-bp PCR product was obtained, then cloned into the pPCR-Script Amp SK (+) plasmid (Stratagene) and sequenced (model CEQ 8000, Beckman-Coulter) using the CEQ DTCS Quick Start Kit (Beckman-Coulter) and T3 sequencing primer.

The second independent analysis of the Chilean Blob was carried out in Auckland, New Zealand (by author CO). Genomic DNA was extracted with phenol/chloroform from three subsamples taken from an original 10-g, ethanol-preserved piece of tissue which was shipped to New Zealand by Ms. Cabrera. An 800-bp portion of the mtDNA control region, proximal to the Pro-tRNA gene, was amplified by PCR from two of the subsamples, using primer sequences Dlp-1.5 (Dalebout *et al.*, 1998) and Dlp-8G (Lento *et al.*, 1998; Pichler *et al.*, 2001). The temperature profile consisted of a 2-min preliminary denaturing period at 94 °C, followed by 35 cycles of 30-s denaturing at 94 °C, 40 s of annealing at 54 °C, and 40 s extension at 72 °C. Amplification and subsequent cycle sequencing were improved by the addition of an M13 tag to the 5′ end of the Dlp-1.5 primer. The PCR products were sequenced (model ABI3100, Applied Biosystems) in both directions, using the BigDye cycle sequencing kit, with M13Dlp-1.5 and Dlp-8G as the sequencing primers.

In addition to the Chilean Blob, we attempted, in Tampa, to extract DNA from samples of all the other remains. However, either because the samples of the other blobs were too small or because their preservation was wrong, only the Nantucket Blob yielded amplifiable DNA. A single, 800-bp PCR product was obtained from the Nantucket Blob, using the temperature profile of Carr *et al.* (2002) and the sequencing procedure that we described above. Subsequently, primers designed to the D-loop region of whale mitochondrial DNA (Wada *et al.*, 2003) were also used to amplify a single 1100-bp PCR product from the Nantucket Blob, which was sequenced as described above using T3 and T7 primers. The amplification conditions were an initial 90-s denaturation at 94 °C, 30 cycles of a 30-s denaturation at 94 °C, a 30-s annealing at 55 °C, and a 45-s extension at 72 °C, followed by a final 240-s extension at 72 °C.

Results

Fine structure

The microscopic anatomy of all the carcasses, including the Chilean Blob, is virtually identical (Figs. 2, 3). These large masses consist almost entirely of pure collagen fibers arranged in cross-hatched layers, often perpendicular to each other. This arrangement is exactly that of the collagen fiber infrastructure of freshly preserved humpback whale blubber (Fig. 2) (see also Pierce *et al.*, 1995) and is totally unlike the fine structure of octopus or squid mantle, which consists mostly of muscle fibers with only a few collagen fibers (Pierce *et al.*, 1995). Furthermore, al-

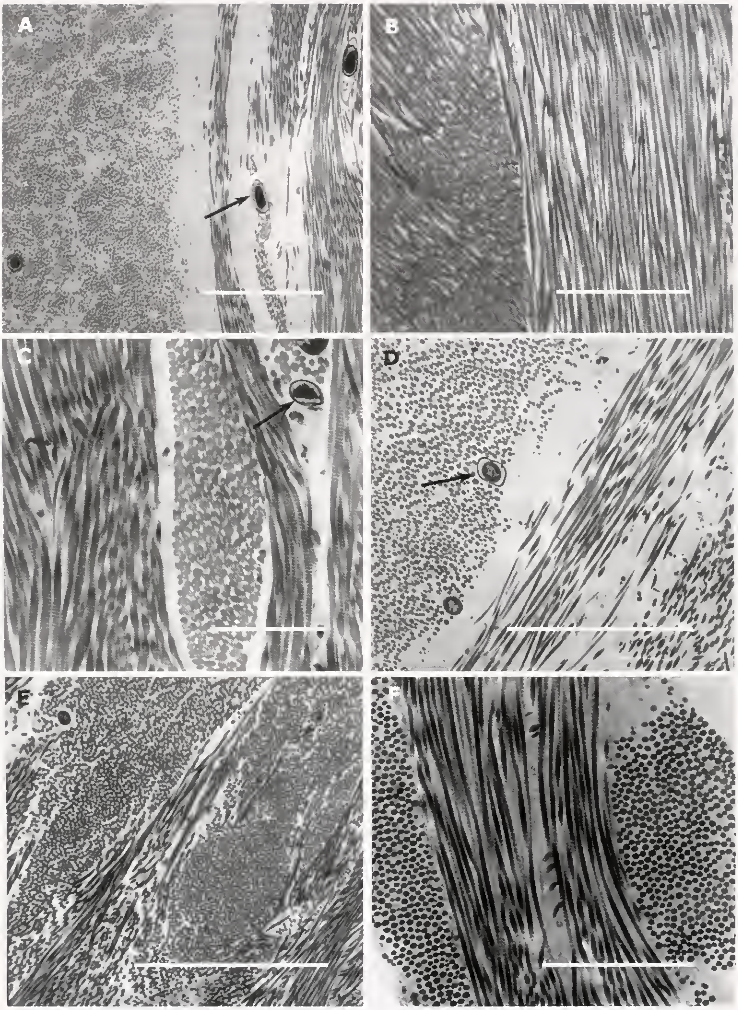

Figure 2. Electron micrographs of sections of tissue from various monsters. (A) St. Augustine carcass (from Pierce *et al.*, 1995); scale bar = 5 μm. (B) Bermuda Blob 1 (from Pierce *et al.*, 1995); scale bar = 5 μm. (C) Tasmanian West Coast Monster; scale bar = 2 μm. (D) Bermuda Blob 2; scale bar = 5 μm. (E) Nantucket Blob; scale bar = 5 μm. (F) Humpback whale blubber (from Pierce *et al.*, 1995); scale bar = 2 μm. In all cases, the tissues are composed entirely of collagen fibers arranged in layers of perpendicularly running fiber bundles. No cellular elements were found. Bacteria were often present amidst the fibers in the carcasses and can be seen in A, C, and D (arrows).

though the fiber layers in the blobs are much thicker than those in vertebrate skin, the arrangement of the collagen fibers in the two sites are similar (See Discussion). Virtually no cellular remnants, other than bacteria and bacterial cysts, were found in any of the carcasses, reflecting their advanced state of decay.

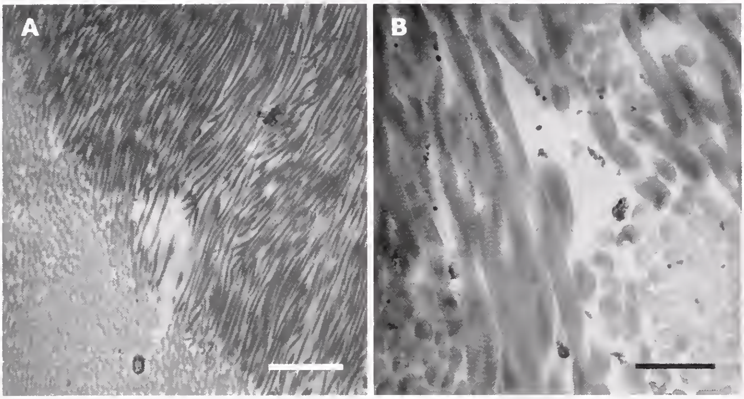

Figure 3. Electron micrographs of tissue sections from the Chilean Blob. (A) Lower magnification. Scale bar = 2 μm. (B) The banding pattern on the fibers is evident. As with the other carcasses, no cellular structures were present, but bacteria (bottom center of A) were often seen. Scale bar = 1 μm.

Amino acid composition

The amino acid compositions of the hydrolysates of all the carcasses were very similar, and they were also diagnostic of collagen. The amino acids in each blob hydrolysate consisted of about 30% glycine residues, and all contained residues of hydroxyproline and hydroxylysine (Table 1).

DNA sequences

The 587-bp consensus sequence (Genbank accession number AY582746) obtained from four sequencing runs on the DNA extracted in Tampa from the Chilean carcass was 100% identical to the mitochondrial *nad2* gene sequence of *P. catadon* (Genbank accession numbers AJ277029, AF414121) (Fig. 4). Sequencing of the PCR product ob-

Table 1

Comparative amino acid compositions of the blob tissue samples following acid hydrolysis (values are amino acid residues/1000 residues)

Amino acid	Chilean	St Augustine[a]	Bermuda 1[a]	Bermuda 2	Tasmanian	Nantucket
Asp	28	50	52	42	31	45
Thr	22	28	27	19	19	23
Ser	40	45	47	36	50	35
OH-Pro	90	54	79	113	84	146
Pro	213	169	88	182	92	136
Glu	63	82	83	62	78	63
Gly	314	330	339	298	363	280
Ala	96	106	113	94	133	94
Val	13	18	25	21	22	22
Cys	0	0	0	0	0	0
Met	4	0	0	3	1	3
Ile	8	11	14	10	11	11
Leu	25	28	32	23	30	25
Tyr	3	0	0	0	0	6
Phe	12	14	16	12	15	14
OH-Lys	11	15	13	26	7	20
Lys	21	0.4	10	18	12	25
His	6	4	6	0	0	8
Arg	29	48	55	42	51	45

[a] Data taken from Pierce *et al.*, 1995.

```
                  1                                                         60
Physeter catadon  TAATACTAACTATATCCCTACTCTCCATTCTCATCGGGGGTTGAGGAGGACTAAACCAGA
Chilean Blob      TAATACTAACTATATCCCTACTCTCCATTCTCATCGGGGGTTGAGGAGGACTAAACCAGA

                  61                                                       120
Physeter catadon  CTCAACTCCGAAAAATTATAGCTTACTCATCAATCGCCCACATAGGATGAATAACCACAA
Chilean Blob      CTCAACTCCGAAAAATTATAGCTTACTCATCAATCGCCCACATAGGATGAATAACCACAA

                  121                                                      180
Physeter catadon  TCCTACCCTACAATACAACCATAACCCTACTAAACCTACTAATCTATGTCACAATAACCT
Chilean Blob      TCCTACCCTACAATACAACCATAACCCTACTAAACCTACTAATCTATGTCACAATAACCT

                  181                                                      240
Physeter catadon  TCACCATATTCATACTATTTATCCAAAACTCAACCACAACCACACTATCTCTGTCCCAGA
Chilean Blob      TCACCATATTCATACTATTTATCCAAAACTCAACCACAACCACACTATCTCTGTCCCAGA

                  241                                                      300
Physeter catadon  CATGAAACAAAACACCCATTACCACAACCCTTACCATACTTACCCTACTTTCCATAGGGG
Chilean Blob      CATGAAACAAAACACCCATTACCACAACCCTTACCATACTTACCCTACTTTCCATAGGGG

                  301                                                      360
Physeter catadon  GCCTCCCACCACTCTCGGGCTTTATCCCCAAATGAATAATTATTCAAGAACTAACAAAAA
Chilean Blob      GCCTCCCACCACTCTCGGGCTTTATCCCCAAATGAATAATTATTCAAGAACTAACAAAAA

                  361                                                      420
Physeter catadon  ACGAAACCCTCATCATACCAACCTTCATAGCCACCACAGCATTACTCAACCTCTACTTCT
Chilean Blob      ACGAAACCCTCATCATACCAACCTTCATAGCCACCACAGCATTACTCAACCTCTACTTCT

                  421                                                      480
Physeter catadon  ATATACGCCTCACCTACTCAACAGCACTAACCCTATTCCCCTCCACAAATAACATAAAAA
Chilean Blob      ATATACGCCTCACCTACTCAACAGCACTAACCCTATTCCCCTCCACAAATAACATAAAAA

                  481                                                      540
Physeter catadon  TAAAATGACAATTCTACCCCACAAAACGAATAACCCTCCTGCCAACAGCAATTGTAATAT
Chilean Blob      TAAAATGACAATTCTACCCCACAAAACGAATAACCCTCCTGCCAACAGCAATTGTAATAT

                  541                                         587
Physeter catadon  CAACAATACTCCTACCCCTTACACCAATACTCTCCACCCTATTATAG
Chilean Blob      CAACAATACTCCTACCCCTTACACCAATACTCTCCACCCTATTATAG
```

Figure 4. Alignment of sperm whale *nad2* nucleotide sequence with that of the PCR product from the Chilean Blob DNA. The sequences are identical.

tained from the Chilean Blob in the Auckland extraction had a 552-bp consensus sequence (Genbank accession number AY 582747) that was 99% identical to the mitochondrial control region sequence of *P. catadon* (Genbank accession numbers AJ277029, X72203, M93154). The sequence obtained in Auckland for the Chilean Blob differed by a single nucleotide from the three *P. catadon* sequences in the database (Fig. 5). The first 429-bp consensus sequence obtained from the Nantucket Blob DNA was 99% identical with the mitochondrial *nad2* gene sequence of *Balaenoptera physalus* (finback whale) (Genbank accession number X61145); only a single nucleotide was different (data not shown). The subsequent 1055-bp consensus sequence (Genbank accession number AY58748) obtained from 2–4 sequencing runs on the Nantucket Blob DNA was 99% identical to the control region of *B. physalus* mitochondrial DNA (Genbank accession number X61145), with only six nucleotide differences (Fig. 6).

Discussion

The molecular results reported here provide irrefutable evidence that the Chilean carcass was the highly decomposed remains of a sperm whale. The nearly 100% match between the two gene sequences obtained in our PCR experiments and the *Physeter catadon* gene sequences leaves no other possibility. The match between the Nantucket Blob DNA and the control region mitochondrial DNA of *Balaenoptera physalus* is equally robust, leaving no doubt about the specific identity of that relic. The six nucleotide differences observed were consistent with variation within the fin whale species and may indicate a different subpopulation from the previously published sequence (Arnason *et al.*, 1991), although even if this is case, both sequences were from specimens of North Atlantic origin. Unfortunately, our attempts to extract usable DNA from the other monsters were not successful, due most likely to some combination of

```
                  1                                                         60
Physeter catadon  CATCATAGATAAATACAAACCCACAGTGCTATGTCAGTATTAAAAATAACCCACCCAATT
Chilean Blob      CATCATAGATAAATACAAACCCACAGTGCTATGTCAGTATTAAAAATAACTCACCCAATT
                                                                    -

                  61                                                       120
Physeter catadon  ACATCTTTCCTACTCCCGACCATACCAATGCCCCCATGCCAATATTCAGCGTTCTCCCTG
Chilean Blob      ACATCTTTCCTACTCCCGACCATACCAATGCCCCCATGCCAATATTCAGCGTTCTCCCTG

                  121                                                      180
Physeter catadon  TAAATGTATACATGTACACGCTATGTATAATAGTGCATTCAATTATTTTCACTACGATCA
Chilean Blob      TAAATGTATACATGTACACGCTATGTATAATAGTGCATTCAATTATTTTCACTACGATCA

                  181                                                      240
Physeter catadon  GTGAAAGCTCGTATTAAATCTTATTAATTTTACATATTACATAAAATTATGGATCGTACA
Chilean Blob      GTGAAAGCTCGTATTAAATCTTATTAATTTTACATATTACATAAAATTATGGATCGTACA

                  241                                                      300
Physeter catadon  TAGGACATATCCTTAAATCAACTCCAGTCCCCTGAAATTATGAGCTCTCGGATCAGACCA
Chilean Blob      TAGGACATATCCTTAAATCAACTCCAGTCCCCTGAAGTTATGAGCTCTCGGATCAGACCA
                                                      -

                  301                                                      360
Physeter catadon  CGAGCTTGATCACCATGCCGCGTGAAACCAGCAACCCGCTTGGCAGGGACTCACTATTAT
Chilean Blob      CGAGCTTGATCACCATGCCGCGTGAAACCAGCAACCCGCTTGGCAGGGACTCACTATTAT

                  361                                                      420
Physeter catadon  TGTATCTCAGGCCCATTCCTCGAAAGCCGTGCTACTCCGTGGTTTTTCCAAGGCCTCTAG
Chilean Blob      TGTATCTCAGGCCCATTCCTCGAAAGCCGTGCTACTCCGTGGTTTTTCCAAGGCCTCTAG

                  421                                                      480
Physeter catadon  TTGCAATTCTCAGGGTCATAACTCGAGGCACCTGCGCTAGTTCCAGCTTTTTCCAAGGCC
Chilean Blob      TTGCAATTCTCAGGGTCATAACTCGAGGCACCTGCGCTAGTTCCAGCTTTTTCCAAGGCC

                  481                                                      540
Physeter catadon  TCGGCTTGGACCTGAGAGCAGGAGCCTCCACCCTATTAATCACTCACGGGGGGAGTTATA
Chilean Blob      TCGGCTTGGACCTGAGAGCAGGAGCCTCCACCCTATTAATCACTCACGGGGGGAGTTATA

                  541
Physeter catadon  GGCATCTGGTCG
Chilean Blob      GGCATCTGGTCG
```

Figure 5. Alignment of sperm whale mtDNA control region nucleotide sequence with that of the PCR product from the Chilean Blob DNA. Nucleotide differences are indicated in **boldface** and underlined.

method of preservation, small sample size, or advanced stage of decomposition. However, when the microscopic anatomy and biochemical composition of the Chilean and Nantucket Blobs are compared with those of the other remains, similarities are manifest. Thus, there is no doubt that they are all derived from the same type of organism.

The amino acid composition of the hydrolysates of all the blobs consists of about 30% glycine residues along with some hydroxyproline and hydroxylysine residues. Only collagen has such an amino acid composition (Eastoe, 1955; Kimura *et al.*, 1969). While there are some differences among the amino acid compositions of the blob hydrolysates—likely resulting from differences in preservation as well as species—the results indicate that all the blobs, including the Chilean and Nantucket, are large masses of collagen.

The collagenous matrix of the blobs is confirmed by their fine structure. They are all composed of bundles of long, banded fibers that are similar in their dimensions, not only to each other, but also to the collagen fibers in rat tail tendon (see Pierce *et al.*, 1995). The bundles of fibers are arranged parallel to each other in layers, and each layer is sandwiched between perpendicularly oriented layers of other fiber bundles. The fiber layering pattern is similar to the arrangement of collagen fibers in vertebrate dermis (Moss, 1972), and identical to the collagen fiber pattern in humpback whale blubber and in all the other blobs. In addition, the unimodal fiber diameter and the tight packaging of the fibers in the Chilean Blob and the others is characteristic of mammalian dermis, including pygmy sperm whale blubber (Craig *et al.*, 1987) and our humpback blubber control. Collagen is much less abundant in octopus and squid mantle, which are composed primarily of muscle; and the few collagen fibers present in these molluscan species are not arranged in the network (Pierce *et al.*, 1995) so obvious in the Chilean Blob and the other blob tissue samples. Thus, both the biochemical and microscopic analyses show clearly that the Chilean

```
                      1                                                         60
Balaenoptera physalus CCTCCCTAAGACTCAAGGAAGAAGTATTACACTCCACCATCAGCACCCAAAGCTGAAGTT
Nantucket Blob        CCTCCCTAAGACTCAAGGAAGAAGTATTACACTCCACCATCAGCACCCAAAGCTGAAGTT

                      61                                                       120
Balaenoptera physalus CTACATAAACTATTCCCTGAAAAAGTATATTGTACAATAACCACAGGACCACAGTACTAT
Nantucket Blob        CTACATAAACTATTCCCTGAAAAAGTATATTGTACAATAACCACAGGACCACAGTACTAT

                      121                                                      180
Balaenoptera physalus GTCCGTATTGAAAATAACTTGCCTTATTAGATATTATTATGTAACTCGTGCATGCATGTA
Nantucket Blob        GTCCGTATTGAAAATAACTTGCCTTATTAGATATTATTATGTAACTCGTGCATGTATGTA
                                                                            -
                      181                                                      240
Balaenoptera physalus CTTCCACATAATTAATAGCGTCTTTCCATGGGTATGAACAGATATACATGCTATGTATAA
Nantucket Blob        CTTCCACATAATTAATAGCGTCTTTCCATGGGTATGAACAGATATACATGCTATGTATAA

                      241                                                      300
Balaenoptera physalus TTGTGCATTCAATTATTTTCACCACGAGCAGTTGAAGCTCGTATTAAATTTTATTAATTT
Nantucket Blob        TTGTGCATTCAATTATTTTCACCACGAGCAGTTGAAGCTCGTATTAAATTTTATTAATTT

                      301                                                      360
Balaenoptera physalus TACATATTACATAATATGTATTAATAGTACAATAGCGCATGTTCTTATGCATCCCCAGAT
Nantucket Blob        TACATATTACATAATATGTATTAATAGTACAATAGCGCATGTTCTTATGCATCCCCAGGT
                                                                                -
                      361                                                      420
Balaenoptera physalus CTATTTAAATCAAATGATTCCTATGGCCGCTCCATTAGATCACGAGCTTAGTCAGCATGC
Nantucket Blob        TTATTTAAATCAAATGATTCTTATGGCCGCTCCATTAGATCACGAGCTTAGTCAGCATGC
                      -                   -
                      421                                                      480
Balaenoptera physalus CGCGTGAAACCAGCAACCCGCTTGGCAGGGATCCCTCTTCTCGCACCGGGCCCATCACTC
Nantucket Blob        CGCGTGAAACCAGCAACCCGCTTGGCAGGGATCCCTCTTCTCGCACCGGGCCCATTAATC
                                                                             - -
                      481                                                      540
Balaenoptera physalus GTGGGGGTAGCTATTTAATGATCTTTATAAGACATCTGGTTCTTACTTCAGGACCATATT
Nantucket Blob        GTGGGGGTAGCTATTTAATGATCTTTATAAGACATCTGGTTCTTACTTCAGGACCATATT

                      541                                                      600
Balaenoptera physalus AACTTAAAATCGCCCACTCGTTCCCCTTAAATAAGACATCTCGATGGGTTAATTACTAAT
Nantucket Blob        AACTTAAAATCGCCCACTCGTTCCCCTTAAATAAGACATCTCGATGGGTTAATTACTAAT

                      601                                                      660
Balaenoptera physalus CAGCCCATGATCATAACATAACTGAGGTTTCATACATTTGGTATTTTTTTATTTTTTTTG
Nantucket Blob        CAGCCCATGATCATAACATAACTGAGGTTTCATACATTTGGTATTTTTTTATTTTTTTTG

                      661                                                      720
Balaenoptera physalus GGGGGCTTGCACGGACTCCCCTATGACCCTAAAGGGTCTCGTCGCAGTCAGATAAATTGT
Nantucket Blob        GGGGGCTTGCACGGACTCCCCTATGACCCTAAAGGGTCTCGTCGCAGTCAGATAAATTGT

                      721                                                      780
Balaenoptera physalus AGCTGGGCCTGGATGTATTTGTTATTTGACTAGCACAACCAACATGTGCAGTTAAATTAA
Nantucket Blob        AGCTGGGCCTGGATGTATTTGTTATTTGACTAGCACAACCAACATGTGCAGTTAAATTAA

                      781                                                      840
Balaenoptera physalus TGGTTACAGGACATAGTACTCCACTATTCCCCCCGGGCTCAAAAAACTGTATGTCTTAGA
Nantucket Blob        TGGTTACAGGACATAGTACTCCACTATTCCCCCCGGGCTCAAAAAACTGTATGTCTTAGA


                      841                                                      900
Balaenoptera physalus GGACCAAACCCCCCTCCTTCCATACAATACTAACCCTCTGCTTAGATATTCACCACCCCC
Nantucket Blob        GGACCAAACCCCCCTCCTTCCATACAATACTAACCCTCTGCTTAGATATTCACCACCCCC

                      901                                                      960
Balaenoptera physalus CTAGACAGGCTCGTCCCTAGATTTAAAAGCCATTTTATTTATAAATCAATACTAAATCTG
Nantucket Blob        CTAGACAGGCTCGTCCCTAGATTTAAAAGCCATTTTATTTATAAATCAATACTAAATCTG

                      961                                                     1020
Balaenoptera physalus ACACAAGCCCAATAATGAAAATACATGAACGCCATCCCTATCCAATACGTTGATGTAGCT
Nantucket Blob        ACACAAGCCCAATAATGAAAATACATGAACGCCATCCCTATCCAATACGTTGATGTAGCT

                      1021                           1055
Balaenoptera physalus TAAACACTTACAAAGCAAGACACTGAAAATGTCTA
Nantucket Blob        TAAACACTTACAAAGCAAGACACTGAAAATGTCTA
```

Figure 6. Alignment of fin whale mitochondrial control region nucleotide sequence with that of the PCR product from the Nantucket Blob DNA. Nucleotide differences are indicated in **boldface** and underlined.

Blob has the characteristics of all the other blobs and is the remains of the collagen matrix of whale blubber—as are they all.

The results, taken together, leave no doubt that all of the blobs examined here—St. Augustine, Bermuda 1, Bermuda 2, Tasmanian West Coast, Nantucket, and Chilean—represent the decomposed remains of great whales of varying species. Once again, to our disappointment, we have not found any evidence that any of the blobs are the remains of gigantic octopods, or sea monsters of unknown species.

Acknowledgments

This study was supported by resources from the Department of Biology at the University of South Florida. We thank Dr. Charles Potter of the Smithsonian Museum of Natural History, Washington, DC, for kindly providing the sample of humpback whale blubber from a specimen in the Museum's collection. We also thank Dr. Shiro Wada of the National Institute of Fisheries Science, Yokohama, Japan, for advice on the PCR conditions for the Nantucket Blob.

Literature Cited

Arnason, U., A. Gullberg, and B. Widegren. 1991. The complete nucleotide sequence of the mitochondrial DNA of the fin whale, *Balaenoptera physalus*. *J. Mol. Evol.* **33:** 556–568.

Carr, S. M., H. D. Marshall, K. A. Johnstone, L. M. Pynn, and G. B. Stenson. 2002. How to tell a sea monster: molecular discrimination of large marine animals of the North Atlantic. *Biol. Bull.* **202:** 1–5.

Craig, A. S., E. F. Eikenberry, and D. A. D. Parry. 1987. Ultrastructural organization of skin: classification on the basis of mechanical role. *Connect. Tissue Res.* **16:** 212–223.

Dalebout, M., A. Van Helden, K. Van Waerebeek, and C. S. Baker. 1998. Molecular genetic identification of southern hemisphere beaked whales (Cetacea: Ziphiidae). *Mol. Ecol.* **7:** 687–695.

Eastoe, J. E. 1955. The amino acid composition of mammalian collagen and gelatin. *Biochem. J.* **61:** 589–600.

Kimura, S., Y. Nagoka, and M. Kubota. 1969. Studies on marine invertebrate collagens. I. Some collagens from crustaceans and molluscs. *Bull. Jpn. Soc. Sci. Fish.* **35:** 743–748.

Lento, G. M., M. J. Dalebout, and C. S. Baker. 1998. Species and individual identification of whale and dolphin products for sale in Japan by mtDNA sequences and nuclear microsatellite profiles. Report (SC/50/O8) to the Scientific Committee of the International Whaling Commission, Oman.

Moss, M.L. 1972. The vertebrate dermis and the integumental skeleton. *Am. Zool.* **12:** 27–34.

Pichler, F. B., D. Robineau, R. N. P. Goodall, M. A. Meyer, C. Olavarría, and C. S. Baker. 2001. Origin and radiation of Southern Hemisphere coastal dolphins (genus *Cephalorhynchus*). *Mol. Ecol.* **10:** 2215–2223.

Pierce, S. K., G. N. Smith, Jr., T. K. Maugel, and E. Clark. 1995. On the giant octopus (*Octopus giganteus*) and the Bermuda Blob: homage to A. E. Verrill. *Biol. Bull.* **188:** 219–230.

Verrill, A. E. 1897a. The supposed great Octopus of Florida: certainly not a cephalopod. *Am. J. Sci.* 4th series, **3:** 355.

Verrill, A. E. 1897b. The Florida monster. *Science* **5(114):** 392.

Verrill, A. E. 1897c. The Florida sea monster. *Science* **5(116):** 476.

Wada, S., M. Oishi, and T. K. Yamada. 2003. A newly discovered species of living baleen whale. *Nature* **426:** 278–281.

Wall, L. E. 1981. The west coast monster, 1962. *Tasmanian Naturalist* **103:** 2–6.

Reference: *Biol. Bull.* **206:** 134–143. (June 2004)
© 2004 Marine Biological Laboratory

Chemical and Visual Communication During Mate Searching in Rock Shrimp

ELIECER R. DÍAZ[1] AND MARTIN THIEL[1,2,*]

[1] *Universidad Católica del Norte, Facultad de Ciencias del Mar, Larrondo 1281, Coquimbo, Chile; and*
[2] *Centro de Estudios Avanzados en Zonas Áridas (CEAZA), Coquimbo, Chile*

Abstract. Mate searching in crustaceans depends on different communicational cues, of which chemical and visual cues are most important. Herein we examined the role of chemical and visual communication during mate searching and assessment in the rock shrimp *Rhynchocinetes typus.* Adult male rock shrimp experience major ontogenetic changes. The terminal molt stages (named "robustus") are dominant and capable of monopolizing females during the mating process. Previous studies had shown that most females preferably mate with robustus males, but how these dominant males and receptive females find each other is uncertain, and is the question we examined herein. In a Y-maze designed to test for the importance of waterborne chemical cues, we observed that females approached the robustus male significantly more often than the typus male. Robustus males, however, were unable to locate receptive females *via* chemical signals. Using an experimental set-up that allowed testing for the importance of visual cues, we demonstrated that receptive females do not use visual cues to select robustus males, but robustus males use visual cues to find receptive females. Visual cues used by the robustus males were the tumults created by agitated aggregations of subordinate typus males around the receptive females. These results indicate a strong link between sexual communication and the mating system of rock shrimp in which dominant males monopolize receptive females. We found that females and males use different (sex-specific) communicational cues during mate searching and assessment, and that the sexual communication of rock shrimp is similar to that of the American lobster, where females are first attracted to the dominant males by chemical cues emitted by these males. A brief comparison between these two species shows that female behaviors during sexual communication contribute strongly to the outcome of mate searching and assessment.

Introduction

Mating systems are expressions of the strategies that both sexes use to find each other and mate (Shuster and Wade, 2003). These strategies, mediated by population demography and ecological variables, depend on specific communication systems between the sexes, which facilitate mate finding and subsequently aid in regulating the mating process (Salmon, 1983). In crustaceans, sexual communication is based on visual, chemical, and acoustic cues (Salmon, 1983; Hughes, 1996; Bushmann, 1999), but chemical signals are of major importance in most aquatic species (Atema, 1995). In many species, individuals are dispersed over variable distances, and mating partners need to locate each other during the searching phase. To better understand the mating system of a species, it is particularly important to know which sex is searching for the other and to identify the communicational cues used during mate searching and assessment.

Chemical communication in aquatic crustaceans may act (1) over distance *via* waterborne odors or (2) by direct contact *via* chemo-tactile signals (Salmon, 1983). Odors may be emitted by either sex to attract potential mates over variable distances (*e.g.*, Dunham, 1978; Atema and Cobb, 1980; Bamber and Naylor, 1996; Bushmann and Atema, 1997). For example, in *Homarus americanus* (Cowan, 1991) and *Callinectes sapidus* (Bushmann, 1999), the female is guided towards the male by a pheromone in the male's urine. In contrast, in *Chionoecetes opilio*, the male is guided by an ecdysteroid from pubescent and multiparous

Received 15 December 2003; accepted 15 March 2004.

[*] To whom correspondence should be addressed. E-mail: thiel@ucn.cl

females (Bouchard *et al.*, 1996). Similarly, in *Carcinus maenas,* waterborne signals from the premolt female evoke searching in males (Bamber and Naylor, 1996). Contact chemoreception, which usually occurs when males and females touch each other during assessment and mating (see Salmon, 1983), has been reported for many crustaceans (Borowsky, 1991; Kelly and Snell, 1998; Correa and Thiel, 2003a).

Visual sexual communication involves cues such as color, shape, and size of morphological structures or resources (*e.g.*, shelters), often in connection with elaborate courtship behaviors (*e.g.*, Latruffe *et al.*, 1999; Christy *et al.*, 2003). Visual signals are reported mostly for crustaceans from terrestrial environments (Salmon, 1983; Burggren and McMahon, 1988; Backwell *et al.*, 1998; Pope, 2000), but also occur in some species from shallow aquatic environments (Hatziolos and Caldwell, 1983; Hughes, 1996; Acquistapace *et al.*, 2002). When visual signals are used in the aquatic environment, they are often accompanied by chemical cues (see review by Salmon, 1983). Combined visual and chemical signals have been reported in the snapping shrimp *Alpheus heterochaelis* (Hughes, 1996), in smasher stomatopods (Christy and Salmon, 1991; Marshall *et al.*, 1999), and in freshwater crayfish (Acquistapace *et al.*, 2002).

Most studies examining sexual communication in crustaceans focus on signal perception in only one sex, either the males or females (Salmon, 1983; Christy and Salmon, 1991; Bamber and Naylor, 1996; Bouchard *et al.*, 1996; Kamio *et al.*, 2002). Similarly, many studies focus exclusively on either visual cues (*e.g.*, Marshall *et al.*, 1999) or chemical cues (*e.g.*, Cowan, 1991), these being the two most important ones in aquatic crustaceans. Several studies, though, have demonstrated that both sexes are involved in signal exchange (Atema and Voigt, 1995; Bushmann, 1999) and that often more than one sense is employed during crustacean communication (Hughes, 1996). In particular, when individuals assess each other, they may base their decision on multiple signals (Sneddon *et al.*, 2003). This should be expected primarily during sexual communication in those species where members of one or both sexes show strong preferences for specific individuals of the opposite sex.

The rock shrimp *Rhynchocinetes typus* Milne Edwards 1837, which is abundant on shallow subtidal hard bottoms along the coasts of the southeastern Pacific (*e.g.*, Caillaux and Stotz, 2003), presents a mating system described as "neighborhood of dominance" (Correa and Thiel, 2003a). Male rock shrimp reach sexual maturity in the female-like typus stage, and during growth they pass through several intermedius stages before reaching the terminal molt stage, named robustus. The robustus males feature highly developed 1st pereopods and 3rd maxillipeds, and they are dominant over the ontogenetically younger stages. Robustus males have high resource-holding potential and can defend females during the entire mating process (Correa *et al.*, 2003), and they also have larger sperm supplies than subordinate typus males (Hinojosa and Thiel, 2003). Receptive females prefer to mate with robustus males (Díaz and Thiel, 2003; Thiel and Hinojosa, 2003) even though these are comparatively rare in natural populations (Correa and Thiel, 2003b). Consequently, it can be expected that both robustus males and receptive females have developed efficient sexual communication to find each other. Receptive females might utilize visual signals such as the distinct morphological characteristics of robustus males to identify them. The robustus males might in turn use visual cues such as tumults developing around receptive females to identify and locate them. Tumults are agitated aggregations of several typus males that attempt to gain access to the receptive female. These tumults are visible over distances of several shrimp body lengths, and it is possible that robustus males perceive these tumults and approach the receptive female. However, since visual cues might be of minor importance in coastal habitats with limited visibility, chemical cues might also be important during sexual communication of rock shrimp.

In the present study, we examined whether receptive females and robustus males of the rock shrimp utilize chemical cues, visual cues, or both to locate and assess a potential mating partner.

Materials and Methods

Experiments were conducted during austral summer (February to April, water temperatures: 14.8–18.9 °C) and spring (September to October, 13.0–15.2 °C) of 2002 in a flowing seawater laboratory located near Bahía La Herradura, Coquimbo, Chile (29°59′S, 79°21′W). Shrimp were collected from the field by using a diver-operated suction sampler and were maintained in the laboratory in tanks with flowing and aerated seawater. They were fed fish and molluscs *ad libitum.* Females and males were held in separate tanks each containing up to 30 shrimp. Every morning the tanks with the females were examined to identify recently molted females, which are receptive 24 h after molting. The molted females were individually held in containers (surface area 20 cm × 20 cm and height 15 cm) with flowing seawater until the following day, when they were used in the experiments (for further details, see Correa *et al.*, 2003; Hinojosa and Thiel, 2003). After each replicate, the receptivity of the female was confirmed by allowing it to mate with a robustus male—if the female did not mate during this opportunity, the replicate was eliminated. The males used for the experiments were either in the terminal molt stage (robustus males) or in the intermolt phase (typus males). All individuals were used only once in these experiments, except where noted otherwise.

Chemical communication experiments

We used a Y-maze (Fig. 1A) to examine whether waterborne chemical cues play a role during mate searching in receptive females and robustus males. Seawater entered the Y-maze through two small branches, which converged in the choice chamber. The flow speed in the two branches was ~1 cm s^{-1}. In the upstream part of each branch was a shelter for the shrimp designated as a potential sender of chemical cues; shrimp were randomly assigned to one of the two branches. The shelter was separated from the branches by a barrier of multiple layers of black mesh that prevented mechanical and visual contact, but allowed water to pass. The shrimp to be tested was placed downstream in the choice chamber under a plastic bell with holes allowing contact with the surrounding water. The acclimation period was 30 min for females and 60 min for males: preliminary experiments had shown that robustus males require more time to calm down after handling than females. Following release, the tested shrimp was observed for 30 min, and after each experiment the tank was washed three times with fresh water.

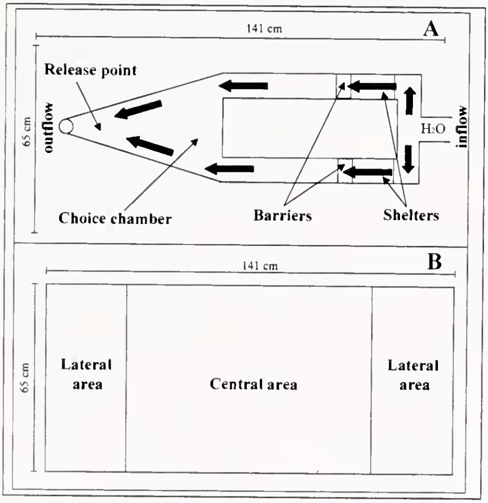

Figure 1. The experimental set-up. (A) The Y-maze used to study the importance of chemical cues that receptive females and dominant robustus males employ to locate potential mating partners. The tested individual was released downstream in the choice chamber; from there it could select one of the upstream branches leading to the shelter of a target individual from the opposite sex. (B) The seawater tank used to study the importance of visual cues employed by receptive females and dominant robustus males to locate their respective potential mating partners. The tested individual was released in the central compartment, while the target individuals from the opposite sex were placed in the lateral compartments. The central compartment was hermetically separated from the lateral compartments by a sealed glass window.

Receptive females: Are receptive females guided by chemical cues in locating robustus males? One typus male was placed in the upstream shelter in one branch of the Y-maze, and one robustus male was placed in the upstream shelter of the other branch. After releasing a receptive female, we observed it for a maximum of 30 min. If the female spent 10 continuous minutes in one branch of the Y-maze, the male in the corresponding shelter was considered to be the chosen male. If the receptive female did not show a preference for either branch during the 30 min of observation, the replicate was considered as a no-choice. We conducted 12 replicates and used a χ^2 goodness-of-fit test to determine whether females chose robustus males more frequently than they chose typus males.

Robustus males: Are robustus males guided by chemical cues in locating receptive females? This experiment was divided into two parts, which differed by the absence or presence of typus males with the females. In part 1, a receptive female and a nonreceptive female were separately placed in the shelters at the upstream part of each branch of the Y-maze. After releasing the robustus male, we observed it for a maximum of 30 min. If the male stayed in one branch of the Y-maze for a continuous 10-min period, the female in the corresponding shelter was considered to be the chosen female. At the conclusion of part 1, the robustus male was again placed at the end of the choice chamber, where it was re-acclimated for 15 min. During this time, two typus males were added to the shelter of each female to induce mating interactions with the receptive female. Following release of the robustus male, observations were conducted as in part 1. In both parts (n = 18 replicates for part 1, n = 17 for part 2), we used a χ^2 goodness-of-fit test to determine whether robustus males oriented to the receptive female more often than to the nonreceptive female. In addition, we used a two-tailed Student's t-test for independent samples to compare the reaction times (start of experiment until the robustus male chooses a female).

Visual communication experiments

The visual cues used during mate searching were examined by providing visual signals to the receptive female and the dominant robustus male. The experiments were conducted in a large indoor tank (surface area 141 cm × 65 cm and height 30 cm) filled to a water level of 20 cm. This tank was divided into three compartments separated from each other by hermetically sealed glass windows (Fig. 1B). The observations were conducted during daylight hours (1100 to 1600). The tested shrimp (receptive female or robustus male) was placed in the central compartment where it was acclimated behind a glass fence (allowing it to see in all directions). The lateral compartments contained the shrimp that were used to generate visual signals (see below). The duration of the observation differed between the sexes (60 min for robustus males, 90 min for females) since previous studies had shown that robustus males usually seize receptive females within 60 min (Correa *et al.*, 2000), but females may delay mate choice for more than 60 min (Díaz and Thiel, 2003).

Receptive females: Can receptive females distinguish between typus and robustus males via *visual cues?* Each experiment used two males—a robustus and a typus—and randomly assigned one to each lateral compartment, where they were tethered to the bottom of the experimental tank. Tethering prohibited the males from actively courting the female behind the glass window and limited the visual signal to the morphological characteristics of the male. During the experiment, some males attempted to move once the female approached their glass window, but they were kept in place by the tether. Males were tethered 24 h before the start of the experiment, which was sufficient for them to acclimatize.

Following an acclimation period of 30 min, the receptive female was released in the central compartment of the tank, and her behavior was registered for 90 min. We quantified the following variables: (a) time of first visit to each male, (b) duration and frequency of individual visits to each male, and (c) male attended by the female at the end of the experiment. We use the term visit to refer to the female touching the glass window of the respective male. Finally, we tested the null hypothesis that the frequencies of the first visit and the last visit to either male were similar by using a χ^2 goodness-of-fit test. We also tested whether the total duration of visits by the female to each male differed between typus and robustus males by using the two-tailed Student's t-test for dependent samples.

Robustus males: How important are visual cues for the robustus male? We examined this question using tumults generated by typus males around a receptive female. These tumults are visible over distances of several shrimp body lengths, and we hypothesized that they could indicate the presence of a receptive female to robustus males. We used different numbers of typus males together with a receptive female to test whether (1) tumults were produced, (2) the frequency of visual cues increased with increasing numbers of typus males, and (3) robustus males reacted to these visual cues.

Different numbers (2, 3, 4, 8, and 12) of typus males were placed in each lateral compartment 24 h before the start of the experiment. For a given treatment, the same number of typus males were always put in each lateral compartment. At the end of the acclimation period of the males, a receptive female was introduced into one lateral compartment, while a nonreceptive female was introduced into the other lateral compartment. Females were assigned randomly to each lateral compartment, where they were acclimated under a transparent plastic bell (made from the upper part of a plastic bottle) for 15 min before the start of the experiment. Because of a shortage of receptive females, replication of the different treatments (number of typus males) was unequal, ranging from $n = 8$ (two typus males) to $n = 5$ (two treatments, with four and eight typus males, respectively). The experiment lasted for 60 min after release of the females.

To assess whether the number and intensity of visual signals depended on the number of typus males, we counted the number of tumults per treatment and determined the total mating time of the receptive female with different numbers of typus males. Two Kruskal-Wallis tests (both two-tailed) were conducted to test for significant differences in these variables. While the robustus male was being acclimated for 15 min behind a glass fence in the central compartment, the females were introduced to the lateral compartments. After release of the male, we observed its behavior for 60 min and counted the number and duration of its visits to each of the two lateral compartments. Using a χ^2 goodness-of-fit test, we compared the number of males visiting the receptive and the nonreceptive female during the first and last visits. To examine whether the robustus male used visual signals to locate the receptive female, we calculated the total duration of visits to each female. Three independent parametric tests were run: (a) a one-way ANOVA to compare the total visit duration by the robustus male to the receptive female between the different typus treatments, (b) a parallel one-way ANOVA to compare the total visit duration by the robustus male to the nonreceptive female between the different typus treatments, and (c) a one-tailed Student's t-test for dependent samples to determine whether the total visit duration by the robustus male (pooling all typus treatments) was longer for the receptive than for the nonreceptive females (Zar, 1999).

Statistical analysis

To assess frequencies of choices made by either robustus males or receptive females in the different experiments, we conducted χ^2 goodness-of-fit tests. All other data were tested for homogeneity of variances using the Cochran C-test. If the original data failed the normality test, they were $\ln(x + 1)$ transformed. A Student's t-test was used when variances were homogeneous. One-way ANOVAs were used to test for significant difference between treatments, followed by a *post hoc* Tukey test. If variances were not homogeneous after transformation, we conducted nonparametric Kruskal-Wallis tests, followed by a *post hoc* Dunn test. All tests were carried out with a significance level of $\alpha = 0.05$.

Results

Chemical communication

Receptive females: Are receptive females guided by chemical cues in locating robustus males? Following release, most females (10 of 12) chose the branch with the robustus male. When the plastic acclimation bell was removed, these ten females went directly to the robustus male (mean ± SD: 1.22 ± 2.14 min). Only one female remained for 30 min in the choice chamber. The female that chose the typus male entered and left the typus branch twice before finally staying with the typus. The difference between the females choosing the robustus male and those choosing other options was significant ($\chi^2 = 13.5$, $\chi^2_{0.05,2} = 5.991$, $P = 0.001$).

Robustus males: Are robustus males guided by chemical cues in locating receptive females? Following release, most robustus males in part 1 (female without typus males) failed to make a choice for the receptive female ($\chi^2 = 4$, $\chi^2_{0.05,2} = 5.991$, $P = 0.135$). Of the 18 animals tested, 4 chose the receptive female, 4 chose the nonreceptive female, and 10 made no choice. The robustus males that selected the branch with the receptive female were not faster to react (mean ± SD: 4.33 ± 2.75 min) than the robustus males that selected the nonreceptive female (mean ± SD: 6.85 ± 5.63 min) (t-test: $t = -0.805$, $t_{0.05(2),6} = 2.447$, $P = 0.452$); the other males reacted late or never left the choice chamber during the 30-min observation period. After the introduction of two typus males to the female shelters (part 2), more robustus males chose the branch with the receptive female, but differences were not significant ($\chi^2 = 2.24$, $\chi^2_{0.05,2} = 5.991$, $P = 0.329$). Of the 17 animals tested, 8 chose the receptive female, 3 chose the nonreceptive female, and 6 made no choice. Also during the second part, robustus males that selected receptive females were not faster to react (mean ± SD: 6.69 ± 5.37 min) than those that selected nonreceptive females (mean ± SD: 3.06 ± 3.43 min) (t-test: $t = 1.062$, $t_{0.05(2),8} = 2.306$, $P = 0.319$).

Visual communication

Receptive female: Can receptive females distinguish between typus and robustus males via *visual cues?* Following their release, receptive females started to move continuously without staying for long near the lateral compartments of the aquarium. There was no clear pattern of choice in favor of either of the two male forms (typus or robustus). When comparing the number of visits to the two males, there was no significant preference for either male, neither during the first visit ($\chi^2 = 0.0769$, $\chi^2_{0.05,1} = 3.841$, $P = 0.78$ after Yates correction) nor during the last visit ($\chi^2 = 2.48$, $\chi^2_{0.05,2} = 5.991$, $P = 0.28$) (Table 1). Similarly, there were no significant differences in the total duration of visits to either male (t-test: $t = -0.432$, $t_{0.05(2),12} = 2.179$, $P = 0.674$). Females spent on average less than 10 min near the compartment of either male (mean ± SD: robustus 8.3 ± 24.4 min; typus 6.3 ± 11.6 min).

Robustus males: How important are visual cues for the robustus male? As predicted, tumults were generated by the typus males around the receptive female, but no tumults were observed near the nonreceptive female. Each tumult lasted only a few seconds, and generally the larger typus male succeeded in mating with the female. The frequency of tumults increased positively in relation to the number of typus males in the different treatments. Significant differences in the number of tumults were found between treatments with 2 and 8 typus males (Kruskal-Wallis $H = 12.602$, df = 4, $n = 30$, $P = 0.013$) (Fig. 2A). Another possible visual signal for the robustus male might be generated by mating of the receptive female with one of the typus males. Matings were observed in all treatments, and there were no significant differences in the total mating time between treatments (Kruskal-Wallis $H = 6.301$, df = 4, $n = 30$, $P = 0.178$) (Fig. 2B). In summary, many visual signals potentially attractive for the robustus males were generated in the lateral compartment with the receptive female.

When comparing the number of visits between the two females, there was no significant preference for either female, neither during the first visit (see Table 2) nor the last visit (see Table 3). The total duration of visits by the robustus males to the receptive female was not significantly affected by the numbers of typus males in each treatment (one-way ANOVA $F_{4,25} = 1.962$, $P = 0.131$) (Fig. 3A). The visit duration of robustus males to the receptive female reached lowest values in the treatment with the highest densities of typus males, but there were no significant differences to the other treatments (the absence of significant

Table 1

Visual communication experiment: choices made by receptive females when presented with a robustus male and a typus male

Choice	First visit	Last visit
Robustus male	7	7
Typus male	6	3
No choice	—	3

Presented are the first visit and the last visit to one of the lateral compartments with a male behind the glass window.

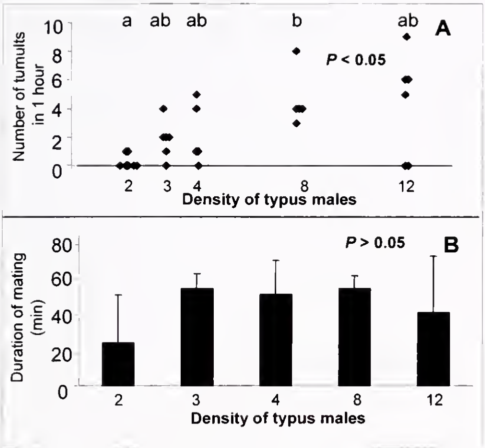

Figure 2. (A) Number of tumults produced in 1 h; different letters indicate treatments with significant differences (*post hoc* test, Dunn $q = 3.073$, $P < 0.05$); (B) Total mating time (mean + SD) of the receptive female with typus males in the respective treatments; note that occasionally a female mated with more than one male.

differences should be interpreted cautiously since the power of the statistical test is very low; $P = 0.253$). The total duration of visits by robustus male to the nonreceptive female also was not affected by the typus treatments (one-way ANOVA $F_{4,25} = 0.089$, $P = 0.984$) (Fig. 3B). Since no differences between typus treatments were found, we pooled all replicates and calculated the total visit duration of the robustus males to each lateral compartment (with receptive female and nonreceptive female, respectively) (Fig. 3C). The total visit duration to the receptive female glass window was on average twice as long as to the nonreceptive female (t-test: $t = -2.039$, $t_{0.05(1),29} = 1.699$, $P = 0.025$).

Table 2

Visual communication experiment: number of robustus males that chose, in the first visit, either a receptive or a nonreceptive female when the females were presented in the presence of various numbers of typus males

Treatment (# of typus males)	Female Receptive	 Nonreceptive	χ^2	df	P
2	3 (3.5)	4 (3.5)	0.1	1	0.705
3	2 (3)	4 (3)	0.6	1	0.414
4	3 (2.5)	2 (2.5)	0.2	1	0.654
8	4 (2.5)	1 (2.5)	1.8	1	0.179
12	5 (3)	1 (3)	2.6	1	0.102
		TOTAL χ^2 =	5.4	5	
χ^2 grouped	17 (14.5)	12 (14.5)	0.8	1	0.353
Heterogeneity χ^2		4.6	4.6	4	>0.05

In parentheses are the expected frequencies of first visit. The P value corresponding to heterogeneity >0.05 means that treatments are homogeneous and can be analyzed as a whole. In the treatment with 2 typus males, one robustus male did not make any choice for either female during the observation time, and consequently was not included in this analysis.

Table 3

Visual communication experiment: number of robustus males that chose, in the last visit, either a receptive or a nonreceptive female when the females were presented in the presence of various numbers of typus males

Treatment (# of typus males)	Female Receptive	 Nonreceptive	χ^2	df	P
2	3 (3.5)	4 (3.5)	0.14	1	0.705
3	4 (3)	2 (3)	0.67	1	0.414
4	4 (2.5)	1 (2.5)	1.8	1	0.179
8	4 (2.5)	1 (2.5)	1.8	1	0.179
12	4 (3)	2 (3)	0.67	1	0.414
		TOTAL χ^2 =	5.08	5	
χ^2 grouped	19 (14.5)	10 (14.5)	2.79	1	0.094
Heterogeneity χ^2			2.29	4	>0.05

In parentheses are the expected frequencies of last visit. The P value corresponding to heterogeneity >0.05 means that treatments are homogeneous and can be analyzed as a whole. In the treatment with 2 typus males, one robustus male did not make any choice for either female during the observation time, and consequently was not included in this analysis.

Discussion

Our results show that receptive females and robustus males use different cues during sexual communication. Receptive females locate their potential mating partners by using chemical cues, whereas robustus males find females mostly by using visual cues. The results suggest that females and males adopt sex-specific roles during the searching and assessment phase. Thus *Rhynchocinetes typus*, like the lobster *Homarus americanus* (Bushmann and Atema, 2000), is a crustacean species in which females locate dominant males *via* chemical signals. In both species, females preferentially mate with dominant males, which defend females during the mating process. This suggests that sexual communication in *R. typus* (and *H. americanus*) is closely linked to their mating system, as will be discussed in the following section.

Chemical communication

Chemical cues are used by a variety of crustaceans during sexual communication. In many species such as the shore

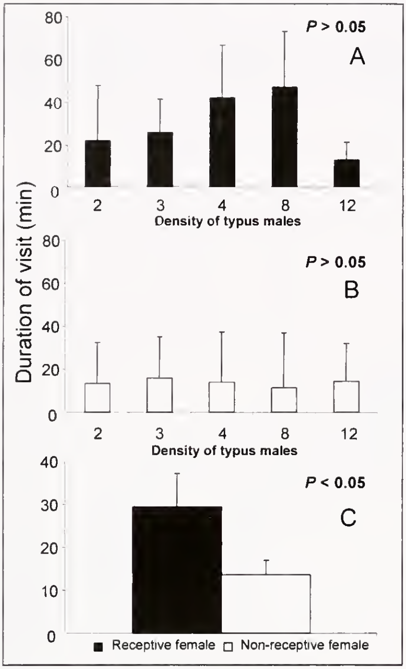

Figure 3. Total visit duration (mean + SD) of robustus males to the (A) receptive female and (B) nonreceptive female in respective treatments; $P > 0.05$ indicates no significant differences between treatments. (C) Total visit duration (mean + SD) of robustus males to the respective females after pooling among all treatments; $P < 0.05$ indicates significant differences between visits to respective females.

crab *Carcinus maenas*, snow crab *Chionoecetes opilio*, and helmet crab *Telmessus cheiragonus*, females advertise their reproductive status and attract males *via* waterborne chemical signals (Bamber and Naylor, 1996; Bouchard *et al.*, 1996; Kamio *et al.*, 2002). This does not appear to be the case in *Rhynchocinetes typus*, where males do not locate receptive females *via* chemical cues. Most crustacean species possess highly efficient chemoreceptive capabilities that allow them to evaluate their environment (Derby and Steullet, 2001). We believe that this is also true for *R. typus*, and that males would be able to perceive the presence of a receptive female if appropriate chemical signals were available. Since males of this species apparently cannot identify a receptive female *via* waterborne chemical cues, it appears that receptive females do not release waterborne chemicals advertising their reproductive status. When typus males were together with females, there was a slight tendency for robustus males to approach the receptive females, but the experimental set-up did not allow distinguishing whether this was in response to chemicals released by the females or by typus males attending them. Rock shrimp typically live at high densities (Caillaux and Stotz, 2003), and there are usually many males for each receptive female (Correa and Thiel, 2003b). Female rock shrimp might have no problem in obtaining a mating partner, and thus the adaptive advantage in attracting males *via* waterborne chemical signals would be slight. It is also possible that *R. typus*, which inhabits complex and wave-exposed rocky shore environments, lives in a habitat where communication *via* chemical cues is complicated by turbulent flow. However, the fact that female rock shrimp locate males *via* waterborne chemical cues suggests that chemical communication in the habitat of *R. typus* is not negatively influenced by the hydrodynamic regime.

In some crustacean species, males advertise their presence to females. For example, in the lobster *Homarus americanus*, females are attracted to dominant males *via* chemical signals (Bushmann and Atema, 1997, 2000). Similarly, in the blue crab *Callinectes sapidus*, females appear to key in on chemical signals from males (Gleeson, 1991; Bushmann, 1999). Males of these crustacean species typically advertise their status to other individuals *via* chemical signals released in the urine (*e.g.*, Breithaupt and Atema, 2000; Zulandt Schneider *et al.*, 2001; Breithaupt and Eger, 2002). These signals often are used during agonistic encounters to establish dominance status, and females might exploit these signals to locate dominant males. This could explain why and how females of *R. typus* find dominant robustus males *via* chemical signals. Robustus males occasionally engage in agonistic interactions (Correa *et al.*, 2003), and during these encounters they may employ chemical signals similar to those of male lobsters and crayfish. During the searching phase, female rock shrimp may utilize these chemical signals to locate robustus males, which they prefer as mates (Díaz and Thiel, 2003; Thiel and Hinojosa, 2003).

Visual communication

Since robustus males feature distinct morphological characteristics, it could have been expected that receptive females would use visual cues to distinguish between males. Females of some other decapod crustaceans choose males on the basis of visual cues such as size of body structures or shelter, which are reliable indicators of the fitness of an individual (Atema and Cobb, 1980; Christy, 1987). The results of the current study suggest that females do not approach the robustus males on the basis of visual signals. In general, visual signals are uncommon during sexual communication of aquatic crustaceans (see Salmon, 1983). Only in particular groups of stomatopods (Hatziolos and

Caldwell, 1983; Christy and Salmon, 1991; Marshall *et al.*, 1999) and in the snapping shrimp *Alpheus heterochaelis* (Hughes, 1996) are visual signals known to play an important role during intersexual communication, probably because both species live in tropical waters where visibility usually is high. Similarly, females of terrestrial crustaceans use visual signals to find males (Christy and Salmon, 1991; Pope, 2000). The importance of visual signals for sexual communication in terrestrial and clear-water environments appears to be related to the better light conditions and visibility. The apparent inability of female rock shrimp to select robustus males *via* visual cues in our study does not prove that females do not use visual cues to recognize robustus males. Female rock shrimp that received both chemical and visual cues avoided robustus males initially (see Díaz and Thiel, 2003). The experiments with the robustus males demonstrated that visual cues also play a role during intersexual communication in *R. typus*. Robustus males are guided visually to the tumults or matings developing around receptive females. A similar phenomenon has been reported for the horseshoe crab *Limulus polyphemus*, where additional males are attracted to satellite males around the receptive female apparently by visual cues (Barlow *et al.*, 1982), but this occurs in shallow waters and is aided by chemical signals (Hassler and Brockmann, 2001). These observations suggest that in the marine environment, once crustaceans are close to potential mating partners, that is, during the assessment phase, visual cues (often accompanied by chemical cues) may gain in importance.

Visual cues are important for judging the size of an opponent during agonistic encounters (*e.g.*, Caldwell and Dingle, 1979; Atema and Cobb, 1980). This occurs when individuals are within a few body lengths of each other. In addition to chemical signals (Breithaupt and Atema, 2000) and moderate agonistic interactions (Karavanich and Atema, 1998), visual signals may also serve to establish and maintain dominance status. In rock shrimp, visual communication occurs during agonistic encounters when robustus males appear to gauge the size of their opponents (*e.g.*, Correa *et al.*, 2003). This might explain why male lobsters and shrimps have evolved visual skills to distinguish conspecifics (opponents and receptive females).

Sexual communication and mating system of rock shrimp

The mating system of rock shrimp has been characterized as "neighborhoods of dominance" (Correa and Thiel, 2003a) in which dominant males monopolize a receptive female and defend it against subordinate males (Correa *et al.*, 2003). In *Rhynchocinetes typus*, females have a strong preference for these dominant males (Díaz and Thiel, 2003; Thiel and Hinojosa, 2003). The mating system of *R. typus* thus shows strong similarities to that of *Homarus americanus*. In this species, dominant males that inhabit shelters also form neighborhoods of dominance (*e.g.*, Karnofsky *et al.*, 1989), and reproductive females exhibit preferences for dominant males (Atema *et al.*, 1979; Atema, 1986; Bushmann and Atema, 2000), even leading to female molt-staggering (Cowan and Atema, 1990).

In contrast to many other decapod species, female rock shrimp and lobsters do not attract males *via* waterborne chemical signals. In both species, harassment from subordinate males may represent a high cost for females (*e.g.*, Cowan, 1991; Thiel and Hinojosa, 2003). To avoid approaches and rambunctious harassment from subordinate males, female rock shrimp and lobsters may thus hide their reproductive status (they remain "chemically quiet" *sensu* Atema, 1995) until they reach the vicinity of a dominant male. Male lobsters are residents in shelters and accept only mature females into their shelter (Cowan, 1991). The same might be true for rock shrimp, where one or several robustus males often occupy large spaces in open shelters (pers. obs.). These dominant males usually are dispersed and difficult to locate visually in their shelters. Consequently, receptive females are attracted to these areas by chemical cues, as shown herein for rock shrimp and by Bushmann and Atema (1997) for *H. americanus*. Once in the vicinity of a dominant male, females may no longer hide their reproductive status but rather permit assessment by that male. In lobsters, this appears to occur *via* chemical cues (Atema and Cowan, 1986), which reduce male aggression and later facilitate successful mating (Bushmann and Atema, 1997). Waterborne chemical signals most likely play only a minor role during mate assessment in *R. typus*, since they would attract large numbers of subordinate males. Visual cues arising from activities developing around the receptive female are apparently sufficient to attract a dominant male within a short period of time and induce it to monopolize the female. Thus the assessment phase seems to be brief and simple in rock shrimp, even though in other crustaceans it involves sophisticated signals and requires substantial time (Christy, 1987; Cowan, 1991; Bushmann, 1999). For rock shrimp, we propose a hypothetical mating scenario in which females molt at night and subsequently (or before molting) approach areas with dominant males. Females then become receptive during the day, when visual cues can be used by the robustus males to locate and monopolize receptive females in their vicinity.

In summary, this comparison of sexual communication in rock shrimp and lobster further underlines the important role of female behavior during mate searching and assessment. Females may significantly influence the outcome of the mating process by hiding their reproductive status before reaching the neighborhood of dominant males.

Acknowledgments

We are grateful to I. Hinojosa and T. Chr. van Son for help in collecting shrimp. Our special thanks go to W. Stotz and D. Lancellotti for their unconditional support during this study. Helpful comments from A. Baeza and from two anonymous reviewers helped to improve the original manuscript.

Literature Cited

Acquistapace, P., L. Aquiloni, B. A. Hazlett, and F. Gherardi. 2002. Multimodal communication in crayfish: sex recognition during mate search by male *Austropotamobius pallipes*. *Can J. Zool.* **80:** 2041–2045.

Atema, J. 1986. Review of sexual selection and chemical communication in the lobster, *Homarus americanus*. *Can. J. Fish. Aquat. Sci.* **43:** 2283–2290.

Atema, J. 1995. Chemical signals in the marine environment: dispersal, detection, and temporal signal analysis. *Proc. Natl. Acad. Sci. USA* **92:** 62–66.

Atema, J., and J. S. Cobb. 1980. Social behavior. Pp. 409–450 in *The Biology and Management of Lobsters*. J. S. Cobb and B. F. Phillips, eds. Academic Press, NY.

Atema, J., and D. F. Cowan. 1986. Sex-identifying urine and molt signals in lobster *Homarus americanus*. *J. Chem. Ecol.* **12:** 2065–2080.

Atema, J., and R. Voigt. 1995. Behavior and sensory biology. Pp. 313–348 in *The Biology of the Lobster,* Homarus americanus, J. R. Factor, ed. Academic Press, New York.

Atema, J., S. Jacobsen, E. Karnofsky, S. Oleszko-Szuts, and L. Stein. 1979. Pair formation in the lobster, *Homarus americanus:* behavioral development, pheromones and mating. *Mar. Behav. Physiol.* **6:** 277–296.

Backwell, P., M. Jennions, N. Passmore, and J. Christy. 1998. Synchronized courtship in fiddler crabs. *Nature* **391:** 31–32.

Bamber, S. D., and E. Naylor. 1996. Chemical communication and behavioural interaction between sexually mature male and female shore crabs (*Carcinus maenas*). *J. Mar. Biol. Assoc. UK* **76:** 691–699.

Barlow, R. B., L. C. Ireland, and L. Kass. 1982. Vision has a role in *Limulus* mating behavior. *Nature* **296:** 65–66.

Borowsky, B. 1991. Patterns of reproduction of some amphipod crustaceans and insights into the nature of their stimuli. Pp. 33–49 in *Crustacean Sexual Biology,* R. T. Bauer and J. W. Martin, eds. Columbia University Press, New York.

Bouchard, S., B. Sainte-Marie, and J. N. McNeil. 1996. Indirect evidence indicates female semiochemicals release male precopulatory behaviour in the snow crab, *Chionoecetes opilio* (Brachyura: Majidae). *Chemoecology* **7:** 39–44.

Breithaupt, T., and J. Atema. 2000. The timing of chemical signaling in dominance fights of male lobsters (*Homarus americanus*). *Behav. Ecol. Sociobiol.* **49:** 67–78.

Breithaupt, T., and P. Eger. 2002. Urine makes the difference: chemical communication in fighting crayfish made visible. *J. Exp. Biol.* **205:** 1221–1231.

Burggren, W. W., and B. R. McMahon. 1988. *Biology of the Land Crabs*. Cambridge University Press, Cambridge.

Bushmann, P. J. 1999. Concurrent signals and behavioral plasticity in blue crab (*Callinectes sapidus* Rathbun) courtship. *Biol. Bull.* **197:** 63–71.

Bushmann, P. J., and J. Atema. 1997. Shelter sharing and chemical courtship signals in the lobster *Homarus americanus*. *Can. J. Fish. Aquat. Sci.* **54:** 647–654.

Bushmann, P. J., and J. Atema. 2000. Chemically mediated mate location and evaluation in the lobster, *Homarus americanus*. *J. Chem. Ecol.* **26:** 883–899.

Caillaux, L. M., and W. Stotz. 2003. Distribution and abundance of *Rhynchocinetes typus* Milne Edwards (Crustacea: Decapoda: Rhynchocinetidae) in different benthic community structures in northern Chile. *J. Mar. Biol. Assoc. UK* **83:** 143–150.

Caldwell, R. L., and H. Dingle. 1979. The influence of size differential on agonistic encounters in the mantis shrimp, *Gonodactylus viridis*. *Behaviour* **69:** 255–264.

Christy, J. H. 1987. Competitive mating, mate choice and mating associations of brachyuran crabs. *Bull. Mar. Sci.* **41:** 177–191.

Christy, J. H., and M. Salmon. 1991. Comparative studies of reproductive behavior in mantis shrimps and fiddler crabs. *Am. Zool.* **31:** 329–337.

Christy, J. H., P. R. Y. Backwell, and U. Schober. 2003. Interspecific attractiveness of structures built by courting male fiddler crabs: experimental evidence of a sensory trap. *Behav. Ecol. Sociobiol.* **53:** 84–91.

Correa, C., and M. Thiel. 2003a. Mating systems in caridean shrimp (Decapoda: Caridea) and their evolutionary consequences for sexual dimorphism and reproductive biology. *Rev. Chil. Hist. Nat.* **76:** 187–203.

Correa, C., and M. Thiel. 2003b. Population structure and operational sex ratio in the rock shrimp *Rhynchocinetes typus* (Decapoda: Caridea). *J. Crustac. Biol.* **23:** 849–861.

Correa, C., J. A. Baeza, E. Dupré, I. A. Hinojosa, and M. Thiel. 2000. Mating behavior and fertilization success of three ontogenetic stages of male rock shrimp *Rhynchocinetes typus* (Decapoda: Caridea). *J. Crustac. Biol.* **20:** 628–640.

Correa, C., J. A. Baeza, I. A. Hinojosa, and M. Thiel. 2003. Male dominance hierarchy and mating tactics in the rock shrimp *Rhynchocinetes typus* (Decapoda: Caridea). *J. Crustac. Biol.* **23:** 33–45.

Cowan, D. F. 1991. The role of olfaction in courtship behavior of the American lobster *Homarus americanus*. *Biol. Bull.* **181:** 402–407.

Cowan, D. F., and J. Atema. 1990. Moult staggering and serial monogamy in American lobsters, *Homarus americanus*. *Anim. Behav.* **39:** 1199–1206.

Derby, C. D., and P. Steullet. 2001. Why do animals have so many receptors? The role of multiple chemosensors in animal perception. *Biol. Bull.* **200:** 211–215.

Díaz, E. R., and M. Thiel. 2003. Female rock shrimp prefer dominant males. *J. Mar. Biol. Assoc. UK* **83:** 941–942.

Dunham, P. J. 1978. Sex pheromones in Crustacea. *Biol. Rev.* **53:** 555–583.

Gleeson, R. A. 1991. Intrinsic factors mediating pheromone communication in the blue crab, *Callinectes sapidus*. Pp. 17–32 in *Crustacean Sexual Biology,* R. T. Bauer and J. W. Martin, eds. Columbia University Press, New York.

Hassler, C., and H. J. Brockmann. 2001. Evidence for use of chemical cues by male horseshoe crabs when locating nesting females (*Limulus polyphemus*). *J. Chem. Ecol.* **27:** 2319–2335.

Hatziolos, M. E. and R. L. Caldwell. 1983. Role reversal in courtship in the stomatopod *Pseudosquilla ciliata* (Crustacea). *Anim. Behav.* **31:** 1077–1087.

Hinojosa, I. A., and M. Thiel. 2003. Somatic and gametic resources in male rock shrimp, *Rhynchocinetes typus:* effect of mating potential and ontogenetic male stage. *Anim. Behav.* **66:** 449–458.

Hughes, M. 1996. The function of concurrent signals: visual and chemical communication in snapping shrimp. *Anim. Behav.* **52:** 247–257.

Kamio, M., S. Matsunaga, and N. Fusetani. 2002. Copulation pheromone in the crab *Telmessus cheiragonus* (Brachyura: Decapoda). *Mar. Ecol. Prog. Ser.* **234:** 183–190.

Karavanich, C., and J. Atema. 1998. Individual recognition and memory in lobster dominance. *Anim. Behav.* **56:** 1553–1560.

Karnofsky, E. B., J. Atema, and R. H. Elgin. 1989. Field observations of social behavior, shelter use, and foraging in the lobster, *Homarus americanus*. *Biol. Bull.* **176:** 239–246.

Kelly, L. S., and T. W. Snell. 1998. Role of surface glycoproteins in mate-guarding of the marine harpacticoid *Tigriopus japonicus*. *Mar. Biol.* **130:** 605–612.

Latruffe, C., P. K. McGregor, and R. F. Oliveira. 1999. Visual signalling and sexual selection in male fiddler crabs *Uca tangeri*. *Mar. Ecol. Prog. Ser.* **189:** 233–240.

Marshall, J., T. W. Cronin, N. Shashar, and M. Land. 1999. Behavioural evidence for polarisation vision in stomatopods reveals a potential channel for communication. *Curr. Biol.* **9:** 755–758.

Pope, D. S. 2000. Testing function of fiddler crab claw waving by manipulating social context. *Behav. Ecol. Sociobiol.* **6:** 432–437.

Salmon, M. 1983. Courtship, mating systems; and sexual selection in decapods. Pp. 143–169 in *Studies in Adaptation: The Behavior of Higher Crustaceans*. S. Rebach and D. Dunham, eds. John Wiley & Sons, New York.

Shuster, S. M., and M. J. Wade. 2003. *Mating Systems and Strategies*. Princeton University Press, Princeton, NJ.

Sneddon, L. U., F. A. Huntingford, A. C. Taylor, and A. S. Clare. 2003. Female sex pheromone-mediated effects on behavior and consequences of male competition in the shore crab (*Carcinus maenas*). *J. Chem. Ecol.* **29:** 55–70.

Thiel, M., and I. Hinojosa. 2003. Mating behavior of female rock shrimp *Rhynchocinetes typus* (Decapoda: Caridea)—indication for convenience polyandry and cryptic female choice. *Behav. Ecol. Sociobiol.* **55:** 113–121.

Zar, J. H. 1999. *Biostatistical Analysis*. 4th ed. Prentice Hall, Upper Saddle River, NJ.

Zulandt Schneider, R. A., R. Huber, and P. A. Moore. 2001. Individual and status recognition in the crayfish, *Orconectes rusticus:* the effects of urine release on fight dynamics. *Behaviour* **138:** 137–153.

Reference: *Biol. Bull.* **206:** 144–151. (June 2004)
© 2004 Marine Biological Laboratory

Remarkable Longevity of Dilute Sperm in a Free-Spawning Colonial Ascidian

SHERI L. JOHNSON[1,*] AND PHILIP O. YUND[2]

[1] *School of Marine Sciences, Darling Marine Center, University of Maine, Walpole, Maine 04573; and*
[2] *Marine Sciences Center, University of New England, Biddeford, Maine 04005*

Abstract. Many benthic marine invertebrates reproduce by releasing sperm into the sea (free-spawning), but the amount of time that sperm are viable after spawning may have different consequences for fertilization, depending on the type of free-spawner. In egg-broadcasting marine organisms, gamete age is usually assumed to be irrelevant because of the low probability of contact between dilute sperm and egg. However, direct dilution effects might be reduced in egg-brooding free-spawners that filter dilute sperm out of the water column, and sperm longevity may play a role in facilitating fertilization in these taxa. We investigated the effects of time, temperature, and mixing on the viability of naturally released sperm of the colonial ascidian *Botryllus schlosseri*. Our data indicate that *B. schlosseri* sperm have a functional life span that is considerably longer than those of the sperm of many other marine invertebrate taxa (half-life of ~16 to 26 h), are able to fertilize eggs at extremely low external sperm concentrations (*ca.* 10^1 sperm ml^{-1}), and have a longevity that varies with temperature. It is possible that such prolonged sperm longevity may be achieved by reductions in motility, reactivation of quiescent sperm by chemical cues, or intermittent swimming.

Introduction

Sperm longevity in free-spawning marine invertebrates (organisms that release sperm into the environment; Giese and Kanatani, 1987; Levitan, 1998) that broadcast their eggs is typically assumed to be irrelevant to field fertilization because hydrodynamic processes may rapidly dilute gametes after release (Vogel *et al.*, 1982; Pennington, 1985; Denny, 1988; Denny and Shibata, 1989; Levitan, 1991, 1995; Levitan and Peterson, 1995). However, dilution also has an indirect effect on fertilization by controlling sperm longevity (Levitan *et al.*, 1991). Longevity is generally high when sperm are concentrated (on the order of many hours), but longevity decreases considerably after dilution (to a functional life span of only tens of minutes; Pennington, 1985; Levitan *et al.*, 1991; Powell *et al.*, 2001; Baker and Tyler, 2001). The mechanism underlying this phenomenon is termed the "respiratory dilution effect"; the amount of energy consumed by sperm is a function of motility, and concentrated sperm can maintain a lower metabolic state than dilute sperm (reviewed by Chia and Bickell, 1983). However, sperm are generally assumed to be diluted below effective concentrations well before the viable life of the gamete has expired (*i.e.*, the direct effects of dilution overwhelm indirect effects; Pennington, 1985; Levitan *et al.*, 1991; Levitan, 1995; but see Williams and Bentley, 2002).

In contrast to egg-broadcasters, many free-spawners that retain eggs for internal fertilization (*i.e.*, egg-brooders) may use filter-feeding or suspension-feeding mechanisms to concentrate dilute sperm from the water throughout a prolonged period of egg viability (Yund, 2000; Pemberton *et al.*, 2003b). If females can overcome direct dilution effects and obtain sperm from distant males, adaptations that increase sperm longevity (*e.g.*, inactivity, intermittent swimming, and activation by chemical cues) may be important in fertilization in the field. Sperm longevity is thought to enhance fertilization in some internally fertilizing ascidians (Bishop, 1998; Pemberton *et al.*, 2003b) and bryozoans (Manríquez *et al.*, 2001).

Because many marine invertebrates spawn under a wide range of temperatures (Andronikov, 1975), thermal effects may have important consequences for gamete longevity. A few studies have examined the effects of temperature on sperm viability (Andronikov, 1975; Greenwood and Ben-

---

Received 13 January 2004; accepted 14 April 2004.

* To whom correspondence should be addressed. E-mail: sherij@maine.edu

nett, 1981; Manríquez *et al.*, 2001), but effects on longevity have received little attention. Temperature has a direct effect on all metabolic processes (Hochachka and Somero, 1984); hence higher temperatures might be expected to reduce longevity (Greenwood and Bennett, 1981). However, increased temperature also decreases water viscosity (Dorsey, 1968; Jumars *et al.*, 1993), which can profoundly affect the energy requirements of small organisms (such as sperm) that swim in a low Reynolds number environment (Denny, 1993; Podolsky and Emlet, 1993; Fuiman and Batty, 1997; Hunt von Herbing, 2002). If sperm are subject to both direct metabolic effects and viscosity effects, the overall thermal effects on longevity and fertilization may be complex.

In this study, we use the colonial ascidian *Botryllus schlosseri* (Pallas, 1766) as a model system to experimentally investigate the effects of time, temperature, and mixing on the viability of naturally released sperm. Physical disturbance created by mixing might alter longevity patterns by inducing or suppressing swimming or by physically damaging gametes (Mead and Denny, 1995; Denny *et al.*, 2002). *Botryllus schlosseri* has been the subject of several laboratory and field fertilization studies (*e.g.*, Grosberg, 1991; Yund and McCartney, 1994; Yund, 1995, 1998; Stewart-Savage *et al.*, 2001). Released sperm exit the colony through the exhalent siphon and rapidly disperse into the surrounding seawater (Milkman, 1967). Sperm are then acquired by another colony, and fertilization takes place internally. *Botryllus schlosseri* is a geographically widespread species (Grosberg, 1988), so colonies experience a wide range of temperature regimes during the reproductive season (*e.g.*, Yund and Stires, 2002).

Materials and Methods

Study organism and culture

Botryllus schlosseri is a sessile colonial ascidian that inhabits shallow waters and harbors throughout New England and other temperate regions of the world (Van Name, 1945). Colonies are cyclical hermaphrodites with alternating female and male phases occurring in repetitive sexual cycles (Milkman, 1967; Grosberg, 1988). This sexual cycle is linked to a zooid-replacement cycle. Over a 7–10 day period (length depends on temperature; Grosberg, 1982), a new generation of zooids (buds) grow and expand and then assume the function of the older zooids, which are quickly resorbed. Eggs are fertilized as the new sexual generation of zooids replaces the old generation (hereafter referred to as takeover, Milkman, 1967); once fertilized, the eggs develop into embryos that are released as tadpole larvae at the end of the cycle (Grosberg, 1991). Sperm release commences about 16 h after the start of a cycle and continues for several days, so colonies are functionally male throughout most of the reproductive cycle (Stewart-Savage and Yund, 1997). Colonies neither self-fertilize nor store sperm (Stewart-Savage *et al.*, 2001).

Colonies of *B. schlosseri* were collected from the Damariscotta River, Maine. Animals were grown on glass microscope slides (7.6 × 5.1 cm) in the flowing seawater system at the University of Maine's Darling Marine Center and monitored. When colonies with at least 20 eggs were approaching takeover (late stage 5 through early stage 6; Milkman, 1967), they were isolated (at least 12 h before siphon opening) in 50 ml of unfiltered sperm-free seawater (aged at least 7 days in the dark at 15 °C) at 15 °C and fed phytoplankton (*Isochrysis* or *Tetraselmis* sp.) at densities of approximately 10^5 cells ml^{-1}. Water and food were changed daily. Colonies were determined to have completed siphon opening when phytoplankton were present in the digestive tract, indicating that eggs had been ovulated, and these colonies were subsequently treated as virgin females for the experiment.

Sperm collection and aging

For each experimental trial, naturally spawned sperm were obtained by isolating 24 colonies in 200 ml of sperm-free seawater (see above) for 4 h during peak sperm release (Stewart-Savage and Yund, 1997). A 15-ml sample of the undiluted solution was collected to determine the sperm concentration. Sperm were then quickly diluted 100-fold: 160 ml of mixed sperm suspension were added to 16. l of aged seawater (15 °C) and mixed. We immediately collected a sample and used it to obtain an initial fertilization level. The remaining suspension was then aliquotted into four glass containers, each containing 3.8 l. The aliquots were then aged under experimental conditions, consisting of all combinations of two temperatures (15 °C and 22 °C) and two mixture treatments (mixed and unmixed). Mixed suspensions were constantly stirred with a magnetic mixer. The 15 °C and 22 °C temperatures were selected to represent the range under which spawning normally occurs in the Damariscotta River estuary (Yund and Stires, 2002). Each container was sampled at 8, 24, 48, and 72 h. We sampled two areas of the unmixed container. One sample was removed from the top, and then a second sample was carefully pipetted off the bottom while minimizing disturbance to the solution. By contrast, the sample from the mixed solution integrated different heights within the container. This sampling scheme yielded three experimental treatments: top and bottom of the unmixed solution, and the mixed solution. Differences between the top and bottom treatments might reveal aspects of sperm behavior (*e.g.*, buoyant or upward-swimming sperm *vs.* immotile sinking or downward-swimming sperm), while the mixed treatment tests the effects of physical disturbance and aeration on sperm viability.

Sperm counts were determined by concentrating a fresh aliquot (13.5 ml) of the undiluted sperm suspension by two orders of magnitude through centrifugation. Polyvinyl alcohol (Sigma-Aldrich; 1.5 ml of a 1 g ml^{-1} solution) was added to the sperm solution before centrifugation to prevent sperm from adhering to container surfaces. The concentrated suspension (150 μl) obtained by centrifugation was fixed with 25% gluteraldehyde and subsequently counted on a hemacytometer (three samples, two counts each). Raw hemacytometer counts were multiplied by a dilution factor to obtain the concentration of the aging and fertilization solution. Because of the low concentration of *B. schlosseri* sperm, all 25 squares of the hemacytometer had to be scored to obtain non-zero counts. Consequently, our values are probably accurate only to the nearest order of magnitude.

Fertilization assays

All fertilization assays were conducted in 50-ml chambers with virgin female colonies. At each time point, 40 ml of each experimental solution was transferred into the chambers along with 5 ml (10^5 cells ml^{-1}) of algae. The fertilization assays were then incubated at the relevant experimental temperature for 4 h. At the end of the incubation, colonies were rinsed with aged seawater to terminate the collection of sperm and were returned to isolation. All colonies were maintained at a constant temperature to standardize development times. After 16–20 h, an incision was made in each zooid, and the unfertilized eggs and developing embryos were counted with the aid of a stereomicroscope. Results are expressed as percent fertilization. A total of 14 trials were conducted over two reproductive seasons. Sperm-free controls were not included, because colonies were isolated in sperm-free seawater well in advance of siphon opening. In addition, stage of embryo development was assessed as a control for the timing of fertilization, to ensure that fertilizations were the product of the sperm we added. Some of the embryos in six female colonies were too far along in development (*i.e.*, >24 h), and so must have been the product of fertilization by contaminating sperm prior to our experiment. Data from these individuals were excluded from the analysis.

Statistical analysis

All percent fertilization data were arcsine transformed to meet normality assumptions. A few fertilization assays were omitted during the experiment, due either to the death of experimental animals or to a shortage of virgin females at appropriate time points. Consequently, fertilization data were analyzed with a software package that accommodates an unbalanced design (Proc GLM ver. 6.07, SAS Institute, Cary, North Carolina). A repeated-measures ANOVA with trial nested within treatment and temperature was conducted. The effects of temperature and treatment were tested against the nested term, and all effects involving time were tested against the residual error. Type III sums of squares are reported for all sources of variation. Significance was determined at the 5% level. An additional multi-way ANOVA assessed whether egg number differed among times, temperatures, and treatments to test whether effects in the main analysis could have been an artifact of variation in egg number.

Sperm half-life

Two sperm half-life estimates were generated by treating time as a continuous variable. For each temperature, a logarithmic regression of mean percent fertilization (not transformed), averaging across all treatments, was conducted with time as the dependent variable. Sperm half-lives were calculated from these equations by solving for the time at which fertilization dropped to half of the initial (0 h) value. Estimates obtained from our data were compared to previously published half-lives of other free-spawning marine invertebrates. We used data previously reviewed by Manríquez *et al.* (2001), but included published values for other egg-brooding taxa.

Results

Effects on sperm viability

The analysis of variance results indicate a highly significant overall effect of time, with a decrease in percent fertilization with increasing sperm age for *Botryllus schlosseri* (Table 1). Fertilization of eggs was still possible using naturally spawned sperm that had been aged 72 h. At an average sperm concentration of approximately $1.38 \times 10^1 \pm 0.13 \times 10^1$ (SE) sperm ml^{-1}, initial fertilization was about 61%, and after 72 h decreased only to about 25% of the starting level (Fig. 1). Temperature also had a significant effect (Table 1), with fertilization generally higher when sperm were aged at 15 °C than at 22 °C (Fig. 1).

We were unable to detect any significant effect of treat-

Table 1

Results of repeated-measures nested ANOVA on percent fertilization

Source	df	SS III	*F* ratio	*P*
Time	3	8.77	14.32	**0.0001**
Time*Temp	3	0.47	0.77	0.5134
Time*Treat	6	0.79	0.08	0.9195
Time*Temp*Treat	6	0.74	0.60	0.7265
Error a: Residual[1]	159	32.48		
Temp	1	1.03	5.21	**0.0252**
Treat	2	0.16	0.40	0.6698
Temp*Treat	2	0.03	0.09	0.9169
Error b: Trial(Temp*Treat)[2]	78	15.40		

[1] Error a: used to test all effects involving time.

[2] Error b: used to test treatment and temperature effects.

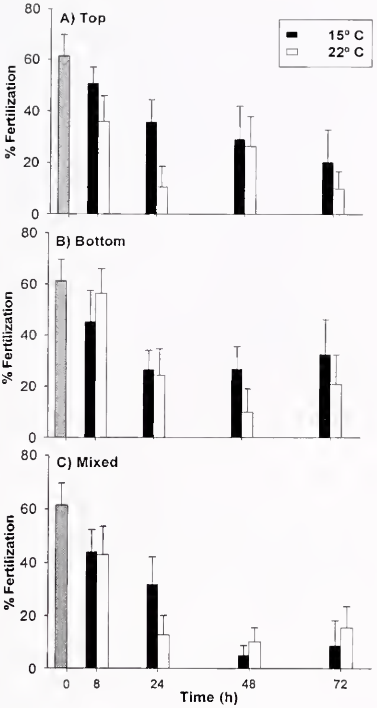

Figure 1. Viability of *Botryllus schlosseri* sperm measured as fertilization (%) of eggs over time (A) at the top (unmixed suspension), (B) at the bottom (unmixed suspension), and (C) in the mixed treatment. Data are means (±SE) of all trials. The 0 h sample (indicated by the gray bar) represents the fertilization potential of the sperm solution prior to manipulation, and so is identical for all temperatures and treatments. Average working sperm concentration was 1.38×10^1 sperm ml^{-1}.

ment, nor were any of the interaction effects significant (Table 1). Average egg numbers were 50.2 ± 0.8 (SE) and did not vary significantly with time, temperature, or treatment ($F_{9,251} = 0.92$, $P = 0.45$).

Sperm half-lives

Logarithmic regressions of fertilization with time were highly significant for both temperatures (15 °C, $r^2 = 0.967$, $P < 0.01$; 22 °C, $r^2 = 0.790$, $P < 0.05$). Sperm half-lives (the time at which fertilization drops to 50% of its initial level) were estimated at both temperatures, using the following logarithmic regression equations: 15 °C, % fertilization = −29.369 log (time) + 72.291; 22 °C, % fertilization = −31.375 log (time) + 68.456. The resulting half-lives were 26.3 h at 15 °C and 16.1 h at 22 °C (Fig. 2).

Comparison with data from several other free-spawners, including two egg-brooders and multiple egg-broadcasters, reveals that dilute *B. schlosseri* sperm have substantially greater longevity than dilute sperm of most other free-spawners (Fig. 3). Similar sperm half-lives in egg-broadcasters have been documented only at sperm concentrations many orders of magnitude greater than those used in our experiment (*e.g.*, Williams and Bentley, 2002). As a group, the three egg-brooders in our comparison have greater sperm half-lives at low concentrations than all of the egg-broadcasters (Fig. 3).

Discussion

Sperm longevity in free-spawning invertebrates

The functional life span reported here for *Botryllus schlosseri* sperm is considerably longer than previously reported for the dilute sperm of any other free-spawning marine invertebrate, and orders of magnitude greater than the qualitative estimate for this species (based in part on motility) previously reported by Grosberg (1987). A substantial number of fertilizations still occurred with 48- and 72-h-old sperm. In the few trials in which fertilization did not drop to zero by 72 h, sperm suspensions were aged and retested after an additional 24 h (*i.e.*, at 96 h). These samples also resulted in a low level of fertilization (13.8%; unpubl. data).

Williams and Bentley (2002) reported similar sperm longevity in a free-spawner (the polychaete *Arenicola*), but only at a sperm concentration four orders of magnitude higher than the 10^1 sperm ml^{-1} reported here. High longevity of concentrated sperm is predicted by the respiratory

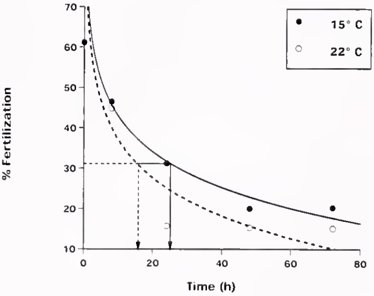

Figure 2. Viability of *Botryllus schlosseri* sperm measured as a function of mean (±SE) fertilization (%) of eggs over time at 15 °C and 22 °C. The value for each point is the grand mean of the top, bottom, and mixed treatments averaged across all trials. Best-fit logarithmic regression lines used to estimate sperm half-lives are plotted for each temperature: 15 °C (solid line) and 22 °C (dashed line). Half-lives were calculated as the time needed for fertilization to decrease to 50% of the initial value, as indicated by the dotted lines.

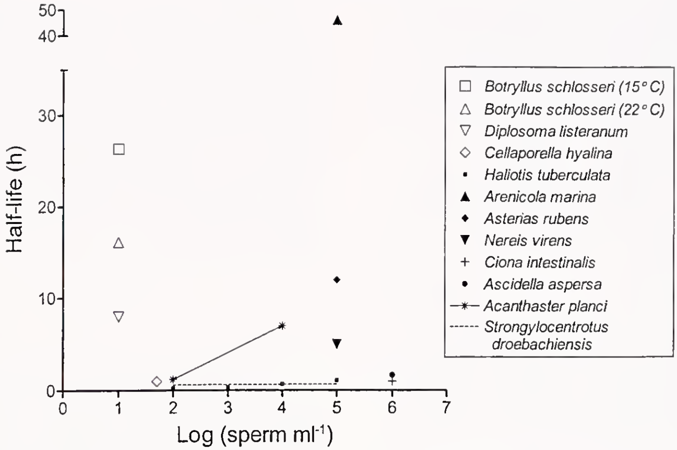

Figure 3. Sperm half-life (h) measured as a function of sperm concentration (log sperm ml^{-1}) in a variety of free-spawning marine invertebrates (*sensu* Manríquez *et al.*, 2001, with additional values from this study and the literature). *Botryllus schlosseri*, this paper; *D. listeranum*, Bishop, 1998; *C. hyalina*, Manríquez *et al.*, 2001; *H. tuberculata*, Powell *et al.*, 2001; *A. marina*, *N. virens*, and *A. rubens*, Williams and Bentley, 2002; *C. intestinalis* and *A. aspera*, Bolton and Havenhand, 1996; *A. planci*, Benzie and Dixon, 1994; *S. droebachiensis*, Levitan, 1993). Lines connect different values reported for individual species at multiple sperm concentrations. The four open symbols represent brooders; the remaining closed symbols are broadcasters.

dilution effect (Chia and Bickell, 1983), but the combination of high longevity and very low concentration has not previously been reported. In addition, *Arenicola* is an egg-broadcasting species that retains its eggs in a burrow and pumps sperm-laden water past them (Williams *et al.*, 1997). Consequently, it appears to function much like an egg-brooder (Williams and Bentley, 2002). Prolonged motility has been observed in two species of deep-sea echinothuriid sea urchins, *Araeosoma fenestratum* and *Sperosoma antillense* (Young, 1994); but sperm concentrations were not reported and fertilization was not assayed. The presence of lipid stores attached to the mitochondria of these sperm may enable the sperm to swim for prolonged times (Eckelbarger *et al.*, 1989; Young, 1994). However, the role of lipid stores in swimming has been questioned (Eckelbarger, 1994).

The only free-spawners known to have comparable sperm longevity at low concentration (Fig. 3) are another brooding ascidian, *Diplosoma listeranum* (Bishop, 1998), with an estimated sperm half-life of 8 h at 10^1 sperm ml^{-1}, and a brooding bryozoan, *Cellaporella hyalina*, with an estimated sperm half-life of 1 h at 10^1–10^2 sperm ml^{-1} (Manríquez *et al.*, 2001). This pattern suggests that sperm longevity may be consistently higher in egg-brooding invertebrates than in egg-broadcasters. However, this relationship may break down when more taxa are studied. Some brooders lack any apparent mechanism to efficiently collect dilute sperm from distant males *via* a filter-feeding or suspension-feeding mechanism (*e.g.*, brooding corals).

Although the other two brooding taxa have dilute sperm longevities greater than those of the broadcasting species, the longevities of *D. listeranum* and *C. hyalina* are nevertheless somewhat lower than in *B. schlosseri*. In contrast to these two species, *B. schlosseri* lacks the ability to store sperm (Stewart-Savage *et al.*, 2001). *D. listeranum* and *C. hyalina* can both store sperm for several months (Bishop and Ryland, 1991; Bishop and Sommerfeldt, 1996) and weeks (Manríquez, 1999), respectively. In the absence of a mechanism to store sperm, extended sperm longevity in *B. schlosseri* may represent an alternative adaptation to further enhance fertilization.

The high longevity of sperm in active filter-feeding or suspension-feeding brooders raises the question of how very dilute sperm can remain viable for such an extended period of time. A sperm's life span is based on its consumption of energy reserves (usually phospholipids; Harumi *et al.*, 1990), which is a function of the amount of energy consumed for motility. If *B. schlosseri* sperm are taken up passively through filter-feeding mechanisms, sperm may need to swim only short distances (*i.e.*, within the maternal zooid) to reach an egg. Consequently, longevity would be prolonged if sperm were relatively inactive while in the water column, and then activated within the maternal zooid.

The activation of dilute, inactive sperm by egg exudates has been reported in some broadcast-spawning solitary ascidians (Miller, 1974; Bolton and Havenhand, 1996; Jantzen *et al.*, 2001) and in abalone (Riffell *et al.*, 2002). Similarly, packets of bryozoan sperm alter their flagellar waveforms when released, thus probably saving energy and enhancing longevity, but increase the generation of waveforms to enter the maternal zooids (Temkin and Bortolami, 2004). *B. schlosseri* sperm might also conserve energy through intermittent swimming after release, as suggested for another colonial ascidian (Bishop, 1998). The continued presence of sperm in our top sample (Fig. 1A) after many hours supports this interpretation, but might also have been due to convection currents within the sperm-aging containers. We have never observed much activity in *B. schlosseri* sperm obtained from testes macerates, but it is possible that sperm are activated prior to natural release. Mixing had no effect on longevity (Table 1), so physical disturbance apparently does not activate sperm.

Temperature effects

This study suggests that temperature has a small but significant influence on longevity. The estimated half-life for sperm aged at 15 °C was 10 h longer than for those kept at 22 °C. *B. schlosseri* is found as far north as Newfoundland and south to North Carolina, and so experiences a wide range of temperature regimes (Pollock, 1998). Within the Damariscotta River estuary, water temperatures during spawning season can be as high as 22 °C at landward sites and as low as 13 °C in seaward sites (Yund and Stires, 2002).

Temperature directly controls metabolic activity in all cells, which influences energy consumption and survival (Hochachka and Somero, 1984). Due to temperature compensation, changes in sperm viability are expected to be minimal in eurythermal species that routinely spawn over a wide range of temperatures (Andronikov, 1975; Manríquez *et al.*, 2001). However, actual fertilization levels have been shown to decrease with increased temperature, due to mechanical damage or exhaustion of energy reserves (in a temperate sea urchin; Greenwood and Bennett, 1981). But any strictly metabolic approach to understanding temperature effects on sperm may be overly simplistic. Recent work on other small organisms has indicated that temperature effects may overestimate direct metabolic expenditures (Podolsky and Emlet, 1993; Fuiman and Batty, 1997; Hunt von Herbing, 2002). Water viscosity decreases with increasing temperature (Dorsey, 1968; Vogel, 1984; Denny, 1993; Jumars *et al.*, 1993), thus altering the energetic requirements of swimming. For example, Podolsky and Emlet (1993) demonstrated that an increase in temperature from 12 °C to 22 °C increased swimming speed in sand dollar larvae, and that about 40% of the speed increase and 67% of the Q_{10} could be attributed to the effect of reduced viscosity. This viscosity effect should be even more pronounced in smaller organisms (like sperm) that inhabit lower Reynolds number environments (Vogel, 1984), and most evident at lower temperatures where changes in viscosity are most pronounced (Jumars *et al.*, 1993). However, viscosity effects will only be relevant during times when sperm are actually swimming, or if viscosity stimulates swimming behavior.

It is also possible that temperature did not have a direct effect on sperm longevity *per se,* but rather an indirect effect *via* fertilization. The fertilization assays were conducted at the same temperatures used for aging the sperm suspensions. The clearance rates of some filter-feeders increase with temperature (Riisgard and Manríquez, 1997; Lisbjerg and Peterson, 2001; Turker *et al.*, 2003), but the ramifications for sperm capture in brooders have not yet been explored. Consequently, we cannot exclude the possibility that temperature affected the rate at which sperm were removed from the suspensions, as well as the viability of sperm.

Potential evolutionary implications

Because there is a trade-off between sperm velocity and longevity, it has been suggested that fast sperm are advantageous under conditions of sperm competition, and long-lived sperm are advantageous under conditions of sperm limitation (Levitan, 1993, 2000). Although *B. schlosseri* possesses extremely long-lived sperm, this species does not experience sperm limitation in nature (fertilization levels in nature are generally >85%; Phillippi *et al.*, 2004), and male-phase colonies in experimental populations compete for access to eggs (Yund and McCartney, 1994; Yund, 1995, 1998). Similarly, other brooding free-spawners with high sperm longevity are not thought to be sperm-limited, and they exhibit reproductive traits (*e.g.*, sperm storage, female choice) that are typically associated with sperm competition (Bishop, 1996, 1998; Bishop *et al.*, 2000; Pemberton *et al.*, 2003a). Hence the trade-off between velocity and longevity may not apply to brooders, but only to egg-broadcasting free-spawners.

Overall, *Botryllus schlosseri* appears to promote fertilization through the longevity of water-born sperm and through the ability to concentrate dilute sperm from the water column. The substantial longevity of dilute sperm reported here potentially allows viable sperm to disperse a great distance from a source population. In the field, most eggs are fertilized by sperm from nearby sources (Grosberg, 1987; Yund, 1995, 1998), but eggs in isolated colonies can be fertilized from distances of 40 m or more (Yund and McCartney, 1994). Given the often high density of *B. schlosseri* colonies in nature (>1000 colonies m^{-2} at some sites; Grosberg, 1982) and the fact that colonies continuously dribble sperm over a period of 4–5 days (Stewart-

Savage and Yund, 1997), more sperm are probably released than are utilized locally. This surplus is likely to be advected away by currents and could contribute greatly to gene flow between populations if sperm remain viable during their journey. Sperm dispersal could be of particular importance to gene flow in an organism like *B. schlosseri* that has a very short-lived larval stage (Grosberg, 1987; Yund, 1995).

Acknowledgments

A. Phillippi, K. Murdock, B. Cole, B. Gensheimer, and J. Stewart-Savage assisted with animal culture. W. Hatleman provided statistical advice. We thank A. Phillippi, J. Grabowski, C. Young, and an anonymous reviewer for reading and suggesting changes that improved the manuscript. Financial support was provided by the National Science Foundation (OCE-01-17623) and the Gulf of Maine Foundation. This is contribution number 393 from the Darling Marine Center.

Literature Cited

Andronikov, V. B. 1975. Heat resistance of gametes of marine invertebrates in relation to temperature conditions under which the species exist. *Mar. Biol.* **30:** 1–11.

Baker, M. C., and P. A. Tyler. 2001. Fertilization success in the commercial gastropod *Haliotis tuberculata. Mar. Ecol. Prog. Ser.* **211:** 205–213.

Benzie, J., and P. Dixon. 1994. The effects of sperm concentration, sperm:egg ratio, and gamete age on fertilization success in crown-of-thorns starfish (*Acanthaster planci*) in the laboratory. *Biol. Bull.* **186:** 139–152.

Bishop, J. D. D. 1996. Female control of paternity in the internally fertilizing compound ascidian *Diplosoma listeranum.* I. Autoradiographic investigation of sperm movements in the female reproductive tract. *Proc. R. Soc. Lond. B* **263:** 369–376.

Bishop, J. D. D. 1998. Fertilization in the sea: are the hazards of broadcast spawning avoided when free-spawned sperm fertilize retained eggs? *Proc. R. Soc. Lond. B* **265:** 725–731.

Bishop, J. D. D., and J. S. Ryland. 1991. Storage of exogenous sperm by the compound ascidian *Diplosoma listeranum. Mar. Biol.* **108:** 111–118.

Bishop, J. D. D., and A. D. Sommerfeldt. 1996. Autoradiographic investigation of uptake and storage of exogenous sperm by the ovary of the compound ascidian *Diplosoma listeranum. Mar. Biol.* **125:** 663–670.

Bishop, J. D. D., A. J. Pemberton, and L. R. Noble. 2000. Sperm precedence in a novel context: mating in a sessile marine invertebrate with dispersing sperm. *Proc. R. Soc. Lond. B* **267:** 1107–1113.

Bolton, T. F., and J. N. Havenhand. 1996. Chemical mediation of sperm activity and longevity in the solitary ascidians *Ciona intestinalis* and *Ascidiella aspera. Biol. Bull.* **190:** 329–335.

Chia, F.-S., and L. R. Bickell. 1983. Echinodermata. Pp. 545–620 in *Reproductive Biology of Invertebrates,* K. G., and R. G. Adiyodi, eds. John Wiley, New York.

Denny, M. W. 1988. *Biology and Mechanics of the Wave-swept Environment.* Princeton University Press, Princeton, NJ.

Denny, M. W. 1993. *Air and Water.* Princeton University Press, Princeton, NJ.

Denny, M. W., and M. F. Shibata. 1989. Consequences of surf-zone turbulence for settlement and external fertilization. *Am. Nat.* **134:** 859–889.

Denny, M. W., E. K. Nelson, and K. S. Mead. 2002. Revised estimates of the effects of turbulence on fertilization in the purple sea urchin, *Strongylocentrotus purpuratus. Biol. Bull.* **203:** 275–277.

Dorsey, N. E. 1968. *Properties of Ordinary Water-Substance in All Its Phases: Water-Vapor, Water, and All the Ices.* Hafner, New York.

Eckelbarger, K. J. 1994. Ultrastructural features of gonads and gametes in deep-sea invertebrates. Pp. 137–157 in *Reproduction, Larval Biology and Recruitment in the Deep-Sea Benthos,* C. M. Young and K. J. Eckelbarger, eds. Columbia University Press, New York.

Eckelbarger, K. J., C. M. Young, and J. L. Cameron. 1989. Modified sperm ultrastructure in four species of soft-bodied echinoids (Echinodermata: Echinothuriidae) from the bathyal zone of the deep sea. *Biol. Bull.* **177:** 230–236.

Fuiman, L. A., and R. S. Batty. 1997. What a drag it is getting cold: partitioning the physical and physiological effects of temperature on fish swimming. *J. Exp. Biol.* **200:** 1745–1755.

Giese, A. C., and H. Kanatani. 1987. Maturation and spawning. Pp. 251–329 in *Reproductive Biology of Invertebrates,* Vol. 9, A. C. Giese, J. S. Pearse, and V. B. Pearse, eds. Boxwood Press, Pacific Grove, CA.

Greenwood, P. J., and T. Bennett. 1981. Some effects of temperature-salinity combinations on the early development of the sea urchin *Parechinus angulosus* (Leske). Fertilization. *J. Exp. Mar. Biol. Ecol.* **51:** 119–131.

Grosberg, R. K. 1982. Ecological, genetical, and developmental factors regulating life history variation within a population of the colonial ascidian *Botryllus schlosseri* (Pallas) Savigny. Ph.D. dissertation. Yale University, New Haven, CT.

Grosberg, R. K. 1987. Limited dispersal and proximity-dependent mating success in the colonial ascidian *Botryllus schlosseri. Evolution* **41:** 372–384.

Grosberg, R. K. 1988. Life-history variation within a population of the colonial ascidian *Botryllus schlosseri.* I. The genetic and environmental control of seasonal variation. *Evolution* **42:** 900–920.

Grosberg, R. K. 1991. Sperm-mediated gene flow and the genetic structure of a population of the colonial ascidian *Botryllus schlosseri. Evolution* **45:** 130–142.

Harumi, T., R. De Santis, M. R. Pinto, and N. Suzuki. 1990. Phospholipid utilization in ascidian *Ciona intestinalis* spermatozoa during swimming. *Comp. Biochem. Physiol.* **96A:** 263–265.

Hochachka, P. W., and G. N. Somero. 1984. *Biochemical Adaptation.* Princeton University Press, Princeton, NJ.

Hunt von Herbing, I. 2002. Effects of temperature on larval fish swimming performance: the importance of physics to physiology. *J. Fish. Biol.* **61:** 865–876.

Jantzen, T. M., R. de Nys, and J. N. Havenhand. 2001. Fertilization success and the effects of sperm chemoattractants on effective egg size in marine invertebrates. *Mar. Biol.* **138:** 1153–1161.

Jumars, P. A., J. W. Deming, P. S. Hill, L. Karp-Boss, P. L. Yager, and W. B. Dade. 1993. Physical constraints on marine osmotrophy in an optimal foraging context. *Mar. Microb. Food Webs* **7:** 121–159.

Levitan, D. R. 1991. Influence of body size and population density on fertilization success and reproductive output in a free-spawning invertebrate. *Biol. Bull.* **181:** 261–268.

Levitan, D. R. 1993. The importance of sperm limitation to the evolution of egg size in marine invertebrates. *Am. Nat.* **141:** 517–536.

Levitan, D. R. 1995. The ecology of fertilization in free-spawning invertebrates. Pp. 123–156 in *Ecology of Marine Invertebrate Larvae,* L. McEdward, ed. CRC Press, Boca Raton, FL.

Levitan, D. R. 1998. Sperm limitation, gamete competition, and sexual selection in external fertilizers. Pp. 175–217 in *Sperm Competition and Sexual Selection,* T. R. Birkhead and A. P. Moller, eds. Academic Press, San Diego, CA.

Levitan, D. R. 2000. Sperm velocity and longevity trade off each other and influence fertilization in the sea urchin *Lytechinus variegatus*. *Proc. R. Soc. Lond. B* **267:** 531–534.

Levitan, D. R., and C. Petersen. 1995. Sperm limitation in the sea. *Trends Ecol. Evol.* **10:** 228–231.

Levitan, D. R., M. A. Sewell, and F.-S. Chia. 1991. Kinetics of fertilization in the sea urchin *Strongylocentrotus franciscanus:* interaction of gamete dilution, age, and contact time. *Biol. Bull.* **181:** 371–378.

Lishjerg, D., and J. K. Petersen. 2001. Feeding activity, retention efficiency, and effects of temperature and particle concentration on clearance rate in the marine bryozoan *Electra crustulenta. Mar. Ecol. Prog. Ser.* **215:** 133–141.

Manríquez, P. H. 1999. Mate choice and reproductive investment in the cheilostome bryozoan *Celloporella hyalina* (L.). Ph.D. thesis, University of Wales, Bangor, UK.

Manríquez, P. H., R. N. Hughes, and J. D. D. Bishop. 2001. Age-dependent loss of fertility in water-borne sperm of the bryozoan *Celleporella hyalina. Mar. Ecol. Prog. Ser.* **224:** 87–92.

Mead, K. S., and M. W. Denny. 1995. The effects of hydrodynamic shear stress on fertilization and early development of the purple sea urchin *Strongylocentrotus purpuratus. Biol. Bull.* **188:** 46–56.

Milkman, R. 1967. Genetic and developmental studies on *Botryllus schlosseri. Biol. Bull.* **132:** 229–243.

Miller, R. L. 1974. Sperm behavior close to *Hydractinia* and *Ciona* eggs. *Am. Zool.* **14:** 1250.

Pemberton, A. J., L. R. Noble, and J. D. D. Bishop. 2003a. Frequency dependence in matings with water-borne sperm. *J. Exp. Biol.* **16:** 289–301.

Pemberton, A. J., R. N. Hughes, P. H. Manríquez, and J. D. Bishop. 2003b. Efficient utilization of very dilute sperm: sperm competition may be more likely than sperm limitation when eggs are retained. *Proc. R. Soc. Lond. B* **270:** 223–226.

Pennington, J. T. 1985. The ecology of fertilization of echinoid eggs: the consequences of sperm dilution, adult aggregation, and synchronous spawning. *Biol. Bull.* **169:** 417–430.

Phillippi, A., E. Hannan, and P. O. Yund. 2004. Fertilization in an egg-brooding colonial ascidian does not vary with population density. *Biol. Bull.* **206:** 152–160.

Podolsky, R. D., and R. B. Emlet. 1993. Separating the effects of temperature and viscosity on swimming and water movement by sand dollar larvae (*Dendraster excentricus*). *J. Exp. Biol.* **176:** 207–221.

Pollock, L. W. 1998. *A Practical Guide to the Marine Animals of Northeastern North America.* Rutgers University Press, New Brunswick, NJ.

Powell, D. K., P. A. Tyler, and L. S. Peck. 2001. Effect of sperm concentration and sperm ageing on fertilization success in the Antarctic soft-shelled clam *Laternula elliptica* and the Antarctic limpet *Nacella concinna. Mar. Ecol. Prog. Ser.* **215:** 191–200.

Riffell, J. A., P. J. Krug, and R. K. Zimmer. 2002. Fertilization in the sea: the chemical identity of an abalone sperm attractant. *J. Exp. Biol.* **205:** 1439–1450.

Riisgård, H. U., and P. Manríquez. 1997. Filter-feeding in fifteen marine ectoprocts (Bryozoa): particle capture and water pumping. *Mar. Ecol. Prog. Ser.* **154:** 223–239.

Stewart-Savage, J., and P. O. Yund. 1997. Temporal pattern of sperm release from the colonial ascidian, *Botryllus schlosseri. J. Exp. Biol.* **279:** 620–625.

Stewart-Savage, J., A. Phillippi, and P. O. Yund. 2001. Delayed insemination results in embryo mortality in a brooding ascidian. *Biol. Bull.* **201:** 52–58.

Temkin, M. H., and S. B. Bortolami. 2004. Waveform dynamics of spermatozeugmata during the transfer from paternal to maternal individuals of *Membranipora membranacea. Biol. Bull.* **206:** 35–45.

Turker, H., A. G. Eversole, and D. E. Brune. 2003. Effect of temperature and phytoplankton concentration on Nile tilapia *Oreochromis niloticus* (L.) filtration rate. *Aquac. Res.* **34:** 453–459.

Van Name, W. G. 1945. The North and South American ascidians. *Bull. Am. Mus. Nat. Hist.* **84:** 1–476.

Vogel, H., G. Czihak, P. Chang, and W. Wolf. 1982. Fertilization kinetics of sea urchin eggs. *Math. Biosci.* **58:** 189–216.

Vogel, S. 1984. *Life in Moving Fluids.* Princeton University Press, Princeton, NJ.

Williams, M. E., and M. G. Bentley. 2002. Fertilization success in marine invertebrates: the influence of gamete age. *Biol. Bull.* **202:** 34–42.

Williams, M. E., M. G. Bentley, and J. D. Hardege. 1997. Assessment of field fertilization success in the infaunal polychaete *Arenicola marina* (L.). *Invertebr. Reprod. Dev.* **31:** 189–197.

Young, C. M. 1994. The biology of external fertilization in deep-sea echinoderms. Pp. 179–200 in *Reproduction, Larval Biology and Recruitment in the Deep-Sea Benthos,* C. M. Young and K. J. Eckelbarger, eds. Columbia University Press, New York.

Yund, P. O. 1995. Gene flow via the dispersal of fertilizing sperm in a colonial ascidian (*Botryllus schlosseri*): the effect of male density. *Mar. Biol.* **122:** 649–654.

Yund, P. O. 1998. The effect of sperm competition on male gain curves in a colonial marine invertebrate. *Ecology* **79:** 328–339.

Yund, P. O. 2000. How severe is sperm limitation in natural populations of marine free-spawners? *Trends Ecol. Evol.* **15:** 10–13.

Yund, P. O., and M. A. McCartney. 1994. Male reproductive success in sessile invertebrates: competition for fertilizations. *Ecology* **75:** 2151–2167.

Yund, P. O., and A. Stires. 2002. Spatial variation in population dynamics in a colonial ascidian (*Botryllus schlosseri*). *Mar. Biol.* **141:** 955–963.

Reference: *Biol. Bull.* **206:** 152–160. (June 2004)
© 2004 Marine Biological Laboratory

Fertilization in an Egg-Brooding Colonial Ascidian Does Not Vary With Population Density

AIMEE PHILLIPPI[1,*], ELLEN HAMANN[2], AND PHILIP O. YUND[1,†]

[1] *School of Marine Sciences, Darling Marine Center, University of Maine, Walpole, Maine 04573; and*
[2] *Biology Department, Augustana College, Sioux Falls, South Dakota 57197*

Abstract. The possibility that free-spawning marine organisms may be subject to fertilization failure at low population density (due to the effects of sperm dilution) has sparked much interest, but these effects have been demonstrated only in a few species that broadcast their eggs. Some egg-brooding species may overcome dilution effects by filtering low concentrations of sperm from seawater and fertilizing eggs throughout an extended period of time. We examined the effects of population density and size on fertilization in *Botryllus schlosseri,* a hermaphroditic colonial ascidian that free-spawns sperm, but broods eggs. We experimentally manipulated the size and density of mating groups and surveyed fertilization levels in natural populations that varied in density. Fertilization was not affected by variation in population size or density in either the experimental or natural populations. Near the end of the reproductive season, some eggs may have been fertilized too late to complete development, suggesting a temporal form of sperm limitation that has not been considered in other systems. We also detected greater variability in fertilization levels at lower population density. Nevertheless, these results suggest that caution must be used in extrapolating reported density effects on fertilization to all taxa of free-spawners; density effects may be reduced in brooders that have efficient sperm collection mechanisms.

Introduction

Population growth is often limited by the recruitment of new individuals. Because most marine organisms produce orders of magnitude more gametes than offspring that successfully recruit (Morgan, 1995), sources of reproductive loss have received much recent attention. Larval mortality may be the biggest bottleneck for many species (Thorson, 1950; Strathmann, 1985; Roughgarden *et al.,* 1988). However, in free-spawning marine taxa (*i.e.,* those that release sperm into the surrounding seawater), fertilization has also attracted attention as a possible stage of significant reproductive loss (Pennington, 1985; Oliver and Babcock, 1992; Sewell, 1994; Levitan and Petersen, 1995; Lasker *et al.,* 1996; Coma and Lasker, 1997a).

Fertilization will not be successful if the distance between spawning individuals is too great. Experimental studies have documented decreasing fertilization with distance from a sperm source in diverse taxa of marine free-spawners (Pennington, 1985; Yund, 1990, 1995; Levitan, 1991; Levitan *et al.,* 1991, 1992; Brazeau and Lasker, 1992; Oliver and Babcock, 1992; Babcock *et al.,* 1994; Benzie and Dixon, 1994; Benzie *et al.,* 1994; Yund and McCartney, 1994; Levitan and Young, 1995; Lasker *et al.,* 1996; Coma and Lasker, 1997a, b; Meidel and Yund, 2001; Metaxas *et al.,* 2002). As a logical consequence of these distance effects, reproduction in low-density populations may be limited by fertilization when individuals are separated by distances greater than the dispersal distance of fertilizing sperm. Fertilization failure at low population density (a form of negative density-dependent population dynamics known as an Allee effect; Levitan *et al.,* 1992) has been investigated in commercially harvested species and considered in the development of management programs (Jamieson, 1993; Quinn *et al.,* 1993; Myers *et al.,* 1995; Pfister and Bradbury, 1996; Liermann and Hilborn, 1997; Levitan and Sewell, 1998; Shelton and Healey, 1999; Frank and Brickman, 2000). Models, coupled with laboratory experiments on the effects of variation in sperm concentration on fertilization,

---

Received 3 December 2003; accepted 16 March 2004.

[*] To whom correspondence should be addressed. E-mail: aimeep@maine.edu

[†] Current Address: Marine Science Center, University of New England, Biddeford, ME 04005.

have predicted declining fertilization levels with decreasing population size or density for free-spawners that broadcast their eggs (Levitan, 1991; Levitan and Young, 1995; Claereboudt, 1999; Metaxas *et al.*, 2002). Field experiments with three egg-broadcasting species of sea urchins have supported the predicted trend (Levitan, 1991; Levitan *et al.*, 1992; Wahle and Peckham, 1999). Density has also been predicted to have a greater effect on fertilization when populations are small (Levitan and Young, 1995), suggesting the need to simultaneously evaluate the effects of population size and density (Levitan *et al.*, 1992).

To date, research on how the density and size of a population affects fertilization has focused on organisms that broadcast eggs, but variation in density may have very different consequences for free-spawners that fertilize eggs internally (brooders). In external fertilizers, both gametes are subject to dilution; in brooders, only sperm are diluted. If brooders are able to capture or concentrate dilute sperm, fertilization levels may be high even when individuals are far apart and few in number (Yund, 2000).

We examined the effects of population density on fertilization in *Botryllus schlosseri* (Pallas, 1766), a sessile, hermaphroditic, free-spawning colonial ascidian with internal fertilization. Sperm limitation has been demonstrated under experimental conditions in the field (Yund and McCartney, 1994; Yund, 1995), and populations are characterized by substantial spatial and temporal variation in population density (Yund and Stires, 2002). However, fertilization levels in natural spawns have not previously been reported, nor have density effects on fertilization been rigorously evaluated. Past manipulations (designed to test for sperm competition) have manipulated male density but not total population density (Yund and McCartney, 1994; Yund, 1995, 1998). We conducted a mix of manipulative field experiments and surveys of spawning in natural populations in the Damariscotta River estuary (Maine) during the summers of 1999 and 2000. Population size and density were manipulated in experimental populations to independently test the effects of these two factors. Density effects were also assessed in natural spawns by deploying laboratory-cultured colonies in populations that varied in density in space and time.

Materials and Methods

Study organism and culture

Botryllus schlosseri is a colonial ascidian with a sexual cycle coupled to an asexual zooid replacement cycle, which is synchronous throughout the colony. Asexually produced buds form and develop along the sides of the functioning generation of zooids that are brooding embryos and releasing sperm. Concurrent with or shortly after the release of fully developed embryos as larvae, the old generation of zooids is resorbed and the new zooids (formerly buds) start to feed and begin the next cycle (Milkman, 1967). Eggs are viable to be fertilized as soon as the siphons of the new zooids open, but if fertilized more than 24 h after siphon opening, they are unlikely to complete development before the end of the asexual cycle (Stewart-Savage *et al.*, 2001a). Sperm release occurs over a period of several days, and does not peak until a few days after siphon opening (Stewart-Savage and Yund, 1997). The duration of the sexual-asexual cycle is temperature dependent (Grosberg, 1982). Colonies are not able to aggregate, spawn synchronously (Stewart-Savage and Yund, 1997), self-fertilize (Stewart-Savage *et al.*, 2001a), or store sperm (Stewart-Savage *et al.*, 2001a). Although eggs are generally fertilized by neighbors when other colonies are nearby (Yund and McCartney, 1994; Yund 1995), spatially isolated colonies can be fertilized by sperm from more than 40 m away (Yund, 1998).

Colonies of *B. schlosseri* on rocks and shells were collected from the Damariscotta River estuary, Maine, by divers and transported to the laboratory. Fragments of each colony were explanted onto microscope slides and maintained in a flowing seawater system at the University of Maine's Darling Marine Center (Walpole, Maine). Animals cultured on glass can be examined under a microscope to assess egg production and stage in the reproductive cycle. Colonies for the manipulative experiment and the field survey were selected on the basis of sexual stage. Male-phase colonies (those releasing sperm) were deployed at about stage three (by the criteria of Milkman, 1967). Female-phase colonies (those with eggs ready to be fertilized) were deployed at late stage four or early stage five (Milkman, 1967), just prior to takeover by the new asexual generation of zooids. Females were recovered between stages 3 and 4 in the subsequent cycle (total cycle duration ranged from 7–10 days), prior to the release of brooded larvae. All embryos were then surgically removed from the zooids for enumeration. The percent of eggs fertilized was calculated as the number of larvae brooded upon return from the field divided by the number of eggs brooded prior to deployment, multiplied by 100. Data from colonies that were unhealthy, damaged, or dead upon return from the field were excluded.

Population size and density manipulation

We examined the potentially independent effects of population size and density on fertilization during the summer of 2000 by manipulating population size and colony spacing in experimental populations. Our experimental design employed four combinations of two population size treatments (4 and 16 colonies; Fig. 1) and two density treatments (equivalent to 13 and 157 colonies per square meter, calculated on the basis of the separation distances between the centers of the colonies). Population sizes in this experiment were smaller than many natural populations, but comparable to colony numbers on isolated pieces of hard substratum.

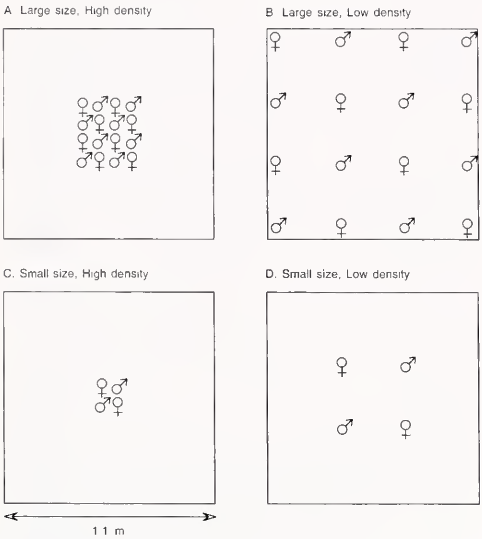
A Large size, High density
B Large size, Low density
C. Small size, High density
D. Small size, Low density
11 m

Figure 1. Design of mating arrays used in the four experimental treatments to assess the effects of population size and density on fertilization levels of *Botryllus schlosseri*. Symbols indicate the functional gender of a colony during an experiment; all colonies are actually hermaphrodites. Colony positions in the two high-density arrays are not quite to scale (colonies were closer together than the size of the symbols permits; 5 cm apart on center). Populations consisted of either 4 or 16 colonies, while density corresponded to 13 *vs.* 157 colonies m^{-2}.

Density treatments spanned most of the reported range for natural variation in this estuary (about 5 to 170 colonies per square meter; Yund and Stires, 2002), though for logistical reasons we were unable to explore the very lowest densities observed in nature. Experimental populations were assembled by mounting laboratory-cultured colonies growing on 2.5 × 7.6 cm glass microscope slides on 1.21-m^{-2} sheets of 0.6-cm-thick marine plywood that were in turn mounted on top of flat concrete patio blocks weighing 40 kg. Colonies were arranged so that male and female phases alternated as nearest neighbors (Fig. 1). Female colonies brooded an average of 59 eggs (±2.5 SE).

Assembled arrays were deployed in a 4-m-deep (at mean low water) channel in the Damariscotta River between an island (Carlisle Island) and the mainland. The substratum in this channel is soft sediment, so *B. schlosseri* does not occur naturally. Past experiments in this location have indicated only minor contamination from natural sperm as long as local experimental males are present (Yund, 1998). Currents are dominated by tidal exchange, are largely bidirectional, and are non-zero 95% of the time (Yund and McCartney, 1994). The arrays were lowered from the surface by means of lines, so the orientation of the colonies with respect to tidal currents was not known. Each array was separated from its nearest neighbor by at least 30 m.

Four replicate trials were conducted of all four treatment combinations, with one replicate of each treatment performed simultaneously. Because each 16-colony (large population) array potentially yielded fertilization levels for four times as many females as the 4-colony (small population) arrays (8 *vs.* 2 females per trial), we conducted two extra trials of the small population size treatments to produce more equitable replication across treatments. Owing to the loss of data on some females that did not survive through their deployment, we obtained an average of 5.5 fertilization values per replicate trial for the large population size treatments, and 1.7 for the small population size treatments. The percent of eggs fertilized was arcsin-transformed to meet ANOVA assumptions, and then this dependent variable was analyzed by an ANOVA package that accommodates an unbalanced design (Statistica '99, Statsoft, Inc.) with population size, population density, and trial as the three main effects. The data were initially analyzed with interaction effects included in the model. No interactions between any of the main effects were significant, so the analysis was repeated excluding interaction effects to maximize power for the main effects. We also performed a power analysis to assess our ability to detect differences among treatments.

Natural spawning populations

To assess fertilization levels in natural spawns, we deployed laboratory-cultured female-phase colonies in two field populations in the Damariscotta River during the summer of 1999. The two populations were located adjacent to the shores of small islands in the river. The seaward site was located at Carlisle Island (hereafter CI), while the landward site (DM) was at Glidden Ledge (see Yund and Stires, 2002, for a map and additional site information). The DM site experiences warmer temperatures during the summer, which decreases the duration of each reproductive cycle (Yund and Stires, 2002). Egg production is much higher at DM, apparently because of greater food availability (Stewart-Savage *et al.*, 2001b). Both sites exhibit seasonal variation in population density, with peak densities occurring in August, but peak density is typically about seven times greater at DM than at CI (Yund and Stires, 2002).

To assess fertilization levels in the field, female-phase colonies growing on 2.5 × 7.6 cm microscope slides were placed individually in open-sided plastic slide boxes that were attached to a cinderblock-weighted rope supported by a surface buoy. Colonies were oriented upside down to reduce the effects of sedimentation, and were located approximately 0.5 m above the substratum. Three to eight (mean = 5.5 ± 0.3 SE) colonies were deployed at each site approximately weekly from early June to mid-August, and at site CI through the end of September. Colonies were positioned along a transect oriented parallel to the shore, and spaced about 7 m from their nearest neighbor.

Egg counts prior to deployment averaged 105 per colony (± 12 SE). All colonies remained in the field through the beginning of the next asexual generation (hereafter termed takeover) and the full period of egg viability, so that eggs were fertilized by naturally available sperm. Fertilization levels were determined as described above. Throughout most of the season, all embryos within a colony were at the same developmental stage. The presence of a mixture of developmental stages indicated that embryos lagging in development were fertilized later than the others (Meidel and Yund, 2001). Typically, all embryos surgically removed from a colony were at about stage four, and possessed a tail that wrapped completely around the embryo (Milkman, 1967). Embryos at a tail-bud stage or earlier (by the criteria of Milkman, 1967) were at least 24 h behind in development and therefore were reported as unlikely to complete development (Stewart-Savage *et al.* 2001a).

Throughout the reproductive season, we surveyed the density of *B. schlosseri* colonies at both sites monthly. Density surveys, made with the aid of scuba, involved counting all of the colonies present in eight randomly deployed 0.64-m^{-2} quadrats. We did not measure the size distribution, reproductive status, or reproductive output of the colonies because past work (Stewart-Savage *et al.*, 2001b; Yund and Stires, 2002) permits reasonable inference about variation in these variables between sites. A subset of the field fertilization data was used to assess the possible relationship with population density. Fertilization values obtained during three week-long intervals (including the weeks immediately before, during, and after the week of a population survey) were paired with the associated population density survey for analysis. Fertilization values obtained outside of these intervals could not be reliably associated with a density and so were excluded from this portion of the analysis. The possible relationship between fertilization and population density was assessed by regression. We also calculated the variance in fertilization at each density and used a variety of nonlinear regressions to explore possible relationships between variance in fertilization and population density.

Results

Population size and density manipulation

Fertilization levels were consistently high (>80%) in all four combinations of population size and density treatments (Fig. 2). The effect of trial was significant, but neither population size nor density affected fertilization levels in experimental populations (Table 1). Results from the power analysis indicated that replication was sufficient to detect differences between treatments as small as 7.5% for density effects and 8.7% for population size effects at $\alpha = 0.05$.

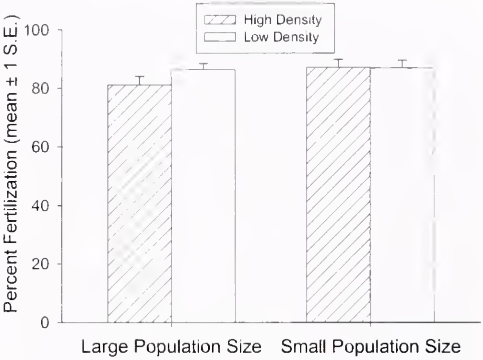

Figure 2. Mean field fertilization levels of *Botryllus schlosseri* colonies in the four population size and density treatments. Error bars represent one standard error.

Natural spawning populations

As reported for 1996 and 1997 (Yund and Stires, 2002), population density increased at the landward site (DM) throughout the summer and declined after September (Fig. 3). However, peak density at DM was substantially lower than recorded in both earlier years (65 *vs.* ~ 170 colonies m^{-2}; Yund and Stires, 2002). Nevertheless, peak density was more than an order of magnitude higher than density early in the season. Densities at the seaward site (CI) were generally lower than at DM and exhibited less variation during the season (Fig. 3).

Mean fertilization levels at both sites were greater than 70% throughout the season, with only two exceptions (Fig. 3). The mean fertilization at DM in week 24 was slightly lower owing to the almost complete fertilization failure of one female colony (note the very high variance for this mean in Fig. 3). Towards the very end of the reproductive season the seaward site showed a slight trend toward declining fertilization (90% to 66% in weeks 37 to 40; Fig. 3).

Beginning at week 38, embryos removed from colonies that had been deployed at site CI varied greatly in developmental staging (in contrast to all earlier weeks when the embryos within a colony were all at the same developmental stage). Embryos at earlier developmental stages would have had insufficient time to complete development before the colony began a new asexual generation and the old zooids were resorbed (Stewart-Savage *et al.*, 2001a). By week 40, although 66% of eggs were fertilized, we estimate that only 39% of eggs would have resulted in fully developed larvae (Fig. 3).

There was no relationship between fertilization level and natural population density (Fig. 4A); the regression of percent of eggs fertilized on the log of density was not signif-

Table 1

Analysis of variance results for effects of population size and density on fertilization in the manipulative experiment

Effect	df	MS	SS	*F*-ratio	*P*
Size	1	2.699	2.699	0.031	0.862
Density	1	63.378	63.378	0.718	0.401
Trial	5	229.251	1146.254	2.596	0.035
Error	55	88.300	4856.505		

icant ($P = 0.250$, $r^2 = 0.016$). The power analysis indicated that a slope estimate of double the value obtained would have been necessary for significance at $\alpha = 0.05$. In contrast to the absence of a pattern in overall fertilization level, a nonlinear (exponentially declining) relationship did exist between the variance in fertilization and colony density ($r^2 = 0.7115$, $0.010 < P < 0.025$; Fig. 4B).

Discussion

Effects of population size and density on fertilization

Population density did not significantly affect fertilization in either experimental or natural populations of *Botryllus schlosseri* (Figs. 2, 3, 4; Table 1), although density varied across more than an order of magnitude and spanned most of the range relevant to local populations (Yund and Stires, 2002). Mean fertilization levels were generally very high (Figs. 2, 3). In the experimental manipulation, population size also had no effect on fertilization (Fig. 2; Table 1). This result contrasts with previous work on a species that broadcasts its eggs (the red sea urchin *Strongylocentrotus franciscanus*), in which population size was found to have an interactive effect (with density) on fertilization levels (Levitan *et al.*, 1992).

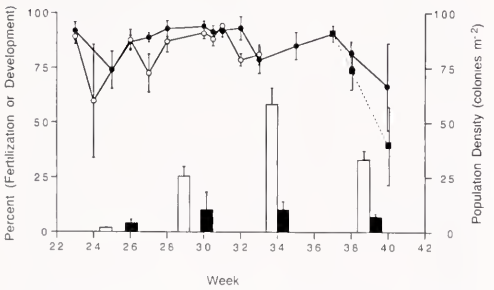

Figure 3. Percent of eggs fertilized (circles), embryos completing development (squares), and population density estimates (bars) for two natural populations of *Botryllus schlosseri*. Open bars and circles represent population DM; solid bars, circles, and squares represent population CI. Error bars represent one standard error.

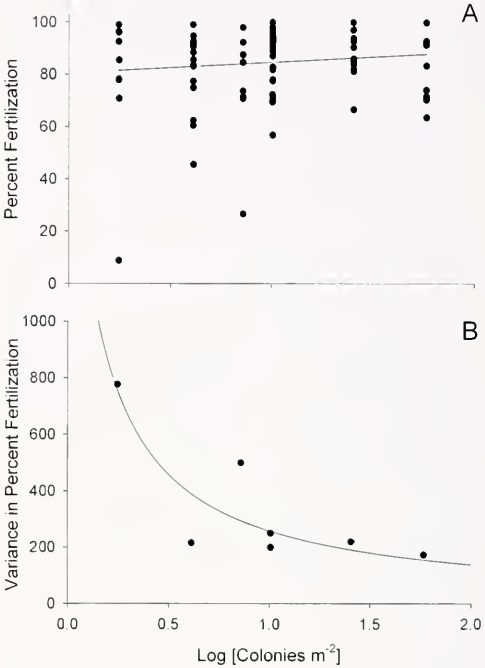

Figure 4. (A) Effect of colony density of natural populations on overall fertilization levels of *Botryllus schlosseri*. The plotted linear regression line is not significant. (B) Effect of colony density on variance in fertilization. The plotted exponential regression is significant at $P < 0.01$.

While overall fertilization levels did not change significantly with population density (Fig. 4A), the variance in fertilization in natural populations did increase at lower density (Fig. 4B), indicating that reduced population density may result in greater variation in fertilization among different individuals. The very high variance in fertilization at the lowest population density was heavily influenced by a single colony that exhibited exceptionally low fertilization (8.8%). However, such individual effects may be relevant to natural populations and should not be dismissed as outliers.

Because *B. schlosseri* is a colonial species, population density alone is an imperfect predictor of population-wide reproductive output. Juvenile colonies delay sexual reproduction until they achieve a minimum size (Boyd *et al.*, 1986; Chadwick-Furman and Weissman, 1995). Reproductive output in sexually mature colonies is highly variable and subject to both genetic (Grosberg, 1988; Yund *et al.*, 1997) and environmental (Newlon *et al.*, 2003) influences. Nevertheless, temporal variation in density is a reasonable first approximation of average gamete production at the population level, because it indicates times of population growth and contraction. Unlike many other colonial invertebrates, *B. schlosseri* rarely exhibits fragmentation (Grosberg, 1982). Consequently, recruitment of sexually produced larvae is essential for population growth (Yund and Stires, 2002).

In surveys, sperm appeared to become somewhat more limiting at the very end of the sample period. At that time, the annual reproductive season was ending and populations were shrinking (Fig. 3; Yund and Stires, 2002), so any marginal fertilization effect is best viewed as a minor component of a larger trend in population dynamics. Overall fertilization values exhibited only a slight downward trend, but the timing of fertilization varied more substantially (Fig. 3). The presence of embryos at various developmental stages indicated that fertilization within each brood occurred over a wider time span than during the rest of the reproductive season. Embryos at an earlier developmental stage at the conclusion of our sample intervals would probably not have had sufficient time to complete development before the adult zooids were resorbed and the next asexual generation began (Stewart-Savage *et al.*, 2001a). Therefore, delayed fertilizations are unlikely to have produced viable progeny, and so may represent a form of temporal sperm limitation. Sperm availability may have been reduced at this time of year from decreases in both population density and energy allocated to sperm production (Stewart-Savage *et al.*, 2001a). A crash in the local phytoplankton population each autumn (Incze *et al.*, 1980) is consistently associated with smaller testes and lower egg production in *B. schlosseri* (unpubl. data).

Comparison with results from other taxa

The effects of population size and density on fertilization have been investigated in other free-spawning marine invertebrates. Field experiments with three species of sea urchins used eggs retained in Nitex mesh bags and either induced males to spawn or used sperm-filled syringes to simulate males. Increasing the number or density of spawning individuals increased fertilization in all three species (Levitan, 1991; Levitan *et al.*, 1992; Wahle and Peckham, 1999). Ultimately, the differing consequences of population size and density for fertilization in sea urchins and ascidians can probably be explained by the different spawning strategies of these taxa. Sea urchins broadcast both sperm and eggs, so rapid gamete dilution may have a greater impact on sperm-egg encounters than in brooders, where egg retention prevents the dilution of female gametes. However, all three of the sea urchin studies cited above manipulated gametes so that eggs were held at fixed concentrations in sperm-permeable containers. Consequently, though egg dilution may be important in natural spawns, it played no role in the experimental results reported in these papers. Hence the proximate explanation for the difference between our results and those of the sea urchin studies must involve a process other than egg dilution.

As part of a reproductive strategy that involves retaining eggs internally, brooders usually possess some mechanism for capturing sperm. The method by which sperm enter a female-phase *B. schlosseri* colony is not known, but all indications are that this organism is exceedingly efficient at acquiring dilute, long-lived sperm from the water (Johnson and Yund, 2004). Additionally, fertilization in *B. schlosseri* is a time-integrated process with eggs viable to be fertilized for 24 h (Stewart-Savage *et al.*, 2001a). Consequently, it seems probable that sperm are filtered out of the water as a by-product of feeding activity, which is likely to involve the processing of a relatively large volume of water. If so, sperm would in effect be concentrated, limiting the impact of sperm dilution. Thus increased efficiency of sperm collection coupled with time-integrated fertilization, rather than reduced egg dilution, may explain the absence of density effects on fertilization in *B. schlosseri.*

Density effects on fertilization have also been explored in the internally fertilizing Queen conch, *Strombus gigas*, which does not free-spawn, but instead transfers sperm by copulation. At very low adult densities (<100/ha or $<0.01/\text{m}^2$), reproductive success was found to be density dependent in *S. gigas* (Stoner and Ray-Culp, 2000). However, above a critical density, evidence for Allee effects in *S. gigas* dissipated as the frequency of observed reproductive behavior plateaued. By analogy, sperm limitation is to be expected in *B. schlosseri* at some very low population density. However, that density condition does not appear to occur in the Damariscotta River estuary.

Although previous studies of fertilization in egg-brooding free-spawners have not directly addressed the effects of population density, a comparison of reported efficiencies of sperm capture is nonetheless illuminating. Both the colonial ascidian *Diplosoma listerianum* and the bryozoan *Celleporella hyalina* achieve maximum fertilization at sperm concentrations on the order of 10^2 ml^{-1}, in contrast to the 10^4–10^5 ml^{-1} concentrations required for fertilization in sea urchins (Pemberton *et al.*, 2003). When sperm from a single male-phase *D. listerianum* colony were diluted in a 3840-l tank, the male was nevertheless able to sire abundant progeny with 20 female-phase colonies (Bishop, 1998). Consequently, these two brooding species appear likely to have ecological fertilization dynamics similar to those of *B. schlosseri.* In marked contrast to these results, female colonies of the brooding octocoral *Briareum asbestinum* were severely sperm limited when placed only 5 m away from a male, and reproductive success was positively correlated with male density (Brazeau and Lasker, 1992). Though based on a very limited number of brooding species, the comparison between the octocoral and the bryozoans and asidians hints at another general principle. Bryozoans, like ascidians, are active suspension feeders who use feeding structures to filter sperm or sperm packets from the seawater (Temkin, 1994, 1996), whereas octocorals are passive suspension feeders. Although the mechanism by which sperm gain access to brooded eggs is unknown in octocorals, this taxon lacks a feeding mechanism that could be co-opted for sperm capture. So while active suspension-feeding brooders may be largely immune to sperm limitation in nature, passive suspension-feeding brooders may be among the most sperm-limited of marine invertebrates (Yund, 2000).

Comparison with previous results for B. schlosseri

It is useful to view our results within the context of past fertilization studies on *B. schlosseri.* A series of papers on sperm competition focused on relative male reproductive success, but also incidentally quantified levels of egg fertilization. While Atkinson and Yund (1996) found no significant difference in the proportion of eggs fertilized in combinations of high and low population density and size, three other studies (Yund and McCartney, 1994; Yund 1995, 1998) did report increased fertilizations with increased male density. If male density (past studies) has more of an effect than total population density (this study) on fertilization, fertilization in *B. schlosseri* may be more sensitive to the male:female ratio than to absolute density. At the level of individual gametes (*i.e.,* the cellular level), this pattern in turn suggests that fertilization levels may be dictated more by sperm:egg ratios than by the absolute sperm concentration. Yund (1998) also used a rare biochemical marker for paternity determination and showed that nearby males monopolize fertilizations as long as the quantity of sperm they produce is greater than some threshold level. When local sperm production is below that threshold, eggs are fertilized nevertheless, but the sperm come from more distant sources. This result helps explain how eggs can be fertilized under a broad range of density conditions.

Maximum field fertilization levels

Fertilization levels for *B. schlosseri* were generally quite high, but even in the most dense conditions still averaged less than 100%. Fertilization levels in colonies placed in natural populations averaged 85.6% throughout the entire sampling season (Fig. 3); levels in the experimental populations were also very close to 85% (Fig. 1). Although it is tempting to interpret these data as evidence of a low level of sperm limitation, another explanation is more likely. Reproductive success below 100% may have been the result not of unsuccessful fertilization, but of unsuccessful development of embryos because of outbreeding depression (Grosberg, 1987). Due to the philopatric dispersal of larvae (that is, dispersal that keeps the larvae near their site of origin), *B. schlosseri* colonies typically live in kin groups (Grosberg, 1987, 1991; Yund and O'Neil, 2000), and consequently mate with relatives (Grosberg, 1987, 1991). Because the normal mating system involves inbreeding, this species may be subject to outbreeding depression (Grosberg, 1987). Our experimental manipulation assembled populations that lacked genetic structure, and our survey introduced randomly selected genotypes into natural populations. Thus, all fertilizations were the product of out-crossed matings. Grosberg (1987) has previously reported that outcrossing reduces the success of both fertilization and subsequent embryo development. The cumulative effect of outbreeding depression (through larval hatching) that he predicted is consistent with the 15% failure that we observed. Because we assayed fertilization by successful development, our approach would not have distinguished early developmental failures from fertilizations that did not occur.

Alternatively, recent ecological work on the occurrence of polyspermy in marine invertebrates (*e.g.,* Franke *et al.,* 2002) suggests a different explanation for our observed 85% fertilization maximum. All of the eggs in our colonies may have been fertilized, but some may have been fertilized by more than one sperm. Because embryos resulting from polyspermic fertilization would have failed to develop, and we assayed fertilization in terms of successful development, our results could also have incorporated the effects of polyspermy. Although we are convinced that polyspermy plays an important role in the fertilization dynamics of many marine free-spawners (Yund, 2000), we are skeptical of this explanation for our own results. All evidence suggests that successful fertilization in *B. schlosseri* tends to be a time-integrated process in which dilute sperm are slowly acquired from the water. If this scenario is valid, then eggs are unlikely to be subject to the high short-term sperm concentrations necessary to cause polyspermy. Furthermore, effective polyspermy blocks are present in ascidians (*e.g.,* Lambert *et al.,* 1997). Even when eggs of *B. schlosseri* are subjected in laboratory experiments to sperm concentrations much higher than those found in nature, we see no evidence of polyspermy (unpubl. data). In addition, if polyspermy had been an important factor in our experiments, fertilization levels (as assayed by development) should have declined at higher population densities.

Acknowledgments

Cheryl Wapnick, Lisa Onaga, and Basma Mohammad assisted with animal culture, and Sheri Johnson provided helpful comments on an earlier version of the manuscript. Funding was provided by the National Science Foundation (OCE-97-30354, OCE-01-22031, and OCE-01-17623).

Literature Cited

Atkinson, O. S., and P. O. Yund. 1996. The effect of variation in population density on male fertilization success in a colonial ascidian. *J. Exp. Mar. Biol. Ecol.* **195:** 111–123.

Babcock, R. C., C. N. Mundy, and D. Whitehead. 1994. Sperm diffusion models and *in situ* confirmation of long-distance fertilization in the free-spawning asteroid *Acanthaster planci*. *Biol. Bull.* **186:** 17–28.

Benzie, J. A. H., and P. Dixon. 1994. The effects of sperm concentration, sperm:egg ratio, and gamete age on fertilization success in crown-of-thorns starfish (*Acanthaster planci*) in the laboratory. *Biol. Bull.* **186:** 139–152.

Benzie, J. A. H., K. P. Black, P. J. Moran, and P. Dixon. 1994. Small-scale dispersion of eggs and sperm of the crown-of-thorns starfish (*Acanthaster planci*) in a shallow coral reef habitat. *Biol. Bull.* **186:** 153–167.

Bishop, J. D. D. 1998. Fertilization in the sea: are the hazards of broadcast spawning avoided when free-spawned sperm fertilize retained eggs? *Proc. R. Soc. Lond. B* **265:** 725–731.

Boyd, H. C., S. K. Brown, J. A. Harp, and I. L. Weissman. 1986. Growth and sexual maturation of laboratory-cultured Monterey *Botryllus schlosseri*. *Biol. Bull.* **170:** 91–109.

Brazeau, D. A., and H. R. Lasker. 1992. Reproductive success in the Caribbean octocoral *Briareum asbestinum*. *Mar. Biol.* **114:** 157–163.

Chadwick-Furman, N. E., and I. L. Weissman. 1995. Life histories and senescence of *Botryllus schlosseri* (Chordata, Ascidiacea) in Monterey Bay. *Biol. Bull.* **189:** 36–41.

Claereboudt, M. 1999. Fertilization success in spatially distributed populations of benthic free-spawners: a simulation model. *Ecol. Model.* **121:** 221–233.

Coma, R., and H. R. Lasker. 1997a. Small-scale heterogeneity of fertilization success in a broadcast spawning octocoral. *J. Exp. Mar. Biol. Ecol.* **214:** 107–120.

Coma, R., and H. R. Lasker. 1997b. Effects of spatial distribution and reproductive biology on *in situ* fertilization rates of a broadcast-spawning invertebrate. *Biol. Bull.* **193:** 20–29.

Frank, K. T., and D. Brickman. 2000. Allee effects and compensatory population dynamics within a stock complex. *Can. J. Fish. Aquat. Sci.* **57:** 513–517.

Franke, E. S., R. C. Babcock, and C. A. Styan. 2002. Sexual conflict and polyspermy under sperm-limited conditions: *in situ* evidence from field simulations with the free-spawning marine echinoid *Evechinus chloroticus*. *Am. Nat.* **160:** 485–496.

Grosberg, R. K. 1982. Ecological, genetical, and developmental factors regulating life history variation within a population of the colonial ascidian *Botryllus schlosseri* (Pallas) Savigny. Ph.D. dissertation, Yale University, New Haven, CT.

Grosberg, R. K. 1987. Limited dispersal and proximity-dependent mating success in the colonial ascidian *Botryllus schlosseri*. *Evolution* **41:** 372–384.

Grosberg, R. K. 1988. Life-history variation within a population of the colonial ascidian *Botryllus schlosseri*. I. The genetic and environmental control of seasonal variation. *Evolution* **42:** 900–920.

Grosberg, R. K. 1991. Sperm-mediated gene flow and the genetic structure of a population of the colonial ascidian *Botryllus schlosseri*. *Evolution* **45:** 130–142.

Incze L. S., R. A. Lutz, and L. Watling. 1980. Relationship between effects of environmental temperature and seston on growth and mortality of *Mytilus edulis* in a temperate northern estuary. *Mar. Biol.* **57:** 147–156.

Jamieson, G. S. 1993. Marine invertebrate conservation: evaluation of fisheries over-exploitation concerns. *Am. Zool.* **33:** 551–567.

Johnson, S. L., and P. O. Yund. 2004. Remarkable longevity of dilute sperm in a free-spawning colonial ascidian. *Biol. Bull.* **206:** 144–151.

Lambert C., H. Goudeau, C. Franchet, G. Lambert, and M. Goudeau. 1997. Ascidian eggs block polyspermy by two independent mechanisms: one at the egg plasma membrane, the other involving the follicle cells. *Mol. Reprod. Dev.* **48:** 137–143.

Lasker, H. R., D. A. Brazeau, J. Calderon, M. A. Coffroth, R. Coma, and K. Kim. 1996. *In situ* rates of fertilization among broadcast spawning gorgonian corals. *Biol. Bull.* **190:** 45–55.

Levitan, D. R. 1991. Influence of body size and population density on fertilization success and reproductive output in a free-spawning invertebrate. *Biol. Bull.* **181:** 261–268.

Levitan, D. R., and C. Petersen. 1995. Sperm limitation in the sea. *Trends Ecol. Evol.* **10:** 228–231.

Levitan, D. R., and M. A. Sewell. 1998. Fertilization success in free-spawning marine invertebrates: review of the evidence and fisheries implications. *Can. Spec. Publ. Fish. Aquat. Sci.* **125:** 159–164.

Levitan, D. R., and C. M. Young. 1995. Reproductive success in large populations: empirical measures and theoretical predictions of fertilization in the sea biscuit *Clypeaster rosaceus*. *J. Exp. Mar. Biol. Ecol.* **190:** 221–241.

Levitan, D. R., M. A. Sewell, and F.-S. Chia. 1991. Kinetics of fertilization in the sea urchin *Strongylocentrotus franciscanus:* interaction of gamete dilution, age, and contact time. *Biol. Bull.* **181:** 371–378.

Levitan, D. R., M. A. Sewell, and F.-S. Chia. 1992. How distribution and abundance influences fertilization success in the sea urchin *Strongylocentrotus franciscanus*. *Ecology* **73:** 248–254.

Liermann, M., and R. Hilborn. 1997. Depensation in fish stocks: a hierarchic Bayesian meta-analysis. *Can. J. Fish. Aquat. Sci.* **54:** 1976–1984.

Meidel, S. K., and P. O. Yund. 2001. Egg longevity and time-integrated fertilization in a temperate sea urchin (*Strongylocentrotus droebachiensis*). *Biol. Bull.* **201:** 84–94.

Metaxas, A., R. E. Scheibling, and C. M. Young. 2002. Estimating fertilization success in marine benthic invertebrates: a case study with the tropical sea star *Oreaster reticulatus*. *Mar. Ecol. Prog. Ser.* **226:** 87–101.

Milkman, R. 1967. Genetic and developmental studies on *Botryllus schlosseri*. *Biol. Bull.* **132:** 229–243.

Morgan, S. G. 1995. Life and death in the plankton: larval mortality and adaptation. Pp. 279–321 in *Marine Invertebrate Larvae*, L. McEdward, ed. CRC Press, New York.

Myers, R. A., N. J. Barrowman, J. A. Hutchings, and A. A. Rosenberg. 1995. Population dynamics of exploited fish stocks at low population levels. *Science* **269:** 1106–1108.

Newlon, A. W. III, P. O. Yund, and J. Stewart-Savage. 2003. Phenotypic plasticity of male, female, and asexual reproduction in a colonial ascidian, *Botryllus schlosseri*. *J. Exp. Zool.* **297A:** 180–188.

Oliver, J., and R. Babcock. 1992. Aspects of the fertilization ecology of broadcast spawning corals: sperm dilution effects and *in situ* measurements of fertilization. *Biol. Bull.* **183:** 409–417.

Pemberton, A. J., R. N. Hughes, P. H. Manriquez, and J. D. D. Bishop. 2003. Efficient utilization of very dilute sperm: sperm competition may be more likely than sperm limitation when eggs are retained. *Proc. R. Soc. Lond. B (Suppl.)* **270:** S223–S226.

Pennington, J. T. 1985. The ecology of fertilization of echinoid eggs: the consequences of sperm dilution, adult aggregation, and synchronous spawning. *Biol. Bull.* **169:** 417–430.

Pfister, C. A., and A. Bradbury. 1996. Harvesting red sea urchins: recent effects and future predictions. *Ecol. Appl.* **6:** 298–310.

Quinn, J. F., S. R. Wing, and L. W. Botsford. 1993. Harvest refugia in marine invertebrate fisheries: models and applications to the red sea urchin *Strongylocentrotus franciscanus*. *Am. Zool.* **33:** 537–550.

Roughgarden, J., S. Gaines, and H. Possingham. 1988. Recruitment dynamics in complex life cycles. *Science* **241:** 1460–1466.

Sewell, M. A. 1994. Small size, brooding, and protandry in the apodid sea cucumber *Leptosynapta clarki*. *Biol. Bull.* **187:** 112–123.

Shelton, P. A., and B. P. Healey. 1999. Should depensation be dismissed as a possible explanation for the lack of recovery of the northern cod (*Gadus morhua*) stock? *Can. J. Fish. Aquat. Sci.* **56:** 1521–1524.

Stewart-Savage, J., and P. O. Yund. 1997. Temporal pattern of sperm release from the colonial ascidian, *Botryllus schlosseri. J. Exp. Zool.* **279:** 620–625.

Stewart-Savage, J., A. Phillippi, and P. O. Yund. 2001a. Delayed insemination results in embryo mortality in a brooding ascidian. *Biol. Bull.* **201:** 52–58.

Stewart-Savage, J., A. Stires, and P. O. Yund. 2001b. Environmental effect on the reproductive output of *Botryllus schlosseri.* Pp. 311–314 in *Biology of Ascidians,* H. Sawada, H. Yokosama, and C.C. Lambert, eds. Springer-Verlag, Tokyo.

Stoner, A. W., and M. Ray-Culp. 2000. Evidence for Allee effects in an over-harvested marine gastropod: density-dependent mating and egg production. *Mar. Ecol. Prog. Ser.* **202:** 297–302.

Strathmann, R. R. 1985. Feeding and non-feeding larval development and life-history evolution in marine invertebrates. *Annu. Rev. Ecol. Syst.* **16:** 339–361.

Temkin, M. H. 1994. Gamete spawning and fertilization in the gymnolaemate bryozoan *Membranipora membranacea. Biol. Bull.* **187:** 143–155.

Temkin, M. H. 1996. Comparative fertilization biology of gymnolaemate bryozoans. *Mar. Biol.* **127:** 329–339.

Thorson, G. 1950. Reproductive and larval ecology of marine bottom invertebrates. *Biol. Rev.* **25:** 1–45.

Wahle, R. A., and S. H. Peckham. 1999. Density-related reproductive trade-offs in the green sea urchin, *Strongylocentrotus droebachiensis. Mar. Biol.* **134:** 127–137.

Yund, P. O. 1990. An *in situ* measurement of sperm dispersal in a colonial marine hydroid. *J. Exp. Zool.* **253:** 102–106.

Yund, P. O. 1995. Gene flow *via* the dispersal of fertilizing sperm in a colonial ascidian (*Botryllus schlosseri*): the effect of male density. *Mar. Biol.* **122:** 649–654.

Yund, P. O. 1998. The effect of sperm competition on male gain curves in a colonial marine invertebrate. *Ecology* **79:** 328–339.

Yund, P. O. 2000. How severe is sperm limitation in natural populations of marine free-spawners? *Trends Ecol. Evol.* **15:** 10–13.

Yund, P. O., and M. A. McCartney. 1994. Male reproductive success in colonial invertebrates: competition for fertilizations. *Ecology* **75:** 2151–2167.

Yund, P. O., and P. G. O'Neil. 2000. Microgeographic genetic differentiation in a colonial ascidian (*Botryllus schlosseri*) population. *Mar. Biol.* **137:** 583–588.

Yund, P. O., and A. Stires. 2002. Spatial variation in population dynamics in a colonial ascidian (*Botryllus schlosseri*). *Mar. Biol.* **141:** 955–963.

Yund, P. O., Y. Marcum, and J. Stewart-Savage. 1997. Life-history variation in a colonial ascidian: broad-sense heritabilities and tradeoffs in allocation to asexual growth and male and female reproduction. *Biol. Bull.* **192:** 290–299.

Reference: *Biol. Bull.* **206:** 161–172. (June 2004)
© 2004 Marine Biological Laboratory

Induction of Settlement of Larvae of the Sea Urchin *Holopneustes purpurascens* by Histamine From a Host Alga

REBECCA L. SWANSON[1,4,*], JANE E. WILLIAMSON,[1,4,†], ROCKY DE NYS[1,4,‡],
NARESH KUMAR[2,4], MARTIN P. BUCKNALL[3], AND PETER D. STEINBERG[1,4]

[1] *School of Biological, Earth & Environmental Sciences,* [2] *School of Chemical Sciences,*
[3] *Bioanalytical Mass Spectrometry Facility,* [4] *Center for Marine Biofouling & Bio-Innovation,*
University of New South Wales, Sydney 2052, Australia

Abstract. Larvae of the Australian sea urchin *Holopneustes purpurascens* are induced to settle and metamorphose (termed settlement herein) by a water-soluble compound produced by the red alga *Delisea pulchra,* the main host plant of new recruits. The settlement cue for *H. purpurascens* had previously been identified as a floridoside-isethionic acid complex, and this paper presents new evidence correcting that finding. The actual settlement cue produced by *D. pulchra* was isolated from the polar extract by cation-exchange chromatography and identified as histamine, using one- and two-dimensional nuclear magnetic resonance spectrometry. The chemical identity of the cue was confirmed by gas chromatography–mass spectrometry (GC-MS) and matrix-assisted laser desorption/ionization–time-of-flight mass spectrometry. Synthetic histamine and histamine at 4.5 μM isolated from *D. pulchra* both induced rapid settlement in 80%–100% of the larvae of *H. purpurascens.* Lower concentrations of histamine (0.9–2.3 μM) induced larval settlement, but this response varied from 0%–90%. The histamine content of two host plants of *H. purpurascens*—*D. pulchra* and *Ecklonia radiata*—and of four other common species was quantified using GC-MS. *D. pulchra* had the highest histamine content, which is consistent with *H. purpurascens* recruiting to this species. Histamine was also detected in the seawater surrounding these host algae. This is the first time that a settlement cue has been quantified in the habitat of a marine organism.

Introduction

Most marine invertebrates have complex life histories in which a dispersive larval phase alternates with benthic juvenile and adult phases. The demography of such species is highly dependent on larval recruitment to a favorable habitat (Pawlik, 1992; Underwood and Keough, 2000), and the question of how planktonic larvae locate an appropriate benthic habitat in which to settle has long been a focus for marine biologists. The current view is that hydrodynamic processes dominate at large spatial scales (meters, kilometers), with active habitat selection becoming progressively more important at smaller spatial scales (centimeters, millimeters, micrometers) (Keough and Downes, 1982; Mullineaux and Butman, 1991; Harvey and Bourget, 1997; Zimmer and Butman, 2000).

Active habitat selection requires that larvae discriminate among potential settlement sites, which is possible through the detection of habitat-specific cues. Many laboratory experiments have confirmed that larvae from a diverse range of phyla respond both behaviorally (settlement—sinking to the bottom for substrate exploration) and morphologically (metamorphosis—ontogenesis into the benthic form) to such physical factors of a habitat as light (Maida *et al.,*

Received 24 October 2003; accepted 8 April 2004.

[*] To whom correspondence should be addressed. E-mail: r.swanson@unsw.edu.au

[†] Current address: Department of Biological Sciences, Macquarie University, NSW 2109 Australia.

[‡] Current address: School of Marine Biology & Aquaculture, James Cook University, QLD 4811 Australia.

Abbreviations: CX, cation-exchange; F-I, floridoside-isethionic acid; GC-MS, gas chromatography–mass spectrometry; HPLC, high-performance liquid chromatography; ISTD, internal standard; MALDI-TOF MS, matrix-assisted laser desorption/ionization–time-of-flight mass spectrometry; NMR, nuclear magnetic resonance; SSW, sterile seawater.

1994), surface orientation (Raimondi and Morse, 2000), flow conditions (Mullineaux and Butman, 1991), crevices (Keough and Downes, 1982), and surface texture (Berntsson *et al.*, 2000). Larvae can also be induced to settle and metamorphose (collectively termed settlement in this paper) by surface-bound or waterborne chemical cues, which are thought to indicate a suitable habitat for the benthic stage (Hadfield and Paul, 2001). The source of such chemical cues (inducers) may be conspecifics (Burke, 1986), host organisms (Williamson *et al.*, 2000), prey (Hadfield and Scheuer, 1985), or biofilms (Wieczorek and Todd, 1998).

The chemical cues for larval settlement that have been isolated from natural sources within the habitat appear to be diverse; however, most have been only partially characterized. These include small peptides (the sand dollar *Dendraster excentricus*—Burke, 1984; the oyster *Crassostrea virginica*—Zimmer-Faust and Tamburri, 1994; the jellyfish *Cassiopea xamachana*—Fleck and Fitt, 1999), uncharacterized low-molecular-weight water-soluble compounds (the nudibranch *Phestilla sibogae*—Hadfield and Pennington, 1990; the cephalaspidean *Haminaea callidegenita*—Gibson and Chia, 1994), carbohydrates (the coral *Agaricia humilis*—Morse and Morse, 1996; the ascoglossan *Alderia modesta*—Krug and Manzi, 1999), and glycoproteins (the barnacle *Balanus amphitrite*—Clare and Matsumura, 2000).

In contrast to the numerous partially characterized inducers, there are only a few examples in which the chemical structure of a settlement cue isolated from a natural source has been determined. Delta-tocopherols from *Sargassum tortile* induced settlement of the hydroid *Coryne uchidai* (Kato *et al.*, 1975), jacarone isolated from the red alga *Delesseria sanguinea* induced settlement of the scallop *Pecten maximus* (Yvin *et al.*, 1985), narains and anthosamines A and B isolated from marine sponges induced settlement of ascidian larvae (Tsukamoto *et al.*, 1994, 1995), and lumichrome isolated from conspecifics induced settlement of larvae of the ascidian *Halocynthia roretzi* (Tsukamoto *et al.*, 1999). In most cases, the ecological relevance of these compounds *in situ* is not clear, either because the source of the settlement cue is not necessarily related to the recruitment patterns of the organism (Yvin *et al.*, 1985; Tsukamoto *et al.*, 1994, 1995), or because the availability of the cue to settling larvae has not been demonstrated (Tsukamoto *et al.*, 1999).

A naturally occurring characterized settlement cue that appears to strongly affect the demography of the sea urchin *Holopneustes purpurascens* Agassiz 1872 (Temnopluridae: Echinodermata) was recently reported by Williamson *et al.* (2000). *H. purpurascens* is an endemic Australian echinoid that lives in shallow subtidal habitats in the canopy of macroalgae, particularly *Delisea pulchra* Greville (Montagne) 1844 and *Ecklonia radiata* (C. Agardh) J. Agardh 1898 at Bare Island, Sydney (Williamson *et al.*, 2000, 2004). Although abundant on both host plants, the smaller size classes of *H. purpurascens* were most abundant on *D. pulchra*, with the smallest size class (test diameter ≤ 5 mm) found only on that species. This suggested that *D. pulchra* might produce a settlement cue for larval *H. purpurascens* (Williamson *et al.*, 2000). Fresh pieces of *D. pulchra* (but not *E. radiata*) and seawater collected *in situ* near *D. pulchra* plants induced settlement in larvae of *H. purpurascens*. The water-soluble cue was subsequently isolated and characterized as a complex between the sugar floridoside and isethionic acid (F-1 complex; Williamson *et al.*, 2000).

During further research on this system, we obtained inductive fractions that contained isethionic acid but not floridoside, and we were also unable to reproduce a synthetic F-1 complex that induced settlement of larval *H. purpurascens*. Subsequently, we hypothesized that the F-1 complex was not a natural settlement cue for this urchin. This paper identifies the true nature of this chemical cue from *D. pulchra* for settlement of *H. purpurascens* larvae, correcting the previous finding of Williamson *et al.*, (2000). In addition, we quantify the settlement cue in host and non-host algae of *H. purpurascens*—the first time that a natural settlement cue has been quantified in the habitat of a marine organism.

Materials and Methods

Study site

All animals and algae used in this study were collected from sublittoral habitats (1–3 m depth) at Bare Island (33° 59' 38" S, 151° 14' 00" E) at the north head of Botany Bay, Sydney, Australia. At this site individuals of *Holopneustes purpurascens* are primarily found wrapped in the laminae of the brown kelp *Ecklonia radiata* (Laminariales: Phaeophyta) or in the fronds of the red foliose alga *Delisea pulchra* (Bonnemaisonales: Rhodophyta). A more detailed description of this habitat and the ecology of this system are found in Wright and Steinberg (2001) and Williamson *et al.* (2004).

Preparation of the polar extract of Delisea pulchra

The results of Williamson *et al.* (2000) indicated that any settlement cues were contained within the polar fraction of the crude extract of *D. pulchra*. A polar extract of *D. pulchra* was thus prepared from 1.0 kg (wet weight) of algae collected from Bare Island. Epibiota were removed, the plants blotted dry, and the thallus exhaustively extracted in methanol (OmniSolv, EM Science). The methanol extract was filtered (Whatman #1), dried by rotary evaporation *in vacuo* at 40 °C, and partitioned between dichloromethane (OmniSolv) and Milli-Q water. The Milli-Q phase was filtered (Whatman #1) and dried *in vacuo* at 40 °C. The dried crude polar extract was dissolved in absolute ethanol three times, pooling each extract, and dried *in vacuo* at 40 °C to yield the polar extract.

Isolation of the settlement cue in Delisea pulchra *by bioassay-guided fractionation*

High-performance liquid chromatography. The polar extract of *D. pulchra* was fractionated using reversed-phase high-performance liquid chromatography (HPLC—Adsorbosil C18 column, 5-μm particle size, 250 mm × 4.6 mm, Waters R410 RI-detector) (100% Milli-Q water at 1 ml · min^{-1}). The polar extract was dissolved in Milli-Q water (50 mg · ml^{-1}), filtered (0.22 μm), and manually injected (20 μl). HPLC resolved two major peaks, peak 1 with a retention time (rt) of 2.7 min, and peak 2 with rt = 3.4 min (Fig. 1A). Each peak fraction was collected from multiple injections and dried by rotary evaporation *in vacuo* at 40 °C. Peak fractions were tested for bioactivity in settlement assays and analyzed by ^{1}H- and ^{13}C-nuclear magnetic resonance (NMR) spectroscopy (Bruker DMX 500).

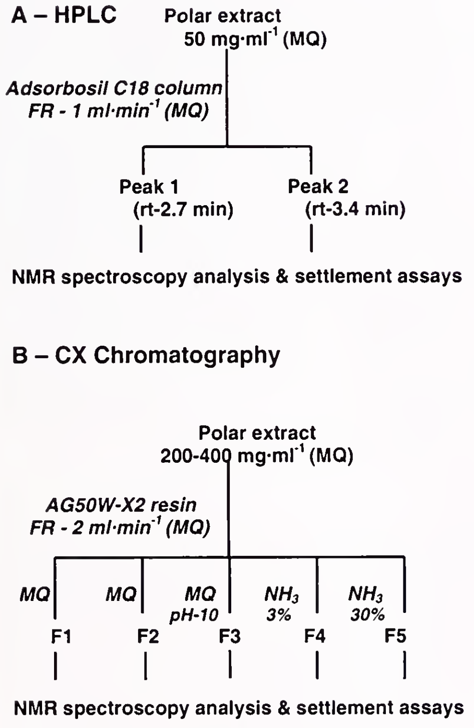

Figure 1. Diagram of the bioassay-guided fractionation of the polar extract of *Delisea pulchra*, using either reversed-phase HPLC (A) or cation-exchange (CX) chromatography (B). MQ = Milli-Q water, FR = flow rate, rt = retention time, F = fraction.

Cation-exchange chromatography. The settlement cue could not be isolated as a pure fraction using HPLC, so an alternative procedure, cation-exchange (CX) chromatography, was used to fractionate the polar extract of *D. pulchra*. CX resin (AG50W-X2 [H+ form], BioRad) in Milli-Q water was poured into a 50-ml burette, taking care to exclude air bubbles. The resin (25-ml bed volume) was equilibrated with Milli-Q water at 2 ml · min^{-1} until the eluant was pH 5–6. The polar extract of *D. pulchra* (1–2 g) was dissolved in 5 ml of Milli-Q water, filtered (0.22 μm), and gently loaded onto the column. Unbound compounds were collected in 100 ml of Milli-Q water (fraction 1) and another 100 ml of Milli-Q water (fraction 2). Retained compounds were eluted using a series of basic solutions: 30 ml of dilute NH_3 in Milli-Q water (pH 10; fraction 3), 30 ml of 3%-NH_4OH w/w (fraction 4), and 30 ml of 30%-NH_4OH w/w (fraction 5, Fig. 1B). Fractions 1–5 were collected as controls, using the same method but without loading any *D. pulchra* extract on the column; none of these fractions had any subsequent activity. CX-fractions were dried in a centrifuge *in vacuo* (speed-vac SVC200, Savant), tested for bioactivity in settlement assays, and analyzed by ^{1}H-NMR spectroscopy.

Identification of isolated settlement cue

Nuclear magnetic resonance spectroscopy. Bioassay-guided fractionation of the polar extract of *D. pulchra* by cation-exchange chromatography yielded one active fraction (CX-fraction 5, F5). The inducing compound in F5 was identified by ^{1}H and ^{13}C-NMR experiments (D_2O), and a high-field two-dimensional ^{1}H-^{15}N HMBC NMR experiment (d_4 MeOH, Bruker DMX 500). To confirm the putative structure of F5 as histamine, 3 mg of F5 was dissolved in D_2O and analysed by ^{1}H-NMR spectroscopy. Synthetic histamine (3 mg) was added to F5 and the sample reanalysed. The ^{1}H-NMR spectra of the unspiked F5 sample and the spiked F5 sample were then compared.

Gas chromatography–mass spectrometry. NMR spectroscopy analyses identified the isolated settlement cue as histamine, and this was confirmed by gas chromatography–mass spectrometry (GC-MS). Putative (naturally isolated) histamine (1 mg) and synthetic histamine (1 mg) were derivatized with heptafluorobutyric anhydride (Aldrich) and then acetic anhydride (Aldrich), using the method of Barancin *et al.* (1998). Derivatized samples were diluted 100-fold in ethyl acetate before analysis. A Zebron ZB-5 column (15 m, 0.25 μm × 0.25 mm ID; Phenomenex) was used on a

Hewlett Packard (HP) 5980 series II gas chromatograph equipped with an HP5971A or HP5972 mass selective detector. Injections (2 μl) were in the splitless mode with an inlet pressure of 170 kPa. The injection port was held as 290 °C and the interface at 300 °C. The gas chromatograph was held at 90 °C for 2 min and ramped at 10 $°C \cdot min^{-1}$ to 200 °C, then at 50 $°C \cdot min^{-1}$ to 310 °C and held for 2 min (17.2 min per run). Helium was used as the carrier gas. The mass selective detector was operated in scan mode (m/z 50–550). The average retention times of derivatized putative histamine and derivatized synthetic histamine were recorded from five injections of each sample (mean ± SD, $n = 5$). The electron impact ion-spectra of derivatized putative histamine and derivatized synthetic histamine were compared.

Matrix-assisted laser desorption/ionization–time-of-flight mass spectrometry. The elemental formula of putative histamine was determined by matrix-assisted laser desorption/ionization–time-of-flight mass spectrometry (MALDI-TOF MS) (Bucknall *et al.*, 2002). A Perseptive Voyager DE STR (Perseptive Biosystems, Framingham, MA) MALDI-TOF MS was operated in both positive-ion linear delayed-extraction mode and reflector delayed-extraction mode for accurate mass analysis. The test samples were prepared in acetonitrile/Milli-Q water (50:50) and contained either 100 $ng \cdot \mu l^{-1}$ of putative histamine or synthetic histamine. α-Cyano-4-hydroxycinnamic acid (5 $mg \cdot ml^{-1}$) prepared in acetonitrile/Milli-Q/trifluoroacetic acid (80:20:0.02) was used as the matrix. Glycine (500 $ng \cdot \mu l^{-1}$) and [sarcosine-^{15}N-methyl-d$_3$]creatinine · HCl (5 $ng \cdot \mu l^{-1}$, Cambridge Isotope Laboratories #DNLM-2171) were added as internal mass calibrants for accurate mass determinations. An accurate mass for the putative protonated histamine molecular ion $[M+H]^+$ was determined by 10 repeat analyses of each sample. The mean molecular weight was calculated for these mass spectra and compared with both the theoretical molecular weight for histamine and the molecular weight measured for synthetic histamine using the same analytical technique. The standard deviation for these mass measurements was taken as an estimate of the mass measurement error.

Settlement assays

H. purpurascens larvae were cultured as previously described (Williamson *et al.*, 2000). Larvae reached competency (*i.e.*, become developmentally ready for settlement) within 6 days, as recognized by the presence of five well-developed tube feet. All settlement assays were done at 19 °C with a 12-h-light/12-h-dark regime, in 40-mm petri dishes and 5 ml of sterile seawater (SSW). Replicates were randomly assigned among treatments, with 10–15 replicates per treatment and one 6-day larva per replicate dish. We were unable to use multiple larvae per dish in these assays because this species is a "dribble" spawner and generally yields low numbers of larvae (settlement is not gregarious; Williamson *et al.*, 2000). Larvae were added once all petri dishes were prepared, and percent settlement (*i.e.*, percent metamorphosed) was recorded at set time intervals.

HPLC peak fractions. Peak 1 and peak 2 fractions were tested against larvae to determine the presence of a settlement cue. Peak fractions were dissolved in Milli-Q water (10 $mg \cdot ml^{-1}$ stock solution) and aliquots of each stock solution were added to assigned petri dishes for final test concentrations of 25 $\mu g \cdot ml^{-1}$ of peak 1 and 51 $\mu g \cdot ml^{-1}$ of peak 2. A floridoside-isethionic complex sample ("F-1 complex") from the previous study (Williamson *et al.*, 2000) was also tested in the assay at a final concentration of 76 $\mu g \cdot ml^{-1}$. Pieces of fresh *D. pulchra* (~10 mg) were used as a positive control, and Milli-Q water and SSW were used as the negative controls. Percent settlement was scored after 18 h (n = 12 replicates per treatment).

Cation-exchange fractions. Each CX-fraction (F) was tested against larvae to determine the presence of a settlement cue. F1, F2, F3, F4 and the polar extract of *D. pulchra* (used as a positive control) were dissolved in Milli-Q water at 5 $mg \cdot ml^{-1}$. Aliquots of the appropriate fraction were added to the petri dish to give final test concentrations of 50 $\mu g \cdot ml^{-1}$ for each treatment. F5 was dissolved in Milli-Q water at 100 $\mu g \cdot ml^{-1}$, and aliquots were added to assigned petri dishes for final test concentrations of 0.1–1.0 $\mu g \cdot ml^{-1}$ (much lower concentrations of F5 were tested because of a low yield in F5). Initial settlement assays showed that only F5 induced settlement; therefore, CX-control-fraction 5 (CF5) was tested in future settlement assays as the procedural control. CF5 was dissolved in Milli-Q water at 100 $\mu g \cdot ml^{-1}$ and tested at 1.0 $\mu g \cdot ml^{-1}$. Milli-Q water and SSW were used as the negative controls. Percent settlement was scored after 1 h (n = 10 replicates per treatment).

Natural versus *synthetic histamine.* Settlement assays were used to compare the responses of larvae to (i) natural histamine isolated using CX chromatography, (ii) synthetic histamine, and (iii) synthetic histamine run through the same procedure used to isolate natural histamine. Stock solutions of 900 μM of each histamine treatment were prepared in Milli-Q water, and aliquots of the appropriate stock solution added to assigned petri dishes for final test concentrations of 0.9–9.0 μM. Pieces of fresh *D. pulchra* (~10 mg) and 50 $\mu g \cdot ml^{-1}$ of the polar extract *D. pulchra* were used as the positive controls, and Milli-Q water and SSW were used as the negative controls. Percent settlement was scored after 1 h (n = 12 replicates per treatment).

Delisea pulchra *treated with antibacterial agents.* Because some marine bacteria produce histamine (Fujii *et al.*, 1997), the identification of histamine as the settlement cue (see Results) raises the possibility that the bacterial biofilm on the surface of *D. pulchra* may be the source of the cue. To test this, the ability of *D. pulchra* to induce settlement after various antibacterial treatments was examined in a settlement assay. Antibacterial treatments were adapted from previous studies in which treatments were shown to be effective in reducing surface bacteria (Xue-Wu and Gordon, 1987; Aguirre-Lipperheide and Evans, 1993; Johnson and Sutton, 1994). Seven plants of *D. pulchra* were collected from Bare Island and brought back to the laboratory, where portions of each plant were allocated to each of seven treatments. There were six antibacterial treatments and a procedural control. All antibacterial treatments included a 5-min soak in a 10% betadine-SSW solution, followed by three rinses in SSW and a 24-h treatment in either (1) SSW (the "soak" treatment); (2) SSW containing 20 $\mathrm{mg \cdot l^{-1}}$ streptomycin (Aldrich), 10 $\mathrm{mg \cdot l^{-1}}$ penicillin G (Aldrich), and 10 $\mathrm{mg \cdot l^{-1}}$ kanamycin (Aldrich; "SPK" treatment); (3) SSW containing 10 $\mathrm{mg \cdot l^{-1}}$ ciprofloxacin (Bayer, "ciprofloxacin" treatment); (4) SSW after pieces of *D. pulchra* were gently wiped across an agar plate, before and after the 24-h soak, to physically remove bacteria ("wipe" treatment); and the combination treatments (5) "wipe + SPK", and (6) "wipe + ciprofloxacin." The procedural control was a 24-h soak in SSW without the initial betadine soak ("soak control" treatment). The next day, subsections of several *D. pulchra* plants were collected as a "fresh control" treatment and used in the settlement assay on that day. Pieces of *D. pulchra* (~10 mg) from each treatment were added to assigned sterile petri dishes, and percent settlement was scored after 20 h ($n = 15$ replicates per treatment).

Quantitative analysis of histamine in various algae

If histamine is a natural settlement cue for this urchin, we would expect *D. pulchra*, the primary host plant of new recruits of *H. purpurascens*, to have higher levels of histamine than other algae in the habitat. To test this, we quantified the histamine content of six species of algae from the habitat of *H. purpurascens*. The two primary host plants (*D. pulchra* and *E. radiata*) and four other prominent species of algae (*Amphiroa anceps, Corallina officinalis, Homeostrichus olsenii,* and *Sargassum vestitum*) were collected from Bare Island in January 2003. Five replicates of each alga were analyzed, with each replicate consisting of three small sections taken from different parts of one thallus, which were then pooled into a single sample for analysis (2–4 g wet-weight). A polar extract of each algal sample was prepared as described above. Polar extracts were dissolved in Milli-Q water (200 μl) and acidified with 50 μl of glacial acetic acid. [α, α, β, β-d$_4$]Histamine · 2HCl (1 μg, Cambridge Isotope Laboratories, #DLM 2911) was added to each sample as the internal standard (ISTD). Strong cation-exchange solid-phase extraction cartridges (50 mg, Alltech) were equilibrated with Milli-Q water (5 ml) at a flow rate of 1 $\mathrm{ml \cdot min^{-1}}$, and the sample was loaded. Unbound compounds were eluted in 2 ml of Milli-Q water (fraction 1) and another 2 ml of Milli-Q water (fraction 2). All retained compounds were eluted in 1 ml of 30% NH_4OH w/w (fraction 3) and dried in a speed vac. Standards that contained 1-μg ISTD and either 0.1, 0.5, 1.0, 5.0, or 10 μg of synthetic histamine were prepared. Standards and fraction 3 samples were derivatized with heptafluorobutyric anhydride and acetic anhydride using the method of Barancin *et al.* (1998).

A DB-5MS column (15 m, 0.25 μm × 0.25 mm ID, J & W Scientific) and a packed liner (3% SP-2250, Supelco; Smythe *et al.*, 2002) were installed on the GC-MS instrument previously described, and the same run conditions were used. The mass selective detector was operated in selected ion monitoring mode using ions characteristic of the analyte (derivatized histamine—*m/z* 94, 307, 349) and the ISTD (*m/z* 97, 311, 353). Extracted ion chromatograms were used to manually integrate the area under each ion peak (which is proportional to the amount of analyte in the sample). For each standard and sample, the areas of the analyte ions (*m/z* 94, 307, 349) were added together and the areas of the ISTD ions (*m/z* 97, 311, 353) were added together. The ratio of the combined areas of analyte:ISTD in standards was used to generate a standard curve. The histamine content of the samples was calculated by reference to the standard curve and expressed in terms of micrograms per gram (wet weight) of algal tissue ($\mu\mathrm{g \cdot g^{-1}}$).

After checking that the data met the assumptions of the test, the histamine content of different algae was transformed [$\ln(x + 1)$] and compared by using a one-factor analysis of variance. We excluded *A. anceps* and *C. officinalis* from the analysis because no histamine was detected in these species. Bonferroni's post hoc test was used to determine which species differed in their histamine contents (SYSTAT ver. 7.0). We were concerned that one high value for *D. pulchra* might be unduly influencing our analysis, but the outcome was unchanged when we repeated the analysis with this value omitted. Therefore, we report the results of the initial analysis.

Reanalysis of samples from Williamson et al. *(2000)*

Samples remaining from the study published in Williamson *et al.* (2000) were analyzed by GC-MS for the presence of histamine. Any histamine in the old samples was isolated using cation-exchange solid phase extraction cartridges, as outlined previously for isolating algal histamine, and then derivatized with heptafluorobutyric anhydride and acetic anhydride, using the method of Barancin *et al.* (1998) for quantitative GC-MS analysis.

Results

Isolation of the settlement cue in Delisea pulchra *by bioassay-guided fractionation*

HPLC fractions—NMR spectroscopy analysis and settlement assays. The polar extract of *Delisea pulchra* was separated into two fractions using HPLC (peak 1 and peak 2, Fig. 1A). These were analyzed by NMR spectroscopy (1-min ^{1}H- and 30-min ^{13}C-NMR experiments) and tested in settlement assays. Peak 1 displayed the pattern of isethionic acid (Barrow *et al.,* 1993), as determined by ^{1}H- and ^{13}C-NMR spectroscopy, as well as some additional signals that were not characteristic of floridoside (see next section). The ^{13}C-NMR spectrum of peak 2 corresponded to previously published data for floridoside [α-D-galactopyranosyl-(1-2)-glycerol] (Karsten *et al.,* 1993). Therefore, the isethionic acid and floridoside components of the F-1 complex eluted separately, in peak 1 and peak 2, respectively. Peak 1 induced settlement of *Holopneustes purpurascens* larvae in settlement assays, but peak 2 did not (Fig. 2). Four batches of peak 1 (25 $\mu g \cdot ml^{-1}$) induced 80%–100% settlement in five assays, whereas neither of two batches of peak 2 (51 $\mu g \cdot ml^{-1}$) induced settlement in two assays (representative data shown in Fig. 2). These data suggested that the F-I complex is not a settlement cue for *H. purpurascens* and that peak 1 (which lacked floridoside) contained the settlement cue.

Isethionic acid and taurine were the major compounds in peak 1, as determined by ^{1}H- and ^{13}C-NMR spectroscopy and comparison with synthetic samples. When isethionic acid (1–25 $\mu g \cdot ml^{-1}$), sodium isethionate (15–30 $\mu g \cdot ml^{-1}$), and taurine (1–13 $\mu g \cdot ml^{-1}$) were tested in settlement assays with *H. purpurascens* larvae, none of these compounds induced settlement (data not shown). Different combinations of these compounds were tested together (*e.g.,* 15 $\mu g \cdot ml^{-1}$ of isethionic acid and taurine) in case two cues were required for settlement of *H. purpurascens.* There was no settlement in the combination treatments (data not shown). Following these results, we hypothesized that one or more trace compounds in peak 1, not yet detected by NMR analysis, were inducing settlement. To test this, a larger amount of peak 1 was collected and a much longer (24-h) ^{13}C-NMR experiment run on the sample. The ^{13}C-NMR spectrum showed about 20 additional carbon signals not detected previously by NMR spectroscopy, indicating that additional compounds were present in peak 1 in trace amounts. The finding that peak 1 induced settlement of larvae of *H. purpurascens* but the identified major components (isethionic acid, taurine) in peak 1 did not implied that one of the compounds present in trace amounts was the settlement cue.

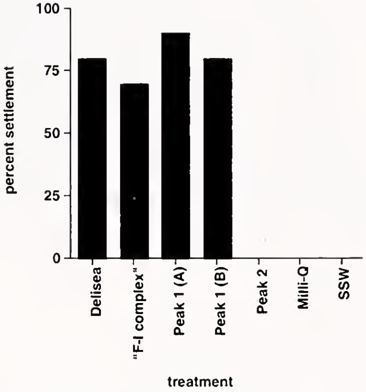

Figure 2. The settlement (%) of larvae of *Holopneustes purpurascens* after 18 h incubation with fresh *Delisea pulchra* (~10 mg) or HPLC peak fractions of the polar extract of the alga. Peak 1 (batch A or B) was tested at 25 $\mu g \cdot ml^{-1}$, peak 2 was tested at 51 $\mu g \cdot ml^{-1}$, and a floridoside-isethionic acid complex sample ("F-I complex") from Williamson *et al.* (2000) was tested at 76 $\mu g \cdot ml^{-1}$. Milli-Q water and sterile seawater (SSW) were included as the negative controls (n = 10).

Cation-exchange fractions—settlement assay. The settlement cue could not be isolated as a pure fraction using HPLC, so the polar extract of *D. pulchra* was fractionated using CX chromatography (Fig. 1B). Five CX-fractions (F) were obtained and tested in settlement assays; only F5 induced settlement of larvae of *H. purpurascens* (Fig. 3). F5 at a concentration of 1.0 $\mu g \cdot ml^{-1}$ induced 100% settlement in larvae after 1 h, 0.5 $\mu g \cdot ml^{-1}$ induced 70% settlement, and 0.1–0.25 $\mu g \cdot ml^{-1}$ did not induce settlement. There was no settlement in the control fraction CF5 (1.0 $\mu g \cdot ml^{-1}$) and SSW treatments (Fig. 3).

Identification of the settlement cue for Holopneustes purpurascens

Nuclear magnetic resonance spectroscopy. The ^{1}H-NMR (D_2O) spectrum of F5 showed proton signals at δ 2.76 (2H, t, J 7.0 Hz, H2), 3.03 (2H, t, J 8.2 Hz, H1), 6.86 (1H, s 2H, imidazole H), and 7.57 (s, 1H, imidazole H). The ^{13}C-NMR (D_2O) and DEPT spectra of F5 showed carbon signals at δ 25.9, 39.5 (CH_2); 116.4, 136.5 (CH) and 134.0 (quaternary C). These signals supported the assignment of F5 as histamine (2-[1*H*-imidazol-4-yl]-ethylamine, MW 111.15). The structure of F5 was further confirmed by a high-field two-dimensional ^{1}H-^{15}N HMBC NMR experiment in which the methylene triplet at 2.76 ppm showed two three-bond correlations to the ethylamine NH_2 group and the imidazole nitrogen. The identity of F5 was further confirmed by a spiking experiment. All F5 signals increased in intensity and no additional signals were detected, confirming the identity of F5 as histamine.

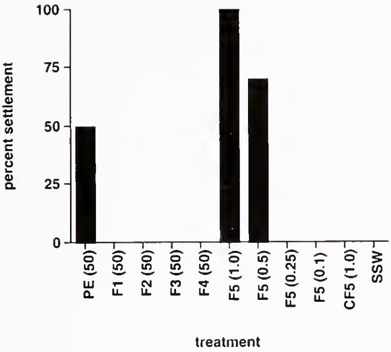

Figure 3. The settlement (%) of larvae of *Holopneustes purpurascens* after 1 h incubation with the polar extract of *Delisea pulchra* (PE) and cation-exchange fractions (F) of the PE. The different test concentrations of each treatment are shown in brackets ($\mu g \cdot ml^{-1}$); note the lower concentrations for F5 and the procedural control (CF5). Sterile seawater (SSW) was used as the negative control (n = 10).

Gas chromatography–mass spectrometry. The identity of putative histamine (F5) isolated from *D. pulchra* was confirmed using GC-MS. The retention times (rt) of the heptafluorobutyrlacyl derivative of putative histamine (rt = 9.728 ± 0.0045, mean ± SD, n = 5) and synthetic histamine (rt = 9.732 ± 0.0045, mean ± SD, n = 5) were nearly identical, suggesting that they were the same compound. The electron-impact ion spectra of both derivatized compounds displayed the same major fragment ions (m/z—54, 69, 81, 94, 138, 169, 226, 307, 349) and overall fragmentation pattern, confirming that they were the same compound. The electron-impact ion spectra for derivatized histamine matched that reported in the literature (Barancin *et al.*, 1998).

Matrix-assisted laser desorption/ionization–time-of-flight mass spectrometry. The elemental formula of putative histamine isolated from *D. pulchra* was confirmed by accurate mass measurements using MALDI-TOF MS. The measured accurate mass of the putative protonated histamine molecular ion $[M+H]^+$ was 112.08878 ± 0.0026 (n = 10, mean ± SD), and the measured mass for synthetic histamine was 112.08853 ± 0.0025 (n = 10, mean ± SD). The measured masses of the two samples were different by only 2.2 ppm. These values were different from the calculated monoisotopic mass for protonated histamine (112.08692—elemental formula $C_5H_{10}N_3$) by only 15 ppm for synthetic protonated histamine and 17 ppm for putative protonated histamine. This is most likely due to measurement bias introduced by the very different chemical properties of histamine, glycine, and creatinine (the internal calibrants).

An elemental calculator was used to generate all possible elemental formulas with a mass of approximately 112.08878. The nearest other candidate was $C_6H_{10}NO$ at 112.07569 with a difference of 117 ppm from the measured mass of putative protonated histamine. This difference was much higher than 17 ppm (difference of measured mass for putative histamine relative to calculated mass for $C_5H_{10}N_3$), confirming that the putative protonated histamine had the elemental formula of $C_5H_{10}N_3$.

The response of Holopneustes purpurascens *larvae to natural and synthetic histamine*

Natural histamine isolated from *D. pulchra* by using CX chromatography, synthetic histamine, and synthetic histamine eluted from CX resin all resulted in very similar responses in larvae when assayed concurrently (Fig. 4). More than 80% of the *H. purpurascens* larvae settled within an hour of incubation in 4.5 and 9 μM natural and synthetic histamine. The lowest test concentration of synthetic histamine that consistently induced rapid settlement of all larvae was 4.5 μM (in 10 separate assays). Larvae exhibited a more variable response to 0.9 and 2.3 μM histamine, both within and across different batches (Fig. 4). Up to 80% of larvae settled in response to 0.09–0.45 μM synthetic histamine, but only after long incubation times (up to 96 h) or as larval age increased to 13–21 days (data not shown).

Response of larvae to Delisea pulchra *after antibacterial treatments*

In response to *D. pulchra* that had received antibacterial treatments, larvae of *H. purpurascens* settled at levels equivalent to (or greater than) those in response to control

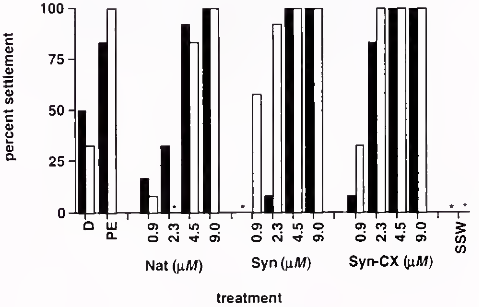

Figure 4. The settlement (%) of larvae of *Holopneustes purpurascens* after 1 h incubation with fresh *Delisea pulchra* (~10 mg), its polar extract (50 $\mu g \cdot ml^{-1}$) and 0.9–9.0 μM of natural histamine isolated from *D. pulchra* (Nat), synthetic histamine (Syn), or synthetic histamine eluted from cation-exchange resin (Syn-CX). Sterile seawater (SSW) was used as a negative control. Data from two experiments using different batches of larvae are shown (black and white bars). * Indicates no settlement in treatment (n = 12).

D. pulchra treatments (Fig. 5). SSW did not induce settlement.

Quantitative analysis of histamine content in algae

The histamine content of six algal species was determined by GC-MS (Table 1). *D. pulchra,* the alga on which new recruits of *H. purpurascens* are found (Williamson *et al.,* 2000), had the highest histamine content of all algae surveyed. Histamine was not detected in any samples of *Amphiroa anceps* or *Corallina officinalis.* The histamine content of *D. pulchra, Ecklonia radiata, Homeostrichus olsenii,* and *Sargassum vestitum* differed significantly from each other ($F_{3,16} = 9.903$, $P = 0.0006$). Pairwise comparisons showed that the histamine content of *D. pulchra* ($11.82 \pm 6.56\ \mu g \cdot g^{-1}$) was significantly higher than the histamine content of *E. radiata* ($1.28 \pm 1.01\ \mu g \cdot g^{-1}$, $P = 0.0092$), *S. vestitum* ($0.35 \pm 0.32\ \mu g \cdot g^{-1}$, $P = 0.0016$), and *H. olsenii* ($0.25 \pm 0.09\ \mu g \cdot g^{-1}$, $P = 0.0015$). The amount of histamine in different *D. pulchra* plants was highly variable, ranging from 1.88–34.22 $\mu g \cdot g^{-1}$ wet weight of algal tissue. The variability in histamine levels of *E. radiata* was also high, with no histamine detected in two samples, yet another contained 4.73 $\mu g \cdot g^{-1}$ wet weight of algal tissue. Likewise, histamine was not detected in three of the *S. vestitum* samples analyzed, but another contained 1.48 $\mu g \cdot g^{-1}$ wet weight of algal tissue. The *H. olsenii* plants analyzed showed consistently low levels of histamine, ranging from 0.05–0.46 $\mu g \cdot g^{-1}$ (wet weight) of algal tissue.

Table 1

The histamine content of six algal species was significantly different (ANOVA, $F_{3,16} = 9.903$, $P = 0.0006$*)*

Species	Histamine ($\mu g \cdot g^{-1}$ [ww]) mean ± SE, $n = 5$
Delisea pulchra	11.82 ± 6.56
Ecklonia radiata	1.28 ± 1.01*
Sargassum vestitum	0.35 ± 0.32*
Homeostrichus olsenii	0.25 ± 0.09*
Corallina officinalis	nd
Amphiroa anceps	nd

* Indicates species in which histamine content differs significantly from *D. pulchra* (pairwise comparisons, $P < 0.0092$); nd, not detected; ww, wet weight.

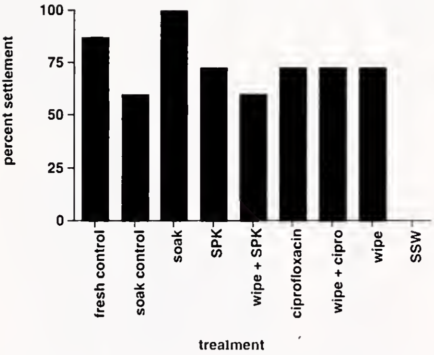

Figure 5. The settlement (%) of larvae of *Holopneustes purpurascens* after 20 h incubation with *Delisea pulchra* subjected to antibacterial treatments. All antibacterial treatments included a 5-min soak in a 10% betadine solution, followed by 3 rinses in sterile seawater (SSW) and a 24-h treatment in either SSW ("soak"); SSW containing streptomycin (20 $mg \cdot l^{-1}$), penicillin G (10 $mg \cdot l^{-1}$) and kanamycin (10 $mg \cdot l^{-1}$, "SPK"); or SSW containing ciprofloxacin (10 $mg \cdot l^{-1}$, "ciprofloxacin"). Other treatments involved wiping pieces of *D. pulchra* across an agar plate gently, to physically remove bacteria, before and after a 24-h soak in SSW ("wipe"), SSW containing SPK ("wipe + SPK"), or SSW containing ciprofloxacin (10 $mg \cdot l^{-1}$, "wipe + cipro"). *D. pulchra* soaked in SSW for 24 h (without betadine soak) was the procedural control ("soak control"), fresh *D. pulchra* was used as a positive control ("fresh control"), and SSW was used as a negative control ($n = 15$).

Reanalysis of samples from Williamson et al. *(2000)*

Several samples remaining from the previous study were analyzed by GC-MS for the presence of histamine. Histamine was detected in F-I complex fractions from *D. pulchra* (1.5–46 $\mu g \cdot mg\ [sample]^{-1}$) in a synthetic F-I complex sample (0.35 $\mu g \cdot mg\ [sample]^{-1}$), and in a batch of floridoside used to make the synthetic complexes (0.45 $\mu g \cdot mg\ [sample]^{-1}$).

Discussion

Habitat-specific cues play an important role in the settlement of many benthic marine invertebrates (Pawlik, 1992; Hadfield and Paul, 2001). Larvae presumably maximize their chances of post-settlement survival by responding to habitat-specific cues, as settlement in a preferred habitat should provide shelter and food to the vulnerable juvenile life-history phase (Gosselin and Qian, 1997). Chemical cues for larval settlement are derived from conspecifics (Burke, 1986), host organisms (Williamson *et al.,* 2000), prey (Hadfield and Scheuer, 1985), or biofilms (Wieczorek and Todd, 1998); they include a diverse range of compounds from small peptides (Zimmer-Faust and Tamburri, 1994) to complex macromolecules (Clare and Matsumura, 2000). The complete characterization of chemical settlement cues has, however, proved difficult because of the low endogenous or environmental levels of such compounds and the rapid dilution of water-soluble cues. Few studies have definitively characterized settlement cues (reviewed by Hadfield and Paul, 2001; Steinberg *et al.,* 2001).

Williamson *et al.* (2000) reported on one such putative characterized cue, a metabolite complex isolated from the red algal host *Delisea pulchra* that induced settlement in larvae of the sea urchin *Holopneustes purpurascens.* At Bare Island (Sydney, Australia), *H. purpurascens* is found primarily on two algal hosts, *D. pulchra* and *Ecklonia radiata,* with the smallest size class (test diameter ≤ 5 mm) only found on *D. pulchra.* Larvae metamorphosed in response to pieces of *D. pulchra* and the polar extract, but not to pieces or extracts of *E. radiata* (Williamson *et al.*, 2000). A water-soluble cue was implicated when seawater collected near *D. pulchra* plants *in situ* also induced settlement of larvae. The settlement cue in *D. pulchra* was isolated and characterized as the floridoside-isethionic acid (F-I) complex (Williamson *et al.*, 2000).

New evidence presented in this paper shows that histamine, not the F-I complex, is a natural inducer of settlement in *H. purpurascens.* The settlement cue was isolated from the polar extract of *D. pulchra* by using bioassay-guided fractionation by cation-exchange chromatography. The isolated compound at 0.5 $\mu g \cdot ml^{-1}$ induced settlement in 80%–100% of larvae within an hour. The settlement cue was identified as histamine using NMR spectroscopy, and this was confirmed by GC-MS and MALDI-TOF MS. The response of larvae to synthetic histamine in settlement assays mirrored their response to natural histamine isolated from *D. pulchra. D. pulchra,* the primary plant on which new recruits of *H. purpurascens* are found, had the highest average histamine content (11.82 ± 6.56 $\mu g \cdot g^{-1}$ wet weight), approximately an order of magnitude higher than other algae surveyed. Seawater collected near *D. pulchra* plants in the study by Williamson *et al.* (2000) induced rapid settlement of larval *H. purpurascens*; however, those samples were used completely in bioassays and are therefore not available for histamine analysis. We have since detected histamine in seawater surrounding *D. pulchra* and *E. radiata* (at concentrations ranging from 20 to 70 n*M*), but not in samples 2 m away from the macroalgae. A comprehensive analysis of histamine levels in seawater will be reported in another manuscript. Although the histamine concentrations measured in seawater do not induce rapid settlement in larvae that have just attained competence, this concentration can induce settlement of *H. purpurascens* larvae over longer time periods and in older larvae (data not shown). In addition, the natural habitat may contain other settlement cues that if detected in conjunction with histamine, may lower the threshold concentration of histamine required for rapid induction of settlement. These findings support our proposal that histamine released from macroalgae is a natural settlement cue for *H. purpurascens.*

Reanalysis of samples from the study by Williamson *et al.* (2000) provides an explanation for the incorrect conclusion that the F-I complex is a settlement cue for larvae of *H. purpurascens.* The F-I complex was isolated from the polar extract of *D. pulchra,* using reversed-phase HPLC and methanol as the mobile phase, and eluted as a single peak (Williamson *et al.*, 2000). ^{13}C-NMR spectroscopy analysis of this peak showed only ^{13}C-signals for floridoside and isethionic acid (Williamson *et al.*, 2000). However, trace amounts of histamine were also present but not detected, because their levels were below the limit of detection for ^{13}C-NMR spectroscopy. Histamine elutes in the first peak from reversed-phase (C18) columns regardless of the mobile phase, so any histamine in the polar extracts of *D. pulchra* used by Williamson *et al.* (2000) would have co-eluted with the F-I complex fraction. Consequently, the "F-I complex" samples contained histamine, detected here using GC-MS, and induced settlement of *H. purpurascens* larvae. Although a synthetic F-I complex induced rapid settlement in *H. purpurascens* larvae in the previous study (Williamson *et al.*, 2000), not all batches induced settlement (R. de Nys, pers. obs.). The synthetic F-I complexes were made using natural floridoside isolated from *D. pulchra* and synthetic isethionic acid. The floridoside used to make the synthetic F-I complex was contaminated by histamine and thus induced settlement. Confirming this, histamine was detected by GC-MS in a floridoside sample (used for preparation of the synthetic complex) and a synthetic F-I complex sample prepared by Williamson *et al.* (2000). In summary, histamine was present in trace amounts in the "F-I complex" samples that induced settlement of larval *H. purpurascens* in the previous study, and histamine was the inductive compound in the "F-I complex" samples.

The finding that histamine is a natural settlement cue for *H. purpurascens* is of considerable interest in the context of linking ecological patterns with physiological mechanisms. Histamine is a biogenic amine produced by the decarboxylation of the amino acid histidine. It is one of five primary biogenic amines in invertebrates, along with serotonin, octopamine, dopamine, and tyramine (Blenau and Baumann, 2001). Biogenic amines, all decarboxylation products of amino acids, play critical roles in initiating and controlling behavior, and in the physiology of invertebrates, by acting as classical neurotransmitters, neuromodulators, and neurohormones (Katz, 1995; Beltz, 1999). For example, dopamine activates hunting behavior in an opisthobranch mollusc (Norekyan and Satterlie, 1993), and serotonin controls aggressive behavior in crustaceans (Huber *et al.*, 1997). The photoreceptors in all classes of arthropod eyes are histaminergic; that is, they synthesize histamine and use it as their neurotransmitter (Stuart, 1999). Also, histamine is thought to be an inhibitory neurotransmitter in the stomatogastric and cardiac ganglia and the sensory system of lobsters (Claiborne and Selverston, 1984; Bayer *et al.*, 1989; Hashemzadeh-Gargari and Freschi, 1992). Importantly, in the context of this study, histamine directly gates a chloride channel in the receptor cells of the olfactory pathway of lobsters (McClintock and Ache, 1989). Fast neurotransmitters directly gate ion channels, which leads to fast behavioral and physiological outcomes. We have observed that the settlement response of *H. purpurascens* to histamine is rapid, with complete metamorphosis within half an hour. This fast response is consistent with the notion that the larvae of *H. purpurascens* have specific receptors that bind histamine and act directly on ion channels, leading to rapid settlement.

Neurotransmitters, or their precursors, have been suggested to mimic the function of natural settlement cues (Morse, 1985; Bonar *et al.*, 1990). The best-known example is the gamma-aminobutyric acid (GABA)-mimetic peptide (or peptides), present on the surface of crustose coralline algae, which Morse and colleagues proposed as a settlement cue for abalone (Morse *et al.*, 1979, 1984). Another example comes from oyster larvae, where L-3, 4-dihydroxyphenylalanine (L-DOPA) induced stereotypical searching behavior, while epinephrine and norepinephrine induced metamorphosis (Coon *et al.*, 1985). Endogenous levels of neurotransmitters, and their precursors, also appear to modulate the behavioral and physiological processes accompanying settlement (Coon and Bonar, 1987; Pires *et al.*, 2000). Our findings show that a naturally produced neurotransmitter is in fact a settlement cue for larvae, a phenomenon that may be widespread in the marine environment.

The finding that histamine, rather than the F-I complex, is a settlement cue for *H. purpurascens* potentially complicates the previous interpretations of the relationship between settlement cues and the demography of this sea urchin (Williamson *et al.*, 2000, 2004). Histamine, a simple breakdown product of the amino acid histidine, may be broadly distributed across the natural habitat of *H. purpurascens;* for example, in algal and animal tissue, and in bacterial communities living on their surfaces. For histamine to be an ecologically relevant settlement cue, its distribution in the natural habitat must relate to the recruitment patterns of *H. purpurascens*. This was in fact the case. The histamine content of the algae surveyed was consistent with the recruitment patterns of the organism, with much higher levels of histamine measured in *D. pulchra*, the primary plant on which we find new recruits.

D. pulchra had the highest average histamine content ($11.82 \pm 6.56\ \mu g \cdot g^{-1}$ wet weight), ranging from 1.88 to 34.22 $\mu g.g^{-1}$ wet weight. Similarly, levels of histamine varied for *E. radiata*, with concentrations ranging from 0 to 4.73 $\mu g.g^{-1}$ wet weight. Since only subsections of plants (not whole plants) were extracted, these results may reflect within-plant variation, within-species variation, or both. Future histamine analyses will extract whole plants, as well as specific regions of thalli, to directly test these possibilities. The low (or absent) levels of histamine typically measured in *E. radiata* samples may explain why pieces and extracts of *E. radiata* did not induce settlement in the study by Williamson *et al.* (2000). However, we have observed that some pieces of *E. radiata* do induce settlement of *H. purpurascens*, which is consistent with the variation we measured in levels of histamine in the alga. Given this, and the large biomass of *E. radiata* kelp beds in the natural habitat of *H. purpurascens, E. radiata* may contribute to environmental levels of histamine, inducing the settlement of larvae in this habitat. Histamine was not detected in the turfing coralline algae *Corallina officinalis* and *Amphiroa anceps,* although they induce settlement of larvae of *H. purpurascens* (Williamson *et al.*, 2000; R. Swanson, pers. obs.) and provide a habitat for new recruits (R. Swanson, pers. obs.). Larger samples of *A. anceps* (up to 180 g wet weight) were extracted and no histamine was detected. The coralline algae may produce a different settlement cue for *H. purpurascens,* or histamine may only be produced and released *in situ*—for example, by surface-associated bacteria.

Finally, the two possible sources of histamine in *D. pulchra* are the host alga or the surface-associated bacterial community (or both). *D. pulchra* treated with various antibacterial agents still induced high levels of settlement in *H. purpurascens,* suggesting that the host alga produces the histamine. A bacterial source of histamine is, however, possible, as a known histamine-producing bacterium, *Photobacterium phosphoreum* (Fujii *et al.*, 1997) is a constituent of the microbial community on local algal species (M. Watson, UNSW Australia; pers. comm.). If histamine-producing bacteria are colonizing algal surfaces within the habitat, then it is possible that they produce and release histamine to seawater, which could lead to the induction of settlement of *H. purpurascens.*

Conclusion

Many larval species have the ability to respond to low-molecular-weight, water-soluble settlement cues (Hadfield and Scheuer, 1985; Zimmer-Faust and Tamburri, 1994; Boettcher and Targett, 1996; Lambert *et al.*, 1997; Fleck and Fitt, 1999). This paper has presented evidence that histamine is a natural settlement cue for the sea urchin, *H. purpurascens,* correcting the previous study of Williamson *et al.* (2000). Histamine at 4.5 μM induces settlement (metamorphosis) in 80%–100% of *H. purpurascens* larvae within half an hour, fulfilling two essential criteria for an effective water-soluble settlement cue: (1) larvae must perceive low concentrations of inducer, and (2) larvae must respond rapidly to the inducer. *D. pulchra* had the highest histamine content of all the species surveyed, consistent with the recruitment patterns of *H. purpurascens.* In a preliminary analysis, we detected histamine in seawater near *D. pulchra* and *E. radiata* plants, but not in seawater collected 2 m away, supporting our proposal that histamine leaches from algae that produce this settlement cue. This hypothesis is consistent with the finding of Williamson *et al.* (2000) that seawater collected very near to *D. pulchra* induced settlement in larvae of *H. purpurascens.* We have shown that histamine, an invertebrate neurotransmitter, is also a natural settlement cue for larvae of *H. purpurascens,* linking the physiology and ecology of the organism.

Acknowledgments

This research was supported by an Australian Postgraduate Award to RLS, an ARC Research Fellowship to RdN, an ARC Large Grant to PDS and RdN, and the Center for Marine Biofouling and Bio-Innovation. We thank the Bioanalytical Mass Spectrometry Facility at UNSW for access to equipment, and Dr. Dustin Marshall for advice on statistical analysis. We especially thank Dr. Tim Charlton for his invaluable assistance with analytical methods.

Literature Cited

Aguirre-Lipperheide, M., and L. V. Evans. 1993. A sterilization protocol for the Dictyotales (Phaeophyceae). *J. Phycol.* **29:** 243–251.

Barancin, C. E., J. C. Smoot, R.H. Findlay, and L. A. Actis. 1998. Plasmid-mediated histamine biosynthesis in the bacterial fish pathogen *Vibrio anguillarum. Plasmid* **39:** 235–244.

Barrow, K. D., U. Karsten, and R. J. King. 1993. Isethionic acid from the marine red alga *Ceramium flaccidum. Phytochemistry* **35:** 1429–1430.

Bayer, T. A., T. S. McClintock, U. Grunert, and B. W. Ache. 1989. Histamine-induced modulation of olfactory receptor neurons in two species of lobster, *Panulirus argus* and *Homarus americanus. J. Exp. Biol.* **145:** 133–146.

Beltz, B. S. 1999. Distribution and functional anatomy of amine-containing neurons in decapod crustaceans. *Microsc. Res. Tech.* **44:** 105–120.

Berntsson, K. M., P. R. Jonsson, M. Lejhall, and P. Gatenholm. 2000. Analysis of behavioral rejection of micro-textured surfaces and implications for recruitment by the barnacle *Balanus improvisus. J. Exp. Mar. Biol. Ecol.* **251:** 59–83.

Blenau, W., and A. Baumann. 2001. Molecular and pharmacological properties of insect biogenic amine receptors: lessons from *Drosophila melangoster* and *Apis mellifera. Arch. Insect Biochem. Physiol.* **48:** 13–38.

Boettcher, A. A., and N. M. Targett. 1996. Induction of metamorphosis in queen conch, *Strombus gigas* Linnaeus, larvae by cues associated with red algae from their nursery grounds. *J. Exp. Mar. Biol. Ecol.* **196:** 29–52.

Bonar, D. B., S. L. Coon, M. Walch, R. M. Weiner, and W. Fitt. 1990. Control of oyster settlement and metamorphosis by endogenous and exogenous chemical cues. *Bull. Mar. Sci.* **46:** 484–498.

Bucknall, M., K. Y. C. Yung, and M. W. Duncan. 2002. Practical quantitative biomedical applications of MALDI-TOF mass spectrometry. *J. Am. Soc. Mass Spectrom.* **13:** 1015–1027.

Burke, R. D. 1984. Pheromonal control of metamorphosis in the Pacific sand dollar. *Dendraster excentricus. Science* **225:** 440–441.

Burke, R. D. 1986. Pheromones and the gregarious settlement of marine invertebrate larvae. *Bull. Mar. Sci.* **39:** 323–331.

Claiborne, B. J., and A. I. Selverston. 1984. Histamine as a neurotransmitter in the stomatogastric nervous system of the spiny lobster. *J. Neurosci.* **4:** 708–721.

Clare, A. S., and K. Matsumura. 2000. Nature and perception of barnacle settlement pheromones. *Biofouling* **15:** 57–71.

Coon, S. L., and D. B. Bonar. 1987. Pharmacological evidence that alpha-1 adrenoceptors mediate metamorphosis of the Pacific oyster *Crassostrea gigas. Neuroscience* **23:** 1169–1174.

Coon, S.L., D. B. Bonar, and R. M. Weiner. 1985. Induction of settlement and metamorphosis of the Pacific oyster *Crassostrea gigas* (Thunberg) by L-DOPA and catecholamines. *J. Exp. Mar. Biol. Ecol.* **94:** 211–221.

Fleck, J., and W. K. Fitt. 1999. Degrading mangrove leaves of *Rhizophora mangle* Linne provide a natural cue for settlement and metamorphosis of the upside down jellyfish *Cassiopea xamachana* Bigelow. *J. Exp. Mar. Biol. Ecol.* **234:** 83–94.

Fujii, T., A. Hiraishi, T. Kobayashi, R. Yoguchi, and M. Okuzumi. 1997. Identification of the psychrophilic histamine-producing marine bacteria previously referred to as the N-group bacteria. *Fish. Sci.* **63(5):** 807–810.

Gibson, G. D., and F.-S. Chia. 1994. A metamorphic inducer in the opisthobranch *Haminaea callidegenita:* partial purification and biological activity. *Biol. Bull.* **187:** 133–142.

Gosselin, L. A., and P. Y. Qian. 1997. Can bacterivory alone sustain larval development in the polychaete *Hydriodes elegans* and the barnacle *Balanus amphitrite*? *Mar. Ecol. Prog. Ser.* **161:** 93–101.

Hadfield, M. G., and V. J. Paul. 2001. Natural chemical cues for settlement and metamorphosis of marine invertebrate larvae. Pp. 431–461 in *Marine Chemical Ecology,* J. B. McClintock and B. J. Baker, eds. CRC Press, Boca Raton, FL.

Hadfield, M. G., and J. T. Pennington. 1990. Nature of the metamorphic signal and its internal transduction in larvae of the nudibranch *Phestilla sibogae. Bull. Mar. Sci.* **46:** 455–464.

Hadfield, M. G., and D. Scheuer. 1985. Evidence for a soluble metamorphic inducer in *Phestilla sibogae:* ecological, chemical and biological data. *Bull. Mar. Sci.* **37:** 556–566.

Harvey, M., and E. Bourget. 1997. Recruitment of marine invertebrates onto arborescent epibenthic structures: active and passive processes acting at different spatial scales. *Mar. Ecol. Prog. Ser.* **153:** 203–215.

Hashemzadeh-Gargari, R. M., and J. E. Freschi. 1992. Histamine activates a chloride conductance in motor neurons of the lobster cardiac ganglion. *J. Neurophysiol.* **68:** 9–15.

Huber, R., K. Smith, A. Delago, K. Isaksson, and E. A. Kravitz. 1997. Serotonin and aggressive motivation in crustaceans: altering the decision to retreat. *Proc. Natl. Acad. Sci. USA* **94:** 5939–5942.

Johnson, C. R., and D. C. Sutton. 1994. Bacteria on the surface of crustose coralline algae induce metamorphosis of the crown-of-thorns starfish *Acanthaster planci. Mar. Biol.* **120:** 305–310.

Karsten, U., K. D. Barrow, and R. J. King. 1993. Floridoside, L-isofloridoside, and D-isofloridoside in the red alga *Porphyra columbina. Plant Physiol. Biochem.* **103:** 485–491.

Kato, T., A. S. Kumanireng, I. Ichinose, Y. Kitahara, Y. Kakinuma, M. Nishihira, and M. Kato. 1975. Active components of *Sargassum tortile* effecting the settlement of swimming larvae of *Coryne uchidai. Experientia* **31:** 433–434.

Katz, P. S. 1995. Intrinsic and extrinsic neuromodulation of motor circuits. *Curr. Opin. Neurobiol.* **5:** 799–808.

Keough, M. J., and B. J. Downes. 1982. Recruitment of marine invertebrates: the role of active larval choices and early motility. *Oecologia* **54:** 348–352.

Krug, P. J., and A. E. Manzi. 1999. Waterborne and surface-associated carbohydrates as settlement cues for larvae of the specialist marine herbivore *Alderia modesta. Biol. Bull.* **197:** 94–103.

Lambert, W. J., C. D. Todd, and J. D. Hardege. 1997. Partial characterization and biological activity of a metamorphic inducer of the dorid nudibranch *Adalaria proxima* (Gastropoda: Nudibranchia). *Invertebr. Biol.* **116:** 71–81.

Maida, M., J. C. Coll, and P. W. Sammarco. 1994. Shedding new light on scleractinian coral recruitment. *J. Exp. Mar. Biol. Ecol.* **180:** 189–202.

McClintock, T. S., and B. W. Ache. 1989. Histamine directly gates a chloride channel in lobster olfactory receptor neurons. *Proc. Natl. Acad. Sci. USA* **86:** 8137–8141.

Morse, A. N. C., and D. E. Morse. 1996. Flypapers for coral and other planktonic larvae. *Bioscience* **46(4):** 254–262.

Morse, A. N. C., C. A. Froyd, and D. E. Morse. 1984. Molecules from cyanobacteria and red algae that induce larval settlement and metamorphosis in the mollusc *Haliotis rufescens*. *Mar. Biol.* **81:** 293–298.

Morse, D. E. 1985. Neurotransmitter-mimetic inducers of larval settlement and metamorphosis. *Bull. Mar. Sci.* **37:** 697–706.

Morse, D. E., N. Hooker, H. Duncan, and L. Jensen. 1979. Gamma-aminobutyric acid, a neurotransmitter, induces planktonic abalone larvae to settle and begin metamorphosis. *Science* **204:** 407–410.

Mullineaux, L. S., and C. A. Butman. 1991. Initial contact, exploration and attachment of barnacle (*Balanus amphitrite*) cyprids settling in flow. *Mar. Biol.* **110:** 93–103.

Norekyan, T. P., and R. Satterlie. 1993. Neuronal analysis of hunting behavior of the pteropod mollusc *Clione limacina*. *Neurosci. Behav. Physiol.* **23:** 11–23.

Pawlik, J. R. 1992. Chemical ecology of the settlement of benthic marine invertebrates. *Oceanogr. Mar. Biol. Annu. Rev.* **30:** 273–335.

Pires, A., R. P. Croll, and M. G. Hadfield. 2000. Catecholamines modulate metamorphosis in the opisthobranch gastropod *Phestilla sibogae*. *Biol. Bull.* **198:** 319–331.

Raimondi, P. T., and A. N. C. Morse. 2000. The consequences of complex larval behavior in a coral. *Ecology* **81:** 3193–3211.

Smythe, G. A., O. Braga, B. J. Brew, R. S. Grant, G. J. Guillemin, S. J. Kerr, and D. W. Walker. 2002. Concurrent quantification of quinolic, picolinic, and nicotinic acids using electron-capture negative-ion gas chromatography–mass spectrometry. *Anal. Biochem.* **301:** 21–26.

Steinberg, P. D., R. de Nys, and S. Kjelleberg. 2001. Chemical mediation of surface colonization. Pp. 335–387 in *Marine Chemical Ecology*, J. B. McClintock and B. J. Baker, eds. CRC Press, Boca Raton, FL.

Stuart, A. E. 1999. From fruit flies to barnacles, histamine is the neurotransmitter of arthropod photoreceptors. *Neuron* **22:** 431–433.

Tsukamoto, S., H. Kato, H. Hirota, and N. Fusetani. 1994. Narains: *N,N*-dimethylguanidinium styryl sulfates, metamorphosis inducers of ascidian larvae from a marine sponge *Jaspis* sp. *Tetrahedron Lett.* **35:** 5873–5874.

Tsukamoto, S., H. Kato, H. Hirota, and N. Fusetani. 1995. Pipecolate derivatives, anthosamines A and B, inducers of larval metamorphosis in ascidians, from a marine sponge *Anthosigmella aff. raromicrosclera*. *Tetrahedron* **51:** 6687–6694.

Tsukamoto, S., H. Kato, H. Hirota, and N. Fusetani. 1999. Lumichrome—a larval metamorphosis-inducing substance in the ascidian *Halocynthia roretzi*. *Eur. J. Biochem.* **264:** 785–789.

Underwood, A. J., and M. J. Keough. 2000. Supply-side ecology: the nature and consequences of variations in recruitment of intertidal organisms. Pp. 183–200 in *Marine Community Ecology*, M. D. Bertness, S. D. Gaines, and M. E. Hay, eds. Sinauer Associates, Sunderland, MA.

Wieczorek, S. K., and C. D. Todd. 1998. Inhibition and facilitation of settlement of epifaunal marine invertebrate larvae by microbial biofilm cues. *Biofouling* **12:** 81–118.

Williamson, J. E., R. de Nys, N. Kumar, D. G. Carson, and P. D. Steinberg. 2000. Induction of metamorphosis in the sea urchin *Holopneustes purpurascens* by a metabolite complex from the algal host *Delisea pulchra*. *Biol. Bull.* **198:** 332–345.

Williamson, J. E., D. G. Carson, R. de Nys, and P. D. Steinberg. 2004. Demographic consequences of an ontogenetic shift by a sea urchin in response to host plant chemistry. *Ecology* **85:** 1355–1371.

Wright, J. T., and P. D. Steinberg. 2001. Effect of variable recruitment and post-recruitment herbivory on local abundance of a marine alga. *Ecology* **82:** 2200–2215.

Xue-wu, L., and M. E. Gordon. 1987. Tissue and cell culture of the New Zealand *Pterocladia* and *Porphyra* species. *Hydrobiologia* **151:** 147–154.

Yvin, J. C., L. Chevolet, A. M. Chevolet-Maguer, and J. C. Cochard. 1985. First isolation of jacarone from an alga, *Delesseria sanguinea:* a metamorphosis inducer of *Pecten* larvae. *J. Nat. Prod.* **48:** 814–816.

Zimmer, R. K., and C. A. Butman. 2000. Chemical signaling processes in the marine environment. *Biol. Bull.* **198:** 168–187.

Zimmer-Faust, R. K., and M. N. Tamburri. 1994. Chemical identity and ecological implications of a waterborne, larval settlement cue. *Limnol. Oceanogr.* **39:** 1075–1087.

Reference: *Biol. Bull.* **206:** 173–187. (June 2004)
© 2004 Marine Biological Laboratory

Fitness Consequences of Allorecognition-Mediated Agonistic Interactions in the Colonial Hydroid *Hydractinia [GM]**

DAVID L. FERRELL

Department of Biological Science, Florida State University, Tallahassee, Florida 32306-1100

Abstract. In sessile and sedentary organisms, competition for space may have fitness consequences that depend strongly on ecological context. Colonial hydroids in the genus *Hydractinia* use an inducible defense when encountering conspecifics, and intraspecific competition is common in natural populations, often resulting in complete overgrowth of subordinate competitors. My goal in this study was to quantify the impacts of agonistic interactions in *Hydractinia [GM]* (an undescribed species from the Gulf of Mexico) in terms of three primary fitness components: colony survival, growth rate, and immature gonozooid production. The results demonstrate that the fitness consequences of intraspecific competition depend on the size at which competitive encounters are initiated and the growth form (an indicator of competitive ability) of the competitors. Moreover, some competing colonies consistently produced more immature gonozooids than the controls without competition, and they exhibited extremely low mortality even after 90 days of growth. These results have several ramifications. First, agonistic interactions do not always proceed to competitive elimination. Second, the increase in production of immature gonozooids—an investment in future reproduction—in response to intraspecific competition supports the hypothesis that indeterminately growing organisms increase sexual reproductive effort when growth becomes limiting. Lastly, in light of known ontogenetic variation in the ability of *Hydractinia* to differentiate among genetically related colonies, strongly size-dependent fitness consequences are consistent with an adaptive, kin-discriminating allorecognition system.

Introduction

Competition for space often imposes limitations on the fitness of sessile and sedentary organisms when a scarcity of hard substrata limits survival, growth, and reproduction (Buss, 1986). Much effort has been dedicated to discerning the effects of spatial competition on these fitness components (reviewed in Jackson, 1977, 1985; Buss, 1986, 1990; Sebens, 1986). Direct competition for space can result in overgrowth (reviewed in Buss and Jackson, 1979) in both heterospecific and conspecific interactions. However, competitive exclusion through overgrowth (or other processes) is not inevitable; competitors may be restricted spatially but coexist, even on densely colonized surfaces (Francis, 1973; Purcell, 1977; Karlson, 1980; Yund *et al.*, 1987).

Spatially restricted coexistence ultimately limits the size of colonial invertebrates that might otherwise exhibit indeterminate growth (Harvell and Grosberg, 1988). Because reproductive potential usually increases with colony size, size limits have the potential to impose reproductive costs. Consequently, many authors (Abrahamson, 1975; Hughes and Cancino, 1985; Harvell and Grosberg, 1988) have hypothesized that indeterminately growing clonal organisms should maximize fitness by increasing sexual allocation when extrinsic factors limit growth. This prediction has been supported by empirical data on diverse invertebrate taxa (Hauenschild, 1954; Braverman, 1974; Yamaguchi, 1975; Stebbing, 1980; Harvell and Grosberg, 1988).

In many colonial marine invertebrates (including sponges, cnidarians, bryozoans, and ascidians), conspecific interactions are mediated by allorecognition systems that

---

Received 20 August 2002; accepted 2 April 2004.

* [*GM*] is the designation given by Cunningham *et al.* (1991) to a species of *Hydractinia* that is found in the Gulf of Mexico but has not been formally described. *Reference:* C. W. Cunningham, L. W. Buss, and C. Anderson. 1991. Molecular and geological evidence of shared history between hermit crabs and the symbiotic genus *Hydractinia*. Evolution **45:** 1301–1316.

E-mail: ferrell@bio.fsu.edu

restrict somatic fusion to self or close kin, thereby limiting spatial competition and spatially restricted coexistence to unrelated individuals (Buss, 1987, 1990; Grosberg, 1988). For taxa in which encounters between relatives are common (often because of limited dispersal of sexually produced progeny), allorecognition may serve as an adaptive mechanism of kin recognition (Grosberg and Quinn, 1986; Hart and Grosberg, 1999). If intraspecific competition is associated with extremely high costs, such as the energetic cost of agonistic behavior and the risk of injury or competitive exclusion (Buss *et al.*, 1984), then intergenotypic fusion may be favorable despite the potentially severe fitness costs associated with it (Buss, 1982, 1987; Rinkevich and Loya, 1983; Barki *et al.*, 2002; Rinkevich, 2002). Conversely, if low costs accompany non-fusion, then fusion may be too costly an alternative. Thus, the fitness consequences of intraspecific competitive encounters provide insight into whether the evolution of allorecognition systems is adaptive.

Colonial hydroids in the genus *Hydractinia* inhabit shells occupied by hermit crabs, where they often encounter conspecifics (Yund *et al.*, 1987; Buss and Yund, 1988; Yund and Parker, 1989; Hart and Grosberg, 1999; Ferrell, 2004). A genetically coded allorecognition system determines whether contacting colonies will fuse (Grosberg *et al.*, 1996; Mokady and Buss, 1996) or attempt to overgrow one another (Ivker, 1972; Buss *et al.*, 1984). Here I present the results of laboratory experiments demonstrating that the fitness consequences of agonistic interactions between colonies of the undescribed species *Hydractinia [GM]* depend on the size at which competitive encounters are initiated and the growth form of the colonies involved. The context-dependent nature of competitive outcomes affects the production of immature reproductive zooids—an investment in future reproduction—and permits an assessment of whether allorecognition in *Hydractinia* is adaptive.

Materials and Methods

Hydractinia [GM], *study species*

Cunningham *et al.* (1991) constructed a phylogeny of the genus *Hydractinia* that consists of two distinct clades. One clade includes *H. symbiolongicarpus* and *H. [GM]*, which do not overlap in their geographic distribution. *H. symbiolongicarpus* has a northwestern Atlantic distribution, but *H. [GM]* is found only in the Gulf of Mexico. Mating experiments reveal nearly complete infertility between colonies collected in the Gulf and the northwestern Atlantic, indicating that *H. [GM]* is a new, undescribed species (pers. comm., C.W. Cunningham, Duke University).

Hydractinia [GM], as well as many Atlantic *Hydractinia* species (Yund *et al.*, 1987; Buss and Yund, 1988, 1989; Frank *et al.*, 2001), encrusts the surface of gastropod shells occupied by pagurid hermit crabs. Colonies are gonochoristic and polymorphic, possessing specialized reproductive polyps, or gonozooids, on which the gametes are produced. Sexual reproduction occurs during broadcast-spawning events in which gametes are released in response to light cues (Bunting, 1894; Ballard, 1942; Levitan and Grosberg, 1993). The crawling planula larva of *Hydractinia* attaches itself to a gastropod shell inhabited by a passing hermit crab (Yund *et al.*, 1987). Metamorphosis subsequently occurs on the shell surface. When two or more colonies recruit to the same shell, the colonies usually grow into contact. The resulting competitive interactions occur commonly in nature (Yund *et al.*, 1987; Buss and Yund, 1988; Yund and Parker, 1989; Hart and Grosberg, 1999; Ferrell, 2004).

Allorecognition and agonistic interactions in Hydractinia

The adaptive significance of kin fusion to the allorecognition system of *Hydractinia* is uncertain (Feldgarden and Yund, 1992; Yund and Feldgarden, 1992; Grosberg, 1992). In laboratory assays, the probability of fusion remains high between full siblings or between parent and offspring, but it drops precipitously between colonies of lesser relatedness (Hauenschild, 1954, 1956; Müller, 1964; Ivker, 1972; Grosberg *et al.*, 1996). If kin interactions are rare in the field, however, discrimination between kin and non-kin may simply reflect imperfect discrimination of self from non-self (Feldgarden and Yund, 1992; Yund and Feldgarden, 1992). Although kin interactions may be common in natural populations of *H. symbiolongicarpus* (Hart and Grosberg, 1999), adaptive kin/non-kin discrimination should persist only if kin fusion results in a net increase in a genotype's fitness relative to non-fusion.

Upon contact with genetically unrelated conspecific tissue, *Hydractinia* colonies do not fuse but instead usually mount a well-characterized agonistic response (Ivker, 1972; Buss *et al.*, 1984). The ability to mount an agonistic attack, or competitive ability, has a strong genetic basis and depends directly on colony growth form (Buss and Grosberg, 1990). (See Fig. 1 for an illustration of growth forms.) Some individuals grow solely by expansion of continuous, unbranching tissue ("mat" phenotypes), whereas others grow primarily by proliferating thin branches of tissue, or stolons ("stoloniferous" phenotypes). Colonies exhibit continuous variation between these two morphological extremes ("intermediate" phenotypes). In agonistic interactions, existing stolons swell due to the recruitment of nematocytes (cells bearing the nematocysts) and discharge of nematocysts (highly specialized stinging organelles) (Buss *et al.*, 1984). These "hyperplastic stolons" (Ivker, 1972) discharge nematocysts in an attempt to competitively exclude the opposing colony by tissue destruction and subsequent overgrowth (Buss and Grosberg, 1990). Thus, colonies with greater stolon proliferation (stoloniferous phenotypes) have an increased capacity to mount an agonistic response and competitively exclude others in laboratory competitive interactions between small colonies (Buss and Grosberg, 1990).

Multiple *Hydractinia* colonies may recruit to near or distant sites on a gastropod shell depending on shell morphology (Yund *et al.*, 1987; Buss and Yund, 1988; Yund and Parker, 1989) and size (Buss and Yund, 1988). As a result, conspecific encounters in *Hydractinia* may occur between small or large colonies, because colonies grow to different extents before contact. Previous studies have emphasized the importance of intraspecific competition between small, juvenile colonies (Buss and Yund, 1988; Buss and Grosberg, 1990), but agonistic interactions between large colonies have been documented in modern and historical populations (Buss and Yund, 1988), and are not uncommon in *H. [GM]* (Ferrell, 2004). Yund *et al.* (1987) used a single pair of competing genotypes to document competitive reversals and prolonged agonistic contests (possibly standoffs) between relatively large colonies. However, the generality of size-dependent competitive outcomes among conspecifics and the effect of growth form in competitive encounters between larger colonies remain largely unexplored.

Laboratory studies

In July 2000, I hand-collected five large, well-established, sexually mature colonies (designated colonies I–V hereafter) of *H. [GM]* from shallow water (1–1.5 m deep) in St. Joseph's Bay, Florida, located in the northeastern Gulf of Mexico. Each colony occupied an individual gastropod shell (*Fasciolaria lilium hunteria, F. tulipa, Polinices duplicatus*, or *Phyllonotus pomum*) inhabited by the hermit crab *Pagurus pollicaris*. In the laboratory, small pieces of tissue, or explants, including four or five gastrozooids were excised with a scalpel and transferred with watchmaker's forceps to plain glass microscope slides (7.64 cm × 3.82 cm, 1.1–1.3 mm thick). These tissue explants were held in the desired position using a single monofilament thread (8-lb. test) and kept in artificial seawater (Instant Ocean Sea Salt, ©1994; temperature = 24 °C, salinity = 32 ppt) in a single aquarium. Tissue explants attached to the glass substrate within a few days. This technique was used to establish all experimental replicates (described in detail below).

Two factors were manipulated in this experiment: (1) inter-competitor spacing and (2) relative competitive ability of competing colonies. Two competitive treatments were established by placing tissue explants from two different field-collected colonies on glass slides at 4-mm or 12-mm apart, resulting in interactions between small and large colonies, respectively, after subsequent colony growth. Such competitive interactions were established between all 10 pairwise combinations of the five experimental colonies. As a control, I also established each experimental colony singly on separate glass slides. All competing pairs and controls were replicated five times, yielding 125 experimental units [(10 pairs × 2 distances × 5 replicates) + (5 controls × 5 replicates) = 125 units]. Glass slides were mounted vertically on one of three acrylic plastic racks lined with nine plastic columns for attachment. Five slides could be mounted in each plastic column, generating five rows of slides on each rack. All slide positions were assigned randomly with respect to rack, column, and row. The three racks, including all glass slides, were maintained in artificial seawater in a single aquarium, as described above. Two underwater pumps ensured adequate circulation. Colonies were fed daily (3–4 h) to repletion with 2-day-old brine shrimp nauplii (Ocean Star International, Inc., Pro 100).

At 15, 30, 60, 80, and 90 days, each experimental unit was examined under a dissection microscope. Survival, colony width and length (omitted at the 80-d interval), and the number of immature gonozooids were recorded. The colonized surface area, defined here as the area covered by connecting stolon tips with straight lines or tracing the edge of mat tissue, was estimated by measuring colony width and length and then calculating the ellipsoid area [= $\pi \times (\text{length}/2) \times (\text{width}/2)$]. The surface-area growth rate of colonies was then calculated (= ellipsoid area/time). Digital computer images were obtained from 53 additional laboratory-cultured *H. [GM]* colonies established from clonal explants, and linear regression was performed to evaluate the appropriateness of estimated ellipsoid area as an indicator of colonized surface area, which was calculated using SigmaScan Pro 4 software. Additionally, the presence or absence of contact between competitors was noted to estimate the time in contact for all replicates. For example, after 90 d of growth, the estimated time in contact for conspecifics in contact after only 15 d would be 75 d.

After 65 d of growth, all control replicates of each of the five experimental colonies were analyzed morphometrically to determine colony growth form (*i.e.*, relative allocation to mat and stolonal tissue). In the absence of substrate limitation, mat and stolon growth rates remain constant throughout ontogeny (McFadden *et al.*, 1984; Blackstone and Yund, 1989). Consequently, morphological assessment at this time can be considered to represent conditions throughout the experiment (0–90 d).

I used a Nikon camera (60-mm lens) interfaced to a computer to obtain and store black-and-white images of the colonies. After tracing all tissue (stolonal or mat) of each replicate (see Fig. 1 for examples), I used SigmaScan Pro 4 software to perform the morphometric measurements needed to calculate the shape metric developed by Blackstone and Buss (1991). The unitless shape metric [= perimeter/(area)$^{0.5}$] is a reliable quantitative indicator of growth form in *Hydractinia* and other organisms that have similar colony development. Higher values correspond to increasingly stoloniferous phenotypes. The biomass surface area covered by mat tissue and individual stolons was also determined by using SigmaScan Pro 4 software. Note that the biomass surface area determined from these images of control-treatment colonies was calculated differently than the estimated ellipsoid surface area used to evaluate growth rate in all experimental units. Calculations of the shape metric and biomass growth rate allowed *a posteriori* assessment of the competitive ability of the five experimental colonies used in this study. The competitive-dominance hierarchy constructed using biomass growth rate and shape metric determinants was then compared to the actual competitive hierarchy based on the outcomes (in terms of colony survival) of the pairwise competitive encounters between all colonies.

Statistical analysis

I used Contingency χ^2 tests of independence to evaluate whether colony survival was associated with (1) intercolony spacing, (2) colony identity, and (3) competitor identity. In cases in which expected values were sufficiently small (≤ 5), Fisher's exact test of independence was used instead.

Initially, three-way analyses of variance (ANOVA) were used to explore the effects of slide position on the two continuous response variables (surface-area growth rate and number of immature gonozooids) after 90 days of growth. The main effects of rack (3), column (9), and row (5) were examined, as well as all possible interactions (JMP, ver. 3.2.6). Then, mixed-model, two-way ANOVAs were used to analyze the surface-area growth rate and the number of immature gonozooids after 90 days of growth. Separate ANOVA models were employed for each of the five experimental colonies to meet model assumptions of independence. The main effects of distance between competing colonies (fixed; 4 *vs.* 12 mm) and competitor identity (random; genotype of competitor) were explored, as well as the interactions between these two main factors. For each distance treatment group, contrasts comparing colony performance against each competitor were performed (12 total contrasts, family level $\alpha = 0.05$, Bonferroni adjusted $\alpha = 0.0042$; Sokal and Rohlf, 1995). Differences from control colonies in growth and reproductive variables were examined separately for the 4-mm and 12-mm treatments with one-way ANOVAs; contrasts comparing control *versus* competitive treatment colonies were performed (4 total contrasts, family level $\alpha = 0.05$, Bonferroni adjusted $\alpha = 0.0125$; Sokal and Rohlf, 1995). In addition, the relationship between immature gonozooid production and quantitative estimates of colony growth form (*i.e.*, shape metric) was examined using simple linear regression analysis for the 4-mm and 12-mm treatments. Natural logarithmic and square root data transformations were used when necessary to meet model assumptions of normality and homoscedasticity.

One-way ANOVAs were used to compare the mean biomass growth rate and mean shape metric of control replicates of the five experimental colonies. All pairwise comparisons were performed (10 total contrasts, family level $\alpha = 0.05$, Bonferroni adjusted $\alpha = 0.005$; Sokal and Rohlf, 1995).

Results

Effects of slide position

For both surface-area growth rate and number of immature gonozooids, two ANOVA models were explored for the effects of slide position. The first included all possible interactions as factors in the model [rack (3), column (9), row (5), rack*column, rack*row, column*row, rack*column*row]. However, in the absence of statistically significant interactions, data were pooled and reanalyzed including only the main effects of rack, column, and row. Neither of these statistical models identified significant effects of slide position with regard to surface-area growth rate or number of immature gonozooids. Consequently, slide position was ignored in all subsequent analyses.

Morphological assessment

Growth forms of experimental colonies included those that were entirely mat and those that were highly stoloniferous as well as intermediate types (Fig. 1). For ease of interpretation, I assigned Roman numerals I–V to colonies according to the extent of stolon proliferation. After 65 d of growth, none of the control replicates (established in the absence of competition) of colony I possessed any peripheral stolons branching out from the central ectodermal mat. In contrast, control replicates of colony V were highly stoloniferous, with most growth occurring *via* stolon rather than as mat tissue. Control replicates of colonies II, III, and IV displayed intermediate growth forms with various proportions of mat and stolon tissue.

Figure 1 compares quantitative estimates of growth form and growth rate of the experimental colonies. The growth rate, in terms of biomass area covered after 65 d of growth, was similar among experimental colonies, except colony V. Although ANOVA results indicated a difference in the mean biomass area of the colonies ($F_{4,20} = 6.76$, $P = 0.001$), Bonferroni pairwise comparisons (adjusted $\alpha = 0.005$) suggested that this is attributable solely to colony V, which produced biomass coverage at a rate greater than the others. The clear differences in growth form of colonies I, II, III, and IV (Fig. 1) did not result in significant differences in biomass production. Thus, morphological variation in *H. [GM]* does not necessarily reflect differences in the rate of biomass production. In contrast to biomass growth rate, the shape metric reveals a relationship between morphology and the growth differences between experimental colonies. As with biomass growth rate, ANOVA showed overall

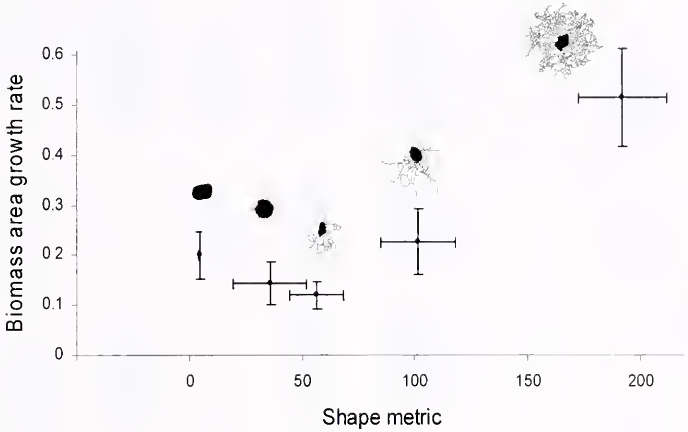

Figure 1. Variation in growth rate and colony morphology among *Hydractinia [GM]* experimental colonies. Roman numerals I–V were assigned to colonies according to the extent of stolonal proliferation for ease of interpretation. The colony outlines illustrate mat (I), highly stoloniferous (V), and intermediate growth morphologies (II, III, IV). These are representative tracings of images obtained from control replicates ($n = 5$) of experimental colonies I–V after 65 d of growth. Colonies are not drawn to scale. The biomass growth rate (mm^2/day) reflects the total area covered by both stolonal and mat tissue encrusting the surface of a glass slide after 65 d of growth. The shape metric (= perimeter/$(area)^{0.5}$), developed by Blackstone and Buss (1991), is a unitless indicator of colony growth morphology calculated using the total perimeter and area covered by stolonal and mat tissue combined.

highly significant differences in the mean shape metric ($F_{4,20} = 24.78$, $P < 0.001$). However, Bonferroni pairwise comparisons indicated that the mean shape metric of colonies IV and V both differ significantly from all other colonies. The colonies can be ranked in order of decreasing allocation to stolon growth: V > IV > III = II = I. The "equal" (=) symbol denotes no statistical difference.

None of the five control replicates of colony I exhibited any stolon growth. This attribute reflects a qualitative morphological distinction between colony I and the other four colonies. Thus, while morphometric analysis did not indicate significant quantitative differences in stolon production between colony I and colonies II and III, an important qualitative difference was observed. Noting the absence of stolons in colony I, the experimental colonies can be ranked in order of decreasing stolon production as follows: V > IV > III = II > I.

Survival

Colony survival differed markedly as a function of intercolony spacing. After only 30 d of growth, competing colonies that had been established 4-mm apart experienced reduced survival compared to those established 12-mm apart or in the absence of competition ($\chi^2_{calc} = 27.3$, $\chi^2_{crit,\ 0.05} = 3.8$, df = 1, $P < 0.001$), and these differences in survival remained significant for the duration of the experiment. For example, after 60 d of growth, survival of 4-mm colonies dropped to 55% and was significantly lower than the 85% survival seen in 12-mm colonies after 90 d ($\chi^2_{calc} = 42.7$, $\chi^2_{crit,\ 0.05} = 3.8$, df = 1, $P < 0.001$). After 90 d, colonies in the 4-mm treatment showed less than half the survival rate of those in the 12-mm treatment (42% compared to 85%; $\chi^2_{calc} = 39.9$, $\chi^2_{crit,\ 0.05} = 3.8$, df = 1, $P < 0.001$; Fig. 2). Thus, competitive encounters between smaller colonies incur greater (or at least earlier) mortality than encounters between larger colonies. By contrast, all control colonies had 100% survival, suggesting that intraspecific competition caused the observed mortality.

Although mortality costs from competition were most intense in small-colony encounters (4-mm treatment), the five experimental colonies differed in all cases with respect to the onset of significant mortality. Differences in mortality between 4-mm and 12-mm treatments were statistically significant (Fisher's exact test, $P < 0.01$) only after 90 d in colony V, the most stoloniferous colony. In contrast, significant mortality differences between these treatments were evident much earlier in other colonies (30 d in colonies I, III, and IV; 60 d in colony II). Colonies in the 4-mm treatment did not exhibit significantly different mortality when pooled over all competitors (*i.e.*, data pooled within

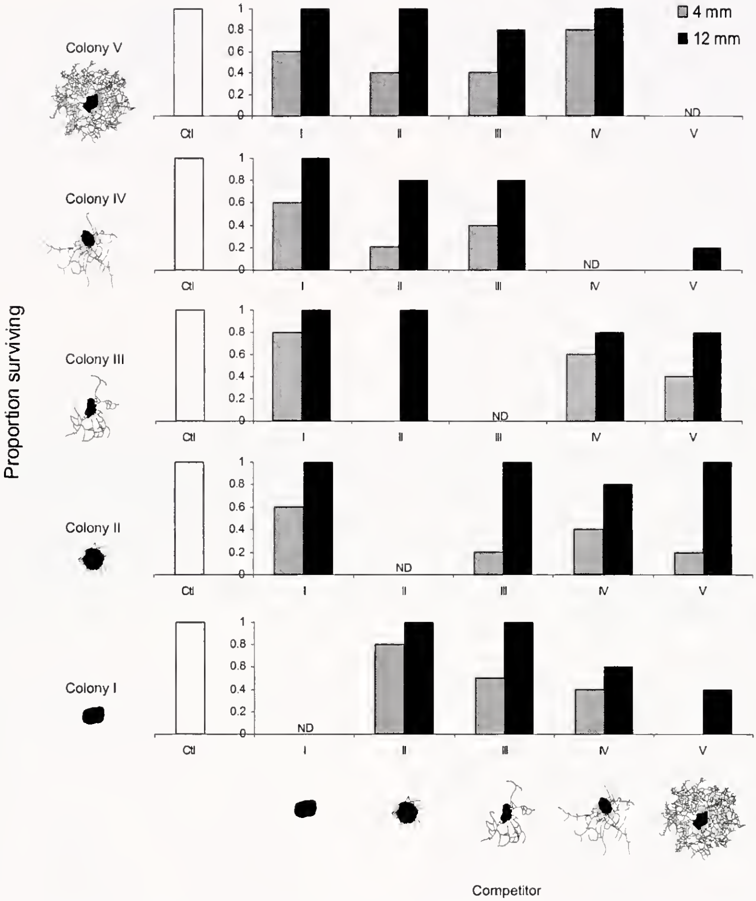

Figure 2. Colony survival as a function of competitor identity and intercolony spacing (4-mm or 12-mm). The proportion of colonies surviving after 90 d in competition with each of four competitors is illustrated for 4-mm and 12-mm treatments. The performance of control replicates is included for reference. Colonies are not drawn to scale. ND = no data.

each colony row in Fig. 2; $\chi^2_{\text{calc}} = 1.7$, $\chi^2_{\text{crit, 0.05}} = 9.5$, df = 4, $P > 0.05$). Although 4-mm clones experienced some mortality in all competitive pairings (Fig. 2), some 4-mm competitors imposed greater overall mortality than others (*i.e.*, data pooled within each competitor column in Fig. 2; $\chi^2_{\text{calc}} = 12.2$, $\chi^2_{\text{crit, 0.05}} = 9.5$, df = 4, $P < 0.05$). Colonies were least likely to survive competition with colony V and most likely to survive competition with colony I.

Survival after 90 d in 12-mm treatments was not significantly different among colonies when pooled over all competitors (*i.e.*, data pooled within each colony row in Fig. 2; $\chi^2_{\text{calc}} = 8.63$, $\chi^2_{\text{crit, 0.05}} = 9.5$, df = 4, $P > 0.05$). Most of the observed mortality occurred among replicates of colonies I and IV, however. Mortality in all other colonies (II, III, and V) was nearly negligible, as survival was 90% or higher. As in 4-mm treatments, some 12-mm competitors imposed greater overall mortality than others (*i.e.*, data pooled within each competitor column in Fig. 2; $\chi^2_{\text{calc}} = 15.7$, $\chi^2_{\text{crit, 0.05}} = 9.5$, df = 4, $P < 0.01$). In 12-mm competitive encounters in which mortality occurred (Fig. 2), colonies were killed by competitors IV and V almost exclusively.

Overall, colonies V and I were the superior and inferior competitors, respectively. Competitive relationships between intermediate competitors were less distinct, with the genotypes that exhibited the more stoloniferous growth forms generally dominating (Fig. 2).

Growth rate

Estimates of ellipsoid area were highly correlated with measurements of colonized surface area ($R^2 = 94.9\%$, $n = 53$), and were therefore used as an indicator of surface-area growth rate for experimental colonies. Colonies established 4 mm apart often suffered marked reductions in growth rate relative to controls; Bonferroni comparisons indicated that all competitor treatments (except one) were significantly different from controls for colonies IV and V, but not significantly different for colonies I, II, and III (Table 1, Fig. 3). In contrast, the growth rate of those in the 12-mm treatment was most often similar to controls; Bonferroni comparisons indicated that no competitor treatments were significantly different from controls, with two exceptions in colony V (Table 1, Fig. 3). Differences in growth rate after 90 d between 4-mm and 12-mm treatments were statistically significant for colonies II, IV, and V (Table 2).

Some competitors inflicted greater costs in growth rate than others did. After 90 d, differences in growth rate depending on competitor identity were significant for all colonies except for the two most mat-like phenotypes, colonies I and II (Table 2, Fig. 3). Instead, the effect of competitor identity was not statistically significant for colonies I ($P = 0.604$) and II ($P = 0.406$), indicating a uniform cost in terms of growth rate regardless of the degree of attack presented by a competitor. For those colonies (III, IV, and V) in which growth rate varied significantly between competitors, Bonferroni comparisons were generally unable to differentiate statistically which competitors imposed greater growth rate costs than others. The two exceptions were colony III in the 4-mm treatment, which exhibited a significantly greater growth rate in competition with colony I than with colony II (Fig. 3); and colony IV in the 12-mm treatment, which showed a significantly greater growth rate in competition with colony I than with colony V (Fig. 3). In both cases, colony I imposed less reduction in growth rate during intraspecific competition. After 90 d of growth, in no case was the interaction between competitive treatment (4-mm and 12-mm) and competitor identity significant (Table 2). Thus, the relative ability of competitors to impose growth-rate costs did not vary between the two treatments. In other words, the severity of the growth reduction imposed by competitors did not depend on whether the competing colonies were large or small.

Table 1

Summary of one-way ANOVAs examining differences between control and competing colonies ($t = 90$ d) in 4-mm and 12-mm treatments

Variable	Focal colony	Treatment	$F_{4,20}$	Significant Bonferroni comparisons
Surface-area growth rate				
	I	4 mm	0.86	—
		12 mm	0.31	—
	II	4 mm	1.32	—
		12 mm	1.18	—
	III	4 mm	2.79	—
		12 mm	3.78*	—
	IV	4 mm	6.41**	control vs. II, III, V
		12 mm	4.59**	—
	V	4 mm	8.46***	control vs. I, II, III, IV
		12 mm	3.83*	control vs. III, IV
Number of immature gonozoids				
	I	4 mm	0.91	—
		12 mm	0.93	—
	II	4 mm	13.29***	control vs. I, III, IV, V
		12 mm	5.73**	control vs. III (+)
	III	4 mm	1.39	—
		12 mm	8.82***	control vs. I (+), II (+)
	IV	4 mm	3.45*	control vs. III, V
		12 mm	0.34	—
	V	4 mm	2.86	control vs. II
		12 mm	1.17	—

Note: Bonferroni comparisons indicate lower values than controls except where indicated with a plus symbol (+). * = $P < 0.05$, ** = $P < 0.01$, *** = $P < 0.001$.

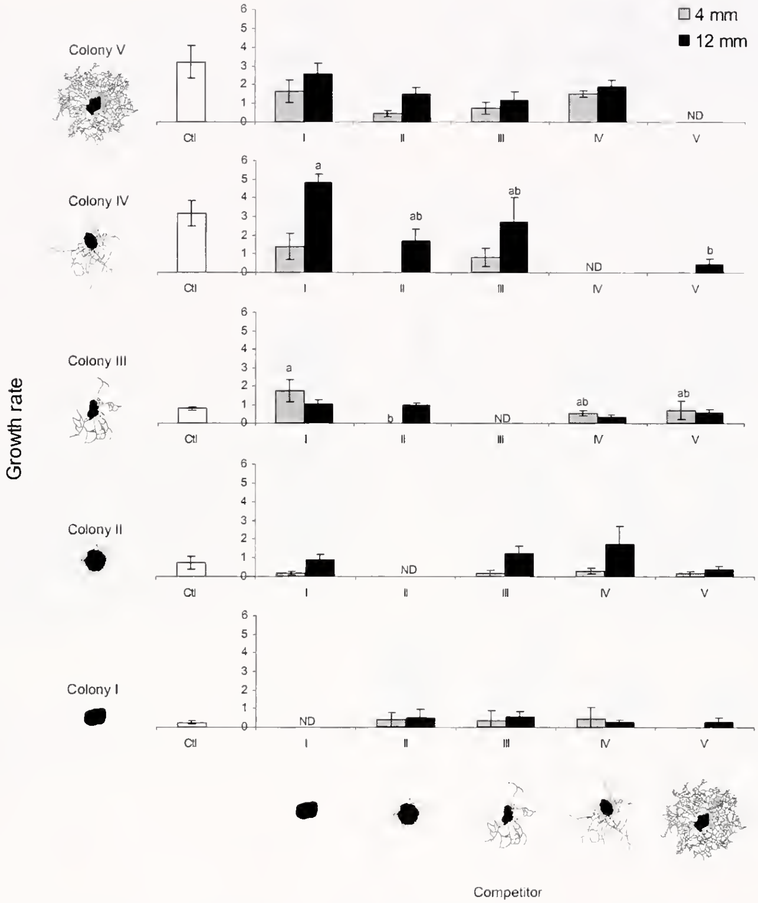

Figure 3. Surface-area growth rate as a function of competitor identity and intercolony spacing (4-mm or 12-mm). The mean (± SE) surface-area growth rate (mm^2/d) after 90 d in competition with each of four competitors is illustrated for 4-mm and 12-mm treatments. The performance of control replicates is included for reference. Bonferroni pairwise comparisons (adjusted $\alpha = 0.0042$) indicated no significant differences in means, with the following exceptions: colony III, 4-mm; colony IV, 12-mm. Significantly different means are indicated by different lowercase letters. Colonies are not drawn to scale. ND = no data.

Production of immature gonozooids

The number of immature gonozooids differed remarkably as a function of intercolony spacing for four out of five experimental colonies. Whereas 4-mm colonies invested very little or no energy into immature gonozooids (Fig. 4), 12-mm colonies exhibited immature gonozooid investment that was similar to control colonies initially (up to 30 d), and then in some cases greater than controls for the remainder of the experiment (see analysis below).

After 90 d, differences in immature gonozooid production between 4-mm and 12-mm treatments were highly significant for all colonies except colony I (Table 3, Fig. 4). All 4-mm competitive treatments exhibited immature gonozooid production similar to or less than controls (Table 1, Fig. 4). In contrast, 12-mm competitive treatments exhibited immature gonozooid production similar to or greater than controls (Table 1, Fig. 4).

All instances of augmented production of immature

Table 2

Summary of two-way ANOVAs examining the effects of intercolony distance and competitor genotype on surface-area growth rate (t = *90 d)*

Focal colony	Source	df	MS	F-ratio
I	Distance	1	0.136	0.441
	Competitor	3	0.192	0.625
	Interaction	3	0.113	0.366
	Error	32	0.308	
II	Distance	1	2.138	15.063***
	Competitor	3	0.142	1.000
	Interaction	3	0.087	0.612
	Error	32	0.142	
III	Distance	1	0.001	0.002
	Competitor	3	1.999	3.975*
	Interaction	3	1.223	2.433
	Error	32	0.503	
IV	Distance	1	5.184	20.843***
	Competitor	3	2.057	8.271***
	Interaction	3	0.278	1.116
	Error	32	0.249	
V	Distance	1	5.247	6.490*
	Competitor	3	3.409	4.220*
	Interaction	3	0.347	0.429
	Error	32	0.808	

Note: Results of individual ANOVAs are given for focal colonies I, II, III, IV, and V. * = $P < 0.05$, *** = $P < 0.001$.

gonozooids involved poor competitors (I, II, III) exhibiting mat or mat-like (intermediate) growth forms (Fig. 4). By summing the shape metrics of each competing pair, the interactions can be ranked according to the morphological attributes of the encounter. Mat-mat encounters have the lowest sums; stoloniferous-stoloniferous encounters have the greatest. Simple linear regression analysis revealed a highly significant, negative relationship between production of immature gonozooids and the sum of the shape metrics ($F_{1,18} = 26.0$, $P < 0.0001$), accounting for a majority (R^2 = 60.1%) of the variation in immature gonozooid production in 12-mm colonies (Fig. 5). This relationship was not detected in 4-mm colonies ($F_{1,18} = 1.3$, $P = 0.26$), which showed much less variability in immature gonozooid production (Fig. 4).

Discussion

Competitive dynamics in *Hydractinia [GM]* clearly depend on the ecological context in which intraspecific competition transpires. The size of colonies upon encountering conspecifics and the growth form, or competitive ability, of competitors both strongly influenced the fitness consequences of agonistic interactions. Interactions between small colonies generally imposed greater costs in colony survival, growth rate, and investment in future reproduction. Superior competitors typically eliminated their opponents in small-colony encounters, but only the most dominant colonies competitively excluded others in larger-colony interactions. In certain conditions, competing colonies consistently increased their investment in future reproduction (relative to controls without competition) and exhibited zero mortality, although reduced growth was often evident. These findings indicate that (1) agonistic interactions do not always result in the elimination of inferior competitors, (2) colonies may increase production of immature gonozooids—an investment in future reproduction—as a result of growth limitation by conspecifics, and (3) ontogenetic changes in allorecognition-mediated fusibility may be due in part to heavily size-dependent fitness consequences of non-fusion.

Competitive outcomes

The fitness consequences of intraspecific competition in *H. [GM]* were heavily size-dependent. Not only may the duration of encounters between larger colonies be prolonged, but also the outcome may be entirely different. Whereas encounters at small size usually result in competitive exclusion (Ivker, 1972; Buss *et al.*, 1984; Yund *et al.*, 1987; Buss and Grosberg, 1990; this study), this may not always be true for the encounters of larger colonies. Indeed, when given a distinct size advantage over its superior interspecific competitor, the colonial hydroid *Podocoryne carnea, Hydractinia* colonies often survived interspecific contests and formed intercolony boundaries stable for 2–3 months (McFadden, 1986). Work with other spatial competitors of *Hydractinia* on artificial substrata similarly suggests that colonies may persist by inhibiting the growth of adjacent competitors rather than by attempting overgrowth (Karlson, 1978). In the present study, mat and mat-like *Hydractinia* phenotypes accrued zero mortality in intraspecific competitive interactions initiated between larger colonies.

Yund *et al.* (1987) also report coexistence, rather than overgrowth, of two competing *Hydractinia* genotypes established at distant recruitment sites after 9.5 weeks of growth. Even after 18 weeks, only four of eight replicates had resulted in exclusion of one of the two genotypes, despite significant differences in growth rate (and presumably competitive ability) between them. Had such interactions been investigated between genotypes with relatively low and similar growth rates (as in the present study), Yund *et al.* (1987) might have observed even less or no overgrowth in large-colony competitive interactions. Yund *et al.* (1987) proposed that the costs of non-fusion are actually much greater in interactions between large colonies. This conclusion implies that complete overgrowth, albeit prolonged, will proceed in all competitive encounters. If this

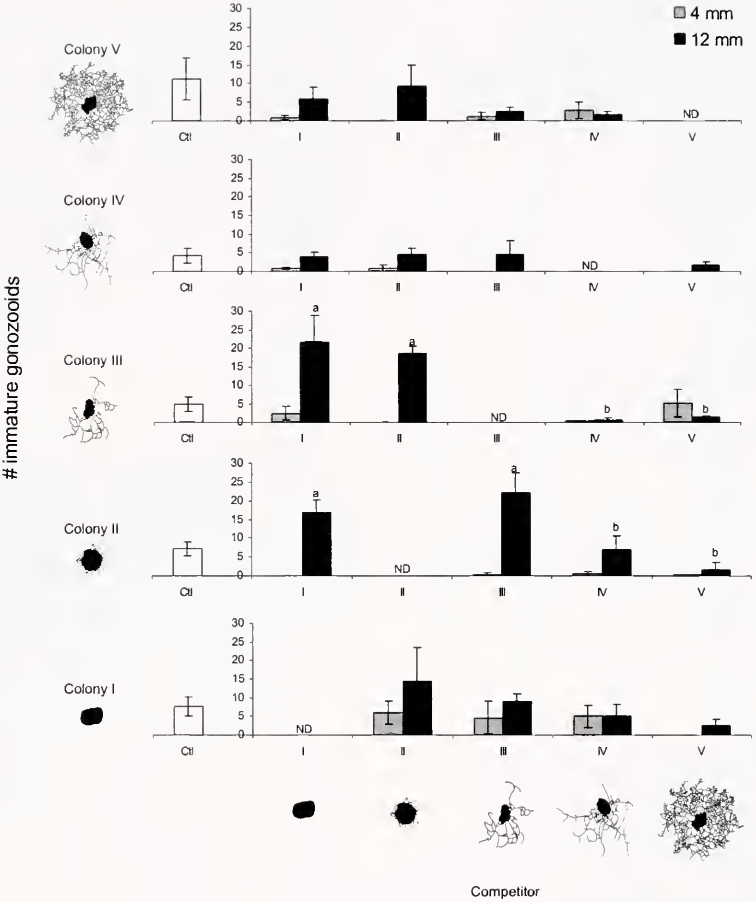

Figure 4. Immature gonozooid production as a function of competitor identity and intercolony spacing (4-mm or 12-mm). The mean (± SE) number of gonozooids per colony after 90 d in competition with each of four competitors is illustrated for 4-mm and 12-mm treatments. The performance of control replicates is included for reference. Bonferroni pairwise comparisons (adjusted α = 0.0042) indicated no significant differences in means, with the following exceptions: colony III, 12-mm; colony V, 12-mm. Significantly different means are indicated by different lowercase letters. Colonies are not drawn to scale. ND = no data.

were the case, fitness costs indeed would be more severe, because even the "winner" faces the immense energetic costs of such a prolonged struggle. My results are consistent with this interpretation in that highly stoloniferous colonies showed evidence of overgrowth regardless of intercolony spacing; however, in the absence of highly stoloniferous phenotypes, this does not appear to be the case. Overgrowth, while likely predominating in many *Hydractinia* populations as a result of recruitment patterns and available gastropod substrata (Buss and Yund, 1988; Yund and Parker, 1989), may not be the inevitable product of intraspecific competition in *H. [GM]*.

Differences in the outcome of competitive encounters based on colony size are important ecologically and evolutionarily only if the frequency of encounters between small and large colonies varies predictably in natural populations.

Table 3

Summary of two-way ANOVAs examining the effects of intercolony distance and competitor genotype on the number of immature gonozooids (t = *90 d)*

Focal Colony	Source	df	MS	*F*-ratio
I	Distance	1	4.589	3.603
	Competitor	3	3.238	2.542
	Interaction	3	0.899	0.706
	Error	32	1.274	
II	Distance	1	32.876	71.472***
	Competitor	3	3.390	7.369***
	Interaction	3	3.660	7.958***
	Error	32	0.460	
III	Distance	1	13.850	22.761***
	Competitor	3	4.546	7.471***
	Interaction	3	6.002	9.864***
	Error	32	0.608	
IV	Distance	1	17.125	22.011***
	Competitor	3	1.384	1.779
	Interaction	3	0.200	0.257
	Error	32	0.778	
V	Distance	1	6.750	8.456**
	Competitor	3	0.098	0.123
	Interaction	3	1.387	1.737
	Error	32	0.798	

Note: Results of individual ANOVAs are given for focal colonies I, II, III, IV, and V. ** = $P < 0.01$, *** = $P < 0.001$.

Field surveys indicate that competitive interactions between large colonies occur regularly in some *H. [GM]* populations with a frequency that varies predictably with the availability of different sizes and types of gastropod shells (Ferrell, 2004). Shell size and morphology affect the likelihood that multiple larvae will recruit to distant positions on a shell (Buss and Yund, 1988; Yund and Parker, 1989). Yund and Parker (1989) acknowledge that a sizeable portion of interactions may occur between large colonies in certain *Hydractinia* species. However, the mean shell length (~42 mm) of encrusted gastropod shells in some *H. [GM]* populations (Ferrell, 2004) greatly exceeds even the maximum shell length (~25 mm) utilized in many northwestern Atlantic *Hydractinia* populations (as reported in Buss and Yund, 1988). On bigger shells, the spacing between colonies can be greater; thus competitive interactions between extremely large colonies, in which overgrowth seems increasingly improbable, occur in *H. [GM]* (pers. obs.). As in other marine cnidarians (*e.g.*, Francis, 1973; Karlson, 1980; Purcell, 1977), agonistic behavior may result in territorial defense of spatial resources rather than competitive exclusion.

Production of immature gonozooids—an investment in future reproduction

Not only were instances of overgrowth attributable to colony morphology, but immature gonozooid production (and growth rate to a lesser degree) also varied as a function of the morphology of the competitors. When growth rate differed significantly among opponents, the less stoloniferous competitor experienced the greater in growth rate and produced few immature gonozooids, or none at all. These results are consistent with expectations of the intensity of aggression based on colony growth form.

Although production of immature gonozooids was higher in colonies encountering less formidable opponents (*i.e.*, mat or mat-like intermediate growth forms), production in some cases was even higher than in the controls. This effect was not apparent in small-colony interactions, in which overgrowth proceeded much more rapidly. Even *Hydractinia* colonies with as few as two feeding polyps are capable of producing mature gonozooids (Hauenschild, 1954; Müller, 1964); nevertheless, their extreme vulnerability to overgrowth and the scarcity of tissue not directly involved in colony defense most likely kept the small colonies from producing many gonozooids. Only colonies of mat and mat-like intermediate morphologies increased their production of immature gonozooids. Hauenschild (1954) made several observations of *Hydractinia* that shed light on this trend: (1) the formation of mat tissue is a precondition for the production of gonozooids, (2) gonozooids form much earlier in mat colonies, (3) entirely mat phenotypes produce gonozooids naturally, even when occupying an unlimited substrate, (4) intermediate phenotypes do not develop gonozooids unless confronted with growth limitations, and (5) stoloniferous colonies require full colonization of surface before gonozooids arise. Thus, the greater production of immature gonozooids observed in mat and mat-like intermediates is simply a by-product of their larger supply of mat tissue upon which to form gonozooids, coupled with an earlier onset of sexual reproduction. If Hauenschild's (1954) third observation is true, it may explain why the entirely mat phenotype, unlike the mat-like intermediate phenotypes, did not increase production of immature gonozooids substantially above control levels. (Table 1, Fig. 4). That is, with no growth limitations (as in the control treatment), the entirely mat phenotype would still exhibit significant immature gonozooid production, whereas the intermediate phenotypes, which react in this manner only in growth-limiting conditions, would not.

I explored two alternate explanations for the observed patterns in immature gonozooid production. First, perhaps the interacting pairs benefiting from positive effects on immature gonozooid production were relatives. None of the interacting colonies exhibited the fusion one might expect if they were genetically related. However, about 50% of *Hy-*

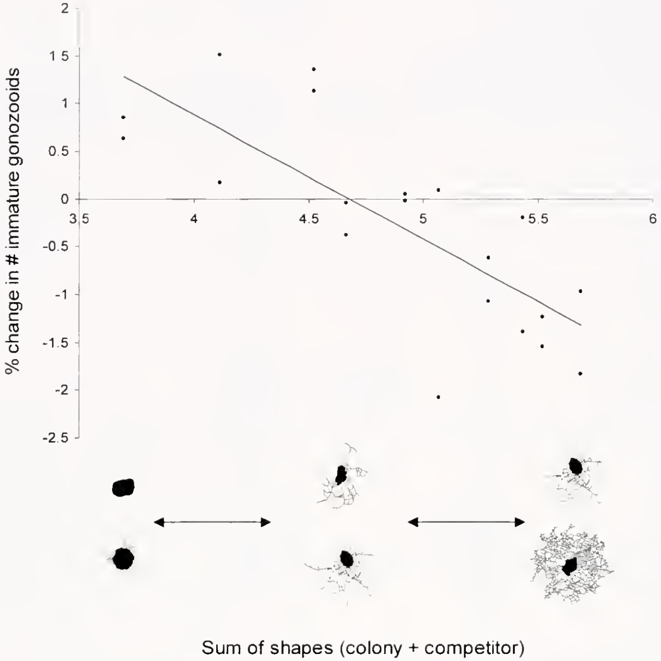

Figure 5. Simple linear regression analysis of immature gonozooid production *vs.* the sum of shape metrics of competing colonies established 12-mm apart. The mean percent change in the number of immature gonozooids per colony (relative to controls) in each competitive pair after 90 d is plotted with respect to the sum of the shape metrics of both colonies in a given competitive encounter. By summing the shape metrics of each competing pair, the interactions can be ranked according to the morphological attributes of the encounter. Mat-mat encounters have the lowest sums; stoloniferous-stoloniferous encounters have the greatest. Data represent the mean immature gonozooid production of each colony in each of 10 competitive pairs. Both axes have been ln-transformed. The negative relationship is highly significant ($P < 0.0001$) and explains 60.1% (R^2) of the variation in immature gonozooid production. See "Materials and Methods" section for explanation of shape metric.

dractinia full siblings do not fuse upon contact (Grosberg *et al.*, 1996), and non-fusing kin could conceivably exhibit reduced aggression accompanied by reduced fitness costs. On the other hand, the probability of finding close relatives of *H. [GM]* on separate shells is extremely low (as indicated by extremely low rates of fusion between such colonies in laboratory assays; D.L. Ferrell, unpubl. data), and this explanation requires that three of the five experimental colonies (I, II, and III) be closely related. Consequently, this first possibility is unlikely. A second explanation could be found in the gender of the competitors. It is conceivable that only male-female (M-F) interactions result in increased production of immature gonozooids. In this experiment, only colony I was female. Unfortunately, only two of the four clear instances of augmented immature gonozooid production involved M-F pairs, suggesting these data may be inconclusive with regard to this explanation. There are six other M-F interactions, however, and only one (I *vs.* II) of these shows any evidence of increased production. Because the majority of M-F interactions contradict this hypothesis, the second explanation also appears unlikely. In contrast, the growth form of the interacting colonies explains much of the variation in immature gonozooid production (Fig. 5).

Because the rate at which *H. [GM]* extends across a substratum increases with stolon proliferation, mat and mat-like phenotypes grow more slowly. Although dissimilar morphologies may not differ in the rate of tissue production (*y*-axis of Fig. 1), they differ considerably in the rate at which a colony expands from its initial site of establishment. The surface-area growth rate measurement used in this study reflected this rate of expansion. ANOVA comparing the mean surface-area growth rate of control colonies revealed significant differences between the five experimental colonies ($F_{4,20} = 17.9$, $P < 0.001$; Fig. 3). Bonferroni comparisons (adjusted $\alpha = 0.008$) further indicated that the surface-area growth rates of colonies IV and V are both greater than those of colonies I, II, and III, but not significantly different from one another. Thus, colonies IV and V extended outward (*via* stolons) more quickly than colonies I, II, and III. As a result, competitive encounters involving colonies IV and V most likely initiated contact with competing conspecifics sooner than others did.

The greater production of immature gonozooids observed in some encounters in the 12-mm treatment might be attributable to the timing of contact between competitors such that more recently contacting colonies showed less reduction in production. Indeed, greater immature gonozooid production was observed in more slowly extending mat and mat-like phenotypes (*i.e.*, colonies I, II, III). However, these competitive encounters yielded greater immature gonozooid production not only relative to other competing colony pairs, but also relative to control replicates, suggesting that the increases were not attributable solely to the timing of contact between conspecifics. Moreover, when the multiple regression model for immature gonozooid production (12-mm treatment) included the estimated time in contact as an independent variable, the result indicated negligible explanatory power for this added variable. The growth phenotypes of competitors (*i.e.*, sum of shape metrics) remained significantly correlated with immature gonozooid production even after the time in contact between competitors was accounted for (Table 4). Interestingly, time in contact was not statistically significant in this model (Table 4). After a second independent variable (time in contact) was added to the model, the R^2 increased only slightly, from 60.1% to 62.9% (Table 4), indicating that time in contact explained very little of the variation in immature gonozooid production.

Recent experiments have shown that the number of immature gonozooids is a strong, statistically significant indicator of the number of mature gonozooids borne by a colony upon sexual maturation (D. L. Ferrell, unpubl. data). These data, together with the findings reported here and the observations of Hauenschild (1954), support pre-existing ideas about reproductive allocation in clonal organisms. Because reproductive potential typically increases with growth, indeterminately growing clonal organisms should be expected to postpone sexual reproductive effort until growth becomes limiting (Abrahamson, 1975; Hughes and Cancino, 1985; Harvell and Grosberg, 1988). A variety of growth-limiting factors have been shown to accelerate the onset of sexual maturity or increase sexual reproductive investment in clonal plants (reviewed in Abrahamson, 1980) and animals (Braverman, 1974; Yamaguchi, 1975; Stebbing, 1980; Harvell and Grosberg, 1988). Abrahamson (1975) and Harvell and Grosberg (1988) identified intraspecific competition in particular as a growth-limiting factor that triggers increased reproductive allocation. In many cnidarian agonistic interactions, competitors may experience reductions in growth or reproductive investment, or even be overgrown entirely (reviewed in Grosberg, 1988). However, when the agonistic assault is unlikely to result in overgrowth, it appears that *H. [GM]* increases reproductive allocation in response to intraspecific competition.

Table 4

Summary of multiple regression analysis of the effects of growth form and duration of contact between competitors on immature gonozooid production in colonies established 12-mm apart (t = *90 d)*

	Coefficient	P-value
Constant	+5.183	0.001
Sum of shape metrics	−0.487	0.002
Time in contact	−0.594	0.203

Note: The sum of the shape metrics of both colonies in a competitive pair, an indicator of growth form of the interacting colonies (see Fig. 5), and the length of time that the competing colonies had been in contact were included as explanatory variables of the mean percent change in the number of immature gonozooids possessed by each colony. The overall R^2 for this regression model was 62.9%.

Adaptive allorecognition and costs of competition

An adaptive allorecognition system is molded evolutionarily by the fitness consequences of the behavioral alternatives it mediates. Extremely high costs associated with non-fusion increase the likelihood that intercolony fusion will optimize colony fitness in intraspecific competitive interactions. Despite potentially severe costs of fusion between genetically distinct but closely related colonies (Buss, 1982, 1987; Rinkevich and Loya, 1983; Barki *et al.*, 2002; Rinkevich, 2002), fusion may still increase fitness. On the other hand, if the costs of non-fusion and fusion are comparable, allorecognition systems may be nonadaptive or linked to other adaptive processes (Chadwick-Furman and Weissman, 2003). The current paper demonstrates that non-fusion entails significantly different fitness costs depending on the size and competitive ability of competitors. Thus, fusion behavior is likely to be adaptive in some ecological scenarios, but not others. As a consequence, complexities should be expected in the allorecognition system of *Hydractinia* if it functions adaptively in governing intergenotypic fusion.

The immediate costs of rejection were clearly greater in interactions between small colonies than between larger colonies. Small colonies experienced significantly greater fitness costs in terms of colony survival, growth rate, and immature gonozooid production. Competitively inferior colonies suffer higher rates of mortality (by definition) and are typically eliminated, whereas dominant colonies generally survive but suffer significant setbacks in growth and reproduction.

Because the size of the competitors affects the fitness consequences in conspecific interactions, it probably also affects the selective pressures that influence allorecognition (assuming its adaptive kin-discriminatory role) in *Hydractinia.* Interestingly, the allorecognition system of *Hydractinia* exhibits ontogenetic variation in full-sibling fusibility, or the tendency to fuse (Shenk and Buss, 1991; R.K. Grosberg, Univ. of California, Davis, pers. comm.). Shenk and Buss (1991) claim that fusibility declines with ontogeny and that some colonies disengage from fusion behavior with the onset of sexual maturity, suggesting that the costs of fusion are greater at this time. On the other hand, while noting some sort of ontogenetic effect, others have been unable to corroborate the decreased fusibility with colony ontogeny and the coupling of sexual maturity with the onset of rejection (Gild *et al.*, 2003; R.K. Grosberg, pers. comm.). Moreover, the costs of intergenotypic fusion may be greatest early in ontogeny (R.K. Grosberg, pers. comm.) and are probably not averted by delayed rejection (Gild *et al.*, 2003). That is, subsequent colony separation may provide little protection from somatic cell parasitism, the primary cost thought to accompany fusion, in which one genotype in a chimera contributes very little to somatic growth while contributing greatly to gamete production (Buss, 1982). Unfortunately, these conflicting reports make it difficult to incorporate the size-dependent variability in the costs of non-fusion reported in this study into a discussion of the possible adaptive significance of changes in fusibility with colony ontogeny.

My findings have a straightforward interpretation if the fitness costs of fusion truly increase with ontogeny and, hence, colony size. In this scenario, low costs of non-fusion would be accompanied by increased costs of fusion later in ontogeny. Thus, fusion would not be favorable in competitive interactions between large colonies, and decreased fusibility with ontogeny (Shenk and Buss, 1991) would be expected. Initially, it would seem that this expectation would be valid even if the costs of fusion actually were heavily skewed in favor of intense costs early in ontogeny. However, given intensified costs of early ontogenetic fusion, the costs of fusion late in ontogeny could be even lower than the low, but measurable, costs of non-fusion I have reported here. An opposite trend in fusibility then would be expected. Of course, ridding ourselves of such speculative deliberations depends on identifying and quantifying the fitness consequences of fusion in *Hydractinia* and understanding whether these consequences vary with colony ontogeny. Nevertheless, recognizing that the costs of non-fusion vary ontogenetically (Yund *et al.*, 1987, this study), the presence of ontogenetic variation in fusibility is consistent with an adaptive allorecognition system intended to distinguish kin from non-kin.

Several avenues for future research remain unexplored. Long-term monitoring of prolonged encounters is needed to verify the nature of their dynamics and eventual outcome (overgrowth or coexistence). In particular, estimates of lifetime reproductive output, although difficult to obtain, would be most helpful. This study reveals that, in some circumstances, reproductive allocation may be modified in the presence of conspecifics, even in species that exhibit agonistic behavior. Similar effects may have been previously overlooked in other cnidarians with analogous inducible defenses. Lastly, close examination and quantification of the costs of fusion is needed to better evaluate the adaptiveness of kin fusion in *Hydractinia.*

Acknowledgments

R. Mariscal provided guidance and the necessary equipment to design and execute these experiments. W. Herrnkind, L. Keller, D. Levitan, R. Mariscal, and three anonymous reviewers provided many helpful comments on earlier versions of this manuscript.

Literature Cited

Abrahamson, W. G. 1975. Reproductive strategies in dewberries. *Ecology* **56:** 721–756.

Abrahamson, W. G. 1980. Demography and vegetative reproduction. Pp. 89–106 in *Demography and Evolution in Plant Populations*, O. T. Solbrig, ed. University of California Press, Berkeley, CA.

Ballard, W. W. 1942. The mechanism for synchronous spawning in *Hydractinia* and *Pennaria. Biol. Bull.* **82:** 329–339.

Barki, Y., D. Gateño, D. Graur, and B. Rinkevich. 2002. Soft-coral natural chimerism: a window in ontogeny allows the creation of entities comprised of incongruous parts. *Mar. Ecol. Prog. Ser.* **231:** 91–99.

Blackstone, N. W., and L. W. Buss. 1991. Shape variation in hydractiniid hydroids. *Biol. Bull.* **180:** 394–405.

Blackstone, N. W., and P. O. Yund. 1989. Morphological variation in a colonial marine hydroid: a comparison of size-based and age-based heterochrony. *Paleobiology* **15:** 1–10.

Braverman, M. 1974. The cellular bases of morphogenesis and morphostasis in hydroids. *Oceanogr. Mar. Biol.* **12:** 129–221.

Bunting, M. 1894. The origin of sex cells in *Hydractinia* and *Podocoryne* and the development of *Hydractinia. J. Morphol.* **9:** 203–246.

Buss, L. W. 1982. Somatic cell parasitism and the evolution of somatic tissue compatibility. *Proc. Natl. Acad. Sci. USA* **79:** 5337–5341.

Buss, L. W. 1986. Competition and community organization on hard surfaces in the sea. Pp. 517–536 in *Community Ecology*, T. Case and J. Diamond, eds. Harper and Row, New York.

Buss, L. W. 1987. *The Evolution of Individuality.* Princeton University Press, Princeton, NJ.

Buss, L. W. 1990. Competition within and between encrusting invertebrates. *Trends Ecol. Evol.* **5:** 352–356.

Buss, L. W., and R. K. Grosberg. 1990. Morphogenetic basis for phenotypic differences in hydroid competitive behavior. *Nature* **343:** 63–66.

Buss, L. W., and J. B. C. Jackson. 1979. Competitive networks: nontransitive competitive relationships in cryptic coral reef environments. *Am. Nat.* **113:** 223–234.

Buss, L. W., and P. O. Yund. 1988. A comparison of recent and historical populations of the colonial hydroid *Hydractinia. Ecology* **69(3):** 646–654.

Buss, L. W., and P. O. Yund. 1989. A sibling species of *Hydractinia* in the northeastern United States. *J. Mar. Biol. Assoc. UK* **69:** 857–874.

Buss, L. W., C. S. McFadden, and D. R. Keene. 1984. Biology of Hydractiniid hydroids. 2. Histocompatibility effector system/competitive mechanism mediated by nematocyst discharge. *Biol. Bull.* **167:** 139–158.

Chadwick-Furman, N. E., and I. L. Weissman. 2003. Effects of allogeneic contact on life-history traits of the colonial ascidian *Botryllus schlosseri* in Monterey Bay. *Biol. Bull.* **205:** 133–143.

Cunningham, C. W., L. W. Buss, and C. Anderson. 1991. Molecular and geologic evidence of shared history between hermit crabs and the symbiotic genus *Hydractinia. Evolution* **45(6):** 1301–1316.

Feldgarden, M., and P. O. Yund. 1992. Allorecognition in colonial marine invertebrates: does selection favor fusion with kin or fusion with self? *Biol. Bull.* **182:** 155–158.

Ferrell, D. L. 2004. Gastropod shell size and morphology influence conspecific interactions in an encrusting hydroid. *Mar. Ecol. Prog. Ser.* (In press).

Francis, L. 1973. Clone specific segregation in the sea anemone *Anthopleura elegantissima. Biol. Bull.* **144:** 64–72.

Frank, U., T. Leitz, and W. A. Müller. 2001. The hydroid *Hydractinia:* a versatile, informative cnidarian representative. *Bioessays* **23:** 963–971.

Gild, S., U. Frank, and O. Mokady. 2003. Allogeneic interactions in *Hydractinia*\#: is the transitory chimera beneficial? *Int. J. Dev. Biol.* **47:** 433–438.

Grosberg, R. K. 1988. The evolution of allorecognition specificity in clonal invertebrates. *Q. Rev. Biol.* **63:** 377–412.

Grosberg, R. K. 1992. To thine own self be true? An addendum to Feldgarden and Yund's report on fusion and the evolution of allorecognition in colonial marine invertebrates. *Biol. Bull.* **182:** 454–457.

Grosberg, R. K., and J. F. Quinn. 1986. The genetic control and consequences of kin recognition by the larvae of a colonial ascidian. *Nature* **322:** 456–459.

Grosberg, R. K., D. R. Levitan, and B. B. Cameron. 1996. Evolutionary genetics of allorecognition specificity in the colonial hydroid *Hydractinia symbiolongicarpus. Evolution* **50:** 2221–2240.

Hart, M. W., and R. K. Grosberg. 1999. Kin interactions in a colonial hydrozoan (*Hydractinia symbiolongicarpus*): population structure on a mobile landscape. *Evolution* **53:** 793–805.

Harvell, C. D., and R. K. Grosberg. 1988. The timing of sexual maturity in clonal animals. *Ecology* **69(6):** 1855–1864.

Hauenschild, C. von. 1954. Genetische und Entwicklungphysiologische Untersuchungen über Intersexualität und Gewebeheverträlichkeit bei *Hydractinia echinata* Flem. *Wilhelm Roux's Arch. Entwicklungsmech. Org.* **147:** 1–41.

Hauenschild, C. von. 1956. Über die Vererbung einer Gewebebeverträlichkeits bei dem Hydroidpolypen *Hydractinia echinata. Z. Naturforsch.* **11б:** 132–138.

Hughes, T. P., and J. M. Cancino. 1985. An ecological overview of cloning in Metazoa. Pp. 153–186 in *Population Biology and Evolution of Clonal Organisms*, J. B. C. Jackson, L. W. Buss, and R. E. Cook, eds. Yale University Press, New Haven.

Ivker, F. B. 1972. A hierarchy of histo-compatibility in *Hydractinia echinata. Biol. Bull.* **143:** 162–174.

Jackson, J. B. C. 1977. Competition on marine hard substrata: the adaptive significance of solitary and colonial strategies. *Am. Nat.* **111:** 743–767.

Jackson, J. B. C. 1985. Distribution and ecology of clonal and aclonal benthic invertebrates. Pp. 297–355 in *Population Biology and Evolution of Clonal Organisms*, J. B. C. Jackson, L. W. Buss, and R. E. Cook, eds. Yale University Press, New Haven.

Karlson, R. H. 1978. Predation and space utilization patterns in a marine epifaunal community. *J. Exp. Mar. Biol. Ecol.* **31:** 225–239.

Karlson, R. H. 1980. Alternative competitive strategies in a periodically disturbed habitat. *Bull. Mar. Sci.* **30:** 894–900.

Levitan, D. L., and R. K. Grosberg. 1993. The analysis of paternity and maternity in the marine hydrozoan *Hydractinia symbiolongicarpus* using randomly amplified polymorphic DNA (RAPD) markers. *Mol. Ecol.* **2:** 315–326.

McFadden, C. S. 1986. Laboratory evidence for a size refuge in competitive interactions between the hydroids *Hydractinia echinata* (Flemming) and *Podocoryne carnea* (Sars). *Biol. Bull.* **171:** 161–174.

McFadden, C. S., M. J. McFarland, and L. W. Buss. 1984. Biology of hydractiniid hydroids. 1. Colony ontogeny in *Hydractinia echinata. Biol. Bull.* **166:** 54–67.

Mokady, O., and L. W. Buss. 1996. Transmission genetics of allorecognition in *Hydractinia symbiolongicarpus* (Cnidaria: Hydrozoa). *Genetics* **143:** 823–827.

Müller, W. 1964. Experimentelle Untersuchungen über Stockentwicklung, Polypdifferenzierung und Sexualchimären bei *Hydractinia echinata. Wilhelm Roux's Arch. Entwicklungsmech.* **155:** 181–268.

Purcell, J. E. 1977. Aggressive function and induced development of catch tentacles in the sea anemone *Metridium senile* (Coelenterata, Actiniaria). *Biol. Bull.* 153: 355–368.

Rinkevich, B. 2002. Germ cell parasitism as an ecological and evolutionary puzzle: hitchhiking with positively selected genotypes. *Oikos* **96:** 25–30.

Rinkevich, B., and Y. Loya. 1983. Oriented translocation of energy in grafted corals. *Coral Reefs* **1:** 243–247.

Rinkevich, B., and Y. Loya. 1985. Intraspecific competition in a reef coral: effects on growth and reproduction. *Oecologia* **66:** 100–105.

Sebens, K. P. 1986. Spatial relationships among encrusting marine organisms in the New England subtidal zone. *Ecol. Monogr.* **56:** 73–96.

Shenk, M. A., and L. W. Buss. 1991. Ontogenetic changes in fusibility in the colonial hydroid *Hydractinia symbiolongicarpus. J. Exp. Zool.* **257:** 80–86.

Sokal, R. R., and F. J. Rohlf. 1995. *Biometry*, 3rd ed. W. H. Freeman, New York.

Stebbing, A. R. D. 1980. Increase in gonozooid frequency as an adaptive response to stress in *Campanularia flexuosa.* Pp. 27–32 in *Developmental and Cellular Biology of Coelenterates*, P. Tardent and R. Tardent, eds. Elsevier, New York.

Yamaguchi, M. 1975. Growth and reproductive cycles of the marine fouling ascidians *Ciona intestinalis, Styela plicata, Botrylloides violaceous*, and *Leptoclinum mitsukurii* at Aburatsubo-Moroiso Inlet (central Japan). *Mar. Biol.* **29:** 253–259.

Yund, P. O., and M. Feldgarden. 1992. To thine own self be true? Yes! Thou canst not then be false to any other. A reply to Grosberg. *Biol. Bull.* **182:** 458–459.

Yund, P. O., and H. M. Parker. 1989. Population structure of the colonial hydroid *Hydractinia* sp. nov. C in the Gulf of Maine. *J. Exp. Mar. Biol. Ecol.* **125:** 63–82.

Yund, P. O., C. W. Cunningham, and L. W. Buss. 1987. Recruitment and postrecruitment interactions in a colonial hydroid. *Ecology* **68:** 971–982.

Reference: *Biol. Bull.* **206:** 188–196. (June 2004)
© 2004 Marine Biological Laboratory

Effects of Hypercapnic Hypoxia on the Clearance of *Vibrio campbellii* in the Atlantic Blue Crab, *Callinectes sapidus* Rathbun

JEREMY D. HOLMAN, KAREN G. BURNETT, AND LOUIS E. BURNETT*

Grice Marine Laboratory, College of Charleston, 205 Fort Johnson, Charleston, South Carolina 29412

Abstract. *Callinectes sapidus,* the Atlantic blue crab, encounters hypoxia, hypercapnia (elevated CO_2), and bacterial pathogens in its natural environment. We tested the hypothesis that acute exposure to hypercapnic hypoxia (HH) alters the crab's ability to clear a pathogenic bacterium, *Vibrio campbellii* 90-69B3, from the hemolymph. Adult male crabs were held in normoxia (well-aerated seawater) or HH (seawater with $P\text{O}_2 = 4$ kPa; $P\text{CO}_2 = 1.8$ kPa; and pH = 6.7–7.1) and were injected with 2.5×10^4 *Vibrio* g^{-1} body weight. The animals were held in normoxia or in HH for 45, 75, or 210–240 min before being injected with *Vibrio*, and were maintained in their respective treatment conditions for the 120-min duration of the experiment. *Vibrio* colony-forming units (CFU) ml^{-1} hemolymph were quantified before injection, and at 10, 20, and 40 min afterward. Total hemocytes (THC) ml^{-1} of hemolymph were counted 24 h before (−24 h), and at 10 and 120 min after injection. Sham injections of saline produced no change in the bacterial or hemocyte counts in any treatment group. Among the groups that received bacterial injections, *Vibrio* was almost completely cleared within 1 h, but at 10-min postinjection, *Vibrio* CFU ml^{-1} hemolymph was significantly higher in animals held in HH for 75 and 210–240 min than in those held in normoxia. Within 10 min after crabs were injected with bacteria, THC ml^{-1} significantly decreased in control and HH45 treatments, but not in the HH75 and HH210–240 treatments. By 120 min after injection of bacteria, hemocyte counts decreased in all but the HH45 group. These data demonstrate that HH significantly impairs the ability of blue crabs to clear *Vibrio* from the hemolymph. These results also suggest that HH alters the normal role of circulating hemocytes in the removal of an invading pathogen.

Introduction

Where they occur naturally in coastal waters, hypoxia (low oxygen) and hypercapnia (high carbon dioxide) are believed to contribute to outbreaks of infectious disease, such as mycobacteriosis in fish (Rhodes *et al.*, 2001) and infections with a protozoan parasite in oysters (Anderson *et al.*, 1998). The effects of hypoxia and hypercapnic hypoxia (HH) on disease susceptibility are likely to be multiple and complex, changing not only respiration and circulation, but also immune defense (Burnett, 1997). In laboratory-based studies, we and others have shown that hypoxia and HH can increase the rate of mortality in penaeid or palaemonid shrimp injected with live bacterial pathogens (Le Moullac *et al.*, 1998; Mikulski *et al.*, 2000). Here we asked whether levels of dissolved O_2 and CO_2 that increase mortality rates in shrimp also reduce the rate at which live bacteria are removed from the hemolymph of another crustacean species, *Callinectes sapidus* Rathbun, 1896, the Atlantic blue crab.

Crustaceans employ a broad spectrum of soluble (humoral) factors in immune defense, including non-self recognition proteins, immediate defense molecules such as clotting proteins and prophenoloxidase, and antimicrobial peptides (reviewed by Bachère 1998, 2000). Many of these humoral factors are produced, stored, and released from hemocytes—the major cellular components of the crustacean immune system. In addition, hemocytes can adhere to a pathogen, triggering phagocytosis and production of highly toxic reactive oxygen species (Song and Hsieh, 1994; Gargioni and Barracco, 1998; Muñoz *et al.*, 2000).

Received 2 December 2003; accepted 8 April 2004.

* To whom correspondence should be addressed. E-mail: burnettl@cofc.edu

Abbreviations: CFU, colony-forming unit; HH, hypercapnic hypoxia; PPO, prophenoloxidase; THC, total hemocyte count.

In well-aerated normoxic water, crustaceans rapidly remove bacteria or other large particles from the hemolymph, with a coordinate drop in the total hemocyte count per milliliter of hemolymph (THC ml^{-1}) (White and Ratcliffe, 1982; Martin *et al.*, 1993). Smith and Ratcliffe (1980) and Martin *et al.* (1993, 1998) have suggested that hemocytes aggregate with injected particles to form nodules that become trapped in small capillary beds of well-vascularized tissues such as the gill and the hepatopancreas. This aggregation is believed to involve non-self recognition proteins, prophenoloxidase (PPO), and antimicrobial peptides. In contrast, van de Braak *et al.* (2002) presented evidence that hemocytes become fixed in peripheral organs before taking up bacteria by phagocytosis.

After shrimp received an injection of pathogenic bacteria, those held in hypoxia (Le Moullac *et al.*, 1998) or HH (Mikulski *et al.*, 2000) had higher rates of mortality than animals held under normoxic conditions. Several mechanisms underlie the effects of dissolved gasses on the susceptibility of organisms to a pathogen. Hypoxia and hypercapnia can suppress several key components of the invertebrate immune system that are responsible for killing and clearing bacterial pathogens from tissues. In penaeid shrimp, both hypoxia (Le Moullac *et al.*, 1998) and HH (Mikulski *et al.*, 2000) induced significant decreases in THC ml^{-1} hemolymph while also decreasing resistance to bacterial pathogens. Low O_2 and low pH (induced by high CO_2) independently and additively suppressed *in vitro* production of reactive oxygen species by oyster hemocytes (Boyd and Burnett, 1999), and hypoxia suppressed phagocytosis in the blue shrimp *Litopenaeus stylirostris* (Le Moullac *et al.*, 1998). However, the complexity of the immune responses in the whole organism makes it difficult to attribute changes in disease outcome to any specific defense mechanism.

As an alternative approach to understanding the effects of dissolved O_2 and CO_2 on susceptibility to microbial pathogens in crustaceans, we tested whether hypoxia and hypercapnia can suppress the ability of the blue crab to eliminate live bacteria from its hemolymph. We chose blue crabs because they are hearty organisms that are abundant in estuaries where levels of oxygen and carbon dioxide fluctuate, and they can easily tolerate experimental manipulations such as a bacterial injection and multiple samplings of hemolymph. Animals with prior exposure to HH for 0, 45, 75, or 210–240 min were injected with live *Vibrio campbellii* or saline and were maintained in HH. For control groups, crabs were held in normoxia before and after injection with the same dose of live bacteria or saline. One day before injection (−24 h) and at 10, 20, and 40 min after injection, we monitored the number of colony-forming units (CFU) of bacteria ml^{-1} hemolymph. We also monitored THC ml^{-1} of all experimental animals at −24 h, 10 min, and 120 min postinjection and compared the responses of their circulating hemocytes to bacterial challenge.

Materials and Methods

Male blue crabs were trapped in the creeks of Charleston Harbor, Charleston, South Carolina and transported to the Grice Marine Laboratory where they were held in recirculating seawater at 25 ppt salinity and 24–26 °C. The crabs weighed between 92 and 236 g and were held for a minimum of 3 days prior to experimentation, but no longer than 10 days. The animals were fed frozen fish or shrimp each day, but food was withheld for at least 24 h before the experiments began.

Preparation of the crabs for treatment

A 1-mm hole was drilled in the carapace directly over the heart, creating a port through which saline alone, or saline containing bacteria, was injected directly into the ventricle. The bacteria injected into the heart would then be rapidly distributed throughout the circulatory system. Two similar holes were drilled over the pericardium adjacent to the heart through which hemolymph was withdrawn from the pericardium. Two holes were drilled in case we could not easily withdraw hemolymph from one hole. A thin layer of latex rubber was glued over each hole with cyanoacrylate glue. A needle could be inserted into each hole through the rubber diaphragm and withdrawn easily without causing bleeding. These procedures were performed 2 days prior to experimentation.

Intracardiac (postbranchial) injection of bacteria

The postbranchial point of injection used in the present study is distinct from that used by others who injected pathogens into muscle tissues (Alday-Sanz *et al.*, 2002) or sinuses downstream from the heart (Smith and Ratcliffe, 1980; Martin *et al.*, 1993, van de Braak *et al.*, 2002). Injecting bacteria directly into the single-chambered heart ensures that the bacteria will be rapidly and evenly distributed throughout the circulatory system. The heart of the blue crab distributes hemolymph through seven major arteries (McGaw and Reiber, 2002), and the high cardiac output typical of crabs (McMahon and Burnett, 1990) ensures a uniform distribution throughout the crab's circulatory system, as shown by studies using thermal dilution techniques (Burnett *et al.*, 1981).

The effects of acute exposure to HH on the cardiac output of *C. sapidus* are unknown, but acute hypoxia causes a reduction in heart rate of about 25% (deFur and Mangum, 1979). Cardiac output in crustaceans is often strongly influenced by changes in cardiac stroke volume rather than heart rate, but even with a 25% reduction in cardiac output, mixing and circulation of bacteria injected into the ventricle would still be rapid. Injection of bacteria into the heart avoids the localization of pathogens that can occur for reasons not specifically associated with normal routes of clearance by the whole organism. For example, injecting pathogens into the infrabranchial sinus, which supplies hemolymph to one or more gills, may bias the observed role of the gill in pathogen clearance. In the present study, sampling hemolymph from the pericardial sinus, which is immediately downstream from the gill, ensured that the bacteria sampled had made a complete circuit through the circulatory system.

Preparation of the pathogen

The bacterial pathogen used in these studies was *Vibrio campbellii* 90–69B3, which was originally isolated from diseased shrimp by D. Lightner and L. Mahone (University of Arizona). The 16S rRNA sequence of this strain places it in the *V. parahaemolyticus/V. harveyi* family with 99% identity to *V. campbellii* (unpubl. data, Eric Stabb, University of Georgia). For each assay, *V. campbellii* 90–69B3 (hereafter referred to as *V. campbellii*) was thawed from frozen aliquots, streaked onto tryptic soy agar (TSA) + 2.5% NaCl, and incubated overnight at 25 °C. A separate aliquot was used for each assay. A wooden applicator stick was used to transfer the bacteria from the culture plate to sterile 2.5% NaCl buffered with 10 mmol l^{-1} HEPES adjusted to pH 7.6 (HEPES saline). The concentration of *V. campbellii* was adjusted to an optical density of 0.1 at 540 nm (OD_{540nm}). This OD_{540nm} had previously been determined to equal 1.0×10^8 CFU ml^{-1} (Mikulski *et al.*, 2000). The bacterial suspension was then diluted with HEPES saline to obtain the desired dose for injection.

Assessment of baseline conditions

One day (*i.e.*, −24 h) before each bacterial challenge experiment, two 100-μl samples of hemolymph were withdrawn through the pericardial sampling port. One sample was used to determine whether the crab had detectable levels of live, culturable bacteria in the hemolymph, as measured in the CFU assay. The other sample was used to determine the THC ml^{-1} in the hemolymph. To measure CFU ml^{-1}, one part of hemolymph was diluted with 9 parts HEPES saline. A 150-μl sample of this mixture was suspended in marine agar and plated over TSA and TCBS (thiosulfate citrate bile sucrose) agar plates. TSA supports the growth of a wide range of bacteria; TCBS agar is more selective, and supports the growth of a few species of *Escherichia* and *Vibrio*, including *V. campbellii*. Plates were incubated at 25 °C for 24 h, at which time the number of bacterial colonies was counted and recorded. For each hemolymph sample, bacterial colonies on three replicate plates were counted and averaged. CFU ml^{-1} was calculated according to the formula CFU $plate^{-1} \times 10$ dilution factor/0.15 ml, where CFU is the average number of bacterial colonies counted on three replicate TCBS plates for each 0.15-ml hemolymph sample diluted 10-fold in saline prior to plating. Only crabs whose hemolymph had no CFU on TSA or TCBS plates at the −24 h time point were used in these experiments. The frequency with which CFU are detected in the hemolymph of crabs collected from the field varies considerably with the season. During early to mid-summer, when these experiments were performed, about 10% to 15% were positive for CFU in the hemolymph at −24 h and were rejected for experimental use. The same assay was used to determine CFU ml^{-1} in hemolymph samples taken from crabs after injection of *V. campbellii* or saline, except that the marine agar containing the diluted hemolymph sample was plated only on TCBS plates. This provided a measure of assurance that the bacterial colonies being counted in the hemolymph arose from the injected bacteria.

The THC ml^{-1} in a hemolymph sample was determined as follows. Hemolymph (100 μl) was drawn into a syringe containing 900 μl of ice-cold 10% neutral buffered formalin (Mix and Sparks, 1980). After mixing, an aliquot of the hemocyte suspension was transferred to a hemocytometer for direct counting. Hemocytes were counted in three separate aliquots of each hemolymph sample and averaged for each crab at each time point in these experiments.

Experimental protocol

In a typical experiment (Fig. 1), a crab was transferred to a 17-l glass aquarium in which oxygen and carbon dioxide levels were regulated (Mikulski *et al.*, 2000). For all experiments, the seawater was at first aerated vigorously; and for treatments in normoxia, crabs were held in this well-aerated water (20.7 kPa Po_2 and <0.06 kPa Pco_2) throughout the experiment. At the start of all HH treatments, the oxygen and the carbon dioxide pressures of the water were regulated (Mikulski *et al.*, 2000) to achieve values of 4 kPa Po_2 and 1.8 kPa Pco_2 within 20 to 30 min. The crabs were held in HH for one of three durations prior to injection of bacteria (45, 75, and between 210 and 240 min), and they remained in these HH conditions throughout the experiment (Fig. 1). The crabs were injected with *V. campbellii* suspended in HEPES saline. The bacterial suspension (between 40 μl and 140 μl, depending on the size of the crab) was injected directly into the ventricle. Control animals from the normoxia treatment were injected with the same dose of bacteria.

Crabs were injected with 2.5×10^4 bacteria g^{-1} body weight, to achieve a circulating dose of 1.0×10^5 *V. campbellii* ml^{-1} of hemolymph, assuming a hemolymph volume of 25 ml 100 g^{-1} body weight (Gleeson and Zubkoff, 1977). The dose is slightly below the LD_{50} for

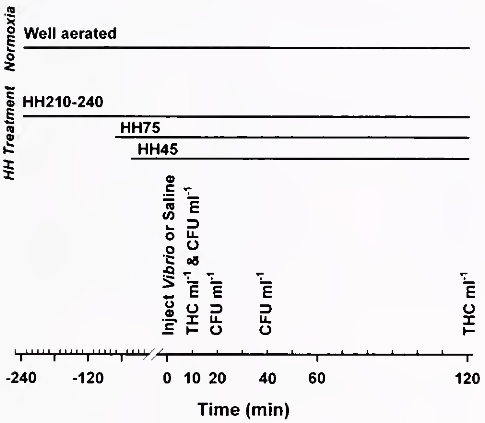

Figure 1. An illustration of the experimental design, indicating the timing of exposure to hypercapnic hypoxia (HH), bacterial injection, and hemolymph withdrawal along with subsequent analyses. Crabs were placed in experimental tanks and HH treatments were initiated at different times prior to the injection of bacteria, which is indicated at time = 0. For example, in the HH210–240 treatment, HH was initiated between 210 and 240 minutes before injection and maintained until 120 min after injection. The normoxia group was held in well-aerated water before and after the injection of bacteria. For the sham injection treatment, crabs were held in one of the HH treatments or in normoxia, then were injected with HEPES-saline at time = 0, and maintained in the same treatment condition for 120 min after injection. Hemolymph samples were taken from animals in all treatment groups at the same time points and for the same assays as illustrated.

juveniles of the penaeid shrimp *Litopenaeus vannamei* (Mikulski *et al.*, 2000).

After the bacteria were injected, animals in HH treatments were maintained in HH and those in normoxic treatments were held in normoxia. Hemolymph was sampled from the pericardium of each crab at 10, 20, 40, and 120 min. Preliminary experiments indicated that these time points would be optimal for discerning the impacts of HH on hemocyte counts and bacterial clearance. At the 10-min time point, two hemolymph samples were withdrawn from the pericardium. One unfixed sample was used to quantify the *Vibrio* CFU ml^{-1} remaining in the hemolymph, as described above. The other sample was fixed in formalin and used to quantify THC ml^{-1} hemolymph, as described above. At the 20-min and 40-min time points, hemolymph was sampled, and the number of CFU ml^{-1} was determined again. Finally, a sample of hemolymph taken at 120 min was fixed in formalin to monitor THC ml^{-1}. The crab was then removed from the aquarium, frozen, and ultimately autoclaved and discarded.

To control for the effects of injection and hemolymph sampling, sham experiments were performed for each treatment (normoxia, HH45, HH75, and HH210–240) by injecting a sterile solution of HEPES saline into the ventricle as described above. Hemolymph was sampled at the time points indicated above (Fig. 1), and *V. campbellii* and hemocytes were quantified. During all injections and samplings, the animals remained submerged in the aquarium, either in normoxic or HH water, with minimal disturbance. The crab was near the top of the 17-l aquarium on a plastic platform, where it was completely immersed and free to move. To inject bacteria or sample hemolymph, the crab remained immersed but was lifted so that the injection or sampling ports on its carapace were raised to the surface of the water.

Aseptic techniques were used when working with the bacteria, and all waste material was autoclaved or disinfected with 2% chlorine bleach. Experimental tanks were rinsed with 2% bleach daily, and the filtration systems were rinsed with fresh water daily.

Data analysis

SigmaStat 3.0 software was used to perform all statistical analyses. To determine whether the amount of bacteria in the hemolymph changed as a function of time after injection, a one-way ANOVA was performed on the *V. campbellii* CFU ml^{-1} hemolymph at 10, 20, and 40 min within each treatment group. All tests for normality (Kolmogorov-Smirnov test) failed; therefore, a Kruskal-Wallis ANOVA on ranks test was used. When differences within a treatment group were detected, the Student-Newman-Keuls method was used for multiple comparisons between individual time points.

To determine whether there were differences at individual times among treatment groups, a one-way ANOVA was performed on CFU ml^{-1} data at 10, 20, and 40 min across all treatment groups (normoxia, HH45, HH75, and HH210–240). As above, all tests for normality (Kolmogorov-Smirnov test) failed, so a Kruskal-Wallis ANOVA on ranks test was used. When the test indicated a significant effect of treatment within a time, a Dunn's test was used, because of unequal sample sizes, to compare HH treatments with the normoxic value.

To determine whether there were differences in THC ml^{-1} at one day prior to the initiation of the experiments, a one-way ANOVA was performed for the crabs across all normoxic and HH treatments. For subsequent analysis, THC ml^{-1} data at 10 and 120 min were normalized to the −24 h counts for an individual crab. A one-way ANOVA was performed on normalized THC ml^{-1} for each normoxic and HH treatment group as a function of time after sham and bacterial injections. All tests for normality (Kolmogorov-Smirnov test) or equal variances failed and, therefore, a Kruskal-Wallis ANOVA on ranks test was used. When a significant effect of time within a treatment group was indicated, a comparison of 10-min and 120-min counts with

−24 h counts was performed using Dunnett's test (equal sample sizes).

Results

Clearance of bacteria from the hemolymph

The theoretical maximum *Vibrio* CFU ml^{-1} hemolymph after injection is $1 \times 10^5\ \text{ml}^{-1}$. This value is based on the known number of bacteria injected and assumes a homogeneous distribution of bacteria in the hemolymph as well as a hemolymph volume of 25 ml per 100-g crab (Gleeson and Zubkoff, 1977). Patterns of bacterial clearance were similar in all treatment groups: when the crabs were injected with bacteria, *V. campbellii* CFU ml^{-1} hemolymph declined precipitously to very low levels within 10 min after injection and became almost undetectable after 40 min (Table 1, Fig. 2). Even though most of the bacterial clearance occurred before the 10-min measurement, the decrease between the CFU ml^{-1} at 10 min and the value at 40 min was significant in all treatment groups. Comparisons between 10 and 20 min and between 20 and 40 min revealed significant differences in some, but not all, cases (Table 1, Fig. 2).

Comparisons of different treatments at single time points after injection of *V. campbellii* revealed significant differences in CFU ml^{-1} at 10 min between the normoxic treatment and the HH75 treatment and between the normoxic treatment and the HH210–240 treatment (Kruskal-Wallis ANOVA on ranks and Dunn's multiple comparison procedure, $P = 0.002$); but there were no differences between the normoxic and the HH45 treatments (Fig. 2). With treatment as a variable, differences were detected 20-min postinjection (Kruskal-Wallis ANOVA on ranks, $P = 0.027$), but no differences among the individual treatments were found using Dunn's multiple comparison procedure. No differences were detected among treatments at 40-min postinjection when treatment was used as a variable (Kruskal-Wallis ANOVA on ranks, $P = 0.131$). No bacterial colonies were detected at any time in the hemolymph samples from animals that received sham injections of saline (data not shown).

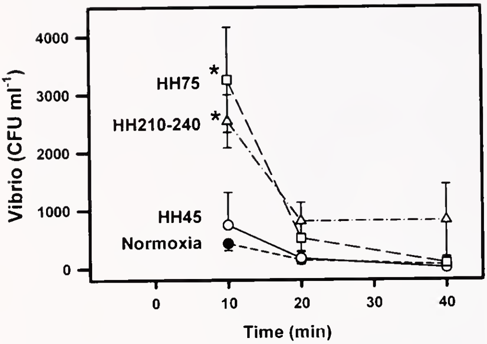

Figure 2. Colony-forming units (CFU) ml^{-1} of *Vibrio campbellii* circulating in the hemolymph at different times after injection plotted as a function of treatment in well-aerated normoxic water or in hypercapnic hypoxia water ($P\text{CO}_2$ = 1.8 kPa, $P\text{O}_2$ = 4 kPa). Crabs were exposed to normoxia or to hypercapnic hypoxia (HH) for different times (given in minutes), then injected with bacteria at time = 0, and for the subsequent duration of the experiments were held in well-aerated (normoxia) or HH water. At time = 0, crabs were injected with 2.5×10^4 *V. campbellii* g^{-1} body weight to achieve a theoretical circulating concentration of 100×10^3 CFU (colony-forming units) ml^{-1} hemolymph. Levels of bacteria in hemolymph (CFU ml^{-1}) are shown at 10, 20, and 40 min after injection. Mean values ± standard error are shown. Significant differences between the normoxic treatment and the HH treatment occurred only at 10 min after injection and are indicated by an asterisk (*).

Table 1

Statistical analysis of the colony-forming units (CFU) ml^{-1} of Vibrio campbellii *in the hemolymph of crabs at different times following injection*

			P value: Pairwise comparisons using Student-Newman-Keuls method		
Treatment	*n*	*P* value: Kruskal-Wallis ANOVA	10 and 20 min	10 and 40 min	20 and 40 min
Normoxia	8	0.005	NS	<0.05	NS
HH45	4	0.005	NS	<0.05	<0.05
HH75	7	<0.001	<0.05	<0.05	<0.05
HH210–240	9	0.008	<0.05	<0.05	NS

Tests for normality failed on one-way ANOVA; therefore, data within a treatment group were tested for differences using a Kruskal-Wallis ANOVA on ranks. Values at different time intervals within a treatment were compared pairwise using the Student-Newman-Keuls method. HH, hypercapnic hypoxia; NS, nonsignificant.

Hemocyte counts

The THC ml^{-1} in hemolymph of crabs prior to treatment (−24 h) was the same across all treatment groups (ANOVA, $P = 0.557$; Figs. 3 and 4). No treatment group that received a sham injection ($n = 17$) showed a significant difference in circulating hemocyte counts at any time (Kruskal-Wallis ANOVA on ranks, $P > 0.155$, Fig. 3). THC ml^{-1} of animals held in normoxia (well-aerated conditions) declined significantly 10 and 120 min after injection with *V. campbellii* (Table 2; Fig. 4). Circulating hemocyte counts declined in the HH 45 (hypercapnic hypoxia 45-min) treatment group 10 min after injection of *V. campbellii*, but at 120 min, the count was not detectably different from the baseline count at −24 h (Table 2, Fig. 4). When crabs were held in HH for 75 min and then injected with *V. campbellii*, there was no change in THC ml^{-1} after 10 min, but the hemocyte concentration declined significantly after 120

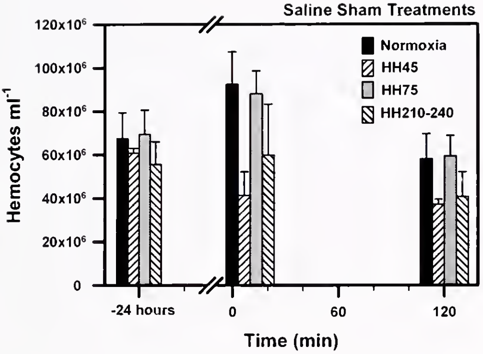

Figure 3. Total hemocyte counts (THC) ml^{-1} of hemolymph in crabs one day prior to treatment (−24 h) and 10 and 120 min after injection of saline in four treatment groups. Normoxia = crabs in well-aerated water, HH treatments = hypercapnic hypoxia ($P\mathrm{O}_2$ = 4 kPa, $P\mathrm{CO}_2$ = 1.8 kPa) administered for 45, 75, and 210–240 min before the saline injection at time = 0. No significant differences were detected within any treatment between pre-injection (−24 h) THC ml^{-1} and postinjection values at 10 and 120 min. Mean values + standard error are shown.

min. The same pattern of response occurred when crabs were incubated in HH for 210–240 min and then injected with *V. campbellii* (Table 2; Fig. 4).

Discussion

Minutes after being injected with *Vibrio campbellii*, blue crabs rapidly remove the bacteria from their hemolymph. For animals held in well-aerated water, this rapid clearance of bacteria is associated with a significant decline in the concentration of circulating hemocytes. The present study demonstrates that bacterial clearance from the hemolymph of blue crabs is reduced when the animals are held in water that is hypercapnic and hypoxic. Moreover, this reduced ability to clear bacteria is associated with a slower decline in circulating hemocytes after injection of bacteria. Taken together, these findings suggest that the low-oxygen and acidic internal milieu of a blue crab exposed to hypercapnic hypoxia may impair the mechanisms responsible for clearing pathogens from its hemolymph.

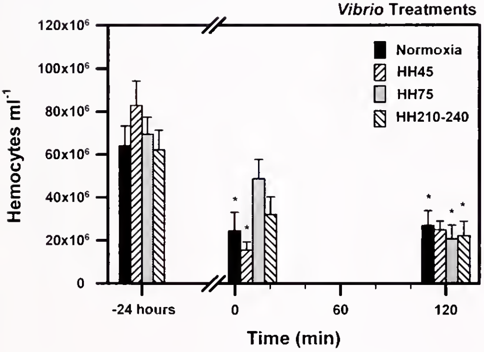

Figure 4. Total hemocyte counts (THC) ml^{-1} of hemolymph in crabs before treatment (−24 h) and 10 and 120 min after injection of *Vibrio campbellii* in four treatment groups. Normoxia = crabs in well-aerated water, HH treatments = hypercapnic hypoxia ($P\mathrm{O}_2$ = 4 kPa, $P\mathrm{CO}_2$ = 1.8 kPa) administered for 45, 75, and 210–240 min before the injection of bacteria. Significant differences within a treatment between pre-injection (−24 h) THC ml^{-1} and postinjected values at 10 and 120 min are indicated by an asterisk (*). Mean values + standard error are shown.

Table 2

Statistical analysis of total hemocyte counts ml^{-1} *(THC* ml^{-1}*) following injection of* Vibrio campbellii

Treatment	*n*	*P* value: Kruskal-Wallis ANOVA	*P* value: Comparison with pretreatment using Dunnett's method	
			10 min	120 min
Normoxia	8	0.002	<0.05	<0.05
HH45	4	<0.001	<0.05	NS
HH75	7	<0.001	NS	<0.05
HH210–240	9	0.044	NS	<0.05

Data were normalized to pretreatment (−24 h) THC ml^{-1} and compared as a function of time. Tests for normality or equal variances failed on one-way ANOVA; therefore, data within a treatment group were tested for differences using a Kruskal-Wallis ANOVA on ranks. THC ml^{-1} at 10 and 120 min after injection were then compared to pretreatment numbers using Dunnett's method. HH, hypercapnic hypoxia; NS, nonsignificant.

The rapid removal of bacteria from the hemolymph of the blue crabs in the present study confirms findings in other crustacean species (Merrill *et al.*, 1979; Smith and Ratcliffe, 1980; White and Ratcliffe, 1982; Martin *et al.*, 1993; van de Braak *et al.*, 2002). The efficiency and the rate of clearance vary with the particular pairing of host and bacterial species. For example, Martin *et al.* (1993) found that the gram-positive bacteria *Bacillus cereus*, *B. subtilis*, and *Aerococcus viridans* were cleared to undetectable levels from the hemolymph of the penaeid shrimp *Sycionia ingentis* within 10 min of injection. The gram-negative bacteria *Pseudomonas fluorescens* and *Vibrio alginolyticus* were reduced, but not eliminated: 7.8% and 23%, respectively, of the bacteria were still free in the hemolymph one hour after injection. The different rates at which bacteria are cleared may reflect the binding specificity of hemolymph components such as lectins (Vargas-Albores *et al.*, 1993, 1997), anti-microbial peptides (Schnapp *et al.*, 1996; Destoumieux *et al.*, 1997; Khoo *et al.*, 1999; Bartlett *et al.*, 2002), the prophenoloxidase (PPO) cascade (Aspàn *et al.*, 1995), and hemocytes (Gargioni and Barracco, 1998).

The present study demonstrates that the rate of bacterial clearance from the hemolymph of blue crabs is reduced when the animals are held in water that is hypercapnic and hypoxic. The systemic respiratory responses of blue crabs to hypoxia are well-documented and are typical of brachyuran crabs (Burnett, 1992, 1997). A quiescent blue crab in well-aerated water has the high postbranchial oxygen pressures ($P\text{O}_2$ = 13 kPa) typical of many water-breathers (deFur *et al.*, 1990). Hemolymph passes through the tissues, where oxygen is consumed, and returns to the infrabranchial sinus just before it passes through the gills, where it is oxygenated. Oxygen pressures of prebranchial hemolymph are as low as 1 kPa (Booth *et al.*, 1982). Thus, a hemocyte circulating freely in the hemolymph is exposed to a wide range of oxygen pressures. During hypoxia, oxygen pressures in the hemolymph fall to levels that, depending on the severity of the ambient $P\text{O}_2$, may be very low. deFur *et al.* (1990) reported oxygen pressures of 2.4 kPa in the postbranchial hemolymph when the ambient $P\text{O}_2$ of the water was 6.7 kPa. The ambient $P\text{O}_2$ used in the present study was lower (4 kPa), forcing the hemolymph oxygen pressures to fall below 2.4 kPa. The main point is that the mechanisms associated with the clearance of bacteria must operate in a very low-oxygen environment within the crab when the animal is exposed to hypoxic water.

In the present study, at 10 min after bacterial injection, crabs in the HH75 and HH210–240 treatments had significantly greater numbers of *V. campbellii* in the hemolymph than the control crabs had (Fig. 2). Thus, the process of bacterial clearance is somehow inhibited by hypercapnic hypoxia. The bacteria are ultimately cleared in all treatments, but it is the rate of clearance that is compromised. These data support the idea that rapid clearance of live bacteria, whether by bactericidal mechanisms in the hemolymph or by physical trapping and removal to peripheral sites, contributes to disease resistance in crustaceans by limiting the spread of free pathogens to other tissues. The effects of hypoxia on bacterial clearance in crustaceans have received limited attention. *Penaeus monodon* exposed to hypoxia (1.8–2.0 mg l^{-1}, $P\text{O}_2$ = 5.4–6.4 kPa) cleared live *V. harveyi* more slowly from the hemolymph than did control animals (Direkbusarakom and Danayadol, 1998). However, results from the treatment groups were highly variable, and the authors questioned the health of some of the animals. The ability of the freshwater prawn *Macrobrachium rosenbergii* to clear live *Enterococcus* was significantly decreased by exposure to hypoxia ($P\text{O}_2$ = 4.4 and 7.0 kPa) for 12 h (Cheng *et al.*, 2002). Neither study (Direkbusarakom and Danayadol, 1998; Cheng *et al.*, 2002) reported the absolute numbers of bacteria in the hemolymph. Since bacteria are generally cleared from crustacean hemolymph within minutes to hours following injection, the results of these two studies are difficult to compare with the present work.

The impacts of hypercapnia alone or in combination with hypoxia on bacterial clearance in crustaceans have been largely neglected. Mikulski *et al.* (2000) reported that hypercapnic hypoxia at 4 kPa O_2, 2 kPa CO_2, and a pH range of 6.8 to 7.0 decreased survival following bacterial challenge in both *Litopeneaus vannamei* and the grass shrimp *Palaemonetes pugio*.

The decline in circulating hemocytes that accompanies the clearance of injected bacteria in crabs from the normoxia treatment is consistent with the role of this cell type in immune defense in crustaceans. This effect mirrors similar declines in the hemocyte counts of crustaceans that have been injected with foreign substances including lipopolysaccharide, β-1,3 glucan (laminaran), or bacteria (Smith and Söderhäll, 1983; Persson *et al.*, 1987; Martin *et al.*, 1993; van de Braak *et al.*, 2002), although this decline is not universally observed (Destoumieux *et al.*, 2000; Cheng and Chen, 2001). Following injection of foreign matter into crustacean tissues, hemocytes move into the injection site to seal the wound and to trap and kill invading bacteria by mechanisms such as melanization (Fontaine and Lightner, 1974; van de Braak *et al.*, 2002). Several studies using *in vitro* and *in vivo* measurements have shown that hemocytes, in the presence of foreign particles, rapidly associate with each other to form aggregates, or nodules (Smith *et al.*, 1984; Martin *et al.*, 1998). Aggregate formation may be mediated by lectins such as LPS-binding protein and β-glucan-binding proteins (Vargas-Albores *et al.*, 1993, 1997), by components of the prophenoloxidase cascade (Aspàn *et al.*, 1995), or by other unidentified receptors on hemocytes. Martin *et al.* (1998) presented evidence that these aggregates grow in size by the adhesion of hemocytes until they become trapped in the narrowest diameter vessels of the body. The extensive capillary network of the gill that supports respiration and osmotic regulation appears to play an important role in the trapping and removal of these nodules (Fontaine and Lightner, 1974; Johnson, 1976; Smith and Ratcliffe, 1980), although this is not observed in all cases (van de Braak *et al.*, 2002). Aggregates of hemocytes with or without associated bacteria have also been reported to accumulate in the heart, the hepatopancreas, and the connective tissues of crabs (Smith and Ratcliffe, 1980) and lobsters (Factor and Beekman, 1990) and in the lymphoid organ of penaeid shrimp (van de Braak *et al.*, 2002).

No significant changes in the concentration of hemocytes occurred in the hemolymph of crabs in the HH75 and HH210–240 treatments at 10 min after injection of bacteria (Fig. 4). It is possible that low pH and low O_2 inhibited aggregate formation by slowing or blocking the interactions of hemocytes with bacteria or with each other. An alternative possibility is that hypercapnic hypoxia may have induced changes in the process by which aggregates were removed from circulation. Several important components of the innate immune system involve oxygen, including respiratory burst reactions that generate toxic reactive oxygen species and reactive nitrogen species as well as phenoloxidase, the terminal enzyme of the PPO cascade. Inhibition of the production of reactive oxygen species was observed in *Crassostrea virginica*, the Eastern oyster, and was related specifically to low levels of oxygen and pH, which occur naturally in the tissues of oysters exposed to hypercapnic hypoxia (Boyd and Burnett, 1999). Phagocytic activity (Direkbusarakom and Danayadol, 1998) and respiratory burst activity (Le Moullac *et al.*, 1998) were decreased in hemocytes of *Penaeus monodon* exposed to hypoxia (25%–30% and 15% air saturation, respectively) as compared to controls in air-saturated water. The latter study also reported an increase in PPO activity associated with low O_2 conditions. Hemocyte phagocytosis, respiratory burst, and PPO activity were significantly reduced in *Macrobrachium rosenbergii* exposed for 24 h to hypoxia (35% air saturation; Cheng *et al.*, 2002). Note that these tests of immune function in *P. monodon* and *M. rosenbergii* were conducted *in vitro* under air-saturated conditions and, therefore, do not necessarily reflect changes in the *in vivo* activity of the enzymes involved.

In the present study, pre-exposure to hypercapnic hypoxia for 75 or 210–240 min significantly reduced the rate at which blue crabs removed bacteria from their hemolymph. These results support the concept that oxygen-dependent mechanisms play an important role in the physical removal and killing of bacterial pathogens. The accumulation of hemocytes and bacteria in the gill that has been observed by others (Smith *et al.*, 1984; Martin *et al.*, 1998) may be an efficient means to assure optimal Po_2 for immune reactions such as the respiratory burst and the PPO cascade. A potential liability of this accumulation in the gill is that aggregates of hemocytes or hemocytes and bacteria might impede hemolymph flow in the microvasculature of the gill lamellae, reducing hemolymph oxygenation and pH. This line of reasoning leads to the suggestion that tissues of the blue crab, and other crustaceans, may become hypoxic as a consequence of mounting an immune defense against a new pathogen or during an active infection. Prior exposure of the animal to hypercapnic hypoxia may reduce the rate of aggregate formation, minimize occlusion of capillaries in the gill, and help to maintain oxygenation of internal tissues, while increasing exposure of internal tissues to bacterial pathogens circulating in the hemolymph. In this study we did not directly test the interplay of respiration, acid-base balance, and immune defense, but these results do provide a framework for testing and understanding how hypercapnic hypoxia may contribute to the outbreaks of infectious disease in coastal waters.

Acknowledgments

This material is based upon work supported by the National Science Foundation under Grant No. IBN-0212921 and REU 99-35204-8555 to KGB and LEB. JDH was supported by the University of North Texas Ronald E. McNair Program. We wish to acknowledge Austin Dantzler and Joe Burgents for technical assistance. Contribution 263 to the Grice Marine Laboratory.

Literature Cited

Alday-Sanz, V., A. Roque, and J. F. Turnbull. 2002. Clearance mechanisms of *Vibrio vulnificus* biotype I in the black tiger shrimp, *Penaeus monodon*. *Dis. Aquat. Org.* **48:** 91–99.

Anderson, R. S., L. L. Brubacher, L. R. Calvo, M. A. Unger, and E. M. Burreson. 1998. Effects of tributyltin and hypoxia on the progression of *Perkinsus marinum* infections and host defence mechanisms in oyster, *Crassostrea virginica* (Gmelin). *J. Fish Dis.* **21:** 371–379.

Aspàn, A., T. S. Huang, L. Cerenius, and K. Söderhäll. 1995. cDNA cloning of prophenoloxidase from the freshwater crayfish *Pacifastacus leniusculus* and its activation. *Proc. Natl. Acad. Sci. USA* 92: 939–943.

Bachère, E. 1998. Shrimp immunity and disease control: an integrated approach. Pp. 129–134 in *Advances in Shrimp Biotechnology*, T. W. Flegel, ed. National Center for Genetic Engineering and Biotechnology, Bankok.

Bachère, E. 2000. Penaeidins, antimicrobial peptides of shrimp: a comparison with other effectors of innate immunity. *Aquaculture* **191:** 71–88.

Bartlett, T. C., B. J. Cuthbertson, E. F. Shepard, R. W. Chapman, P. S. Gross, and G. W. Warr. 2002. Crustins, homologues of an 11.5-kDa antibacterial peptide, from two species of penaeid shrimp, *Litopenaeus vannamei* and *Litopenaeus setiferus*. *Mar. Biotechnol.* **4:** 278–293.

Booth, C. E., B. R. McMahon, and A. W. Pinder. 1982. Oxygen uptake and the potentiating effect of increased hemolymph lactate on oxygen transport during exercise in the blue crab, *Callinectes sapidus*. *J. Comp. Physiol.* **148:** 111–121.

Boyd, J. N., and L. E. Burnett. 1999. Reactive oxygen intermediate production by oyster hemocytes exposed to hypoxia. *J. Exp. Biol.* **202:** 3135–3143.

Burnett, L. E. 1992. Integrated function of respiratory pigments (Compleat Crab Symposium). *Am. Zool.* **32:** 438–446.

Burnett, L. E. 1997. The challenges of living in hypoxic and hypercapnic aquatic environments. *Am. Zool.* **37:** 633–640.

Burnett, L. E., P. L. deFur, and D. D. Jorgensen. 1981. Application of the thermodilution technique for measuring cardiac output and assessing cardiac stroke volume in crabs. *J. Exp. Zool.* **218:** 165–173.

Cheng, W., and J. C. Chen. 2001. Effects of intrinsic and extrinsic factors on the haemocyte profile of the prawn, *Macrobrachium rosenbergii*. *Fish Shellfish Immunol.* **11:** 53–63.

Cheng, W., C.-H. Liu, J.-P. Hsu, and J.-C. Chen. 2002. Effect of hypoxia on the immune response of giant freshwater prawn *Macrobrachium rosenbergii* and its susceptibility to pathogen *Enterococcus*. *Fish Shellfish Immunol.* **13:** 351–365.

deFur, P. L., and C. P. Mangum. 1979. The effects of environmental variables on the heart rates of invertebrates. *Comp. Biochem. Physiol.* **62A:** 283–294.

deFur, P. L., C. P. Mangum, and J. E. Reese. 1990. Respiratory responses of the blue crab *Callinectes sapidus* to long-term hypoxia. *Biol. Bull.* **178:** 46–54.

Destoumieux, D., P. Bullet, D. Loew, A. Van Dorsselaer, J. Rodriguez, and E. Bachère. 1997. Penaeidins, a new family of antimicrobial peptides isolated from the shrimp *Penaeus vannamei* (Decapoda). *J. Biol. Chem.* **272:** 28398–28406.

Destoumieux, D., M. Munoz, C. Cosseau, J. Rodriguez, P. Bulet, M. Comps, and E. Bachere. 2000. Penaeidins, antimicrobial peptides with chitin-binding activity, are produced and stored in shrimp granulocytes and released after microbial challenge. *J. Cell Sci.* **113:** 461–469.

Direkbusarakom, S., and Y. Danayadol. 1998. Effect of oxygen depletion on some parameters of the immune system in black tiger shrimp (*Penaeus monodon*). Pp. 147–149 in *Advances in Shrimp Biotechnology*, T. W. Flegel, ed. National Center for Genetic Engineering and Biotechnology, Bangkok.

Factor, J. R., and J. Beekman. 1990. The digestive system of the lobster, *Homarus americanus*. III. Removal of foreign particles from the blood by fixed phagocytes of the digestive gland. *J. Morphol.* **206:** 293–302.

Fontaine, C. T., and D. V. Lightner. 1974. Observations on the phagocytosis and elimination of carmine particles injected into the abdominal musculature of the white shrimp, *Penaeus setiferus*. *J. Invertebr. Pathol.* **24:** 141–148.

Gargioni, R., and M. A. Barracco. 1998. Hemocytes of the palaemonids *Macrobrachium rosenbergii* and *M. acanthurus*, and of the penaeid *Penaeus paulensis*. *J. Morphol.* **236:** 209–221.

Gleeson, R. A., and P. L. Zubkoff. 1977. The determination of hemolymph volume in the blue crab, *Callinectes sapidus*, utilizing 14C-thiocyanate. *Comp. Biochem. Physiol.* **56A:** 411–413.

Johnson, P. T. 1976. Bacterial infection in the blue crab, *Callinectes sapidus*: course of infection and histopathology. *J. Invertebr. Pathol.* **28:** 25–36.

Khoo, L., D. W. Robinette, and E. J. Noga. 1999. Callinectin, an antibacterial peptide from blue crab, *Callinectes sapidus*, hemocytes. *Mar. Biotechnol.* **1:** 44–51.

Le Moullac, G., C. Soyez, D. Saulnier, D. Ansquer, J. C. Avarre, and P. Levy. 1998. Effect of hypoxic stress on the immune response and the resistance to vibriosis of the shrimp, *Penaeus stylirostris*. *Fish Shellfish Immunol.* **8:** 621–629.

Martin, G. G., D. Poole, C. Poole, J. E. Hose, M. Arias, L. Reynolds, N. McKrell, and A. Whang. 1993. Clearance of bacteria injected into the hemolymph of the penaeid shrimp, *Sicyonia ingentis*. *J. Invertebr. Pathol.* **62:** 308–315.

Martin, G. G., K. Kay, D. Poole, and C. Poole. 1998. *In vitro* nodule formation in the ridgeback prawn, *Sicyonia ingentis*, and the American lobster, *Homarus americanus*. *Invertebr. Biol.* **117:** 155–168.

McGaw, I. J., and C. L. Reiber. 2002. Cardiovascular system of the blue crab *Callinectes sapidus*. *J. Morphol.* **251:** 1–21.

McMahon, B. R., and L. E. Burnett. 1990. The crustacean open circulatory system: a reexamination. *Physiol. Zool.* **63:** 35–71.

Merrill, D. P., S. A. Mongeon, and S. Fisher. 1979. Distribution of fluorescent latex particles following clearance from the hemolymph of the freshwater crayfish *Orconectes virilis* (Hagen). *J. Comp. Physiol.* **132:** 363–368.

Mikulski, C. M., L. E. Burnett, and K. G. Burnett. 2000. The effects of hypercapnic hypoxia on the survival of shrimp challenged with *Vibrio parahaemolyticus*. *J. Shellfish Res.* **19:** 301–311.

Mix, M. C., and A. K. Sparks. 1980. Tanner crab *Chionoecetes bairdi* Rathbun haemocyte classification and an evaluation of using differential counts to measure infection with a fungal disease. *J. Fish Dis.* **3:** 285–293.

Muñoz, M., R. Cedeno, J. Rodriguez, W. P. W. van der Knaap, E. Mialhe, and E. Bachère. 2000. Measurement of reactive oxygen intermediate production in haemocytes of the penaeid shrimp, *Penaeus vannamei*. *Aquaculture* **191:** 89–107.

Persson, M., L. Cerenius, and K. Söderhäll. 1987. The influence of haemocyte number on the resistance of the freshwater crayfish *Pacifastacus leniusculus* Dana, to the parasitic fungus, *Aphanomyces astaci*. *J. Fish Dis.* **10:** 471–477.

Rhodes, M. W., H. Kator, S. Kotob, P. van Berkum, I. Kaattari, W. Vogelbein, M. M. Floyd, W. R. Butler, F. D. Quinn, C. Ottinger, and E. Shotts, E. 2001. A unique mycobacterium species isolated from an epizootic of striped bass (*Morone saxatilis*). *Emerg. Infect. Dis.* **7:** 896–899.

Schnapp, D., G. D. Kemp, and V. J. Smith. 1996. Purification and characterization of a proline-rich antibacterial peptide, with sequence similarity to bactenecin-7, from the haemocytes of the shore crab, *Carcinus maenas*. *Eur. J. Biochem.* **240:** 532–539.

Smith, V. J., and N. A. Ratcliffe. 1980. Host defence reactions of the shore crab, *Carcinus maenas* (L.): clearance and distribution of injected test particles. *J. Mar. Biol. Assoc. UK* **60:** 89–102.

Smith, V. J., and K. Söderhäll. 1983. β-1,3 glucan activation of crustacean hemocytes *in vitro* and *in vivo*. *Biol. Bull.* **164:** 299–314.

Smith, V. J., K. Söderhäll, and M. Hamilton. 1984. β-1,3-glucan induced cellular defense reaction in the shore crab, *Carcinus maenas*. *Comp. Biochem. Physiol.* **77A:** 635–639.

Song, Y. L., and Y. T. Hsieh. 1994. Immunostimulation of tiger shrimp (*Penaeus monodon*) hemocytes for generation of microbicidal substances: analysis of reactive oxygen species. *Dev. Comp. Immunol.* **18:** 201–209.

van de Braak, C. B. T., M. H. A. Botterblom, N. Taverne, W. B. Van Muiswinkel, J. H. Rombout, and W. P. W. Van der Knaap. 2002. The roles of haemocytes and the lymphoid organ in the clearance of injected *Vibrio* bacteria in *Penaeus monodon* shrimp. *Fish Shellfish Immunol.* **13:** 293–309.

Vargas-Albores, F., A. Guzmán-Murillo, and J. L. Ochoa. 1993. A lipopolysaccharide-binding agglutinin isolated from brown shrimp (*Penaeus californiensis* Holmes) haemolymph. *Comp. Biochem. Physiol.* **104A:** 407–413.

Vargas-Albores, F., F. Jimenez-Vega, and G. Yepiz-Plascencia. 1997. Purification and comparison of β-1,3-glucan binding protein from the white shrimp (*Penaeus vannamei*). *Comp. Biochem. Physiol.* **116B:** 453–458.

White, K. H., and N. A. Ratcliffe. 1982. The segregation and elimination of radio- and fluorescent-labelled marine bacteria from the haemolymph of the shore crab, *Carcinus maenas*. *J. Mar. Biol. Assoc. UK* **62:** 819–833.

INDEX

A

Actograph, 103
Adaptable defense: a nudibranch mucus inhibits nematocyst discharge and changes with prey type, 113
Aggression, 173
Alkylphenols, 13
Antioxidants, 13
Ascidian, 95, 144, 152

B

Bacterial clearance, 188
Barnacle, 121
Behavior, 134
Biggers, William J., and Hans Laufer, Identification of juvenile hormone-active alkylphenols in the lobster *Homarus americanus* and in marine sediments, 13
Biological rhythm, 103
Birenheide, Rüdiger, see Tatsuo Motokawa, 4
Bisphenol A, 13
Blubber, 125
Boal, Jean G., see Kendra C. Buresch, 1
Bortolami, S. B., see M. H. Temkin, 35
Botryllus schlosseri, 144, 152
Brittle star, 25
Brooder, 144
Bryozoa, 35
Bucknall, Martin P., see Rebecca L. Swanson, 161
Buresch, Kendra C., Jean G. Boal, Gregg T. Nagle, Jamie Knowles, Robert Nobuhara, Kate Sweeney, and Roger T. Hanlon, Experimental evidence that ovary and oviducal gland extracts influence male agonistic behavior in squids, 1
Burnett, Karen G., see Jeremy D. Holman, 188
Burnett, Louis E., see Jeremy D. Holman, 188

C

Callinectes sapidus, 188
Chemical and visual communication during mate searching in rock shrimp, 134
Chemical
  cues, 134
  sensing, 1
Chemoreception, 65
Chemotaxis, 95
Chilean Blob, 125
Chlorophyll fluorescence, 61
Chromosomal rearrangement, 46
Collagen, 125
Communication, 134
Competition, 173
Conflict chemoreception, 1
Confocal microscopy, 65
Contractile connective tissue, 4
Contraction and stiffness changes in collagenous arm ligaments of the stalked crinoid *Metacrinus rotundus* (Echinodermata), 4
Coral, 61
Cosson, Jacky, see Makiko Ishikawa, 95
Crassostrea
  gigas, 46
  plicatula, 46
  rhizophorae, 46
  virginica, 46
Crayfish, 78
Crustacea, 134
Cue
  chemical, 134
  visual, 134
Curtis, Nicholas E., see Sidney K. Pierce, 125

D

De Nys, Rocky, see Rebecca L. Swanson, 161
Defense, 113
Denny, Mark W., see Natasha K. Li, 121
Density effects, 152
Deposit feeding, 65
Development, 25, 78
  larval, 87
Díaz, Eliecer R., and Martin Thiel, Chemical and visual communication during mate searching in rock shrimp, 134
Differences in the rDNA-bearing chromosome divide the Asian-Pacific and Atlantic species of *Crassostrea* (Bivalvia, Mollusca), 46

E

Echinoderm, 4
Edmunds, Peter J., and Ruth D. Gates, Size-dependent differences in the photophysiology of the reef coral *Porites astreoides*, 61
Effects of hypercapnic hypoxia on the clearance of *Vibrio campbellii* in the Atlantic blue crab, *Callinectes sapidus* Rathbun, 188
Ehlinger, Gretchen S., and Richard A. Tankersley, Survival and development of horseshoe crab *(Limulus polyphemus)* embryos and larvae in hypersaline conditions, 87
Evolution, 134
Experimental evidence that ovary and oviducal gland extracts influence male agonistic behavior in squids, 1

F

Ferrell, David L., Fitness consequences of allorecognition-mediated agonistic interactions in the colonial hydroid *Hydractinia*, 173
Fertilization, 35, 144, 152
Fertilization in an egg-brooding colonial ascidian does not vary with population density, 152
Field studies, 55
Fitness, 103
Fitness consequences of allorecognition-mediated agonistic interactions in the colonial hydroid *Hydractinia*, 173
Floridoside-isethionic acid complex, 161
Forest, D., see Sara M. Lindsay, 65
Free-spawning invertebrate, 144

G

Garry, Kyle, see Paul G. Greenwood, 113
Gates, Ruth D., see Peter J. Edmunds, 61
Greenwood, Paul G., Kyle Garry, April Hunter, and Miranda Jennings, Adaptable defense: a nudibranch mucus inhibits nematocyst discharge and changes with prey type, 113

Growth rate, 173
Gulf of Mexico, 173

H

Hamann, Ellen, see Aimee Phillippi, 152
Hanlon, Roger T., see Kendra C. Buresch, 1
Harper, S. L., and C. L. Reiber, Physiological development of the embryonic and larval crayfish heart, 78
Hemocyte, 188
Histamine, 161
Holman, Jeremy D., Karen G. Burnett, and Louis E. Burnett. Effects of hypercapnic hypoxia on the clearance of *Vibrio campbellii* in the Atlantic blue crab, *Callinectes sapidus* Rathbun, 188
Homarus americanus, 13
Horseshoe crab, 87
Hunter, April, see Paul G. Greenwood, 113
Hybridization barrier, 46
Hydrodynamics, 121
Hypercapnia, 188
Hypersalinity, 87
Hypoxia, 78, 188

I

Identification and activity-dependent labeling of peripheral sensory structures on a spionid polychaete, 65
Identification of juvenile hormone-active alkylphenols in the lobster *Homarus americanus* and in marine sediments, 13
Immunohistochemistry, 65
Indian River Lagoon, 87
Induction of settlement of larvae of the sea urchin *Holopneustes purpurascens* by histamine from a host alga, 161
Innate immunity, 188
Interaction between photoperiod and an endogenous seasonal factor in influencing the diel locomotor activity of the benthic polychaete *Nereis virens* Sars, 103
Invertebrate, 173
Ishikawa, Makiko, Hidekazu Tsutsui, Jacky Cosson, Yoshitaka Oka, and Masaaki Morisawa, Strategies for sperm chemotaxis in the siphonophores and ascidians: a numerical simulation study, 95

J

Jennings, Miranda, see Paul G. Greenwood, 113
Johnson, Sheri L., and Philip O. Yund, Remarkable longevity of dilute sperm in a free-spawning colonial ascidian, 144
Juvenile hormone activity, 13

K

Knowles, Jamie, see Kendra C. Buresch, 1
Komatsu, Miéko, see Hideyuki Tominaga, 25
Kumar, Naresh, see Rebecca L. Swanson, 161

L

Larva, 161
  development of, 87
Last, Kim S., and Peter J. W. Olive, Interaction between photoperiod and an endogenous seasonal factor in influencing the diel locomotor activity of the benthic polychaete *Nereis virens* Sars, 103
Laufer, Hans, see William J. Biggers, 13
Li, Natasha K., and Mark W. Denny, Limits to phenotypic plasticity: flow effects on barnacle feeding appendages, 121
Life history, 103
Limits to phenotypic plasticity: flow effects on barnacle feeding appendages, 121
Lindsay, Sara M., Timothy J. Riordan, Jr., and D. Forest, Identification and activity-dependent labeling of peripheral sensory structures on a spionid polychaete, 65
Limulus polyphemus, 87
Lobster, 13

M

Marine
  invertebrate, 121
  sediments, 13
Maruyama, Yoshihiko K., Occurrence in the field of a long-term, year-round, stable population of placozoans, 55
Massey, Steven E., see Sidney K. Pierce, 125
Mating systems, 134
Maugel, Timothy K., see Sidney K. Pierce, 125
Metamorphosis, 161
Methylfarnesoate, 13
Microscopic, biochemical, and molecular characteristics of the Chilean Blob and a comparison with the remains of other sea monsters: nothing but whales, 125
Model, 95
Molt cycle duration, 87
Morisawa, Masaaki, see Makiko Ishikawa, 95
Morphology, 121
Motokawa, Tatsuo, Osamu Shintani, and Rüdiger Birenheide, Contraction and stiffness changes in collagenous arm ligaments of the stalked crinoid *Metacrinus rotundus* (Echinodermata), 4
Mucus, 113
Mutable connective tissue, 4

N

Nagle, Gregg T., see Kendra C. Buresch, 1
Nakamura, Shoga, see Hideyuki Tominaga, 25
Nematocyst, 113
Nereis virens, 103
Nudibranch, 113

O

Occurrence in the field of a long-term, year-round, stable population of placozoans, 55
Oka, Yoshitaka, see Makiko Ishikawa, 95
Olavarría, Carlos, see Sidney K. Pierce, 125
Olive, Peter J. W., see Kim S. Last, 103
Ontogeny, 78
Osmoregulation, 87
Oxygen consumption, 78

P

Phenotypic plasticity, 121
Pheromones, 1
Phillippi, Aimee, Ellen Hamann, and Philip O. Yund, Fertilization in an egg-brooding colonial ascidian does not vary with population density, 152
Photophysiology, 61
Physiological development of the embryonic and larval crayfish heart, 78
Pierce, Sidney K., Steven E. Massey, Nicholas E. Curtis, Gerald N. Smith, Jr., Carlos Olavarría, and Timothy K. Maugel, Microscopic, biochemical, and molecular characteristics of the Chilean Blob and a comparison with the remains of other sea monsters: nothing but whales, 125
Placozoa, 55
Polychaeta, 103

R

Reiber, C. L., see S. L. Harper, 78
Remarkable longevity of dilute sperm in a free-spawning colonial ascidian, 144
Reproduction, 25, 134

Reproduction and development of the conspicuously dimorphic brittle star *Ophiodaphne formata* (Ophiuroidea), 25
Rhynchocinetes, 134
Ribosomal RNA genes, 46
RIORDAN, TIMOTHY J., JR., see Sara M. Lindsay, 65

S

Salinity tolerance, 87
Sampling
  slide, 55
  substrate, 55
Sea
  anemone, 113
  lily, 4
  monster, 125
  urchin, 161
Sensory ecology, 65
Settlement, 161
Sexual dimorphism, 25
SHINTANI, OSAMU, see Tatsuo Motokawa, 4
Shrimp, 134
Simulation, 95
Siphonophore, 95
Size mortality, 61
Size-dependent differences in the photophysiology of the reef coral *Porites astreoides*, 61
SMITH, GERALD N., JR., see Sidney K. Pierce, 125
Sperm, 35
  half-life, 144
  longevity, 144
Spermatozeugmata, 35
Spionidae, 65
Stalked crinoid, 4
STEINBERG, PETER D., see Rebecca L. Swanson, 161
Strategies for sperm chemotaxis in the siphonophores and ascidians: a numerical simulation study, 95
Survival, 87, 173
Survival and development of horseshoe crab *(Limulus polyphemus)* embryos and larvae in hypersaline conditions, 87
SWANSON, REBECCA L., JANE E. WILLIAMSON, ROCKY DE NYS, NARESH KUMAR, MARTIN P. BUCKNALL, AND PETER D. STEINBERG, Induction of settlement of larvae of the sea urchin *Holopneustes purpurascens* by histamine from a host alga, 161
SWEENEY, KATE, see Kendra C. Buresch, 1

T

TANKERSLEY, RICHARD A., see Gretchen S. Ehlinger, 87
TEMKIN, M. H., AND S. B. BORTOLAMI, Waveform dynamics of spermatozeugmata during the transfer from paternal to maternal individuals of *Membranipora membranacea*, 35
Temperature tolerance, 87
Thermal stress, 61
THIEL, MARTIN, see Eliecer R. Díaz, 134
TOMINAGA, HIDEYUKI, SHOGO NAKAMURA, AND MIÉKO KOMATSU, Reproduction and development of the conspicuously dimorphic brittle star *Ophiodaphne formata* (Ophiuroidea), 25
Trichoplax adhaerens, 55
TSUTSUI, HIDEKAZU, see Makiko Ishikawa, 95

V

Vibrio campbellii, 188
Visual cues, 134

W

WANG, YONGPING, ZHE XU, AND XIMING GUO, Differences in the rDNA-bearing chromosome divide the Asian-Pacific and Atlantic species of *Crassostrea* (Bivalvia, Mollusca), 46
Wave exposure, 121
Waveform dynamics of spermatozeugmata during the transfer from paternal to maternal individuals of *Membranipora membranacea*, 35
Whale, 125
WILLIAMSON, JANE E., see Rebecca L. Swanson, 161

Y

YUND, PHILIP O., see Aimee Phillippi, 152; Sheri L. Johnson, 144

THE BIOLOGICAL BULLETIN

2004 Subscription Rates
Volumes 206-207

***Paid Subscriptions include both print and electronic subscriptions at:** www.biolbull.org

	Institutional*	Individual*
One year subscription (6 issues - 2 volumes)	$325.00	$120.00
Single volume (3 issues)	$165.00	$70.00
Single Issues	$ 75.00	$25.00

*Surface delivery included in above prices.
For prompt delivery, we encourage subscribers outside the U.S. to request airmail service.

Airmail Delivery Charge

U.S. and Canada:	$ 45.00
Mexico:	$ 60.00
All other locations:	$100.00

Orders Must Be Prepaid in U.S. Dollars, Check Payable to The Marine Biological Laboratory

About *The Biological Bulletin*
ISSN: 0006-3185
Frequency: Bimonthly
Number of issues per year: 6
Months of Publication: February, April, June, August, October, December
Subscriptions entered for calendar year
Volume indexes contained in June and December issues
Annual report of the Marine Biological Laboratory contained in August issue
Most back issues available
Claims handled upon receipt
No agency discounts
Internet:
www.biolbull.org

Please address orders to:
Wendy Child
Subscriptions
The Biological Bulletin
Marine Biological Laboratory
7 MBL Street
Woods Hole, MA 02543-1015 U.S.A.
Fax: 508-289-7922 Tel: 508-289-7402 Email: wchild@mbl.edu

Published by the Marine Biological Laboratory
Woods Hole, Massachusetts, 02543 U.S.A.

THE BIOLOGICAL BULLETIN
(www.biolbull.org)
2004 SUBSCRIPTION FORM
(VOLUMES 206-207, 6 ISSUES)

(please print)
NAME: ______________________________
INSTITUTION: ______________________________
ADDRESS: ______________________________
CITY: ______________ **STATE:** ______________
POSTAL CODE: ______________ **COUNTRY:** ______________
TELEPHONE: ______________ **FAX:** ______________
E-MAIL ADDRESS ______________________________

All subscriptions run on the calendar year; price includes both print and online journals

☐ Please send me a 2004 subscription to *The Biological Bulletin* at the rate indicated below:

☐ Individual: $120.00 (6 ISSUES) ☐ Institutional : $325.00 (6 ISSUES)
☐ Individual: $70.00 (3 ISSUES) ☐ Institutional : $165.00 (3 ISSUES)

Check one: ☐ February April June or ☐ August October December

☐ Please send me the following back issue(s): ______________________

☐ Individual: at $25.00 (PER ISSUE) ☐ Institutional : at $75.00 (PER ISSUE)

Delivery Options

_____ Surface Delivery (Surface delivery is included in the subscription price.)
_____ Air delivery (Please add the correct amount to your payment.)

☐ U.S. and Canada: $46.00 ☐ Mexico: $60.00 ☐ All other locations: $100.00

Payment Options

_____ Enclosed is my check or U.S. money order for $ ______payable to The Marine Biological Laboratory

_____ Please charge my ☐ VISA, ☐ MasterCard ☐ Discover Card $________

_____ Please send me an invoice. (Note: Payment must be received before subscription commences.)

Account No.: ______________________ **Exp. Date:** ______________________

Signature: ______________________ **Date:** ______________________

Return this form with your check or credit information to:
Marine Biological Laboratory
Subscription Office ◆ The Biological Bulletin ◆7 MBL Street ◆ Woods Hole, MA 02543-1015

OGL-OCEAN GENOME LEGACY

■ *EXECUTIVE DIRECTOR*

A new not-for-profit foundation devoted to the preservation, distribution and evolutionary genomics of DNA from marine organisms is seeking an **EXECUTIVE DIRECTOR.**

The successful candidate will have a Ph.D. in cell or molecular biology, 4+ years' experience in molecular biology, and be highly motivated to work at the bench. Responsibilities will include the assembly of a small team of scientists for the long-term preservation of marine organism DNA, development of tissue culture techniques for marine invertebrate cells, construction of genome libraries, and evolutionary genomics of special marine transition groups.

The OGL laboratory will be temporarily located at New England Biolabs, Inc., Beverly, MA until a new facility is constructed in Ipswich, MA.

Applicants should send a resume and three references to:
Carol Ann Zapustas, New England Biolabs, Inc.,
32 Tozer Road, Beverly, MA 01915.

OCEAN GENOME LEGACY

An Equal Opportunity Employer.

POSITION ANNOUNCEMENT

Editor-in-Chief
The Biological Bulletin

Start Date: January 2005
Term: Five years, renewable

The Editor-in-Chief is responsible for the overall editorial direction of the *Biological Bulletin*. The Editor-in-Chief appoints Associate Editors and members of the Editorial Board, decides which manuscripts are published, mediates editorial disputes, and sets policy for the journal.

The Editor-in-Chief is an independent contractor who reports to the Director and CEO of the Marine Biological Laboratory. Stipend for the position is $10,000 annually. The *Bulletin's* editorial offices are based in Woods Hole, but the Editor-in-Chief may work from his/her home institution. The Editor-in-Chief is expected to spend some part of the summer months in Woods Hole. Housing for up to one month will be provided in Woods Hole.

The successful candidate for this position will meet the following requirements:

- A broad understanding of biology, and a manifest interest in its diversity and comparative and integrative aspects
- A track-record of publishing in peer-reviewed journals
- Experience reviewing papers for scientific journals
- Proven skill as a substantive editor
- Ability to make tough decisions and willingness to work with other editors to reach a decision on difficult papers
- Demonstrated experience with the editorial process *(e.g.*, serving as an Editor or Associate Editor for a journal similar to the *Biological Bulletin*)
- The willingness and ability to commit the time required, approximately one day per week, to fulfill the duties outlined here for five years.

Job description: The Editor-in-Chief devotes a minimum of six hours per week to the operation of the *Biological Bulletin*. The Editor's ongoing activities include 1) assigning submitted papers to the appropriate Associate Editor; 2) reading reviews and manuscripts to ensure fairness and technical accuracy; 3) writing editorial decision letters based on the reviews; 4) fielding telephone and e-mail queries on a daily basis from authors deciding whether to submit their work to the *Biological Bulletin*, authors who are unhappy about an editorial decision, and Associate Editors requesting guidance on such matters as the identity, availability, and number of reviewers, and editorial decisions and disputes; 5) communicating regularly (by telephone or e-mail) with the Managing Editor and other editorial staff members to plan future issues, to arrange the table of contents, to develop the issue cover, and to discuss organizational issues; 6) editing accepted manuscripts as necessary for substance, accuracy, and clarity; 7) selecting cover photos and writing associated legends; 8) informing editorial staff of noteworthy articles for the media; 9) as the deadline for each issue approaches, deciding which manuscripts will be published.

Nomination packets must include the following:

1. Letter of intent
2. Current CV
3. Vision Statement for the journal

Send nominations to:
Pamela Clapp Hinkle
Managing Editor, *Biological Bulletin*
Marine Biological Laboratory
7 MBL Street
Woods Hole, MA 02543
pclapp@mbl.edu

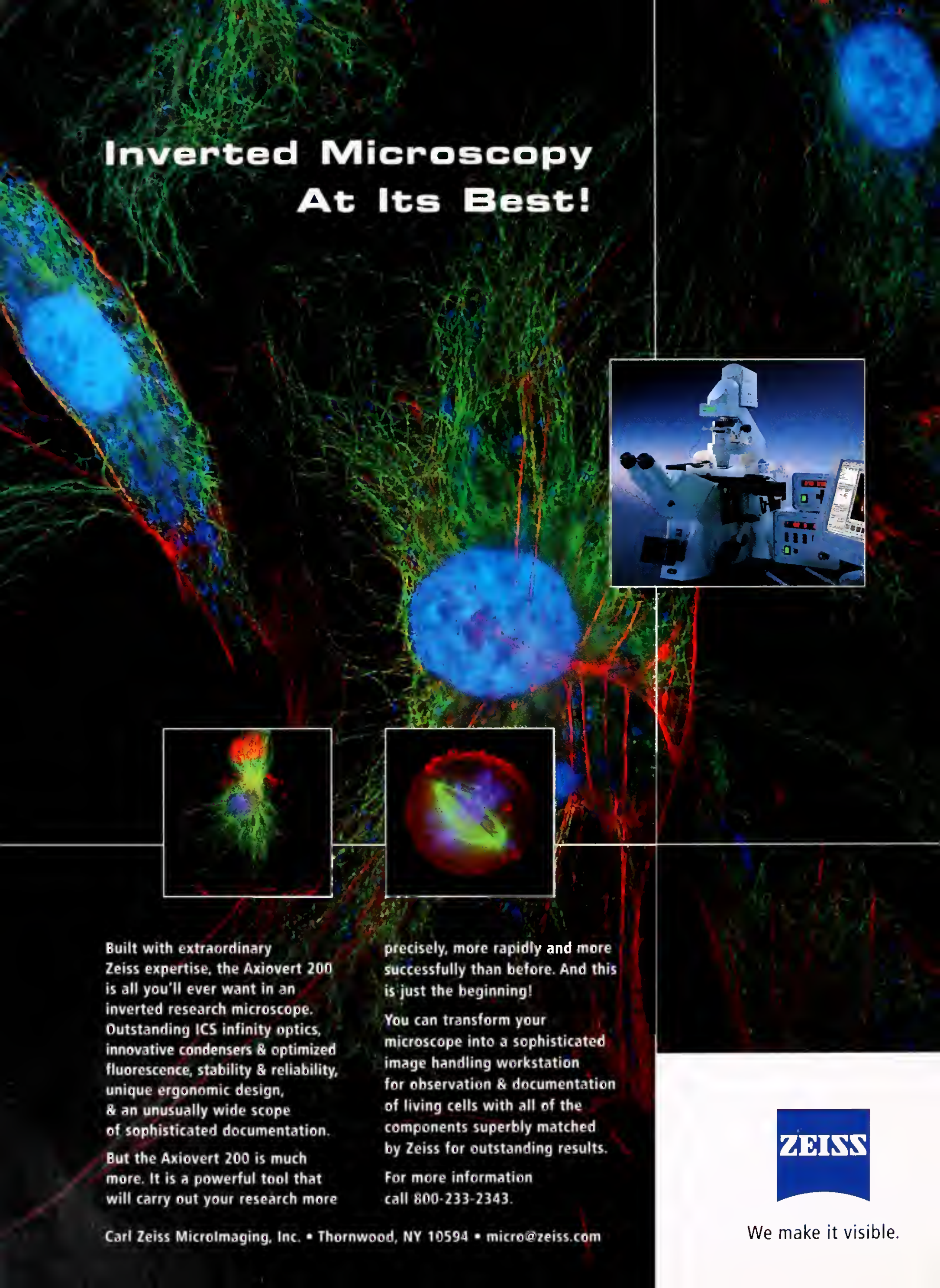

Inverted Microscopy At Its Best!

Built with extraordinary Zeiss expertise, the Axiovert 200 is all you'll ever want in an inverted research microscope. Outstanding ICS infinity optics, innovative condensers & optimized fluorescence, stability & reliability, unique ergonomic design, & an unusually wide scope of sophisticated documentation.

But the Axiovert 200 is much more. It is a powerful tool that will carry out your research more precisely, more rapidly and more successfully than before. And this is just the beginning!

You can transform your microscope into a sophisticated image handling workstation for observation & documentation of living cells with all of the components superbly matched by Zeiss for outstanding results.

For more information call 800-233-2343.

Carl Zeiss MicroImaging, Inc. • Thornwood, NY 10594 • micro@zeiss.com

ZEISS

We make it visible.

MBL/WHOI LIBRARY
WH 1ART U